Modulation of the p53 response: effects of DNA damage and MDM2 overexpression

Mark Clifford Ditzel

Thesis presented to the University of London for
the degree of Doctor of Philosophy

January 2000

Imperial Cancer Research Fund
and
University College London

Abstract

p53 is known to play a major role in the cellular response to stress, capable of mediating either a cell cycle arrest or apoptosis. MDM2 has recently been implicated as a crucial regulator of p53 activity, affecting p53's protein level, transcriptional capabilities and subcellular localisation. An intimate relationship also exists between these two proteins and MDM2's negative regulator, ARF. Transcriptional- and protein-protein-relationships between these proteins have been highlighted through a number of observations, although the regulatory mechanisms governing the relationships remain unclear.

Examination of the irradiation responses of different human cell lines revealed similar increases in p53 expression, but fundamental differences in the p53-inducible MDM2 and p21 protein responses. UV-irradiation induced apoptosis in U2OS cells and reduced the expression of both MDM2 and p21 protein, while only mediating a reduction in *mdm2* mRNA levels. A transient reduction in MDM2 protein, but not mRNA, levels was apparent in a variety of X-ray-irradiated cell lines. Closer examination revealed potential UV- and X-ray-mediated p21 and MDM2 protein degradation events, respectively. These results suggested the temporal importance of MDM2 and p21 protein levels in irradiation-mediated cell cycle arrest and apoptosis. Furthermore, immunofluorescence analysis of irradiated cells also revealed differential p53 and MDM2 subcellular localisation patterns, perhaps reflecting apoptotic-specific spatial processes.

Analysis of ARF-induced and X-ray- and UV-irradiated cells, exhibiting elevated p53 levels, surprisingly showed no negative effects on p53:MDM2 association. Hence, negative regulation of MDM2-mediated p53 degradation seemed to occur downstream of p53:MDM2 association, perhaps at the stage of ubiquitin transfer or the actual proteosomal degradation event.

For Susan Hansford, a mother who I could ask no more of. I wish you and Richard every happiness.

In memory of Victor Albert Ditzel, my father, who will never know.

Acknowledgements

My gratitude to: my supervisor, Dr. Mike Fried, who gave me this opportunity and has taught me many things and the Eukaryotic Genome Organisation and Expression (EGOE) lab members, past and present. Special thanks go out to Dr. Lindseed Alleen (sic) (inspirational scientifically and for lab solidarity), Dr. Martine Lomax (for her clothing effulgence), Trevor Duhig (you bearded beauty), Moira Read (Czar of cell culture), Dr. Jon Gilley (ol' wobbly lips) and Gavin Fox (the nasal leprechaun) for help, advice and very memorable times.

I am very grateful to the Imperial Cancer Research Fund (ICRF) for providing me with a bursary to undertake this PhD and to the members of staff for their general friendliness and helpfulness; providing an exceptional working environment.

Finally, I thank my friends who have lead me onto, and off of many paths, to many destinations and I hope to continue travelling with them.

"The offing was barred by a black bank of clouds, and the tranquil waterway leading to the uttermost ends of the earth flowed sombre under an overcast sky – seemed to lead into the heart of an immense darkness."

'Heart of Darkness'

Table of Contents

List of Figures

CHAPTER FOUR - IMMUNOFLUORESCENCE ANALYSIS

CHAPTER FIVE - GENERAL DISCUSSION

List of Tables

List of Abbreviations

aa	Amino Acid
bp	Base pairs
BrDU	Bromodeoxyuridine
CDK	Cyclin-Dependent Kinase
CDK-I	Cyclin-Dependent Kinase Inhibitor
cDNA	Complimentary Deoxyribonucleic Acid
CHX	Cycloheximide
Con	Control
DN(5)	pCMV-driven p53 $175^{R \Rightarrow H}$ expressing U2OS cell line
ds	Double-stranded
ECL	Enhanced Chemoluminescence
FACS	Fluorescence Assisted Cell Sorting
g	Relative Centrifugal Force
GFP	Green Fluorescent Protein
Gy	Grays
HPV	Human Papilloma Virus
Hrs (hrs)	Hours
IF	Immunofluorescence
IP	Immunoprecipitation
Jm^{-2}	Joules per $Metre^2$
kDa	kilo Dalton
M	Molar
M(5)	pCMV-driven MDM2 overexpressing U2OS cell line
MCS	Multiple Cloning Site
Mins (mins)	Minutes
mRNA	Messenger Ribose Nucleic Acid
NES	Nuclear Export Signal
NLS	Nuclear Localisation Signal
nts	Nucleotides

p3	pcDNA3.1 transfected U2OS cell line
PAGE	Polyacrylamide Gel Electrophoresis
PBS	Phosphate Buffered Saline
PCNA	Proliferating Cell Nuclear Antigen
PCR	Polymerase Chain Reaction
RE	Restriction Enzyme
RPM	Revolutions Per Minute
rRNA	Ribosomal Ribonucleic Acid
RT-PCR	Reverse Transcriptase Polymerase Chain Reaction
SDS	Sodium Dodecyl Sulphate
Secs (secs)	Seconds
ss	Single-Stranded
TUNEL	Terminal
UV	Ultra-violet (C)-irradiation
v/v	Volume per Volume
w/v	Weight per Volume

Chapter One

Introduction

p53

The p53 story has been gathering pace since its discovery in 1979 as a protein complexed with SV40 large T antigen(Lane and Crawford 1979; Linzer and Levine 1979). Over its 20 year career p53 has continued to dominate the centre-stage in cancer biology. Intense research has continued to illuminate p53's activities and regulation of those activities; explaining old and creating new paradoxes. p53's role as being one of the most important tumour suppresser proteins has continued to be strengthened, but concomitantly complicated. Now is an extremely exciting time, due to the emergence of novel p53 regulatory pathways and mechanisms, in addition to the existence of p53 family members. These recent findings are helping to explain past-phenomena and explore the new.

Apart from the initial evidence of mutant p53 being an oncogene(Eliyahu, Raz et al. 1984; Jenkins, Rudge et al. 1984; Parada, Land et al. 1984), a plethora of papers has defined the wild-type function of p53 to be anti-oncogenic or growth-suppressive(Eliyahu, Michalovitz et al. 1989; Finlay, Hinds et al. 1989; Baker, Markowitz et al. 1990; Chen, Chen et al. 1990; Mercer, Amin et al. 1990; Mercer, Shields et al. 1990), mediated through apoptosis or cell cycle arrest. Initial screening of colon cancer patients revealed that *p53* mutations were of unusually high frequencies(Baker, Fearon et al. 1989). Similar elevated mutation frequencies were also apparent in a number of other forms of human and animal cancers(Greenblatt, Bennett et al. 1994; Hollstein, Rice et al. 1994; Hainaut, Hernandez et al. 1998). The nature of the genetic lesions mostly generated missense mutations in one allele producing a faulty protein followed, in a majority of cases, by a reduction to homozygosity. Furthermore, members of Li-Fraumeni cancer-prone families were shown to carry germ-line mutations in the *p53* gene(Malkin, Li et al. 1990; Srivastava, Zou et al. 1990). Championing these observations was the finding that mice homozygous null for *p53*, while developmentally competent, were highly predisposed to cancer(Donehower, Harvey et

al. 1992). Early work with DNA tumour virus antigens shown to target and inhibit p53 function, highlighted an alternative route to p53 inactivation and provided invaluable tools to facilitate its study(Lane and Crawford 1979; Linzer and Levine 1979; Kao, Yew et al. 1990; Scheffner, Takahashi et al. 1992)

Overall analysis reveals that over 50% all tumours carry p53 mutations and in light of recent findings, the majority of the remaining tumours may exhibit defects upstream or downstream in the p53 pathway. As well as "loss of function" mutations, "gain of function" mutations have also been proposed(Dittmer, Pati et al. 1993; Hsiao, Low et al. 1994). Nevertheless, a link between cancer, *p53* mutation and subsequent alteration in its activity has been well established(Greenblatt, Bennett et al. 1994; Hollstein, Rice et al. 1994; Hainaut, Hernandez et al. 1998). The strength of the link has recently lead to the development of novel potential therapeutic agents, ultimately aimed at removing mutant p53 containing cancer cells, either via re-activation or re-introduction of p53(Barinaga 1997; Clayman, el-Naggar et al. 1998; Li, Rakkar et al. 1998) or through direct killing mechanisms dependent on the absence of functional p53(Bischoff, Kirn et al. 1996; Freytag, Rogulski et al. 1998).

p53 presents itself as a key regulator of cancer initiation and progression; an internal sensor of cellular tumourigenic potential. p53 responds to a multitude of different cellular stresses, including: oncogenes(de Stanchina, McCurrach et al. 1998; Palmero, Pantoja et al. 1998; Zindy, Eischen et al. 1998), DNA-damaging agents (reviewed(Ko and Prives 1996)), hypoxia(Graeber, Peterson et al. 1994) and ribonucleotide (rNTP) depletion(Linke, Clarkin et al. 1996).Therefore, on the molecular level it is a key player in part of an ever expanding complex network of networks, integrating multiple signals and controlling, in part, the ultimate level of cellular control, apoptosis. p53 remains the archetypal tumour suppresser protein, a true 'guardian of the genome'(Lane 1992) and hence, the associated organism.

Mutant- and null-p53 models

Li-Fraumeni Syndrome

Li-Fraumeni syndrome (LFS) is a dominantly inherited syndrome, showing a predominance of soft tissue sarcomas, osteosarcomas and breast cancer(Li and Fraumeni 1969). Cells isolated from LFS individuals cultured *in vivo* exhibited genetic instability(Liu, Kraus et al. 1996), defective of G_1 and G_2 cell cycle checkpoints(Liu, Kraus et al. 1996; Goi, Takagi et al. 1997), attenuated apoptosis(Goi, Takagi et al. 1997) and reduced global and long-patch excision nucleotide repair(Mirzayans, Enns et al. 1996). Mutation of the p53 gene was identified as the underlying genetic cause of LFS families, affecting both p53 coding and non-coding regions(Malkin, Li et al. 1990; Srivastava, Zou et al. 1990; Varley, McGown et al. 1997).

p53-null Mouse Models

Several groups developed p53-deficient mice using gene targeting in embryonic stem cells(Donehower, Harvey et al. 1992; Harvey, Vogel et al. 1995). The majority of p53-null mice developed normally, although a fraction of the female null embryos displayed defects in neural tube closure. In later life, p53-null mice developed tumours at a very young age. 75% of p53-null mice developed various tumours at six months, while by ten months all had succumbed to tumours(Donehower, Harvey et al. 1992). Thymic T-cell lymphomas were the most frequent tumour type in the null mice, but B-cell lymphomas, soft-tissue sarcomas, osteosarcomas, testicular teratomas and other types were also observed(Donehower, Harvey et al. 1992; Jacks, Remington et al. 1994; Purdie, Harrison et al. 1994). The tumour spectrum in heterozygous ($p53^{+/-}$) mice differed from p53 null mice, with osteosarcomas and soft tissue sarcomas being more prevalent than lymphomas(Harvey, McArthur et al. 1993; Jacks, Remington et al. 1994). Furthermore, carcinomas occurred more frequently in the p53 heterozygous mice. Interestingly, the heterozygous mice tumour spectrum was similar to signature tumours in Li-Fraumeni patients(Malkin 1994). However, the frequent breast and brain tumours seen in Li-Fraumeni patients are infrequently observed in heterozygous mice.

Analysis of heterozygous p53 mice tumour samples revealed that in approximately 50% of cases, the wild-type p53 allele was retained structurally intact and wild-type in sequence(Venkatachalam, Shi et al. 1998). Similar observations have been observed in approximately half of Li-Fraumeni tumours(Varley, McGown et al. 1997). Thus, p53 may be an exception to the 'two hit' model of tumour suppressers, with simple reductions in p53 dosage level being sufficient for cancer progression. Alternatively, downstream or upstream defects in the p53 pathway may also effectively abrogate p53 function.

Another contributing factor to appearance and growth of tumours lacking p53 may be through increased levels of genomic instability. Cell culture experiments using both human and murine cells showed that the absence of p53 conferred increased aneuploidy, increased rates of drug-induced gene amplification and abnormal centrosome duplication(Livingstone, White et al. 1992; Yin, Tainsky et al. 1992). Correlation of p53 loss with chromosomal instability has also been confirmed in sarcomas and lymphomas from p53-deficient mice(Ventatachalam and Donehower 1998).

Further development of mutant p53 transgenics and multitransgenic (p53 deficient mice overexpressing an oncogene, or lacking a second tumour suppresser protein) mouse models will continue to elucidate p53's role in tumour suppression and mechanisms of tumour progression. In a number of such existing models, it appears that p53 loss results in abrogated tumour cell apoptosis(Howes, Ransom et al. 1994; Pan and Griep 1994; Symonds, Krall et al. 1994; Symonds, Krall et al. 1994) and that this may be a key rate-limiting step in tumour formation. In contrast, other models show no significant affect of p53 status on apoptosis levels, while cell proliferation rates are dramatically affected by p53 loss(Donehower, Godley et al. 1995; Jones, Attardi et al. 1997). Each models' results probably reflects the co-operating oncogene or tumour suppresser used, or the tissue type examined, partially explaining some of the observed differences. Nevertheless, the p53 null mice phenotype has supported many earlier observations made with cultured cells, linking p53 to cell cycle arrest, apoptosis and genomic instability. However, p53 loss can contribute to tumour progression through a variety of mechanisms, some of which have yet to be explained. Use of 'knock-in' mutant p53 transgenic mice and tissue-specific alterations, will play an important role in elucidating novel tumourigenic mechanisms.

Structure and Function of p53[1,2]

Human p53 is a 393 amino-acid protein(Zakut-Houri, Bienz-Tadmor et al. 1985) encoded by an 11 exon gene, the first of which is non-coding, on chromosome 17(Lamb and Crawford 1986; Caron de Fromentel and Soussi 1992). It functions as a transcription factor capable of binding to and transactivating or repressing a number of target genes (see Tables 1.1 and 1.2, respectively). The functional character of the p53 protein was determined by experiments showing that p53 contains a strong transcriptional activation domain within its amino-terminus(Fields and Jang 1990; Raycroft, Wu et al. 1990) and is a tetrameric(Stenger, Mayr et al. 1992; Sturzbecher, Brain et al. 1992), sequence-specific DNA-binding protein(Kern, Kinzler et al. 1991), with a defined cognate site(El-Deiry, Kern et al. 1992; Funk, Pak et al. 1992). Partial proteolysis, domain exchange, X-ray crystallography and evolutionary studies of p53 have defined four main domains(reviewed(Soussi, Caron de Fromentel et al. 1990)): amino-terminal transactivation domain, central core sequence specific DNA-binding domain, oligomerisation domain and the multifunctional carboxyl-terminal domain. Its modular structure with several domains have distinct, but inter-dependent functions.

Analysis of p53 across a range of species revealed five major clusters of amino acid conservation, four of which are within the sequence DNA-binding domain(Soussi, Caron de Fromentel et al. 1990), strongly supporting the role of p53 as a sequence-specific transcription factor.

---

[1] Please refer to Figure 1.1 for the following domain locations.

[2] The majority of comments are applicable to both murine and human p53, although specific amino acid residues shall refer to human p53, unless stated otherwise.

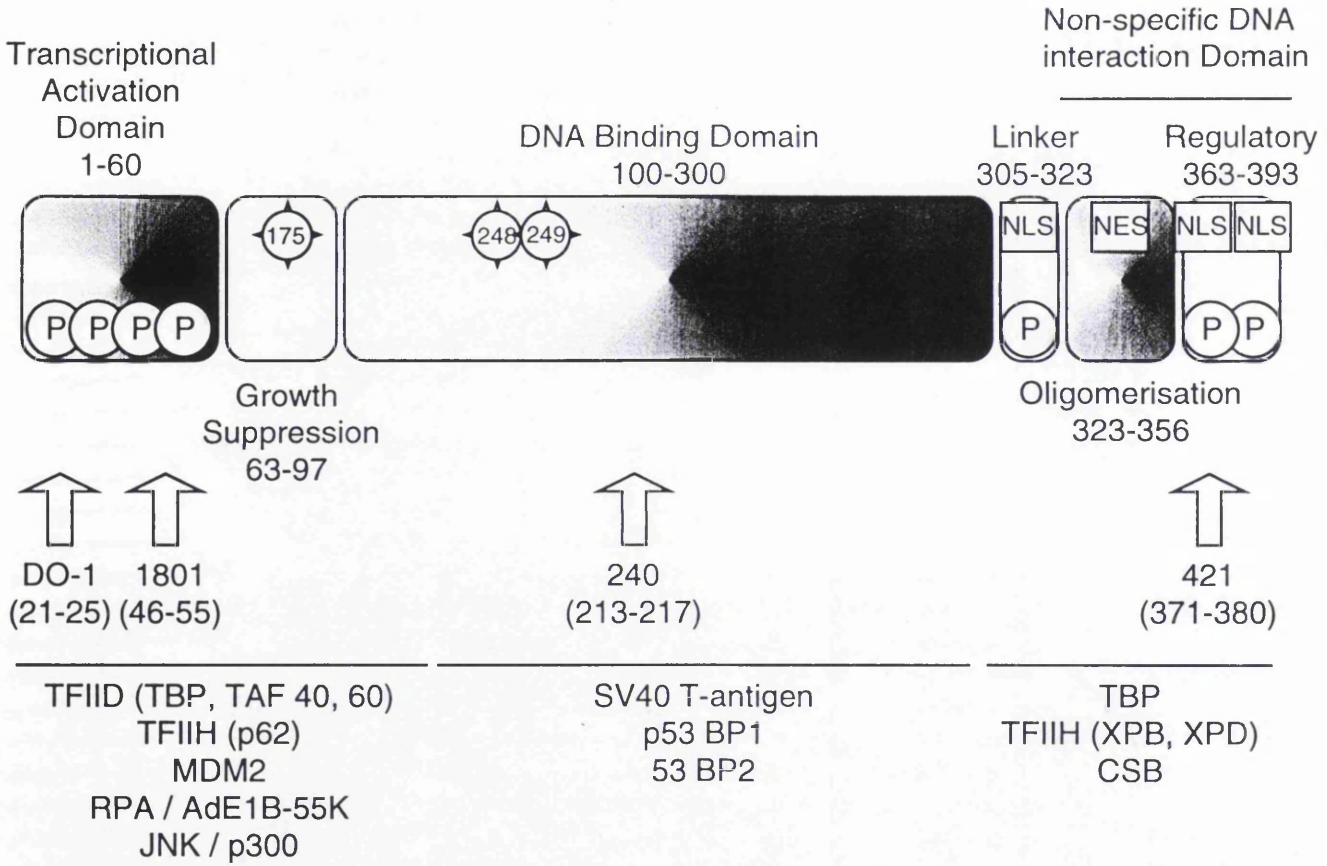

1.1. **Schematic representation of the human p53 polypeptide (aa 1-393)**. Phosphorylation sites are marked by a circled 'P'; three hot-spot mutations used in this study are marked by circled numbers; Nuclear localisation and export signals are marked by boxed 'NLS' and 'NES', respectively; four arrowed anti-p53 antibodies' epitopes, used thoroughout this study, are shown below the diagram; and p53 binding proteins and their approximate binding domains are also indicated below the diagram.

Amino-terminal Transcriptional Transactivation Domain

Initial studies revealed the amino terminus of p53 contained the transcriptional activity of p53(Fields and Jang 1990; Raycroft, Wu et al. 1990), which was further narrowed down to the first 42 amino acids(Unger, Nau et al. 1992). This domain was shown to interact with many factors involved in basal transcription, such as the TATA box-binding protein (TBP) component of TFIID(Horikoshi, Usheva et al. 1995), TBP-associated factors (TAFs), including the $TAF_{II}70$ and $TAF_{II}31$ of TFIID(Lu and Levine 1995; Thut, Chen et al. 1995) and the p62 subunit of the dual transcription/repair factor TFIIH(Xiao, Pearson et al. 1994). This domain bears hallmarks of a transcriptional activator, containing acidic regions that function autonomously when fused to heterologous DNA-binding domains(Pietenpol, Tokino et al. 1994). It also has a very open, antigenic structure, that is reflected in the number of amino-terminal epitopes for various antibodies.

In addition to this domain recruiting the basal transcriptional machinery, it also a target site for at least two negative regulators of p53 function, the cellular protein MDM2[3](Oliner, Pietenpol et al. 1993) and adenovirus E1B 55 kDa(Kao, Yew et al. 1990) proteins. Protein-protein interactions with either protein interfered with p53's transcriptional activity, suggesting that regulation of p53-mediated transcription is important in both a cellular and viral context. Amino acids F19, L22 and W23 were shown to be required for both transcriptional activation and MDM2 binding(Lin, Wu et al. 1995). These crucial amino acids are absolutely conserved between a number of diverse species, but deletion of conserved box I (aa 13-19), does not eliminate transcriptional transactivation, but abolishes MDM2 binding(Marston, Crook et al. 1994). These findings strongly implicate MDM2 as a key regulator of p53 function and will be discussed further in later sections. Mutational analysis of this domain revealed that no single point mutation could eliminate p53's transcriptional transactivation ability(Lin, Chen et al. 1994; Marston, Crook et al. 1994), perhaps explaining the low frequency of mutation in human cancers of this domain(Greenblatt, Bennett et al. 1994; Hollstein, Rice et al. 1994; Hainaut, Hernandez et al. 1998).

---

[3] The majority of comments are applicable to both murine and human MDM2, although specific amino acid residues shall refer to human full length MDM2, unless stated otherwise.

A second transactivation domain has also been described between amino acids 40-83, with W53 and F54 being crucial for activity(Candau, Scolnick et al. 1997). W53 and F54 show an identical motif to L22 and W23, of two hydrophobic residues surrounded by acidic residues.

Proline rich Domain

The core DNA binding domain and the amino-terminal transactivation domain are separated by a region containing five PXXP motifs between amino acids 61 and 94(Walker and Levine 1996), which can form a left-handed polyproline type II helix(Yu, Chen et al. 1994), resembling a SH3 binding site. SH3 domains are a common feature of signal transduction molecules(Cohen, Ren et al. 1995; Pawson 1995) and two known nuclear SH3 proteins have been proposed as candidates for p53 interaction, namely c-Abl(Goga, Liu et al. 1995), a growth-inhibitory tyrosine kinase and BIN1, a MYC-interacting protein (Sakamuro, Sabbatini et al. 1997).

Deletion of amino acids 61-94, did not affect p53's transcriptional activation ability, but eliminated p53's growth arrest ability in tumour cells(Walker and Levine 1996). Similar observations were observed with murine p53, although only apoptotic function was lost, while transcriptional activity, DNA binding, growth arrest and suppression of transformations were all unaffected(Sakamuro, Sabbatini et al. 1997). These results fail to identify the domain as a specific regulator of apoptosis or growth arrest, but suggests a potential role in both.

Central DNA Binding Domain

The sequence-specific DNA binding domain of p53 is located between amino acids 102-292 and is an independently folded domain containing a Zn^{2+} ion that is required for its sequence specific DNA-binding activity(Bargonetti, Manfredi et al. 1993; Halazonetis, Davis et al. 1993; Pavletich, Chambers et al. 1993; Wang, Reed et al. 1993). This domain folds into a four-stranded and five-stranded antiparallel β-sheet that in turn is a scaffold for two α-helical loops that interact directly with the DNA(Cho, Gorina et al. 1994).

Elucidation of the p53 consensus binding site involved *in vitro* binding assays of DNA fragments or double-stranded DNA oligonucleotides and subsequent sequencing of the bound DNA(El-Deiry, Kern et al. 1992; Funk, Pak et al. 1992). The resulting consensus binding site consisted of two copies of the sequence 5′-PuPuPuC(A/T)(T/A)GPyPyPy-3′ separated by 0 to 13 bases. *In vivo* analysis using random genomic DNA fragments cloned upstream of a reporter gene in a yeast screen verified the *in vitro* determined consensus site (Tokino, Thiagalingam et al. 1994). However, in the majority of positives the separation of the consensus site was small or non-existent. Binding sites with four base pair or more spacers exhibited less than 10% transcriptional activity of the directly juxtaposed sites. In addition, p53 binding did not always lead to transcriptional transactivation(Tokino, Thiagalingam et al. 1994), perhaps reflecting the need for other sequences and/or factors and p53's transcriptional repression abilities.

Residues K^{120}, S^{241}, R^{273}, A^{276} and R^{283} make contacts with the phosphate backbone in the major groove of the DNA helix, while K^{120}, C^{277} and R^{280} interact via hydrogen bonds to the DNA bases. R^{248} then makes multiple hydrogen bonds contacts in the minor groove of the DNA helix(Cho, Gorina et al. 1994). Two classes of mutation exist: R^{248} and R^{273}, the two most frequently altered residues, which result in defective contact with DNA and hence the ability of p53 to act as a transcription factor; and other mutations which disrupt the structural basis of the β-sheet and the loop-sheet helix motif that acts as a scaffold for the DNA-binding domain. More than 90% of the missense mutations in p53 reside in this sequence-specific DNA-binding domain, 40% of which are directly implicated in either disrupting the structural integrity of the domain or the altering the DNA contact sites directly(Cho, Gorina et al. 1994; Hollstein, Rice et al. 1994).

Structural mutations altering the conformation of p53 can explain the tumour-derived mutants differing in antibody and heat shock binding, as well as protease resistance. Altered conformation leads to changes in accessibility and presentation of various recognition and binding sites. PAb240, whose epitope amino acids 212-217, is not accessible in the native or wild-type structure, becomes exposed in various mutant conformations(Gannon, Greaves et al. 1990).

The importance of this domain in the function of p53 is not only emphasised through the high frequency of mutations, but also in the localisation of four of the five highly conserved region (boxes II-V) across different species.

Co-operative binding of purified core domains to DNA may be mediated through inter core-domain interactions resulting in DNA bending(Balagurumoorthy, Sakamoto et al. 1995) and looping(Stenger, Tegtmeyer et al. 1994). A positive correlation between the angle of DNA-bending and p53 binding affinity exists, were greater bending angle leads to higher affinity binding(Nagaich, Appella et al. 1997). Higher order structures of DNA, such as stem loop structures and the position of the consensus sites within these structures also determine p53 affinity(Kim, Albrechtsen et al. 1997). Hence, primary and secondary DNA structure can affect p53's DNA binding and transcriptional abilities. Such DNA alterations may be relevant in promoters of p53 target genes that contain p53-binding sites spaced at a distance apart from each other, as in *p21* and *cyclin G* genes, adding an additional regulatory mechanisms controlling expression of p53 responsive genes.

Oligomerisation Domain

Native p53 protein is a tetramer in solution, which requires amino acids 324-355(Stenger, Mayr et al. 1992; Sturzbecher, Brain et al. 1992; Sakamoto, Lewis et al. 1994). Three groups have reported the structure of the tetramerisation domain using both nuclear magnetic resonance (NMR)(Lee, Harvey et al. 1994; Clore, Ernst et al. 1995) and X-ray crystallography(Jeffrey, Gorina et al. 1995). All agreed on a β-sheet-turn-α-helix motif that can homodimerise and is present in p53 tetramers as a pair, or dimer, of dimers. Formation of primary dimers, which is the initial step towards tetramerisation, is formed by hydrophobic interactions between two α-helices and two β-strands, leading to formation of a hydrophobic core. Dimerisation of existing dimers is achieved through a hydrophobic interface.

Mutations in the oligomerisation domain are rarely found in human cancers, although a small number have been identified in Li-Fraumeni patients and may impair tetramerisation and p53 function(Varley, McGown et al. 1996; Ishioka, Shimodaira et al. 1997; Varley, McGown et al. 1997; Lomax, Barnes et al. 1998). Experiments demonstrating the

requirement for p53 oligomerisation for DNA binding(Halazonetis, Davis et al. 1993; Shaulian, Zauberman et al. 1993; Pietenpol, Tokino et al. 1994) are in contradiction to work on the isolated sequence-specific DNA binding core (see earlier section). In some cases, the oligomerisation domain appears dispensable for sequence-specific transactivation(Halazonetis, Davis et al. 1993; Shaulian, Zauberman et al. 1993; Slingerland, Jenkins et al. 1993; Tarunina and Jenkins 1993), but not in others(Halazonetis, Davis et al. 1993; Pietenpol, Tokino et al. 1994). In terms of overall biological significance, many groups have exhibited suppression of transformation in the absence of tetramerisation(Shaulian, Zauberman et al. 1993; Slingerland, Jenkins et al. 1993; Ishioka, Shimodaira et al. 1997).

The type of oligomerisation domain mutation and p53 consensus site used also seems to affect the resultant p53 binding affinity. For example, Ala, but not Leu, substitution of F^{341} results in loss of DNA binding(Waterman, Shenk et al. 1995). Additionally, use of a $pG_{13}CAT$ reporter revealed dimeric p53 was more effective than tetrameric p53 in transcriptional transactivation, while the opposite was observed for the p53CONCAT reporter construct(Thomas, Massimi et al. 1995).

Nuclear Localisation Signals

Three nuclear localisation signals (NLSs) are located within the carboxyl-terminal domain of p53. NLS motifs have been defined as short stretches of basic amino acids with an amino-terminal α-helix-breaking proline or glycine residue(Dang and Lee 1989). All three are required for efficient nuclear localisation, although NLS I (aa 313-322) is the principal localisation signal(Shaulsky, Goldfinger et al. 1990). Mechanisms and regulation of p53's subcellular localisation shall be discussed in later sections.

Non-Sequence specific DNA Binding Domain

The carboxyl-terminal 26 amino acids form an open, protease-sensitive, domain composed of nine basic amino acids residues that bind DNA or RNA readily with some sequence or structural preferences; including DNA ends and internal deletion loops in DNA, as generated

by DNA damage and repair processes(Wang, Reed et al. 1993; Bakalkin, Yakovleva et al. 1994; Bayle, Elenbaas et al. 1995; Lee, Elenbaas et al. 1995; Reed, Woelker et al. 1995). It helps catalyses the re-association of single-stranded-DNA (ssDNA) or –RNA (ssRNA) to double stranded forms(Oberosler, Hloch et al. 1993; Brain and Jenkins 1994; Prives, Bargonetti et al. 1994; Bakalkin, Selivanova et al. 1995; Wu, Bayle et al. 1995).

The non-specific DNA binding activity of p53 was located to amino acids 361-382 and binds the ends of ssDNA of a minimum length of 20 nucleotides as a oligomer(Wang, Reed et al. 1993; Bakalkin, Yakovleva et al. 1994; Selivanova, Iotsova et al. 1996). A second region was localised to amino acids 99-307, which binds internal segments of ssDNA(Bakalkin, Yakovleva et al. 1994). p53 is capable of binding double-stranded DNA (dsDNA), recognising insertion:deletion mismatches(Lee, Elenbaas et al. 1995) and dsDNA containing a two nucleotide ssDNA overhang(Selivanova, Iotsova et al. 1996), predominately as a tetramer. Formation of such DNA lesion/p53 complexes greatly increases the half-life of p53(Lee, Elenbaas et al. 1995).

Carboxyl-terminal Regulatory Domain

There is considerable evidence supporting the need for p53 to undergo a structural/conformational alteration to activate it for sequence-specific binding to DNA. Regulation of a latent, non-DNA binding form of p53 to an active sequence-specific transcriptionally active form is mediated through the basic carboxyl-terminal domain. Deletion of this domain(Hupp, Meek et al. 1992), phosphorylation of S^{378}, by PKC(Takenaka, Morin et al. 1995), or S^{392} by caesin kinase II(Hupp, Meek et al. 1992), or binding of antibody PAb 421 (aa 370-378) or dnaK(Hupp, Meek et al. 1992; Halazonetis, Davis et al. 1993), all activate the central core sequence-specific binding domain (aa 102-292) of p53. Short (20-39 nucleotides) ssDNAs interacting with carboxyl-terminus also activate p53, while longer, dsDNA inhibit p53 sequence-specific binding through the same region(Jayaraman and Prives 1995). Additionally, peptides spanning the carboxyl-terminal 30 amino acids can strongly stimulate DNA binding by full length p53 *in vitro*(Hupp, Sparks et al. 1995).

In addition to PAb 421 stimulating sequence-specific DNA binding, it also inhibits non-specific interactions and reannealing by p53(Bakalkin, Selivanova et al. 1995; Jayaraman and Prives 1995; Wu, Bayle et al. 1995). These results suggested that p53 can exist in two conformations with differing properties, not just with respect to sequence-specific DNA binding. An alternatively spliced form of murine p53, which is most abundant in the G_2 phase of the cell cycle, lacks the carboxyl-terminal domain and has 17 alternative amino acids(Kulesz-Martin, Lisafeld et al. 1994). This murine p53 form was constitutively active for DNA binding(Wu, Liu et al. 1994; Bayle, Elenbaas et al. 1995; Wolkowicz, Peled et al. 1995), but lacked the single-stranded nucleic acid re-annealing function(Wu, Bayle et al. 1995).

Clearly, the carboxyl-terminal domain either sterically or allosterically regulates the ability of p53 to bind to specific DNA sequences at its central core domain. The presence of autoinhibitory domains has been documented in other DNA-binding proteins, such as the Ets protein(Peterson, Skalicky et al. 1995).

Signalling to p53: Activation of p53

p53 is part of a complex network, responding to an vast array of exogenous and endogenous sources of stress- and cellular damage-signals, including: nitric oxide(Forrester, Ambs et al. 1996); ATP accumulation, mediated by adenosine deaminase deficiency(Benveniste and Cohen 1995); hypoxia(Graeber, Peterson et al. 1994; Graeber, Osmanian et al. 1996); ribonucleotide depletion(Linke, Clarkin et al. 1996); irradiation and a whole host of genotoxic and non-genotoxic agents (reviewed(Fornace 1992; Pellegata, Antoniono et al. 1996; Morgan and Kastan 1997; Schwartz and Rotter 1998)). These signals are transmitted by p53 to an ever-expanding list of p53-responsive genes and p53-interacting proteins. The eventual cellular outcome of this signal transmittance relay being either: cell cycle arrest, differentiation or apoptosis(Ko and Prives 1996).

The majority of early work concerned downstream effectors of p53 function, while the components and mechanistics of the upstream affectors were unknown. However, it was known that in response to cellular stress, p53 levels were elevated and became activated as

a sequence-specific transcription factor. Recent findings now reveal there are distinct pathways governing the regulation of p53 activation in response to different cellular stress-signals, with post-translational modifications playing a major role. Additionally, the elucidation of negative regulators of p53, have also revealed alternative mechanisms of p53 activation through abrogation of repression.

Direct recognition and activation of p53 by DNA damage

Single stranded DNA breaks have been shown to be sufficient to activate p53, shown by the introduction of damaged DNA substrates(Huang, Clarkin et al. 1996) and restriction enzymes(Wahl, Linke et al. 1997) by microinjection. p53 has been shown to bind directly to sites of DNA damage including mismatches(Lee, Elenbaas et al. 1995), single stranded DNA(Bakalkin, Yakovleva et al. 1994; Jayaraman and Prives 1995) and stimulate its sequence-specific DNA binding(Jayaraman and Prives 1995; Selivanova, Iotsova et al. 1996). The sensitivity of the p53 pathway to exogenous DNA has meant that standard protocols, such as transfection (including electroporation, calcium phosphate and even some liposome-based reagents) have been reported to activate p53(Renzing and Lane 1995; Rodriguez and Flemington 1999).

p53 Latency

Testicular teratocarcinomas express high levels of wild-type sequence p53, which appears to be functionally inactive with respect to induction of target proteins(Lutzker and Levine 1996). Treatment with retinoic acid induced differentiation and increased p53 transcriptional activity, with a concomitant reduction of p53 protein levels. In contrast, etoposide treatment increased both p53 protein levels and activity, ultimately leading to p53-dependent apoptosis. These results clearly indicate that p53 protein levels and activity can be uncoupled, with one factor not necessarily being directly proportional to the other.

Protein stabilisation of p53

In contrast to many other cellular responses, including the majority of p53's responsive targets, transcriptional induction of p53 is not a major mechanism for the acute up-regulation of p53 following DNA damage. p53 accumulation occurs in the presence of transcriptional and translational inhibitors(Caelles, Helmberg et al. 1994; Price and Park 1994) and has been shown to result from stabilisation of the protein(Maltzman and Czyzyk 1984). Activation of increased DNA-binding and increased expression of genes containing p53-binding sites can also occur without increased p53 protein levels(Price and Park 1994; Selvakumaran, Lin et al. 1994). Under normal conditions, p53 has a short half-life, being targeted for ubiquitin-dependent degradation (see later section).

Post-Translational Activation of p53

Post-translational modification (PTM) of p53 could provide a signal registering a DNA damage event. The existence of multiple p53 phosphorylation sites alone, provides the potential for multiple input signals in response to different types of cellular stress (see below). Such PTMs may cause activational or inhibitory signals, perhaps directly altering the physical property of p53. With PTM sites covering virtually the whole length of the protein, PTM also has the potential to affect p53's protein-macromolecular associations. Co-ordinate regulation of p53 via an array of different PTM permutations may provide a mechanism for selective, adjustable activation/inhibition of one or all of p53 functions and activities. Such a complex control panel of PTM 'switches' could explain some of the conflicting observations documented for p53 activities.

Phosphorylation

Following cellular stress, p53 is phosphorylated upon a number of residues, increasing its stability and transcriptional function (reviewed(Meek 1998)). Many kinase families has been shown to phosphorylate p53, including: DNA-PK, the caesin kinase family, MAP kinases, SAP kinases, CDKs and protein kinase C(Meek 1998). However the importance of p53

phosphorylation in DNA damage-mediated activation and stabilisation of p53, remains controversial(Ashcroft, Kubbutat et al. 1999; Blattner, Tobiasch et al. 1999).

DNA-PK

DNA-dependent protein kinase (DNA-PK), which is activated only in the presence of DNA strand breaks(Nelson and Kastan 1994) and acts primarily during DNA repair(Jackson 1996), has been reported to be required to activate sequence-specific DNA binding by p53 following DNA damage(Woo, McLure et al. 1998). DNA-PK is capable of phosphorylating p53 at Ser^{15} and Ser^{37} *in vitro* and may facilitate p53 activation(Lees-Miller, Chen et al. 1990).

ATM kinase

ATM the gene mutated in ataxia-telangiectasia (AT) patients is though to be one of the major upstream regulators of the p53 response to ionizing radiation-induced damage(Savitsky, Bar-Shira et al. 1995). AT patients show an autosomal recessive disease, characterised by high cancer predisposition, radiation sensitivity, increased chromosome breakage and other physiological symptoms. AT cells shows reduced and delayed accumulation of the p53 protein in response to ionising radiation, indicating that ATM may play a role in relaying the DNA damage events to p53(Kastan, Zhan et al. 1992; Khanna and Lavin 1993). AT cells are also impaired in their ability to induce transcription of p53 target genes, including: *GADD45*, *p21* and *mdm2*(Oliner 1993).

The ATM kinase is capable of phosphorylating p53 on S^{15} and this activity is enhanced in response to ionising radiation, but not UV(Matsushime, Ewen et al. 1992). Furthermore, ATM also seems required for ionizing radiation-induced dephosphorylation of p53 S^{376} which allows specific binding of 14-3-3σ (a potential G_2/M arrest mediator protein)(Ford 1994; Hermeking, Lengauer et al. 1997) to p53, leading to increased sequence-specific DNA-binding activity of p53(Waterman, Stavridi et al. 1998).

ATR Kinase

ATR, a cell cycle checkpoint protein related to DNA-PKCs and ATM, may also function as an upstream regulator of p53 phosphorylation(Lakin, Hann et al. 1999; Tibbetts, Brumbaugh et al. 1999). *In vitro* ATR is capable of phosphorylating both Ser^{15} and Ser^{37}, while expression of a kinase mutant ATR protein reduced Ser^{15} phosphorylation of p53 in response to UV- and γ-irradiation(Tibbetts, Brumbaugh et al. 1999).

Other Kinases/Phosphatases

Phosphorylation of carboxyl-terminal sites of p53 by CDKs has been shown to activate the sequence-specific binding of p53 in a manner specific for the promoters of stress-responsive genes(Wang and Prives 1995; Hecker, Page et al. 1996). While the CDK7-cycH-p36 complex of transcription factor IIH may phosphorylate $Ser^{371, 376, 378, and 392}$ residues of p53(Lu, Fisher et al. 1997).

Serine/Threonine protein phosphatase type 5 (PP5) has been shown to modulate the phosphorylation and DNA binding activity of p53, alleviating G_1 arrest(Zuo, Dean et al. 1998).

Acetylation

In addition to sequence-specific binding, p53 must be able to interact with the transcriptional machinery to function as a transcription factor and influence transcription of target genes. Members of histone acetylase family, p300/CBP, have been shown to bind to p53 and enhance p53-mediated transcription(Avantaggiati, Ogryzko et al. 1997; Gu, Shi et al. 1997; Lill, Grossman et al. 1997). p300 can directly acetylate p53 in the regulatory carboxyl-terminal domain, which activates the p53 sequence-specific DNA binding activity(Gu and Roeder 1997). *In vitro* experiments have identified p53 K^{320} and K^{382} as targets for PCAF and p300, respectively(Sakaguchi, Herrera et al. 1998). These acetylation events enhanced p53's sequence specific DNA binding activity and K^{382} was acetylated in response to DNA

damage. Furthermore, *in vitro* DNA-PK phosphorylated p53 appeared to be a better substrate for acetlytransferases than non-treated p53. This observation may suggest that a network of post-translational modifications may function interdependently.

Redox modulation

Intracellular redox status and its links and effects on p53 are presumably complex, affecting all levels of p53 induction and function. Reactive oxygen species (ROS) are the likely signals leading to p53 induction and additionally, the redox state of p53 itself; affecting its DNA binding and transcriptional functions(Hainaut and Milner 1993). Oxidised p53 loses its sequence-specific DNA-binding abilities, which may reflect the need for certain reduced cysteine residues to bind divalent metal cations and maintain p53 function(Hainaut and Milner 1993).

Furthermore, nitric oxide and thioredoxin reductase have recently been shown to affect p53 conformation and/or transcriptional activity(Calmels, Hainaut et al. 1997). Redox/repair protein Ref-1, also activates DNA binding and transcriptional activities(Jayaraman, Murthy et al. 1997).

It is unknown whether the redox state of p53 may either reflect and/or affect the post-translational modification of p53, perhaps adding another interdependent level of p53 regulation. Discovery of p53-responsive ROS-generating target genes, that may be required for apoptosis(Polyak, Xia et al. 1997), further emphasises the role of redox in all aspects of the p53 signalling pathway

O-glycosylation

EB-1 colon carcinoma cell-derived p53 showed constitutively high levels of p53 DNA binding and transcriptional activity. Analysis revealed O-glycosylation in the carboxyl-terminal regulatory domain, masking the PAb421 epitope, suggesting that O-glycosylation may mimic PAb421-mediated activation of p53(Shaw, Freeman et al. 1996).

Sumoylation

p53 has recently been shown to be post-translationally modified by a small ubiquitin-like molecule, SUMO-1, at a K^{386}(Gostissa, Hengstermann et al. 1999; Rodriguez, Desterro et al. 1999). This modification activated p53's transcriptional activity and will be covered further in later sections.

Downstream mediators of p53 activity

A number of regulatory systems control p53's function through post-transcriptional modifications, affecting its sequence-specific DNA binding activity, conformation, oligomeric state and protein-binding profiles. All of these properties are intimately linked to p53's ability as a transcription factor. A large body of p53-responsive transcriptional target genes have emerged, many of which have unclear functions. However, p53's ability to induce apoptosis in the presence of transcriptional and translational inhibitors(Caelles, Helmberg et al. 1994; Wagner, Kokontis et al. 1994) suggests that non-transcriptional p53 functions are also affected in response to stress stimuli.

Regulation of p53 downstream genes

Transcriptional upregulation of p53-target genes

Analysis of the degeneracy of the p53 DNA-binding site suggests that there may be 400+ p53 target-genes(El-Deiry, Kern et al. 1992). p53 transcriptionally up-regulated targets identified so far, can be loosely grouped into: apoptotic, growth arresting, anti-angiogenic and unknown genes (see Table 1.1). Some of these transcriptional targets and their relevance to apoptosis and cell cycle arrest will be discussed in more detail in later sections.

Table 1. 1. Genes transcriptionally upregulated by p53.

Gene	Group
$p21^{CIP1/WAF-1}$(el-Deiry, Tokino et al. 1993)	Growth arrest
14-3-3σ(Hermeking, Lengauer et al. 1997)	Growth arrest
GADD45(Zhan, Chen et al. 1998)	Growth arrest
B99(Utrera, Collavin et al. 1998)	Growth arrest
Bax(Miyashita and Reed 1995)	Apoptotic
Fas/APO1(Owen-Schaub, Zhang et al. 1995)	Apoptotic
Killer/DR5(Wu, Burns et al. 1997)	Apoptotic
PIGs(Polyak, Xia et al. 1997)	Apoptotic
p85(Yin, Terauchi et al. 1998)	Apoptotic
PAG608(Israeli, Tessler et al. 1997)	Apoptotic
IGF-Bp3(Buckbinder, Talbott et al. 1995)	Apoptotic
Tsp1(Dameron, Volpert et al. 1994)	Anti-angiogenic
BAI1(Nishimori, Shiratsuchi et al. 1997)	Anti-angiogenic
GD-AiF(Van Meir, Polverini et al. 1994)	Anti-angiogenic
Cyclin G(Okamoto and Beach 1994)	Unclear
GML(Furuhata, Tokino et al. 1996)	Unclear
Wip1(Fiscella, Zhang et al. 1997)	Unclear
EI24(Lehar, Nacht et al. 1996)	Unclear
EF-1α(Kato, Sato et al. 1997)	Unclear
HIC-1(Wales, Biel et al. 1995)	Unclear
RTP/rit42(Kurdistani, Arizti et al. 1998)	Unclear
TP53TGI(Takei, Ishikawa et al. 1998)	Unclear
wig-1(Varmeh-Ziaie, Okan et al. 1997)	Unclear
Cathepsin D(Wu, Saftig et al. 1998)	Unclear

In addition to transcriptional upregulation, p53 has also been demonstrated to repress transcription of a number of genes that do not necessarily contain p53 DNA-binding sites. The mechanism of p53 repression is not clear, although the several autonomous transrepression domains of p53 has been implicated(Sang, Chen et al. 1994; Horikoshi, Usheva et al. 1995; Shaulian, Haviv et al. 1995). More recently several groups have determined a role for histone deacetylases (HDACs) in the mechanism of repression by transcription factors, such as Mad/Max(Hassig, Fleischer et al. 1997; Laherty, Yang et al. 1997), pRB(Luo, Postigo et al. 1998) and nuclear hormone receptors(Nagy, Kao et al. 1997). Inhibition of HDAC function by trichostatin A abrogated p53's ability to repress the expression of endogenous p53-target genes.(Murphy, Ahn et al. 1999). Complex formation between the transcriptional co-repressor, mSin3a and the histone deacetylase, HDAC, was also observed. Such complexes were only found with wild-type p53 at the promoter site of the transcriptionally repressed *Map4* gene, but not the transcriptionally upregulated *mdm2* gene, suggesting that p53 is bona fide transcriptional repressor.

p53-repressible target-genes to date can be crudely grouped into serum-inducible, growth promoting, transcription factor and anti-apoptotic genes (see Table 1.2).

Table 1. 2. Genes transcriptionally repressed by p53.

Gene	Group
c-fos(Ginsberg, Oren et al. 1990)	Serum-inducible
IL6(Santhanam, Ray et al. 1991)	Serum-inducible
c-myc(Webster, Resnik et al. 1996)	Growth-promoting
Insulin receptor(Webster, Resnik et al. 1996)	Growth-promoting
IL2 and IL4(Pesch, Brehm et al. 1996)	Growth-promoting
TBP(Pesch, Brehm et al. 1996)	Transcription factor
SP1(Bargonetti, Chicas et al. 1997)	Transcription factor
Thyroid hormone receptor(Bhat, Yu et al. 1997)	Transcription factor
Oestrogen receptor(Yu, Driggers et al. 1997)	Transcription factor
Hypoxia-inducible factor(Blagosklonny, An et al. 1998)	Transcription factor
STAT5(Fritsche, Mundt et al. 1998)	Transcription factor
DP-1(Gopalkrishnan, Lam et al. 1998)	Transcription Factor
Bcl-2(Miyashita, Harigai et al. 1994)	Anti-apoptotic
relA(Ravi, Mookerjee et al. 1998)	Anti-apoptotic
MAP4(Murphy, Hinman et al. 1996)	Anti-apoptotic
hsp70(Agoff, Hou et al. 1993)	Heat shock protein
MDR1(Chin, Ueda et al. 1992)	Drug-resistance
DNA topoisomerase IIα(Wang, Zambetti et al. 1997)	DNA polymerase
wee1(Leach, Scatena et al. 1998)	Kinase
presenilin-1(Roperch, Alvaro et al. 1998)	Unclear
Actin(Guenal, Risler et al. 1997)	Cytoskeletal

Modifiers of p53-mediated transcription

Direct binding of p53 to its consensus recognition sequence is not the only mechanism through which p53 can regulate transcription of its effector genes (see earlier section). The p53-dependent increase in transcription of *GADD45* in response to ionising radiation is thought to be mediated through a consensus binding site in the third intron of the gene(Kastan, Zhan et al. 1992; Hollander, Alamo et al. 1993). In contrast, p53 has been shown to play a role in *GADD45* induction in response to other DNA damaging agents, such as methyl methanesulphonate (MMS) and UV, through a WT1/Egr1 site in the promoter(Zhan, Chen et al. 1998). Activation of transcription via this site requires direct binding by a complex containing both p53 and WT1 (Wilm's Tumour suppresser)(Zhan, Chen et al. 1998). This 'indirect' transcriptional role of p53, suggests that p53 has the potential to influence multiple genes, whether they contain a p53-binding site or not. Other examples of such genes whose induction is attenuated upon p53 disruption, include the stress genes GADD153/CHOP and GADD34/MyD116. Both genes lack detectable p53 binding sites, are not induced by ionising radiation, but are induced by UV and alkylating agents (base-damaging agents)(Gujuluva, Baek et al. 1994; Zhan, Fan et al. 1996).

c-Myc overexpression can also down modulate the basal levels and stress-responsiveness of a number of p53-responsive growth suppression genes, including *gas1*(Lee, Li et al. 1997), *Cyclin D1*(Phillipp, Schneider et al. 1994), *p21$^{CIP1/WAF1}$* (p21) (Hermeking, Funk et al. 1995), *GADD34*, *GADD153* and *GADD45*(Marhin, Chen et al. 1997). The exact mechanism of the interaction of c-Myc with the *GADD45* promoter is unknown, although its effect is mapped to the same Egr1/WT1 binding site that mediates WT1's effect on p53's transcription of the *GADD45* gene(Amundson, Myers et al. 1998).

BRCA1, the tumour suppresser gene associated with familial predisposition to breast and ovarian cancer, whose overexpression in cancer cells can induce a G_1 arrest through a p53-independent induction of p21(Somasundaram, Zhang et al. 1997). BRCA1 can also directly bind to p53(Zhang, Somasundaram et al. 1998). This protein-protein interaction increases p53-dependent transcription from both *p21* and *Bax* promoters(Zhang, Somasundaram et al.

1998). Another link emerges from the findings that *BRCA1* and *BRCA2* transcription may be regulated by DNA damage in a p53-dependent manner(Andres, Fan et al. 1998).

Therefore, a pattern may exist in which proliferative signals may attenuate stress-induction of p53-responsive growth arrest genes, while anti-proliferative signals enhance the responsiveness of the same promoters; perhaps representing yet another level of regulation of the p53 responsive.

Protein-protein interactions

In addition to p53's vast array of transcriptional target genes, an ever-growing body of protein interactions has emerged, which continues to grow (see Table 1.3). Such protein-protein interactions may be stable, or extremely transient in nature. A number of these proteins and relevance to p53 function will be discussed in further detail in later sections.

Many physical and genetic methods have been used for identification of p53-interacting macromolecules, including: co-immunoprecipitation – both *in vitro* and *in vivo*; the yeast two-hybrid hybrid system and phage-display. Co-localisation studies utilising confocal microscopy and fluorescence energy transfer (FRET) can also support protein interaction findings. However, all of the methods have individual problems and therefore need to be supported by each other and mutational analysis. A major problem also revolves around the common occurrence of supra-physiological protein levels in various experiments and the stoichiometry of the interaction, therefore questioning the physiological relevance of that interaction.

Table 1. 3. p53-interacting proteins

Cellular Proteins	Viral Proteins
c-abl(Yuan, Huang et al. 1996)	SV40 large T(Lane and Crawford 1979; Linzer and Levine 1979)
P300/CBP(Lill, Grossman et al. 1997)	Adenovirus 5 and 12 E1b 55k(Kao, Yew et al. 1990)
TFIIH(Xiao, Pearson et al. 1994; Wang, Yeh et al. 1995; Leveillard, Andera et al. 1996)	Adenovirus E4orf6(Dobner, Horikoshi et al. 1996)
HSP70(Pinhasi-Kimhi, Michaalovitz et al. 1986)	HPV E6(Scheffner, Takahashi et al. 1992)
L5 ribosomal protein(Marechal, Elenbaas et al. 1994)	EB virus EBNA-5(Szekely, Selivanova et al. 1993)
MDM2(Momand, Zambetti et al. 1992)	Hepatitis B virus X protein(Feitelson, Zhu et al. 1993)
MDMX(Shvarts, Steegenga et al. 1996)	Human CMV IE84 protein(Speir, Modali et al. 1994)
P53-BP1(Iwabuchi, Bartel et al. 1994)	
P53-BP2(Iwabuchi, Bartel et al. 1994)	**Cellular Proteins (cont'd)**
E2F-1(O'Connor, Lam et al. 1995)	
BRCA1(Zhang, Somasundaram et al. 1998)	Sp100b(Baudier, Delphin et al. 1992)
DP1(O'Connor, Lam et al. 1995)	Sp1(Gualberto and Baldwin 1995)
DNA-PK(Lees-Miller, Chen et al. 1990)	TAFII 31(Lu and Levine 1995)
CK1(Milne, Palmer et al. 1992)	TBP(Seto, Usheva et al. 1992)
JNK(Milne, Campbell et al. 1995)	WT1(Maheswaran, Park et al. 1993)
CKII(Meek, Simon et al. 1990)	Cdc2(Milner, Cook et al. 1990)
PKC(Baudier, Delphin et al. 1992)	RPA(Dutta, Ruppert et al. 1993)
MAPK(Milne, Campbell et al. 1994)	ARF*(Kamijo, Weber et al. 1998)
14-3-3σ(Waterman, Stavridi et al. 1998)	RAD51(Buchhop, Gibson et al. 1997)
REF1(Jayaraman, Murthy et al. 1997)	$p33^{ING1}$(Garkavtsev, Grigorian et al. 1998)
HMG1(Jayaraman, Moorthy et al. 1998)	Vimentin(Klotzsche, Etzrodt et al. 1998)

* ARF refers to both human $p14^{ARF}$ and murine $p19^{ARF}$ proteins.

Regulation of p53 Synthesis

Transcriptional regulation of Human p53 expression

In the majority of studies, regulation of p53 gene transcription has concentrated on either the murine or human genes. Both the murine and human p53 promoter regions were cloned over a decade ago and show over 75% sequence identity(Bienz-Tadmor, Zakut-Houri et al. 1985; Lamb and Crawford 1986; Reisman, Greenburg et al. 1988).

Two promoters have been identified at the 5' end of the human p53 gene(Lamb and Crawford 1986; Reisman, Greenburg et al. 1988) p1 is located upstream of the first exon and is responsible for the major p53 mRNA species, while the second downstream promoter, p2, is responsible for the transcription of a novel gene located within the first intron of the p53 gene(Reisman, Balint et al. 1996).

The majority of the transcriptional regulatory elements found to date lie upstream of the transcription initiation site and include binding sites for a number of transcription factors (see Table 1.4). These proteins control transcription through positive transactivation and negative repression of the p53 promoter activity. In addition, p53 itself has been shown to repress its own promoter in a cell-type specific manner, although direct promoter binding was not demonstrated(Hudson, Frade et al. 1995).

Inactivation of the wild-type p53 function is an extremely common event during tumourigenesis. Many different mechanisms of inactivation exist, affecting all levels of control, including transcription. Many myeloid leukaemia(Prokocimer, Harris et al. 1987), malignant astrocytomas(Stuart, Haffner et al. 1995) and some invasive breast carcinomas(Reisman and Loging 1998) show lack of, or reduced, transcription of wild type *p53* mRNA. Although neither promoter mutation or methylation were shown to mediate the reduction of p53 transcription, *trans*-acting defects could also explain the reduced transcription. Supporting this hypothesis are the findings of PAX-mediated repression of p53 expression in astrocytomas(Stuart, Haffner et al. 1995) and the HTLV type I Tax protein

mediating repression of *p53* transcription, providing a potential mechanism of viral transformation. (Uittenbogaard, Giebler et al. 1995)

More frequent than the loss of expression of the p53 gene, is the finding that mutant forms of the gene are elevated at both mRNA and protein levels. While the majority of work has focused on post-transcriptional stabilisation mechanisms, it has been shown that c-Myc, as a heterodimer with Max, will bind to its recognition site on the p53 promoter and up-regulate *p53* expression(Reisman, Elkind et al. 1993; Roy, Beamon et al. 1994). Numerous studies have identified a positive correlation between the levels of expression of p53 and c-Myc(Chenevix-Trench, Martin et al. 1990; Reisman, Elkind et al. 1993; Roy, Beamon et al. 1994; Rochlitz, Heide et al. 1995; Ben-Yosef, Yanuka et al. 1998; McCormack, Weaver et al. 1998). Moreover, inhibition of c-Myc expression by anti-sense *c-myc* RNA or inhibitory peptides resulted in an inhibition of p53 expression(Roy, Beamon et al. 1994; Giorello, Clerico et al. 1998). Although, in light of the c-Myc stimulation of ARF[4], a post-transcriptional mechanism, most probably involving MDM2 inhibition, can also contribute to c-Myc-mediated p53 accumulation(Zindy, Eischen et al. 1998).

[4] ARF refers to both human $p14^{ARF}$ and murine $p19^{ARF}$ proteins.

Table 1. 4. *p53*-regulatory transcription factors.

Transcription Factor	Binding Site	Effect on p53 Promoter
PAX family(Stuart, Haffner et al. 1995)	+197 to +193	Represses
c-Myc/Max(Roy, Beamon et al. 1994)	-33 to -38	Transactivates
HTLV-type I Tax(Uittenbogaard, Giebler et al. 1995)	-33 to –38	Represses Myc-mediated transactivation
NF-κB(Sun, Shimizu et al. 1995)	-40 to –60	No effect
CPEp53-BP I(Sun, Shimizu et al. 1995)	-50 to –70	Required for promoter response to genotoxic stress
NF1 and YY1(Furlong, Rein et al. 1996)	-91 to –103 –98 to –107	Transactivates
HoxA5(Reisman and Loging 1998)	-115 to –122	Transactivates
Sp1(Reisman and Loging 1998)	-155 to -161	Not determined
PF1(Reisman and Loging 1998)	-170 to -179	Not determined
ETS1/2(Venanzoni, Robinson et al. 1996)	-379 to –391	Not determined

Translational regulation of p53

Post-transcriptional processes represent an important mechanism of p53 upregulation. The importance of translational regulatory mechanisms underlying the expression of p53 has been supported by the findings that murine p53 binds to the 5′ untranslated region of its own mRNA, repressing its translation(Mosner, Mummenbrauer et al. 1995). In contrast to the murine system, human p53 binds to a sequence within the 3′ untranslated region of the human mRNA. Upon γ-irradiation, p53 mRNA translational repression was alleviated, facilitating p53 protein expression and subsequent accumulation(Fu and Benchimol 1997; Fu, Ma et al. 1999). Regardless of the specific mechanism, evidence exists for a negative autoregulatory feedback loop, mediated through regulation of translation. Additionally, thymidylate synthase, an RNA binding protein which regulates its own synthesis through auto-inhibitory translational repression, can also negatively regulate p53 translation(Ju, Pedersen-Lane et al. 1999).

Subcellular Localisation as a Control Mechanism

For p53 to act as a transcription factor it must bind to DNA and hence be located in the nucleus. Nuclear exclusion of wild-type p53 has been observed in diverse neoplasms(Sun, Carstensen et al. 1992; Moll, LaQuaglia et al. 1995; Ueda, Ullrich et al. 1995; Moll, Ostermeyer et al. 1996) and embryonic stem cells(Aladjem, Spike et al. 1998) and many demonstrate an impaired G_1 arrest in response to genotoxic stress(Moll, Ostermeyer et al. 1996). Subcellular sequestration of p53, was shown to be a mechanism of overcoming p53-mediated growth arrest, in REFs overexpressing both activated Ras and p53 135^{Val}(Knippschild, Oren et al. 1996). In contrast, p53 in normal cells is predominantly nuclear in G_1 and is largely cytoplasmic during S and G_2(Shaulsky, Ben-Ze'ev et al. 1990; David-Pfeuty, Chakrani et al. 1996), consistent with its role as a nuclear transcription factor mediating a G_1 checkpoint. In response to stress, p53 is stabilised and transferred and retained in the nucleus(Clarke, Purdie et al. 1993; Fritsche, Haessler et al. 1993; Lowe, Schmitt et al. 1993) where it induces the expression of genes involved in cell cycle arrest or apoptosis. Therefore, an effective mechanism of down-regulating p53 activity is through spatial separation from its downstream effector genes. Additionally, cytoplasmic

sequestration of p53 may also facilitate negative regulation of specific mRNAs, including its own(Mosner, Mummenbrauer et al. 1995). Regulatory mechanisms governing p53 subcellular localisation may involve nuclear and cytoplasmic tethering molecules and/or regulation of physical, nuclear import and export(Middeler, Zerf et al. 1997; Klotzsche, Etzrodt et al. 1998).

NES masking Model

Initially, p53 was thought to localise to the nucleus from the cytoplasm in a linear, unidirectional manner. However, bi-directional, energy dependent, carrier-mediated shuttling of p53 between the nucleus and the cytoplasm was shown to occur(Middeler, Zerf et al. 1997). Analysis of p53's primary sequence determined a leucine-rich sequence of conserved spacing and hydrophobicity, which fitted with the criteria established for a nuclear export signal (NES)(Bogerd, Fridell et al. 1996). Carboxyl-terminal residues between amino acids 340-351 (see Figure 1.1) conformed to this motif, placing it within the tetramerisation domain of p53(Stommel, Marchenko et al. 1999). Mutation analysis of the NES resulted in nuclear accumulation of p53, while wild-type p53 exhibited nuclear and cytoplasmic localisation.

Proteins larger than 40 kDa must use a nuclear export receptor to pass through the nuclear pore(Gerach 1995; Gorlich and Mattaj 1996). Treatment of cells with the leptomycin B, an non-specific inhibitor of CRM1-mediated nuclear export(Fornerod, Ohno et al. 1997; Ossareh-Nazari, Bachelerie et al. 1997; Ullman, Powers et al. 1997), led to p53 nuclear accumulation, suggesting that p53 contains a CRM1-dependent NES which mediates its nuclear cytoplasmic shuttling(Stommel, Marchenko et al. 1999).

p53 tetramerisation has been demonstrated to be important efficient binding to DNA response elements and transcriptional transaction of those target genes(Friedman, Chen et al. 1993; Halazonetis and Kandil 1993; Hainaut, Hall et al. 1994; Hupp and Lane 1994; McLure and Lee 1998). L^{348}, L^{350} mutation revealed reduced tetramerisation, transcriptional and growth suppressive abilities and exhibited constitutive nuclear localisation(Stommel, Marchenko et al. 1999). Furthermore, such inability to achieve nuclear export(Varley,

McGown et al. 1996) and tetramerisation(Ishioka, Shimodaira et al. 1997) are observed in Li-Fraumeni patients with $344^{L \Rightarrow P}$ mutations.

Tetramerised p53 would be the preferred oligomeric state for nuclear p53 to carry out its transcriptional functions (see earlier section). The location of the NES within the oligomerisation domain of p53 suggests that in such a tetrameric state, these signals would be sterically obscured, buried deep within the oligomeric core from nuclear export receptors. Formation of tetrameric p53 within the nucleus would therefore lead to retention of transcriptional active p53 within the nucleus, through the concealment of the p53s' multiple NESs.

Phosphorylation: Tetramer formation and subcellular localisation

Stress-activation of p53 may favour tetramerisation: UV-irradiation leads to phosphorylation of S^{392}, resulting in increased DNA binding and tetramer formation *in vitro*(Sakaguchi, Sakamoto et al. 1997; Sakaguchi, Sakamoto et al. 1997). It is possible that cdk2 and cdc2 are involved in the cell cycle-dependent localisation of p53, since they both phosphorylate p53 after the G_1 restriction point when p53 returns to the cytoplasm(Bischoff, Friedman et al. 1990; Price, Hughes-Davies et al. 1995). Supporting this theory, S^{315} phosphorylation results in reduced tetramer stability *in vitro*(Sakaguchi, Sakamoto et al. 1997; Sakaguchi, Sakamoto et al. 1997) and may therefore represent a mechanism of controlling p53 subcellular localisation.

Analysis of the temperature-sensitive murine p53 135^{Val}, revealed that at the non-permissive temperature, p53 135^{Val} was sequestered in the cytoplasm(Gannon and Lane 1991; Ginsberg, Michael-Michalovitz et al. 1991). Shifting to the permissive temperature, p53 135^{Val} concentrated to the nucleus in a hyperphosphorylated, DNA-binding, transcriptionally active form. Tryptic peptide mapping, revealed amino-terminal phosphorylation occurred only in the nucleus, whereas carboxyl-terminal phosphorylation occurred in both the nucleus and cytoplasm(Martinez, Craven et al. 1997).

Proteins that prevent nuclear importation of p53

Overexpression of Bcl-2 in LNCap prostate carcinoma cell lines demonstrated that Bcl-2 could inhibit X-ray-mediated cell death, by impairing p53 nuclear import(Beham, Marin et al. 1997). The role of Bcl-2 as a regulator of nuclear import is supported by the observation that Bcl-2 may selectively alter import of NF-AT (Nuclear Factor of Activated T-cells) following T-cell activation(Shibasaki, Kondo et al. 1997). Additionally, Bcl-2 and c-Myc overexpression can overcome cell cycle arrest and apoptosis in murine erythroleukemia cells, through cytoplasmic sequestration of p53 during G_1(Ryan and Clarke 1994).

Proteins that bind and influence p53's localisation

Expression of a cytoplasmic, mutant SV40 T-antigen, cT-Ag, defective in its NLS, caused cytoplasmic retention of p53. These results indicate that the nuclear import of p53 can be overcome through complex-formation with another protein. In this scenario, SV40 cT-Ag, acts a cytoplasmic anchor protein, defective in its own ability to translocate into the nucleus. Furthermore, evidence for short-lived cytoplasmic anchors was apparent in cl6 cells, were upon addition of inhibitors of protein synthesis lead to p53 being translocated into the nucleus(Gannon and Lane 1991). Cytoplasmic-sequestering proteins must therefore overcome p53's intrinsic NLSs, either through steric hindrance or allosteric-mediated conformational changes. MDM2 has also been heavily implicated in p53's subcellular localisation and be covered in later sections. Spot-1, a nuclear protein that interacts with the NLS I of p53 through its p(CA)n repeat, may promote p53's nuclear localisation(Elkind, Goldfinger et al. 1995).

Regulation of p53 activity by Degradation

Absolute cellular protein levels are determined by the net result between rate of protein production and degradation. Increased production can be achieved by a variety of mechanisms, although rate-limiting steps in the processes ultimately determine the overall rate of protein synthesis. Potential mechanisms of increased protein production include: gene amplification; mRNA stabilisation; and increased rates of transcription and translation

initiation, elongation and termination. p53 protein degradation is similarly controlled by regulatable steps, determining the specificity and rate of p53 degradation. Two major p53 *in vivo* degradation pathways have been discovered: calpain- and ubiquitin-mediated degradation.

Ubiquitin-mediated degradation and the proteosome

Ubiquitin, a 76 amino acid protein, exists either free or covalently linked to other proteins(Schlesinger, Goldstein et al. 1975; Hershko 1996). It has been shown to be important in a number of important biological processes, including: cell differentiation, cell cycle, embryogenesis, apoptosis, signal transduction, DNA repair, transmembrane and vesicular transport, stress response (including the immune response) and functions of the nervous system(Varshavsky 1997). The vast functional range of the ubiquitin system stems from the diversity of its physiological substrates, whose number is likely to be comparable to phosphokinase substrates. A majority of the ubiquitin-dependent pathways involve processive degradation of ubiquitinated (ubiquitinylated)[5] proteins by the 26S proteosome; an ATP-dependent multisubunit protease comprising of a 20S core and multiple 19S ATPase caps at both ends of the 20S core(Jentsch and Schlenker 1995).

Work in yeast has shown that ubiquitin is also involved in non-proteolytic functions such as endocytosis including: receptor internalisation(Hicke and Riezman 1996) and delivery of proteins to peroxisomes, endoplasmic reticulum and mitochondria(Horak and Wolf 1997; Kolling and Losko 1997). A non-proteolytic, chaperonin function of ubiquitin was determined for mammalian ribosomal biogenesis(Finley, Bartel et al. 1989). Discovery of a small ubiquitin-related modifier (SUMO-1) which can be similarly covalently conjugated to other proteins, has revealed an role in a variety of non-proteolytic processes(Saitoh, Pu et al. 1997).

---

[5] Ubiquitinated shall be used to describe to process of ubiquitin addition, although ubiquitinylated is the correct chemical definition of the process.

Ubiquitination of a protein substrate requires the concerted action of three enzyme classes(Scheffner, Nuber et al. 1995; Hershko 1996): A ubiquitin-activating enzyme (E1s) initially activates ubiquitin in an ATP-dependent reaction through the formation of a thiol ester bond between the carboxyl-terminus of ubiquitin and the thiol group of a specific cysteine residue of E1. Ubiquitin is then transferred to a specific cysteine residue on one of several ubiquitin-conjugating enzymes (E2s). E2 enzymes in turn may transfer the ubiquitin either directly to a substrate or to a third enzyme class known as ubiquitin-protein ligases (E3s). The E3 catalyses the formation of an isopeptide bond between the carboxyl-terminus of ubiquitin and the ε-amino group of lysine residues on target proteins. A substrate may be multiply ubiquitinated through the attachment of additional ubiquitin molecules to specific lysines (K^{48} or K^{63}) of ubiquitin itself, creating linear or branched multi-ubiquitin chains(Hochstrasser 1996).

Cellular-mediated p53 ubiquitination

MDM2 mediated ubiquitination and degradation

The MDM2 protein can inhibit the transcriptional transactivation ability of p53 through binding and masking of its transactivation domain(Momand, Zambetti et al. 1992)(Oliner and Pietenpol et al. 1993). An alternative mechanism that requires the same interaction, causes the ubiquitination of p53 and subsequent degradation by the proteosome(Haupt, Maya et al. 1997; Kubbutat, Jones et al. 1997). This second mechanism, abolishes all of p53's functions, hence MDM2 represents an extremely potent inhibitor of p53 function overall activity. MDM2-mediated p53 degradation will be covered in more detail in later sections.

JNK-mediated ubiquitination and degradation

Jun-N-terminal kinase (JNK) has been shown to target the ubiquitination of a number of associated proteins: c-Jun, JunB and ATF2(Fuchs, Dolan et al. 1996; Fuchs, Xie et al.

1997). Regulation of JNK ubiquitination activity is controlled by phosphorylation of the target proteins, as phosphorylated, but not un-phosphorylated, c-Jun and ATF2 were protected against JNK-mediated ubiquitination. *In vivo* JNK:p53 interactions were preferentially found in non-stressed cells, in comparison to UV-irradiated stressed cells and suggested that JNK may also have a role in ubiquitination and regulation of p53 stability(Fuchs, Adler et al. 1998).

Viral-mediated p53 ubiquitination and degradation

Human Papilloma Virus E6-mediated degradation of p53

The human papillomaviruses (HPVs) play a major role in cervical carcinomas, with 90% of all cases containing 'high risk' HPV DNA (HPV 16 and 18) (reviewed(zur Hausen 1991)). A biochemical basis for the difference in HPV risk classification is correlated with the ability of the HPV E6 protein to bind and target p53 for degradation(Scheffner, Werness et al. 1990; Crook, Tidy et al. 1991), a process involving ubiquitin-dependent proteolysis(Scheffner, Werness et al. 1990). High-risk HPV E6 proteins, acting in concert with a cellular 100kDa E6-associated protein (E6-AP), mediate p53 ubiquitination(Huibregtse, Scheffner et al. 1991). The HPV E6:E6-AP association generates a ubiquitin-ligase function, targeting the ubiquitination and subsequent degradation of p53(Scheffner, Huibregtse et al. 1993; Scheffner, Nuber et al. 1995).

Adenovirus E1B and E4 orf6-mediated degradation of p53

Oncogenic transformation of primary rodent cells by human adenoviruses is a multistep process that is mediated by the co-ordinated expression of viral gene products encoded within early region 1 (E1) (reviewed(Nevins and Vogt 1996)). E1 contains two transcription units, E1A and E1B, which are both necessary and sufficient to transform primary cells in culture. E1A proteins induce cellular DNA synthesis and cell proliferation by virtue of their ability to interact with and modulate the function of several growth-regulatory proteins that control transcription and cell cycle progression. Full manifestation of the transformed phenotype requires expression of two E1B gene products, E1B-19kDa and E1B-55kDa, that

are individually capable of co-operating with E1A to transform cells via independent, but additive pathways

Both E1B proteins promote cellular transformation in part by antagonising apoptosis and growth arrest, which arise from the induction of p53 by E1A(Debbas and White 1993; Lowe and Ruley 1993). E1B-19kDa seems to play a central role in suppression of apoptosis and inhibits both p53-dependent and independent pathways, resembling the action of Bcl-2. E1B-55kDa (reviewed(White 1996)). E1B-19kDa, in contrast, directly binds to p53 and blocks p53-mediated transcriptional activity, blocking growth arrest and apoptosis. The binding of E1B-55kDa and p53 does not disrupt p53's sequence-specific DNA binding activity, but tethers the transcription-repression domain of E1B to p53- target genes, inhibiting transcriptional transactivation by p53.

A third gene product, E4orf6, with transforming activities resembling those of the E1B proteins was discovered, which co-operated with E1A in the transformation of primary cells(Moore, Horikoshi et al. 1996; Nevels, Rubenwolf et al. 1997). It was shown to inhibit both activation and repression of transcription by p53, but in contrast to E1A and E1B, it decreased p53's half-life and resulting in a dramatic reduction in p53 expression levels(Moore, Horikoshi et al. 1996). E4orf6 interacts with both E1B-55kDa(Moore, Horikoshi et al. 1996) and p53(Sarnow, Hearing et al. 1984), suggesting that multiple protein interactions between all three proteins may modulate p53 function and stability.

Calpains

Calpains are a family of calcium-dependent intracellular proteases. Rather than peptide motifs, they recognise structural determinants, the nature of which remains unknown. The nature of calpain-catalysed proteolysis is not digestive but proceeds in a limited manner resulting in only several cleavage events(Saido, Sorimachi et al. 1994).

In vitro analysis of calpain-mediated cleavage of p53 revealed a 46kDa amino-terminal truncated degradation product(Kubbutat and Vousden 1997; Pariat, Carillo et al. 1997). Conserved box I of p53 (aa13-19) was shown to be important in calpain recognition, while

cleavage occurred within the DO-1 epitope (aa20-25)(Kubbutat and Vousden 1997). *In vivo* evidence for calpain-mediated degradation of p53 suggests that it does contribute to p53 degradation, although stronger evidence exists for ubiquitin-mediated p53 degradation. Interestingly, different mutant p53 proteins showed varying degradation profiles, suggesting that mutant p53s adopt a variety of conformations and not purely a singular 'mutant' conformation(Pariat, Carillo et al. 1997).

Role of p53 in DNA damage repair

p53-interacts with component of the DNA repair machinery

p53's ability to bind DNA strand breaks (mediated by multiple DNA damaging agents) and ssDNA and stimulate reannealing of complimentary DNA strands (see earlier section), suggested that it may play a role in DNA repair processes.

The importance of p53 in DNA repair is heavily contradicted through the analysis of p53-deficient cells. A number of groups revealed reduced repair of cellular DNA in wild-type p53-deficient cells(Ford and Hanawalt 1995; Havre, Yuan et al. 1995; Smith, Chen et al. 1995; Wang, Yeh et al. 1995; Ford and Hanawalt 1997; Smith and Fornace 1997), although Li-Fraumeni cells only exhibited defective global DNA repair(Ford and Hanawalt 1995; Ford and Hanawalt 1997), while p53-null mouse fibroblasts displayed normal rates of repair(Ishizaki, Ejima et al. 1994; Sands, Suraokar et al. 1995). Nevertheless, p53 has been demonstrated to bind and affect the activity of components the transcription-coupled DNA repair system. p53 physically with components of the dual function transcription-repair factor, TFIIH(Xiao, Pearson et al. 1994; Wang, Yeh et al. 1995; Leveillard, Andera et al. 1996), including: p62, XPD (ERCC2) and XPB (ERCC3) DNA helicase polypeptides. Furthermore, p53 interacts with the strand-specific repair factor, CSB, a potential helicase protein(Wang, Yeh et al. 1995). While it has been difficult to prove that these protein-protein interactions seen *in vitro* have a physiological role *in vivo*, cells deficient in XP-B or XP-D helicases failed to undergo p53-mediated apoptosis(Wang, Yeh et al. 1995).

Interaction between p53 and the replication protein A (RPA) provided another link with the nucleotide excision repair (NER) process(Dutta, Ruppert et al. 1993). RPA is a ssDNA-binding protein composed of three subunits of 70, 32 and 17 kDa and has roles in DNA replication, NER and recombination (reviewed(Wold 1997)).

p53 effector genes: potential roles in DNA repair

In addition to p53's direct protein-protein interactions with the DNA repair machinery, transcriptionally upregulated p53-effector gene products have also been implicated in DNA repair. Both p21 and GADD45 bind to proliferating cell nuclear antigen (PCNA), a protein required for both DNA replication(Wilcock and Lane 1991) (reviewed(Stillman 1994)) and nucleotide excision repair(Shivji, Kenny et al. 1992; Shivji, Podust et al. 1995). p21 inhibits PCNA-dependent DNA replication, although the actual effect of p21 on NER remains to be clarified(Li, Waga et al. 1994; Shivji, Grey et al. 1994; Waga, Hannon et al. 1994; Pan, Reardon et al. 1995). The *GADD45* gene was transcriptionally upregulated by p53 in response to DNA damage(Kastan, Zhan et al. 1992; Lu and Lane 1993) and can bind to both p21(Kearsey, Coates et al. 1995) and PCNA(Smith, Chen et al. 1994). However, the role of GADD45 in NER remains disputed(Kazantsev and Sancar 1995; Kearsey, Shivji et al. 1995).

Cellular response to p53 activation: the choice between Cell Cycle Arrest and Apoptosis

The complex nature of p53 regulation ensures that the p53-mediated outcomes of cell cycle arrest and apoptosis are correctly initiated in response to the appropriate signals. Unfortunately, both the regulatory mechanisms and the pro-apoptotic or -cell cycle arrest signals involved are far from clear and hence cellular choice.

Activation of p53 may result in a cell cycle arrest, presumably to allow an opportunity for DNA repair to occur before replication or mitosis in an attempt ascertain cellular homeostasis. However, in some cell types p53 activation results in apoptotic cell death as a means of eliminating irreparably damaged cells. The final outcome of p53 activation

depends on many factors, both cellular and extracellular, but is significantly initiated through p53-mediated regulation of downstream effectors, either directly or indirectly.

The responsiveness of p53 to a multitude of physical and oncogene-mediated signals places p53 at the nexus of an extensive web governing cellular viability. However, the determinants and mechanisms of cellular choice between apoptosis and cell cycle arrest are still unclear.

Apoptosis

Programmed cell death or apoptosis can be initiated by a wide variety of stimuli, including developmental signals, cellular stress and disruption of the cell cycle. In contrast, execution of apoptosis utilises a common mechanism, generating characteristic morphologic and biochemical changes. Such apoptotic hallmarks include membrane blebbing, cellular loss of volume, nuclear condensation and DNA fragmentation(Kerr, Wyllie et al. 1972). A number of the key factors involved in the regulation and execution of apoptosis have been identified, facilitated through the genetic analysis of *Caenorhabditis elegans* developmental apoptosis(Hengartner and Horovitz 1994). Apoptotic cell death in the worm requires CED-3 and its activator, CED-4. CED-9(Yuan, Shaham et al. 1993), an anti-apoptotic factor and Egl-1, which binds and inhibits the anti-apoptotic function of CED-9(Conradt and Horovitz 1998), add an additional level of control of apoptosis.

However, the molecular basis of apoptotic signalling in mammalians seems to be far more complex, with large families of CED-9-like proteins having both pro-apoptotic and anti-apoptotic functions. CED-3 mammalian counterparts comprise of a whole family of cysteine proteases, called caspases, which are critical terminal effectors of apoptosis and generate the apoptotic morphology. The CED-4 mammalian activator, Apaf-1, also has a role in activating a downstream a caspase cascade. Such multiple members of these gene families may allow for the independent regulation of effecting apoptosis.

Four classic pathways of apoptotic signalling in mammalian cells have emerged (reviewed(Dragovich, Rudin et al. 1998; Jarpe, Widmann et al. 1998)):

- Initiation by withdrawal of growth factors and regulated by Bcl-2 family members, resulting in mitochondrial cytochrome c release, activation of Apaf-1 and activation of the caspase cascade.
- Cell-surface death receptor-mediated, such as TNF or Fas, which via adapter proteins can recruit and activate caspases.
- DNA-damage mediated, which is in part regulated by p53.
- Sphingomyelin and c-Jun Kinase (JNK)/Stress-activated Protein Kinase (SAPK) pathways.

In all three pathways of cell death caspases play a key role in regulation and execution of apoptosis.

Caspases

Caspases are proteases that cleave substrates after aspartic acids residues(Alnemri, Livingston et al. 1996), initiating proteolytic degradation and ultimately resulting in apoptotic morphology(Casiano, Martin et al. 1996). Multiple mammalian homologues of CED-3 have been identified(Reed 1997). Specific inhibitors of caspases prevent apoptotic morphology, in response to a number of apoptotic signals(Miura, Zhu et al. 1993; Rabizadeh, LaCount et al. 1993). Furthermore, overexpression of most of the known caspases triggers apoptosis in various cell lines (reviewed(Nunez, Benedict et al. 1998)). Caspase-9 has been implicated in a central role of apoptotic induction, as cytochrome(c)-bound Apaf-1 was shown to complex with caspase-9 and initiate apoptotic events *in vitro*(Li, Nijhawan et al. 1997). Interestingly, γ-irradiation- and cytotoxic drug treatment of caspase-9 deficient cells comprised apoptosis, while other pro-apoptotic stimuli responses, including Fas, were unaffected.

Caspase activation requires the proteolytic processing of an inactive proenzyme. The processing sites themselves are caspase consensus sites, suggesting a potential mechanism for an amplification cascade of caspase activation. Once activated, downstream caspases cleave and inactivate proteins crucial for the maintenance of cellular cytoskeleton, DNA repair, signal transduction and cell cycle control(Fraser and Evan 1996; Nagata 1997).

While caspase activation typically results in apoptotic morphology, not all cell death pathways are caspase-dependent and can die in the presence of caspase inhibitors(Hirsch, Marchetti et al. 1997). However, the morphology of the dying cells lack many of the characteristic morphological features of apoptosis, including typical nuclear changes.

p53-dependent apoptosis

Transcriptional roles for p53-mediated apoptosis

Several stimuli can cause p53-depedent apoptosis, including: growth factor withdrawal(Johnson, Chung et al. 1993; Gottlieb, Haffner et al. 1994); DNA damage(Clarke, Purdie et al. 1993; Lowe, Schmitt et al. 1993); cytotoxic drugs(Lowe, Ruley et al. 1993); *myc* overexpression(Hermeking and Eick 1994; Wagner, Kokontis et al. 1994); and E1A expression(Debbas and White 1993; Lowe and Ruley 1993).

Following ionizing radiation, lymphoid and myeloid cell lines usually undergo rapid apoptotic cell death, while most non-lymphoid cell lines tend to die by necrosis or later apoptosis during the first or subsequent mitosis(Radford 1994). Ectopic expression of wild-type p53 in murine myeloid leukaemia cells induces rapid apoptosis(Yonish-Rouach, Resnitzky et al. 1991), but appears to be via both p53-dependent and –independent apoptotic pathways. Thymocytes from p53-null mice are resistant to ionizing radiation-induced apoptosis, but not to apoptosis induced by other stresses, such as gluccocorticoids(Clarke, Purdie et al. 1993). p53-dependent apoptosis can proceed from signals other than ionizing radiation and has been shown to be important for p53 function, as in the case of removing UV-damaged keratinocytes(Ziegler, Jonason et al. 1994).

Several studies indicate that sequence-specific transactivation is a required function for p53-mediated apoptosis in various experimental systems(Sabbatini, Lin et al. 1995; Attardi, Lowe et al. 1996). Furthermore, an increasing number of p53-responsive genes are being associated with apoptosis. 14 new p53-induced genes expressed prior to apoptosis were recently identified(Polyak, Xia et al. 1997). *PAG608*, another newly isolated p53-inducible

gene, can induce apoptosis when transiently expressed in human cell lines(Israeli, Tessler et al. 1997), although the mechanisms involved by which these genes contribute to apoptosis are not well determined.

A large body of work has concentrated on the p53-regulated Bcl-2 family members, which has revealed pro-apoptotic and anti-apoptotic members. Bax is a p53-induced member of the Bcl-2 family(Miyashita, Krajewski et al. 1994; Zhan, Fan et al. 1994), which heterodimerises with Bcl-2 and suppresses apoptosis signalled by a number of stress signals. In contrast Bax homodimers promote apoptosis, leading to the idea that the relative proteins levels in a stressed cell can determine cellular life or death(Oltavi, Milliman et al. 1993). However, Bax expression is neither solely required nor sufficient for radiation-induced apoptosis, as this process still occurs in a p53-dependent manner in thymocytes from *bax*-null mice. Furthermore, Bax overexpression did not restore radiation-induced apoptosis to p53-null cells(Brady, Salomons et al. 1996).

Another member of the Bcl-2 family, Bcl-X_L, is induced by ionizing radiation, as is Bax, in a p53-dependent manner(Zhan, Alamo et al. 1996). Unlike Bax, Bcl-X_L protects against apoptosis, exerting it effects largely through antagonism of Bax(Schott, Apel et al. 1995). Therefore, in response to ionizing radiation, p53 appears to regulate the induction of directly opposing anti- and pro-apoptotic proteins. A rheostat-like mechanism between these two proteins is likely to play a role in the determination of the outcome of the potential apoptotic signal. Bcl-X_L's role in protection from apoptosis has been supported with a correlation between its basal mRNA level and sensitivity to radiation-induced apoptosis in a panel of lymphoid and myeloid lines(Zhan, Alamo et al. 1996).

Fas/Apo-1 is another mediator of apoptosis which is upregulated by p53 in several cell types(Owen-Schaub, Zhang et al. 1995). Binding of the Fas ligand (FasL) to Fas/Apo-1, triggers a cascade of signalling events resulting in activation of the caspases and apoptosis(Enari, Hug et al. 1995; Tewari and Dixit 1995; Schlegel, Peters et al. 1996). Fas-induced apoptosis can be partially abrogated by overexpression of Bcl-2 in some cell types(Itoh, Tsujimoto et al. 1993), indicating cross-talk between branches of the apoptotic pathway.

A member of the TBFR family, *KILLER/DR5*, is also a p53-inducible gene(Wu, Burns et al. 1997). Interaction of DR5 with its ligand, TRAIL, activated the cytoplasmic death domain of DR5 which in turn activated an apoptotic caspase-cascade(Pan, Ni et al. 1997). Both TRID and TRUNND, antagonistic decoy receptors lacking the cytoplasmic tail, are also induced by genotoxic stress and by exogenous expression of p53(Pan, Ni et al. 1997). DR5 and its related decoy receptors compete for TRAIL binding, enhancing or attenuating apoptotic signals, respectively. The finding that all three of these receptors are induced by p53 provides a link between p53 and the caspase cascade. Again, a rheostat-like mechanism exists of p53-induced antagonistic pro- and anti-apoptotic proteins.

In addition to p53's sequence-specific transactivation, p53 also represses the transcription of many genes(Ginsberg, Mechta et al. 1991; Mack, Vartikar et al. 1993; Hall, Campbell et al. 1996), several of which can block p53-mediated apoptosis, including: *bcl-2*(Miyashita, Harigai et al. 1994), *IGF-IR*(Prisco, Hongo et al. 1997), and *MAP-4*(Murphy, Hinman et al. 1996). Such a two-pronged attack of transcriptional activation of pro-apoptotic genes and transcriptional repression of anti-apoptotic genes may represent a failsafe mechanism ensuring apoptosis even with either route being compromised. Alternatively, a dual approach may represent a more efficacious pro-apoptotic approach or allow fine-tuning of the apoptotic signal through incorporation of multiple targets and pathways.

Non-transcriptional roles for p53-mediated apoptosis

While transcription of p53-regulated genes can contribute to the regulation of apoptosis, p53 mutants lacking sequence-specific transactivation function have been shown to induce a slower, less efficient apoptotic response in a cell-type specific manner(Haupt, Barak et al. 1996). p53 can also induce apoptosis without initiating *de novo* protein or RNA synthesis(Caelles, Helmberg et al. 1994; Wagner, Kokontis et al. 1994).

Many p53 protein-protein interactions (see Table 1.3) could also represent another non-transcriptional mechanism of p53-mediated apoptosis. For example, p53 binding to the transcription/repair complex TFIIH, inhibits the helicase activity of its subunits, XP-B and XP-D and such action may be important in generating an apoptotic signal(Wang, Yeh et al.

1995). Expression of p53 in mutant XP-B or XP-D fibroblasts results in an abrogated apoptotic response, restoration of which can be achieved by addition of the appropriate wild-type XP gene(Wang, Vermeulen et al. 1996).

p53 and cell cycle checkpoints

G_0 Arrest

Gas-1 is a membrane protein whose expression maintains cells in G_0 arrest(Del Sal, Ruaro et al. 1995) and is absent in growing or transformed cells. Moreover, Gas1 blocked cellular proliferation of a number of transformed cell lines, with the exception of SV40- or adenovirus-transformed cell lines. The quiescent state mediated by Gas-1 expression was dependent on the presence of p53. Interestingly, mutated $p53^{22,23}$ incapable of transcriptional transactivation, was capable of co-operating with Gas-1 in achieving a G_0 arrest, suggesting the presence of an intrinsic transactivation-independent function(s) of 53.

G_1 Arrest

A cell can arrest its progression through the cell cycle at a number of points following the detection of cellular insult. p53 has mainly been associated with delays in transit through G_1 and G_2, as well as in a mitotic spindle checkpoint. G_1 arrest is a prominent outcome of DNA damage and is induced in many cell types by expression of exogenous wild-type p53. Activation of a G_1 checkpoint in human cells shows a remarkable concordance with functional p53(Hartwell and Kastan 1994; O'Connor 1997). In tumour cell lines, checkpoint activation is transient and many of the cells progress into S phase and cycle normally(Linke, Clarkin et al. 1997). In normal cells, such as human fibroblasts, it appears that p53's role is not to provide a protective delay, but to remove the cell from the cell cycle through a permanent G_1 checkpoint, similar to terminal differentiation(Gadbois, Bradbury et al. 1997). However, irradiated bronchial epithelial cells showed a transient G_1 arrest, reminiscent of the tumour cell line response. In addition, the 'permanently' arrested human fibroblasts re-entered the cell cycle when the cells were trypsinized and re-plated, suggesting a role for cellular-extracellular matrix interactions in cell cycle control after irradiation.

Cells lacking wild-type p53 function are found to lack DNA damage-induced G_1 but not G_2 arrest(O'Connor 1997). Induction of the G_1 arrest is mediated largely by the sequence-specific transactivation function of p53(Hartwell and Kastan 1994). Induction of $p21^{CIP1/WAF1}$ (p21) in response to ionising radiation is dependent on wild-type p53(el-Deiry, Tokino et al. 1993) and was shown to be a G_1 cyclin-dependent kinase (Cdk) inhibitor(Harper, Adami et al. 1993), giving it a clear role in cell cycle arrest.

Exit from G_1 and entry into S-phase requires the activation of G_1-specific cyclin/Cdk complexes. p21 inhibits phosphorylation and activation of Cdk2 associated with Cyclin D or Cyclin E, preventing the phosphorylation of downstream and activation of downstream protein targets required for cell cycle progression(Askew, Ashmun et al. 1991; Radford, Murphy et al. 1994). The crucial target of G_1 cyclin-Cdk phosphorylation is the retinoblastoma protein (pRB), which when hypophosphorylated, binds and sequesters E2F (E2F-1 and DP-1 heterodimer), a transcription factor required for entry into S-phase(Chellappan, Hiebert et al. 1991; Johnson, Schwarz et al. 1993). Exogenous overexpression of p21 results in growth arrest, presumably through inactivation of cyclin/Cdk2 complexes and the subsequent failure of pRB to release E2F(Harper, Elledge et al. 1995). This model is supported by the result of E2F overexpression overcoming a G_1 arrest(Johnson, Schwarz et al. 1993), while p21 null mice are only partially defective in their radiation-induced G_1 arrest(Brugarolas, Chandrasekaran et al. 1995). Therefore, while p21 is a major mediator of G_1 arrest, but not the sole effector.

Roles for p53 in G_2/M Delay

Although earlier studies of p53-mediated cell cycle arrest focused on the G_1 checkpoint, it has become clear that p53 can also contribute to G_2 arrest. Although G_2 arrest in response to ionising radiation-induced damage can occur in the absence of p53(Kastan, Onyekwere et al. 1991; O'Connor, Jackman et al. 1993), p53-regulated genes do participate in the regulation of a G_2 arrest. Inducible p53 systems have shown that p53 overexpression results in a G_1 and G_2 arrest and down regulation of Cyclin B1(Agarwal, Agarwal et al. 1995; Stewart, Hicks et al. 1995).

Caffeine and staurosporine related compounds (protein kinase C inhibitors) can suppress the G_2 checkpoint, which is generally accompanied by increased radioresistance. Interestingly, both checkpoint activation and radioresistance can be decreased preferentially in p53-deficient cells, suggesting that while not required, p53 can contribute to the efficacy of the G_2 arrest(Fan, Smith et al. 1995; Powell, DeFrank et al. 1995; Wang, Fan et al. 1996; O'Connor, Jackman et al. 1997). The CyclinB1/Cdc2 complex is most probably the most important regulatory factor involved in the G_2/M transition(Elledge 1996; O'Connor 1997) and decreased expression of Cyclin B1 and inhibitory phosphorylations of Cdc2 are thought to be the major mediators of G_2 arrest.

Overexpression of GADD45 in normal human fibroblasts has been shown to participate in G_2/M arrest(Wang, Zhan et al. 1999). Attenuation of the arrest was achieved through Cyclin B1 and Cdc25c overexpression(Wang, Zhan et al. 1997). GADD45 has more recently been shown to inhibit activity of the CyclinB1/Cdc2 complex *in vitro* through disruption of the complex, most probably via protein-protein interaction with Cdc2(Zhan, Antinore et al. 1999).

Other p53-regulated genes also may have a role in G_2 arrest. p21 overexpression causes cells to accumulate in both G_1 and G_2 and is also associated with a reduction of Cyclin-B-associated kinase activity(Medema, Klompmaker et al. 1998; Niculescu, Chen et al. 1998). Another ionising radiation-induced protein, 14-3-3σ, when overexpressed results in a G_2 arrest(Hermeking, Lengauer et al. 1997). In addition to it binding p53, 14-3-3σ can bind and sequester phosphorylated Cdc25C, preventing its dephosphorylation and activation of Cdc2(Peng, Graves et al. 1997). BTG2 expression has also been shown to be p53 regulated and its inactivation in embryonic stem (ES) cells led to the disruption of DNA-damage-induced G_2/M arrest. A possible explanation could lie in loss of mCaf1 interaction (the murine homologue of a component of the yeast CCR4 transcriptional regulatory complex) and consequent loss of other cell cycle regulatory genes(Rouault, Prevot et al. 1998).

There is also evidence for cell cycle controls in late G_2 and early M phase that may involve p53. Cells usually do not progress through mitosis in the presence of spindle inhibitors, but p53-null mouse embryo fibroblasts (MEFs) undergo multiple rounds of DNA synthesis without completing chromosome segregation, forming tetraploid and octaploid cells(Cross, Sanchez et al. 1995). Centrosome duplication may also be regulated in part by wild-type p53, as p53-null MEFs frequently produce multiple copies of functionally competent centrosomes during a single cell cycle, thus contributing to genetic instability(Fukasawa, Choi et al. 1996). Furthermore, Human Papilloma Virus (HPV) type 16 E6(Thompson, Belinsky et al. 1997) or SV40 large T antigen(Chang, Ray et al. 1997) expression in normal diploid human fibroblasts, resulted in a decrease of radiation-induced mitotic delay, increased uncoupling of mitosis from completion of replication and a reduced ability to arrest in response to mitotic spindle inhibitors.

In addition to the abolishment of p53 function on G_2/M, specific p53 mutations can confer a gain of function phenotype that interferes with regulation of the spindle checkpoint. A specific class of dominant p53 mutations has been identified in cells from Li-Fraumeni Syndrome patients which specifically interferes with the mitotic spindle checkpoint and promotes genomic instability(Gualberto, Aldape et al. 1998).

p53 was shown to play a critical role in cells which had exited mitotic arrest without undergoing cytokinesis; required during a specific time window to prevent cells from re-entering the cell cycle and initiating another round of DNA synthesis. The mechanism required p21, as p21-null fibroblasts fail to arrest in response to nocodazole treatment and became polyploid(Lanni and Jacks 1998). Thus, the p53-dependent checkpoint following spindle disruption may functionally overlap with the p53-dependent checkpoint following DNA damage.

Selective induction of cell cycle arrest or apoptosis by p53 mutants

Cell cycle arrest and apoptosis are the two activities attributed to p53 in the inhibition of cell growth. Wild-type p53 is capable of activating either pathway dependent on a variety of

relatively unknown cellular and environmental factors. A tumour-derived point mutant (p53 $175^{R\Rightarrow P}$) showed specific loss of apoptotic activity, despite retaining wild-type cell cycle arrest activity(Rowan, Ludwig et al. 1996). Another mutant retained the ability to induce apoptosis, but was unable to generate a cell cycle arrest in some cell types(Haupt, Rowan et al. 1995). Uncoupling between growth arrest and apoptosis has also been demonstrated through the use of several p53 mutant forms(Ishioko, Engler et al. 1993; Kobayashi, Consoli et al. 1995; Sabbatini, Lin et al. 1995).

Analysis of the transcriptional activity of p53 mutants using synthetic consensus sequence promoters, showed that mutations at amino acid 273 attenuated promoter activation(Ludwig, Bates et al. 1996). p53-mediated transcriptional transactivation of most synthetic and natural promoters was abolished, while the artificial consensus binding site promoter, p53CON, was not affected. However, other p53 mutants demonstrated specific loss of *IGF-BP3* and *bax* transcriptional inducibility and impaired apoptotic ability(Friedlander, Haupt et al. 1996; Ludwig, Bates et al. 1996). Therefore, qualitative and quantitative differences in the ability of p53 to regulate different classes of promoter, may have functional consequences for the decision of a cell to undergo apoptosis or cell cycle arrest in response to p53 activation.

Modulation of the cellular response to stress

Survival factors

p53 can clearly stimulate both of the major cellular responses to DNA damage, cell cycle arrest and apoptosis. Additional factors contribute to modulation of the p53 signal to determine the final outcome of p53 activation and accumulation. Factors influencing such a decision may be cell-type specific or dependent on the cellular environment. The presence of growth factors can be a major determinant of the decision in certain cell types; IL-6 can protect M1 myeloid leukaemia cells from p53-induced apoptosis, while erythropoeitin similarly protects DP16 Friend erythroleukaemia cells(Gottlieb and Oren 1996). Following exposure to ionizing radiation, the Ba/f3 murine leukaemia cell line undergoes a p53-dependent cell cycle arrest in the presence of IL-3, but rapid p53-induced apoptosis in its absence(El-Deiry, Harper et al. 1994; Canman, Gilmer et al. 1995). The mouse lymphoma

cell line, DA-1, is similarly dependent on IL-3 for its response to radiation. Exposure of DA-1 cells to DNA damage causes p53 accumulation which leads to growth arrest in the presence of IL-3 and apoptosis without IL-3(Gottlieb, Lindner et al. 1996). In DA-1 cells, the co-operation of IL-3 and p53 in determining apoptosis appears to be mediated through cleavage of pRB by caspase activation following IL-3 withdrawal(Gottlieb and Oren 1998).

pRB and pRb family members

HPV E7 binds to pRB and inactivates its growth suppressive function and E7 overexpressing fibroblast undergo apoptosis in response to ionising radiation, when in the absence of E7, would normally undergo growth arrest in response to the same treatment(White, Livanos et al. 1994). These results suggest a role for pRB in the modulation of the p53 signal from cell cycle arrest to apoptosis. pRB's usual role following stress is the sequestration of E2F, preventing entry in S-phase. Co-expression of E2F-1 and p53 in a fibroblast cell line abolished the 'normal' p53-induced cell cycle arrest and resulted in S-phase progression and apoptosis(Wu and Levine 1994). While, co-expression of E2F-1 and mutant p53, or pRB, however, does not result in apoptosis(Qin, Livingston et al. 1994). In the absence of pRB function, E2F may drive the cell cycle forward into S-phase in the presence of additional growth arrest signals from p53. Such conflicting signals may result in activation of the apoptotic program. While pRB is the only member of its protein family, including p107 and p130, which is frequently mutated in human cancer, it is also possible that alterations in other family members may also contribute to regulation of the cell cycle and apoptosis by p53.

p33^{ING-1}

The candidate tumour-suppresser gene *ING1* was identified using the genetic suppresser element (GSE) methodology(Garkavtsev, Kazarov et al. 1996) and encodes a nuclear protein, p33^{ING1}. Expression of *ING1* was upregulated in senescent human fibroblasts and ectopic expression lead to G_1/S cell cycle arrest or apoptosis in several cell lines(Garkavtsev, Kazarov et al. 1996; Helbing, Veilette et al. 1997). Antisense inhibition of *ING1* expression promoted anchorage-independent growth of mouse epithelial cells,

increased foci formation of NIH3T3 cells and extended the lifespan of human fibroblasts(Garkavtsev, Kazarov et al. 1996).

Comparison of the cellular outcomes of $p33^{ING1}$ overexpression in wild-type and null-p53 cell lines, revealed that only wild-type p53 containing cells exhibited growth inhibition(Garkavtsev, Grigorian et al. 1998). Additionally, the function of p53 as a transcriptional activator was dependent on the presence of $p33^{ING1}$ and suggested that the mechanism for the growth-inhibitory function of $p33^{ING1}$ involved stimulation of p53 transcriptional activity. A physical interaction between p53 and $p33^{ING1}$ was also observed, providing a possible co-operative role for $p33^{ING1}$ in mediating p53 function. Adriamycin-mediated DNA damage and p53 overexpression failed to affect $p33^{ING1}$ expression, suggesting that it was not DNA damage-inducible or regulated by p53 activity. Overall, $p33^{ING1}$ may co-operate with p53 in inducing both cell cycle arrest and apoptosis, although may not determine the actual cellular choice.

The p53 Protein Family

Despite the widespread presence of *p53* mutations in human malignancies, many tumours develop in the absence of any detectable *p53* abnormalities. Analysis of such tumours have revealed other tumour suppressers such as pRB(Benedict, Murphree et al. 1983), NF1(Ballester, Marchuk et al. 1990) (neurofibromatosis) and DPC and APC(Fearon, Hamilton et al. 1987) (colon carcinoma), all of which were initially identified through cytogenic evidence of loss of heterozygosity (LOH). Similar analysis of neuroectodermal tumours suggested the presence of multiple tumours at the subtelomeric region of chromosome 1(Dracopoli, Harnett et al. 1989).

p73

p73 was fortuitously cloned from a COS-cell cDNA library using degenerate oligonucleotides corresponding to IRS-1 binding domains(Kaghad, Bonnet et al. 1997). Two splice variants, α and β, differing in their carboxyl-terminus were subsequently cloned, both of which showed homology to p53: transactivation domain (29% identity with p53 aa 1-45), sequence-specific

DNA binding domain (63% identity with p53 aa 113-290) and p53 oligomerisation (38% identity with p53 aa 319-363). p73β is encoded by transcripts lacking the 96 nucleotides corresponding to exon 13, yielding a 499 amino acid protein.

Key residues of p53's MDM2 binding domain TFSDLW (aa 18-23) are present in p73 as TFEDLW. Other significant residues corresponding to p53 mutational hot spots (R^{175}, G^{245}, R^{248}, R^{249}, R^{273} and R^{282}) are conserved and occupy identical positions in p73. However, no significant homology was detected between the C-terminal domain of p53 (aa 364-393) and p73α or β. Nevertheless, the carboxyl-terminus of p73α shows homology with a number of invertebrate p53 homologues, suggesting that p53 may have evolved from a more primitive, *p73*-like gene. Supporting this, the intron-exon organisation of the *p73* gene was found to be similar to that of the p53 gene.

Oligomerisation studies carried out in the yeast-two hybrid system(Kaghad, Bonnet et al. 1997), revealed p73α to form only weak homotypic interactions, in contrast to p73β, which showed strong homotypic interactions. This observation was also reflected in the propensity for p73β, but not p73α, to form heterotypic interactions with p53. p73 α and β variants also showed weak but detectable interactions .

p63

At the same time as the p73 discovery, another p53 homologue, KET or p63, was discovered(Schmale and Bamberger 1997). Considerable similarities exist between p63 and p73, including isoforms of p63 as a consequence of alternative spicing and the presence of long carboxyl-terminal extensions (SAM domain)(Schmale and Bamberger 1997; Osada, Ohba et al. 1998). Conservation of the MDM2 binding and oligomerisation domains in p63, also raise the possibility of MDM2-mediated regulation and homo- and hetero-oligomerisation of p53 family members.

NBP and p51

NBP, another member that binds to the p53 consensus response elements and enhances transcription, but displays a different sequence preference from p53(Zeng, Levine et al.

1998). Another p53 homologue, p51, was also found to induce apoptosis and suppress transformation in p53-null human cell lines and to transactivate the p21 promoter, although to a lesser extent than p53 itself(Osada, Ohba et al. 1998).

Impact of p53 family members

The discovery of p53 homologues suggests evidence for redundancy in function, potentially explaining a number of observations seen in p53-null mice and cells. However, very little evidence exists that confirms that the family members serve similar or distinct functions in the cell. Examination and comparison of family members' ability to transcriptional regulate p53-responsive genes and interact with known p53-interacting partners needs to be carried out to answer some of these questions. Additionally, comparison of the effect of upstream regulators of p53 and responsiveness and outcome of cellular stress stimuli, could also reveal differential roles and functions for the family members. Hence, 20 years of p53 research findings needs to applied to these new proteins to determine their roles in the cell.

MDM2[6]

Discovery of MDM2 as a proto-oncogene

The initial discovery of *mdm2* (mouse double minute gene 2) amplification in a spontaneously arising tumourigenic Balb/c 3T3 cell line(Cahilly-Snyder, Yang-Feng et al. 1987) and subsequent evidence of transforming activity, suggested that *mdm2* encoded a cellular proto-oncogene(Fakharzadeh, Trusko et al. 1991). A potential molecular mechanism of MDM2 tumourigenesis was discovered when immunoprecipitation analysis revealed MDM2 bound to p53(Momand, Zambetti et al. 1992) and complex formation inhibited p53's transcriptional ability(Oliner, Pietenpol et al. 1993). Transformation and immortalisation assays validated a functional link to p53; transfection of primary rat embryo fibroblasts with co-operating oncogenes, such as E1A and H-*ras*, resulted in the generation of fully transformed cell lines, with either abrogated or mutated p53 expression(Eliyahu, Michalovitz et al. 1989; Finlay, Hinds et al. 1989; Hinds, Finlay et al. 1990). *mdm2* could substitute for E1A as a co-operating oncogene with H-*ras*. However, in sharp contrast with H-*ras* and E1A transformation, H-*ras* and *mdm2* transformants maintained expression of the wild-type p53 in more than 50% of the resulting cell lines(Finlay 1993). Furthermore, transfection of primary rat embryo fibroblasts with *mdm2* alone efficiently immortalised these cells, a process that normally requires functional inactivation of p53(Finlay 1993). A hypothesis was proposed that MDM2 overexpression could provide an alternative route to mutation as a means of inactivating p53.

MDM2 amplification/overexpression in tumours

Cellular transformation of rat embryo fibroblasts and inhibition of wild-type p53 by MDM2 suggested that it may function as an oncogene and promote tumourigenicity. Discovery of the frequent amplification of *mdm2*'s, 12q13-14 chromosomal location in human sarcomas(Oliner, Kinzler et al. 1992), supported the idea of *mdm2* as a proto-oncogene.

---

[6] The majority of comments are applicable to both murine and human MDM2, although specific amino acid residues shall refer to human full length MDM2, unless stated otherwise.

Subsequent analysis of human soft tissue tumours (including osteosarcomas), demonstrated that *mdm2* was amplified in approximately 20% of the samples (reviewed(Momand and Zambetti 1997)). In primary sarcomas and cell lines that were characterised in more detail, amplification of the *mdm2* gene correlated with overexpression of the MDM2 protein, while maintaining wild-type p53 status(Oliner, Kinzler et al. 1992). In addition, *mdm2* amplification was more frequently observed in metastatic or recurrent human osteosarcomas, when compared to primary osteosarcomas, implicating a role for MDM2 in late-stage tumour progression(Ladanyi, Lewis et al. 1995). *mdm2* amplification has been detected in other tumour types, including malignant gliomas, breast cancers and non-small cell lung carcinomas. Interestingly, *mdm2* amplification appears to be more common in cells derived from non-epithelial origin, especially those derived from mesenchyme. However, in addition to *mdm2*, the *CDK4* and *GLI* proto-oncogenes may also be co-amplified at the 12q13-14 locus(Khatib, Matsushime et al. 1993).

Simultaneous mutation of *p53* and overexpression of *mdm2* has been rarely observed. An extensive study of 104 human carcinomas revealed 12 tumours contained mutant *p53*, 10 overexpressed *mdm2* and only one contained both mutant *p53* and *mdm2* overexpression(Florenes, Maelandsmo et al. 1994). Originally, with the knowledge of MDM2-mediated inhibition of p53 function, it was thought that MDM2 overexpression would functionally mimic an inactivating mutant p53 phenotype. Hence, MDM2 overexpression and mutant p53 would be mutually exclusive. Interestingly, a number of studies revealed that cells/tumours containing mutant p53 and overexpressing *mdm2* coincided with increased malignancy and a worse prognosis(Cordon-Cardo, Latres et al. 1994; Marks, Vonderheid et al. 1996). Such observations suggest that p53 mutation and *mdm2* overexpression are not completely redundant.

MDM2 and development

The importance of the relationship between MDM2 and p53 was demonstrated using *mdm2* knockout mice. Mice heterozygous for *mdm2* deletion were viable and phenotypically normal, while loss of *mdm2* resulted in embryonic lethality(Jones, Roe et al. 1995; Montes de Oca Luna, Wagner et al. 1995). Embryos died between implantation and six days of

development and within eight cell divisions, being one of the earliest seen by deletion of a gene affecting proliferation(Montes de Oca Luna, Wagner et al. 1995).

Remarkably, the *mdm2* null phenotype was rescued by deletion of p53, as *p53/mdm2* double-null mice were viable(Jones, Roe et al. 1995; Montes de Oca Luna, Wagner et al. 1995). Such findings strongly implied a major function for MDM2 was as a negative regulator of p53 and supported a role for p53 in development. Interestingly, subtle abnormalities in the double null *mdm2:p53* mice existed, generating very small litters, suggesting that MDM2 may have additional p53-independent function(s) in development(Montes de Oca Luna, Wagner et al. 1995).

Studies with animal models have revealed *mdm2* expression patterns throughout development, although no consistent picture is evident. *mdm2* mRNA in developing Xenopus increases from undetectable levels, peaks at oocyte stage V/VI, then diminishes to barely detectable levels after the blastula stage(Marechal, Elenbaas et al. 1997). This data suggests that MDM2 is required to modulate p53 activity during the early mitoses. A rat developmental model revealed differential MDM2 tissue expression, although a general concomitant increase in MDM2 expression and developmental stage was evident(Ibrahim, Gallimore et al. 1997). However, a ubiquitous low-level mdm2 expression level was found throughout mouse embryonic development(Montes de Oca Luna, Tabor et al. 1996).

MDM2-mediated inhibition of apoptosis and cell cycle arrest

Inhibition of Apoptosis

Several cases of apoptosis were inhibited by MDM2 overexpression, including: p53-dependent apoptosis of p53 Val^{135}-expressing 10(1) cells induced by *c-myc* overexpression(Chen, Wu et al. 1996); apoptosis induced by p53 overexpression in H1299 cells(Haupt, Barak et al. 1996); withdrawal of Granulocyte-macrophage colony-stimulating factor (GM-CSF) in TF-1 cells(Urashima, Teoh et al. 1998) and E2F-1 induced apoptosis in REF-52 cells(Kowalik, DeGregori et al. 1998). Furthermore, expression of antisense *mdm2*

mRNA lead to apoptotic hypersensitivity of human glioblastoma U87-MG cells to cisplatin, while MDM2 overexpression decreased apoptotic sensitivity(Kondo, Barnett et al. 1995).

Inhibition of cell cycle arrest

MDM2 inhibition of γ-irradiation-induced cell cycle arrest has also been documented in RKO colorectal carcinoma cells. Comparison of parental and MDM2 overexpressing isogenic RKO cell lines, revealed significant inhibition of a G_1/S arrest(Chen, Oliner et al. 1994). Analysis of BALB/c 3T3 variants revealed a cell line that showed intact p53 and p21 response when γ-irradiated, but in contrast to the parental cell line, did not undergo significant cell cycle arrest(Nozaki, Masutani et al. 1997). *mdm2* was shown to be constitutively overexpressed, as was*CDK4* and were proposed to contribute to the G_1/S arrest abrogation.

Exogenous expression of MDM2 rescued TGF-β-induced growth arrest in a p53-independent manner, through interference with pRB phosphorylation and maintenance of E2F-1 levels and activity(Sun, Dong et al. 1998). Another p53-independent mechanism of cell cycle arrest abrogation was mediated through inhibition of the pRB-family member, p107-induced G_1 cell-cycle arrest and led to morphological transformation of Saos-2 cells(Dubs-Poterszman, Tocque et al. 1995).

MDM2 and terminal differentiation

A potential regulatory role for MDM2 in muscle differentiation was apparent as *mdm2* overexpression led to inhibition of Myo-D-dependent transcription and differentiation of C2C12 myoblasts(Fiddler, Smith et al. 1996). p53's transcriptional activity was also shown to be required for the *in vitro* differentiation of C2C12 cells, providing a role for p53:MDM2 interplay in determining differentiation(Fiddler, Smith et al. 1996). Study of *mdm2* expression in normal or reconstituted human skin revealed the highest levels of MDM2 protein in the nucleus of the most differentiated layers of the tissue(Dazard, Augias et al. 1997). Therefore, in contrast to muscle differentiation, skin differentiation could be accompanied by increased *mdm2* expression.

MDM2-mediated disruption of DNA replication

Tissue-specific overexpression of MDM2 in normal and p53-null mouse mammary glands inhibited normal development, generating morphological and nuclear abnormalities, cellular hypertrophy and mammary tumours. Closer examination revealed that the cells were undergoing multiple rounds of S-phase re-initiation, but in the absence of mitosis(Lundgren, Montes de Oca Luna et al. 1997). The observed phenotypes were similar in both the $p53^{+/+}$ and p53-null mice, demonstrating a role for MDM2 in the regulation of DNA synthesis, independent of p53.

Loss of p53, either through deletion or mutation, results in centrosome hyperamplification, leading to aberrant mitosis and chromosome instability(Harvey, McArthur et al. 1993; Donehower, Godley et al. 1995). A number of human tumours showing centrosome hyperamplification contain wild-type p53, but show elevated MDM2 protein levels, supporting a possible role for MDM2-mediated disruption of DNA replication(Carroll, Okuda et al. 1999). Although, it is unknown whether this effect is mediated entirely through p53 inhibition.

MDM2 upregulates P-glycoprotein

The overexpression of the multi-drug resistance *mdr1* gene and its product, P-glycoprotein, a membrane-associated ATP-dependent effluxing transport pump, is thought to antagonise chemotherapy of human tumours. Overexpression of *mdm2* in the cell line U87-MG, lead to and the induction of *mdr-1* mRNA and P-glycoprotein(Kondo, Kondo et al. 1996). In addition, MDM2 overexpression confirmed resistance of U87-MG cells to etoposide- or doxorubicin-induced apoptosis(Kondo, Kondo et al. 1996). Wild-type p53 has been implicated in repressing *mdr-1* promoter activity, while mutant p53 enhances *mdr-1* expression(Zastawny, Salvino et al. 1993). Therefore, MDM2 may be inhibiting the suppressive effect of wild-type p53 on *mdr-1* expression.

MDM2-mediated cell cycle arrest

In an attempt to isolate MDM2 overexpressing stable cell lines, MDM2 was shown to be lethal in a number of murine cell lines and normal human keratinocytes; arresting cell-cycle progression at the G_0/G_1 phase(Brown, Thomas et al. 1998). MDM2 was capable of inducing this arrest in cells lacking p16 (NIH3T3) or p53 (null MEF), while other cells were unaffected by MDM2 overexpression (Saos-2, H1299 and U2OS). Two growth inhibitory domains were identified, ID1 (aa155-220) and ID2 (aa272-320), within the central region of MDM2 (see Figure 1.2) and deletion of these domains allowed stable overexpression in cells previously intolerant.

Regulation of the Cyclin A promoter

MDM2, when transiently over-expressed, was found to activate reporter plasmids containing the cyclin A promoter(Leveillard and Wasylyk 1997). However, higher levels of MDM2 expression lead to general repression of many different reporters, including the cyclin A-promoter reporter plasmid(Leveillard and Wasylyk 1997). Endogenous cyclin A expression is repressed during the G_1 phase of cell cycle and activated during S_1 through de-repression of the critical cell-cycle dependent element and the cell-cycle genes homology region elements(Henglein, Chenivesse et al. 1994). p53 has been reported to suppress cyclin A expression(Desdouets, Ory et al. 1996), hence MDM2-mediated inhibition could explain the activation of the cyclin A promoter. However, MDM2 has been documented to harbour intrinsic, p53-independent transcriptional properties, interacting with different components of the transcriptional machinery (see later section).

Structure and Function of MDM2

Full length murine MDM2 protein is composed of 489 amino acids(Fakharzadeh, Trusko et al. 1991). Comparison of human (491 aa)(Oliner, Kinzler et al. 1992), *Xenopus laevis* (473 aa)(Marechal, Elenbaas et al. 1997) and zebrafish (445 aa)(Piette, Neel et al. 1997) MDM2 reveals four major conserved regions (amino acid residues correspond to human MDM2, unless stated otherwise) (see Figure 1.2):

- Region I (46% aa identity, aa 23-108) lacks any obvious sequence domains.
- Region II (63% aa identity, aa 237-260) contains a highly acidic domain.
- Region III (58% aa identity, aa 289-333) contains a potential zinc finger domain.
- Region IV (83% aa identity, aa 460-489) contains a RING-finger domain.
- A putative nuclear localisation (aa 178-185) signal is also conserved

MDM2 Functional domains[7]

p53 association domain

MDM2 was known to complex with p53 and repress its transcriptional transactivation ability(Momand, Zambetti et al. 1992). A number of studies isolated the binding domains for each protein using a variety of techniques (see earlier sections for p53). *In vitro* association assays using amino acids 19-102 demonstrated stable association with p53(Chen, Marechal et al. 1993), which agreed with finding from a yeast two-hybrid assay using amino acids 1-118(Oliner, Pietenpol et al. 1993). Interestingly, the monoclonal antibody 3G5 which recognises an MDM2 epitope around amino acids 61-80(Chen, Marechal et al. 1993; Bottger, Bottger et al. 1997), could immunoprecipitate free MDM2, but not p53:MDM2 complexes(Chen, Marechal et al. 1993); suggesting that 3G5 may be sterically blocked from binding to this epitope by p53, or p53 association may alter the epitope's conformation.

Recent studies have identified key MDM2 amino acids required for the MDM2:p53 interaction. A genetic screen in yeast was employed to select mutations in MDM2 which interfered with its ability to bind p53(Freedman, Epstein et al. 1997). This method identified two mutated residues, $58^{G\Rightarrow D}$ and $77^{C\Rightarrow Y}$, that abrogated p53 association. A number of further mutations were made between amino acids 58 and 77, all of which were severely inhibited in *in vitro* p53 association assays. *In vivo*, MDM2 mutations $58^{G\Rightarrow A}$, $68^{D\Rightarrow A}$ and $75^{V\Rightarrow A}$ failed to inhibit p53-dependent transcriptional activation in a transient transfection system.

---

[7] Please refer to Figure 1.2 for following domain locations.

E2F-1/DP-1 binding domain

MDM2 makes two independent functional contacts with the co-operating, heterodimerising transcription factors, E2F-1 and DP-1(Martin, Trouche et al. 1995). MDM2-mediated stimulation of the transcriptional activity of E2F-1/DP-1 occurs in a p53- and pRB-independent manner. The transcriptional activity of the E2F-1/DP-1 heterodimer is due to the presence of an E2F-1 activation domain, which shares similarity to p53's transactivation domain (26% identity) and overlaps with p53's MDM2-binding domain. Furthermore, the short p53 peptide TFSGLW, shown to be essential for MDM2 binding, is well conserved in E2F-1. In addition, both proteins also bind to the N-terminus of MDM2 (aa 1-220).

The mechanism by which MDM2 stimulates E2F-1/DP-1 activity is still unclear. Simple competition between pRB and MDM2 for E2F-1 binding is possible, due to the adjacent locations of the binding domains on E2F-1. Therefore, simple MDM2-mediated steric hindrance of E2F-1's pRB binding site may be a way of stimulating E2F-1 activity through abrogation of pRB-mediated inhibition. Nevertheless, overexpression of MDM2 may be oncogenic, not only due to inhibition of p53, but also through stimulation of the S-phase promoting E2F-1/DP-1 transcription factors.

Numb binding domain

An amino-terminal fragment of murine MDM2 (aa 1-134) was used to screen a human peripheral lymphocyte yeast two-hybrid cDNA library using the yeast two-hybrid system(Juven-Gershon, Shifman et al. 1998). Numb, a 65 kDa protein proposed to play a role in mammalian and *Drosophila* neural development, was isolated and shown to bind MDM2 *in vitro* and *in vivo*. Amino-terminal truncations of MDM2 initiating at +50 and +62, failed to bind Numb *in vivo*, suggesting a partial overlap with MDM2's p53-binding domain. Interestingly, MDM2 affects Numb in a similar manner to p53 (see later sections); reducing Numb's half-life and modulating its subcellular localisation(Juven-Gershon, Shifman et al. 1998). Such a protein-protein interaction between an important neuroectodermal cell fate regulator and MDM2 may support evidence for MDM2's oncogenic functions; perhaps inhibiting Numb-mediated differentiation state.

p300 binding domain

Transcriptional co-activators p300 and CREB-binding protein (CBP/p300) interact with wild-type and mutant forms of p53 and function by linking a number of cellular activators to components of the basal transcriptional machinery(Lill, Grossman et al. 1997). p53's transcriptional transactivation domain interacts with p300 at both its amino-terminal C/H1 domain and carboxyl-terminal C/H3 domain. MDM2 also interacts with p300's amino-terminal C/H1 domain, subsequently inhibiting any p53:p300 interactions(Wadgaonkar and Collins 1999). Therefore, MDM2 not only binds and masks p53's activation domain from transcriptional activators, but also directly binds and masks a co-activators p53-interaction domains. This dual inhibitory mechanism provides even tighter inhibition of p53's transcriptional ability and/or may provide specific regulation of certain target genes transcription.

Transcriptional repression domain

MDM2 was shown to exhibit transcriptional inhibitory functions, directly repressing basal transcription in the absence of p53. Immunoprecipitation studies revealed that both the small subunit of TFIIE and monomeric TBP are bound by the MDM2(Thut, Goodrich et al. 1997). Such inhibitory action can be possibly explained through MDM2-mediated inhibition of the pre-initiation complex to synthesise RNA.

This additional level of control of p53's activity, may simply enforce MDM2-mediated specificity or facilitate specificity in inhibition of p53 targets, as MDM2 may not inhibit all co-activators. Differential gene expression is regulated through integration of a wide variety of positive and negative transcriptional signals. Hence, co-operative and antagonistic action of multiple transcriptional regulators bound at a promoter, may ultimately determine the effect on the basal transcriptional machinery.

Ribosomal L5 binding domain

The L5 protein has been shown to bind specifically to 5S RNA during ribosomal biogenesis, first in the nucleus and then in the nucleolus, as well as on the large ribosomal subunit of the ribosomes(Steitz, Berg et al. 1988). Immunoprecipitation analysis revealed the existence of ribosomal L5 protein associated with both free MDM2 and p53:MDM2 complexes(Marechal, Elenbaas et al. 1994). Possible functions for such complexes could lie in translational control of specific mRNAs and/or ribosomal biogenesis.

pRB binding domain

pRB:MDM2 complexes were first detected in asynchronous U2OS cells(Xiao, Chen et al. 1995). Interaction was dependent on the carboxyl-terminal region of pRB, but independent of the presence of pRB-bound E2F. Transcriptional studies revealed significant stimulation of E2F activity *in vivo*, consistent with the idea of MDM2:pRB complex formation and subsequent relief of pRB's suppression of E2F activity.

Additionally, studies have revealed that pRB interacts with MDM2 when complexed with p53, regulating MDM2-mediated ubiquitination and degradation of p53(Hsieh, Chan et al. 1999)(see later section). Therefore, MDM2 acts as a bridging molecule binding two of the major tumour suppresser proteins, as a heterotrimer. In such a trimeric complex, p53 retains its transcriptional repression activity, remains transcriptionally inactive (through masking of its transactivation domain by MDM2), but retains it ability to induce apoptosis(Hsieh, Chan et al. 1999). Interestingly, complex formation increased following DNA damage, suggesting that p53-mediated transcriptional repression, not transactivation, may be important for apoptosis.

ARF binding domain

Yeast two-hybrid and immunoprecipitation analysis revealed that the carboxyl-terminal 284 amino acids of MDM2 bound to the full length human ARF(Pomerantz, Schreiber-Agus et al.

1998; Zhang, Xiong et al. 1998). A functional consequence of this interaction was suppression of MDM2-mediated inhibition of wild-type p53 activity. ARF was shown to inhibit MDM2-mediated p53 degradation and transcriptional silencing (see later section).

RING Finger Domain

The carboxyl-terminus of MDM2 contains a non-classical RING-finger domain of the structure $CX_2CX_{13}TXHX_3CX_2CX_{10}CX_2C$ with a stretch of basic residues between the C-terminal cysteine pairs(Boddy, Freemont et al. 1994). RING fingers were originally proposed to be nucleic-acid binding structures, due to the high positive charge of the surface of the RING domain, providing a favoured binding domain for the negatively charged phosphate backbone of nucleic acids(Saurin, Borden et al. 1996). The domain has also been proposed to play a role in forming large multi-protein complexes, such as promyelocytic leukaemia nuclear (PML) bodies(Saurin, Borden et al. 1996).

RNA-Binding

An RNA homopolymer binding assay revealed the RNA-binding activity of MDM2, specifically binding to the homopoly-RNA poly(G) and no others(Elenbaas, Dobbelstein et al. 1996). RNA association was independent of the ribosomal L5 protein interaction (see earlier section) and occurred through the carboxyl terminal RING finger. A single point mutation, $446^{G \Rightarrow S}$ totally abolished the RNA-binding ability(Elenbaas, Dobbelstein et al. 1996). Therefore, MDM2 can interact with both components of the ribosome and RNA, suggesting a potential role in regulating translation.

Oligomerisation Domain

Yeast two-hybrid analysis showed MDM2 homo-oligomerisation, mediated through their RING finger domains(Tanimura, Ohtsuka et al. 1999). Discovery of a closely related MDM2

homologue, MDM-X (see later section) also hetero-oligomerised with MDM2 via their RING-fingers(Tanimura, Ohtsuka et al. 1999).

$TAF_{II}250$ Interaction Domain

MDM2 was found to co-immunoprecipitate with the general transcription factor, TFIID. Two distinct MDM2 regions contacted two different subunits of TFIID, namely the central acidic domain with TBP and carboxyl-terminal RING finger with $TAF_{II}250$(Leveillard and Wasylyk 1997) (see Section X).

NLS and NES Signals

MDM2 has been shown to be a nucleocytoplasmic shuttling protein and contains both a nuclear localisation signal (NLS)(Fakharzadeh, Trusko et al. 1991) and an nuclear export signal (NES)(Roth, Dobbelstein et al. 1998). Both signals are located centrally within MDM2, adjacent to each other and share conserved residues with other known NLS and NES sequences(Roth, Dobbelstein et al. 1998; Tao and Levine 1999). Functionally, the nuclear:cytoplasmic shuttling of MDM2 is required for MDM2-mediated degradation of p53 in the cytoplasm, as inhibition MDM2 nuclear export or import lead to p53 accumulation (see later section).

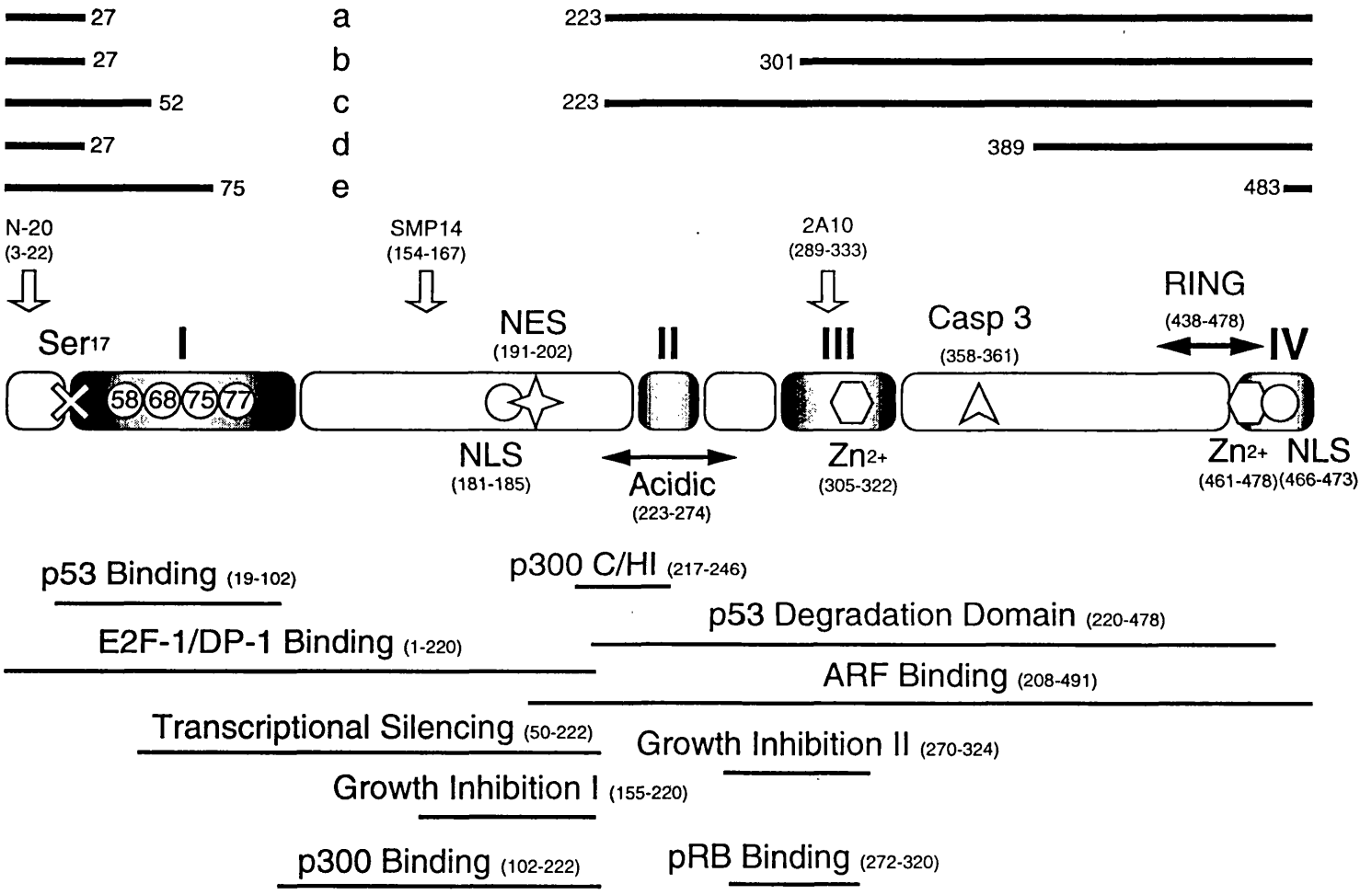

Figure 1.2. Schematic representation of the human MDM2 polypeptide (aa 1-491). MDM2 alternatively splice variants are indicated above the diagram (a-e); three MDM2 antibodies' epitopes, used throughout this study, are also indicated above the diagram; the four conserved regions are marked (I-IV); nuclear localisation and export signals are marked, NLS and NES, respectively; Zinc finger motifs are marked Zn2+; Ser^{17} phosphorylation site is marked with a cross; four important residues for p53 binding are encircled; and MDM2 binding proteins and their binding domains are indicated below the diagram.

Regulation of MDM2 Expression

MDM2 Gene structure

The murine *mdm2* gene structure was determined through sequencing of overlapping clones, isolated from a genomic murine 129 cell phage library(Jones, Ansari-Lari et al. 1996; Montes de Oca Luna, Tabor et al. 1996). Analysis revealed that the *mdm2* gene spans approximately 25kb and is divided into a minimum of 12 exons, ranging in size from 50 to greater than 573bp. While intron sizes ranged from 160bp to 5kb and splice donor and acceptor sites followed the 'GT-AG' rule.

MDM2 Promoters

Using chimeric reporter plasmids, two different murine *mdm2* promoter sequences were identified(Barak, Gottlieb et al. 1994). One promoter conferred upon *mdm2* the ability to be strongly induced by p53, while the other allowed significant expression in the absence of p53.

Barak et al.,(Barak, Gottlieb et al. 1994) showed activation of murine *mdm2* transcription by p53 was achieved through use of an internal promoter, whose activity was strictly dependent on wild-type p53. This promoter, termed P_2, was silent in cells devoid or expressing (non-stressed) basal levels of p53. However, upon transient overexpression of exogenous p53 or DNA-damaged induced endogenous p53, P_2 became strongly induced. This promoter is likely to be associated with the two p53 responsive elements identified within the first intron of the mouse *mdm2* gene(Juven, Barak et al. 1993). Hence a transcript emanating from P_2 would lack exon 1, but may include elements of intron1 and the downstream introns and exons.

In contrast to P_2, the constitutive *mdm2* promoter P_1 is active in p53-null cells, where expression is low, but detectable levels of *mdm2* mRNA and protein product are evident(Barak, Gottlieb et al. 1994). Differences existed between cell lines and the method of p53 induction; use of temperature sensitive p53 mutants in REFs and the myeloid-derived

LTR6 cell lines showed upon switching to the permissive temperature, activation of P_2, but not P_1. In contrast, γ-irradiation of lymphoid-derived DIN cell line activated the P_2 promoter and although less dramatically, the P_1 promoter. Hence, the p53 responsive elements may also function as an intronic enhancer, augmenting transcription from P_1.

Transcripts directed from P_2 differ from P_1 transcripts through the absence of 5' noncoding sequences, as the first two exons of murine *mdm2* are noncoding(Barak, Gottlieb et al. 1994). Hence, both types of transcripts are expected to generate the same translation products. Therefore, it is unexpected that p53 selectively induce transcription from P_2, rather than serving as an enhancer of P_1. *In vitro* translation experiments revealed that the presence of distinct 5' ends direct differential use of in-frame translation initiation codons and affect translational efficiency. Absence of exon 1 (P_2-derived) was shown to facilitate initiation at the first initiation codons (+1/+6), while presence of exon 1 (P_1-derived) lead to the predominantly shorter MDM2 polypeptides, initiated at a later initiation codon (+50). Functionally, such truncated MDM2 polypeptides are incapable of associating with and hence inhibiting p53.

MDM2 Alternative Splicing

Multiple MDM2 proteins and mRNA transcripts have been identified in murine and human cells(Olson, Marechal et al. 1993; Barak, Gottlieb et al. 1994; Haines, Landers et al. 1994; Gudas, Nguyen et al. 1995), although detailed analysis of their origin and biological significance was not determined. RT-PCR analysis of a number of human primary tumour samples revealed alternatively spliced forms of *mdm2* that lacked portions of the p53 binding domain, but were able to transform NIH 3T3 cells(Sigalas, Calvert et al. 1996) (see Figure 1.2). Four of the splice variants lacked regions of the amino-terminus and were confirmed to show reduced p53 binding activity. These results suggested that the transforming activity of some of the splice forms had been p53-independent and mediated through carboxyl-terminal sequences. It was also unlikely that p107, pRb or E2F-1 interactions were involved due to their interaction domains localising to the amino-terminus (see earlier section). Only one of the splice variants (e) encoding the first 75 amino acids and the final eight carboxyl-terminal amino acids, retained p53 binding activity. Additionally,

increased expression of alternatively spliced *mdm2* variants may be correlated to increased malignancy(Sigalas, Calvert et al. 1996; Matsumoto, Tada et al. 1998).

Mechanisms of mdm2 overexpression

In addition to gene amplification, MDM2 overexpression may also be achieved independently of increased gene dosage. Analysis of human leukaemia samples demonstrated that the *mdm2* gene may be maintained at a normal copy number while *mdm2* mRNA levels were dramatically upregulated(Bueso-Ramos, Yang et al. 1993; Watanabe, Hotta et al. 1994). The murine plasmacytoma cell line harbours a *mdm2* gene translocated to the immunoglobulin C κ gene, which generates elevated *mdm2* mRNA(Berberich and Cole 1994). Evidence for translational enhancement exists in a variety of human tumours and occurs in samples with high levels of wild-type p53 protein(Landers, Haines et al. 1994; Landers, Cassel et al. 1997). In agreement with *in vitro* observations, translational enhancement of MDM2 involved a preferential increase in *mdm2* transcription initiated from the p53-dependent internal P_2 promoter(Landers, Cassel et al. 1997)(see earlier section).

The MDM2:p53 relationship

p53:MDM2 Negative Feedback Loop

p53-mediated induction of MDM2 leads to down-regulation of p53 transcriptional transactivation function, by virtue of MDM2's ability to complex with p53. Such interplay creates a p53-MDM2 autoregulatory feedback-loop model(Chen, Oliner et al. 1994), where the induction of MDM2 by p53 is required to reverse the inhibitory effects of p53 on cell cycle progression. Crucial observations leading to the formulation of this model include: *mdm2* being a transcriptionally upregulated target of p53(Barak, Juven et al. 1993; Wu, Bayle et al. 1993) and that MDM2 was a negative regulator of p53's transcriptional activity(Momand, Zambetti et al. 1992; Oliner, Pietenpol et al. 1993). Therefore, the inducer (p53) automatically activates its own repressor (MDM2). Knock-out mice models provided the strongest link between p53 and MDM2, where the additional p53 knockout rescues

mdm2 null mice viability (see earlier section). Additional experiments have provided a direct role of MDM2 in abrogation of p53-mediated cell cycle arrest and apoptosis (see earlier section).

The general outlines of this model have been validated, however its details and additional regulatory mechanisms are beginning to flesh out the basic model.

3D structure of MDM2 bound p53

Xenopus laevis MDM2 (aa 13-118) and human p53 (aa 13-29) were used to create crystals for Multiple Isomorphous Replacement (MIR) structure determination(Kussie, Gorina et al. 1996). Analysis revealed the MDM2 amino-terminal domain formed a twisted-trough structure, with hydrophobic a cleft composed of two helices forming the sides, two shorter helices forming the bottom and a pair of three-stranded β sheets capping each end. The p53 peptide formed an amphipathic α helix, followed by an extended region of three residues. Primary contacts from p53 are made by its α helix, binding the cleft of MDM2, with its hydrophobic face burying all but one of its five hydrophobic amino acids at the interface.

The key to the interface is a triad of hydrophobic and aromatic amino acids of p53: F^{19}, W^{23} and L^{26}, inserted deep into the MDM2 cleft(Kussie, Gorina et al. 1996). These three p53 amino acids are invariant across species(Lin, Chen et al. 1994). Interaction relies extensively on van der Waals contacts and the steric complementarity between the MDM2 cleft and the hydrophobic face of the p53 helix. Only two intermolecular hydrogen bonds augment the interaction.

Biochemical studies in conjunction with the structural information, revealed the mechanism of MDM2-mediated inhibition of p53 transcriptional activity. Several hydrophobic amino acids on the amphipathic helix of p53 have been implicated in contacting basal transcriptional machinery (see earlier sections), hence MDM2 masking of these residues would prevent such interactions.

With the resolution of the crystal structure and determination of the p53-binding pocket a number of residues of MDM2 shown to functionally important can be linked to important structural roles. The monoclonal antibody 3G5's specificity for non-p53 complexed MDM2 can be explained due to its epitope, ^{66}LYDE^{69}, comprising the β3 strand side end of the pocket. Additionally, a number of important residues(Freedman, Epstein et al. 1997) (see earlier section) have been identified that contribute to formation of the hydrophobic pocket, either through intramolecular hydrogen bonds, van der Waals contacts or being intrinsically hydrophobic(Kussie, Gorina et al. 1996).

Phosphorylation of MDM2 by DNA-PK

DNA-dependent protein kinase (DNA-PK) is a nuclear serine/threonine protein kinase with the unique property that its activity is dependent on DNA discontinuities and has been implicated in both double-stranded DNA break repair and recombination (see above). MDM2 has eight potential DNA-PK sites; one of which, S^{17}, is located adjacent to the p53-binding domain was shown to be phosphorylated by DN-PK(Mayo, Turchi et al. 1997). DNA-PK phosphorylated MDM2, revealed significantly inhibition of p53:MDM2 binding with phosphorylated MDM2 (S^{17}).

MDM2-mediated ubiquitination and degradation of p53

Stress-induced p53 stabilisation in response to a variety of stress-stimuli has been shown to mediated mostly through post-transcriptional mechanisms(Maltzman and Czyzyk 1984; Kastan, Onyekwere et al. 1991), but appears to be cell-type dependent(Midgley, Owens et al. 1995).

A series of peptide aldehydes were shown to inhibit the chymotryptic and peptidylglutamyl peptidase activities of the 26S proteosome in cultured cells(Rock, Goldberg et al. 1994). Application of a number of these inhibitors, including MG132, lead to elevated p53 levels in a number of cell lines, presumably through inhibition of ubiquitin-mediated, proteosome-dependent degradation(Maki, Huibregtse et al. 1996). Similar observations(Maki, Huibregtse et al. 1996) were made with the *Streptomyces* metabolite lactacystin, a highly-specific

proteosome inhibitor(Fenteany, Standaert et al. 1995). In addition, HPV E6 had also been documented to mediate p53 ubiquitination, recruiting the ubiquitin-protein ligase, E6-AP, and subverting the cellular ubiquitination machinery into degrading p53 (see earlier section). E6-AP was later shown not to be involved in 'normal' cellular p53 degradation(Beer-Romero, Glass et al. 1997).

Upon transient expression of MDM2 in was reported to mediate ubiquitin-dependent degradation of both endogenous and exogenous p53(Haupt, Maya et al. 1997; Kubbutat, Jones et al. 1997). Moreover, MDM2-mediated degradation of p53 was inhibited by both mutations preventing MDM2:p53 protein-protein interaction and proteosome inhibitors.

MDM2 in vitro *acts a ubiquitin protein-ligase*

In vitro assays using Sf9 insect cell extract in the presence of the ubiquitin-activating enzyme, E1, ubiquitin-conjugating enzyme, UbcH5 and human MDM2, generated polyubiquitinated p53(Honda, Tanaka et al. 1997). MDM2 itself was shown to be ubiquitinated, showing MDM2 had characteristics of an ubiquitin-protein ligase (E3). Ubiquitin is transferred by E1-E2-E3 enzymes, through tranesterification reactions between cysteine residue in the enzymes (see earlier section). Mutation of the carboxyl-terminal C^{464} of MDM2 to alanine abrogated MDM2's E3 activity and prevented p53 ubiquitination.

Role for p300 in MDM2-mediated p53 Degradation

MDM2 and p300 were shown to play an interactive role in the normal process of p53 degradation(Grossman, Perez et al. 1998). A specific p300 binding site (known as the C/H1 domain) bound both MDM2 and p53, while MDM2 and p53 mutants defective in C/H1 binding abrogated MDM2-mediated p53 degradation. Furthermore, exogenous expression of a p300 C/H1 polypeptide enhanced the stability of endogenous p53. p300 serves as a multiprotein binding platform during the integration of certain transcription signals(Kamei, Xu et al. 1996). In comparison, p300 may play a role as a platform, organising catalytic and regulatory factors needed for p53 ubiquitination and degradation.

Two DNA tumour viruses, adenovirus and SV40, have adopted a strategy to abrogate p53 function, using p300 as a common molecular target(Eckner, Ludlow et al. 1996; Lill, Grossman et al. 1997; Somasundaram and El-Deiry 1997). Both these proteins bind p300 and p53, causing stabilisation and inhibition of p53. Such aberrant protein-protein interactions may in addition to interfering with p53's transcriptional functions, inhibit 'normal' protein-protein interactions controlling p53 activity and stability.

MDM2 affects p53 family members functions

The p53 family member, p73, was shown to function as a transcription factor and induce apoptosis following transient overexpression(Jost, Marin et al. 1997; Kaghad, Bonnet et al. 1997). p53 and p73α levels increased following N-acetyl-leucinyl-leucinyl-norleucinal (LLnL) and lactacystin treatment, suggesting that the proteosome regulated both p73α and p53 stability(Balint, Bates et al. 1999).

p73α:MDM2 complexes were observed both *in vitro* and *in vivo*, upon ectopic expression of both proteins(Balint, Bates et al. 1999). Transient transfection assays also revealed that in contrast to p53 levels(Haupt, Maya et al. 1997; Kubbutat, Jones et al. 1997), p73α were not reduced upon MDM2 co-expression(Balint, Bates et al. 1999). Furthermore, in Saos2 cells, p53 levels were slightly elevated in cells co-transfected with MDM2 and p73α, suggesting that the p73α:MDM2 interaction may reduce p53 degradation(Balint, Bates et al. 1999). Interestingly, p73α was also resistant to HPV E6-mediated degradation, revealing that both MDM2- and E6-induced ubiquitin-mediated degradation mechanisms capable of degrading p53, could not degrade p73α. However, similarities between p53 and p73α were observed with respect to MDM2-mediated inhibition of transcriptional transactivation of both proteins (Momand, Zambetti et al. 1992; Oliner, Pietenpol et al. 1993; Balint, Bates et al. 1999).

Overall these results suggest that the relationship between p53 and its family members share some similarities, although differences may provide an additional layer of regulatory control to the p53:MDM2 relationship.

Identification of a sequence element resembling previously characterised NESs(Gorlich and Mattaj 1996) was identified in MDM2(Roth, Dobbelstein et al. 1998), located closely to MDM2's NLS (see Figure 1.2). Comparison between species revealed conserved hydrophobic residues, reminiscent of human immunodeficiency virus (HIV) rev(Fischer, Huber et al. 1995) and human T-cell lymphotrophic virus (HTLV) rex(Bogerd, Fridell et al. 1996) NESs. Mutation of MDM2's L^{205} and I^{208} to alanines significantly impaired MDM2's ability to undergo nuclear-cytoplasmic shuttling in heterokaryon assays. Furthermore, the three p53-binding mutants of MDM2, $58^{G\Rightarrow A}$, $68^{D\Rightarrow A}$ and $75^{V\Rightarrow A}$(Freedman, Epstein et al. 1997) all demonstrated nuclear-cytoplasmic shuttling(Roth, Dobbelstein et al. 1998), demonstrating p53-independent nuclear export. Competition with an SV40 LT NLS-HTLV Rex (NLS-rex) fusion protein, a known competitive inhibitor of HIV Rev export(Katahira, Ishizaki et al. 1995), significantly inhibited the nuclear export of MDM2, suggesting that MDM2 competes with similar nuclear-export pathways to Rev and Rex(Roth, Dobbelstein et al. 1998).

The drug leptomycin B (LMB) blocks the formation of ternary complexes in the nucleus, consisting of CRM1, RanGTP and proteins that contain NES sequences; effectively blocking nuclear export of the NES-containing proteins(Fornerod, Ohno et al. 1997; Fukada, Asano et al. 1997; Ossareh-Nazari, Bachelerie et al. 1997). Addition of LMB to a variety of cell lines containing mutant and wild-type p53 resulted in increased steady-state levels of p53(Freedman and Levine 1998). In the case of MCF-7, LMB addition caused both increased stabilisation and re-localisation of cytoplasmic wild-type p53 into the nucleus.

Analysis of wild-type p53 containing LMB-treated cells, revealed induction of the p53-responsive gene products, p21 and MDM2, while no response was observed in mutant or null-p53 cells(Freedman and Levine 1998). These results indicated that the increases in MDM2 and p21 were dependent on the presence of transcriptionally active, functional p53. Therefore, LMB not only increased p53 protein levels, but additionally activated p53's transcriptional transactivational abilities. The functional outcome of LMB-treatment was cell cycle arrest, which was not entirely mediated through p53, as growth arrest was evident in p53-negative cell lines, H1299 and 10(3) cells.

Mutation of MDM2's NLS or NES sequences inhibited MDM2-mediated degradation of exogenous p53 in *p53/MDM2* double-null cells(Tao and Levine 1999). Similar results were obtained with LMB(Freedman and Levine 1998) and NLS-Rex(Roth, Dobbelstein et al. 1998) treated cells, concluding that MDM2 must shuttle p53 from the nucleus to the cytoplasm to achieve effective degradation. Interestingly, co-expression of wild-type MDM2 with either mutant NLS or NES MDM2 did not affect wild-type MDM2-induced p53 degradation(Tao and Levine 1999). Thus, the mutant MDM2 proteins did not act in a transdominant fashion. Comparatively, HPV-E6-mediated degradation of p53 was also reduced through the action of LMB(Freedman and Levine 1998), demonstrating that both MDM2 and HPV-E6 require nuclear export and the action of cytoplasmic proteosomes.

The ARF:p53:MDM2 relationship

Discovery of ARF[8] as a tumour suppresser protein

Upstream regulators of viral and cellular oncogene-mediated stabilisation of p53 remained unknown until the discovery of ARF. A single murine genetic locus, INK4a, was shown to encode the CDK4/6 inhibitor, $p16^{INKa}$ and another protein $p19^{ARF}$ (ARF)(Quelle, Zindy et al. 1995). $p16^{INK4a}$ is encoded by three closely linked exons (1α, 2 and 3). While an mRNA arising from an alternative first exon (1β) spliced to exon 2, yields a β-transcript. The initiator codon in exon 1β was not in frame with sequences encoding $p16^{INK4a}$ in exon 2, so the β-transcript encoded a novel polypeptide. In the mouse, the 19kD protein ($p19^{ARF}$) consists of 65 amino acids encoded by exon 1β and 105 amino acids arising from the alternative reading frame (ARF) of exon 2(Quelle, Zindy et al. 1995). The human protein terminates further 5' in exon 2, expressing a 14kD protein ($p14^{ARF}$).

Partial deletion of $p16^{INK4a}$ and ARF in mice through elimination of exons 2 and 3 revealed that nullizygous animals were highly prone to tumour development(Serrano, Lee et al. 1996). Mouse embryo fibroblasts (MEFs) explanted from the knock-out mice, unlike wild-

[8] ARF refers to both human $p14^{ARF}$ and murine $p19^{ARF}$ proteins, unless stated otherwise.

type MEFs, did not undergo replicative senescence and could be transformed by oncogenic ras alone. MEFs from p53-null mice exhibited similar properties(Harvey, Sands et al. 1993).

Pure ARF-null mice were created only lacking exon 1β and leaving $p16^{INK4a}$ intact. These mice were phenotypically indistinguishable from that attributed previously to $p16^{INK4a}$ disruption(Kamijo, Zindy et al. 1997). Therefore, ARF was shown to function as a tumour suppresser protein.

Functional link between p53 and ARF

The primary features of ARF-null MEFs is their capacity to be transformed by a single oncogene (oncogenic ras) and to grow as an established cell line(Kamijo, Zindy et al. 1997). Interestingly, approximately 20% of spontaneous, 'normal' MEF-derived cell lines undergo bi-allelic deletion of ARF. MEF lines lacking ARF preserved wild-type p53, whereas those retaining ARF harboured mutant p53. In addition, cells lacking functional p53 were resistant to ARF-mediated cell cycle arrest. However, ARF-null cells exhibited an intact p53 checkpoint in response to ionizing or UV irradiation, suggesting that ARF was not relaying DNA-damage signals to p53.

Exogenous expression of ARF stabilised and activated p53, upregulating p53-responsive genes, including *p21* and *mdm2*(Stott, Bates et al. 1998). Overexpression of ARF in ARF-null NIH-3T3 cells induced expression of a p21 promoter-driven reporter in manner dependent on endogenous p53(Kamijo, Weber et al. 1998). Paradoxically, exogenous overexpression of wild-type p53 in ARF-null cells did not activate the reporter construct, indicating that simple increases in the amount of p53 were insufficient to activate transcription. p53-dependent reporter expression was restored upon introduction of ARF, suggesting that ARF could provide an activation signal that facilitated p53-dependent transcription.

The immortalising oncogenes c-Myc and E1A, shown to co-operate with growth promoting oncogenes in cellular transformation(Land, Parada et al. 1983; Ruley 1983), are also potent inducers of apoptosis(Askew, Ashmun et al. 1991; Evans, Wyllie et al. 1992; Rao, Debbas et al. 1992). A process which is enhanced through serum survival factor deprivation(Evans, Wyllie et al. 1992). These contrasting and contradictory outcomes of extended life versus apoptotic death, can be explained by observations that their overexpression provides strong selective pressure for abrogation of the apoptotic machinery, with ARF being a key target(Zindy, Eischen et al. 1998).

Overexpression of c-Myc, E1A or E2F-1 in primary MEFs rapidly induces ARF gene expression, leading to p53-dependent apoptosis. In contrast, p53-null and ARF-null MEFs are resistant(de Stanchina, McCurrach et al. 1998; Zindy, Eischen et al. 1998). Wild-type or hemizygous ARF MEFs surviving c-Myc overexpression sustain either p53 mutation or ARF loss, bot not both(Zindy, Eischen et al. 1998). Indeed re-introduction of ARF into ARF-null c-Myc or E1A expressing MEFs, resulted in apoptosis. Both Myc and E1A can induce p53 via ARF-dependent and ARF-independent routes, although higher levels of either oncoprotein were required to activate p53 in the absence of ARF. Therefore, c-Myc, E1A and E2F-1 trigger a p53-dependent response, mediated by ARF. Ras may also act in a similar manner(Palmero, Pantoja et al. 1998). The ARF-p53 pathway was not shown to be essential for normal proliferation, but was important in embryonic development. In the model of the developing murine lens, pRB deficiency triggers p53-dependent apoptosis(Morgenbesser, Williams et al. 1994) which is attenuated in lenses lacking $p16^{INKa}$ and ARF(Pomerantz, Schreiber-Agus et al. 1998).

E2F-1

Conditional expression of E2F-1 in Saos-2 cells increased both ARF mRNA and protein levels, resulting in accelerated entry into DNA synthesis and apoptotic cell death(Bates, Phillips et al. 1998). However, use of E2F-1 transcriptional mutants failed to upregulate ARF. Identification of a potential E2F-1 binding site upstream of exon 1β and subsequent fusion of this region to a luciferase gene, revealed E2F-1-dependent activation. Other reports have further linked E2F-1 expression and ARF-induction in the control of apoptosis(Zhu, DeRyckere et al. 1999) and senescence(Dimri, Itahana et al. 2000).

DMP1

DMP1 is a 761 amino acid protein that contains a central DNA-binding domain, composed of three imperfect Myb-like repeats flanked by acidic activating domains at both its amino- and carboxyl-termini(Hirai and Sherr 1996). It binds all three D-cyclins *in vitro* and *in vivo* and is frequently deleted in myeloid leukaemia, suggesting a potential role as a tumour suppresser(Inoue and Sherr 1998). DMP1 bound to a single consensus site in the mouse ARF promoter in electrophoretic mobility shift assays. A reporter construct containing nucleotides –225 to +56 of the ARF promoter fused to the luciferase gene showed DMP1-dependent transcription. In agreement with these results, exogenous expression of DMP1 in wild-type, but not ARF-null, MEFs induced ARF, p53 and p21 expression and caused a cell cycle arrest.

Wild-type p53 represses ARF expression

p53-null MEFs exhibit elevated levels of ARF which upon re-introduction of wild-type p53, decrease to normal levels(Kamijo, Weber et al. 1998). A number of other cell lines, mutant or null for p53 also show elevated ARF. Indeed, Saos-2 cells (p53-null) induced to express

wild-type p53 down-regulated ARF expression(Stott, Bates et al. 1998). Hence, ARF can upregulate p53 expression and p53 in turn, can down-regulate ARF expression; an example of a negative feedback loop.

Physical interaction between MDM2 and ARF

ARF itself was shown to physically interact with MDM2, blocking both MDM2-mediated degradation and transcriptional inhibition of p53(Kamijo, Weber et al. 1998; Pomerantz, Schreiber-Agus et al. 1998; Stott, Bates et al. 1998; Zhang, Xiong et al. 1998). Interaction between the two proteins was dependent on the carboxyl-terminal half of MDM2 and the amino-terminus of ARF (exon 1β-encoded)(Zhang, Xiong et al. 1998).

As MDM2 can interact with p53, ARF may enter into ternary complexes with MDM2:p53 binary complexes, with MDM2 acting as a bridging molecule. Direct ARF:p53 interaction remains controversial, with different group reporting opposing findings: Kamijo et al.(Zhang, Xiong et al. 1998), finding ARF:p53 complexes in the absence of MDM2, while Pomerantz et al.(Pomerantz, Schreiber-Agus et al. 1998), Stott et al.(Stott, Bates et al. 1998) and Zhang et al.(Zhang, Xiong et al. 1998), find no direct interaction.

ARF was reported to accelerate MDM2 turnover in HeLa cell cotransfected with vectors encoding ARF and MDM2(Zhang, Xiong et al. 1998). MDM2 destabilisation, through removal of p53's negative regulator, was proposed as the mechanism underlying p53 accumulation and activation. However, additional investigations have revealed conflicting observations, as ARF overexpression caused MDM2 accumulation in the presence or absence of exogenous p53(Stott, Bates et al. 1998). Verification of ARF-mediated abrogation of MDM2-mediated p53 degradation was demonstrated through co-transfection studies in a number of cell lines(Stott, Bates et al. 1998).

ARF blocks Nuclear Export of p53 and MDM2

Heterokaryon analysis revealed ARF prevented the nuclear-cytoplasmic shuttling of both p53 and MDM2, in conjunction with the formation of p53:MDM2:ARF nuclear bodies(Zhang

and Xiong 1999). An independent heterokaryon assay revealed that upon co-expression of ARF and MDM2, ARF was shown to block nuclear-cytoplasmic shuttling of MDM2 and caused a shift in subnuclear localisation to the nucleolus in a shuttling time-dependent manner(Tao and Levine 1999). Furthermore, ARF was exclusively located to the nucleolus, showing no cytoplasmic presence or nucleoplasmic body formation. Therefore, similar conclusions were drawn with respect to ARF inhibiting nuclear-cytoplasmic shuttling, but via conflicting results

These two sets of results both conclude that ARF prevents MDM2 nuclear-cytoplasmic shuttling, in conjunction with ARF's ability to stabilise p53. However, different nuclear localisation patterns were observed for ARF, MDM2 and p53: Zhang et al(Zhang and Xiong 1999), found the formation of nuclear bodies containing all three proteins, with ARF shifting from the nucleolus to the nucleoplasm; and Tao et al(Tao and Levine 1999; Tao and Levine 1999), found ARF and MDM2 co-localising in the nucleolus with p53's nucleoplasmic localisation unaffected.

MDM2's p53-independent functions

Generally, MDM2 has been shown to exhibit p53-antagonistic actions. This role has been partly engineered due to the majority of work being focused on MDM2 over-expression on p53, while p53-independent effects are only beginning to come to light.

mdm2 Alternative-spliced forms

MDM2 may carry out oncogenic functions independent of p53, in addition to the alternative splice forms generated from different promoters (see earlier section), a number of other alternative splice products were identified(Fakharzadeh, Trusko et al. 1991; Barak, Gottlieb et al. 1994). Five alternatively spliced products are observed in urothelial, ovarian and brain tumours(Sigalas, Calvert et al. 1996; Matsumoto, Tada et al. 1998) (see Figure 1.2). Of these five alternatively spliced *mdm2* products, only (MDM2-e) retained p53-binding capability, although all five could independently transform NIH3T3 cells, suggesting that MDM2 may have p53-independent transforming activity. Alternatively-spliced forms of

MDM2 positively correlated with late stage forms of tumours and in brain tumours, MDM2-b was the most prevalent form, found in both wild-type and mutant p53 containing tumours.

Point mutation of MDM2's Zn^{2+}-finger in Human Cancers

Point mutational inactivation of MDM2 may also contribute to tumour formation. A number of point mutations were found in tumour samples, clustering within the first putative Zn^{2+}-finger domain (aa302-310), the conserved region III(Schlott, Reimer et al. 1997) (see Figure 1.2). Missense, nonsense and frameshift mutations were evident, but it was unclear whether mutations offered loss or gain of function.

MDM2 overexpression in p53-null backgrounds

Comparative tumour susceptibility studies performed on *p53*-null and *p53/mdm2* double-null mice, detected no difference between the different mouse genotypes, in either rate of tumour formation or in the spectrum of tumours. This indicated that physiological levels of MDM2 were not affecting tumourigenesis in the absence of p53(Montes de Oca Luna, Wagner et al. 1995). Embryonic fibroblasts were also examined, revealing indistinguishable rates of proliferation and cell cycle characteristics. However, analysis of p53-null mice overexpressing an *mdm2* transgene caused predisposition to spontaneous tumour formation(Jones, Hancock et al. 1998). Specific skin phenotypes were identified in a similar experiment, where MDM2 overexpression was associated with increased proliferation in the skin basal layer and altered expression of differentiation markers(Alkhalaf, Ganguli et al. 1999).

The MDM2:E2F-1 relationship

Transgenic mice overproducing MDM2 exhibit a disruption of normal cellular proliferation in the mammary gland, in a p53-indepent manner(Lundgren, Montes de Oca Luna et al. 1997). This phenotype is marked by a decrease in mammary epithelial cell number and cells

contain enlarged or multiple nuclei that undergo multiple round of inappropriate DNA replication. A likely S-phase inducing protein E2F-1, shown to bind and stimulated by MDM2, was a likely candidate for mediating MDM2's effect. However, no changes in phenotype were observed between wild-type and E2F-1-null mice, suggesting that E2F-1 was not a critical factor in development of the phenotype. DP-1 or other E2F family members may have provided an alternative mechanism of MDM2-mediated perturbations of DNA replication(Reinke, Bortner et al. 1999).

MDM-X

A protein related to MDM2, termed MDMX, shows a high degree of homology within the amino-terminal p53-binding domain of MDM2 and the amino-terminus of MDMX(Shvarts, Steegenga et al. 1996; Shvarts, Bazuine et al. 1997). Additionally, a central Zn^{2+} finger domain and the carboxyl-terminal RING-finger domain are conserved in both sequence and position. MDMX resembles MDM2 functionally, associating with p53 and suppressing its activity(Shvarts, Steegenga et al. 1996), although its involvement in p53 degradation has not been addressed. However, MDMX is distinct from MDM2 in its p53-inducibility in response to DNA damage(Shvarts, Steegenga et al. 1996). Furthermore, MDMX cannot substitute for MDM2 function in development, due to MDM2-null embryonic lethality(Jones, Roe et al. 1995; Montes de Oca Luna, Wagner et al. 1995).

RT-PCR analysis of MDMX expression revealed the expression of two transcripts encoding full-length MDMX and a carboxyl-terminal deleted MDMX-S protein(Rallapalli, Strachan et al. 1999). Both MDMX and MDMX-S were capable of binding p53. Comparison of the p53-repression activity of the MDMX variants and MDM2, revealed that MDMX and MDM2 exhibited comparable activity, while MDMX-S was a more potent repressor than either MDMX or MDM2(Shvarts, Steegenga et al. 1996; Rallapalli, Strachan et al. 1999). A high degree of similarity in the biochemical interaction between p53 and both of its transcriptional inhibitors, MDM2 and MDMX is conserved(Bottger, Bottger et al. 1999), suggesting an intimate relationship between the two proteins.

An additional twist to the MDMX:MDM2 relationship was revealed through MDM2:MDMX hetero-oligomerisation(Tanimura, Ohtsuka et al. 1999). MDMX:MDM2 protein-protein interactions was initially identified by screening a cDNA library with the carboxyl-terminus (aa 294-491) of MDM2 in a yeast two-hybrid system. Of the positive-interacting MDMX clones, the smallest contained only the carboxyl-terminal 58 amino acids, incorporating the RING-finger domain. Further *in vitro* and *in vivo* association assays suggested that MDMX and MDM2 interacted with each other through their RING-finger domains.

In vivo analysis of the MDMX's protein stability revealed a very stable protein with a half-life in excess of 12 hours(Tanimura, Ohtsuka et al. 1999). Co-expression of full-length, but not RING-finger deleted, MDMX with MDM2 lead to increased MDM2 stability, suggesting that MDMX can stabilise MDM2 through hetero-oligomerisation. These findings add another layer of potential regulation, placing MDMX as both a potential stabiliser and mediator of MDM2 function, as well a potential competitor for p53 binding.

Aim

Information revealed in the Introduction reveals that regulation of p53 function and activity is a complex affair, ultimately governing the cell's fate. The aim of this work was to characterise a p53-centric profile for growth arrested and apoptotic cells, in an attempt to illuminate the differences and similarities between the two cellular outcomes. With the establishment of such profiles, comparison between the two would, perhaps, reveal specific characteristics indicative of a certain cellular response. It was also of interest to analyse the cellular effects of MDM2 and mutant p53 expression, two proteins heavily implicated with inhibitory p53 activities and cancer. Revealing their effects on cellular choice and their potential mechanism(s) of affecting that choice.

Use of different, but complimentary, biochemical and cell biological techniques was thought to provide a more complete cellular overview.

Chapter Two

FACS and Molecular Analysis

Many reports have revealed either p53-dependent cell cycle arrest or apoptosis in response to X-Ray- or 254 ηm Ultra-Violet(C)-irradiation (UV) (see Introduction), while the molecular mechanisms governing the choice between the two responses and their effectors are still unclear. Such cellular choices have drastic implications to the cell and the organism as a whole. Knowledge of the determinants of the choice is particularly relevant to cancer treatment with radiation and radiomimetic drugs. In this situation, individual cell-type responses could determine the appropriate treatment, leading to apoptosis of tumour cells with non-detrimental effects to 'normal' cells.

Both UV- and X-ray-irradiation have direct physical effects on DNA structure: UV causes pyrimidine dimers, bulky photo-adducts that can cause transcriptional stalling and potential DNA replication errors (reviewed(Tornaletti and Pfeifer 1996)); and X-ray-irradiation causes single- and double-stranded DNA breaks, that can detrimentally effect transcription, DNA replication and lead to mutations and deletions through aberrant chromosomal rearrangements (reviewed(Whitaker, Powell et al. 1991; Whitaker 1992; Price 1993)). As well as direct physical DNA damage, irradiation promotes various chemical reactions in other cellular macromolecules and the production of reactive oxygen species (ROS), triggering multiple cellular pathways. Both these forms of irradiation are relevant in a cellular context, due to environmental and medical exposure.

Previous work in the laboratory had shown that fluorescence-assisted cell sorting (FACS) analysis of UV and X-ray treated U2OS cell line elicited a dichotomous response, with respect to apoptosis and cell cycle arrest(Allan and Fried 1999). U2OS is a human osteosarcoma-derived cell line of epithelial morphology(Ponten and Saksela 1967; Diller, Kassel et al. 1990), expressing both of the major tumour suppresser proteins, pRB and p53, in a wild-type state(Florenes, Maelandsmo et al. 1994). However, the p16 promoter is

silenced through methylation(Stott, Bates et al. 1998). Thus, U2OS posed as a suitable candidate for p53-dependent DNA damage studies.

Analysis of apoptotic and arresting U2OS cells was carried out in an attempt to further understand the characteristics and molecular mechanisms governing the choice between apoptosis and cell cycle arrest. Additionally, the effects of p53 $175^{R \Rightarrow H}$ and MDM2 overexpression on cellular choice and response were also investigated. Primarily, Western blot analysis of protein levels was used in conjunction with FACS analysis; a powerful method for determining cell cycle profiles and apoptosis.

The following table contains information concerning the cell lines used throughout this work (see Table 2.1).

Table 2. 1. Summary of cell lines used in this work

Name	Status	Comments
U2OS(Florenes, Maelandsmo et al. 1994; Isfort, Cody et al. 1995)	pRB + p53 WT	Osteosarcoma-derived; elevated *mdm2* mRNA levels
M(x)	pRB + p53 WT	U2OS-derived cell line overexpressing pCMV-driven *mdm2*
p3	pRB + p53 WT	U2OS-derived cell line transfected with pcDNA3.1 (vector only) mimicking parental U2OS
DN(x)	pRB + p53 WT	U2OS-derived cell line overexpressing pCMV-driven *p53* $175^{R\Rightarrow H}$
MG-63(Chandar, Billig et al. 1992)	WT pRB / MT p53	Osteosarcoma-derived cell line
OSA (SJSA)(Florenes, Maelandsmo et al. 1994; Isfort, Cody et al. 1995)	pRB + p53 WT	Osteosarcoma-derived cell line; amplified *mdm2* gene and mRNA levels
U393 (G. Peters, ICRF)	?	Osteosarcoma-derived cell line
Saos-2(Chandar, Billig et al. 1992)	pRB + p53 null	Osteosarcoma-derived cell line
MCF7(Plummer, Adams et al. 1997)	WT pRB+p53	Adenocarcinoma-derived cell line
JAR(Chen, Chen et al. 1994)	?/ WT p53	Choriocarcinoma-derived cell line exhibiting elevated MDM2 levels
HOS(Romano, Ehrhart et al. 1989)	? / MT p53 $156^{R\Rightarrow P}$	Osteosarcoma-derived cell line

FACS Analysis of the Ultraviolet and X-ray responses of U2OS cells

UV-irradiation induces an apoptotic response in U2OS cells

Sub-confluent U2OS cells were UV-irradiated with 30 Jm^{-2} using a laminar flow hood-based germicidal UV(C) bulb. Apoptotic morphology was first visually noticeable at 24 hours post-treatment, revealing morphological distortions, elongated cytoplasmic processes and cellular rounding and detachment (see Figure 2.1). By 48 hours, the majority all of the cells were either showing apoptotic morphology or had detached from the plate.

To ensure that the apoptotic-like morphology was actually apoptosis, FACS analysis was used. Degradation of DNA into nucleosomal and smaller fragments is a characteristic event in apoptosis(Wyllie, Beattie et al. 1981; Gavrieli, Sherman et al. 1992) and both Terminal deoxynucleotidyl transferase-mediated dUTP-biotin nick end-labelling (TUNEL) and sub G_1 analysis both utilise this process to determine apoptosis.

TUNEL analysis determines the number of free DNA ends (generated through inter-nucleosomal DNA cleavage) that are available for labelling and is therefore a measure of DNA fragmentation(Gavrieli, Sherman et al. 1992). One potential problem with this system stems from the fact that DNA repair, recombination and any other non-apoptotic DNA breakage events would be classed as 'apoptotic DNA' and hence may not reflect truly apoptotic DNA. Nevertheless large increases in TUNEL-positive cells can be assumed to represent apoptotic cells. Sub-G_1 analysis reveals the total cellular DNA content through propidium iodide incorporation. Normal cells show a range of DNA content ranging from 2n to 4n, reflecting the replication status of the DNA. Apoptotic cells show DNA content lower than 2n with the actual 'loss' of DNA reflecting nuclease action and sub-detection sized DNA fragments(Wyllie, Beattie et al. 1981).

Examination of UV-treated U2OS revealed both positive TUNEL staining and generation of sub-G_1 populations at 48 hours post-treatment (see Figure 2.2), with both methods yielding similar percentages of apoptotic cells (please note the format of the TUNEL and sub-G_1 graphs). Mock-irradiated control cells showed neither significant TUNEL-positive or sub-G_1 cellular populations. TUNEL analysis of the UV-irradiated cells revealed TUNEL-positive

cells represented by all phases of the cell cycle, including a sub-G_1 population, as determined by propidium iodide staining (reflecting DNA content). Sub-G_1 analysis also revealed formation of a sub-G_1 population at the expense of G_1, S, G_2 and M populations, effectively shifting DNA from higher to lower n values. Percentage loss from S-phase cell populations was the greatest, followed by G_1 and G_2/M. Loss from the G_1/S and G_2/M phases hence accounts for the increase in the sub-G_1 population. These results stress the fact that the observed UV-mediated cell death was apoptosis, an active process in response to UV-mediated cellular damage and simply not cellular atrophy. Significant agreement between the two methods of apoptosis detection lead to sub-G_1 analysis, through ease of use, being subsequently chosen as the major method used to determine apoptosis by FACS analysis.

Comparison of different UV exposure levels, ranging from 5 to 30 Jm^{-2}, revealed increasing degrees of apoptosis with increasing dosage (see Figure 2.3 [II]). A near-linear response was evident, although a potential threshold level of apoptosis-inducing UV-mediated damage (<5 Jm^{-2}), may have been present. Long term culturing of the UV-treated cells, revealed significant numbers of viable colonies that eventually grew to confluence. However, an inverse relationship existed between the number of surviving cells and UV-dose, with very few cells surviving a UV-dose of 30 Jm^{-2} (see Figure 2.3 [III]).

It was of interest to determine whether the cells exhibited any alterations in the cell cycle, or were arrested while undergoing apoptosis. To examine cell cycle arrest Bromodeoxyurindine (BrdU) incorporation was measured following UV treatment. Different UV doses were examined 24 hours post-treatment and all yielded similar results, leading to loss of S and G_2 cells, an apparent increased G_1 population and a loss of well defined DNA-content populations (see Figure 2.4). A non-BrdU-incorporating population, apparently with S phase DNA content (n=3) began to emerge. Presumably, the apoptotic DNA degradation events can account for the sub 2n shift in cellular DNA content and apparent loss of G_2/M cells. A 5 Jm^{-2} UV-dose did reveal a reproducible slight increase in G_2 and showed very little 'DNA drag'. In conclusion, no clear cell cycle arrest was evident at 24 hours post-irradiation, although apoptotic events may have masked such an event or cell cycle arrest may have occurred prior to analysis.

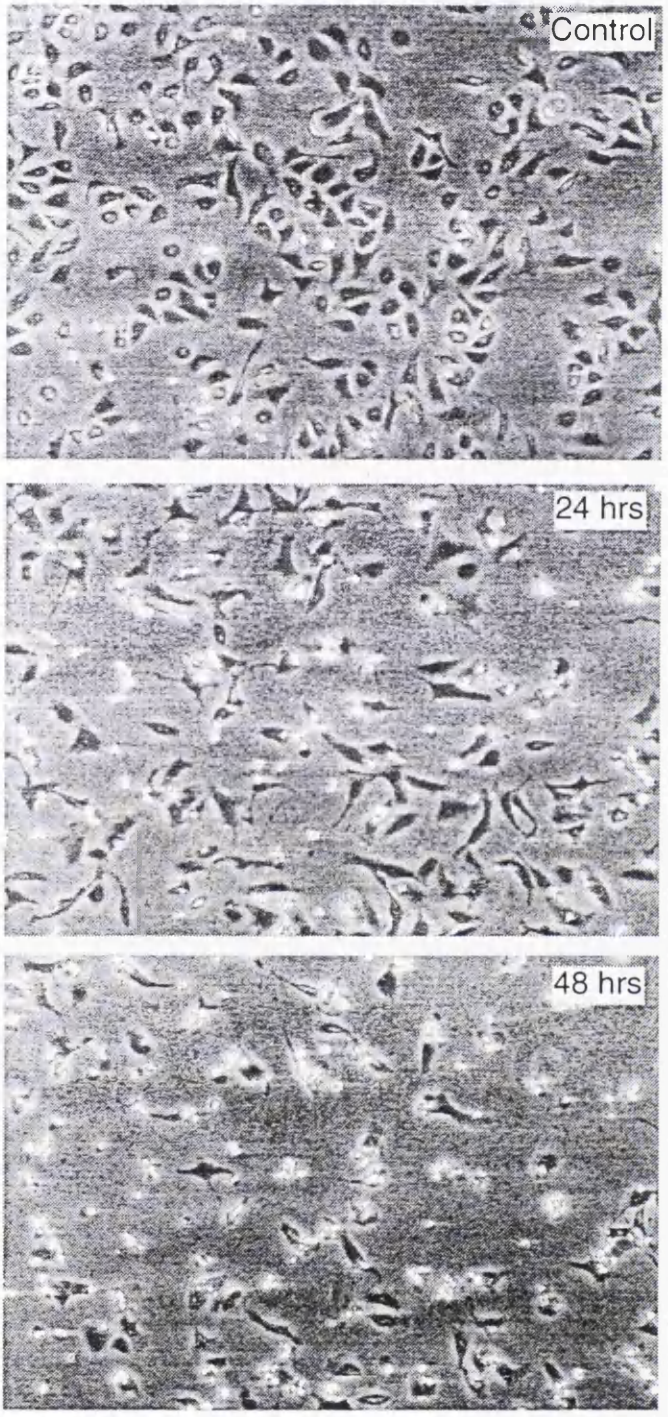

Figure 2.1. 30 Jm-2 UV-irradiation induces apoptotic morphology in U2OS cells. U2OS cells were 30 Jm^{-2} UV-irradiated and examined by time-lapse photography up to 48 hours post-irradiation.

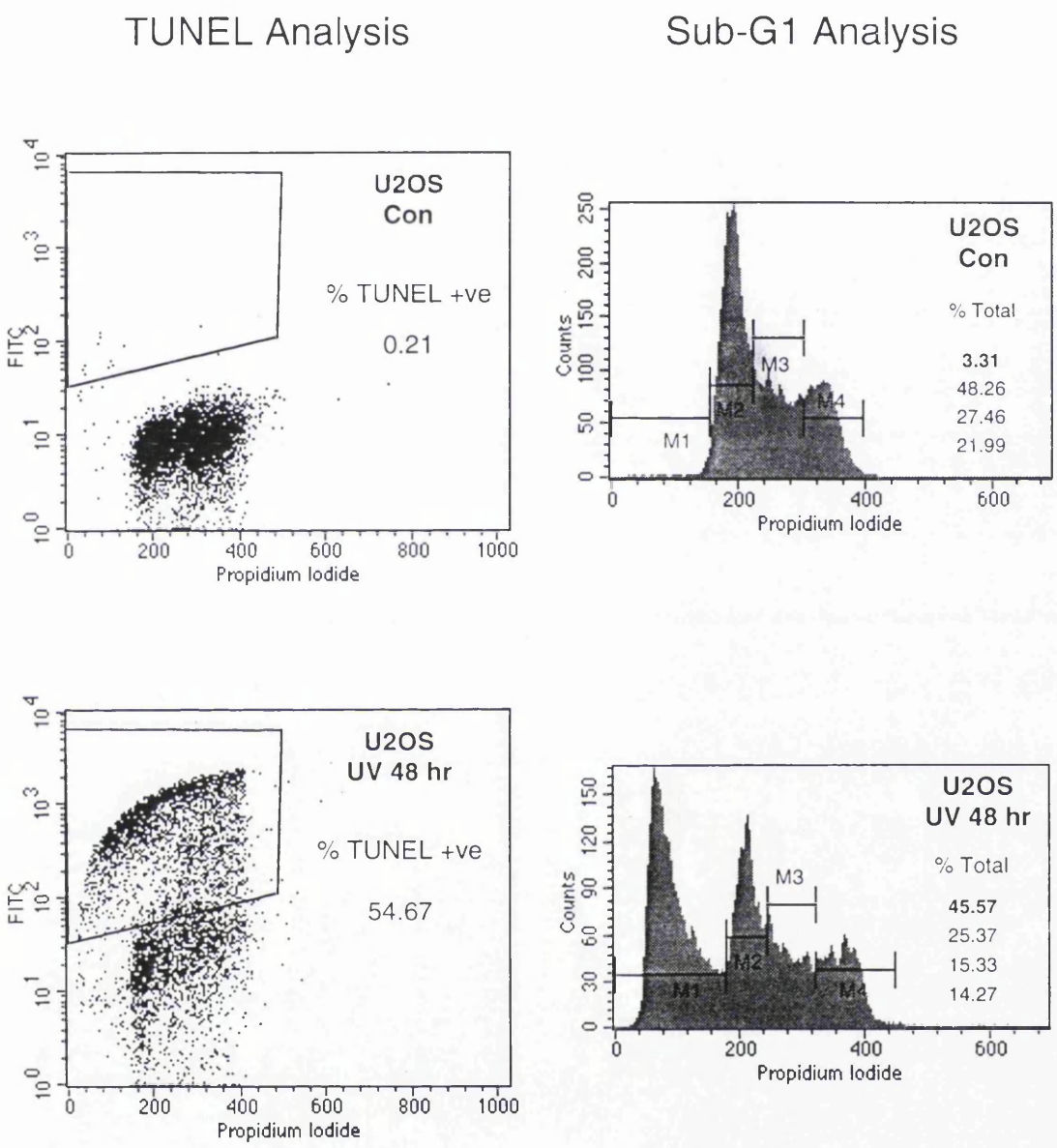

Figure 2.2. 30 Jm-2 UV-irradiation induces TUNEL and sub-G1 positive U2OS cells. U2OS cells were 30 Jm^{-2} UV-irradiated and examined by TUNEL and sub-G1 analysis (as indicated) 48 hours post-irradiation. Sub-G1 percentages (M1) are marked in bold, while G1, S, G2/M cells correspond to M2, M3 and M4,as well as to the relative descending figures alongside the graph, respectively. TUNEL positive cells are boxed off and a coresponding percentage of total cell number analysed is indicated alongside.

I.

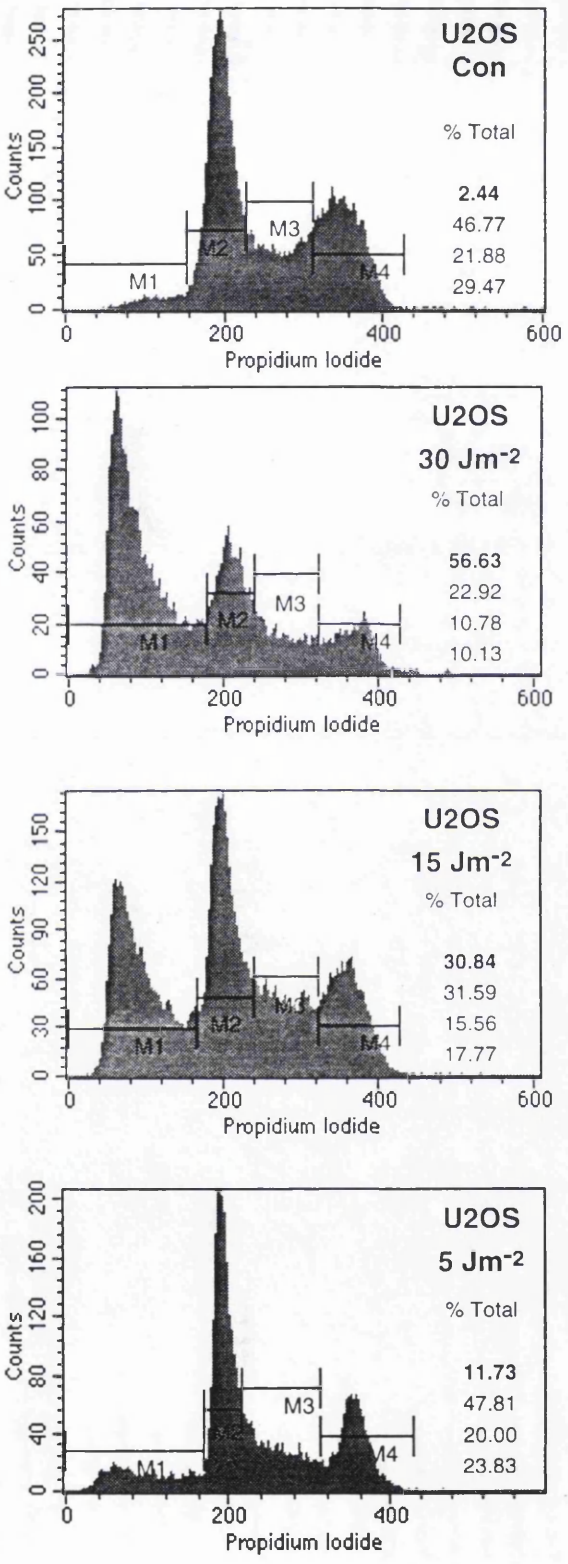

Figure 2.3. Increased UV dose increases U2OS sub-G1 cell populations (two pages). (I) U2OS cells were UV-irradiated with varying doses of UV-irradiation (as indicated) and analysed by sub-G1 analysis 48 hours post-irradiation. Sub-G1 percentages are marked in bold. (II) Graphical representation of (I) sub-G1 data. (III) Number of surviving colonies 7 days post-UV-irradiation (varying doses as indicated).

II.

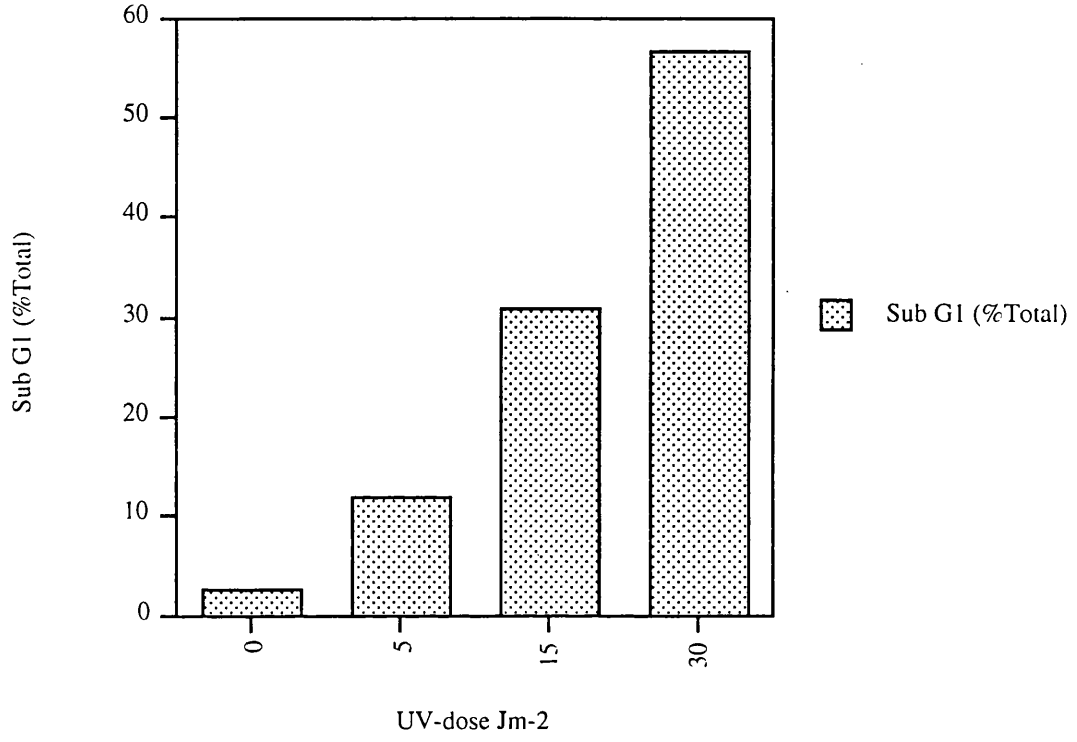
60
50
40
30
20
10
0
Sub G1 (%Total)
0
5
15
30
UV-dose Jm-2
Sub G1 (%Total)

III.

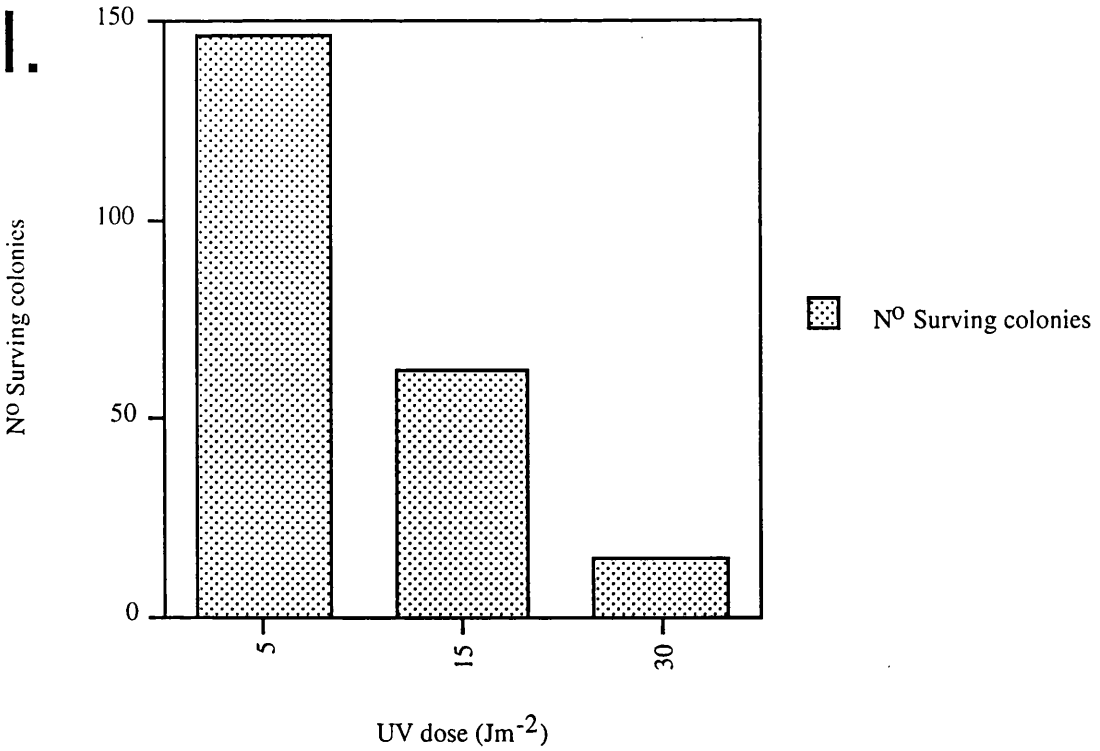
150
100
50
0
N° Surving colonies
5
15
30
UV dose (Jm-2)
N° Surving colonies

I.

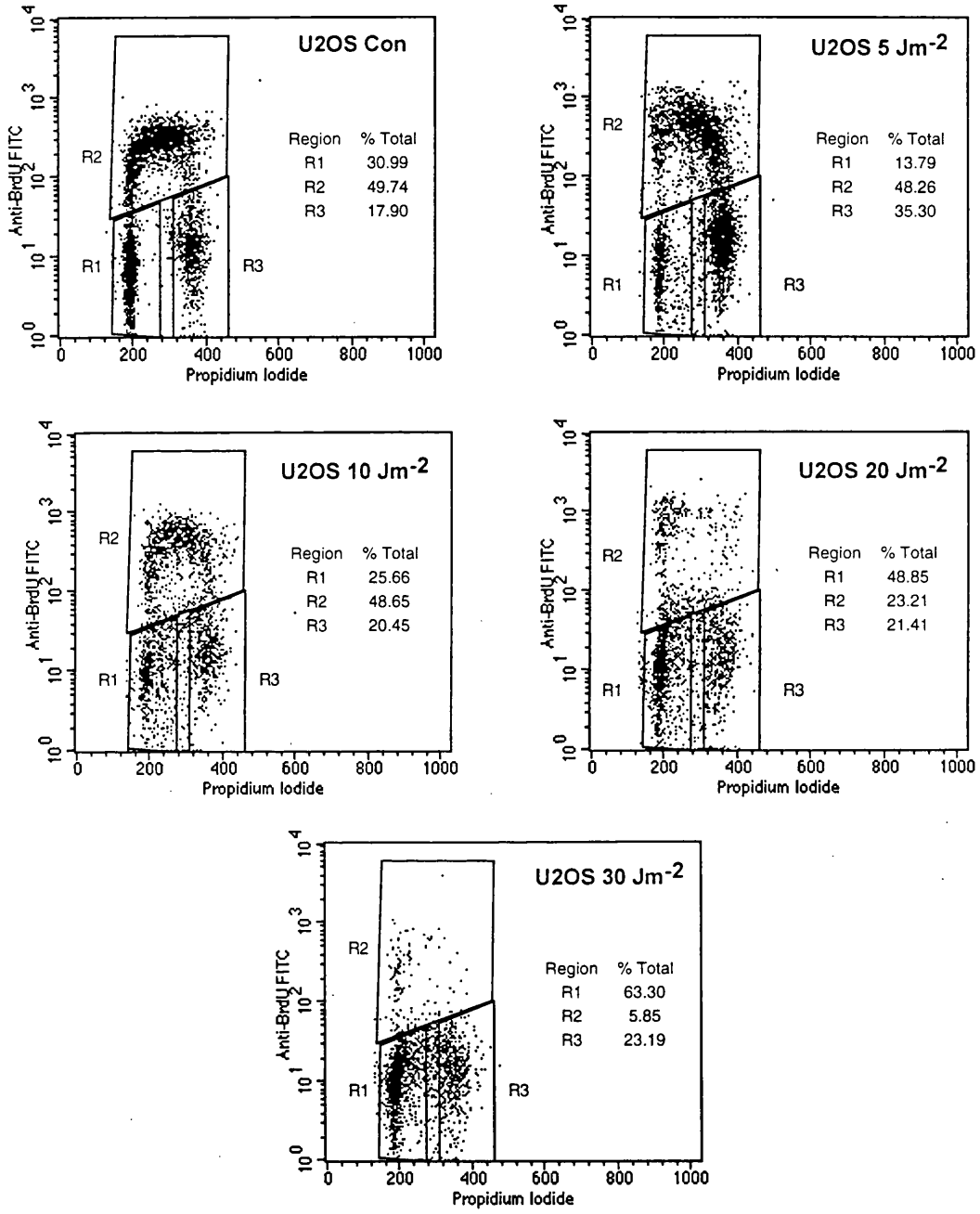

Figure 2.4. UV-irradiation causes perturbations in the cell cycle of U2OS cells (two pages). (I) U2OS cells were UV-irradiated with varying doses of UV-irradiation and analysed by BrdU analysis 24 hours post-irradiation. (II) Graphical representation of (I) S-phase cell data.

II.

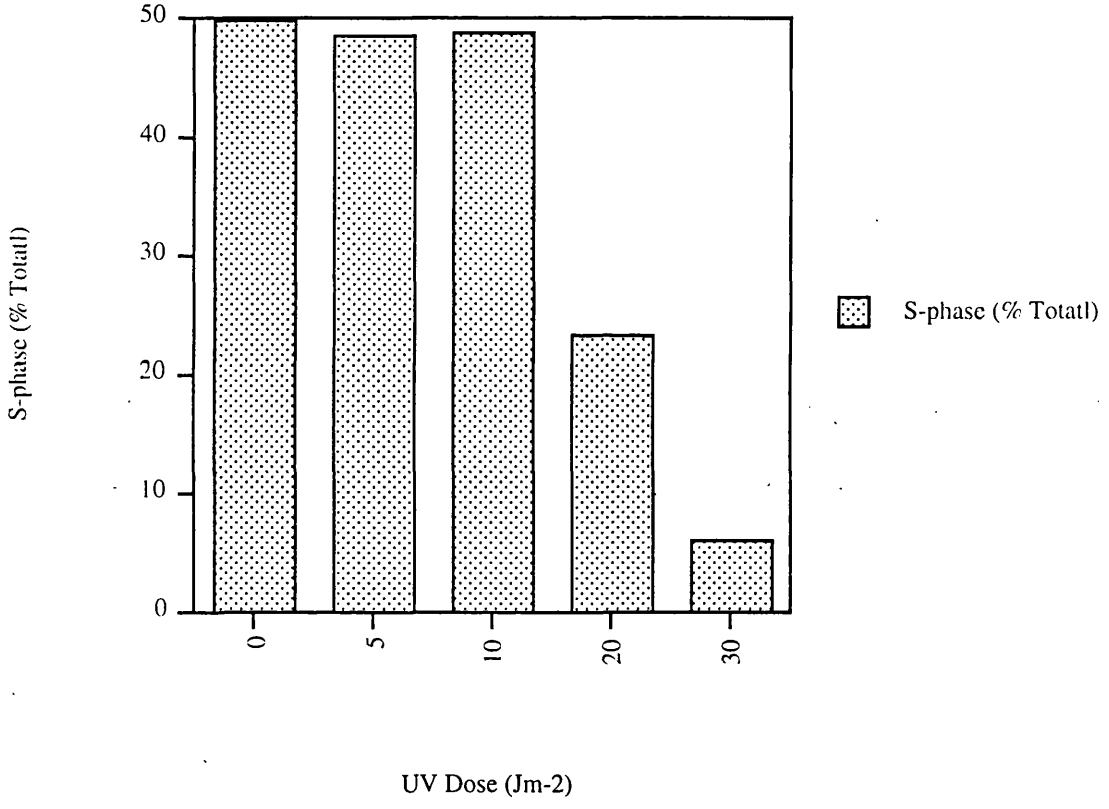
50
40
30
20
10
0
S-phase (% Totatl)
0
5
10
20
30
UV Dose (Jm-2)
S-phase (% Totatl)

UV treatment induces apoptosis in certain cell lines.

To compare the effects of UV-irradiation in other cells, a number osteosarcoma-derived cell-lines were analysed. HOS, MG-63, U393 and U2OS cells were irradiated with 30 Jm^{-2} UV and analysed by sub-G_1 and TUNEL at 24 hours post-treatment. The U2OS and HOS cell lines yielded an apoptotic response while U393 and MG63 cells showed insignificant levels of apoptosis (see Figure 2.5). Further culturing of UV-irradiated MG63 and U393 cells lines failed to exhibit any signs of delayed apoptosis and continued to divide until confluence. These results show that an identical UV dose and dose rates can cause differential effects in different cell lines.

X-ray induces a cell cycle arrest without apoptosis

To examine the X-ray-irradiation response of U2OS, cells were irradiated with 12 Gy and then visually monitored, revealing at approximately 24 hours post-treatment a lack of mitotic events and the emergence of flattened, enlarged cells (see Figure 2.6). At 72 hours post-irradiation, mitotic events were evident and the cells eventually reached confluence. Apoptotic cell morphology or significant cellular detachment was not visible throughout the 72 hour time course. The visible loss of mitosis suggested that the cells were undergoing a cell cycle arrest that was transient due to the re-emergence of mitotic events and eventual plate confluence.

BrdU analysis was used to ensure the cell cycle arrest was actually occurring and to determine where in the cell cycle the cells were arresting. Control, 24, 48 and 72 post-X-ray treatment time points were examined to characterise the apparent cell cycle arrest. BrdU analysis revealed a reduction in BrdU incorporation, hence an emptying of S-phase and an accompanying G_1/S and G_2/M block (see Figure 2.7). G_1:S ratios were used as a measure of the strength of the G_1/S block. This ratio reflects the decrease in S phase entry and the increase in G_1, due to absence of G_1 exit. Thus, the higher the ratio, the greater the arrest (see Figure 2.7 [II]). By 48 hours post-treatment, cells were beginning to cycle with increasing S-phase cell cycling taking place.

It was of interest to consolidate the visual lack of apoptosis with TUNEL data. Such analysis revealed a negligible degree of apoptotic cells that may represent a background level of apoptosis, as a low degree of apoptosis was apparent in the 48 hour-mock control sample. However, the level was insignificant in comparison to the degree obtained with UV-mediated apoptosis (see Figure 2.8 and compare with Figure 2.2). Increasing X-ray doses ranging from 12-20 Gy, all failed to induce TUNEL positive cells. In contrast increased X-ray dose revealed a positive relationship, where increasing X-ray dose increased the G_1/S ratio and emptying of S-phase at 24 hours post-treatment (see Figure 2.8 [II]).

I.

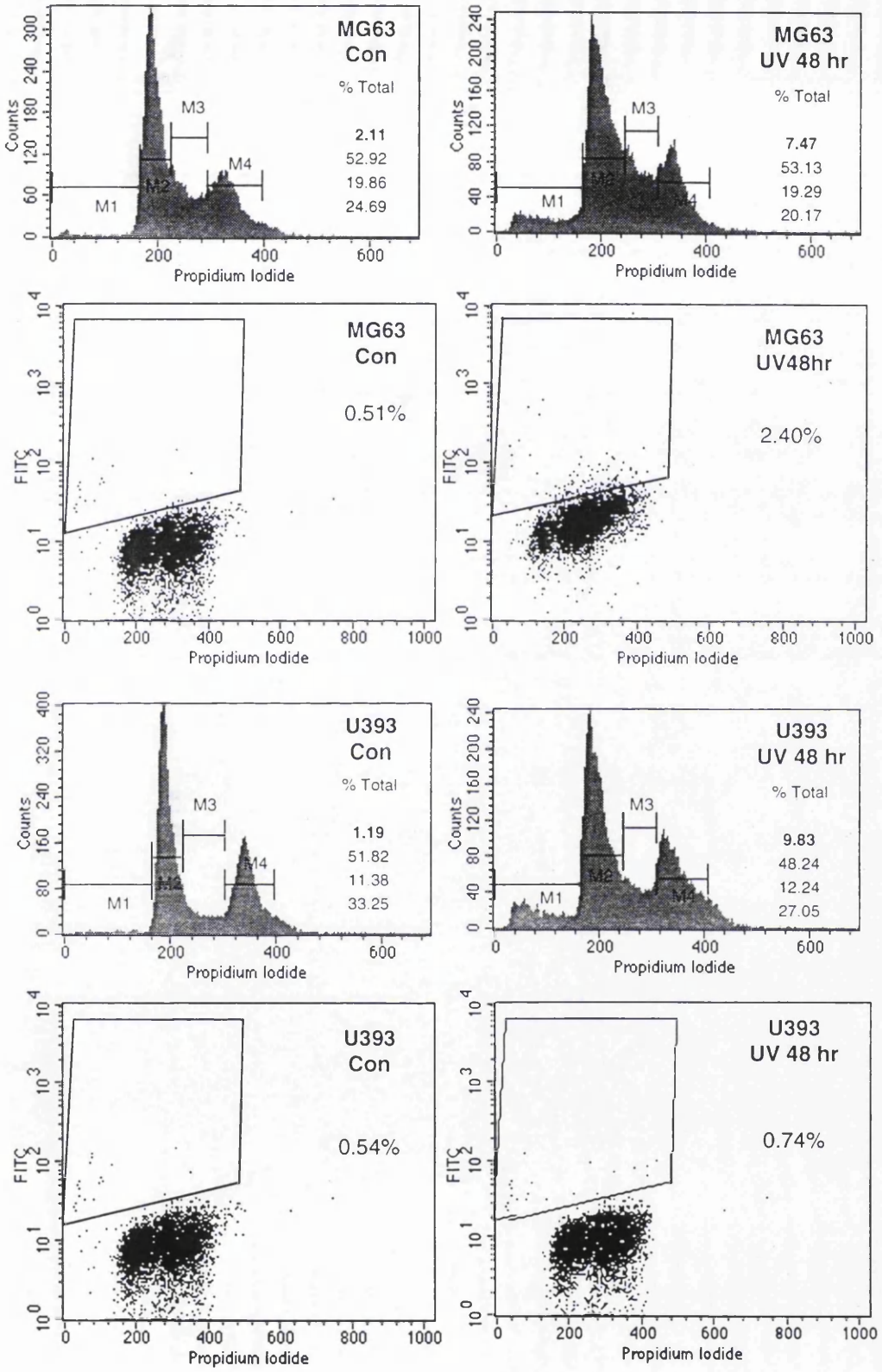

Figure 2.5. 30 Jm-2 UV –irradiation induces apoptosis in only certain cell lines (three pages). (I) Four cell lines (HOS, MG-63, U2OS and HOS) were UV-irradiated and analysed by TUNEL and sub-G1 analysis 48 hours post-irradiation. Sub-G1 percentages are marked in bold. (II) Graphical representation of (I) sub-G1 and TUNEL positive cells.

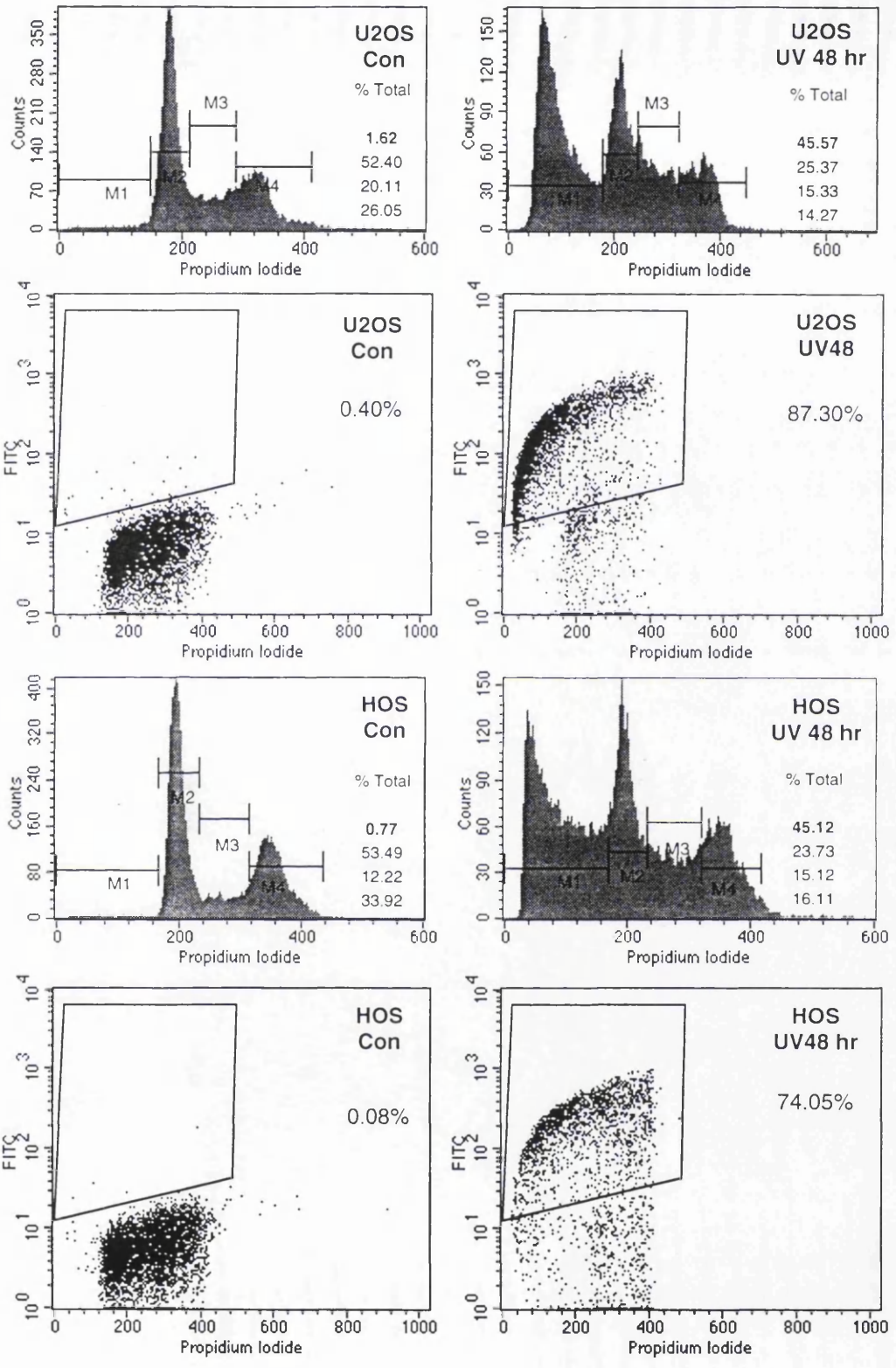
U2OS
Con
% Total
1.62
52.40
20.11
26.05
M1
M2
M3
M4
Counts
Propidium Iodide
U2OS
UV 48 hr
% Total
45.57
25.37
15.33
14.27
U2OS
Con
0.40%
FITC
Propidium Iodide
U2OS
UV48
87.30%
HOS
Con
% Total
0.77
53.49
12.22
33.92
HOS
UV 48 hr
% Total
45.12
23.73
15.12
16.11
HOS
Con
0.08%
HOS
UV48 hr
74.05%

II.

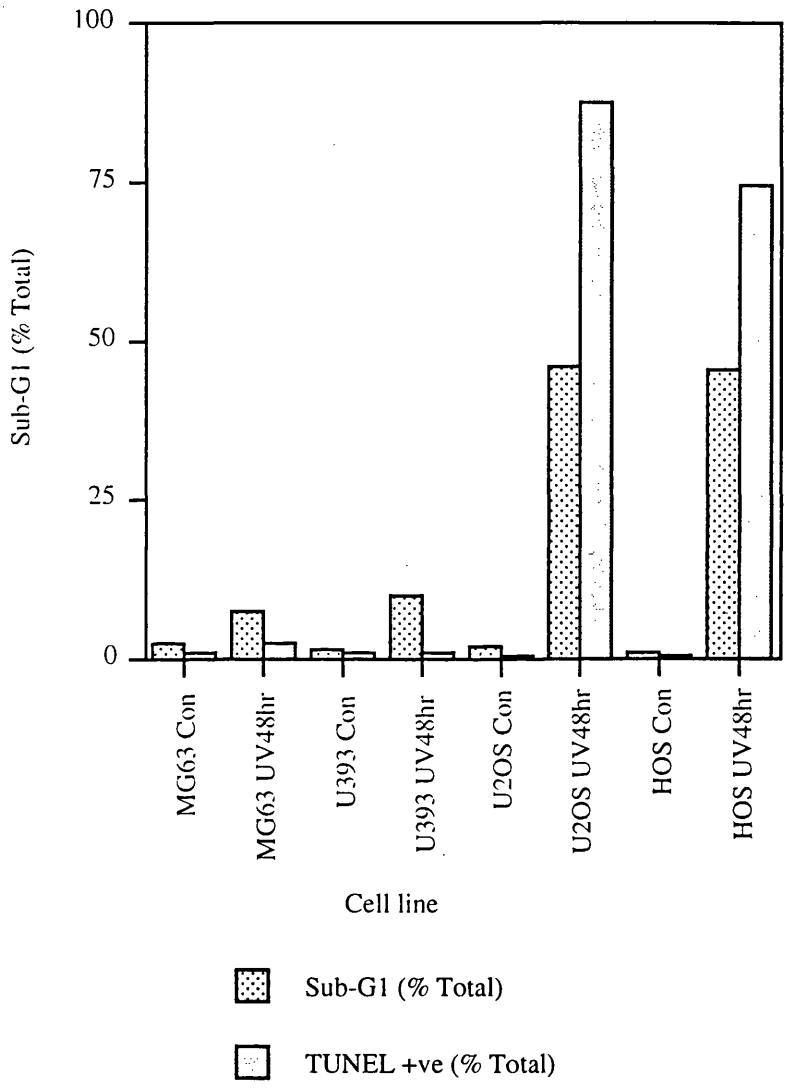
100
75
50
25
0
Sub-G1 (% Total)
MG63 Con
MG63 UV48hr
U393 Con
U393 UV48hr
U2OS Con
U2OS UV48hr
HOS Con
HOS UV48hr
Cell line
Sub-G1 (% Total)
TUNEL +ve (% Total)

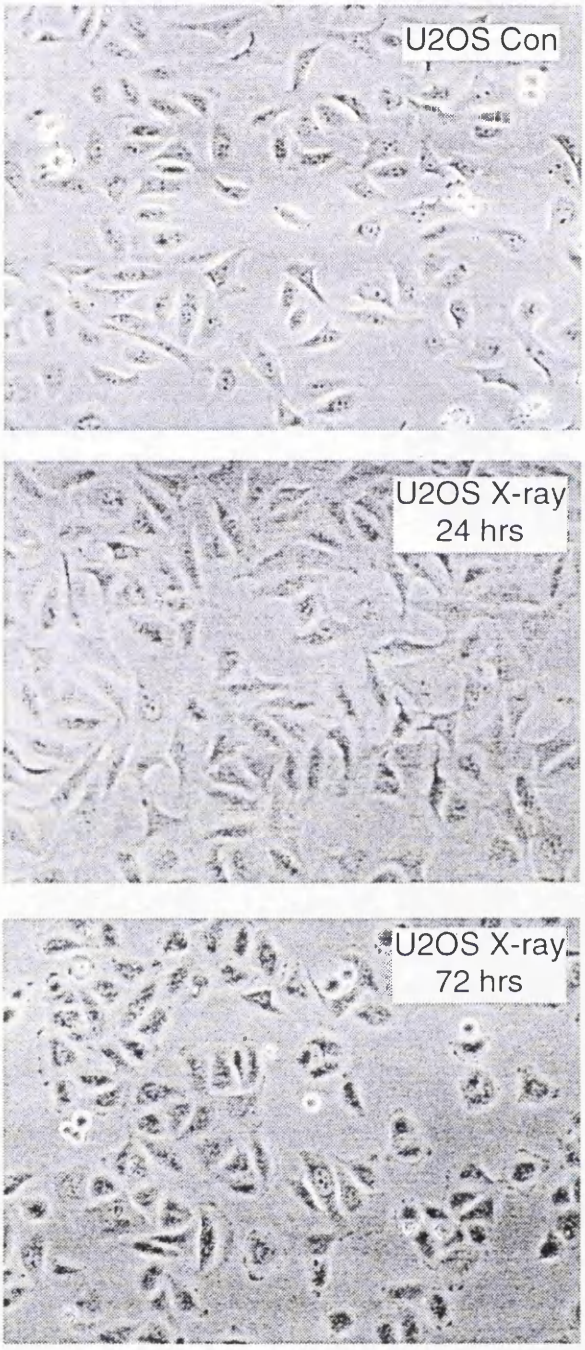

Figure 2.6. 12 Gy X-ray-irradiation induces a transient loss of cytokinesis in U2OS cells. U2OS cells were X-ray-irradiated and examined by time-lapse photography up to 72 hours post-irradiation.

I.

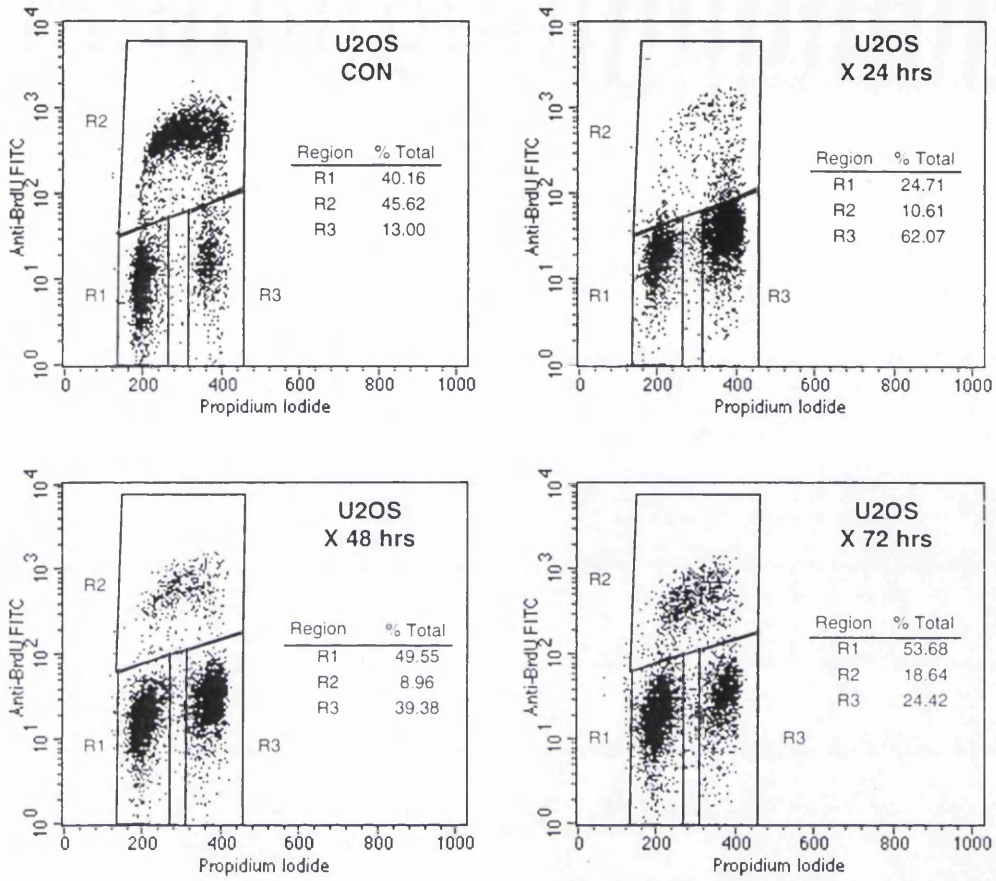

II.

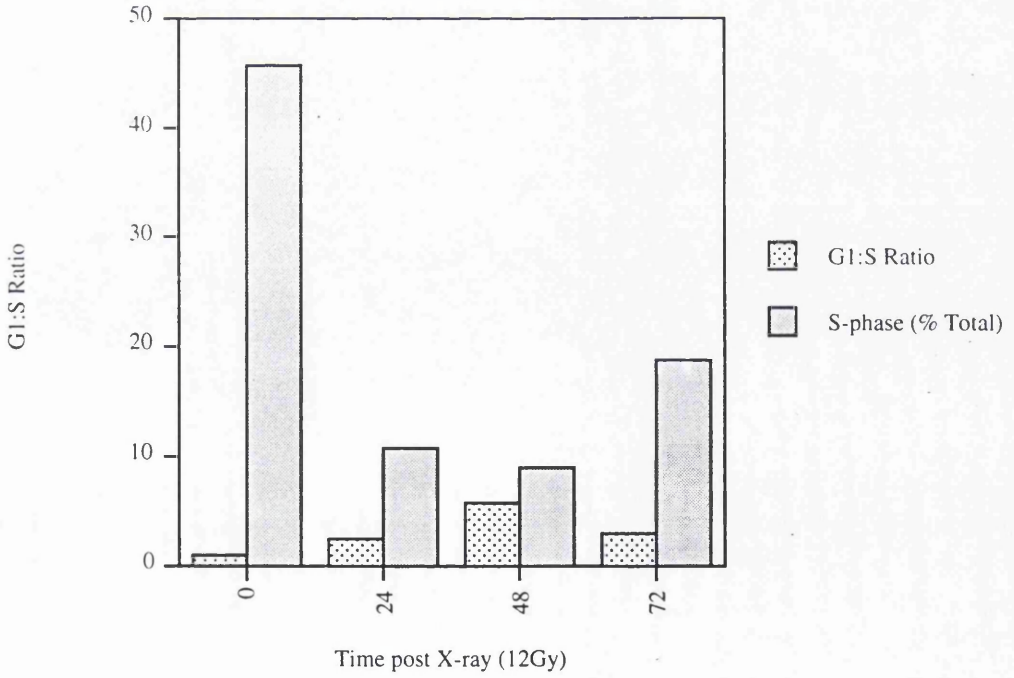

Figure 2.7. 12 Gy X-ray irradiation induces a loss of S-phase cells and a G1/S and G2/M arrest in U2OS cells. (I) U2OS cells were X-ray irradiated and analysed by BrdU analysis at various time points (as indicated) post-irradiation. (II) Graphical representation of (I) S-phase and G1:S ratios.

I.

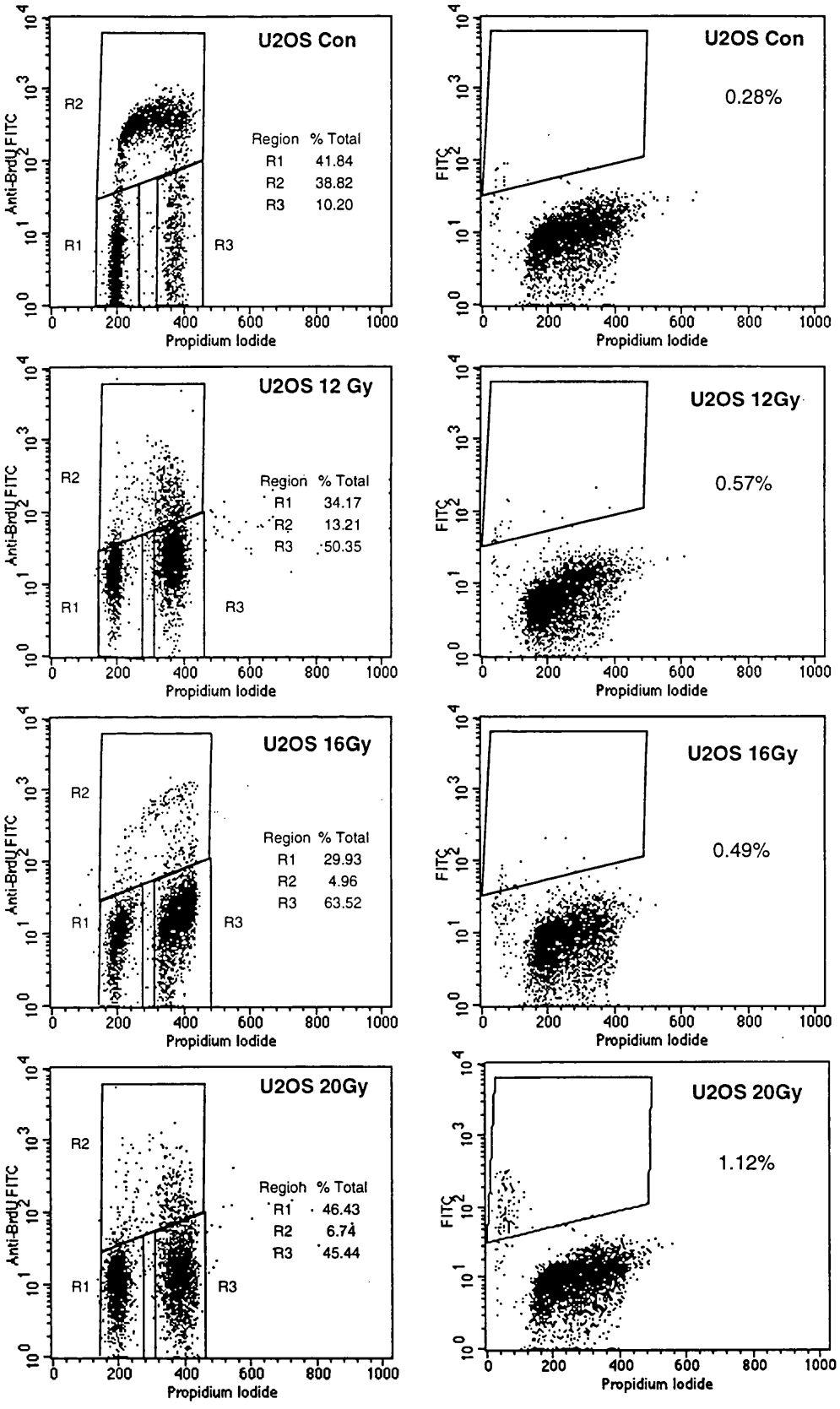

Figure 2.8. Increased X-ray-irradiation dose fails to significantly induce apoptosis in U2OS cells (two pages). (I) U2OS cells were X-ray-irradiated with varying doses (as indicated) and analysed by TUNEL and BrdU analysis 48 and 24 hours post-irradiation, respectively. (II) Graphical representation of (I) G1:S ratios.

II.

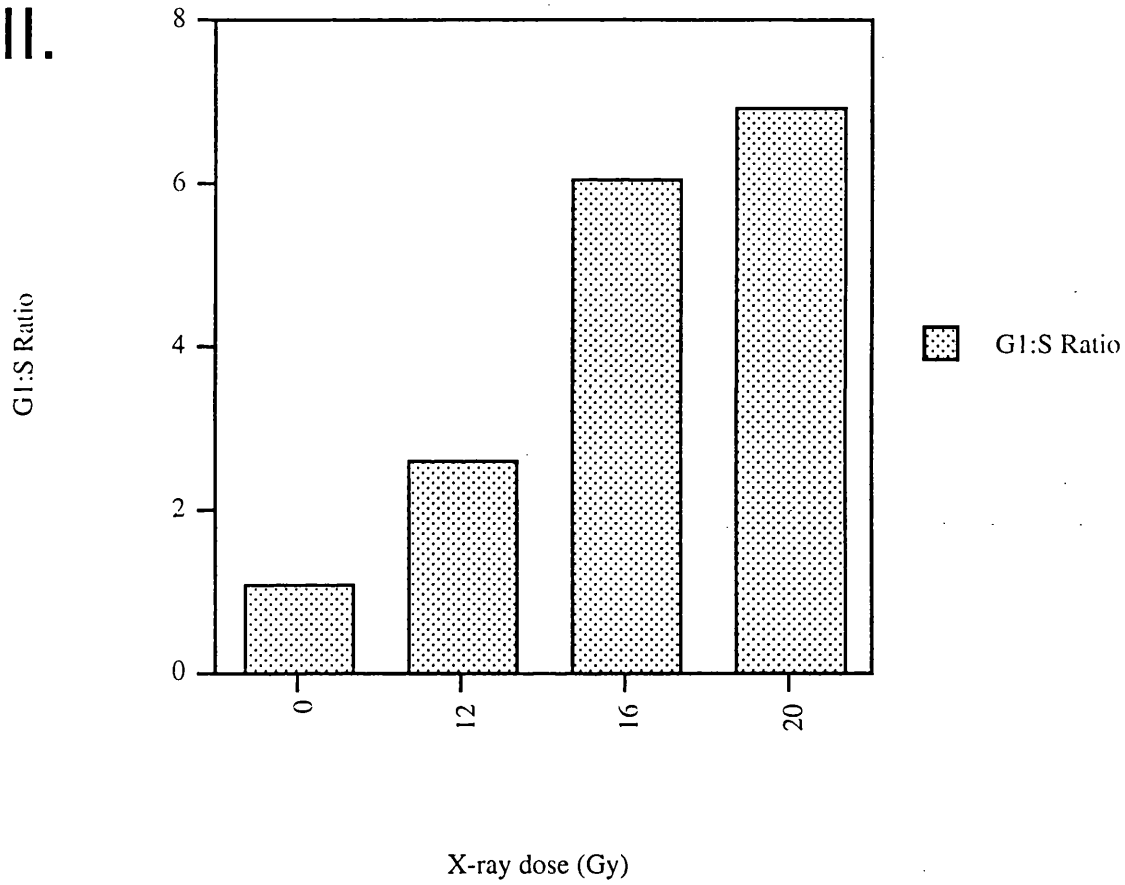

X-ray treatment is capable of inducing both cell cycle arrest and apoptosis in various cell lines

To analyse whether the 12Gy X-ray-irradiation was capable of inducing apoptosis, the different cell lines used for UV-irradiation studies were analysed for cell cycle arrest and sub-G_1. Cells were irradiated with 12 Gy X-rays and analysed by sub-G_1 and BrdU, 72 and 24 hours post-treatment, respectively. Sub-G_1 results revealed a differential response between cell lines, with HOS, MG63 and U393 cells exhibiting sub-G_1 apoptotic populations, while U2OS showed no significant increase in sub-G_1 content (see Figure 2.9). Clear visual apoptosis was evident in U393 and MG63 samples, two cell lines that behave diametrically to U2OS, undergoing apoptosis in response to X-ray, but not to UV. BrdU analysis of HOS (p53 $156^{R \Rightarrow P}$-expressing), MG63 (mutant p53) and U393 cells (unknown status) all exhibited cell cycle perturbations by 48 hrs post-irradiation, mainly generating increased G_2/M populations (see Figure 2.10). Later time points revealed loss of general cell cycle profile definition, however a clear loss of S-phase cells was evident. Mutant-p53 $156^{R \Rightarrow P}$ containing HOS cells at 16 hours post-irradiation showed a massive emptying of G_1 and concomitant accumulation of cells in G_2.

I.

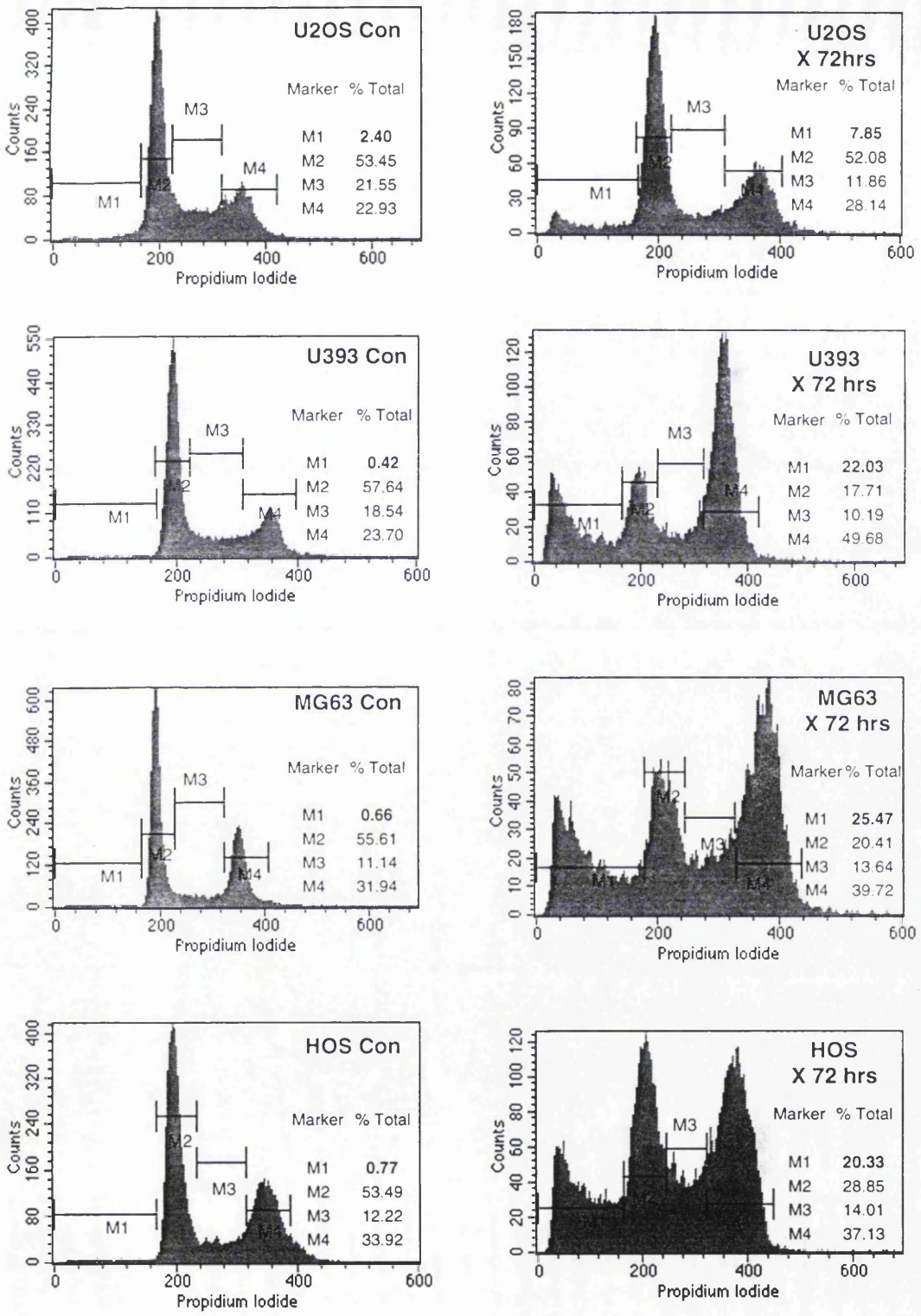

Figure 2.9. 12 Gy X-ray irradiation causes apoptosis in certain cell lines (two pages). (I) Four cell lines (HOS, MG-63, U2OS and HOS) were X-ray-irradiated and analysed by sub-G1 analysis 72 hours post-irradiation. Sub-G1 percentages are marked in bold. (II) Graphical representation of (I) sub-G1values.

II.

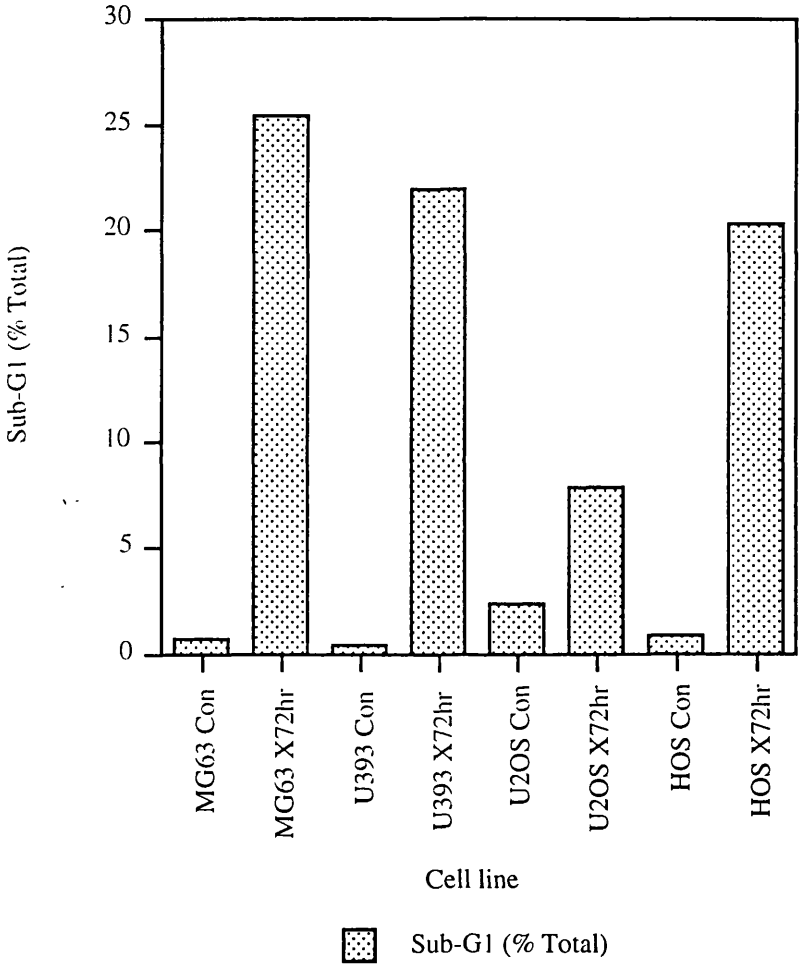
30
25
20
15
10
5
0
Sub-G1 (% Total)
MG63 Con
MG63 X72hr
U393 Con
U393 X72hr
U2OS Con
U2OS X72hr
HOS Con
HOS X72hr
Cell line
Sub-G1 (% Total)

I.

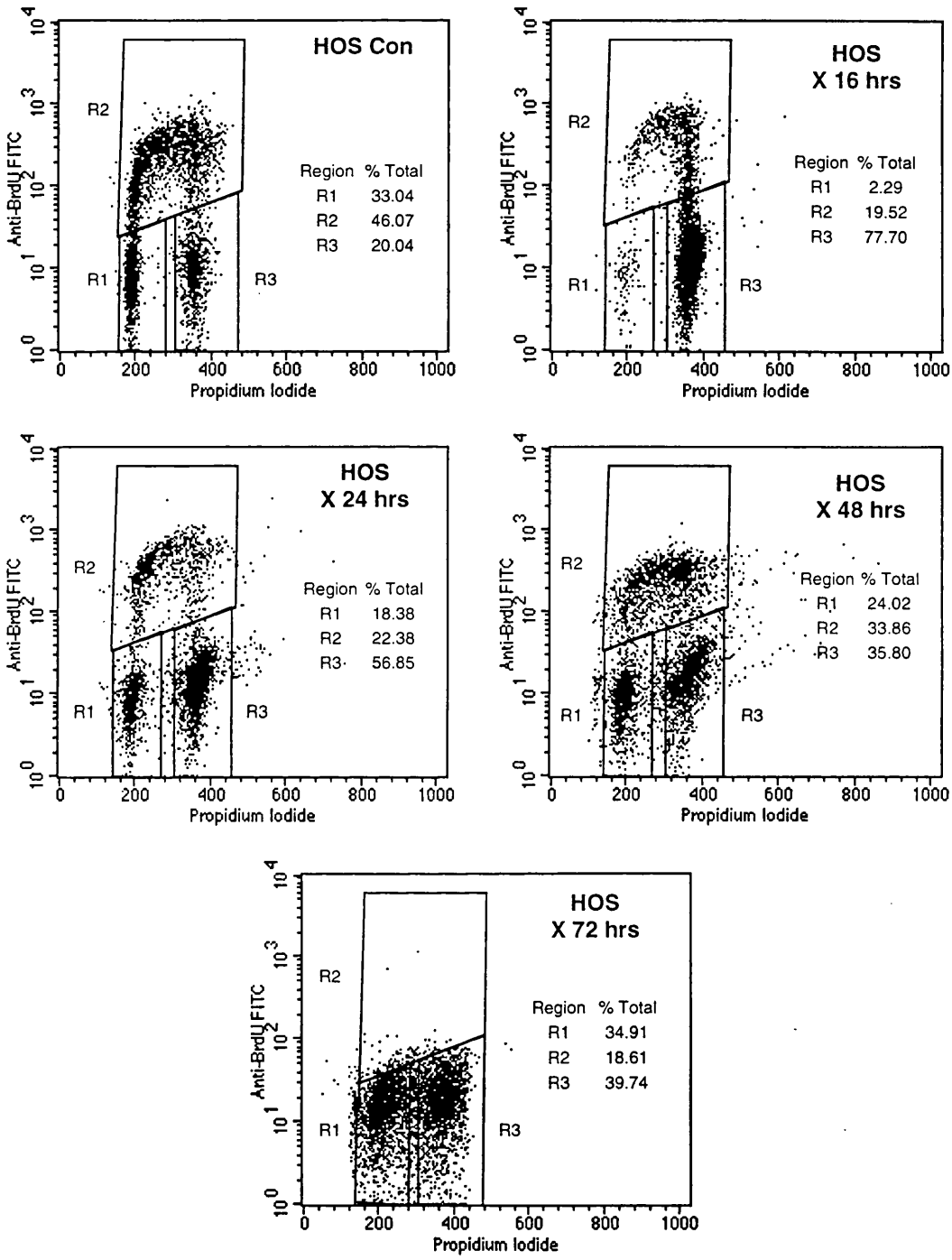

Figure 2.10. 12 Gy X-ray-irradiation causes cell cycle perturbations in a number of cell lines (three pages). (I) Four cell lines (HOS, MG-63, U2OS and HOS) were 12 Gy X-ray-irradiated and analysed by BrdU analysis at various time points (as indicated) post-irradiation. (II) Graphical representation of (I) S-phase values.

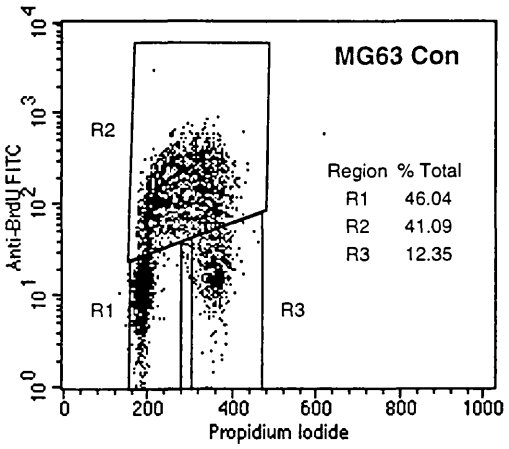
MG63 Con
R2
R1
R3
Region % Total
R1 46.04
R2 41.09
R3 12.35
Anti-BrdU FITC
Propidium Iodide

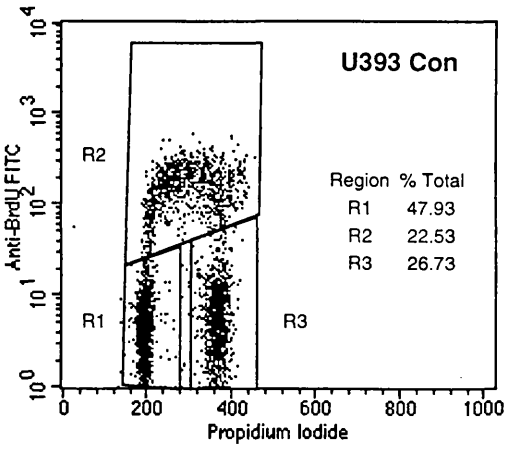
U393 Con
R2
R1
R3
Region % Total
R1 47.93
R2 22.53
R3 26.73
Anti-BrdU FITC
Propidium Iodide

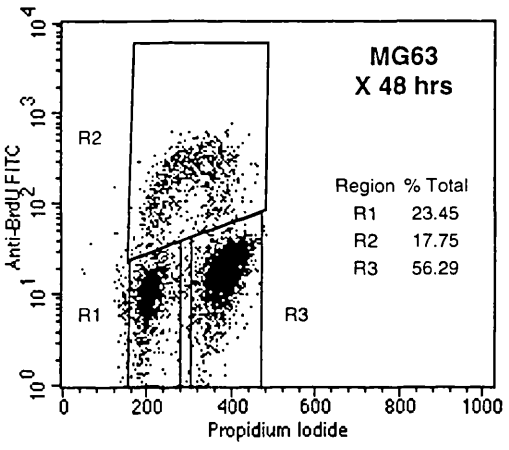
MG63
X 48 hrs
R2
R1
R3
Region % Total
R1 23.45
R2 17.75
R3 56.29
Anti-BrdU FITC
Propidium Iodide

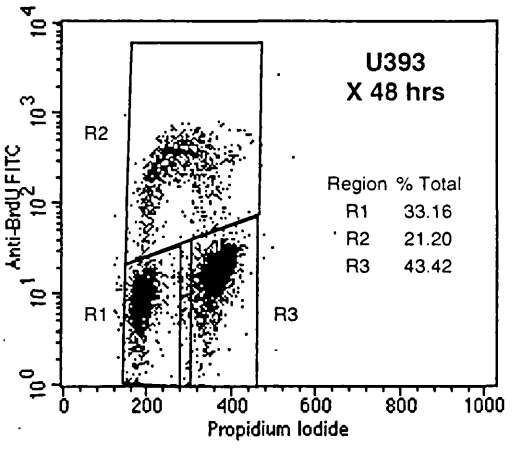
U393
X 48 hrs
R2
R1
R3
Region % Total
R1 33.16
R2 21.20
R3 43.42
Anti-BrdU FITC
Propidium Iodide

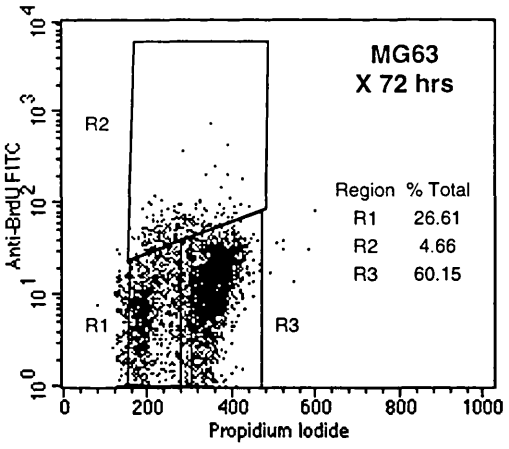
MG63
X 72 hrs
R2
R1
R3
Region % Total
R1 26.61
R2 4.66
R3 60.15
Anti-BrdU FITC
Propidium Iodide

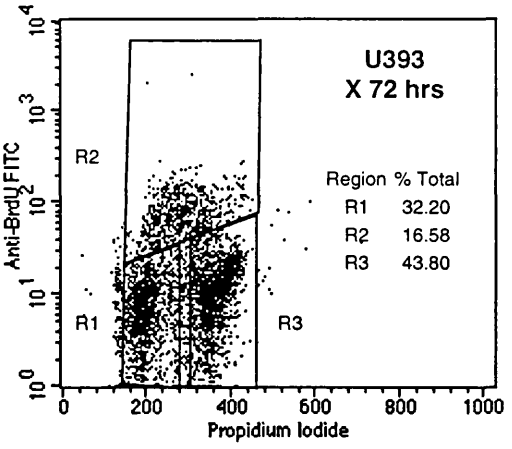
U393
X 72 hrs
R2
R1
R3
Region % Total
R1 32.20
R2 16.58
R3 43.80
Anti-BrdU FITC
Propidium Iodide

II.

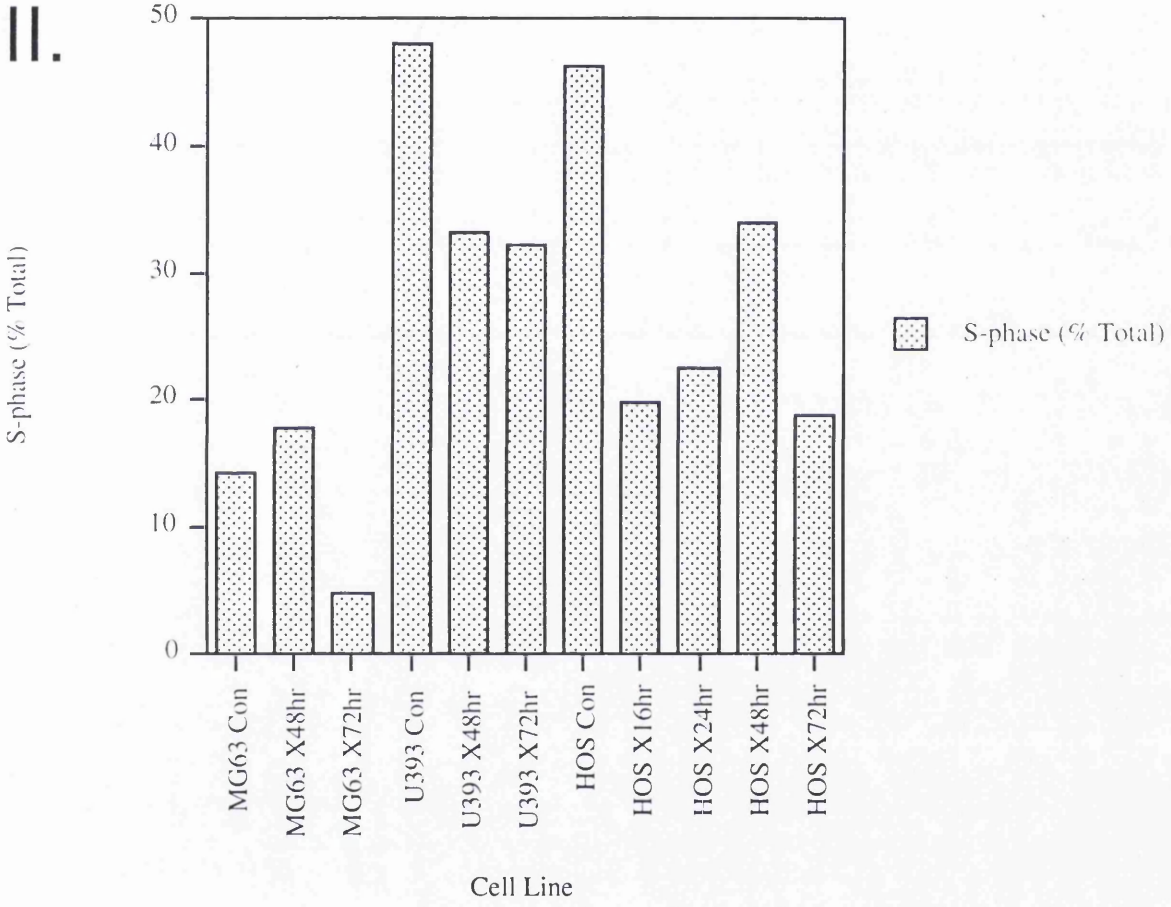
50
40
30
20
10
0
S-phase (% Total)
MG63 Con
MG63 X48hr
MG63 X72hr
U393 Con
U393 X48hr
U393 X72hr
HOS Con
HOS X16hr
HOS X24hr
HOS X48hr
HOS X72hr
Cell Line
S-phase (% Total)

The UV and X-ray responses in U2OS cells are p53-dependent

p53-dependent and –independent cell cycle arrest and apoptosis have been documented within and between cell lines (see Introduction). Therefore, it was of interest to determine whether the X-ray and UV responses in U2OS were p53-dependent or independent. To address this question U2OS cell lines were created using a p53 $175^{A\Rightarrow H}$ dominant negative point mutant, deficient in DNA binding and hence transcriptional activation or repression. Due to its dominant negative nature, hetero-oligomerisation between endogenous wild-type p53 and mutant p53 $175^{A\Rightarrow H}$ would lead to conversation of a wild-type to a mutant conformation(Milner and Medcalf 1991; Milner, Medcalf et al. 1991; Rolley, Butcher et al. 1995; Brachmann, Vidal et al. 1996). pCMV-driven expression of p53 $175^{A\Rightarrow H}$ should lead to unregulated high expression levels and negate wild-type p53 activity. Lindsey Allen had already established a number of clones in a batch of U2OS that were intrinsically more UV-sensitive than the batch examined in the initial UV experiments. Nevertheless, both UV and X-ray analysis revealed dramatic reductions in both apoptosis and cell cycle arrest, in comparison to parental U2OS. To ensure directly comparable data, p53 $175^{A\Rightarrow H}$ stable cell lines were created in the initial U2OS batch. A number of stable cell line were isolated, all of which exhibited extremely high levels of p53 by Western analysis (see Figure 2.11 [I]).

Upon UV analysis of a number of p53 $175^{A\Rightarrow H}$ clones 48 hours post-treatment, cells showed fewer detached or morphologically apoptotic cells, compared to parental U2OS. TUNEL analysis of DN(5) cells revealed virtually total negation of apoptosis (see Figure 2.11 [II]). However, apoptosis most probably was only delayed, as by 72 hours post-treatment cells had begun to round up and detach themselves from the plates.

12 Gy X-ray treatment of a number of DN clones also failed to elicit a G_1/S arrest 24 hours post-irradiation, although the G_2/M checkpoint was still apparent (see Figure 2.12). These findings are in accordance with many reports documenting the need for p53's transcriptional trans-activational ability to induce cell cycle arrest, with the existence of a p53-independent G_2/M arrest. Nevertheless, both sets of these results suggested that both UV- and X-ray-mediated apoptosis and cell cycle arrest, respectively, were significantly affected by p53 $175^{R\Rightarrow H}$ expression.

I.

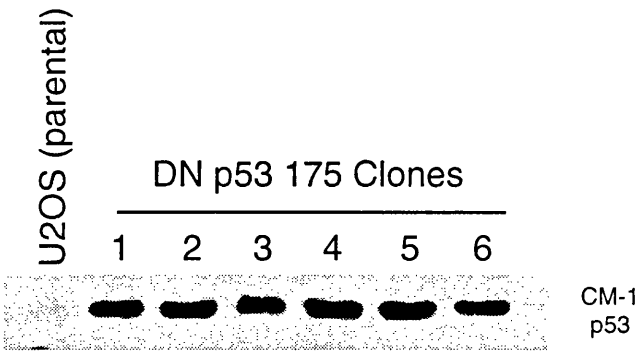

II.

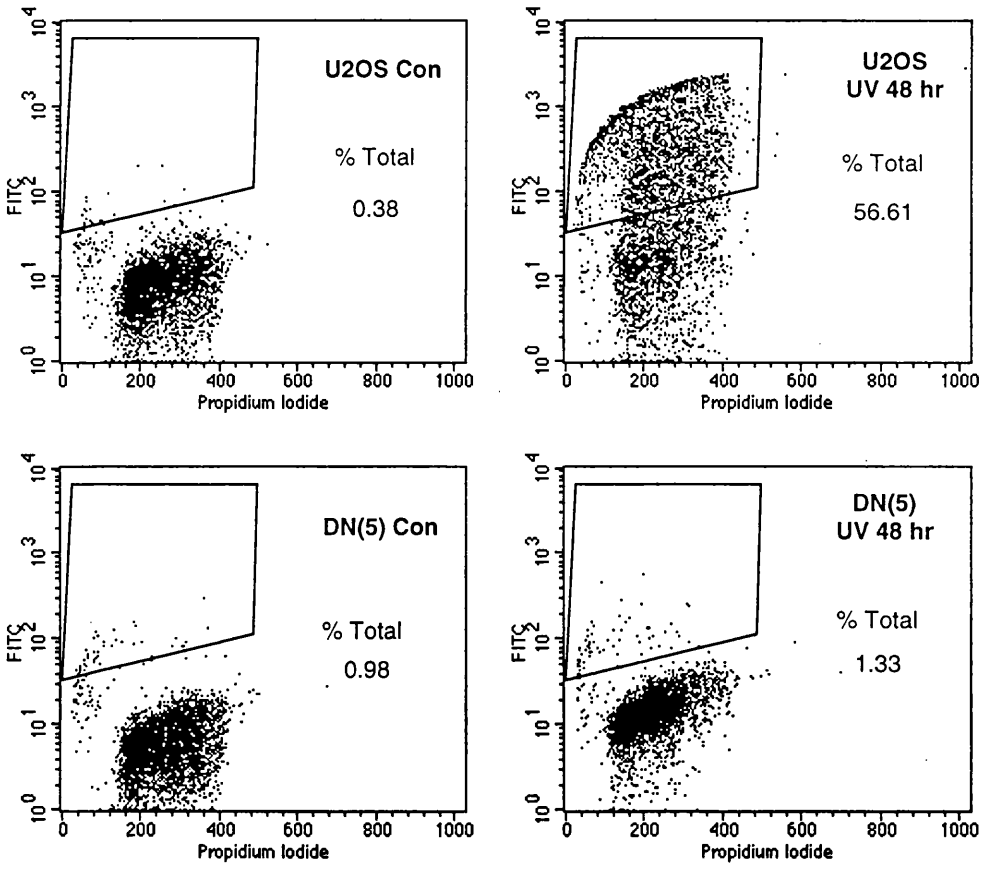

Figure 2.11. Expression of p53 175R⇒H inhibits UV-mediated apoptosis in U2OS cells. (I) Western analysis of p53 expression levels of various p53 175R⇒H expressing U2OS clones (DN clones 1-6) compared to parental U2OS p53 levels. (II) U2OS or DN(5) cells were UV-irradiated with 30 Jm-2 and analysed by TUNEL analysis 48 hours post-irradiation.

I.

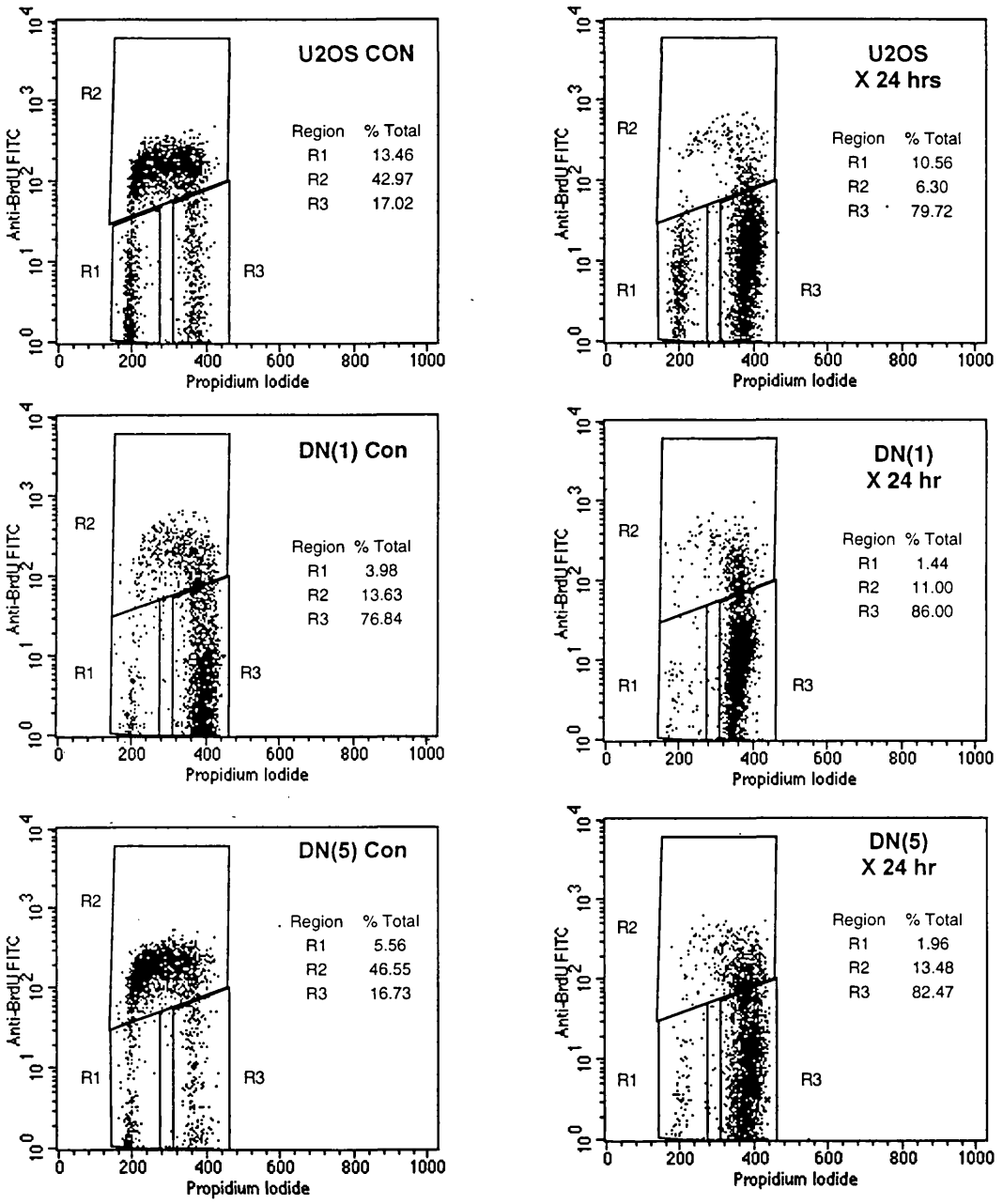

Figure 2.12. Expression of p53 175R⇒H inhibits X-ray-mediated G1/S arrest in U2OS cells (two pages). (I) U2OS or p53 175R⇒H expressing U2OS clones DN(5) and DN(1) were X-ray-irradiated with 12 Gy and analysed by BrdU analysis 24 hours post-irradiation. (II) Graphical representation of (I) G1:S ratios.

II.

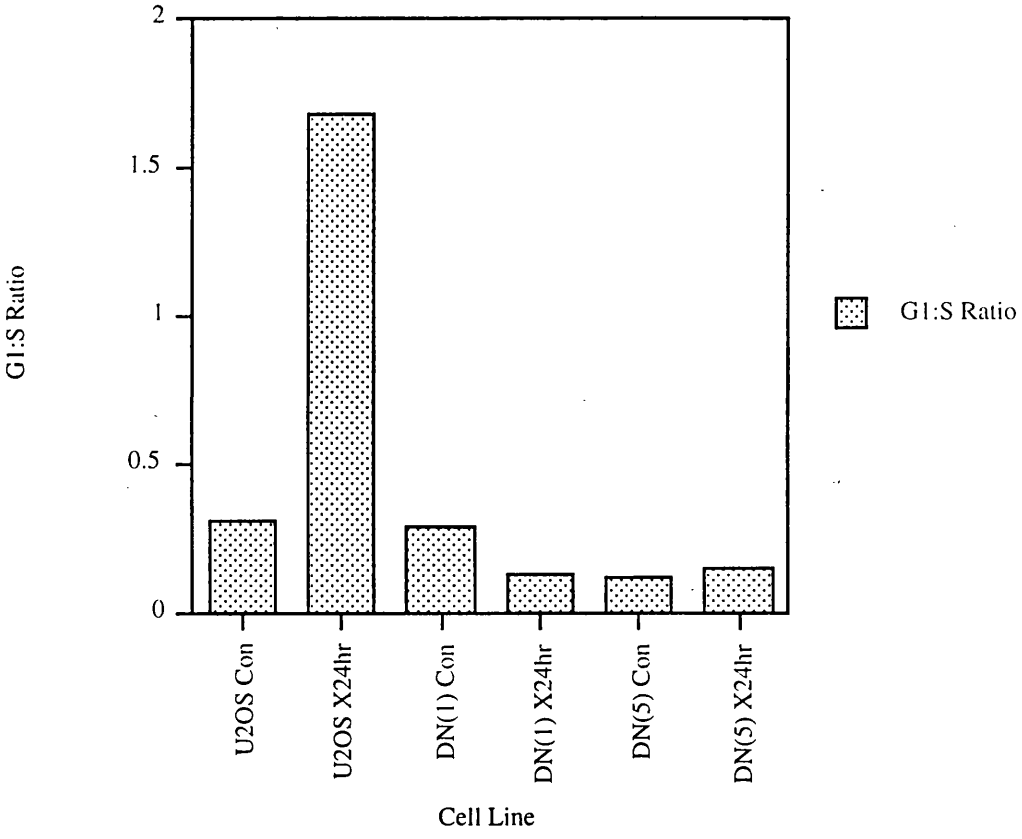
2
1.5
1
0.5
0
G1:S Ratio
U2OS Con
U2OS X24hr
DN(1) Con
DN(1) X24hr
DN(5) Con
DN(5) X24hr
Cell Line
G1:S Ratio

Summary and Discussion

A number of papers have reported either an apoptotic or cell cycle arrest in response to a number of different forms of cellular stress; many of which act through DNA damage (see Introduction). From the irradiation results U2OS cells were shown to be capable of undergoing both types of cell cycle perturbations in response to different forms of irradiation. Furthermore, both responses were shown to be partly p53-dependent. Rarely, has apoptosis and cell cycle arrest been reported in the same cell type. Interestingly both MG-63 and U393 cell lines exhibited opposing responses to U2OS cells in answer to the different forms, but identical doses of irradiation. U2OS cells demonstrated apoptosis in response to UV-, but not, X-ray-irradiation, while the opposite was observed for MG-63 and U393 cells. Furthermore, the p53-mutant cell line, HOS, exhibited apoptotic responses to both UV- and X-ray-irradiation. Therefore, different cell types can react differentially in response to the same dose and form of irradiation.

Cellular choice between apoptosis transient cell cycle arrest or senescence in response to a variety of different signals is important both in respect to individual cells and to the whole organism. Such decisions have strong implications in the prevention of cancer formation, as well as in development. With respect to detrimental irradiation damage such as UV and X-ray, cellular responses are thought to reflect the degree of damage sustained. Frank damage assessment determines apoptosis when cellular damage is beyond feasible repair, while cell cycle arrest allows a 'time out' in an attempt to redress cellular homeostasis. A temporal delay may allow DNA repair mechanisms to remove DNA lesions, preventing generation or perturbation of DNA mutations through DNA replication. Moreover, repair of transcriptionally transcribed damaged DNA also prevents transcriptional stalling and inhibition of gene expression (reviewed(Tornaletti and Pfeifer 1996)). Other stress mechanisms may also repair or remove stress-generated molecules detrimental to the cell, such as oxygen free radicals.

Using the model mentioned above, these results suggest that 30 Jm^{-2} UV-irradiation causes more cellular damage than 12 Gy X-ray irradiation, generating apoptosis instead of cell cycle arrest. In terms of energy exposure, X-ray irradiation delivers more Joules/cell than UV

irradiation, although absorption co-efficients affect the ratio of applied energy to absorbed energy. Direct comparison between the two forms of irradiation in terms of energy delivered is not possible due to differences in their physical nature and modes of cellular damage. X-rays represent ionizing radiation (radiation of sufficient energy to cause ionisation of the medium through which it passes), while UV represents non-ionising radiation. However, UV-irradiation does has the ability to form highly-reactive, free radicals (uncharged atoms or group of atoms with one or more unpaired electrons) (reviewed(Tornaletti and Pfeifer 1996)). UV-irradiation has been well documented to cause disruption of the cellular membranes, releasing ceramide leading to activation of the JNK pathway (reviewed(Fanger, Gerwins et al. 1997; Ip and Davis 1998) and see Introduction). Other macromolecules, other than DNA, including proteins, lipids and RNA may also have the potential to be affected either directly or indirectly by irradiation. Therefore, with such a wide array of potential targets, irradiation can potentially affect the majority of cellular processes. Hence, any observations may not merely reflect DNA damage responses, although DNA is arguably the most important (and examined) individual cellular component to be affected.

To examine the "DNA-damage level' theory, it would be of interest to examine radiomimetic DNA-damaging chemicals that specifically damage DNA without effecting other cellular elements and determine whether different dose levels resulted in different cellular responses. Examination of other stress stimuli may also reveal a pattern linking not dose, but physical form of cellular insult to cellular outcome. The presence of individual 'stress-sensor' proteins to each type of cellular stress seems unlikely due to the huge array of cellular stress signals. Therefore, an internal damage assessment system seems more plausible, although a significant number of damage-assessment proteins must exist to evaluate the wide scope of cellular-damage induced. Potentially co-existing systems could actively either detect certain types of stress-stimuli, pre-damage or passively register the consequences of cellular stress.

An additional point to be added to the 'DNA-damage level' theory, concerns the rate of damage infliction. Conflicting results between irradiation doses may occur due to differences not in the absolute dose level, but in the intensity and duration of the dose. A short, but high dose may cause massive amounts of damage, swamping any cellular defence systems

triggering apoptosis. In contrast a long, but lower dose may be repairable and hence tolerated leading to a transient cell cycle arrest.

Analysis of a number of different cell lines revealed that the choice between apoptosis and cell cycle arrest in not purely determined by type or dose of irradiation. Irradiation-mediated cell cycle arrest and apoptosis were apparently mutually exclusive in U2OS cells. Of particular interest were the opposing cellular responses seen between U2OS and both MG-63 and U393 cell lines; UV-irradiation mediating apoptosis in U2OS, while X-ray irradiation mediated apoptosis in MG-63 and U393 cells. Mutant p53-containing HOS cells exhibited an apoptotic response to both forms of irradiation, suggesting that X-ray- and UV-mediated apoptosis are not mutually exclusive or p53-dependent within a certain cell type. However, partial retention of wild-type apoptotic function(s) in the mutant p53-expressing HOS and MG63 cell lines could not be ruled out.

All of the cell lines analysed were of sarcoma-derived lineage and shared similar morphology. However, U2OS did exhibit the most epithelial-like features in comparison to the more fibroblast-like appearance of the other cell lines. Gross differences in cellular structure and content were unlikely to dramatically affect irradiation-absorption co-efficients and therefore explain the differences in cellular outcome. The determinant(s) of the choice presumably lie in the molecular profiles of the individual cell types, perhaps affecting their sensitivities and/or modulating the irradiation-induced signals. The significance may reflect the importance of the cell type with respect to mutation prevention and stage of differentiation. For example, rapidly dividing progenitor stem cells in comparison to quiescent, fully differentiated cells, may be less tolerant toward stress stimuli due to their progenitor role. Although all of the cell lines were sarcoma-derived and significantly morphologically undifferentiated, they may have represented alternative states of differentiation.

Although X-ray irradiation clearly did not induce apoptosis in U2OS cells, BrdU analysis of UV-irradiated U2OS cells revealed an alteration in BrdU incorporation, possibly reflecting a partial G_1/S arrest or inhibition of DNA synthesis. Upon lower UV doses no such perturbations were apparent, although apoptosis still occurred, albeit to a lesser degree. Sub-G_1 analysis of apoptotic cells revealed a 'slide' effect in DNA content, with G_2 cells

decreasing with a concurrent increase in sub-G_2 content DNA, suggesting that apoptosis can be initiated in G_2/M content cells. This 'slide' in DNA content can be explained through the DNA fragmentation and degradation events of apoptosis, leading to decreased cellular DNA content. Furthermore, TUNEL analysis revealed TUNEL-positive cells throughout all phases of the cell cycle (as determined by DNA content). Overall this evidence suggests that U2OS cells, regardless of cell cycle stage and DNA content, are capable of undergoing apoptosis.

Analysis of a number of dominant-negative p53 $175^{A\Rightarrow H}$ U2OS clones revealed the important role of p53 in both X-ray- and UV-mediated cell cycle and apoptosis, respectively. Absolute dependency on p53 in both processes did differ with the X-ray mediated G1/S block being completely abrogated, while apoptosis was only delayed. Although, with the maintenance of the X-ray mediated G_2/M block, p53's role in cell cycle arrest as a whole, is not omnipotent. Nevertheless, the importance of the G_1/S block is reflected in its ability to prevent DNA-replication errors and mutation generation. In contrast, the G_2/M block can not prevent mutation generation, but can influence mutation perseverance by blocking mitosis and subsequent cell division. Together the two check points provide an effective method of mutation-prevention and -endurance.

With regard to the p53 $175^{A\Rightarrow H}$-mediated delayed apoptosis, an alternative explanation could lie in increased wild-type:mutant ratio. Increased UV-mediated induction of endogenous p53 could have lead to increased functional wild-type homotetramer formation through squelching out mutant p53 $175^{A\Rightarrow H}$. Such an increase could effectively overcome mutant-p53-mediated inhibition, ultimately leading to p53-dependent apoptosis. Also, partial retention of wild-type function of the p53 $175^{A\Rightarrow H}$ mutant, could also explain the reduced kinetics of the apoptotic event.

Maintenance of the G_2/M block seen in the X-ray irradiated p53 $175^{A\Rightarrow H}$ clones, can be explained through either through activation by non-p53-dependent activation, or as with the apoptotic bypass, through partial retention of wild-type function or squelching out of the p53 $175^{A\Rightarrow H}$ mutant.

Overall a delayed apoptotic or partial cell cycle arrest response in DN(5) cells can be explained either via incomplete inhibition of wild-type p53 or a slower p53-independent apoptotic mechanism. The need for p53-dependent transcription in apoptosis remains a moot point (see Introduction). An emerging numbers of p53-interacting proteins (see Table 1.3) reveals the importance of protein-protein interactions in the p53 network. p53's $175^{A \Rightarrow H}$ mutant conformation also may have affected wild-type p53's protein-protein interaction profile, hence explaining its dominant negative p53 effect. However, redundancy in both cellular responses is not only prudent, but also expected due to the emerging p53 protein family members that have also been shown to exhibit tumour suppresser-like properties (see Introduction). p53-family-independent cell cycle arrest and apoptosis are also possible explanations.

FACS Analysis of the effect of MDM2 overexpression on the UV and X-ray responses of U2OS cells

With the discovery of partial p53-dependent apoptotic and cell cycle arrest occurring in U2OS cells, we were interested in examining the effect of MDM2 overexpression on the outcome of irradiation treatment. At the time this work was initiated the majority of work had looked at gene-amplified (endogenous or cosmid stables) murine MDM2 cell lines (see Introduction). It was suggested (K.Vousden, personal communication and later Brown *et al.*(Brown, Thomas et al. 1998)) that human MDM2 overexpression was detrimental to cell growth, although Chen *et al*(Chen, Oliner et al. 1994) had generated colorectal carcinoma-derived, RKO stables overexpressing human MDM2 cDNA.

Clinical evidence describing overexpression (at the mRNA and protein level) of MDM2 in sarcomas, especially osteosarcomas, prompted thoughts that these tumours may be special, with respect to toleration of MDM2 overexpression. The initial work of Oliner *et al*(Oliner, Pietenpol et al. 1993), demonstrated MDM2 : p53 physical interaction and the resulting inhibition of p53's transcriptional activity and hence the importance of MDM2 as a negative regulator of p53. This and subsequent work mainly concentrated on *in vitro* data, while *in vivo*, less was known. Establishing an MDM2 overexpressing U2OS cell line was

intended to facilitate isogenic analysis of different aspects of the MDM2:p53 relationship, as well as the consequences of altering that relationship.

Establishment of U2OS cells overexpressing MDM2 cell lines

U2OS cells were either transfected with full length human MDM2 (pCMV-MDM2) or a control vector-only plasmid (pcDNA3.1). Comparison of vector-only colonies (p3)[9] and pCMV-MDM2 colonies revealed approximately equal numbers, suggesting an absence of extensive detrimental growth effects or lethality. A number of colonies were picked and analysed by Western, revealing a range of elevated MDM2[10] expression levels in comparison to vector-only controls (see Figure 2.13), most probably reflecting the number and location of plasmid integration sites. p53 levels were also examined, revealing no significant differences in expression levels. This observation was unexpected due to the reported role of MDM2 as a mediator of p53's ubiquitin-dependent degradation (see Introduction).

MDM2 overexpression delays UV-induced apoptosis

A number of MDM2 and vector-only clones were UV-irradiated with 30 Jm^{-2} and subsequently analysed by sub-G_1. Correlation between MDM2 expression level and degree of apoptosis suppression was apparent, with vector-only clones showing apoptotic levels equivalent to parental U2OS (see Figure 2.14). Levels of MDM2-mediated inhibition were not as drastic as p53 $175^{A\Rightarrow H}$ levels, although M(5) approached it (see Figure 2.14 and compare with 2.11 [II]). M(5) cells expressing the highest MDM2 levels inhibited apoptosis the most, while M(1) cells showed the opposite. Therefore a rough correlation between MDM2 expression level and degree of apoptosis inhibition was observed (see Figure 14.2 [II]). As with the case of p53 $175^{A\Rightarrow H}$ clones, M(5) cells exhibited only delayed apoptosis, with significant sub-G_1 populations evident at 72 hours post-treatment (see Figure 2.15). Early

---

[9] Please note that parental U2OS and vector-only p3 cell lines were used interchangeably due to their near identical behaviour.

[10] Please note that endogenously- and exogenously-expressed MDM2 proteins in pCMV-MDM2 transfected cells could not be distinguished between, however it was assumed that the increased levels were due to exogenous MDM2 expression.

time points revealed that both M(5) and p3 cell lines showed no significant sub-G_1 populations 8 hours post-irradiation, while by 24 hours a small population had emerged.

MDM2 overexpression inhibits G_1/S cell cycle arrest

In light of the MDM2-mediated inhibitory effects on UV-mediated apoptosis, it was of interest to determine whether similar inhibition occurred with X-ray-mediated cell cycle arrest. Upon 12 Gy X-ray treatment the MDM2 stable clones exhibited different degrees of cell cycle arrest at the G_1/S checkpoint, although all the clones analysed displayed a strong G_2/M arrest (see Figure 2.16). Vector-only control clones exhibited parental behaviour. G_1:S ratios showed some degree of correlation between MDM2 expression levels and inhibition of the G_1/S arrest, with clone M(5) exhibiting the highest degree of inhibition. These results revealed that MDM2 partially abrogated the X-ray-mediated G_1/S, but not the potential p53-independent G_2/M arrest.

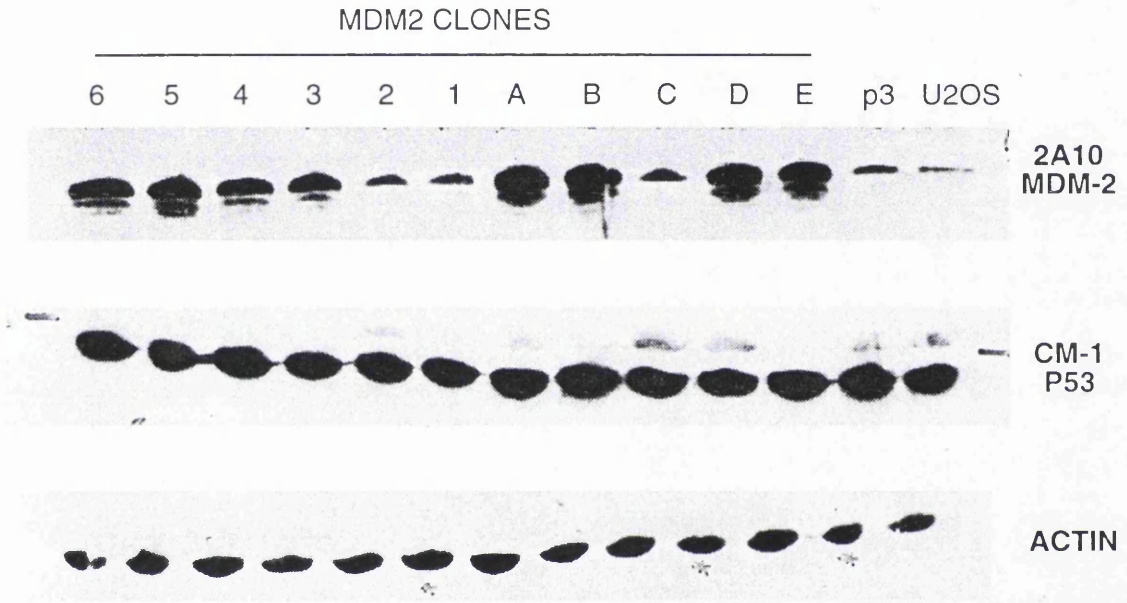

Figure 2.13. Establishment of MDM2 overexpressing U2OS cell lines reveals parental p53 protein levels. U2OS cells were transfected with pCMV-MDM2 and the resultant clones were compared to vector-only (p3) and parental U2OS cells by Western analysis for MDM2, p53 and actin levels (as indicated).

I.

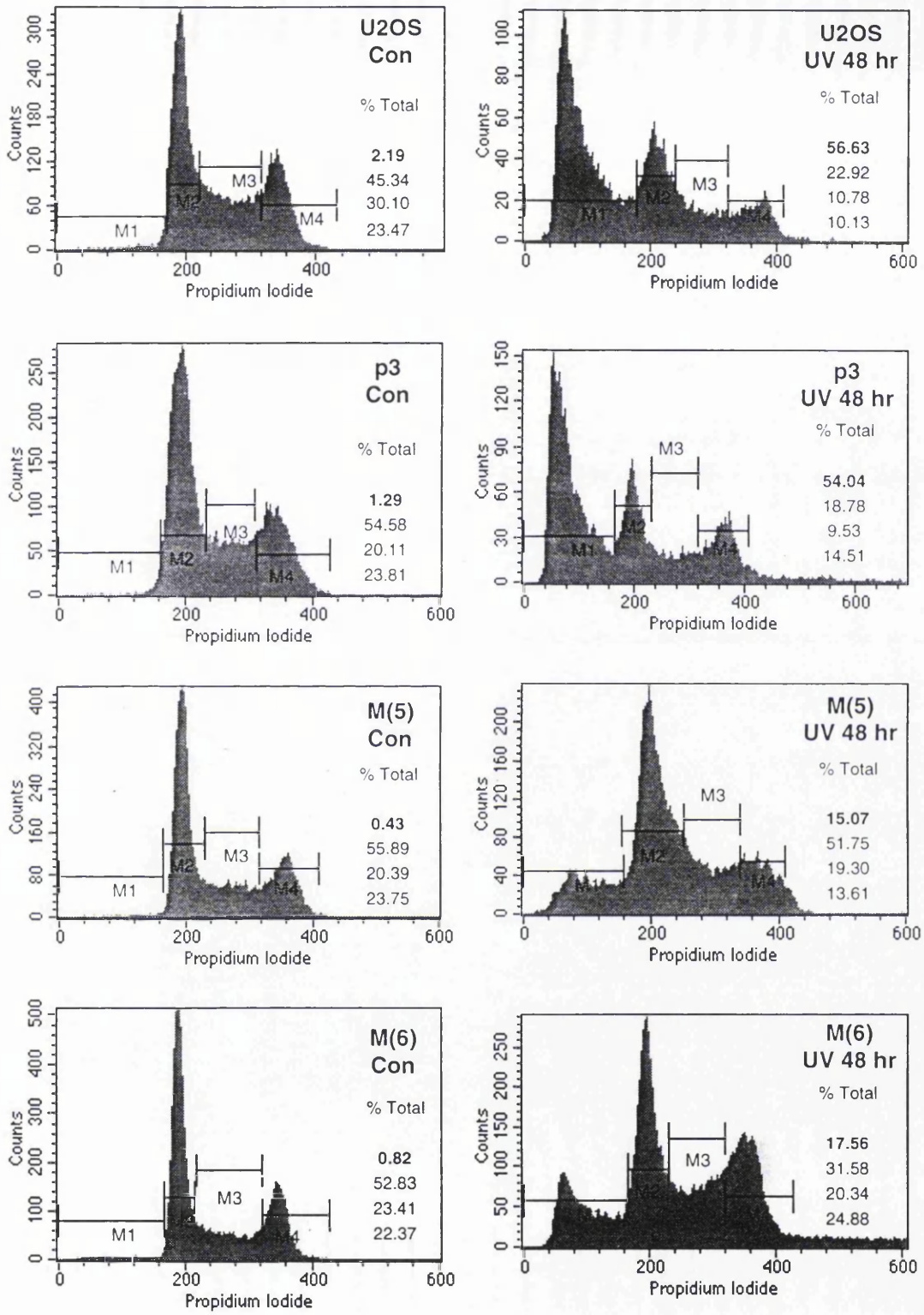

Figure 2.14. MDM2 overexpression inhibits UV-mediated apoptosis in U2OS cells (two pages). (I) U2OS, vector-only (p3) and various MDM2 overexpressing (M(X), as indicated) U2OS clones were UV-irradiated with 30 Jm-2 and analysed by sub-G1 analysis 48 hours post-irradiation. Sub-G1 percentages are marked in bold. (II) Graphical representation of (I) sub-G1 values.

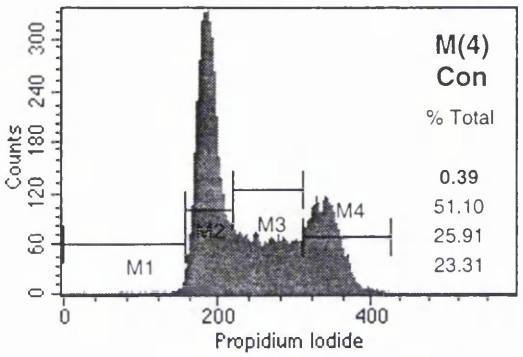
M(4)
Con
% Total
0.39
51.10
25.91
23.31
M1
M2
M3
M4
Counts
Propidium Iodide

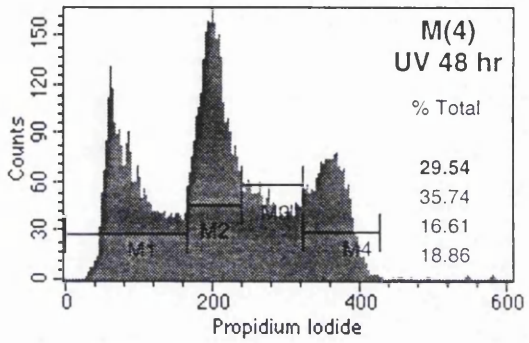
M(4)
UV 48 hr
% Total
29.54
35.74
16.61
18.86
M1
M2
M4
Counts
Propidium Iodide

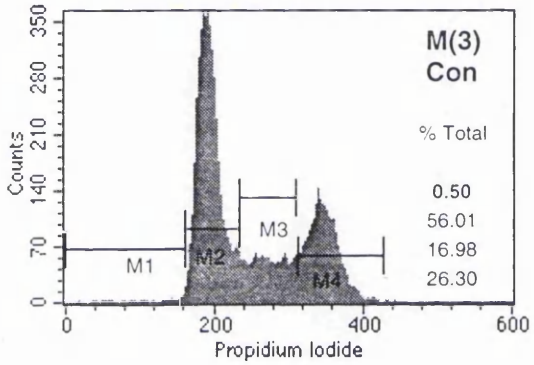
M(3)
Con
% Total
0.50
56.01
16.98
26.30
M1
M2
M3
M4
Counts
Propidium Iodide

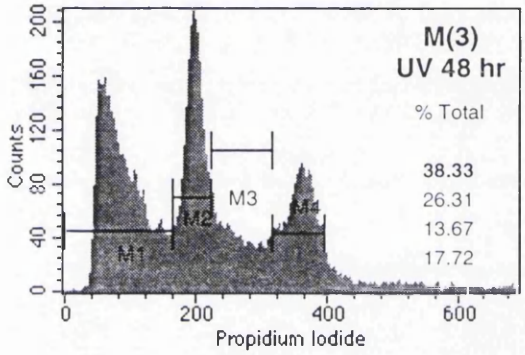
M(3)
UV 48 hr
% Total
38.33
26.31
13.67
17.72
M1
M2
M3
M4
Counts
Propidium Iodide

II.

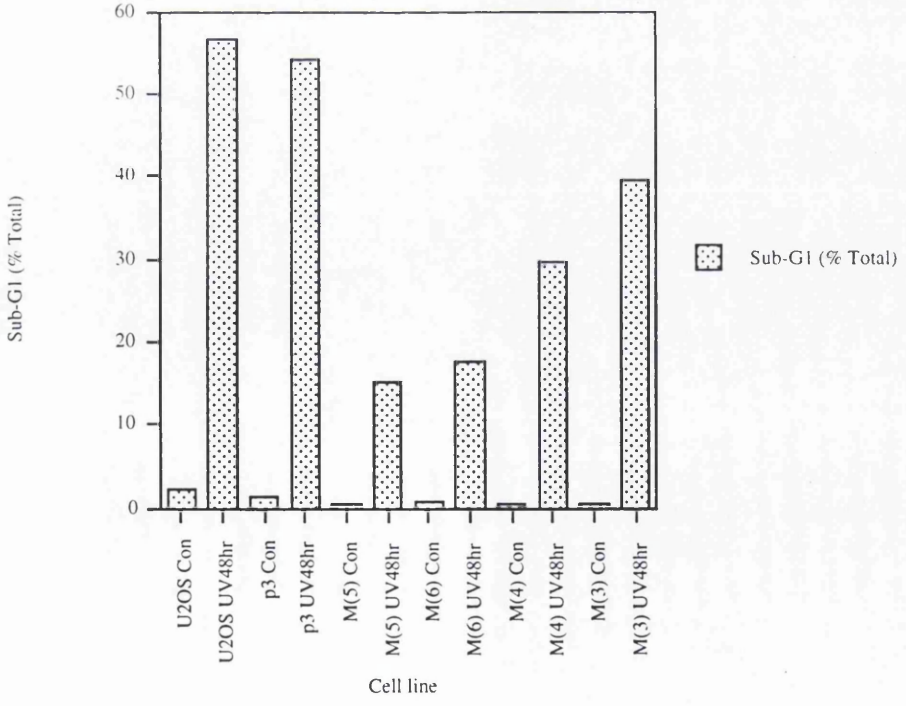
Sub-G1 (% Total)
Cell line
U2OS Con
U2OS UV48hr
p3 Con
p3 UV48hr
M(5) Con
M(5) UV48hr
M(6) Con
M(6) UV48hr
M(4) Con
M(4) UV48hr
M(3) Con
M(3) UV48hr
Sub-G1 (% Total)

I.

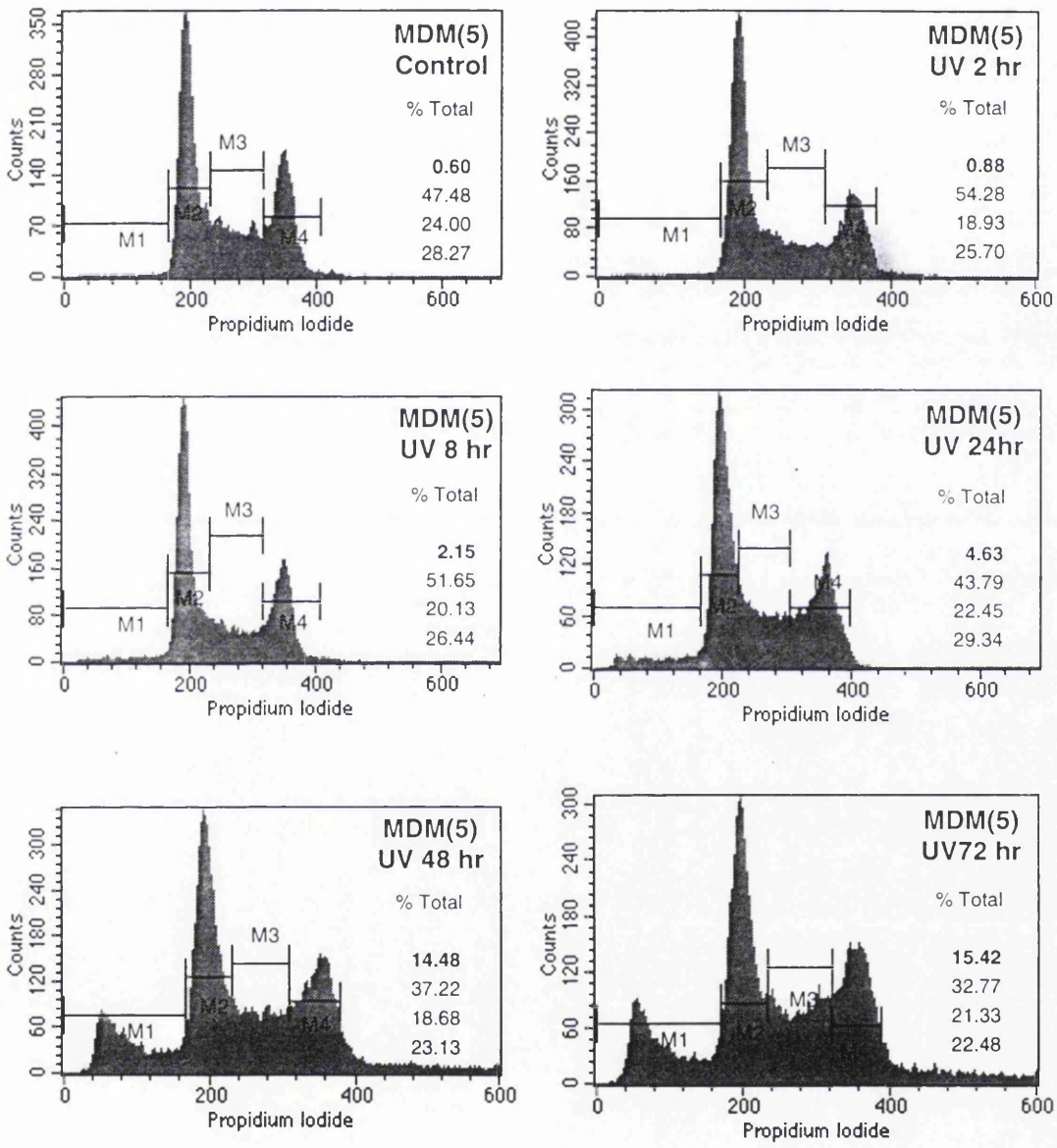

Figure 2.15. MDM2 overexpression delays UV-mediated apoptosis in U2OS cells (three pages). (I) Vector-only and MDM2-overexpressing M(5) U2OS clones were UV-irradiated with 30 Jm-2 and analysed by sub-G1 analysis at varying time points post-irradiation (as indicated). Sub-G1 percentages are marked in bold. (II) Graphical representation of (I) sub-G1 values.

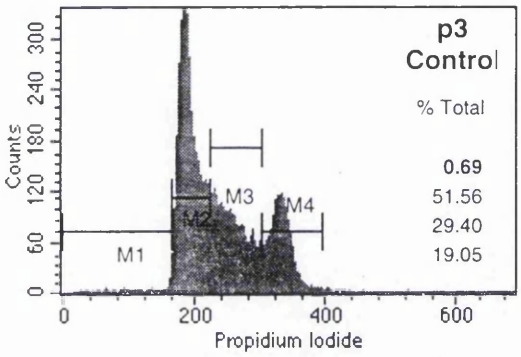
p3
Control
% Total
0.69
51.56
29.40
19.05
M1
M2
M3
M4
Counts
Propidium Iodide

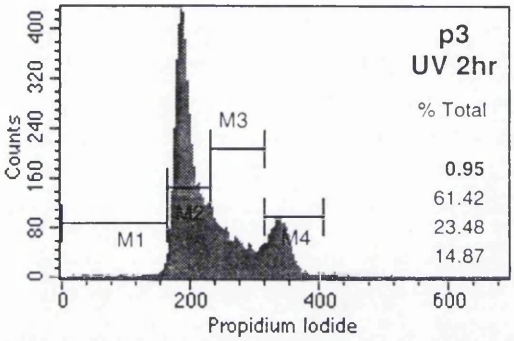
p3
UV 2hr
% Total
0.95
61.42
23.48
14.87
M1
M2
M3
M4
Counts
Propidium Iodide

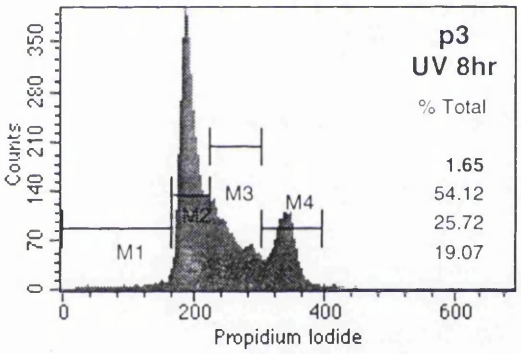
p3
UV 8hr
% Total
1.65
54.12
25.72
19.07
M1
M2
M3
M4
Counts
Propidium Iodide

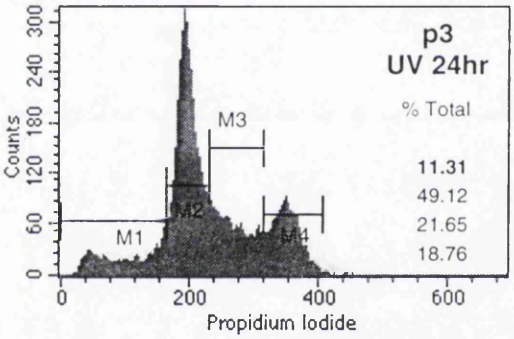
p3
UV 24hr
% Total
11.31
49.12
21.65
18.76
M1
M2
M3
M4
Counts
Propidium Iodide

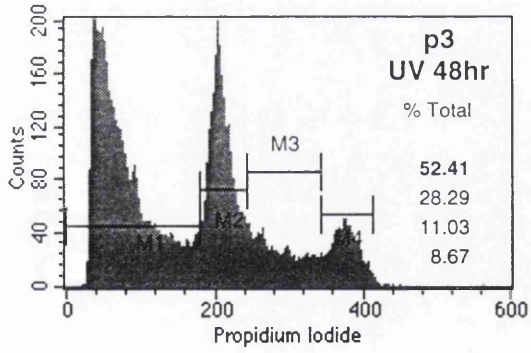
p3
UV 48hr
% Total
52.41
28.29
11.03
8.67
M1
M2
M3
M4
Counts
Propidium Iodide

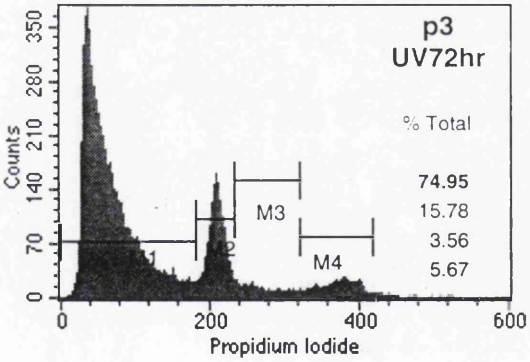
p3
UV72hr
% Total
74.95
15.78
3.56
5.67
M1
M2
M3
M4
Counts
Propidium Iodide

II

II.

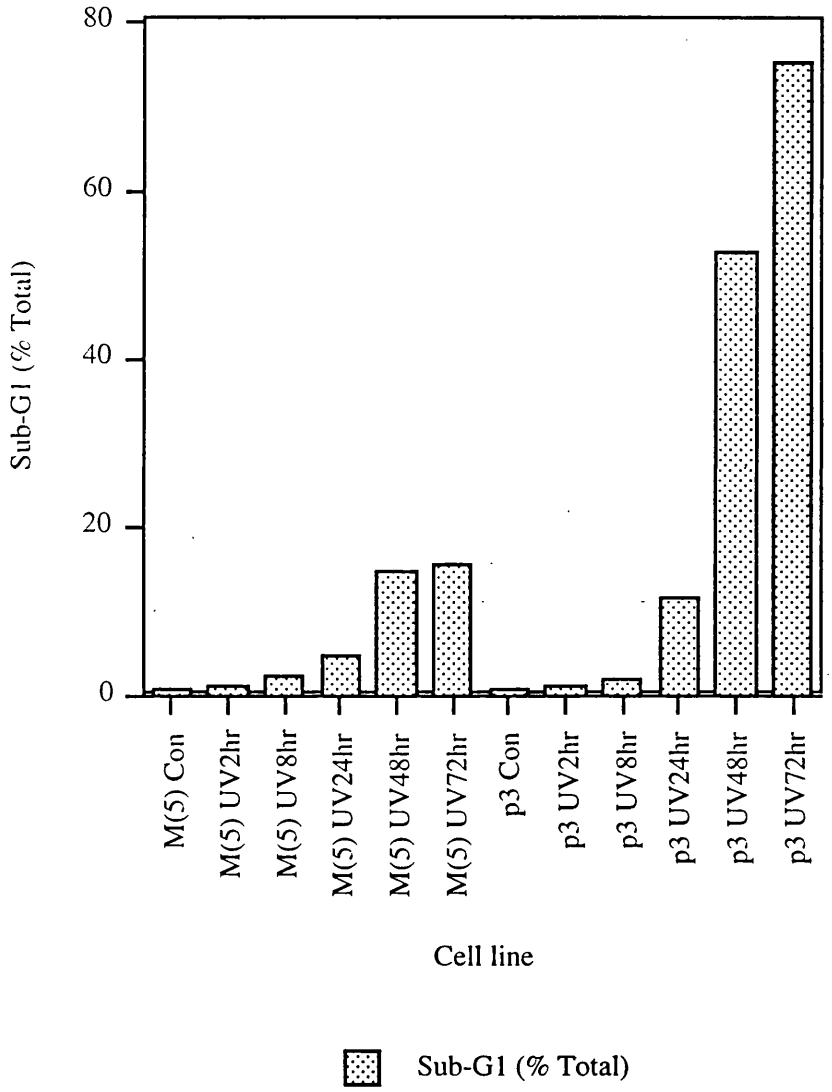
80
60
40
20
0
Sub-G1 (% Total)
M(5) Con
M(5) UV2hr
M(5) UV8hr
M(5) UV24hr
M(5) UV48hr
M(5) UV72hr
p3 Con
p3 UV2hr
p3 UV8hr
p3 UV24hr
p3 UV48hr
p3 UV72hr
Cell line
Sub-G1 (% Total)

I.

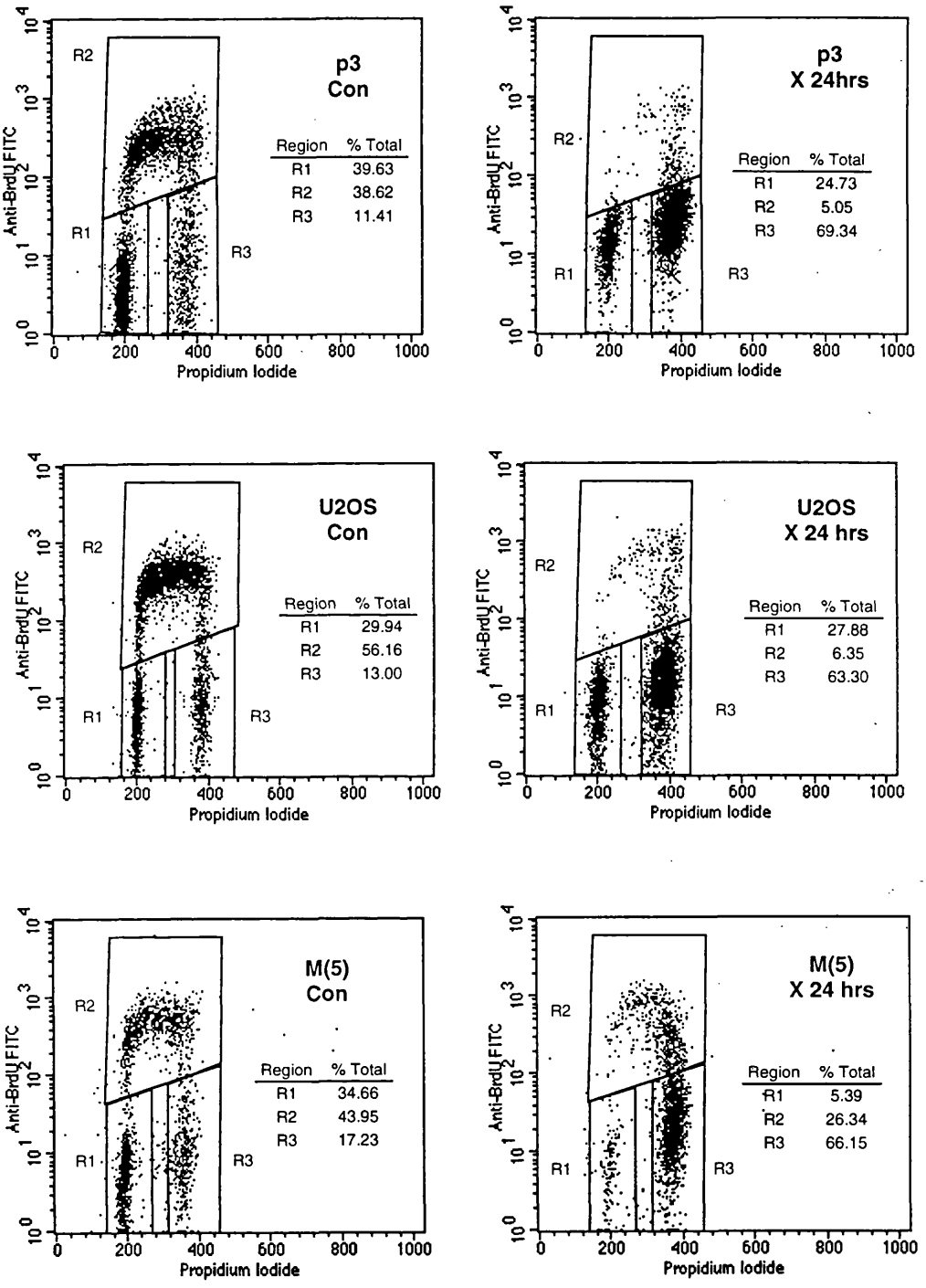

Figure 2.16. MDM2 overexpression inhibits the X-ray-mediated G1/S arrest in U2OS cells (three pages). (I) Parental, vector-only (p3) and MDM2-overexpressing (M(X), as indicated) clones were X-ray-irradiated with 12 Gy and analysed by BrdU analysis 24 hours post-irradiation. (II) Graphical representation of (I) G1:S ratios.

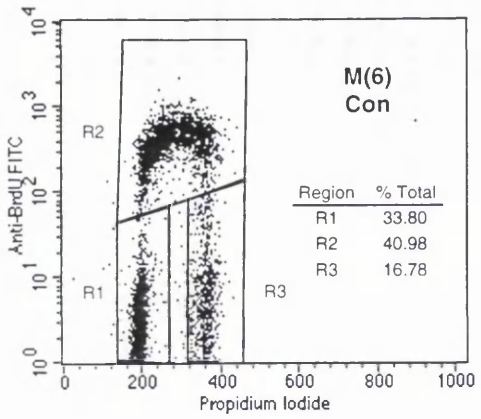
M(6)
Con
Region % Total
R1 33.80
R2 40.98
R3 16.78
R1
R2
R3
Anti-BrdU FITC
Propidium Iodide

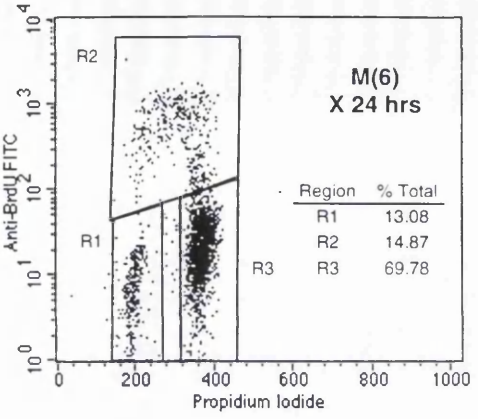
M(6)
X 24 hrs
Region % Total
R1 13.08
R2 14.87
R3 69.78
R1
R2
R3
Anti-BrdU FITC
Propidium Iodide

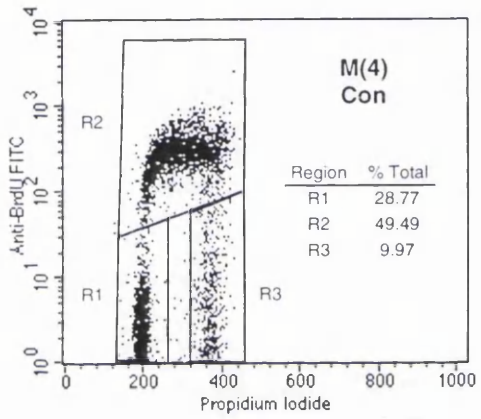
M(4)
Con
Region % Total
R1 28.77
R2 49.49
R3 9.97
R1
R2
R3
Anti-BrdU FITC
Propidium Iodide

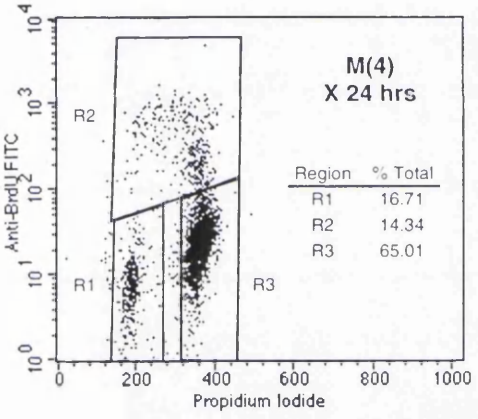
M(4)
X 24 hrs
Region % Total
R1 16.71
R2 14.34
R3 65.01
R1
R2
R3
Anti-BrdU FITC
Propidium Iodide

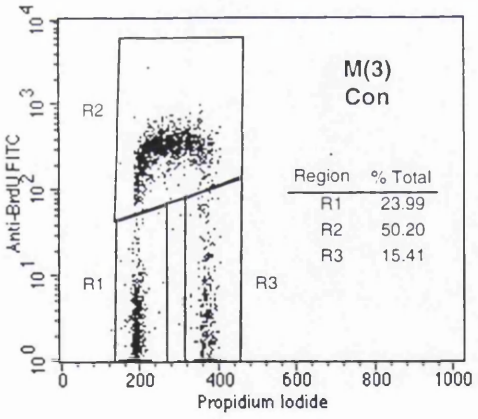
M(3)
Con
Region % Total
R1 23.99
R2 50.20
R3 15.41
R1
R2
R3
Anti-BrdU FITC
Propidium Iodide

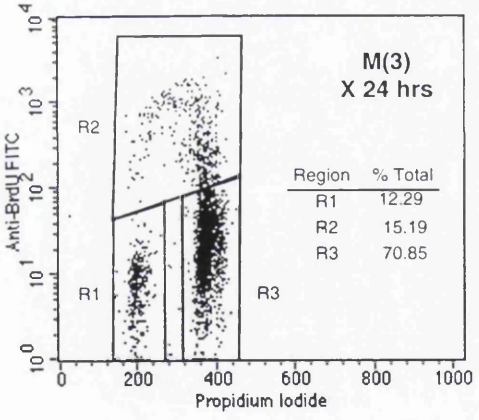
M(3)
X 24 hrs
Region % Total
R1 12.29
R2 15.19
R3 70.85
R1
R2
R3
Anti-BrdU FITC
Propidium Iodide

II.

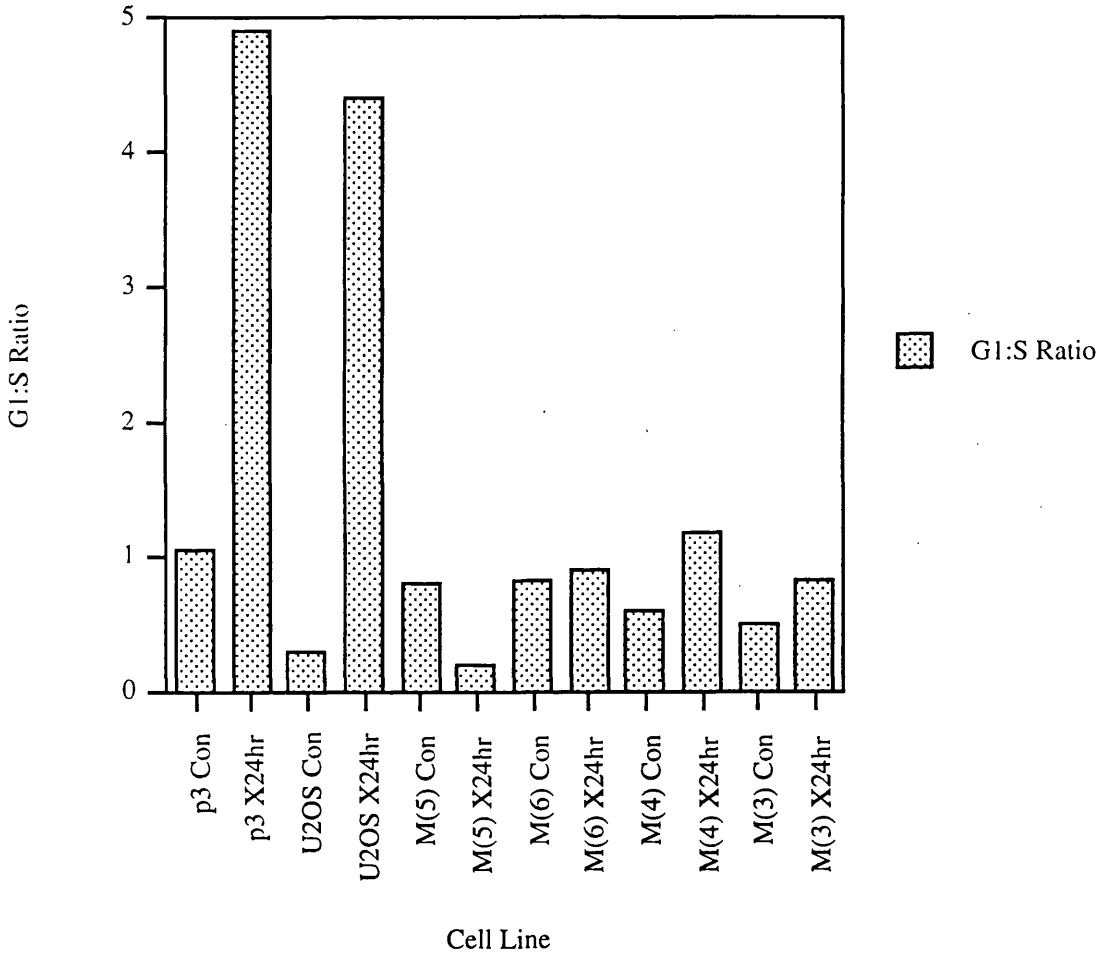
G1:S Ratio
5
4
3
2
1
0
p3 Con
p3 X24hr
U2OS Con
U2OS X24hr
M(5) Con
M(5) X24hr
M(6) Con
M(6) X24hr
M(4) Con
M(4) X24hr
M(3) Con
M(3) X24hr
Cell Line
G1:S Ratio

MDM2 and p53 $175^{A\Rightarrow H}$ overexpression increase the cellular growth rate of U2OS cells.

Due to MDM2's reported interactions with a number of cell cycle regulatory proteins, namely p53, pRB and E2F-1, as well as a role in uncoupling S phase from mitosis (see Introduction), it was of interest to examine the growth rates of the various stable lines generated in U2OS. To take into account increases in cellular mass without cellular division, direct cell number counting was used instead of relying on protein determination methods. MDM2 overexpressing M(5) and p53 $175^{A\Rightarrow H}$ clone DN(5) cells were used for the growth rate analysis, due to their strong expression levels and high levels of apoptotic and G_1:S cell cycle arrest inhibition. 'Normal' growth rates were also determined using both vector-only U2OS stables and parental U2OS cells. As expected a near perfect exponential relationship was apparent for all of the cell lines, although obvious increased growth rates were observed in both the MDM2 and p53 $175^{A\Rightarrow H}$ stable lines in comparison to the parental and vector-control lines, which showed very similar growth rates (see Figure 2.17)

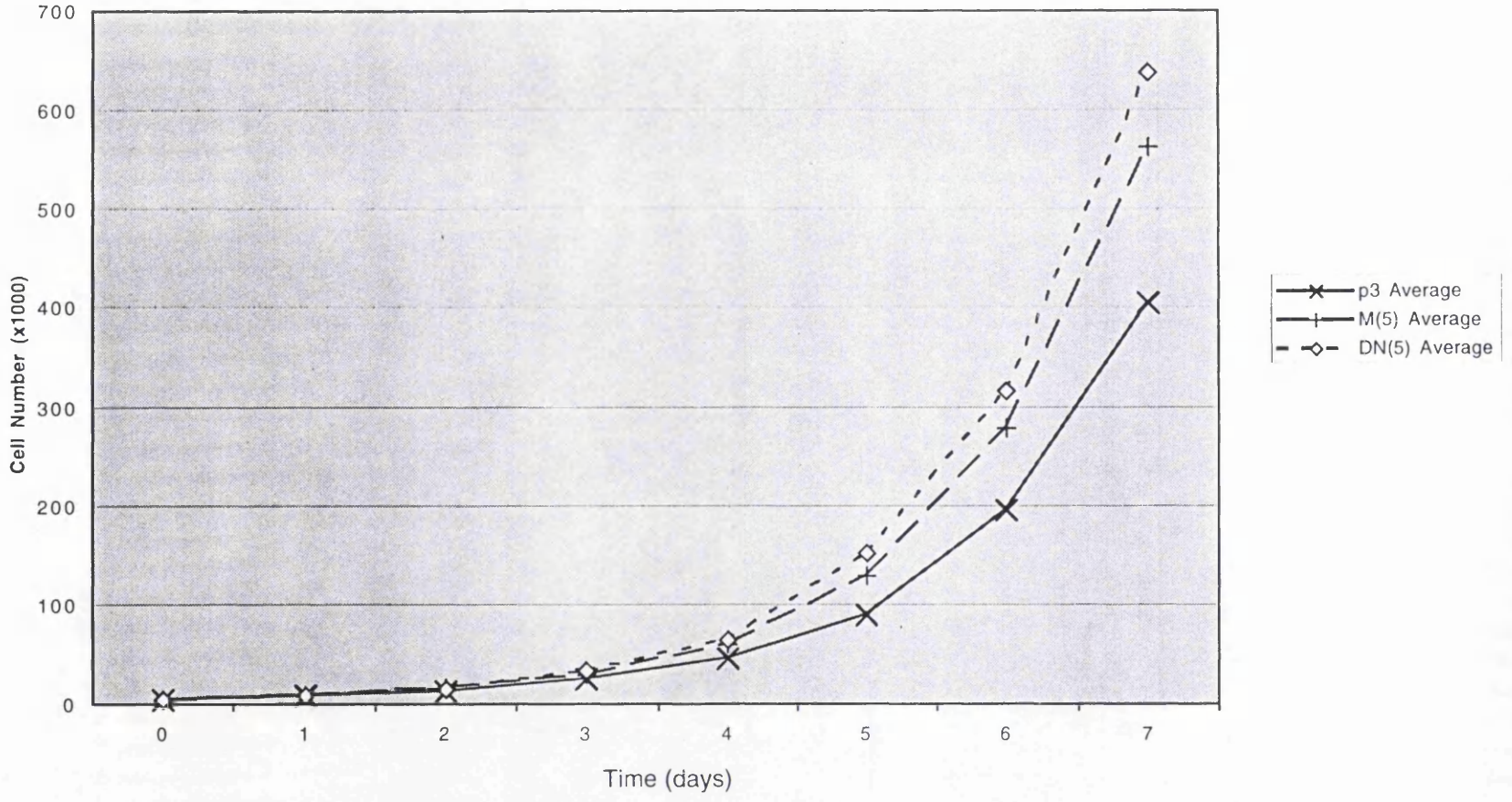

Figure 2.17. MDM2 and p53 175R⇒H expression increase the overall growth rate of U2OS cells. Vector only (p3), MDM2 overexpressing (M[5]) and p53 175R⇒H expressing (DN[5]) U2OS cells were seeded at 10 x10^3 and counted over a seven day time course. The results are an average of two data sets.

Summary and Discussion

The relative ease of generating U2OS clones overexpressing MDM2 suggested that such overexpression was not detrimental to cell growth. The U2OS cells used in this study may tolerate elevated MDM2 expression through specific compensatory cellular alterations in protein expression or post-translational modification mechanisms. Further comparison between MDM2-tolerating and -non-tolerating cell lines may reveal certain cellular prerequisites or abilities to adapt. Of especial interest are sarcomas, which frequently exhibit elevated MDM2 levels.

The lack of excess p53 degradation seen in MDM2 overexpressing U2OS clones, could be explained through responsive homeostatic mechanisms, responding to the elevated MDM2 protein levels. Maintenance of a steady state of p53:MDM2 interaction and/or MDM2-mediated degradation in the MDM2-overexpressing U2OS cell lines, could have been effected through negative regulation of those processes. An alternative to an active homeostatic mechanism, could reflect a passive rate-limiting step of p53:MDM2 association or MDM2-mediated p53 degradation. Such a situation would suggest that simple elevations in MDM2 protein levels could not increase its p53-negative effects due to the dependence on other rate-limiting factors.

Establishment of MDM2 overexpressing cell lines revealed a number of affects on the irradiation-mediated U2OS cellular responses. Both UV-mediated apoptosis and X-ray-mediated cell cycle arrest were, to some degree, attenuated and/or delayed. An obvious correlation between MDM2 expression levels and the degree of abrogation of apoptosis or degree of G1/S cell cycle arrest was apparent. In comparison to the p53 $175^{A \Rightarrow H}$ clones, only M(5), the highest MDM2 overexpressor, showed comparable levels of inhibition.

A detailed sub-G_1 time course of UV-irradiated p3 and M(5) revealed a lack of sub-G_1 cells up to 8 hours post-irradiation. This result does not mean that the apoptotic signals or machinery was not activated, but may reflect the DNA fragmentation-dependent methods of apoptotic determination used. DNA fragmentation represents one of the final stages of apoptosis, and hence may only be detected once apoptosis is effectively completed. These

results do suggest that apoptosis temporally, from apoptotic signal to DNA fragmentation, takes more than 8 hours, but less than 24 hours in U2OS cells. Such a processing time most-probably reflects the temporal transmittance of signals from the apoptotic cause to the apoptotic effectors.

Both p53 $175^{A\Rightarrow H}$ and MDM2 are thought to primarily act by inhibiting p53 function through direct protein-protein interaction, ultimately resulting in alteration of p53's function as a positive and/or negative transcription factor of p53-target genes. Both proteins most probably alter wild-type p53's protein-protein interaction profile, either through direct steric hindrance (as in the case of MDM2) or through conformational changes (as may be the case for both p53 $175^{A\Rightarrow H}$ and MDM2). p53 $175^{A\Rightarrow H}$ primarily acts through preventing p53 sequence-specific DNA binding, while MDM2 acts through masking the transcriptional transactivation domain and/or mediating p53's ubiquitin-dependent degradation. The more direct mechanism of p53-inhibition of p53 $175^{A\Rightarrow H}$ may explain the different efficacy of inhibition seen with MDM2-overexpressing cell lines.

MDM2 overexpressing clones only showed reduced/delayed apoptosis, as in the case with the p53 $175^{A\Rightarrow H}$ clones, although not as effective. Similar explanations can be used to explain the apoptotic delay seen with both p53-inhibtory proteins, with dependency on increasing levels of endogenous wild-type p53 squelching out excess inhibitor proteins, generating unbound wild-type p53 tetramers.

Stable MDM2 overexpression in U2OS revealed that MDM2 overexpression in M(5) was non-detrimental, but actually provided a growth advantage. p53 $175^{A\Rightarrow H}$ expression in stable clone DN(5) provided a greater growth advantage than MDM2-overexpression in M(5) cells, perhaps reflecting a greater p53 $175^{A\Rightarrow H}$-mediated inhibition of p53 function. Inhibition of p53 may lead to faster cell cycle progression, due to abolishment of genome integrity checks and G_1/S restrictions and a reduction in 'natural' apoptosis rates. In addition to MDM2's association with p53, reported interaction with cell cycle proteins, E2F-1 and pRB, may also provide a growth advantage, perhaps promoting the release of E2F-1 from pRB and subsequent stimulation of E2F-1's growth promoting functions (see Introduction). However, the growth advantages were not very dramatic.

Molecular Analysis of the UV and X-ray responses in parental and MDM2- and p53 $175^{A\Rightarrow H}$-expressing U2OS cell lines

Extensive cell cycle analysis of p53 $175^{A\Rightarrow H}$, MDM2 and parental U2OS cell lines had revealed a cell line capable of undergoing both apoptosis and cell cycle arrest, that was inhibited by both p53 $175^{A\Rightarrow H}$ and MDM2 expression (see earlier sections). Therefore it was of interest to try and understand the molecular mechanism involved between the choice of apoptosis and cell cycle arrest and how that choice was effected. Furthermore molecular analysis of the inhibitory mechanisms elicited by p53 $175^{A\Rightarrow H}$ and MDM2 overexpression was also of interest. Hence, Western and Northern blotting techniques were used to examine gene expression.

Protein determination were carried out using the colourimetric 'DC' protein assay (Bio-Rad) system; a Lowry-based chemical reaction which mainly reacts with tyrosine and tryptophan residues. BSA standard graphs covering the average range of protein mass (0-10 μg) were used to determine a trend line formula (see Figure 2.18 [I]), used to convert OD values into protein sample concentrations. Standard graphs were continuously taken. Accuracy concerning equal loading of samples was essential for direct comparisons between direct cell lines' responses. Western analysis of actin levels revealed the assay to be a reliable and reproducible system (see Figure 2.18 [II]).

I.

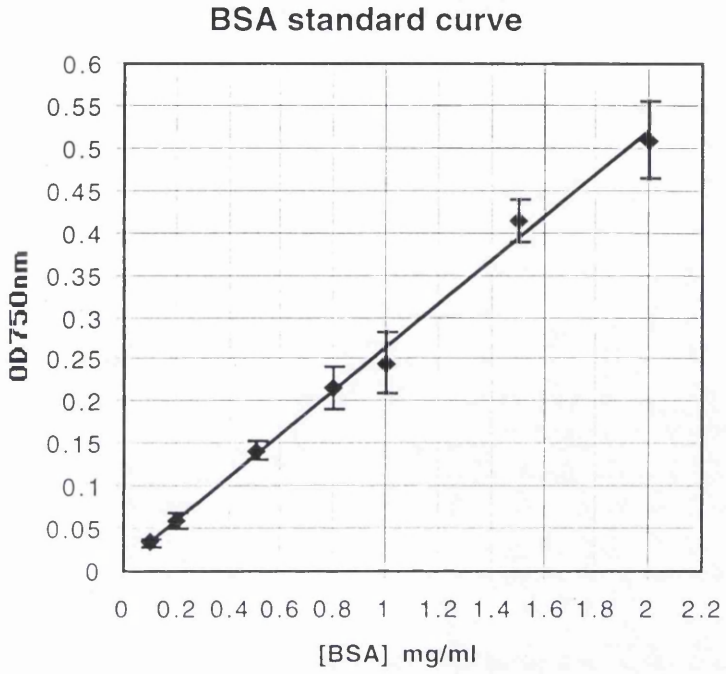

Formula of Line

$y = 0.2555x + 0.0092$

II.

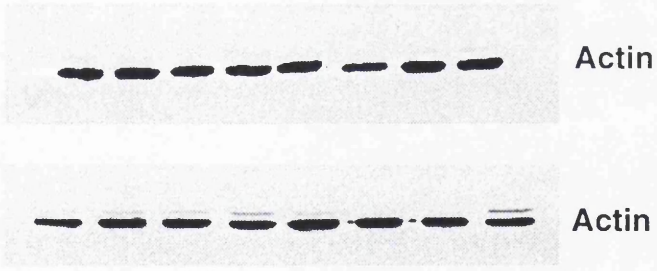

Figure 2.18. Bio-Rad (DC) protein concentration determination represents a reliable and reproducible means of equal protein loading upon Western analysis. (I) Spectrophotometric determination of the optical density of various protein concentrations of DC-assayed bovine serum albumin (BSA) revealed a linear line of best fit. (II) Western analysis of equal DC-determined protein masses revealed equivalent amounts of actin.

Comparison of the protein profiles of UV and X-ray treated U2OS cells

A number of proteins have been implicated in cell cycle arrest and apoptosis, with p53 being a well-documented player. p53 $175^{A \Rightarrow H}$-expressing U2OS FACS analysis had revealed p53 to be important component in both the X-ray mediated cell cycle arrest and the UV-mediated apoptotic responses of U2OS. Many of p53's well-characterised transcriptional targets have been linked to roles in cell cycle arrest and apoptosis, although not necessarily DNA damage-mediated. Analysis of a number of the cell cycle- and apoptotic-implicated proteins was carried out in an attempt to determine a protein profile for apoptotic and cell cycle arrested U2OS cells.

A number of p53-responsive genes were analysed for both forms of irradiation and included (see Introduction): the cyclin-dependent kinase (CDK) inhibitor, $p21^{CIP\text{-}1,\ WAF\text{-}1}$ (p21), which has been shown to induce a G_1/S cell cycle arrest; MDM2, a negative regulator of p53 activity; and components of the apoptotic 'rheostat': Bcl-2 and BAX, anti-apoptotic and pro-apoptotic proteins, respectively. The non-p53-regulated pRB and E2F-1 (a component of the E2F-1/DP-1 heterodimer) proteins were also examined due to their central role in control of cell cycle progression and potential roles in apoptosis and their protein-protein interactions with MDM2 (see Introduction).

X-ray induces p53, p21 and MDM2 protein levels

U2OS cells were X-ray irradiated with 12 Gy as in the cell cycle studies and Western samples were taken at various time points post irradiation (see Figure 2.19 [I]). The time course revealed an induction in p53, MDM2 and p21 levels. No effects on protein expression were seen with Bax or Bcl-2, with stable levels throughout the time course. A small, but reproducible peak in E2F-1 induction was observed eight-ten hour post-irradiation, while a transient dip in MDM2 expression was observed 30 minutes post-irradiation. The X-ray-mediated reduction in MDM2 will be addressed further in later sections.

UV induces p53 and E2F-1 and suppresses p21 and MDM2 protein expression

U2OS cells were irradiated with 30 Jm^{-2} and a range of time points were taken post-irradiation. Western visualisation showed an induction in both p53 and E2F-1 proteins and a reduction in p21 and MDM2 levels, while Bax and Bcl-2 protein levels remained unaffected (see Figure 2.19 [I]). UV-mediated reduction of p21 protein levels shall be addressed in later sections.

30 Jm^{-2} UV irradiation leads to a greater induction in p53 levels than 12 Gy X-ray irradiation

Both UV and X-ray irradiation lead to an induction in p53 levels with the maximum level analysed, obtained at approximately 24 hours post-irradiation. Despite overall p53 induction, degree and rate of induction varied between the two forms of irradiation, with UV-mediated induction being greater in both respects (see Figure 2.19 [II]).

Ser^{392} and Ser^{15} phosphorylation status of p53 post- UV- and X-ray-irradiation

The role of phosphorylation in the control and modulation of a number of cellular proteins' functions is well established. p53 has many phosphorylation sites located within functional domains that could potentially regulate many of p53's properties, namely, oligomerisation and DNA- and protein-binding (see Introduction). Regulation of protein-protein interaction by p53 phosphorylation, could be effected through either modification of the conformational status and/or by direct steric hindrance of binding sites. Two such phosphorylation sites, Ser^{15} and Ser^{392}, have shown to be differentially phosphorylated in response to X-ray- and UV-irradiation(Blaydes and Hupp 1998; Canman, Lim et al. 1998). These phosphorylation sites were examined to investigate whether a similar differential response was evident in U2OS.

Western analysis using phospho-specific antibodies, which are unable to bind non-phosphorylated p53, were used to monitor p53's phosphorylation status post UV- and X-ray-

irradiation. It was of interest to determine whether accumulation of phosphorylated p53 paralleled the 'total' p53 induction seen in both X-ray and UV- irradiated cells. UV-irradiated cells showed both increased Ser^{392} and Ser^{15} phosphorylation, while X-ray irradiated cells revealed no induction in Ser^{392} phosphorylation. Ser^{15} phosphorylation induction in response to X-ray irradiation was detectable but extremely weak 24 hours post-irradiation (see Figure 2.20).

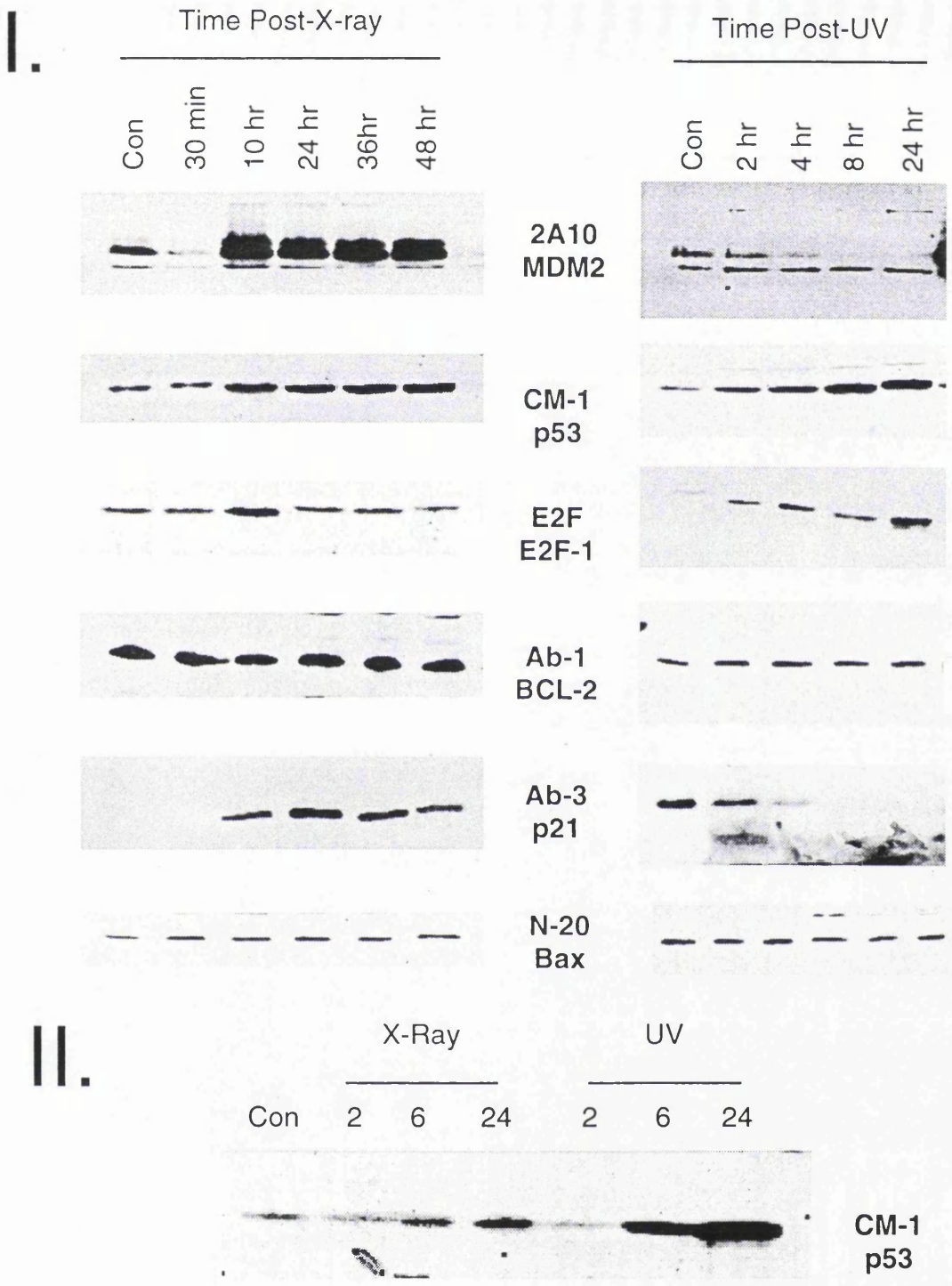

Figure 2.19. Comparison of protein profiles of UV- and X-ray-irradiated U2OS cells. (I) Western analysis of 12 Gy X-ray- and 30 Jm-2 UV-irradiated U2OS cells; U2OS cells were irradiated and analysed by Western blotting at various time points post-irradiation (as indicated) and for the various cellular proteins (as indicated). (II) Comparison of the degree and kinetics of UV- and X-ray-mediated p53 induction; U2OS cells were irradiated and analysed by Western blotting for p53 levels at various time points post-irradiation (as indicated).

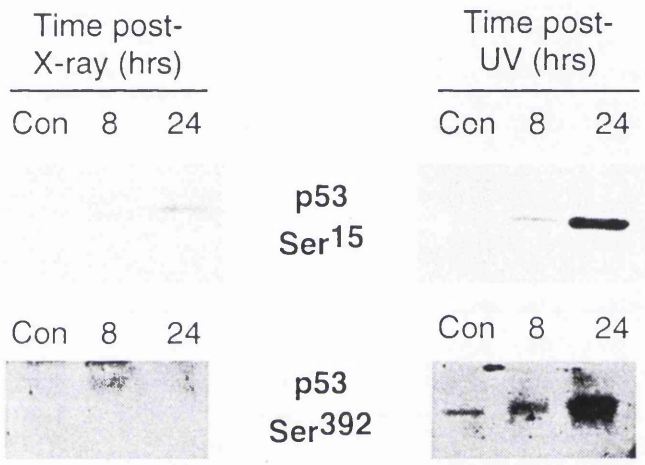

Figure2.20. Irradiation of U2OS cells reveals an increase in p53 Ser15 and Ser392 phosphorylation. U2OS cells were either 12 Gy X-ray- or 30 Jm-2 UV-irradiated and analysed at various time points (as indicated) by Western blotting for p53 phosphorylation using two phospho-specific antibodies (as indicated).

Northern Analysis of X-ray- and UV-irradiated U2OS mRNA reveals differential effects on p21 and mdm2 transcripts

With the observation of irradiation-mediated protein induction and reduction of proteins in U2OS cells, Northern analysis was used to determine if the alterations in protein expression were transcriptionally regulated.

X-ray irradiated U2OS show upregulation of p21 and mdm2 mRNA

Northern analysis of X-ray-irradiated U2OS total cellular RNA revealed a clear induction in both *mdm2* and *p21* mRNA levels, although the *p21* induction was not as marked. The p21 probe yielded a single ≅2 kb transcript, while the MDM2 probe generated a single ≅6.5 kb transcript (see Figure 2.21). Maximum levels were attained at 24 hours post-irradiation, with clear induction seen six hours post-irradiation. These results clearly suggested that the increases in p21 and MDM2 protein levels were, in part, mediated through increased transcription of the respective genes.

UV-irradiated U2OS show a reduction in MDM2 mRNA

Northern analysis of 30 Jm^{-2} UV-irradiated total cellular RNA revealed a steady level of *p21* mRNA throughout the time course. In contrast, *mdm2* mRNA levels showed a rapid reduction in levels, with expression significantly decreased six hours post-irradiation (see Figure 2.21). *mdm2* expression levels remained reduced relative to the control levels throughout the time course, but failed to reduce any further than following the initial reduction at six hours post-irradiation. Further analysis of the UV-mediated loss of *mdm2* transcript is investigated in later sections.

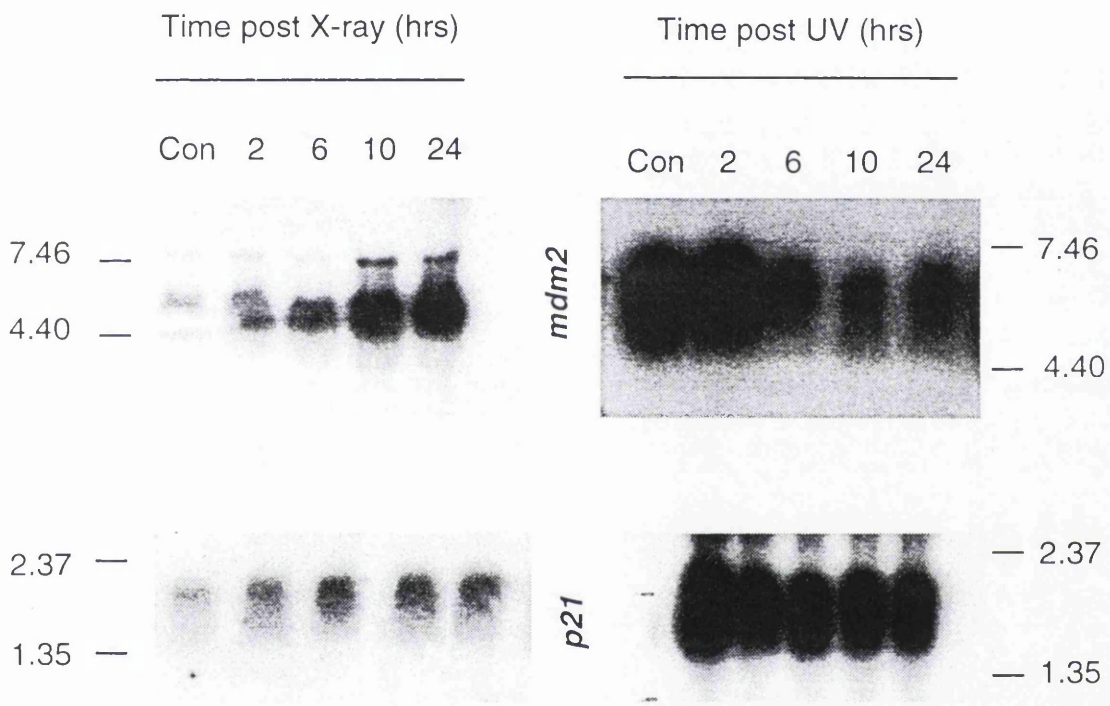

Figure 2.21. Irradiation of U2OS cells reveals differential regulation of p53-regulated genes. U2OS cells were either 12 Gy X-ray- or 30 Jm-2 UV-irradiated and analysed at various time points (as indicated) by Northern blotting using random-hexanucleotide *p21* and *mdm2* primed probes (as indicated). Size markers are indicated on the left-hand side (kb).

Summary and Discussion

Previously it was shown that that X-ray-irradiation of U2OS cells generated a transient p53-dependent G_1/S and p53-independent G_2/M cell cycle arrest, in the absence of apoptosis. In contrast, UV-irradiation caused apoptosis in the absence of any clear cell cycle arrest(Allan and Fried 1999). A question of how these two cellular processes were brought about lead to the molecular analysis of irradiated cells. Analysis of X-ray and UV-irradiated cells revealed partial protein profiles of a number of important gene products previously reported to be involved in apoptosis and/or cell cycle progression/arrest. Differences between the protein profiles upon UV- and X-ray-irradiation were apparent, providing potential explanations for the choice of cellular outcome in response to the different forms of irradiation. Table 2.2 summarises the irradiation protein profiles examined. UV-mediated reduction and induction of MDM2 and E2F-1 proteins, respectively, were also reported in U2OS cells, as was the X-ray-mediated transient peak in E2F-1 levels(Blattner, Sparks et al. 1999).

Table 2. 2. Summary of X-ray- and UV-irradiated U2OS protein profiles.

Protein	30 Jm^{-2} UV	12 Gy X-ray
Ser^{392}	Increases	No Change
Ser^{15}	Increases	Slight increase
p53	Increases	Increases
MDM2	Decreases	Increases
E2F-1	Increases	Transient peak
p21	Decreases	Increases
BCL-2	No Change	No Change
BAX	No Change	No Change

Both forms of irradiation lead to induction of p53, most probably through a post-transcriptional mechanism (see Introduction). Such increases in p53 levels are thought to mediate increased transcriptional trans-activation/repression of p53 target genes involved in either response. However, the need for transcription in apoptosis remains contentious, hence an alternative explanation for increased p53 levels lies in mediating increased

protein-protein interactions. Although absolute increases in p53 levels may suggest increased activity, a number of reports have shown that p53 additionally needs to be converted from a latent to an active conformation for transcriptional activity (see Introduction). UV irradiation created a greater induction of p53 compared to X-ray, perhaps due to stronger inductive and/or stabilisation signals. This difference may simply reflect the differences in energy input levels and damage caused between the two different forms of irradiation, or may truly represent a differential degree of induction of p53 in response to different stimuli. These observations differ slightly from the respective, rapid and transient and the increased and prolonged X-ray- and UV-mediated effects on p53 induction, reported by Lu and Lane(Lu and Lane 1993).

A paradoxical situation exists in the X-ray irradiated cells with increased p53 levels leading to increased p53-dependent transcription of *mdm2.* MDM2, as a negative regulator of p53, should in theory reduce p53 levels through ubiquitin-mediated degradation of p53 and inhibit p53's transcriptional activity both through masking of the domain and degradation. However, p53 levels remained elevated even with concomitant MDM2-induction up to 72 hours post-irradiation. Modification of p53 or MDM2 leading to loss of complex formation could explain this paradox. Alternatively, p53-independent roles for MDM2 in mediating a cell cycle arrest could also explain the need for MDM2 induction. Such properties could perhaps be linked to its ID-1 and ID-2 growth inhibitory domains (see Introduction), with increasing MDM2 levels mediating its own p53-independent cell cycle arrest. Increased MDM2:E2F-1 protein-protein interaction could also perhaps negate E2F-1's cell cycle-promoting and pro-apoptotic roles.

An absence of fluctuation in BAX or BCL2 protein levels was surprising, as p53 has been reported to up-regulate BAX and down-regulate BCL-2 to induce apoptosis, while the opposite has been observed for cell cycle arrest (see Introduction). It is unknown whether U2OS cells were defective in the pathway or what the wild-type status of the BAX and BCL2 proteins were. Although, in addition to direct mutation, cell type specific modifications affecting production and turnover rate may explain the lack of irradiation-mediated effects.

X-ray irradiation induction of p21 was expected, due to its link to negative regulation of the cell cycle (see Introduction and below). Additionally, the observed G_2/M block could be a

result of p21 induction or through the action of the p53-regulated GADD45, with proteins inhibiting some aspect of the Cyclin-B-kinase activity(Wang, Zhan et al. 1999).

Of particular interest were the opposing effects the different irradiation forms had on MDM2 and p21 protein levels. Both *MDM2* and *p21* are p53 transcriptional target genes, and hence expected to be increased in conjunction with p53 accumulation. While X-ray irradiation lead to the expected MDM2 and p21 accumulation, UV-irradiation lead to quite drastic reductions in MDM2 and p21 levels. These apparent dichotomous effects could be causative or simply consequential of the choice between apoptosis and cell cycle arrest.

p53-mediated up-regulation of p21 following DNA damage(el-Deiry, Tokino et al. 1993; Xiong, Hannon et al. 1993; Xiong, Zhang et al. 1993; Di Leonardo, Linke et al. 1994; El-Deiry, Harper et al. 1994) is thought to be an integral part of the p53-mediated growth arrest pathway (see Introduction). p53-mediated p21-induction required the transcriptional transactivation domain of p53(Pietenpol, Tokino et al. 1994) and in the absence of p53, p21 mRNA levels were drastically reduced(el-Deiry, Tokino et al. 1993; Xiong, Zhang et al. 1993; El-Deiry, Harper et al. 1994). Analysis of γ-irradiated p53-null and wild-type mice suggested that p53-dependent regulation of p21 was critical for the response to irradiation(Macleod, Sherry et al. 1995). Furthermore, cultured p21-null MEFs were compromised in their ability to undergo G_1/S growth arrest in response irradiation(Brugarolas, Chandrasekaran et al. 1995). However, p21-null cells exhibited an intermediate phenotype between p53-null and wild-type cells, suggesting that p53 may induce an additional gene that participates in cell cycle arrest. In addition to p21's CKI role, it may induce growth arrest through direct inhibition of DNA synthesis, binding and inhibiting proliferating cell nuclear antigen (PCNA)(Waga, Hannon et al. 1994) a processivity factor for DNA polymerase δ and ε (reviewed)(Kelman 1997).

Analysis of the human HCT116 cell line revealed absolute dependency on p21 to facilitate a G_1/S growth arrest in response to γ-irradiation(Waldman, Kinzler et al. 1995). Interestingly, p21 deletion in HCT116 cells also lead to a DNA repair defect(McDonald, Wu et al. 1996), supporting the idea that p21-mediated cell cycle arrest may prevent replication of damaged

DNA not only through prevention of cell-cycle progression, but perhaps via a more direct DNA-repair mechanism.

Interestingly, p21 has previously been reported to be anti-apoptotic(Gorospe, Cirielli et al. 1997; Bissonnette and Hunting 1998; McKay, Ljungman et al. 1998), as well as pro-apoptotic(Kondo, Barna et al. 1996; Kondo, Kondo et al. 1997), although its mode of action is unclear (see later Summary and Discussion). These findings clearly support the former observations.

UV-mediated reduction of p21 levels may have lead to increased E2F-1 activity through decreased inhibition of CDKs and subsequent increased pRB phosphorylation. Such hyperphosphorylated pRB would then lead to the release of E2F-1 (see Introduction). However, loss of p21 expression was unlikely to account for the actual UV-mediated increase in E2F-1's proteins levels, although it may have accounted for increased E2F-1 activity. A possible explanation lies in the UV-mediated reduction of MDM2 levels, decreasing its protein-protein interaction with E2F-1 and perhaps MDM2-mediated degradation. Although such MDM2-mediated action has not been shown, such a mechanism could be applied to the p53 induction. Increased E2F-1 levels in combination with decreasing MDM2 could have squelched out MDM2 protein-protein inhibition, allowing E2F-1 and p53 to function as an MDM2-unbound pro-apoptotic transcription factor. Reduced MDM2:pRB interactions could also have facilitated release of E2F-1, further strengthening the multiple route to E2F-1 activation. Therefore, reduction of p21 and MDM2 may culminate in increased E2F-1 activity.

E2F-1 was the first identified member of a family of transcription factors (E2F 1-5) which require heterodimerisation with DP-1 or DP-2 for transcriptional regulation of various S-phase genes (reviewed(Slansky and Farnham 1996)). Overexpression of E2F-1 in quiescent mammalian cells can drive S-phase entry(Johnson, Schwartz et al. 1993) and can overcome irradiation-induced G_1 arrest(DeGregori, Kowalik et al. 1995). In addition, ectopic E2F-1 expression triggered apoptosis subsequent to S-phase entry of quiescent cells(Qin, Livingston et al. 1994; Shan and Lee 1994; Wu and Levine 1994; Kowalik, DeGregori et al. 1998). E2F-1-mediated apoptosis was significantly abolished in p53-null(Kowalik, DeGregori et al. 1995) and MDM2 overexpressing cells(Kowalik, DeGregori et al. 1998) and was

enhanced through exogenous p53 expression(Qin, Livingston et al. 1994; Wu and Levine 1994). Of the five known E2F family members, the ability to induce apoptosis is unique to E2F-1(DeGregori, Leone et al. 1997).

In a murine tumour model, deficiency in p53 caused an 85% reduction in apoptosis and an increase in tumour growth, while E2F1-deficiency generated an 80% reduction apoptosis and no affect on tumour growth(Pan, Yin et al. 1998). These results suggest that E2F-1 is required for both growth and apoptosis, possessing properties of both an oncogene and a tumour suppresser gene.

E2F-1's ability to transcriptionally upregulate ARF, provides a direct link between E2F-1 and p53 activation(Bates, Phillips et al. 1998). Nevertheless, E2F-1 must provide an additional apoptotic-specific signal to mediate the apoptotic response, rather than the reported ARF-mediated cell-cycle arrest(Kamijo, Zindy et al. 1997; Stott, Bates et al. 1998; Zhang, Xiong et al. 1998; Kurokawa, Tanaka et al. 1999). E1A expressing, ARF-null MEFs cells undergo attenuated p53-dependent apoptosis(Stanchina, McCurrach et al. 1998), suggesting that ARF can also mediate apoptosis. In this situation E1A-mediated pRB inhibition would provide deregulated E2F-1 activity as a potential apoptotic stimuli.

Similar (5 Gy) X-ray- and ($30Jm^{-2}$) UV-mediated effects on E2F-1 protein levels were reported in U2OS cells(Blattner, Sparks et al. 1999). Interestingly, (20 Jm^{-2}) UV- and (6 Gy) γ-irradiated U2OS cells also induced not only E2F-1 protein levels, but also stimulated its DNA-binding ability(Hofferer, Wirbelauer et al. 1999). Taken with the observations that 30 Jm^{-2} UV-irradiation lead to p53-dependent apoptosis and 12 Gy X-ray irradiation induced a cell cycle arrest (see Chapter Two); E2F-1-mediated transcription may mediate both irradiation-induced cell cycle arrest and apoptosis. The temporal-specific UV-induction of E2F-1 may provide an apoptotic signal, while in contrast, the early X-ray-mediated transient peak in E2F-1 levels may not have been temporally-significant for apoptosis, but instead facilitated a cell cycle arrest.

UV-mediated decreases in MDM2 levels could lead to decreased inhibition of p53 activity, which may be required for apoptosis. Removal of p53's negative regulator could account for both p53 protein accumulation and increased activity. Such a decrease in MDM2 levels

could lead to decreased MDM2:p53 complex-formation, facilitating increased novel protein-protein interactions, through decreased MDM2-mediated steric hindrance. Additionally, removal of MDM2's ID-1 and ID-2 growth inhibitory domains may be needed to facilitate apoptotic dominance over a cell cycle arrest.

In an attempt to determine whether the UV-mediated reductions of the MDM2 and p21 proteins were transcriptionally controlled, Northern analysis was used to compare UV- and X-ray-irradiated U2OS cells. Both *mdm2* and *p21* mRNA transcripts levels increased over time following X-ray irradiation, while *mdm2* mRNA transcript levels reduced post-UV-irradiation. Conversely, *p21* mRNA transcript levels remained constant throughout the time points taken and may have been mediated through UV-mediated enhanced stability of *p21* mRNA(Gorospe, Wang et al. 1998).

From this evidence, decreases in *mdm2* mRNA can explain the reduction in MDM2 protein levels, although whether the reduction in mRNA was due to decreased rates of transcriptional initiation, elongation or termination and/or mRNA stability (methylation capping or splicing etc) cannot be ascertained from these results. An obvious explanation lies in the nature of damage mediated by UV-irradiation; the formation of bulky pyrimidine dimers (6′-4′ photoproducts and cyclopyrimidine dimers) in the *mdm2* gene which could cause transcriptional stalling and hence explain a reduction in mRNA transcript levels. However, the constant levels of *p21* mRNA post-UV-irradiation conflicts with this idea, although increased mRNA stability or smaller-target gene size (which will be discussed later) may explain such differences. Interestingly, *p21* mRNA levels remained unaffected in 50 Jm^{-2} UV-irradiated NIH3T3 cells(Lu, Burbidge et al. 1996), suggesting either rapid repair of the *p21* gene or high mRNA stability. The existence of promoter/enhancer control elements that are UV-irradiation responsive may explain the differential mRNA expression patterns. Stress-responsive positive or negative transcription factors could then mediate such differential responses seen between *mdm2* and *p21* genes. Alternatively, the differences in the irradiation-mediated magnitudes of p53 induction may have facilitated differential induction of p53-target genes, due to different promoter affinities for p53 binding (see Introduction).

In addition to transcriptional regulation, translational or degradative mechanisms could also explain the irradiation-mediated reductions of MDM2 and p21 protein levels and will be addressed in later sections.

Phospho-specific antibodies raised against Ser^{15} or Ser^{392} were used to analyse p53 phosphorylation status following both UV- and X-ray-irradiation. Irradiation-mediated phosphorylation of p53 was proposed to function in controlling the p53:MDM2 interaction (Ser^{15})(Shieh, Ikeda et al. 1997) or activation of p53 from a latent monomeric form to an active tetrameric form (Ser^{392})(Sakaguchi, Sakamoto et al. 1997; Sakaguchi, Sakamoto et al. 1997). UV-irradiation lead to increased levels of both Ser^{15} and Ser^{392} phosphorylation, while X-ray only slightly induced Ser^{15} phosphorylation.

UV-mediated Ser^{392} induction and its reported transcriptional activation of latent p53 cannot be supported from these results, due to lack of evidence for activation of four p53-responsive target proteins, namely: MDM2, p21, BAX and BCL2. However, it cannot be ruled out that activation of other target genes, not investigated, occurred. Additionally, conformational and oligomeric alterations as a consequence of p53 Ser^{392} phosphorylation may have lead to altered protein-protein interactions, facilitating apoptosis. Paradoxically, induction of p53-responsive gene products (MDM2 and p21) were seen upon X-ray irradiation, which failed to increase phosphorylated Ser^{392} levels. The effects of irradiation and p53 Ser^{15} phosphorylation on MDM2:p53 complex formation is addressed further in chapter three.

Comparison of irradiated protein profiles between various cell lines

Analysis of the MDM2 stable cell lines revealed no obvious effects on the protein levels of a number of important cell cycle proteins. Although the 'resting' levels of these proteins were unaltered, upon DNA damage differential regulation of such proteins could explain delayed or abrogated cellular responses observed between M(5) and parental U2OS[11] cells.

[11] Please note that parental U2OS and vector-only p3 cell lines were used interchangeably due to their near identical behaviour.

Therefore, a number of proteins implicated in both apoptosis and cell cycle arrest were analysed for variances.

MDM2 overexpression delays X-ray induction of p53 and p21

From the initial work on parental U2OS cells, it was known that 12 Gy X-ray irradiation lead to an increase in both p53 and p21 protein levels. In an attempt to explain the partial abrogation of the G_1/S cell cycle arrest seen in the MDM2 stable lines, comparison of the magnitude of both p53 and p21 induction was undertaken. The role of p21 in mediating cell cycle arrest is well known and it was of interest to determine whether reduced p21 levels would reflect the reduced G_1/S cell cycle arrest and whether that reduction was due to reduced p53 levels. Indeed, this was the case, with a temporal lag in induction levels, in both p53 and p21 levels, seen in M(5) cells relative to p3 cells (see Figure 2.22 [I]).

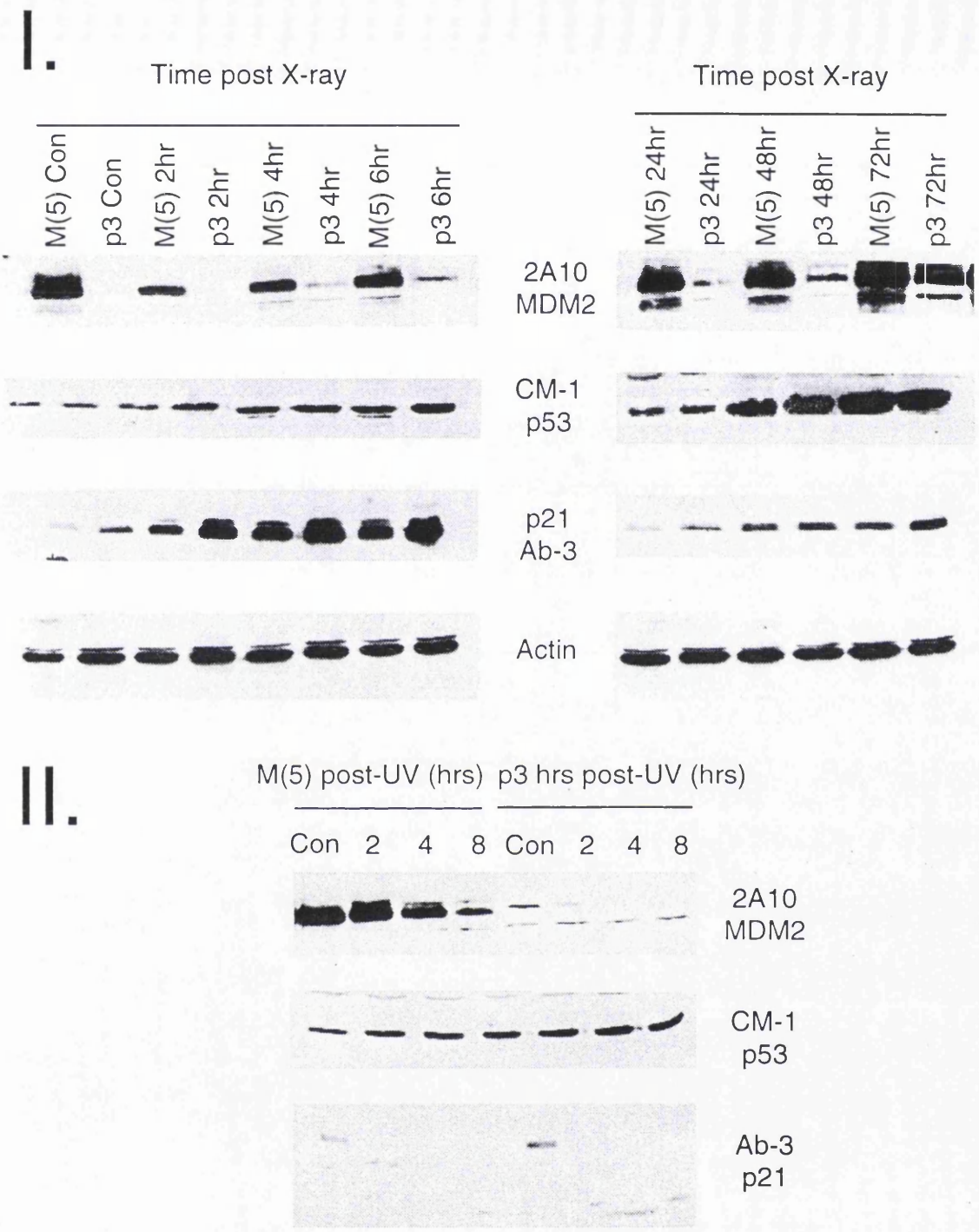

Figure 2.22. MDM2 overexpression alters the irradiation profiles of U2OS cells. (I) Vector-only (p3) and MDM2-overexpressing (M[5]) U2OS cells were X-ray-irradiated with 12 Gy and analysed by Western blotting at various time points post-irradiation (as indicated) for different cellular proteins (as indicated). (II) Vector-only (p3) and MDM2-overexpressing (M[5]) U2OS cells were UV-irradiated with 30 Jm-2 and analysed by Western blotting at various time points post-irradiation (as indicated) for different cellular proteins (as indicated).

X-ray-irradiation causes a transient dip in MDM2 levels and increases p21 in a number of cell lines.

Analysis of the X-ray irradiated MDM2[12] levels revealed a reduction in MDM2 protein levels, prior to subsequent induction, in both M(5) and p3 cells, 0.5-2 hours post-irradiation (see figure 2.19 [I] and 2.22 [I]). Interestingly, a lower ≅50 kDa molecular weight 2A10 MDM2 reactive band was generated in conjunction with loss of the 90 kDa MDM2 band (see Figure 2.23). Unfortunately, the visualisation of the lower molecular weight band was temperamental in its reproducibility. Further analysis of a number of other cell lines, including JAR and OSA cells (both overexpressing endogenous MDM2), revealed a biphasic MDM2 response to X-ray irradiation (see Figure 2.23 and 2.24). Even DN(5) and HOS cells (both mutant p53) showed a transient dip which recovered to control levels by 24 hours post-irradiation (see Figure 2.24).

Comparison of p21 induction showed that DN(5), M(5), OSA and p3 cell lines demonstrated p21 induction in response to 12 Gy X-ray-irradiation (see Figure 2.23). However, DN(5)'s p21 induction was severely attenuated in comparison to p3's p21 induction levels 24 hours post-irradiation. MG63 and U393 cells exhibited contrasting p21 responses: decreasing and remaining unaffected, respectively (see Figure 2.24). HOS cells consistently failed to demonstrate any detectable p21, most probably reflecting its mutant p53 status and mirroring the extremely low levels of p21 seen in DN(5) cells.

Overall OSA, M(5) and p3 cells showed similar patterns of protein induction, with all three inducing p53, p21 and MDM2, albeit to different levels. While all cell lines analysed showed, to some degree, an X-ray-mediated transient dip in MDM2 levels. In the case of p21, three different responses were observed: U393 cells showed no upregulation; MG63 revealed reduced expression; and p3, M(5), OSA and (to a slight extent) DN(5) upregulated p21 expression.

---

[12] Please note that endogenously- and exogenously-expressed MDM2 present in M(5) cells could not be distinguished between. However, due to the massive overexpression of MDM2, the majority of the effects were assumed to be affecting the exogenously-expressed protein.

OSA mimics the X-ray irradiation response of U2OS in both protein induction profile and cellular response.

The initial OSA observations seemed to mimic the X-ray-irradiated protein profile of U2OS cells (see Figure 2.23), with p53, p21 and MDM2 induction. FACS analysis of 12 Gy X-ray-mediated OSA cells revealed that like U2OS, OSA underwent a G_1/S (relatively weak) and G_2/M cell cycle arrest 24 hours post-irradiation and in the absence of apoptosis (see Figure 2.25). Long term culturing of X-ray irradiated OSA revealed that the cell cycle arrest was only transient as the cell eventually grew to confluence.

Further characterisation of the X-ray-irradiated protein profiles of different cell lines

With the quantitative differences in p53 and p21 induction seen between M(5), p3 and DN(5) cells, it was of interest to look for other potential quantitative or qualitative differences. X-ray irradiated DN(5), OSA, M(5) and U2OS samples were analysed for pRB, E2F-1 and p53 Ser^{15} levels.

Western blotting showed no clear alterations in the protein level or phosphorylation status of pRB in either U2OS-derived or OSA cells (see Figure 2.23). However, U2OS has been documented to show over-hyperphosphorylation of pRB(Hofferer, Wirbelauer et al. 1999). E2F-1 levels in all of the U2OS-derived cell lines showed a significant peak in E2F-1 protein levels eight hours post-irradiation, which reduced to control levels by 24 hours post-irradiation. OSA showed a similar pattern, although E2F-1 levels peaked at two hours post-irradiation. This elevated level was maintained until eight hours post-irradiation and then returned to control levels by 24 hours post-irradiation. Phosphorylated p53 Ser^{15} was undetectable in all of the cell lines, except DN(5). This line cell exhibited highly elevated levels in response to X-ray-irradiation, with maximal induction seen as early as two hours post-irradiation. Control levels were also highly elevated in comparison to the undetectable p53 Ser^{15} levels in the other cell lines.

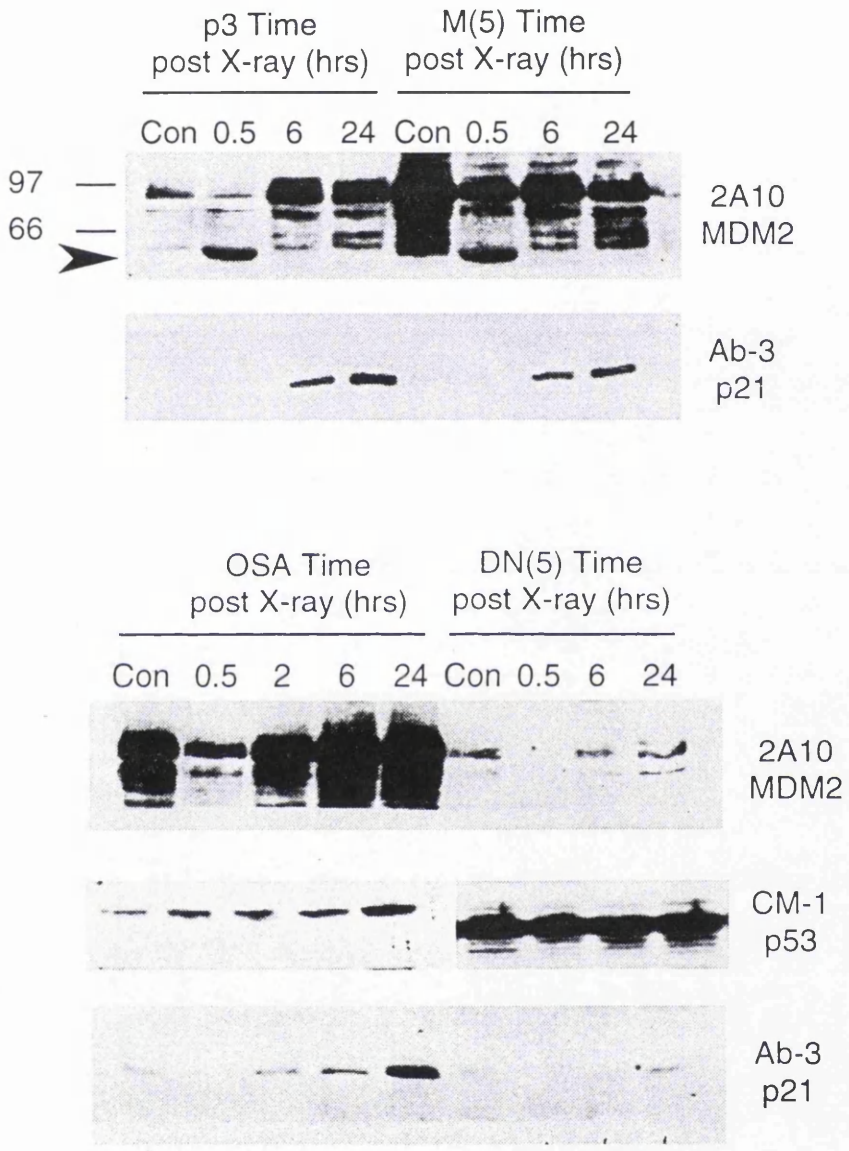

Figure 2.23. 12 Gy X-ray-irradiation of U2OS-derived and OSA cell lines reveals differing protein profiles and a reduction in MDM2 levels. Vector-only (p3), MDM2-overexpressing (M[5]) and p53 175R⇒H expressing U2OS clones and OSA cells were X-ray irradiated and analysed by Western blotting at various time points post irradiation (as indicated) for different cellular proteins. An arrowhead marks a potential 60kDa MDM2 cleavage product.

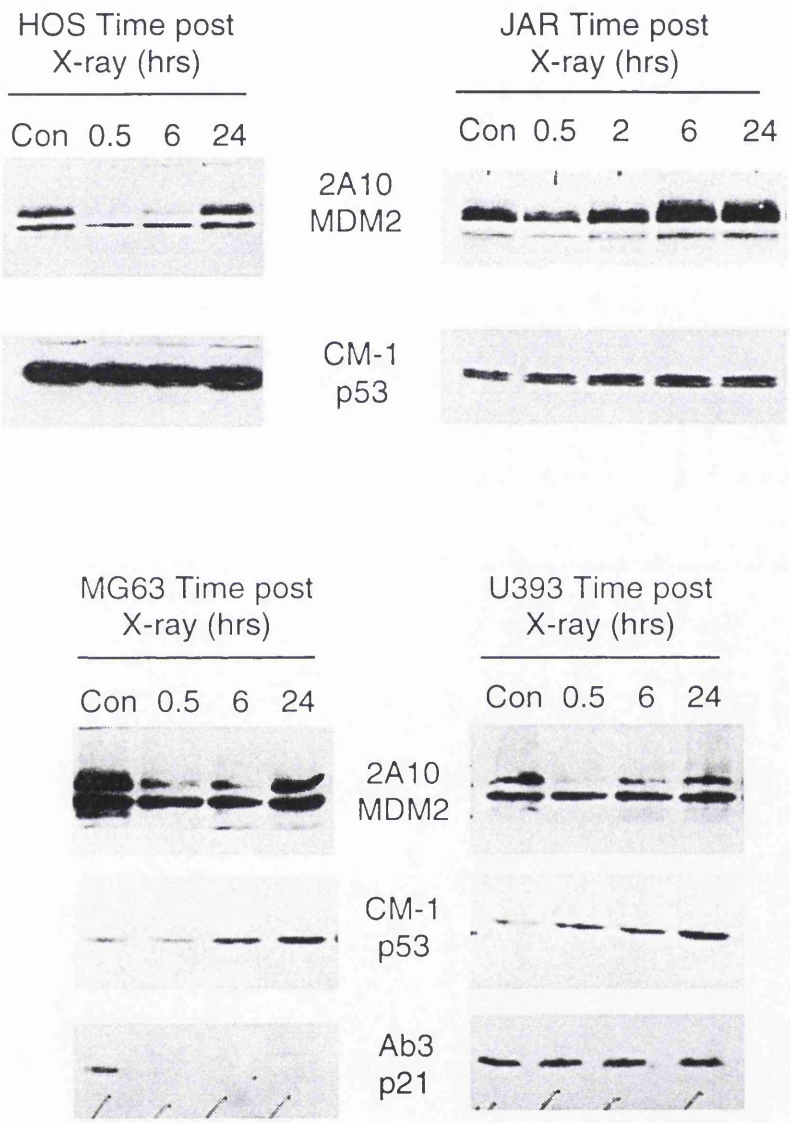

Figure 2.24. 12 Gy X-ray-irradiation of a variety of cell lines reveals differing protein profiles and a reduction in MDM2 levels. HOS, JAR, MG63 and U393 cells were X-ray irradiated and analysed by Western blotting at various time points post irradiation (as indicated) for different cellular proteins.

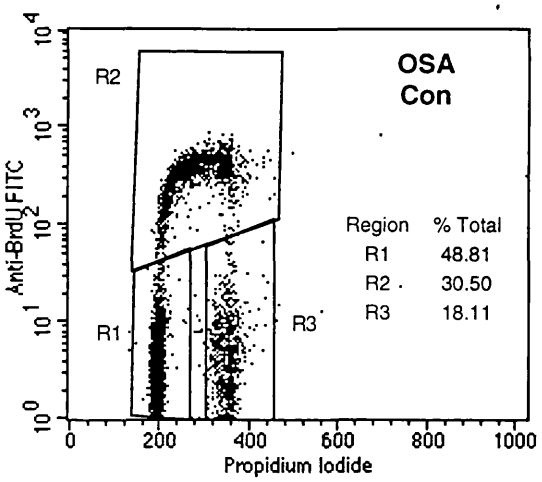

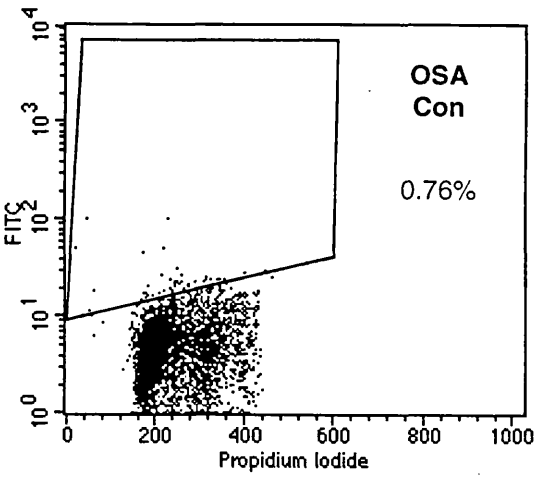

G1:S Ratio = 1.60

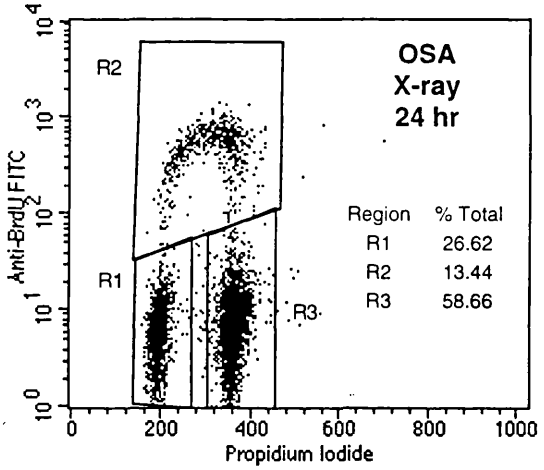

G1:S Ratio = 1.98

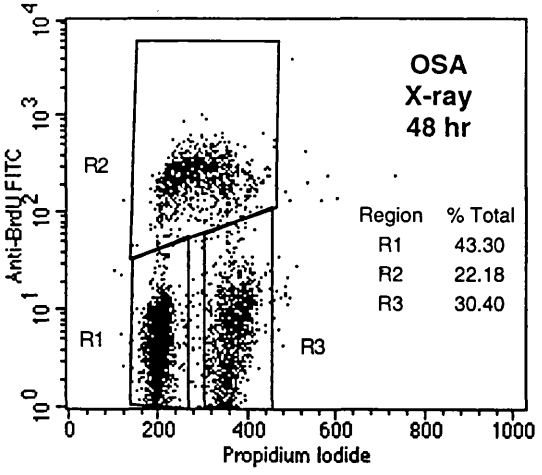

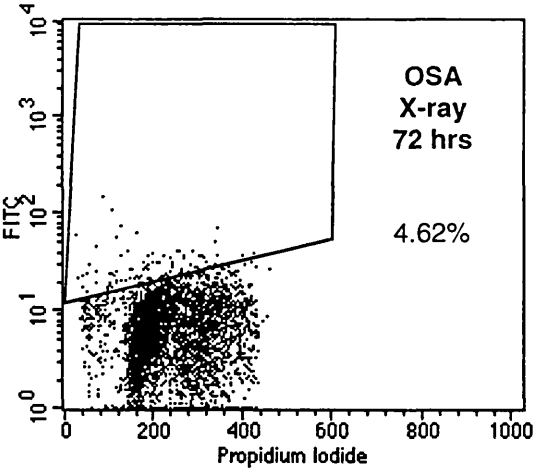

G1:S Ratio = 1.95

Figure 2.25. 12 Gy X-ray-irradiation induces a loss of S-phase cells and a G1/S and G2/M cell cycle arrest and no apoptosis in OSA cells. OSA cells were X-ray irradiated and analysed by BrdU and TUNEL analysis at various time points (as indicated) post-irradiation.

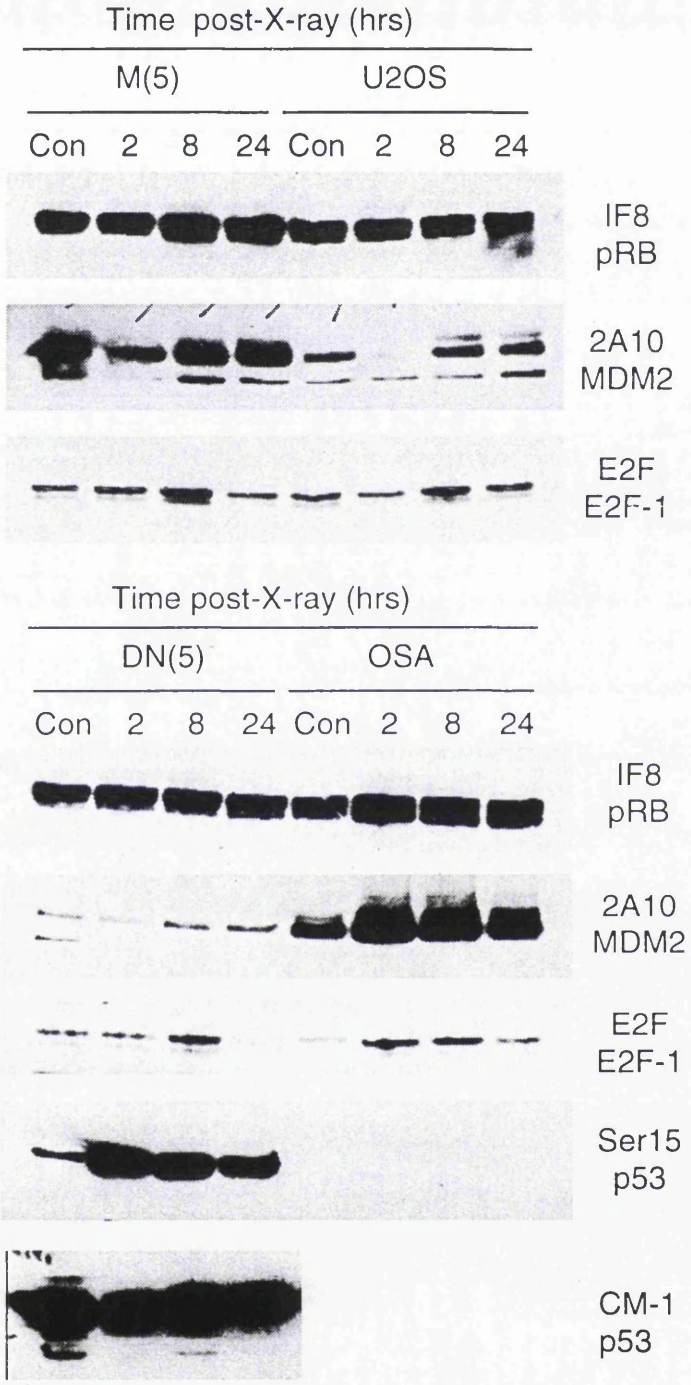

Figure 2.26. 12 Gy X-ray-irradiation of U2OS-derived and OSA cell lines reveals differing protein profiles and a reduction in MDM2 levels. Vector-only (p3), MDM2-overexpressing (M[5]) and p53 175R⇒H expressing U2OS clones and OSA cells were 12 Gy X-ray irradiated and analysed by Western blotting at various time points post irradiation (as indicated) for different cellular proteins (as indicated).

UV-irradiation suppresses both exogenously and endogenously-expressed MDM2

UV-irradiation of M(5) and p3 cells revealed a clear reduction of MDM2 protein levels (see Figure 2.22. [II]). Reductions in MDM2 levels were evident in p3 cells as early as 2 hours post-irradiation, while M(5) cells maintained control levels up until eight hours post-irradiation. p53 induction levels were generally comparable between the two cell lines, although a slight, but reproducible attenuated p53 induction was evident in M(5) cells. Examination of p21 protein levels revealed that both cell lines exhibited similar decreases in p21 protein expression as early two hours post-irradiation.

The wild-type p53 containing cell line, OSA, which has elevated endogenous MDM2 levels was examined following UV-irradiation. Visual and FACS analysis revealed UV-mediated apoptosis of OSA cells (see Figures 2.27 and 2.28 [I]), respectively). However, in comparison to U2OS, OSA cells showed significantly less apoptosis at 48 and 72 hours post-irradiation (compare Figures 2.2 and 2.28 [I]), although the process was merely delayed as the majority of cultured UV-irradiated eventually died.

Western analysis of UV-irradiated OSA cells revealed clear reductions in MDM2 protein levels four hours post-irradiation and continued to remain low until 24 hours post-irradiation, when levels returned to control levels (see Figure 2.28 [II]). p53 accumulated until the last time point, 24 hours post-irradiation. Interestingly, p21 protein could not be detected in control or early UV-treated OSA cells, but by 24 hours post-irradiation p21 levels had massively accumulated. Therefore, OSA had partially mirrored the U2OS-cell UV-irradiation response, although the most striking difference was the recovery of both MDM2 and p21 expression 24 hours post-irradiation.

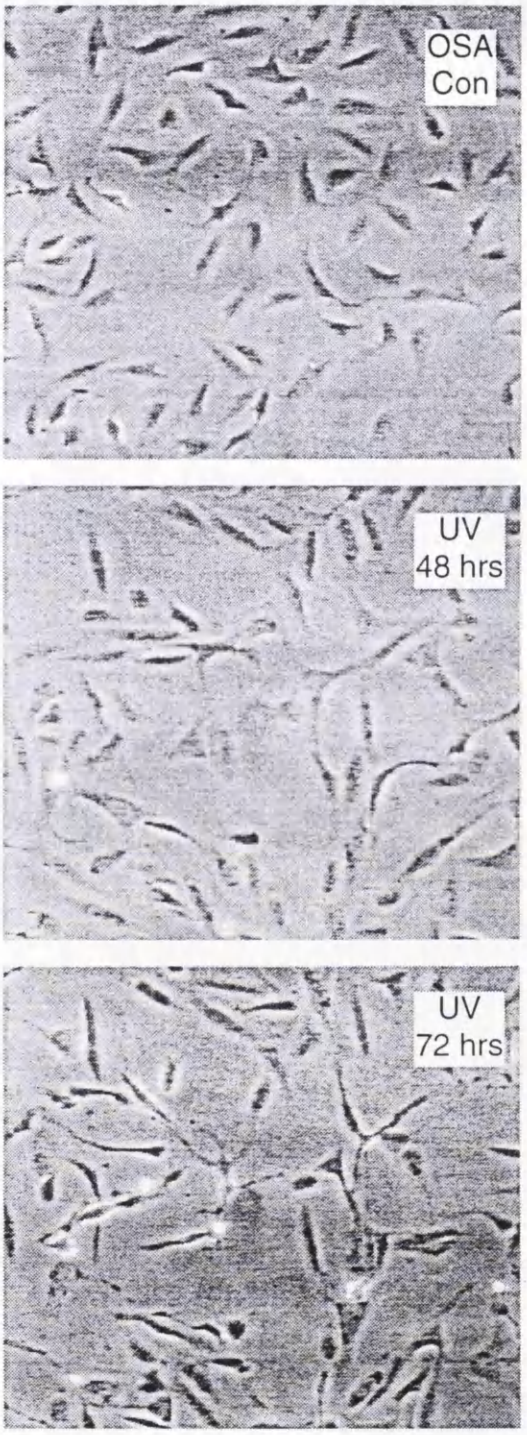

Figure 2.27. 30 Jm-2 UV-irradiation induces apoptotic morphology in OSA cells. OSA cells were 30 Jm^{-2} UV-irradiated and examined by time-lapse photography up to 72 hours post-irradiation.

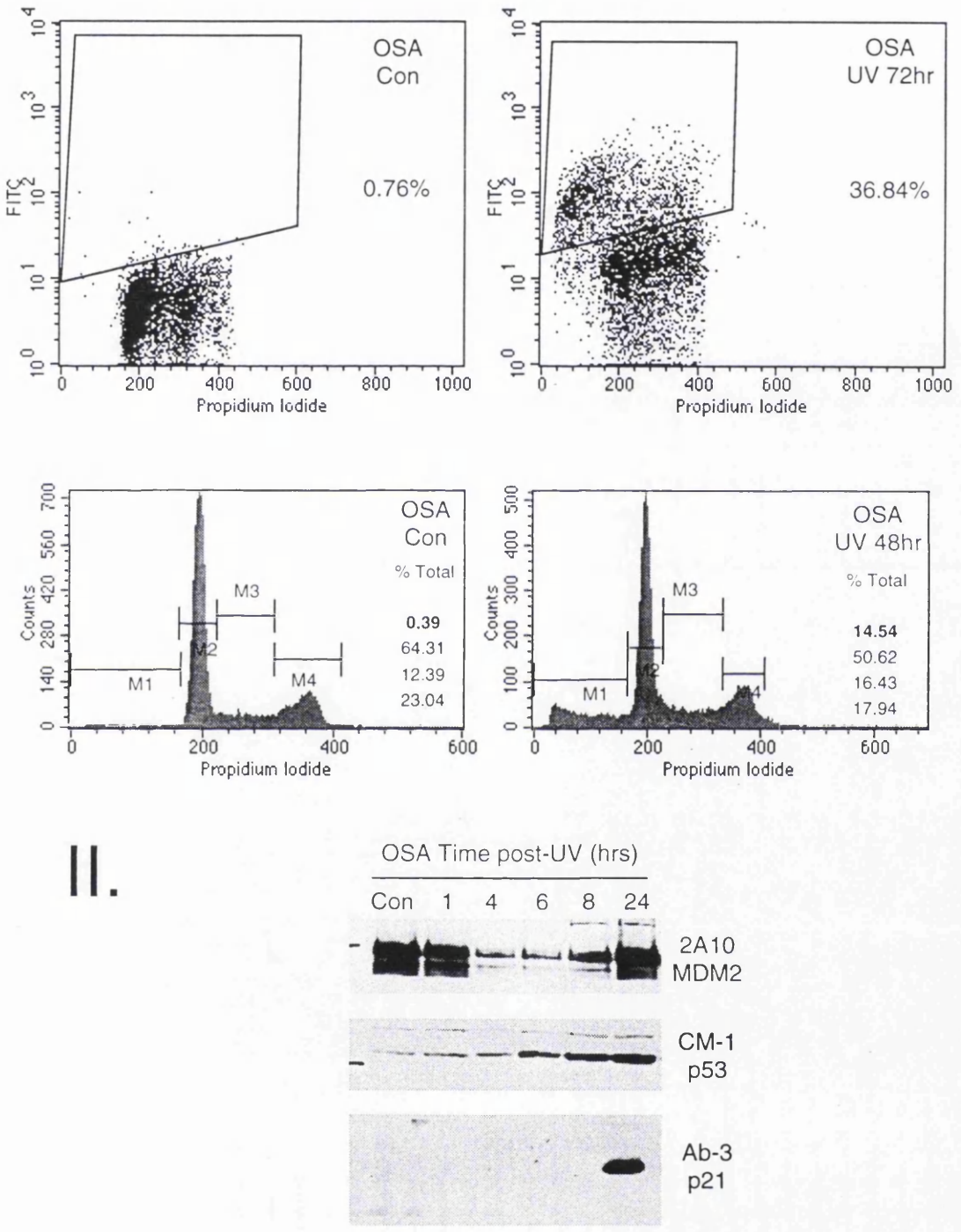

Figure 2.28. OSA cells partially mirror the U2OS UV-mediated apoptotic response. (I) 30 Jm-2 UV-irradiation induces TUNEL- and sub-G1-positive OSA cells; OSA cells were UV-irradiated and examined by TUNEL and Sub-G1 analysis at 72 hours and 48 hours post-irradiation, respectively.(II) Western analysis of 30 Jm-2 UV-irradiated OSA cells; OSA cells were UV-irradiated and analysed by Western blotting at various time points post-irradiation (as indicated) for different cellular proteins (as indicated).

Further characterisation of the UV-irradiated protein profiles of different cell lines

MDM2, E2F-1, pRB and p53 Ser^{15} were examined in an attempt to further characterise the protein profiles of UV-irradiated of the cell lines examined by FACS analysis. pRB protein levels remained constant throughout the 24 hour time course and no obvious phosphorylation-mediated shift in mobility was observed (see Figure 2.29). All three U2OS-derived cell lines (including DN[5]) showed UV-mediated loss of MDM2. However, as mentioned above, OSA showed a bi-phasic response of initial reduction followed by induction. As expected, M(5) cells demonstrated more persistent MDM2 expression following UV-irradiation, compared to U2OS cells, while DN(5) cells showed a more rapid reduction.

All four cell-lines revealed UV-mediated induction of E2F-1, with levels peaking at 24 hours post-irradiation (see Figure 2.29). Similarly, p53 Ser^{15} phosphorylation increased following irradiation, with detectable levels in OSA, M(5) and U2OS 24 hours post-irradiation. As with X-ray irradiation, UV-irradiation of DN(5) cells revealed a massive increase in phosphorylated p53 Ser^{15}, as early as two hours post-irradiation. Phosphorylated p53 Ser^{15} levels continued to increase up to 24 hours post-irradiation, while general p53 levels remained constant.

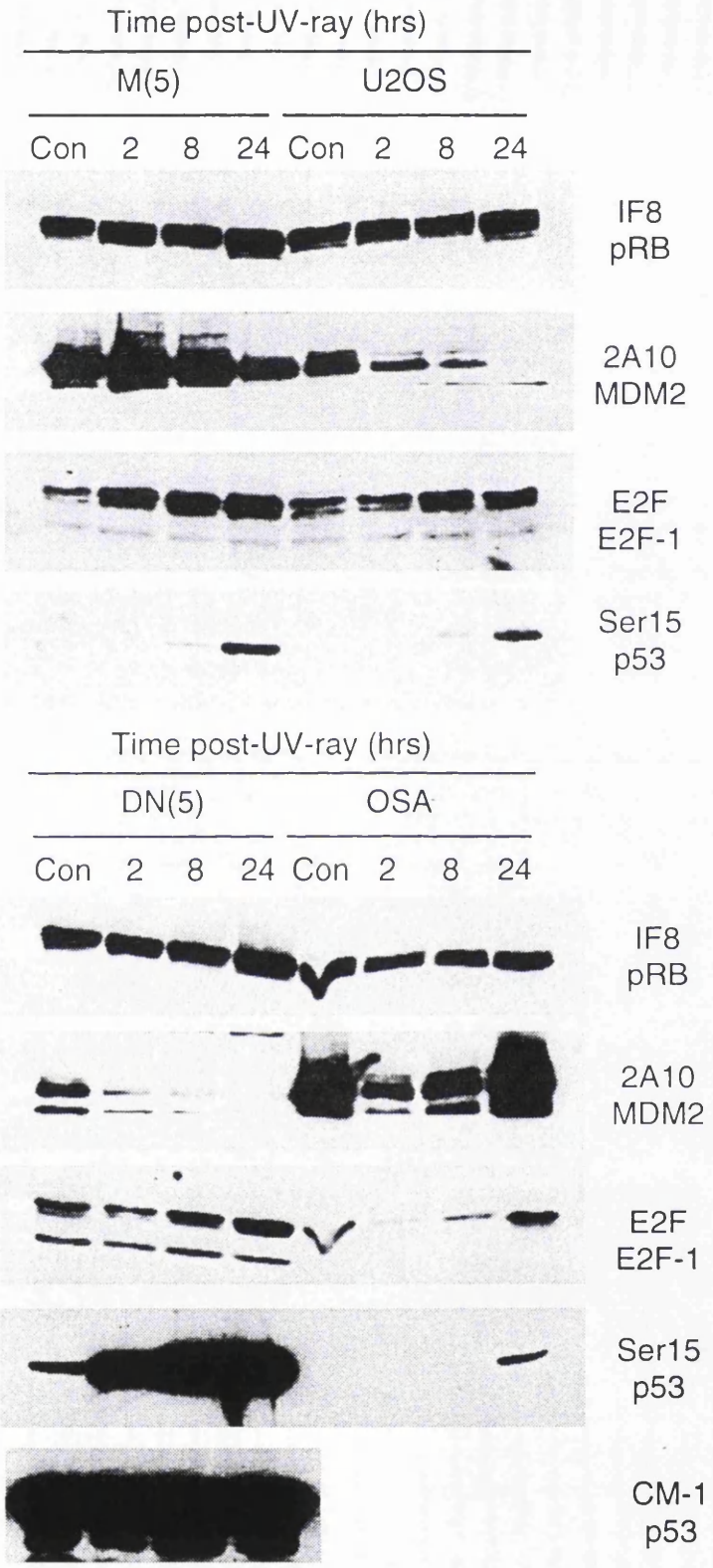

Figure 2.29. 30 Jm-2 UV-irradiation of U2OS-derived and OSA cell lines reveals differing protein profiles and a reduction in MDM2 levels. Vector-only (p3), MDM2-overexpressing (M[5]) and p53 175R⇒H expressing U2OS clones and OSA cells were 30 Jm^{-2} UV-irradiated and analysed by Western blotting at various time points post irradiation (as indicated) for different cellular proteins (as indicated).

Northern blotting reveals no reduction in mdm2 mRNA levels upon X-ray-irradiation

Earlier Northern analysis had revealed no reduction in endogenous *mdm2* mRNA levels in X-ray-irradiated U2OS cells. However, due to the earliest time point being two hour post-irradiation, it was possible that earlier alterations in transcription rates and/or mRNA stability may have occurred, accounting for the X-ray mediated 'dip' in MDM2 protein levels. Therefore, earlier time points were examined.

Total cellular RNA extracted 15, 30, 60 and 120 minutes post-irradiation revealed no reductions in either endogenous or exogenous *mdm2* mRNA levels, in U2OS or M(5), respectively (see Figure 2.30 [I]).

Northern blotting reveals a small reduction in exogenous mdm2 *mRNA following UV-irradiation of M(5) cells.*

The dramatic reduction in endogenous *mdm2* mRNA seen in UV-irradiated U2OS cells (see Figure 2.21) was a possibly explanation for the loss of MDM2 expression in U2OS cells. An explanation of the delayed loss of MDM2 expression seen in M(5) cells was also sought. Examination of the exogenously expressed *mdm2* mRNA in UV-irradiated M(5) cells revealed a gradual reduction, with loss of transcript as early as two hours post-irradiation (see Figure 2.30 [II]). This relatively small reduction in *mdm2* mRNA did not directly match the more dramatic loss of MDM2 protein. Therefore discordance between the mRNA and protein level of MDM2 was apparent, although both showed the overall pattern of UV-mediated loss of expression.

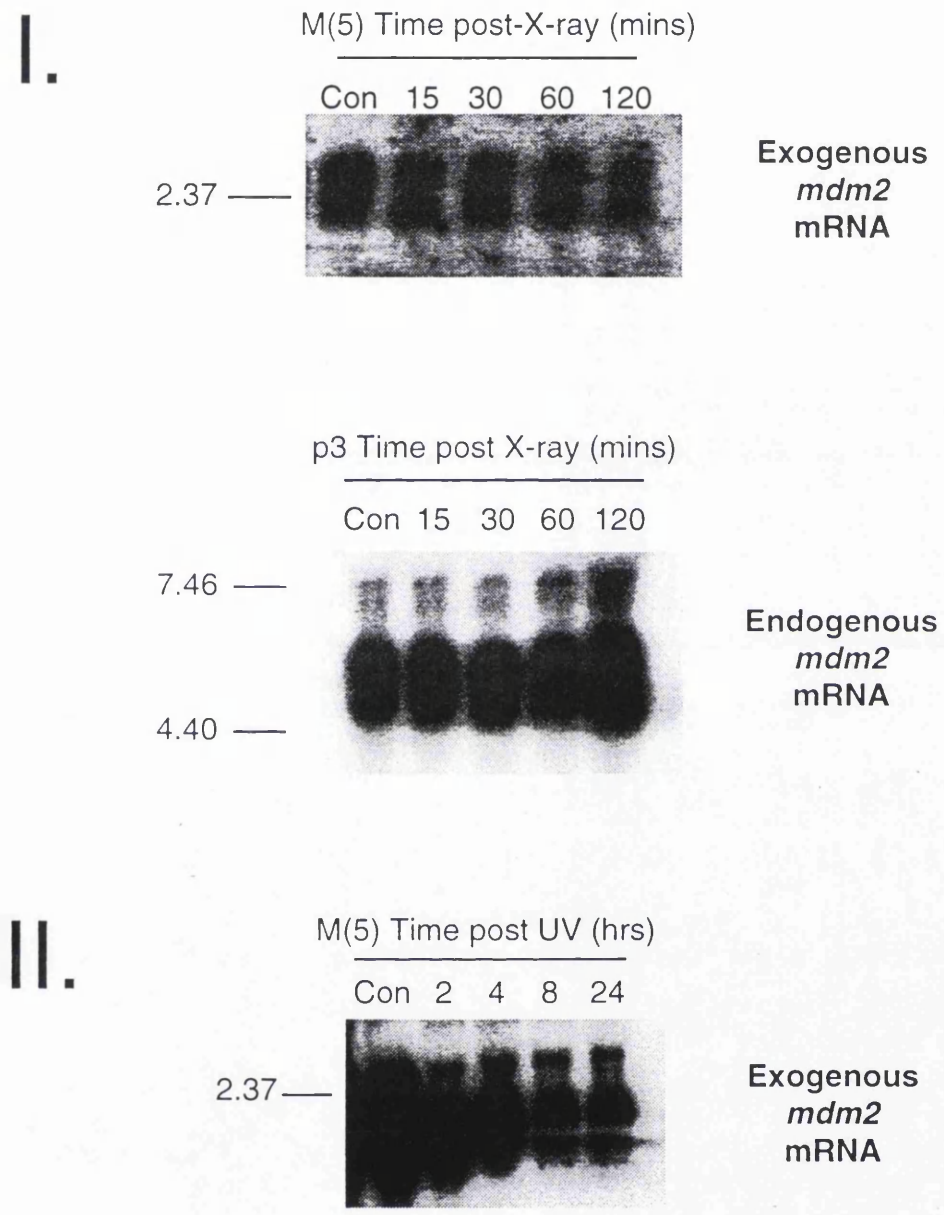

Figure 2.30. Northern analysis of irradiated cell lines reveal different responses. (I) 12 Gy X-ray-irradiation of exogenously (M[5]) and endogenously (p3) expressing U2OS cell lines reveal no reduction in *mdm2* mRNA; Vector-only (p3) and MDM2 overexpressing (M[5]) cell lines were X-ray-irradiated and examined by Northern blotting at different time points post-irradiation (as indicated) using random-hexanucleotide primed *mdm2* probes. (II) 30 Jm-2 UV-irradiation decreases expression of exogenously expressed *mdm2* mRNA; MDM2 overexpressing (M[5]) U2OS cells were UV-irradiated and examined by Northern blotting at different time points post-irradiation (as indicated) as above. Size markers are indicated on the left-hand side (kb).

Summary and Discussion

Comparison of UV- and X-ray-irradiated U2OS cells revealed differences in protein profiles that may determine the cellular outcome between apoptosis and cell cycle arrest. The question of how the MDM2 and p53 $175^{A\Rightarrow H}$ inhibitory effects on apoptosis and cell cycle arrest were addressed by analysing and comparing the protein profiles of parental, M(5) and DN(5) U2OS cell lines.

X-ray irradiation of M(5) cells revealed a delayed/reduced p21- and p53- induction response when compared to control p3 cells. The western analysis performed did not reveal whether the induced levels of p21 and p53 would have eventually obtained p3 levels. Therefore, differentiation between a delayed or attenuated response was not possible. Increased MDM2:p53 complexes through elevated MDM2 levels in M(5) cells and, hence reduced 'free' unbound p53, could explain the inhibition observed. Such increased complex formation would increase the likelihood of MDM2-mediated ubiquitin-dependent degradation (explaining the reduced stabilisation of p53) and increase the transcriptional inhibition of p53. Such transcriptionally inactive p53 would be unable to induce p53 target genes, such as p21. Nevertheless, an induction in both p53 and p21 protein levels was seen in M(5) cells, suggesting that cellular mechanism(s) capable of relieving any MDM2-mediated inhibition were functional in U2OS cells. Simple increases in MDM2 protein level may either take longer to inactivate or the system may be incapable of inhibiting all of the MDM2, hence, reflecting either a delayed or attenuated response, respectively.

In the case of DN(5) cells, reduced p21 expression was expected due to the dominant negative effect of non-DNA binding p53 $175^{A\Rightarrow H}$ on wild-type p53 and therefore its inability to transcriptionally transactivate *p21* transcription. However, regulation of *p21* gene transcription is complex, being regulated in response to a number of signals and transcription factors in a p53-dependent or -independent manner (reviewed(Gartel and Tyner 1999)). Therefore, p53-independent transcriptional activation could explain the presence of p21 in MG-63 and X-ray-irradiated DN(5) cells, in addition to partial retention of wild type p53 functions. E2F-1 strongly transactivates *p21* transcription(Hiyama, Iavarone et al. 1998; Gartel and Tyner 1999) and induced *p21* transcription in melanocytes(Halaban,

Cheng et al. 1998) and melanomas(Trotter, Tang et al. 1997). In light of the UV-mediated increase in E2F-1 protein levels seen in all of the cell lines examined (see Figure 2.29) only OSA cells revealed a concomitant increase in p21 protein levels. Such results suggested that the E2F-1-p21 pathway was either mutated in U2OS cells or sensitive to inhibition by UV-irradiation.

Taking the DN(5) and M(5) cell observations together, there seemed a link between abrogation of p21 induction and attenuation of the X-ray-mediated G_1/S cell cycle. Such findings place p21 as key effector of this checkpoint and p53 as its key regulator. In contrast, retention of the G_2/M checkpoint in both M(5) and DN(5) cells, suggested that p21 had no role in mediating such a cell cycle arrest in X-ray-irradiated U2OS cells. Steady state levels of p21 were severely reduced in p53 $175^{R\Rightarrow H}$ expressing clones in comparison to parental U2OS, while induction of p21 upon X-ray irradiation was severely attenuated, but did show a small increase. Such an increase can be explained through increased X-ray-irradiated-induction of wild-type p53, squelching out p53 $175^{R\Rightarrow H}$ inhibition and increasing the likelihood of wild-type homotetramerisation and formation of transcriptionally-active DNA-binding forms. Another possibility could depend on p53-independent induction of p21 transcription, which has been reported by in a number of cell lines(Wagner, Kokontis et al. 1994; Macleod, Sherry et al. 1995; Gartel and Tyner 1999). Examination of the stabilisation of p53 was not possible due to the very high expression levels of p53 in DN(5). Upon exposure to ECL film the film's maximum exposure threshold was rapidly reached, preventing detection of any further increases.

X-ray irradiated M(5), DN(5), U2OS and OSA cells exhibited transient reductions in both endogenous and exogenous expressed MDM2 protein levels 30 minutes – 1 hour post-irradiation. A number of other cell lines also exhibited the same molecular response, suggesting that this was not just unique to the U2OS cell line. The occurrence in DN(5) and HOS cells containing mutant p53, suggested that it was not p53-dependent and affected MDM2 protein expression whether derived from the p53-dependent (P1) or –independent (P2) mdm2 promoter (see Introduction).

A transient reduction in MDM2 protein may have lead to decreased MDM2-mediated p53 degradation and a concomitant rapid induction in p53 protein levels. However, a drastic burst of p53 induction was not seen and both p53 and MDM2 protein levels increased simultaneously after the reduction in MDM2 levels. Transient reductions in MDM2 levels may also generate a temporal window for achieving a temporal 'burst' of non-MDM2 complexed p53 activity; facilitating transcriptional induction/repression of p53 target genes or protein-protein interactions. Such an event may facilitate activation of components of the cell cycle arrest machinery, such as p21. Furthermore p53 stabilisation events may occur, when p53:MDM2 complexes are reduced, leaving uncomplexed p53 available for stabilising modifications to prevent re-association with MDM2.

X-ray irradiation has been reported to inhibit transcription, altering the chromatin DNA and chromatin topology(Ljungman and Hanawalt 1992; Ljungman and Hanawalt 1995) and causing nicks in the DNA(Luchnik, Hisamutdinov et al. 1988). However, Northern analysis of X-ray-irradiated M(5) and p3 cells revealed no reductions in *mdm2* expression, suggesting that the MDM2 dip was the result of post-transcriptional mechanism(s). Evidence for a potential ≅50 kDa MDM2 cleavage or alternative splice product was sometimes apparent in X-ray-irradiated M(5) cells, coinciding with the reduction in the 90kDa MDM2 species. Interestingly, MDM2 has been reported to be processed by caspase-3 in apoptotic and non-apoptotic cells and contains a carboxyl-terminal caspase site, which upon cleavage yields a ≅60 kDa cleavage product(Chen, Marechal et al. 1997; Pochampally, Fodera et al. 1998; Pochampally, Fodera et al. 1999). The X-ray-mediated MDM2 reduction is investigated in later sections.

The extremely transient nature of the MDM2 reduction could reflect the need to generally restrain p53 activity, perhaps to prevent generation of apoptotic signal(s). However, these results suggested that MDM2-mediated degradation of p53 was negatively regulated throughout the time course analysed.

E2F-1 protein levels peaked in all four cell lines approximately eight hours post-irradiation along with the recovery and induction of MDM2 levels. Such co-induction may be totally co-incidental, although in light of the reported MDM2:E2F-1 protein interaction and

augmentation of E2F-1 activity, a functional link is possible. However, E2F-1's role as a mainly pro-apoptotic protein and promoter of S-phase conflicts with the FACS observations of cell cycle arrest in the absence of apoptosis. Nevertheless, the subsequent reduction in E2F-1 levels may have prevented the cell from entering an apoptotic process.

Examination of p53 Ser^{15} phosphorylation in OSA, M(5) and U2OS cells revealed no detectable increases following X-ray irradiation, although a small and faintly detectable increase in X-ray-irradiated U2OS had been detected previously (see Section 2.20). Antibody ageing could explain the lack of detection, as increased protein loads also generated no signal. However, DN(5) cells exhibited easily detectable control levels of phosphorylated p53 Ser^{15}, which was greatly elevated following irradiation. Alterations in general p53 expression levels in DN(5) cells were extremely difficult to determine due to extremely high levels, although no obvious effects were seen upon X-ray irradiation. This result shows that mutant p53 $175^{R \Rightarrow H}$ presents itself as an efficient target for Ser^{15} phosphorylation and could occur in the absence of increasing p53 levels. Such excessive levels of p53 phosphorylation may simply reflect the elevated p53 levels in DN(5) cells, or a desperate cellular overcompensation event in an attempt to bring about a cell cycle arrest through hyper-phosphorylation of p53. Due to the inability to detect Ser^{15} phosphorylation in other cell lines it was impossible to determine whether increasing p53 Ser^{15} occurred in the other cell lines and hence mirrored the trend seen in DN(5) cells. The role of Ser^{15} phosphorylation and its effect on MDM2:p53 association shall be covered in later sections.

No alterations in the protein levels of pRB occurred following X-ray-irradiation. It was expected that through the increasing p21 levels and subsequent CDK-inhibition, pRB's phosphorylation status would have been altered. Surprisingly, no shift in apparent molecular weight was evident, suggesting that X-ray-mediated cell cycle arrest and p21 itself was not affecting pRB's phosphorylation status. Therefore p21's role as a CDK-inhibitor, with respect to pRB-kinases, may not have brought about the irradiation-induced cell cycle arrest. Alternatively, p21's alternative role as an inhibitor of PCNA function may have facilitated the G_1/S arrest.

UV-irradiated M(5) cells revealed a slight delay/reduction in p53 induction in comparison to p3 cells. Similar observations were seen in X-ray irradiated M(5) and p3 cells, although the

difference was less marked than the X-ray-response (see Figure 2.22). This delay in induction again can be attributed to MDM2 mediated inhibition of p53 accumulation, most probably through increased degradation of p53 or perhaps MDM2-mediated steric hindrance of stabilisation sites.

UV-mediated loss of p21 was observed in both M(5) and p3 cells, suggesting that p21 was not providing any of the anti-apoptotic/delaying effects seen in M(5) cells upon FACS analysis. UV-irradiation of OSA cells revealed, in contrast to M(5) and p3 cells, a delayed upregulation of p21 protein. TUNEL analysis revealed a significant degree of apoptotic cells 72 hours post-irradiation, although significantly lower than U2OS cells. Such differences in the extent of apoptosis may be reflected in the increased levels of anti-apoptotic p21 in OSA cells 24 hours post-irradiation. However, the drastic induction of p21 at 24 hours post-irradiation did not prevent apoptosis, but merely delayed it relative to the UV-irradiation response of U2OS. Furthermore, the anti-apoptotic role of p21 cannot be applied to DN(5)'s apoptotic delay, as p21 levels were undetectable throughout a 24 hour time course

The previously observed reduction of MDM2 levels in U2OS following UV-irradiation was also evident in a number of cell lines, including M(5) and DN(5). OSA cells, likewise showed a reduction in MDM2 levels which, unlike M(5), DN(5) and U2OS cells, recovered to control levels 24 hours post-irradiation. Long-term reductions in MDM2 levels, in comparison to the X-ray-mediated transient reduction, may generate a longer temporal window of opportunity for p53 activation. This may reflect the need for 'free' non-MDM2-complexed p53 to orchestrate a major active-cellular process, such as apoptosis. Alternatively, MDM2 may be providing a p53-independent anti-apoptotic function that needs to be removed, explaining why M(5) cells were more resistant to apoptosis than p3 cells. However, the same explanation cannot be applied to DN(5) cells which exhibited the lowest levels of MDM2, but the highest degree of apoptosis protection.

UV-mediated reduction of MDM2 occurred with exogenously and endogenously expressed MDM2, in M(5) and U2OS, OSA and DN(5), respectively. Furthermore MDM2 was lost post-UV-irradiation in a p53-independent manner, in DN(5) cells. These observations suggested that the reduction mechanism was independent of specific transcriptional control, but could be attributed to more general transcriptional inhibition. Northern analysis also showed that

both exogenous and endogenous *mdm2* mRNA was reduced following UV-irradiation. However, in the case of exogenous *mdm2*, significant amounts of mRNA were still present, suggesting that in addition to reduced transcription, translational and post-translational mechanisms may have also contributed to MDM2's loss of expression. A potential candidate for the non-specific reduction in *mdm2* mRNA could lie in UV-mediated pyrimidine dimer formation leading to transcriptional stalling and decreased rates of transcription(Mellon, Spivak et al. 1987; Donahue, Yin et al. 1994).

UV-mediated general transcriptional inhibition of *mdm2* mRNA remained a viable explanation for the loss of MDM2 protein expression. However, no loss of *p21* mRNA expression was observed, therefore failing to explain the loss of p21 protein expression (see Figure 2.21). The differential UV-responses between *p21* and *mdm2* mRNA and between exogenous and endogenous *mdm2* expression may be linked to differences in gene size. An obvious link between gene size and the number of UV-induced pyrimidine dimers exists, where smaller genes, unless extremely pyrimidine-rich, should suffer less pyrimidine-dimer formation than larger genes. Hence, smaller genes should suffer less UV-mediated damage and therefore be repaired quicker. An additional layer of control is determined by the transcription-coupled nucleotide excision pathway (NER), where the rate of gene transcription could determine the rate of DNA damage detection and therefore influence the rate of repair(Kolodner and Marsischky 1999).

The exogenously expressed *mdm2* cDNA and the sequences required for its expression, including the CMV-promoter, rabbit β-globin ribosome-entry site and polyadenylation terminator sequences, comprises ≅4 kb. Human *mdm2* must be at least equivalent to or greater than the ≅5.5 kb size of the mRNA transcript detected by Northern analysis (see Figure 2.21). Considering that the endogenous ≅5.5kb mRNA most probably represents an intronless-transcript (the murine *mdm2* gene ≅25kb(Jones, Ansari-Lari et al. 1996; Montes de Oca Luna, Tabor et al. 1996)), the human *mdm2* gene must be significantly larger than the exogenous *mdm2* target site of ≅4 kb. Hence, the endogenous *mdm2* gene would, in theory, suffer greater pyrimidine-dimer formation than the smaller exogenous mdm2 expression cassette. This combined with the potential presence of multiple sites of exogenous *mdm2* integration in M(5) cells, was the most likely explanation for the continued

expression of exogenous of *mdm2*. Additional differences between the endogenous and exogenous mRNA stability and translatability could also explain the perseverance of exogenous MDM2 mRNA and protein expression, respectively.

Although UV-damaged DNA would inhibit transcription, DNA repair mechanism should, in theory, be able to repair such DNA damage within 24 hours(Ljungman and Zhang 1996). UV-mediated reduction of DNA repair, perhaps reflecting the shut down of certain process in an apoptotic cell, may explain the permanent UV-mediated loss of endogenous and exogenous mRNA transcripts. An interesting observation was the re-occurrence of MDM2 protein in OSA cells levels 24 hours post UV-irradiation, suggesting that *mdm2* mRNA expression had resumed.

MDM2 was initially reported to be induced by UV-irradiation in a p53-dependent manner(Perry, Piette et al. 1993). However, MDM2 induction was delayed when the cells were irradiated with a higher UV dose (20 Jm^{-2}) and correlated with the recovery of DNA synthesis and entry into S-phase. Similar delayed MDM2 induction was observed in 20 Jm^{-2} UV-irradiated primary REF cells, with MDM2 induction occurring 8-12 hours post-irradiation(Wu and Levine 1997). Examination of mRNA levels post-UV-irradiation (20 Jm^{-2}) showed that *mdm2* mRNA decreased and then increased in parallel with MDM2 protein levels(Wu and Levine 1997), while *p21* showed an immediate induction of mRNA levels. *GAPDH* mRNA levels also showed no alterations in levels, suggesting that non-specific, UV-mediated inhibition of RNA pol II was not occurring. Low-dose UV-irradiation generated immediate induction of both *mdm2* and *p21* mRNAs, suggesting that UV-dose was a critical factor affecting *mdm2* expression. Similar UV-mediated *mdm2* mRNA and protein levels were observed in p53-null cells, although subsequent mRNA or protein induction was not seen.

The lack of high dose UV-mediated reduction in *p21* and *GAPDH* mRNA levels, suggested that *mdm2* mRNA induction was initially selectively suppressed(Wu and Levine 1997). Actinomycin D-chase experiments, revealed that UV-irradiation did not affect *mdm2* mRNA stability. Therefore, such suppression was perhaps mediated by a UV-inducible factor capable of blocking p53 binding to the UV-(Saucedo, Carstens et al. 1998) and p53-inducible(Juven, Barak et al. 1993; Wu, Bayle et al. 1993) P_2 promoter or simply repressing

mdm2 expression. The latter model seems more likely, due to both high- and low- dose UV-irradiated p53 binding to an *mdm2* gene fragment containing the two p53 binding sites, with the same degree(Saucedo, Carstens et al. 1998).

In addition to the general inhibition of MDM2 expression seen with high-dose UV-irradiation, low-doses of UV (4 Jm^{-2}) induced, in a p53-dependent manner, a 76 kDa murine MDM2 protein in wild-type p53 MEFs(Saucedo, Myers et al. 1999). This 76 kDa MDM2 protein sub-species was generated from alternative splicing of exon three or an internal translational-initiation event. Therefore, UV-irradiation has the potential to create a non-p53 binding MDM2 protein, with the potential for loss and/or gain of function.

Overall, UV-irradiation is capable of reducing and inducing MDM2 protein levels, which may reflect cell type specificity (including sensitivity to UV) and dosage. UV-irradiation also mediates alterations in MDM2's functional capabilities, affecting *mdm2* mRNA alternative splicing.

Evidence for active MDM2 degradation following X-ray irradiation

Northern analysis revealed that the transient dip in MDM2 protein levels present in a variety of cell lines, was not due to transcriptional downregulation of *mdm2* mRNA. Furthermore, the large reduction in the exogenously expressed pCMV-driven MDM2 protein in M(5) cells, also suggested that the dip was not due to specific transcriptional control. The role of p53 in mediating the dip was also unlikely due to a clear MDM2 dip in the mutant p53-containing cell lines (HOS and DN[5]). The presence of the transient dip in a number of other cell lines also suggested that this was not a property unique to U2OS cells. The dip may have simply reflected physical damage to non-transcriptional components of the cellular expression machinery (translational and post-translational) inhibiting its ability to express MDM2 protein. To partially address this question cycloheximide and lactacystin were used in an attempt to determine whether the dip was an active process or simply a passive consequence of cellular damage.

Lactacystin increases MDM2, p21 and p53 protein expression

Eight hours treatment with 10μM lactacystin (a non-reversible inhibitor of the proteosome(Fenteany and Schreiber 1998)) was shown to increase MDM2 protein levels in M(5), U2OS and OSA cells, while no increase was seen in DN(5) cells (see Figure 2.31). Additionally, MDM2 induction in M(5) and OSA cells seemed more dramatic in comparison to the increase seen in p3 cells, although accurate relative increases were not measured. A concurrent increase in p53 and p21 levels was also observed in all four cell-lines. However, the induction of p21 and p53 seen in the mutant p53 $175^{R\Rightarrow H}$ expressing DN(5) cell line was severely attenuated in comparison to the p3 response. These results suggested that all three of the examined proteins were directly or indirectly upregulated through lactacystin-mediated inhibition of proteosome function.

Lactacystin treatment supports a potential X-ray-dependent degradation event

In an attempt to determine whether lactacystin-mediated stabilisation of MDM2 could counteract the X-ray-mediated MDM2 reduction seen 30 minutes post-irradiation, M(5) cells were treated with lactacystin and X-ray irradiation. Lactacystin has been reported to induce apoptosis in a variety of cell lines (Imajoh-Ohmi, Kawaguchi et al. 1995; Delic, Masdehors et al. 1998; Grimm and Osborne 1999; Kitagawa, Tani et al. 1999; Wagenknecht, Hermisson et al. 1999), so minimal exposure times were required to reduce the influence of any apoptotic effects. Cells were therefore treated with 10μM lactacystin or DMSO for four hours and then either mock or X-ray-irradiated and samples were taken 30 minutes post-irradiation. X-ray irradiation of lactacystin pre-treated cells revealed a reduction in MDM2 levels in comparison to lactacystin-only treated cells, suggesting that the X-ray-mediated reduction was somewhat inhibited (see Figure 2.32 [I]). Furthermore, X-ray-irradiated lactacystin-treated cells exhibited elevated MDM2 levels in comparison to non-lactacystin treated, X-ray irradiated cells, suggesting that lactacystin-treatment was partially attenuating the X-ray-mediated reduction. Use of both MDM2 2A10 and N-20 antibodies revealed the same results. The experiment was also carried out in p3 cells, revealed the same pattern as

M(5) cells (see Figure 2.32 [II]), suggesting that both exogenously and endogenously expressed MDM2 were similarly affected.

Overall these results suggested that X-ray irradiation reduced MDM2 through both proteosome-dependent and -independent routes of degradation, although incomplete inhibition of the proteosome or translation could not be ruled out.

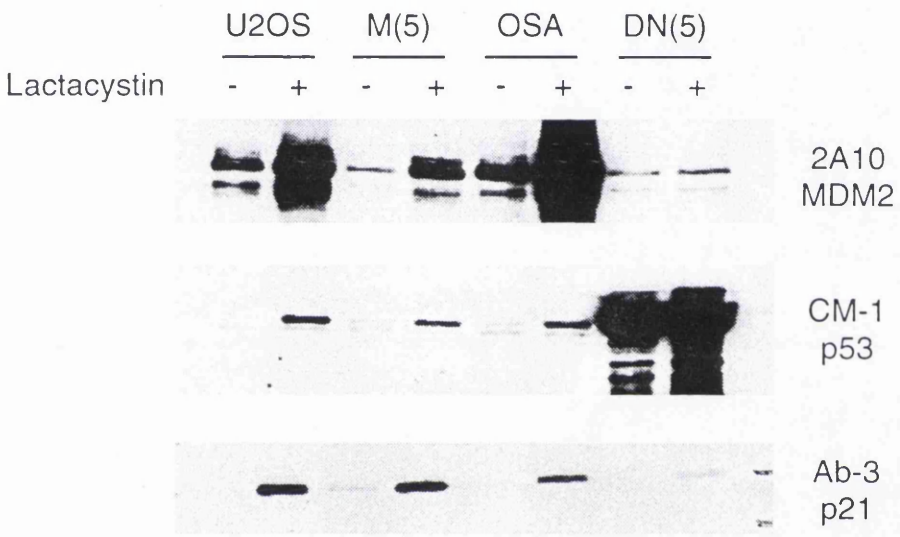

Figure 2.31. Lactacystin increases the expression of a number of cellular proteins. Parental, MDM2 overexpressing (M[5]) and p53 175R⇒H)DN[5]) U2OS clones and OSA cells were treated for eight hours with 10 μM lactacystin (+) or DMSO only (-) and examined by Western blotting for different cellular proteins (as indicated).

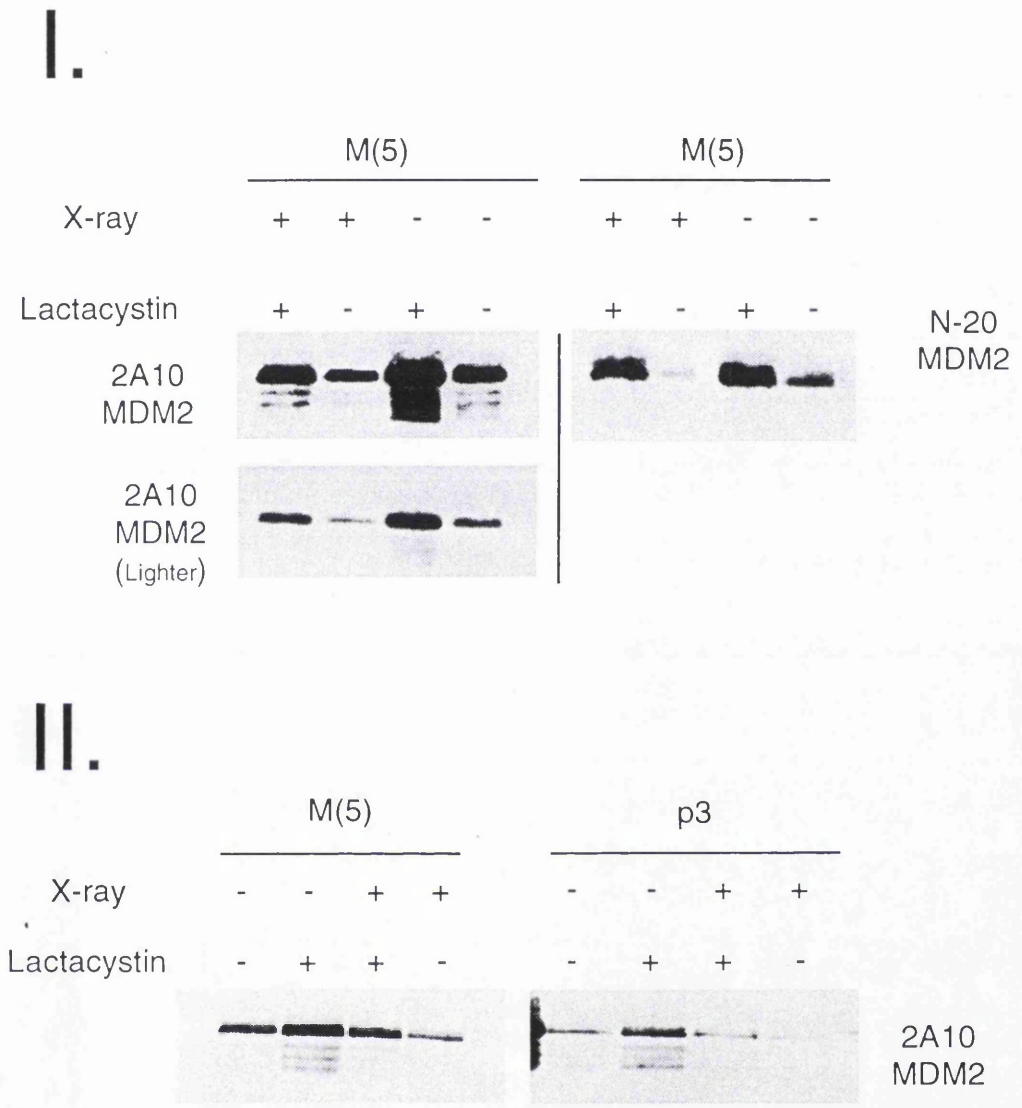

Figure 2.32. Lactacystin partially abrogates the X-ray-mediated reduction in MDM2 protein levels. (I) MDM2 overexpressing U2OS cells (M[5]) cells were treated with 10μM lactacystin (+) or DMSO (-) for four hours prior to 12 Gy X-ray-irradiation (+) or mock-irradiation (-) and subsequent lysis 30 minutes post-irradiation. Samples were then examined by Western blotting for MDM2 with two different antibodies, 2A10 and N-20 (as indicated). A lighter exposure of the 2A10 Western analysis is also shown (lighter). (II) Vector-only (p3) and MDM2-overexpresing U2OS cells were treated as above and compared by Western analysis.

Cycloheximide treatment reveals both a potential X-ray-dependent MDM2 degradation event and the need for translational control in p53 induction

As X-ray-irradiated Northern data of U2OS and M(5) cells revealed no obvious reduction in *mdm2* mRNA levels, X-ray-mediated inhibition of translation could have explained the reduction in MDM2 protein levels. Therefore, cycloheximide (CHX), a potent inhibitor of translational polypeptide-chain elongation(Oleinick 1977) was used to determine maximal inhibition levels of MDM2 translation. With MDM2 translation totally inhibited any X-ray mediated translational effects would not cause any additional reductions in MDM2 protein levels, while any post-translational effects would.

Treatment of M(5) cells with 10 and 100 μg/ml of CHX revealed similar levels of protein reduction two hours post treatment. Such results suggested that maximal levels of inhibition had been achieved using 10μg/ml. Therefore, M(5) cells were treated with 10μg/ml CHX for two hours, irradiated with 12 Gy X-ray irradiation and then lysed for Western analysis 0.5, 1 and 4 hours post-irradiation.

Comparison of CHX- and X-ray-irradiated cells with untreated cells revealed a reduction in MDM2 levels, with CHX causing the greater reduction (see Figure 2.33). However, dual-treated (CHX and X-ray-irradiated) cells exhibited even lower levels of MDM2 than CHX-treated cells alone, suggesting that CHX and X-ray irradiation could co-operate in reducing MDM2 levels. A similar pattern was seen with the ≅90kDa MDM2 protein with both MDM2 2A10 and N-20 antibodies. In contrast an N-20-reactive ≅60kDa band showed no alterations in expression levels following any treatment.

Overall these results suggested that a post-translational mechanism was contributing to the X-ray-induced loss of MDM2 expression.

In addition to MDM2 analysis, p53 and p21 levels were examined post-irradiation. Both proteins' levels reduced upon the addition of cycloheximide, revealing the importance of either transcriptional or translational regulation in the maintenance of their steady state

protein levels. Furthermore, p53 and p21 induction was severely attenuated four hours post-irradiation, with protein levels below that of untreated control levels. These results directly support the importance of translational regulation of p53 and p21 in response to X-ray irradiation, rather than just being reliant upon protein stabilisation.

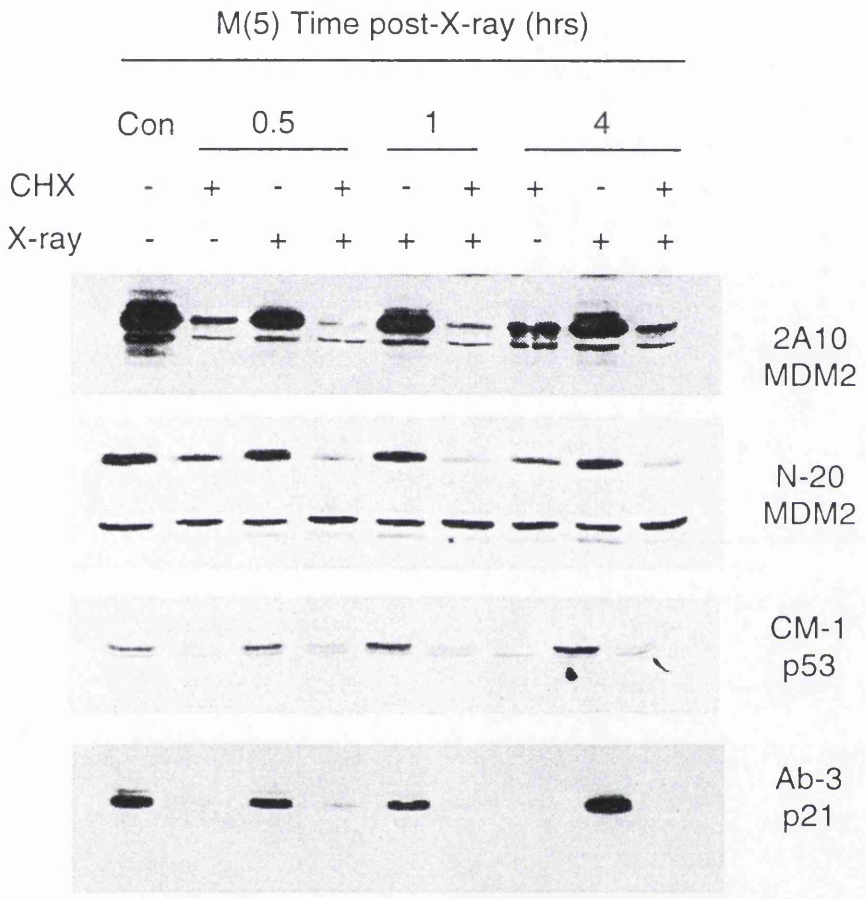

Figure 2.33. Cycloheximide fails to prevent the X-ray-mediated reduction in MDM2 protein levels. MDM2 overexpressing (M[5]) U2OS cells were treated with 10μg/ml cycloheximide (+), or not (-), for two hours and then either 12 Gy X-ray- (+) or mock (-) –irradiated and lysed at various time points post-irradiation (as indicated). Samples were then examined by Western blotting for MDM2 with two different antibodies, 2A10 and N-20 and other cellular proteins (as indicated).

Lactacystin and cycloheximide analysis of p21 reveals a potential UV-mediated p21-degradation event

U2OS cellular p21 protein expression was reduced in response to UV-irradiation, while no reduction in *p21* mRNA expression was apparent (see Figure 2.19 and 2.21, respectively). As with the X-ray mediated reduction in MDM2 expression, irradiation-mediated inhibition of translation or active degradation could have accounted for the loss of p21 expression. Therefore, as with the X-ray analysis, lactacystin and CHX were used to determine the UV-irradiation mechanisms involved.

U2OS cells were either treated with 10μM lactacystin or 10μg/ml CHX for four hours prior to UV- or mock-irradiation and samples were then taken two and six hours post-irradiation (see Figure 2.34 [I]). As seen before, lactacystin increased p21 expression, while UV-irradiation reduced it. Dual-treated (lactacystin and UV-irradiated) cells showed intermediate levels of p21 expression, suggesting that lactacystin-mediated inhibition of the proteosome partially counteracted the UV-mediated loss of p21 expression. CHX analysis revealed a reduction in p21 protein levels two hours after CHX addition (see Figure 2.34 [II]). Furthermore, dual-treated (CHX and UV-irradiated) cells showed a massive reduction in p21 protein levels. Comparison of the UV- and dual-treated cells revealed lower p21 levels in the dual-treated cells, suggesting that UV-irradiation and CHX could co-operate in the reduction of p21 protein expression. These results suggested that UV-irradiation was mediating a post-translational reduction in p21 levels.

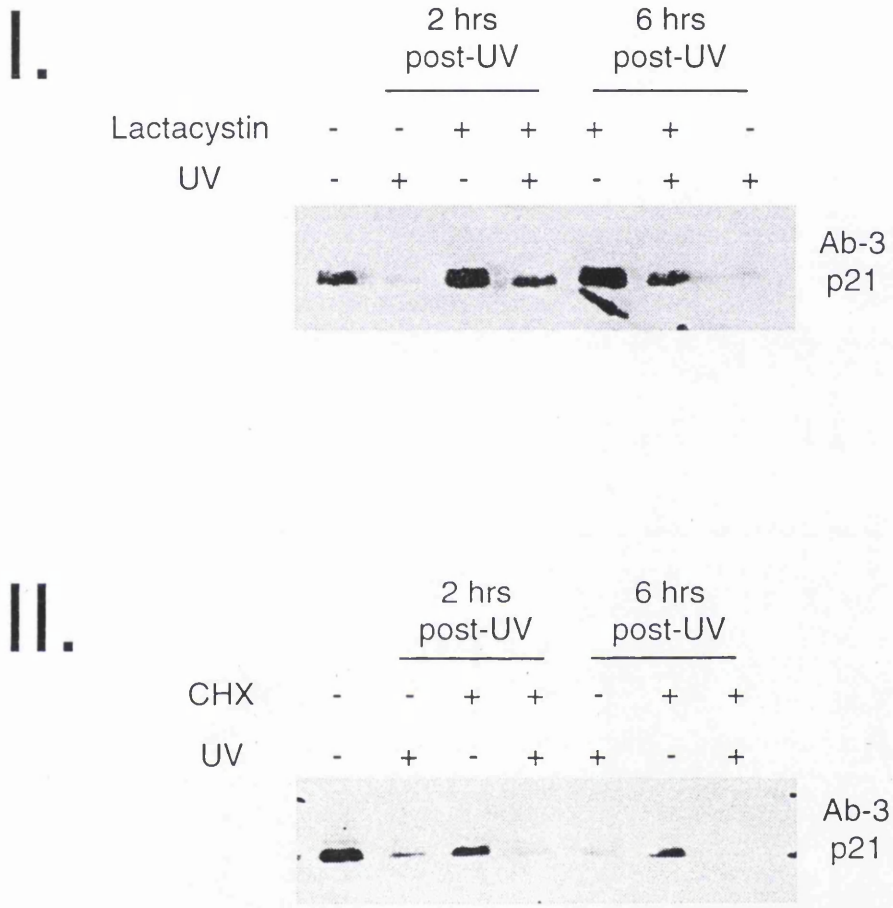

Figure 2.34. Lactacystin and cycloheximide analysis supports a UV-mediated p21 degradation event. (I) MDM2-overexpressing (M[5]) U2OS cells were treated with 10μM lactacystin (+) or DMSO (-) for four hours prior to 30 Jm-2 UV(+)- or mock (-)-irradiation and lysed at various time points post-irradiation (as indicated). Samples were then examined by Western blotting for p21. (II) MDM2-overexpressing (M[5]) U2OS cells were treated with 10μg/ml cyclohexmide (+), or not (-), for two hours prior to 30 Jm-2 UV(+)- or mock (-)-irradiation and lysed at various time points post-irradiation (as indicated). Samples were then examined by Western blotting for p21.

Forced overexpression of p21 delays apoptosis

Transcriptional-independent and potentially active degradative loss of p21 levels was evident in UV-mediated apoptotic U2OS cells (see earlier sections). Therefore, the importance of reduced p21 protein levels in the UV-mediated cellular response of U2OS was investigated. Many previous reports had shown that overexpression of p21 could protect cells from apoptotic stimuli(Gorospe, Cirielli et al. 1997; Bissonnette and Hunting 1998; Allan and Fried 1999). Lindsey Allan had generated a number of Ponasterone A (Pon A)-inducible p21 stable U2OS cell lines (pIND p21 [1-3]), which upon Pon A addition underwent a G_1/S and G_2/S cell cycle arrest (see Figure 2.35 [I]).

Western analysis of Pon A-induced and mock-treated pIND p21 clones revealed a significant increase in p21 protein levels and a concomitant loss of hyperphosphorylated pRB (see Figure 2.35 [II]). PonA-induced clones also showed the emergence of a lower molecular band of ≅16 kDa, which was not present in mock-treated cells. Interestingly, upon p21 induction E2F-1 levels decreased.

Pon A-induced pIND p21 (1) cells overexpressing p21 24 hours prior-to- and 30 hours post-30 Jm^{-2}-UV-irradiation, significantly reduced apoptosis in comparison to un-induced pIND p21 (1) control cells (see Figure 2.36). However, apoptosis was only delayed, as increasing TUNEL-positive cells and apoptotic cells were visually evident by 120 hours post-irradiation, supporting previous findings(Allan and Fried 1999).

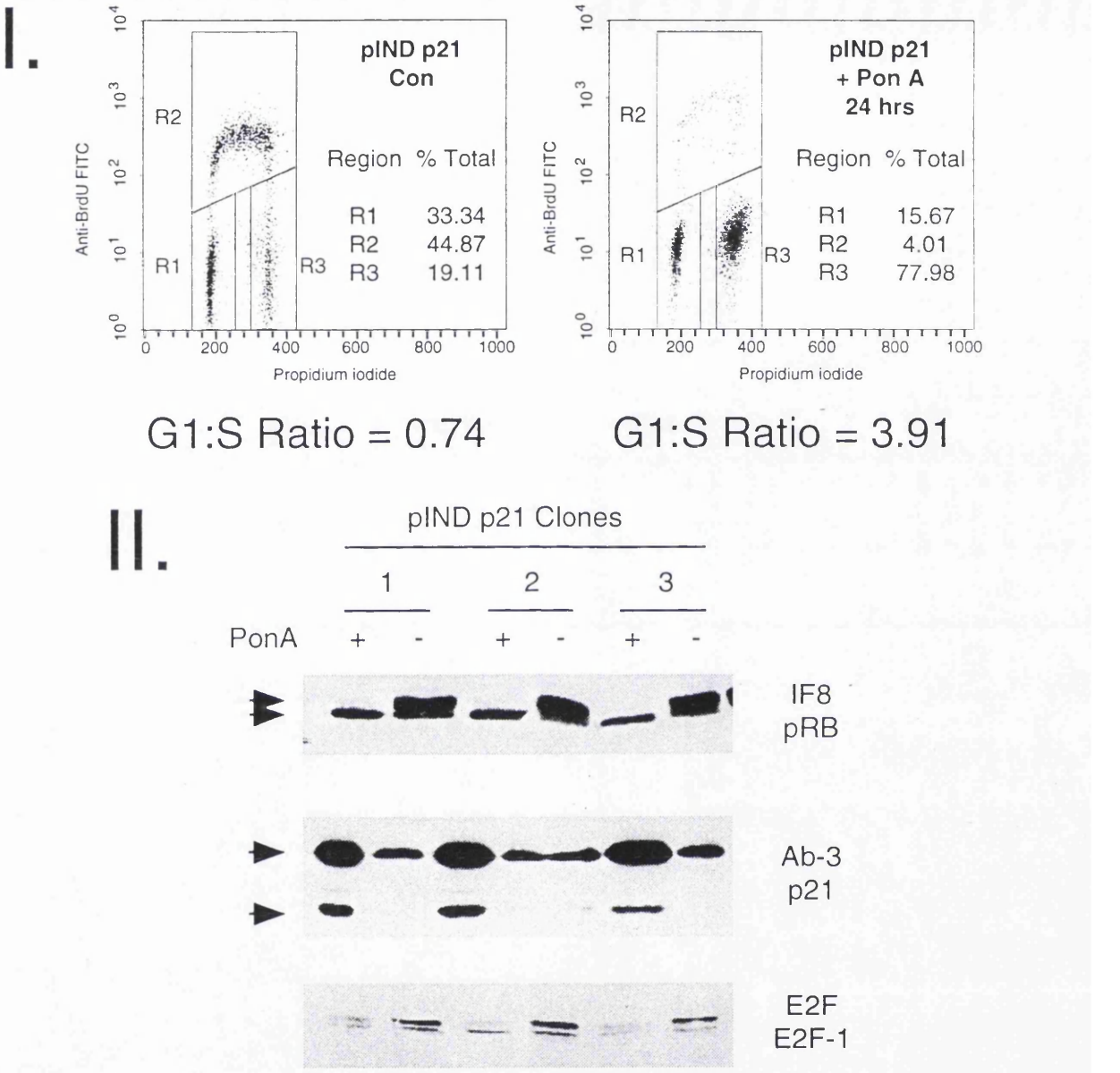

Figure 2.35. Ectopic p21 overexpression induces pRB hypophosphorylation and a G1/S and G2/M cell cycle arrest. (I) Ectopic p21 overexpression induces a G1/S and G2/M cell cycle arrest; pIND p21 (2) U2OS cells were PonA-induced (as below) and analysed by BrdU analysis 24 hours post-treatment. (II) Enforced p21 overexpression suppresses pRB hyperphosphorylation and E2F-1 protein levels; pIND p21U2OS clones were either treated with 5μM Ponasterone A (PonA) (+) or ethanol (-) and analysed by Western blotting 24 hours post-treatment for different cellular proteins (as indicated). Hyper-(upper) and hypo-(lower) phosphorylated pRB are indicated with arrowheads; as are the full-length (upper) and a potential 16kDa p21 cleavage product (lower).

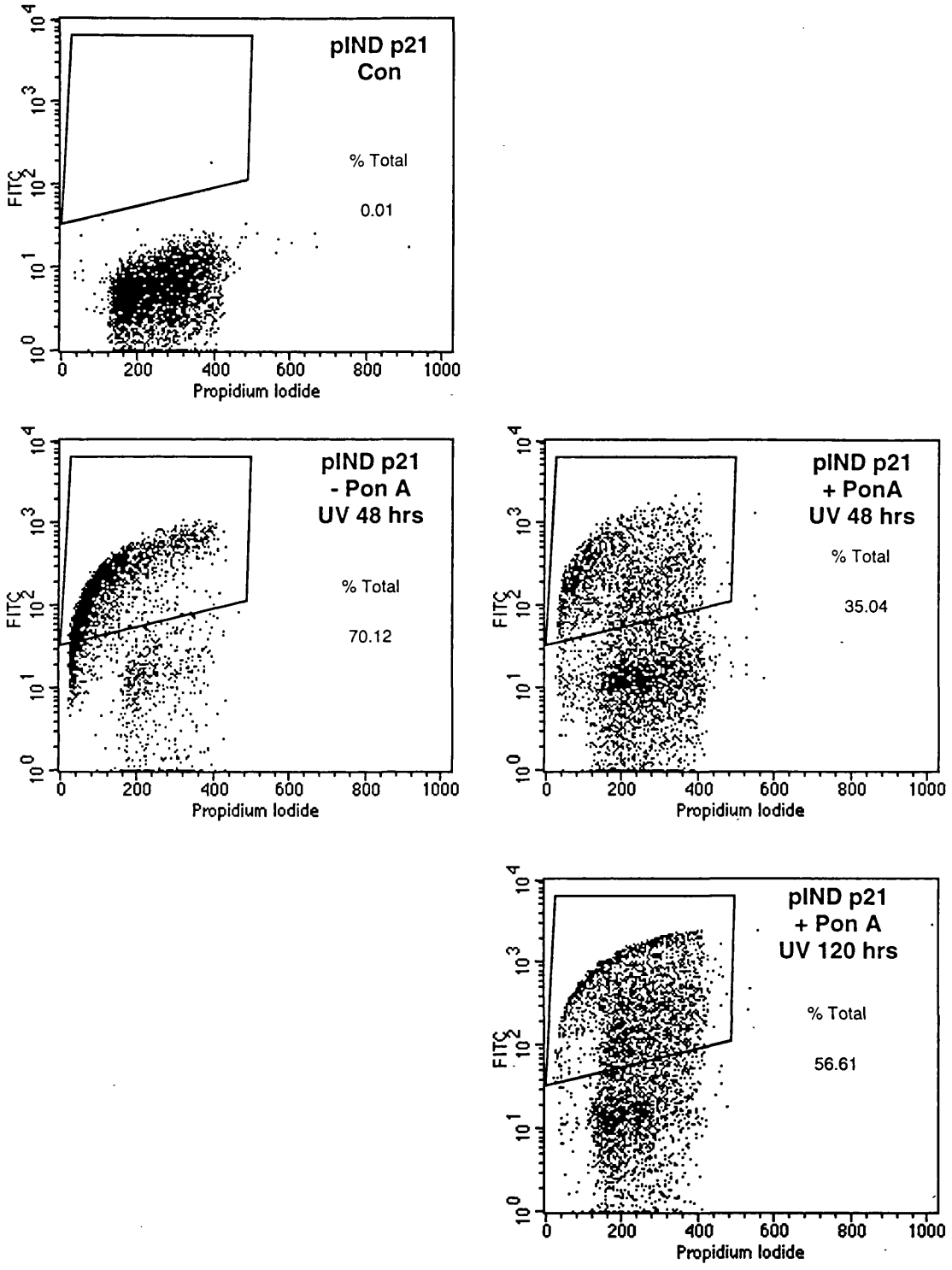

Figure 2.36. Ectopic p21 overexpression delays 30 Jm-2 UV-mediated apoptosis in U2OS cells. pIND p21U2OS clones were either treated with 5μM Ponasterone A (PonA) (+) or ethanol (-) and 30 Jm-2 UV-irradiated. Fresh PonA was added every 24 hours (where necessary) and BrdU analysis was carried out on cells at various time points (as indicated).

Summary and Discussion

Lactacystin treatment generally increased the levels of MDM2, p21 and p53 in three wild-type p53 expressing cell lines (OSA, M(5) and p3). In contrast, DN(5) cells only exhibited slightly increased p21 and p53 levels, while no affect was seen on MDM2 protein levels. The transcriptional-compromised state of p53 $175^{R\Rightarrow H}$, suggests that the MDM2 increases seen in the wild-type p53 cells was due to p53-mediated transcriptional- or perhaps, translational-upregulation of *mdm2* mRNA. Therefore, MDM2 may not be a true degradation target of the proteosome, which has been suggested(Chang, Lee et al. 1998). However, deletion and mutation analysis of MDM2's RING-finger domain stabilised MDM2 expression(Kubbutat, Ludwig et al. 1999) and supported a role for MDM2-ubiquitination as a degradatory mechanism. A possible explanation for this observation being abrogation of auto-ubiquitination, as seen with the other E3 ubiquitin-protein ligase, E6-AP(Nuber, Schwarz et al. 1998). The large increase seen in exogenous-expressing MDM2 M(5)-cells could have been attributed to p53-dependent increases of the endogenous MDM2 protein, rather than inhibited degradation of the exogenous MDM2.

In support of the idea of p53-mediated induction of MDM2, lactacystin-treated OSA cells showed a massive accumulation of MDM2, which may have reflected its amplified *mdm2*-gene status(Florenes, Maelandsmo et al. 1994). In such a situation increases in p53 levels may facilitate huge increases in *mdm2* expression, due to rate-limiting levels of p53 available for promoter binding no-longer being a factor.

In contrast to MDM2, the p53-upregulated p21 protein was slightly increased in lactacystin-treated DN(5) cells, suggesting that p21 may represent a *bona fide* proteosome-dependent target protein(Blagosklonny, Wu et al. 1996; Maki and Howley 1997; Fukuchi, Maruyama et al. 1999). Alternatively, a p53-independent mediated p21-induction or differential p53 DNA binding affinities to the *p21* and *mdm2* promoters could also explain the induction (see Introduction).

The observed UV-mediated loss of p21 protein expression could not be explained through the loss of *p21* mRNA. However, in addition to transcriptional and mRNA stability control

(see above), p21 is regulated at both translational and post-translational levels. Discordance between *p21* mRNA and protein levels in various cell lines upon genotoxic stress revealed the importance of post-transcriptional mechanisms in the expression of the p21 protein(Gudas, Nguyen et al. 1995; Macleod, Sherry et al. 1995; Lu, Burbidge et al. 1996; Butz, Geisen et al. 1998). Ubiquitin-dependent degradation of p21 may be influenced by p21's association with PCNA and CDKs(Cayrol, Knibiehler et al. 1998; Rousseau, Cannella et al. 1999) and the transcription factor, C/EBPα(Timchenko, Wilde et al. 1996; Timchenko, Harris et al. 1997), supporting a potential degradative role in regulating p21 protein levels.

Lactacystin partially blocked both the X-ray and UV-mediated reduction in MDM2 and p21 protein levels, respectively. Incomplete inhibition of the proteosome or conflicting lactacystin-mediated increases and proteosome-independent decreases in p21 levels could explain the partial effects. Similarly, cycloheximide analysis of the respective X-ray- and UV-mediated MDM2 and p21 degradation events, demonstrated the likely existence of a post-translational event mediating the reduction of both proteins. However, more efficient irradiation-mediated translational-inhibition downstream of the cycloheximide-mediated polypeptide chain-elongation step inhibition, could also explain the reduction in protein levels.

Interestingly, camptothecin treated (wild-type p53) A549 cell(Zhang, Fujita et al. 1999) or growth factor-deprived (wild-type p53) HUVEC cells(Levkau, Koyama et al. 1999) underwent apoptosis and exhibited caspase-mediated cleavage of p21 into a 15 kDa fragment. Cleavage of p21 during apoptosis resulted in loss of the carboxyl-terminal 52 amino acids(Levkau, Koyama et al. 1999; Zhang, Fujita et al. 1999), a region incorporating it's NLS(el-Deiry, Tokino et al. 1993), PCNA binding domain(Waga, Hannon et al. 1994) and recently identified second cyclin-binding site(Adams, Seller et al. 1996; Ball, Lain et al. 1997). Consistent with these observation, nuclear localisation, PCNA binding and the ability of carboxyl-terminal truncated p21 (p21ΔC) to inhibit both cell cycle progression and apoptosis were severely abrogated in comparison to wild-type p21(Levkau, Koyama et al. 1999; Zhang, Fujita et al. 1999). Therefore, caspase-mediated cleavage of p21 represents an alternative method to transcriptional-control of down-regulating p21 levels and overall function, perhaps facilitating apoptosis. Additionally, caspase-mediated cleavage of p21, as

with MDM2 (see Introduction), may allow modulation of p21's functional activities, creating potential competitive-inhibitors of wild-type function and possibly imbuing a gain of function.

Cycloheximide analysis also revealed the loss of X-ray-mediated p53 and p21 induction. The X-ray mediated induction of p21 was expected to abrogated due to the need for p53-mediated transcriptional upregulation of the *p21* gene. However, the majority of work concerning p53 induction in response to cellular stress has been shown to be a result of protein-stabilisation (see Introduction). However, in agreement with Fu *et al.*, 1999(Fu, Ma et al. 1999) these results suggested that for X-ray mediated p53-induction, translation of *p53* mRNA was required, rather than just protein stabilisation. One possible explanation for lack of protein stabilisation depends on the availability of p53 protein to be stabilised following cycloheximide block. The relatively short half-life of p53 in U2OS cells(Haupt, Maya et al. 1997; Kubbutat, Jones et al. 1997) may have resulted in complete loss of p53 protein expression, hence preventing protein stabilisation. However, faint p53-CM-1-reactive bands were visible in the cycloheximide-treated samples.

A note of caution surrounds all of the cycloheximide and lactacystin data, due to the global protein effects initiated through inhibition of translation and proteosome-dependent degradation, respectively. Alterations of the protein levels of various positive and negative regulators of protein could directly or indirectly alter the levels of the proteins analysed. Therefore, the lack of specificity creates an extremely complicated picture where clear conclusions can rarely be made.

Analysis of the Pon A-inducible p21 U2OS cell lines revealed that p21 overexpression was capable of mediating hypo-phosphorylation of pRB, suggesting that the p21:CDK:pRB pathway was intact. Interestingly, earlier work had shown that X-ray-irradiation of various cell lines caused the induction of p21, while no alteration in pRB phosphorylation was observed (see Figure 2.19 [1] and 2.26). In contrast, Pon A-induction of pIND p21 U2OS cells lead to the conversion of hyper- to hypo-phosphorylated pRB and initiated a cell cycle arrest. Therefore both X-ray- and Pon A-mediated p21 lead to a G_1/S and G_2/M cell cycle arrest, but only differentially affected pRB's phosphorylation status. Indirect X-ray-mediated p21 induction via p53 most probably triggers multiple effects, that may explain the difference seen with PonA-mediated direct p21-induction. Interestingly, ARF-mediated cell cycle arrest

has been reported to cause pRB hypo-phosphorylation in U2OS cells(Stott,. Bates et al. 1998). Therefore, these results suggest that the differences in pRB phosphorylation may reflect the differences between DNA damage and oncogene-mediated cell cycle arrest. Differential emphasis on p21's two major roles as a mediator of cell cycle arrest, namely, as an inhibitor of CDKs and PCNA, may explain the molecular differences and the overall cellular-outcome similarities. Additionally, the ectopic expression of p21 in pINDp21 U2OS cells may generate effects which are normally modulated with concomitant p53 induction.

Upon Pon-A induction of p21, pIND p21 U2OS cells revealed a reduction in E2F-1 protein levels, possibly reflecting a link to the loss of hyperphosphorylated pRB. Hypohophorylated-pRB-sequestered-E2F-1 may be intrinsically more unstable that free E2F-1, perhaps related to the formation of potential E3 ubiquitin protein-ligase-like complexes with pRB and MDM2(O'Connor, Lam et al. 1995; Xiao, Chen et al. 1995; Hsieh, Chan et al. 1999). Loss of E2F-1 expression reflects the p21-mediated inhibition of S-phase progression, and hence may be causal in the G_1/S cell cycle arrest. Interestingly, p21 induction generated both a G_1/S and a G_2/M cell cycle arrest, implicating it in both of the checkpoints. Conflicting results were obtained with DN(5) cells which exhibited an extremely attenuated X-ray-mediated p21 response and failed to arrest at G_1/S, but did exhibit a strong G_2/M arrest. Again, differences between the direct- and indirect-routes of p21 induction or activation may explain the differential results.

Overexpression of p21 prior to, during and post-UV-irradiation caused a significant delay in apoptosis, paralleling the results obtained with the mutant p53 $175^{R \Rightarrow H}$. Both of these results suggested that although apoptosis could be delayed, the apoptotic signal remained and eventually overcame any anti-apoptotic measures(Polyak, Waldman et al. 1996). Such apoptotic dominance mediated by slower, redundant or p53-independent pathways (see Introduction) would therefore ensure eventual active cellular-death.

Potential mechanisms for p21-mediated anti-apoptotic mechanism revolve around its protein-protein interaction with PCNA and various kinases. In combination with p53-mediated upregulation of PCNA upon DNA damage(Xu and Morris 1999), p21-binding to PCNA may stimulate its role in DNA repair. Increased rates of repair of UV-mediated DNA damage would perhaps reduce the rate of apoptosis, by reducing the amount and temporal

persistence of the DNA damage 'signal'. Furthermore, p21 association with nuclear cyclin-cdk2 complexes, a potential effector of apoptosis(Levkau, Koyama et al. 1999), may prevent the execution of apoptosis.

Both PonA-induced-pINDp21 and DN(5) U2OS cell lines exhibited delayed UV-mediated apoptotic response. p21 itself may provide an antagonistic anti-apoptotic signal, while mutant p53 may act by simply not registering the cellular stress event. These two different processes are highlighted through the differential use of p21. UV-irradiated DN(5) cells lacked any p21 induction, demonstrating that, in contrast to the pIND p21 clone, p21 played no role in the delaying apoptotic mechanism. Furthermore, M(5)'s anti-apoptotic mechanism was not mediated through a temporal maintenance of p21 protein levels, suggesting that multiple routes of apoptotic suppression exist.

Although the role of p21 in cell cycle arrest is relatively well established, its function in promoting or inhibiting apoptosis remains unclear. The observation that p21-null MEFs still underwent thymocytic apoptosis, but exhibited deficiencies in G_1 cell cycle arrest(Deng, Zhang et al. 1995), further supported p21's role in growth arrest. However, in several studies upregulation of p21 was observed in cases of p53-dependent apoptosis: γ-irradiation of pRB-deficient cell lines up-regulated p21 levels and induced apoptosis, as did p21-overexpression alone(Kondo, Kondo et al. 1997); and cisplatin treatment of U87-MG cells lead to p53-dependent induction of p21 and apoptosis, while ectopic p21 overexpression also induced apoptosis(Kondo, Barna et al. 1996).

In contrast to the above, a number of papers have documented p21's protective role in apoptosis. Irradiation of BaF3 cells, in the absence of IL-3, lead to p53-dependent apoptosis with attenuated p21 induction(Canman and Kastan 1998). However, exogenous p21overexpression provided consistent, but partial protection from irradiation-mediated apoptosis. Other examples include: etoposide-induced apoptosis of 293T cells(Zhang, Fujita et al. 1999); p53-induced apoptosis of p21-null MEFs(Gorospe, Cirielli et al. 1997); and prostaglandin-mediated apoptosis of RKO cells(Gorospe, Wang et al. 1996). Additionally, enforced p21 expression also protected cells from p53-independent apoptosis: X-ray- or adriamycin-induced apoptosis of DLD-1 cells (mutant p53)(Lu, Yamagishi et al. 1998); UVB-

induced apoptosis of A431 (mutant p53)(Bissonnette and Hunting 1998); and γ-irradiation and doxorubicin-induced apoptosis of H1299 cells(Wang, Blandino et al. 1999). Therefore, p21 is capable of blocking a step of apoptosis common to both p53-dependent and –independent apoptosis, placing p21 as a key regulator of apoptosis.

DNA Damage- and ARF–mediated stabilisation of p53 and MDM2

Induction of p53 has mainly been studied through two different sets of cellular stress stimuli; direct physical cellular damage and viral or oncogene-mediated signals. All the stimuli have been reported to upregulate p53 as a result of post-translational modification, increasing p53 stability and hence, protein half-life. Recently, ARF[13] has been reported to control the oncogene-mediated upregulation of p53 through inhibition of MDM2-mediated p53 degradation (see Introduction). While DNA damaging agents are not thought to induce ARF(Kamijo, Zindy et al. 1997; Stott, Bates et al. 1998), they may act through activation of a number of protein kinases, leading to inhibition of the MDM2:p53 interaction and subsequent inhibition of MDM2-mediated degradation. Therefore, it was of interest to see how DNA damage, a ARF-independent p53 stabilising route and ARF-induction would affect p53 induction and the subsequent cellular outcome.

Establishment of an inducible ARF U2OS cell line was attempted using the PonA system, which was successfully used to generate inducible p21 cell lines. Unfortunately, transfection of an ARF pIND expression vector consistently failed to generate any colonies. Around this time F.Stott et al(Stott, Bates et al. 1998) published an IPTG-inducible ARF system in U2OS cell line (NARF6) which was generously donated and used for all of the subsequent ARF studies.

---

[13] ARF generally refers to both human $p14^{ARF}$ and murine $p19^{ARF}$, although the subsequent work used human $p14^{ARF}$.

ARF induces p53, MDM2 and p21 accumulation

48 hours post-1mM IPTG induction of NARF(6) cells, a G_1/S and G_2/M cell cycle arrest is evident, in the absence of any apoptosis(Stott, Bates et al. 1998). A clear emptying of S-phase was evident 24 hours post-induction, accompanying a large accumulation of G_1 cells with a huge increase in G_2 cell numbers (see Figure 2.35 [I]). Western analysis showed upregulation of MDM2, ARF, p53 and p21 levels as early as four hours post-IPTG induction, which continued to increase until the last time point at 24 hours post-IPTG induction (see Figure 2.35 [II]). Of particular note was the emergence of a slightly higher molecular weight 2A10-reactive MDM2 band, most noticeable 24 hours post-induction. This resulted suggested either ARF-mediated post-translational modification of MDM2 or *mdm2* alternative splicing.

Ectopic ARF-expression does not alleviate UV-mediated reductions in MDM2 or p21 protein levels

Both ARF and UV-irradiation induced p53 levels and it was of interest to see whether UV-irradiation and ectopic ARF-expression could co-operate in p53 induction. Additionally, the outcome of the contrasting p21 and MDM2 responses seen between the two treatments (ARF-mediating induction and UV-mediating reduction of both proteins) was also examined, with respect to protein levels and cellular outcome.

NARF(6) cells were either UV-or mock-irradiated and/or IPTG-induced and various time points were taken to compare relative protein levels. MDM2 analysis revealed no detectable prevention of UV-mediated loss of expression, with dual-treated (IPTG and UV-irradiated) cells exhibiting undetectable levels of MDM2, 24 hours post-treatment (see Figure 2.38). Similarly, ARF-overexpression also failed to alleviate UV-mediated loss of p21 expression. ARF- and UV-mediated p53 induction showed similar levels and kinetics, with no detectable co-operative effects upon dual treatment. One detectable difference between IPTG-treated and UV-/IPTG-treated cells was an attenuated ARF-induction in the dual treated cells. Dual treated ARF levels, in comparison to IPTG-alone treated cells, were significantly reduced at 24 hours post-treatment.

Ectopic ARF expression does not attenuate UV-mediated apoptosis

With the absence of any protein profile differences in UV-irradiated cells in the presence of ectopic ARF expression, it was of interest to determine whether the cellular outcome was modulated. A theory being the opposing nature of the ARF-mediated cell cycle arrest and its associated p21 induction would perhaps attenuate UV-mediated apoptosis. Visually, dual- and UV-treated NARF(6) cells both revealed apoptotic morphology and cellular detachment by 48 hours post-irradiation. To validate these observations, sub-G_1 analysis was carried out on such cells. In agreement with the protein profiles, apoptosis was not affected by the presence of elevated ARF as both treatments yielded similar sub-G_1 values (see Figure 2.39).

Ectopic ARF expression attenuates X-ray-mediated MDM2 reductions and shows a degree of co-operativity with p53 induction

With observations of ARF causing the induction of MDM2 protein levels, it was of interest to see whether such expression could alleviate the X-ray-mediated transient dip in MDM2 protein levels. NARF(6) cells were either IPTG-induced for 5, 10 or 24 hours prior to X-ray irradiation and then lysed 30 minutes post-irradiation. These samples were then compared with the relevant IPTG-induced samples. A significant attenuation in the degree of the X-ray-mediated dip was seen at all time points, with the most dramatic effects with 10 and 24 hour IPTG pre-treatment (see Figure 2.40). Interestingly, ARF-mediated MDM2 induction clearly induced the formation of two ≅90kDa bands, which can also be seen in Figure 2.37 [II].

Analysis of p53 levels revealed a small, but detectable additive effect upon UV-irradiated/IPTG-induced NARF(6) cells in comparison to individually-treated cells. This increase was also mirrored in the slightly elevated phosphorylated Ser^{15} levels of the dual-treated cells in comparison to X-ray-irradiated levels. Interestingly, IPTG-induced alone p53 showed very low levels of Ser^{15} phosphorylation in comparison to X-ray irradiated samples.

Differences mimicking the general pattern of Ser^{15} phosphorylation pattern were observed with E2F-1 protein levels 8 and 24 hours post-IPTG-induction, with only irradiated cells showing increased E2F-1 levels in comparison to IPTG-only treated cells. IPTG-mediated

p21 induction was not significantly affected by X-ray-irradiation, with near identical levels of p21 in IPTG or IPTG/X-ray treated cells.

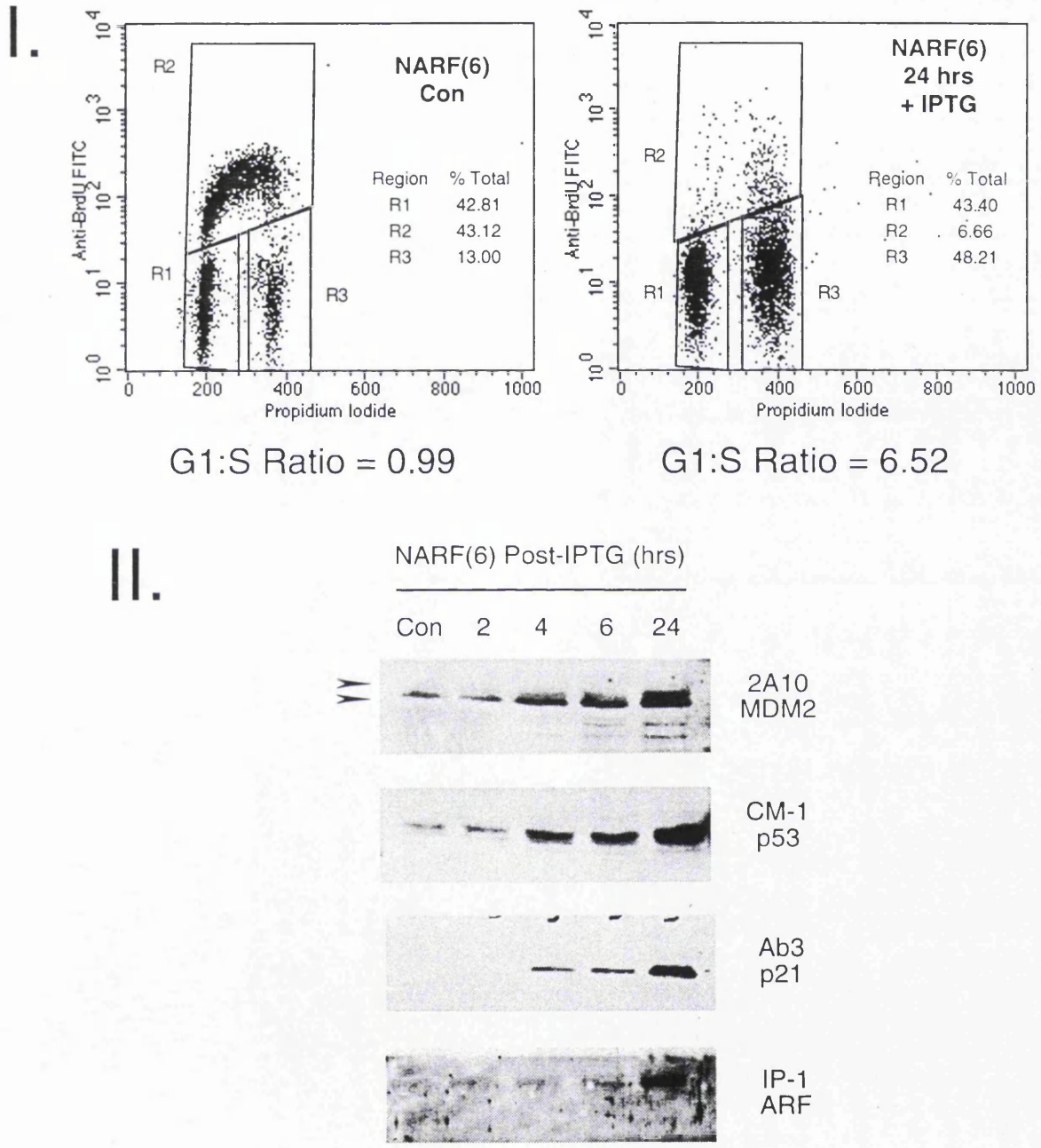

Figure 2.37. Ectopic p14ARF overexpression induces MDM2, p53 and p21 proteins and a cell cycle arrest. (I) Ectopic p14ARF overexpression induces a G1/S and G2/M cell cycle arrest; NARF(6) cells were treated with 1mM IPTG and examined by BrdU analysis 24 hours post-treatment. (II) p14ARF expression increases the protein levels of various cellular proteins; p14ARF-inducible NARF(6) were treated with 1mM IPTG and examined by Western blotting at various time points post-treatment (as indicated) for different cellular proteins (as indicated). Two different (p14ARF-mediated) molecular weight MDM2 bands are indicated by arrowheads.

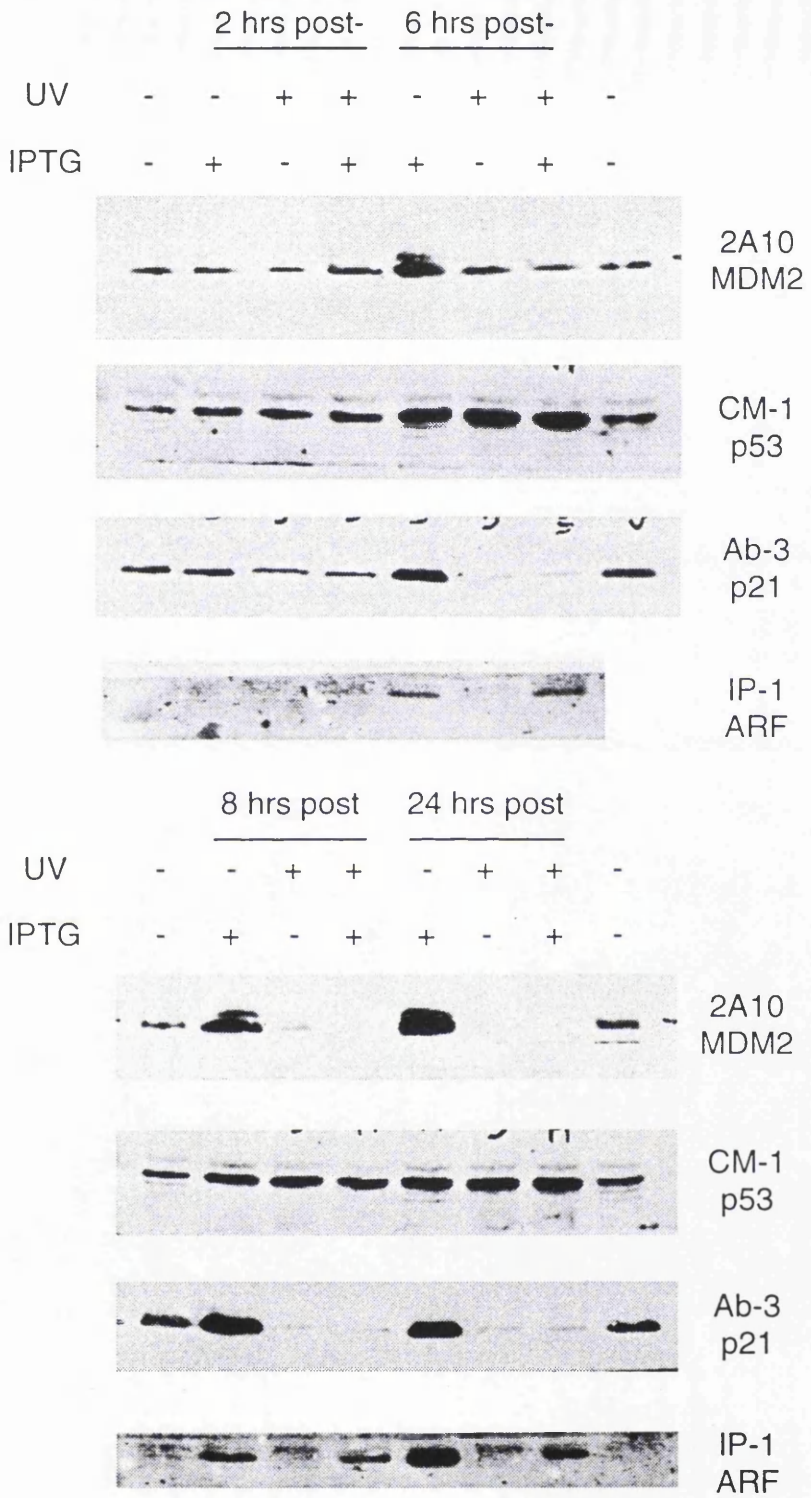

Figure 2.38. p14ARF-overexpression does not alleviate UV-mediated reduction in MDM2 or p21 protein levels. NARF(6) cells were either treated with 1mM IPTG (+), or not (-) and then either 30 Jm-2 UV- or mock-irradiated and lysed at various time points post-treatment (as indicated). Samples were then analysed by Western blotting for different cellular proteins.

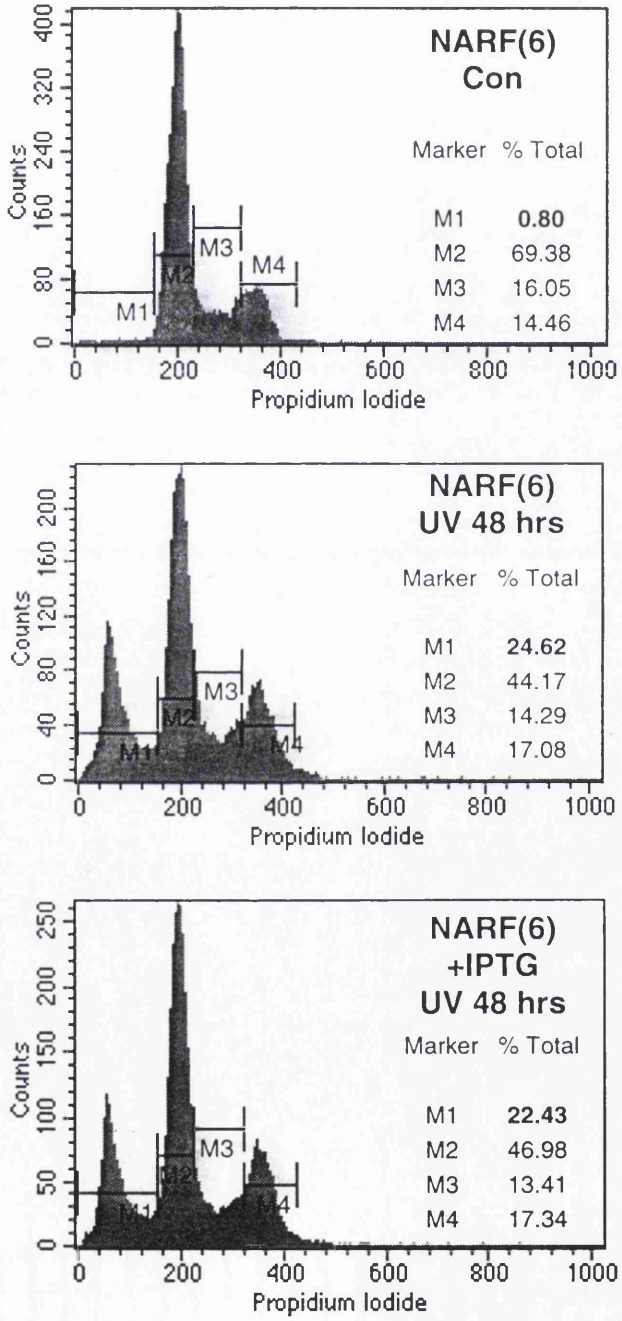

Figure 2.39. p14ARF-overexpression does not affect UV-mediated apoptosis of U2OS cells. NARF(6) cells were either treated with 1mM IPTG, or not and then 30 Jm-2 UV-irradiated. Cells were analysed by sub-G1 analysis 48 hours post-irradiation. Sub-G1 percentages are marked in bold.

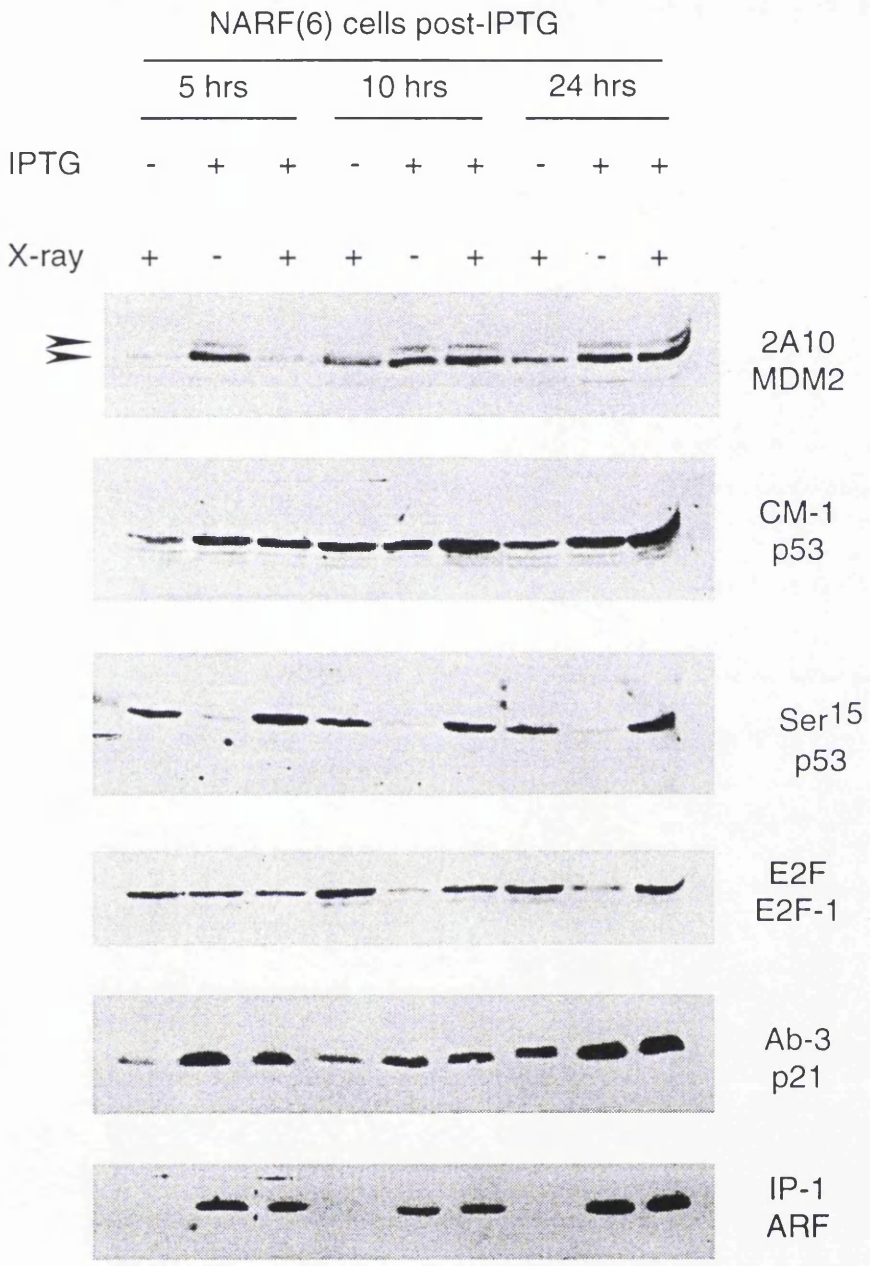

Figure 2.40. p14ARF-overexpression attenuates the X-ray-mediated reduction in MDM2 protein levels. NARF(6) cells were treated with 1mM IPTG, or not and then either 12 Gy X-ray- or mock irradiated at varying time points post-IPTG treatment (as indicated). Cells were lysed 30 minutes post-irradiation and analysed by Western blotting for different cellular proteins (as indicated). Two different (p14ARF-mediated) molecular weight MDM2 bands are indicated by arrowheads.

ARF and X-ray irradiation show some degree of additive effect in generation of a G_1/S and G_2/M cell cycle arrest

Due to both X-ray and ARF expression leading to cell cycle arrest, it was of interest to determine how the two signals would act together, perhaps either generating a stronger cell cycle arrest or conversion into an apoptotic signal. To investigate this, cells were simultaneously X-ray- and IPTG-treated and analysed by BrdU 24 hours post-treatment. Analysis consistently showed a stronger cell cycle arrest of dual-treated (IPTG- and X-ray-treated) cells, in comparison to X-ray irradiated cells (see Figure 2.41). Long-term culturing failed to reveal any signs of apoptosis and the cells grew to confluence.

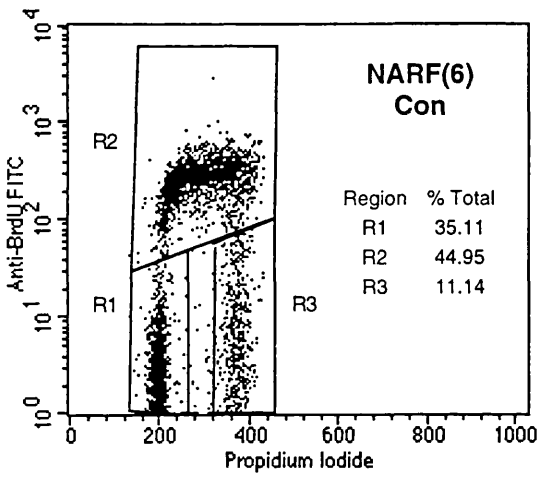

G1:S Ratio

0.78

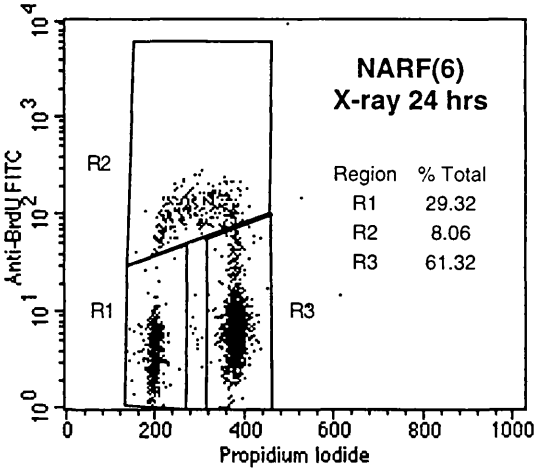

G1:S Ratio

3.64

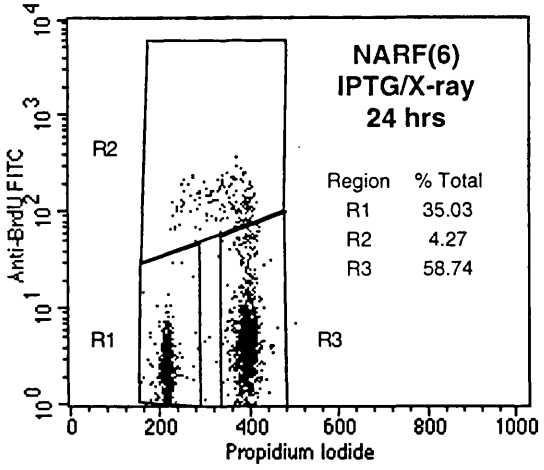

G1:S Ratio

8.20

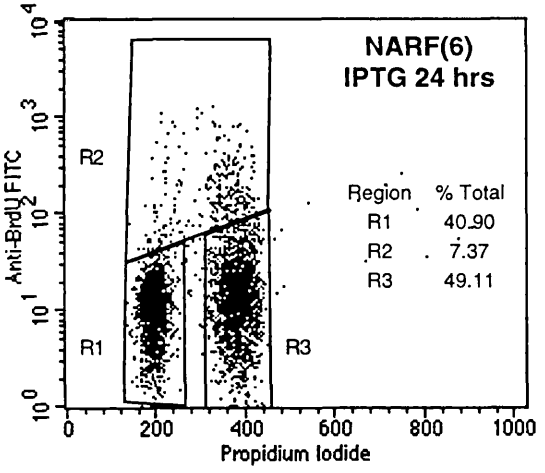

G1:S Ratio

5.55

Figure 2.41. p14ARF co-operates with X-ray-irradiation in induction of G1/S and G2/M cell cycle arrest. NARF(6) cells were either treated with 1mM IPTG, or not and then 12 Gy X-ray-irradiated and examined by BrdU analysis 24 hours post-irradiation.

Summary and Discussion

Discovery of ARF's function as the mediator of oncogene-stimulated p53 induction, revealed a component of a p53 activation pathway that was not utilised by DNA damage-stimulated p53 induction(Kamijo, Zindy et al. 1997; Stott, Bates et al. 1998). These two separate pathways were simultaneously triggered to determine whether they would act together in an additive or synergistic manner in p53 induction and determine the outcome and/or the efficacy of the cellular response - being either a cell cycle arrest or apoptosis. Initial attempts to generate inducible-ARF cell lines failed to generate viable colonies, suggesting that the construct was 'leaky' in its expression of ARF. Such basal expression may have produced enough ARF to mediate a cell cycle arrest and prevent cellular growth.

NARF(6) cells, as reported by Stott et al(Stott, Bates et al. 1998), exhibited a G_1/S and G_2/M cell cycle arrest upon IPTG treatment. Protein analysis revealed a p53 and p21 induction, similar to the X-ray mediated protein profile, prompting questions whether both X-ray- and ARF- induced cell cycle arrests used similar mechanisms. ARF is though to mediate its affects on p53 through abrogation of MDM2-mediated inhibition, generating transcriptionally active p53 (see Introduction). Increased transcriptionally active p53 was observed through the induction of the two p53-responsive proteins, p21 and MDM2. Although, the DNA damage response does not require ARF, X-ray-mediated p53 induction may use a similar mechanistic approach to generate similar protein-profiles and overall cellular outcomes. However, in light of earlier cycloheximide analysis, X-ray-mediated p53-induction seemed dependent on translation. However, distinction between the need for direct translation of *p53* mRNA or perhaps an ARF-like p53-stabilising protein was unascertainable. Overall, the similarity between ARF- and X-ray-mediated responses further supports the role of p21 and MDM2 in generation of a cell cycle arrest and/or protection from apoptosis.

The observed p53 accumulation in NARF(6) cells, although mediated through ARF may ultimately use a similar mechanism(s) of p53 induction, as X-ray irradiation. Interestingly, X-ray and IPTG-induced NARF(6) cells did show a small degree of additive induction of p53. The additive nature of two treatments can be explained through the two stimuli acting within the same pathway, which is not maximally activated in either individual response.

Alternatively, two separate pathways could converge upon p53 and act together, increasing the degree of p53 induction. The additive p53 protein level effect was also reflected in the additive increase in the degree of G_1/S cell cycle arrest of X-ray and IPTG-treated NARF(6) cells. However, no significant differences in p21 protein levels were observed between X-ray- and X-ray/IPTG-treated NARF(6) cells. Perhaps, suggesting the existence of p21-independent cell cycle arrest functions, although differential p21 activity could have also explained the observations.

Increased p53 Ser^{15} phosphorylation of dual-treated cells suggested that ARF could co-operate with X-ray-irradiation in Ser^{15} phosphorylation. In the light of DN(5) cell's p53 Ser^{15} studies, where elevated mutant p53 $175^{A \Rightarrow H}$ levels also resulted in increased Ser^{15} levels, IPTG-induced p53 may have merely produced a larger target pool of p53 for X-ray-activated kinases.

The general pattern of X-ray-mediated p53 Ser^{15} phosphorylation was mirrored by the E2F-1 expression pattern (see Figure 2.40). The lack of p53 Ser^{15} phosphorylation and E2F-1 induction in un-irradiated cells suggested that such events were unnecessary for the ARF-mediated cell cycle arrest, although such events may been required for X-ray-mediated cell cycle arrest.

Observation of ARF-mediated increased MDM2 levels in NARF(6) cells, prompted thoughts that ARF may have countered the irradiation-induced loss of MDM2 expression seen earlier. MDM2 Western analysis of the UV-irradiated or dual treated cells revealed no such stabilisation, suggesting that the UV-induced repression of MDM2 expression was dominant over the ARF-mediated stabilisation. In contrast to UV-irradiation, ARF expression significantly affected the X-ray-mediated loss of MDM2 expression. Pre-induction of ARF inhibited the X-ray-mediated loss of two major ≅90 kDa 2A10-reactive bands, with more specific loss of the upper band. ARF-mediated post-translational modification may explain the apparent differences in molecular weight between the two bands, as the upper band was only evident in ITPG-induced NARF(6) cells. The results suggested that ARF expression could alleviate X-ray-mediated loss of both ≅90 kDa MDM2 forms. An explanation of ARF's MDM2-protective effects may either reside in it's ability to upregulate p53 expression and

hence MDM2 expression, or perhaps via its physical interaction with MDM2, shielding it from degradation. From these results it was possible to demonstrate the existence of antagonistic actions between the X-ray-mediated reduction and the ARF-mediated induction of MDM2. However, it could not be determined whether the antagonism was through a net increase in MDM2 production or via direct inhibition of the X-ray-mediated reduction process.

UV- and IPTG-treated NARF(6) cells showed comparable p53 induction levels to both UV-irradiated or IPTG-treated NARF(6) cells. If the two processes acted through the same pathways of p53 stabilisation, UV-mediated stabilisation may represent maximal levels of induction for that pathway, therefore any additional signals would not been translated into increased p53 stabilisation. The same argument can be applied to if the two stimuli act through two separate pathways. For example, the UV-mediated loss of MDM2 expression may have effectively negated the ARF-effect by removing ARF's target protein (MDM2). ARF-expression also failed to affect the UV-mediated loss of p21 expression, suggesting that the UV-mediated protein profile was dominant over the ARF-mediated protein profile. In addition to decreasing MDM2 and p21 expression, exogenous ARF expression was also inhibited at 24 hours-post irradiation in comparison with non-irradiated IPTG-treated NARF(6) cells. Specific transcriptional or translational down-regulation of exogenous ARF-expression seemed unlikely, suggesting a more general inhibition of global gene expression (as seen for UV-mediated loss of MDM2 expression – see earlier sections). Nevertheless, the inducibility and detection of ARF (albeit reduced) showed that the gene expression machinery (transcription/translation) was still capable of functioning post-30Jm^{-2}-UV-irradiation.

Analysis of the cellular outcome of IPTG-induction and UV-irradiation of NARF(6) cells showed apoptosis to be the dominant cellular response(Polyak, Waldman et al. 1996), perhaps reflecting the importance of removing UV-damaged cells. UV-irradiated cells showed the same degree of apoptosis as IPTG-treated UV-treated cells, suggesting that common components of the cell cycle arrest and apoptotic machinery were not used or that any ARF-mediated anti-apoptotic effects were ineffective and totally overwhelmed. The UV-mediated apoptotic dominance was reflected in the dominant protein profile, with loss of p21 and MDM2, two known anti-apoptotic proteins. These results provided yet another link between the potential active suppression of gene expression and apoptosis.

Stable overexpression of MDM2 in U2OS cells does not effect the protein levels of a number of known MDM2 interacting proteins

Stable overexpression of MDM2 does not cause increased degradation of p53

Transient transfection of MDM2 into a number of cell lines, including U2OS, had been reported to cause the rapid degradation of p53(Haupt, Maya et al. 1997; Kubbutat, Jones et al. 1997). Western analysis of a number of the MDM2 overexpressing U2OS clones (M[x]) revealed similar p53 levels to parental and vector-only (p3) cell lines (see Figures 2.12 and 2.42 [I]), suggesting that stable transfection of MDM2 was incapable of mediating excess p53 degradation.

To ensure that exogenous MDM2 was capable of causing the reported rapid degradation of p53 in M(5) cells, MDM2:CD8 (a cell surface marker allowing positive selection of transfectants – see Material and Methods) co-transfections were carried out. CD8-positive transfectants were sorted 24 hours post-transfection and the p53 and MDM2 levels were examined by Western analysis. MDM2-transfected cells showed a significant degree of p53 reduction in comparison to vector only cells, suggesting that transient overexpression of MDM2 could lead to rapid degradation of p53 in M(5) cells (see Figure 2.42 [II]).

pRB and E2F-1 protein levels are unaffected by MDM2 overexpression

Two documented proteins that interact with MDM2 have roles in both apoptosis and cell cycle arrest, namely E2F-1 and pRB, respectively. In light of the reported ubiquitin protein-ligase E3 function of MDM2, it was possible through the protein-protein interaction that either of these proteins may have been targeted for MDM2-mediated ubiquitin-dependent degradation. Hence, both of these proteins were analysed in a number of MDM2 clones and compared to vector only and parental cells. Western blot analysis revealed no significant differences in protein levels or pRB phosphorylation status in comparison to vector-only or parental control levels (see Figure 2.42 [I]).

MDM2 or p53 175$^{R\Rightarrow H}$ overexpression does not affect ARF expression

ARF had been reported to bind MDM2 and abrogate MDM2-mediated inhibition of p53's functions (see Introduction). Lack of MDM2 lethality and absence of excess p53 degradation in MDM2-overexpressing U2OS cell lines could be explained through up-regulation of the MDM2-inhibitor, ARF. However, examination of ARF protein levels in M(x) cell lines revealed no detectable up-regulation when compared to vector-only and parental control levels (see Figure 2.42 [I]).

Stott et al(Stott, Bates et al. 1998) had reported a link between mutant/null p53 status and positive ARF detection, suggesting that wild-type p53 suppressed ARF expression. ARF levels were analysed in mutant p53 175$^{A\Rightarrow H}$ expressing in DN clones, to assess the impact of mutant p53 expression in U2OS cell. However, Western analysis failed to show any alterations in levels in comparison to parental U2OS cells (see Figure 2.43).

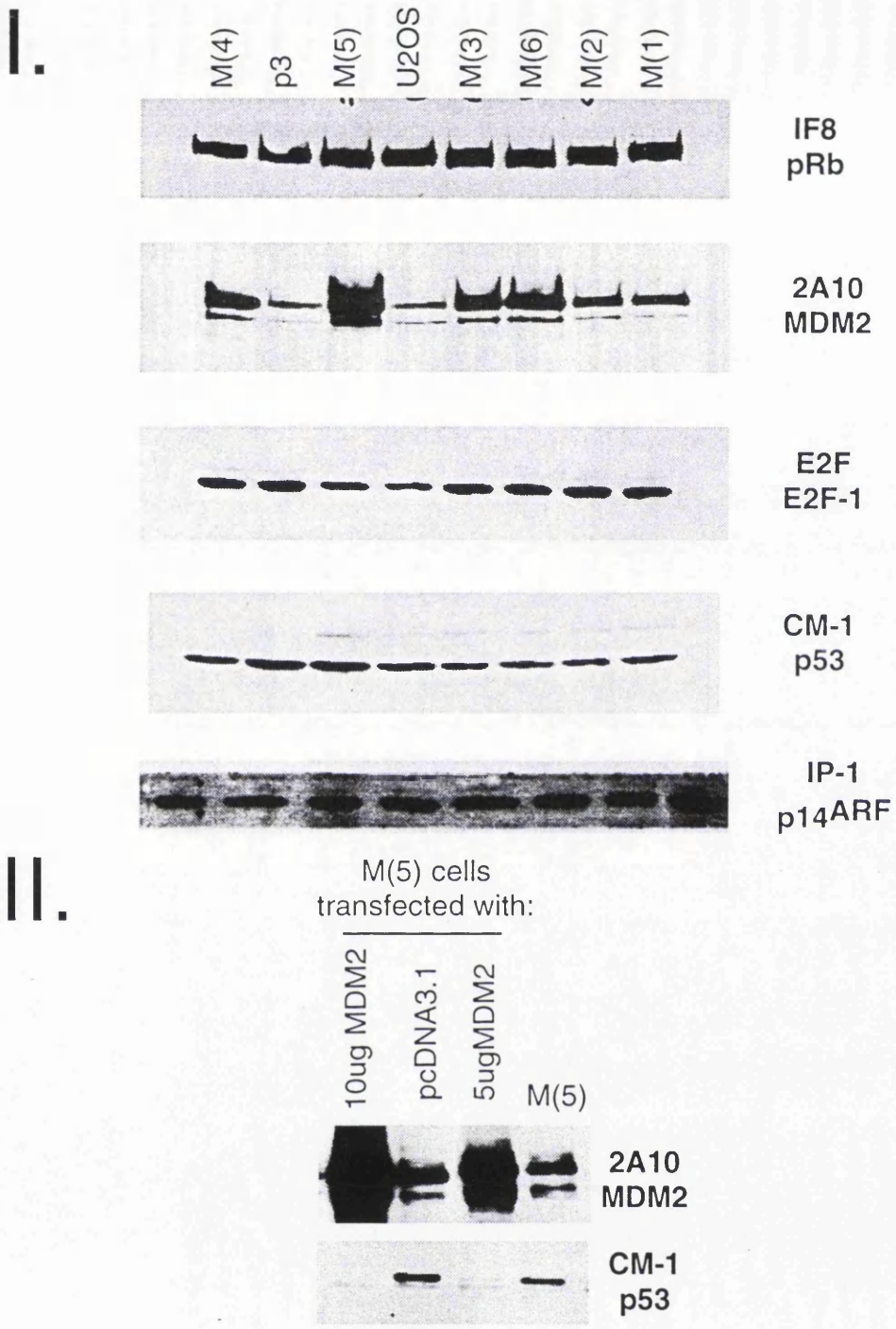

Figure 2.42. Effect MDM2 overexpression on different cellular proteins' expression levels. (I) MDM2 overexpression does not affect the protein levels of a number of associated cellular proteins; Parental, vector-only (p3) and MDM2-overexpressing (M[X]) U2OS cell lines were analysed by Western analysis for various cellular proteins (as indicated). (II) Transient transfection of MDM2 reduces p53 protein levels in U2OS cells; U2OS cells were transiently co-transfected with 10 or 5 μgs of pCMV-MDM2 or pcDNA3.1 (vector-only) and pCMV-CD8 and sorted for CD8 positive cells (1:5 ratio – see Material and Methods) 24 hours post-transfection. Samples were then analysed by Western blotting for MDM2 and p53 expression. M(5) = untreated direct Western lysate.

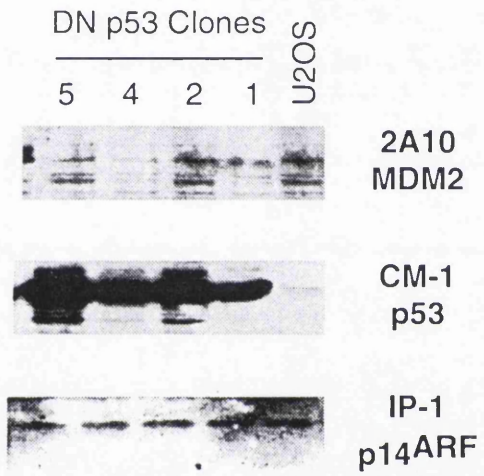

Figure 2.43. p53 175R⇒H expression does not upregulate p14ARF expression in U2OS cells. Parental and p53 175R⇒H expressing (DN[X]) U2OS clones were analysed by Western blotting for different cellular proteins (as indicated).

Lack of amino- and carboxyl-terminal MDM2 -fragment stable generation in U2OS cells

In an attempt to analyse the relative importance of various domain in the observation previously made with full length MDM2, two partially overlapping amino-(NT) and carboxyl-(CT)-terminal MDM2 expression constructs were made (see Figure 2.44). The NT-construct (aa 1-360) contained the p53-binding domain, NLS, NES, acidic domain and a Zn^{2+}-finger domain, as well as N-20, SMP14 and 2A10 antibody epitopes; while the CT-construct (aa 275-491) contained the caspase-3 cleavage sites, both Zn^{2+}-fingers and a RING finger domain, as well as the 2A10 antibody epitope. Of especial interest were the potential dominant-negative effects these constructs may have had on MDM2 function.

Transfection of M(5) and parental U2OS cell lines and subsequent selection repeatedly generated colonies lacking detectable overexpression of the fragments (see Figure 2.45). The expected molecular weight of full-length MDM2 is 55.2 kDa, while the observed molecular weight is approximately 90 kDa. Adjusting for the observed/expected molecular weights, estimation of the adjusted molecular weight for the NT and CT constructs were 40 and 66 kDa, respectively. Using the same molecular weight adjustment, the alternative slice variants MDM2 b and c would produce similar size protein products of 40 and 65 kDa, respectively. Hence overexpression of either construct could have lead to increased expression of potentially pre-existing bands, although no such increases were evident. Sequencing of both constructs revealed an acceptable Kozak sequence(Kozak 1981), start codon and absence of mutations in the MDM2 coding regions.

Upon transient transfection of U2OS cells, the amino-terminal construct failed to generate a detectable increase in an existing band or appearance of a novel band, suggesting that either the fragment was extremely detrimental to cell growth or was not expressed at detectable levels (see Figure 2.46). Alternatively, both protein products were extremely unstable. However, upon transfection of the carboxyl-terminal fragment a novel ≅60 kDa band was clearly evident, absent from untransfected and mock-transfected control cells.

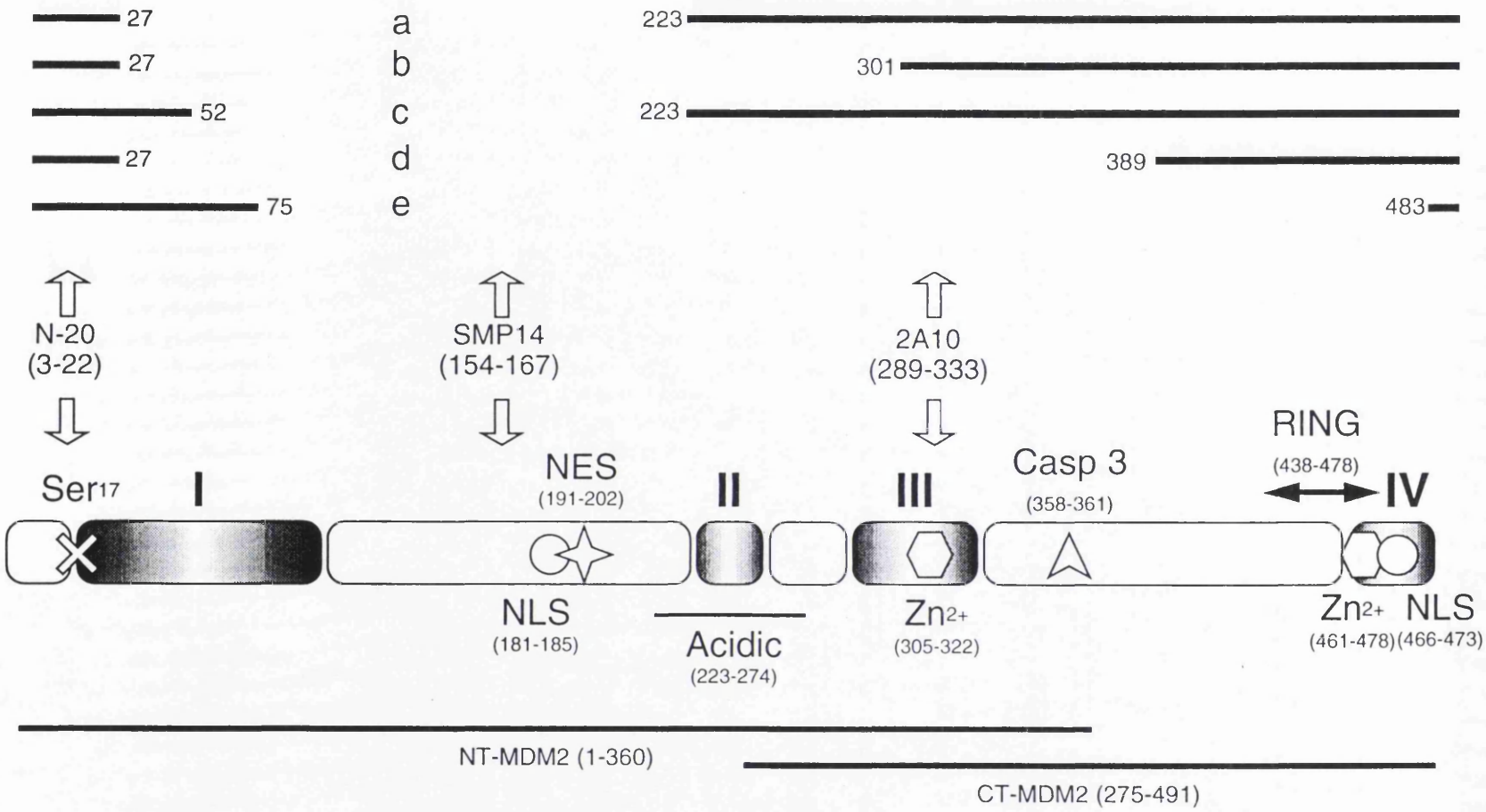

Figure 2.44. Schematic representation of the human MDM2 polypeptide and the regions encoded by the amino- and carboxyl-terminal constructs. MDM2 alternatively splice variants are indicated above the diagram (a-e); three MDM2 antibodies' epitopes, used throughout this study, are also indicated above the diagram; the four conserved regions are marked (I-IV); nuclear localisation and export signals are marked, NLS and NES, respectively; Zinc finger motifs are marked Zn2+; amino-(NT) and carboxyl-terminal (CT) encoding regions are indicated below the diagram.

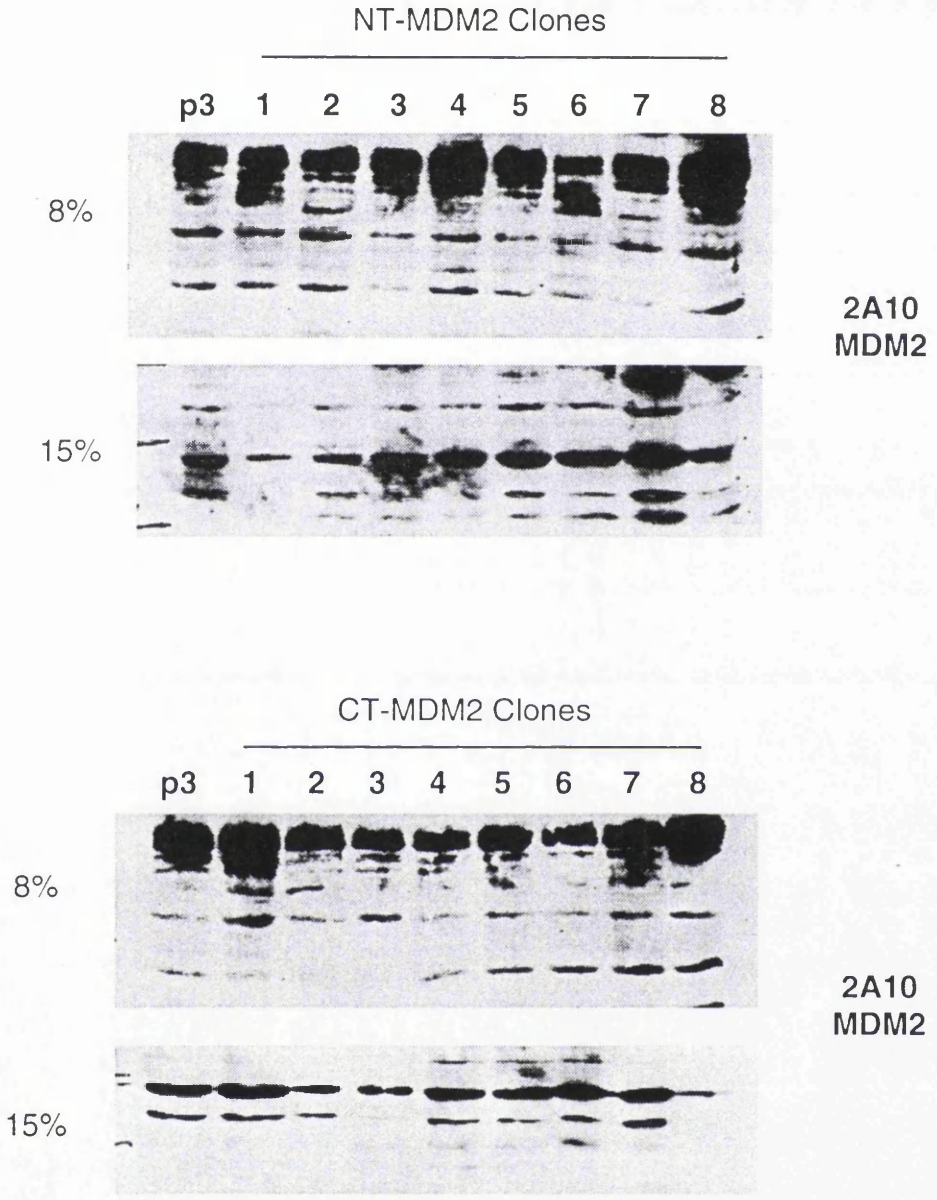

Figure 2.45. Attempt to establish amino- and carboxyl-terminal expressing U2OS cell lines. U2OS cells were separately transfected with amino- and carboxyl-terminal MDM2-pcDNA3.1 constructs. The resulting clones (NT[X] and CT[X]) were compared to vector-only (p3) and parental U2OS cells by Western analysis with anti-MDM2 antibody, 2A10. 8% and 15% gel PAGE was used to cover any discrepancies in molecular weight determination (see text).

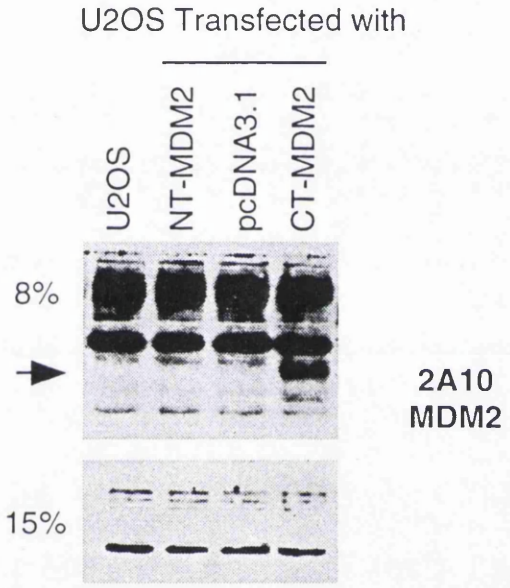

Figure 2.46. Transient expression of amino and carboxyl-terminal MDM2 in U2OS cells. U2OS cells were transiently transfected with pcDNA3.1 (vector only) and amino-(NT) and carboxyl-terminal (CT) MDM2-pcDNA3.1 constructs and analysed 24 hours post-transfection by Western analysis for MDM2. 8% and 15% gel PAGE was used to cover any discrepancies in molecular weight determination (see text). A potential ≅60kDa carboxyl-terminal MDM2 band is indicated by an arrowhead.

Summary and Discussion

Analysis of the MDM2 overexpressing U2OS clones unexpectedly revealed parental protein-levels of p53. Evidence for MDM2-mediated degradation of p53 upon transient transfection was corroborated showing that the mdm2 cDNA construct used in stable transfections was functional, as was M(5)'s cellular p53 degradation machinery. A possible explanation for the lack of increased p53 degradation in the MDM2 cell lines lies in the prevention of p53:MDM2 interaction through: modification of either protein (phosphorylation etc) blocking binding sites or altering binding competent conformations; differential protein compartmentalisation; and/or increased levels of a competitor protein. Inhibition of the actual degradation mechanism itself, through reduced ubiquitination (shown to be the mediated by MDM2(Haupt, Maya et al. 1997; Kubbutat, Jones et al. 1997)) may also explain the parental p53 protein levels. The massive and rapid overexpression of MDM2 by transfection in comparison to stable moderate increases, could have 'swamped' any regulatory/modification machinery designed to prevent excessive p53 degradation; while stable expression of MDM2 may have provided time for an adaptive response by such regulatory mechanisms. Investigation of p53:MDM2 protein association and both proteins' subcellular localisation patterns are covered in following chapters.

The INK4a promoter in U2OS cells may be methylated(Stott, Bates et al. 1998) and unresponsive to p53 regulation, but may generate a low basal transcript level, explaining the detection of ARF protein expression (see Figure 2. 42 [I]). On Western analysis a strong 19kDa non-specific band was evident, which was cut off prior to antibody detection and may have improved detection of the endogenous ARF by effectively concentrating the available antibody.

ARF was reported to bind to MDM2 and inhibit its p53-degradative effect, therefore representing a potential explanation for the absence of increased p53 degradation in MDM2-overexpresing U2OS cell lines. Examination of a number of MDM2 overexpressing cell lines for increased ARF levels revealed no increases over parental control cell lines. Reported existence of a p53:ARF negative feedback loop, mediated through p53's repression of ARF expression, lead to the examination of the p53 $175^{A \Rightarrow H}$ cells lines. These cell lines also failed

to show increased ARF levels. Lack of p53 $175^{A\Rightarrow H}$-mediated ARF induction and low levels in the U2OS cell lines examined could again be explained through ARF promoter methylation, and hence, lack or responsiveness. Another explanation lies in partial retention of wild-type ARF repression function in the p53 $175^{A\Rightarrow H}$ mutant, although the two sets of results suggested that elements of the MDM2:p53: ARF feedback loop were defective in the U2OS cell line.

As well as p53, MDM2 has been documented to interact with E2F-1 and pRB, both of which are involved in cell cycle progression. The observed growth advantage of M(5) over parental U2OS (see Figure 2.17), prompted thoughts that MDM2 may be inhibiting pRB, perhaps through degradation of pRB, negating its growth suppressive role through facilitating E2F-1 release and driving cell cycle progression. Enhancement of E2F-1 activity by MDM2 and in conjunction with the potential pRB effects, MDM2 would provide a potent growth stimulus. Furthermore, MDM2's other p53-independent role as a potential oncogene may also contribute directly to a growth advantage (see Introduction). Examination of E2F-1 and pRB protein levels in a number of MDM2 overexpressing clones exhibited no effects, suggesting that MDM2-mediated degradation or stabilisation of either protein was not contributing to the MDM2-mediated growth advantage. However, the absence of protein level alterations cannot rule out MDM2-mediated effects or modifications on pRB or E2F-1 protein activities.

In an attempt to separate p53-dependent and –independent MDM2 effects and localise the anti-apoptotic and anti-G_1/S effects of MDM2, amino-terminal (NT) and carboxyl-terminal (CT) MDM2 fragments were used to try and generate stable cell lines. Repeated attempts failed to generate cell lines overexpressing either fragment, suggesting that expression was detrimental to cell growth or lethal. Transient expression of NT-MDM2 failed to generate either increases in existing or formation of novel 2A10-reactive bands, suggesting that that the fragment was not being expressed or was extremely unstable. However, transient expression of CT-MDM2 generated a novel 2A10-reactive band of ≅60 kDa, suggesting that the protein was reasonably stable. It is possible that the fragments were acting in a dominant negative fashion, competing with endogenous MDM2 for p53 binding (amino terminal fragment) or the ubiquitination machinery (carboxyl-terminal fragment). Competition between the fragments and endogenous MDM2 with either process could ultimately lead to

p53 accumulation and perhaps cell cycle arrest or apoptosis, explaining the lack of stable clone generation. Competition between any number of other MDM2 interacting proteins could also explain detrimental growth effects (p300/E2F-1/pRB/RNA etc).

Chapter Three

Immunoprecipitation Analysis

The physical interaction of the MDM2:p53 complex determines all the known roles of MDM2's effects on p53's function. Without the interaction, MDM2 can neither facilitate its ubiquitin-mediated degradation or transcriptional inhibition of p53 (see Introduction). It is therefore intuitive for the cell to have a regulatable control over this interaction.

A number of questions had arisen through analysis of the MDM2, p53 $175^{A\Rightarrow H}$ and parental U2OS cell lines and their DNA damage responses. Of particular interest was how U2OS could tolerate MDM2 overexpression and not show an increase in p53 degradation or cell cycle arrest (via its reported growth inhibition domains, ID-1 and ID-2), as seen in the MDM2-overexpressing U2OS cell lines. One possible explanation of the former observation being negative regulation of p53:MDM2 complex formation, leading to decreased MDM2-mediated degradation; potential mechanisms being either through subcellular compartmentalisation, competitor proteins, or modification of either protein. A possible explanation of the lack of MDM2 ID-1/ID-2-mediated cell cycle arrest could be explained through regulation of the reported MDM2:E2F-1 complex. Positive regulation of this complex may induce MDM2-mediated stimulation of E2F-1/DP-1, providing positive growth signals. Alternatively, negative regulation of the MDM2:E2F-1 interaction may reduce potential MDM2-mediated degradation of E2F-1, hence maintaining a positive growth signal. Potential answers to these questions were sought through relevant co-immunoprecipitation analysis.

Complex formation between the dominant-negative mutant p53 $175^{R\Rightarrow H}$ and MDM2 was also examined to determine whether MDM2 could bind the non DNA-binding mutant conformation. Inhibition of such an interaction, and hence MDM2-mediated degradation could have explained the extremely high p53 $175^{R\Rightarrow H}$ expression levels observed in DN(5) cells (see Figure 2.26).

DNA damage effects on the p53:MDM2 complex profile post-DNA damage were also examined, in an attempt to explain the irradiation-mediated increase in p53 levels (see Chapter Two). It was expected that p53:MDM2 complex levels would decrease upon irradiation, reducing MDM2-mediated degradation and facilitating p53 induction. Decreased complex formation could also facilitate p53-dependent activation/repression of target genes and/or allow protein-protein interactions, through alleviation of MDM2-mediated allosteric effects or steric hindrance. In the case of X-ray-mediated p53 induction, a concomitant induction in MDM2 was observed. This paradoxical increase in p53 and its negative regulator could also be explained through decreased protein-protein interaction.

Of the potential post-translational mechanisms governing p53:MDM2 interaction, the majority of work has concentrated on the role of phosphorylation. Phosphorylation represents a well established, powerful cellular mechanism involved in regulating a number of pathways involving transforming and transmitting signals to a number of cellular macromolecules. Many kinases have been shown to phosphorylate p53, both *in vitro* and *in vivo*, at a number of residues; of these kinases, a number are activated by DNA damaging agents or events (X-ray, UV and ss and dsDNA breaks), perhaps forming an upstream link from p53 to cellular stress events (reviwed(Meek 1998) and see Introduction). Evidence presented in chapter two revealed an increase in Ser^{15} and Ser^{392} phosphorylation in response to irradiation (see Figures 2.20, 2.26 and 2.29). Immunoprecipitation analysis of irradiated cells was carried in an attempt to determine whether phosphorylation of these residues correlated with alterations in the levels of MDM2:p53 complexes.

Investigation of p53:MDM2 complexes was addressed using the direct method of co-immunoprecipitation assays.

Optimisation of Immunoprecipitation conditions

Previous co-immunoprecipitation (co-IP) studies had used *in vitro* or *in vivo* radiolabelled proteins to aid detection, presumably due to difficulties in visualising co-IPd proteins. Due to the respective non-physiological nature and radiological-cellular stress and DNA damage mediated by such procedures, a less intrusive *in vivo* system was desired. With the

establishment of U2OS cell lines overexpressing MDM2 and p53 $175^{A \Rightarrow H}$ it was thought that detection of p53:MDM2 complexes would be facilitated, allowing use of direct, non-radiolablled immunoprecipitation (IP) methods.

Choice of Antibodies

Initially, the mouse monoclonal, 2A10 and rabbit polyclonal, N-20, which had been used previously for Western analysis (see Chapter Two), were used for IP analysis. N-20's MDM2-binding epitope (aa 3-22), is directly adjacent to MDM2's p53 binding domain (aa 23-108). All of the six hMDM2 splice forms contain at least amino acids 1-27, hence N-20 would be expected to bind all six forms. Although N-20's ability to recognise all six splice forms was extremely useful, concerns over the proximity to the p53 binding domain raised questions whether it would co-IP p53-complexed MDM2, due to possible epitope obstruction by p53. 2A10's epitope, (amino acids 289-333) meant that it would only recognise three splice forms, full-length and (a) and (c), but was significantly carboxyl-terminal to the p53 binding domain, reducing the chance of p53-mediated steric hindrance (see Figure 1.2 for the location of MDM2 antibody epitopes).

Many anti-human, or cross-reacting, p53 antibodies have been reported, the majority of which are capable of immunoprecipitating p53. Initially, four commonly used mouse monoclonal antibodies, 421 (aa 371-380), 1801 (46-55), DO-1 (aa 21-25) and 240 (aa 213-217) and one rabbit polyclonal, CM-1, were used to IP p53 (see Figure 1.1 for the location of p53 antibody epitopes). The vacinity of DO-1's epitope to the MDM2 binding domain, raised concerns that it would not be able to co-immunoprecipitate MDM2 complexed p53.

Choice of Immunoprecipitation Buffers

Buffer conditions are another crucial factor for successful IPs, determining whether complexed proteins remain complexed. Variables determining the release of the protein from the cell (lysis) and maintenance of the protein-proteins complexes include: salt concentration, type of detergent, pH and presence of divalent cations. In general, non-ionic and amphoteric detergents are gentler on proteins than ionic detergents. In addition to buffer

environment effects on proteins, protease action also needs to be addressed, to prevent protein degradation. Protease inhibition was carried in the presence of a 'cocktail' of inhibitors, covering a wide range of activities (see Materials and Methods).

Control Immunoprecipitations revealed a contaminating p53-reactive band with protein-A-, but not protein-G-sepharose

Unfortunately negative controls, lacking immunoprecipitating antibodies, resulted in the detection, albeit upon significantly high exposure times (15 minutes), of a band migrating at approximately 53kD (the molecular weight of p53). Identical negative controls carried out in SAOS-2 cells (p53-null) also revealed the presence of a 53 kDa, DO-1 reactive band, implying that the band was not p53 (see Figure 3.1 [I]). Pre-clearing with protein-A sepharose also failed to significantly reduce the band's intensity, suggesting a large excess of available protein. Due to the number of wash steps, it was unlikely that the protein was being carried through the immunoprecipitation process non-specifically. Therefore, it was likely that it was binding directly to the protein-A sepharose. Exchanging protein-A for protein-G sepharose completely eliminated the 53 kDa band, while not affecting immunoprecipitation of p53 and MDM2. However, later experiments utilised agarose-conjugated 1801 and SMP-14 antibodies, therefore removing the protein-G sepharose step altogether.

Inability to detect co-immunoprecipitates in Pomerantz Immunoprecipitation Buffer

Pomerantz et al(Pomerantz, Schreiber-Agus et al. 1998), had successfully used an IP buffer for MDM2:p53 and ARF:MDM2 co-IPs and hence was chosen for the initial experiments. Cells were lysed directly on the plate with the IP buffer (NP-40 PBS-based including a cocktail of protease inhibitors – see Material and Methods). Preliminary experiments revealed a number of strong bands running at approximately 50 and 90 kDa, both of which interfered with MDM2 and p53 detection. These bands proved to be the components of the antibodies used, most probably reduced or non-reduced heavy and light chains, detected by the 2° Western antibody. To minimise detection of the heavy and light chains of the

immunoprecipitating antibody, 1° and 2° Western antibodies used were of different species to the immunoprecipitating antibody. Especial care was taken in minimising the risk of non-specific bands through multiple washing in large wash of the IP buffer volumes.

To determine whether different antibodies would reveal co-IP proteins, perhaps due to conformational specificity or epitope location, a panel of available p53 antibodies were tested for immunoprecipitation. Again, all of the antibodies successfully directly immunoprecipitated their respective proteins, albeit at different levels, but failed to generate detectable co-immunoprecipitates (see Figure 3.1 [II]).

Both the MDM2 mouse monoclonal, 2A10 and rabbit polyclonal, N-20, successfully immunoprecipitated (IPd) MDM2 in U2OS cells. p53 was also IPd efficiently by the rabbit polyclonal, CM-1 and the mouse monoclonal, DO-1. However, Western detection of both the MDM2 and p53 IPs failed to detect any co-IPd proteins (see Figure 3.1 [III]).

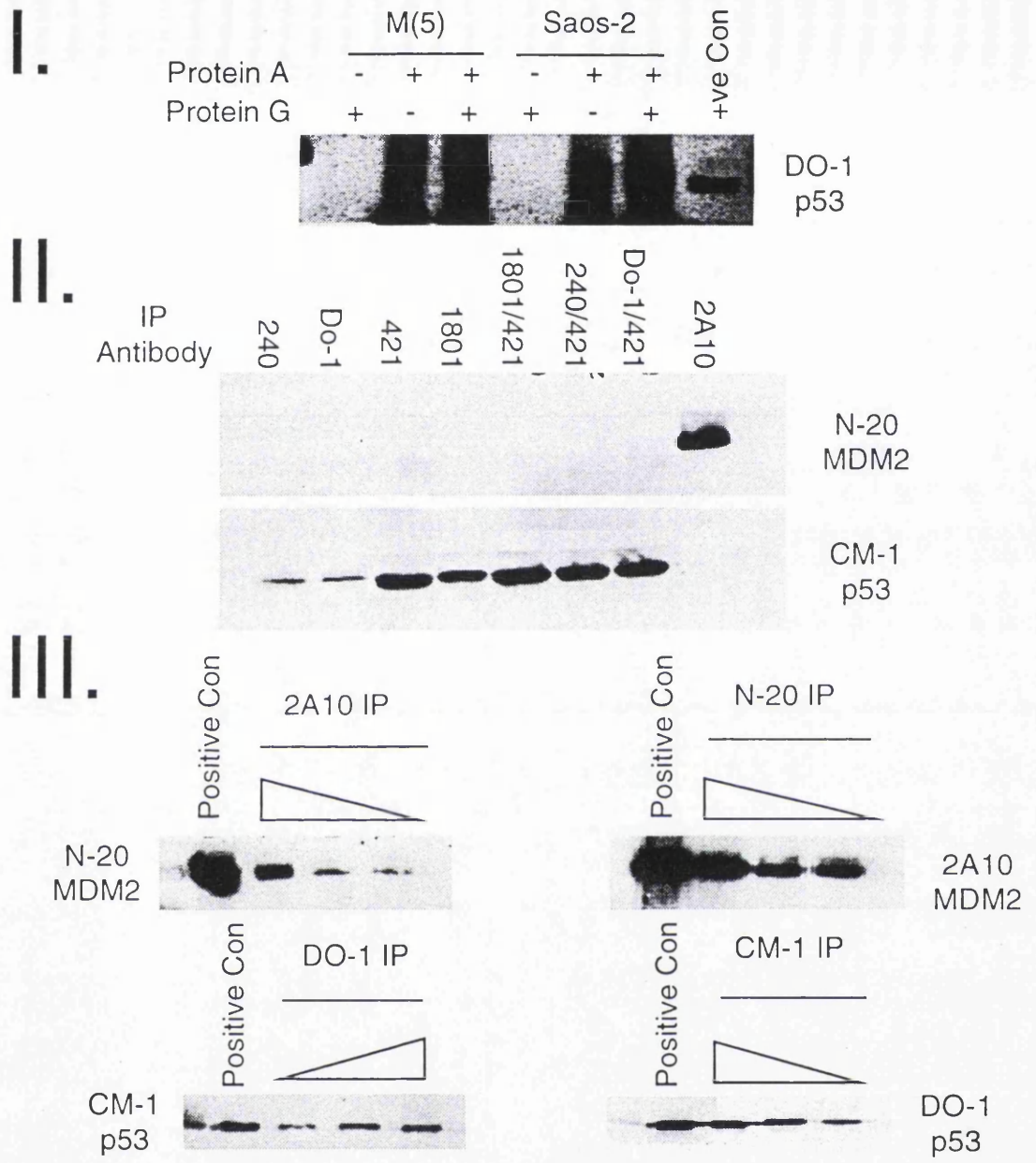

3.1. **Importance of Immunoprecipitation (IP) buffers in the detection of p53:MDM2 protein complexes**. (I) Protein A-, but not G-sepharose detects a ≅53kDa DO-1-reactive band; M(5) and Saos2 cells were mock-IPd (lacking antibody) with either protein A- or G-sepharose and examined by Western analysis. +ve Con = M(5) direct lysate to show p53. (II) Various anti-p53 antibodies fail to detect co-IP MDM2 in Pomerantz IP buffer; Various p53 antibodies (as indicated) and the MDM2 antibody, 2A10, were used to IP U2OS lysates in Pomerantz IP buffer. Western analysis revealed the expected directly-IPd proteins, but no co-IPd proteins. (III) Various MDM2 and p53 antibodies in Pomerantz IP buffer fail to co-IP p53 or MDM2 proteins, respectively; Various p53 and MDM2 antibodies (as indicated) were used to IP U2OS lysates in Pomerantz IP buffer. Western analysis revealed the expected directly-IPd proteins, but no co-IPd proteins. DO-1 and N-20 antibodies concentrations were 0.5, 1 and 2 μg/ml; 2A10 were 50, 100, 150 μl/ml and CM-1 were 0.5, 1, 1.5 μl/ml (see Materials and Methods). Positive Con = M(5) direct lysate.

Detection of co-immunoprecipitates using RIPA and NP-40 Immunoprecipitation Buffers

In an attempt to facilitate detection of co-IPs, other buffers were investigated, namely RIPA and NP-40. Both buffers are polyoxyethylene (9) *p-t*-octyle phenol (Nonidet P-40 [NP-40]) based; a detergent which shows effective solublisation, but is a weak protein denaturant. RIPA buffer in addition, has sodium deoxycholate (DOC), a moderate denaturant and sodium dodecylsulphate, a potent solublisation agent and denaturant.

IP analysis with these buffers consistently yielded co- and direct IPs for MDM2 and p53 using a number of antibodies. DO-1 (p53) and 2A10 and N-20 (MDM2) directly IPd p53 and MDM2, respectively, as well as the respective co-IP proteins. However, the p53 rabbit polyclonal antibody, CM-1, consistently failed to co-IP MDM2, while direct p53 IP levels were significantly high. Comparison between the MDM2-overexpressing, M(5) and vector-only (p3) cell lines, revealed increased MDM2:p53 complex levels in both p53 and MDM2 IPs (see Figure 3.2). M(5) and p3 IPd similar levels of p53 with DO-1, while much more MDM2 was co-IPd with M(5). This vast difference in co-IPd p53 was not as well reflected in the reciprocal 2A10 and N-20 IPs, although a significant difference was seen.

Further IP analysis of parental U2OS, p3, M(5) and M(4) (another MDM2 overexpressing U2OS cell line – see Figure 1.13), revealed similar results of increased MDM2:p53 complexes in cells with elevated MDM2 protein levels (see Figure 3.3).

NP-40 IP buffer was used over RIPA in the majority of the subsequent immunoprecipitation studies due to cleaner, stronger and clearer band generation upon Western analysis. Additionally, all IPs were carried out for four hours post-IP-antibody addition, unless otherwise stated.

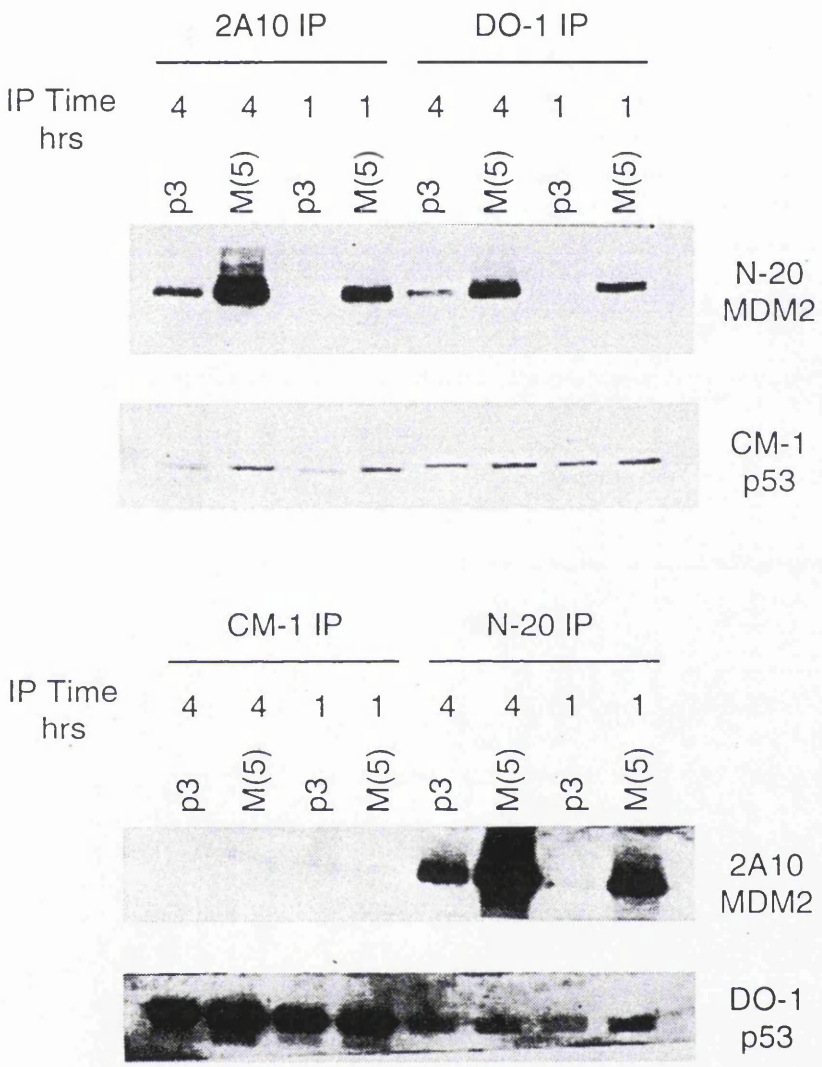

Figure 3.2. Detection of p53:MDM2 complexes using p53 and MDM2 antibodies. M(5) and p3 NP-40 IP buffer lysates were examined by IP analysis using various p53 and MDM2 antibodies (as indicated). IPs were analysed 1 or 4 hours (as indicated) post-IP-antibody addition and examined by Western analysis for MDM2 and p53 proteins. Mouse antibody IPs were detected by Western analysis using rabbit antibodies and vice versa.

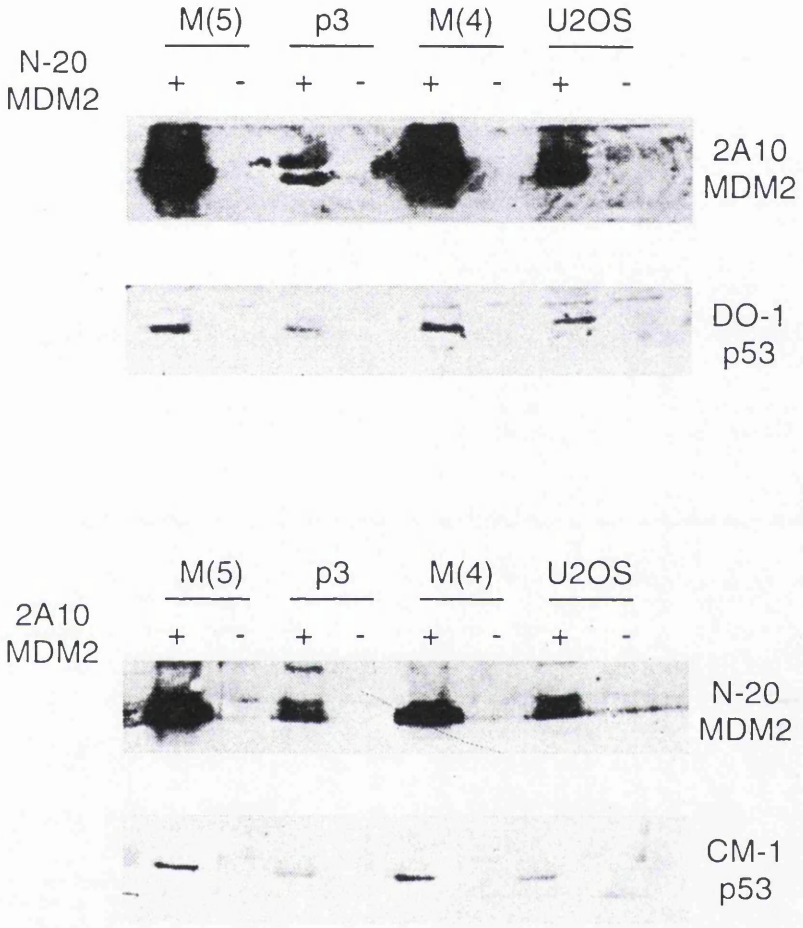

Figure 3.3. Detection of increased p53:MDM2 complexes in MDM2 overexpressing U2OS cell lines. M(5), M(4), p3 and parental U2OS NP-40 IP buffer lysates were examined by IP analysis using rabbit N-20- (+) or mouse 2A10-MDM2 antibodies (+) or no IP antibody (-), followed by Western analysis using mouse 2A10 and DO-1 and rabbit N-20 and CM-1, respectively.

Summary and Discussion

These results revealed the importance of immunoprecipitation conditions in facilitating the detection of protein-protein interactions and the potential problems of using protein A-sepharose in conjunction with p53 detection. The differences in specificity of protein A versus G sepharose in antibody sub-type binding, may explain the differences in binding the contaminating p53-reactive protein. Use of p53-null Saos-2 cells, revealed that the 53 kDa band was not p53, but was capable of binding the p53 monoclonal antibody, DO-1. The presence of large amounts of proteins may generate non-specific, promiscuous interactions with antibodies, possibly explaining the apparent antibody binding.

Of the three MDM2 antibodies tested, all three recognised both free and p53-complexed MDM2. Co-precipitation of p53 with the MDM2 rabbit polyclonal antibody, N-20, which binds the amino terminus of MDM2 near the p53 binding-domain, suggested that the N-20 epitope was not masked by MDM2-complexed p53. Additionally, co-precipitation of MDM2 with the p53 monoclonal antibody DO-1, which binds an epitope near the MDM2 binding domain, also suggested that the epitope was not masked by p53-complexed MDM2. However, due to the oligomeric nature of p53, one molecule of MDM2 bound to tetrameric p53, may only mask one of the four DO-1 epitopes, allowing non-saturated MDM2:p53 complexes to be immunoprecipitated. The failure of the p53 rabbit polyclonal antibody, CM-1, to co-immunoprecipitate MDM2 could be explained through MDM2-mediated obstruction of its major epitope. However, preferential binding of unbound p53 remained another possible explanation. Alternatively, CM-1 mediated conformational changes may have actively resulted in dissociation of the MDM2:p53 complex, resulting in immuno-precipitation of un-complexed p53.

Initial comparison of the M(5) and p3 cell lines revealed increased MDM2:p53 complexes in the MDM2-overexpressing M(5) cells. Both vector only p3 and parental U2OS cells demonstrated similar levels of MDM2:p53 complexes, suggesting that the p3 clone selection process had no effect on complex regulation. As a result p3 and U2OS cells were used interchangeably in the following studies. Both of the MDM2 overexpressing cell lines (M[5] and M[4]) demonstrated elevated complex levels in comparison to vector-only (p3) or

parental U2OS cells. Such increased MDM2:p53 complexes and hence MDM2-mediated transcriptional inactivation of p53, could explain both the reduced p21 and p53 induction in response to X-ray irradiation seen in chapter two. These results also partially explain the observation of delayed apoptosis and abrogated G_1/S cell cycle arrest observed in M(5) in chapter two, through delayed p53 and p21 induction, respectively.

Comparison of cell lines and effects of MDM2 or p53 overexpression

In a further attempt to characterise the cell lines examined in chapter two, p53:MDM2 complexes were examined between the isogenic M(5), DN(5) and parental U2OS cell lines, as well as OSA, a cell line showing high levels of endogenous MDM2 protein. Explanation of the non-detrimental phenotype observed in MDM2 overexpressing M(5) cells, was sought by examining p53:MDM2 complex levels between M(5) and OSA cells. Both cells exhibit similar levels of MDM2 and p53 proteins, while they differed in their method of overexpression: as a result of endogenous gene amplification in OSA cells and possible exogenous gene amplification and enforced CMV-promoter expression in M(5) cells. It was of interest to see whether OSA exhibited similar levels of MDM2:p53 complexes in an attempt to determine whether the cells had the potential for positively or negatively regulating complex formation. Alternatively, to see whether complex formation was simply reflected by absolute MDM2 or p53 protein levels.

Analysis of the M(5) cell line in comparison to the isogenic parental U2OS cell line, allowed investigation into the effects of up-regulation of MDM2, partly independent of the transcription-mediated MDM2-p53 negative-feedback loop. Isogenic analysis of DN(5) also facilitated the investigation of increased p53 levels on p53:MDM2 complex levels in a functionally compromised, mutant p53 cell line, presumably defective in the p53-mediated transcriptional activity of the MDM2-p53 negative-feedback loop.

Lactacystin treatment increases p53:MDM2 complex formation

To investigate the effects of inhibition of proteosomal degradation on p53:MDM2 association, the four cells lines under investigation were treated with 10μM of lactacystin for eight hours prior to immunoprecipitation analysis[14]. MDM2 and p53 IPs were carried out on lactacystin-treated and mock-treated control cells and revealed significant increases in direct immunoprecipitates relative to control samples, although DN(5) did not strictly follow this pattern (see Figure 3.4 [I]). Generally, in accordance with increased direct levels of immunoprecipitates, co-immunoprecipitates were also increased in all of the cell lines examined, even in DN(5), albeit very slightly.

Comparison of the amount of SMP14-IPd MDM2 between the pre-lactacystin-treated cell lines revealed OSA to IP the most, followed by M(5), U2OS and DN(5) (see Figure 3.4 [I]). This pattern was not exactly the same post-lactacystin-treatment, with M(5) cells exhibited the most IPd MDM2, revealing the most dramatic increase, followed by OSA, U2OS and DN(5) cells. A second lower molecular weight 2A10-reactive band was also increased following lactacystin treatment. The order of IPd MDM2 levels was mirrored in the degree of co-IPd p53 with respect to OSA, M(5) and U2OS cells, although M(5) cells, which IPd the most MDM2 following lactacystin-treatment, co-IPd less p53 than OSA cells. However, the most striking observation concerned DN(5) cells, which in spite of the lowest IPd MDM2 levels, exhibited the highest co-IPd p53, pre- and post-lactacystin treatment. Although, the increase of co-IPd p53 after lactacystin-treatment in DN(5) cells was not very significant in comparison to the other three cells lines.

Overall observations made with SMP14 IPs were paralleled in the 1801 IPs, with lactacystin treatment clearly increasing the amount of directly IPd p53 (see Figure 3.4 [I]). DN(5) cells

---

[14] Although 2A10, N-20, and DO-1 in combination with protein-G sepharose had been successfully used for IP, agarose-conjugated SMP14 and 1801 monoclonal antibodies with NP-40 IP buffer were used in subsequent experiments, unless otherwise stated. The use of agarose-conjugated antibodies provided a clearer and more user-friendly method of p53 and MDM2 immunoprecipitation capable of visualising p53:MDM2 complexes.

IPd the most p53 pre-treatment, followed by U2OS, M(5) and OSA cells. OSA and M(5) cells revealed the most significant increases in IPd p53 levels, matching U2OS levels, while detection of an increase in DN(5) cells was not clear due to exposure problems. Co-IPd MDM2 levels were the highest in DN(5) cells pre-lactacystin-treatment, paralleling the highest levels of IPd p53. However, both M(5) and OSA cells exhibited more co-IPd MDM2 than U2OS, while exhibiting lower levels of IPd p53. The most significant increases in co-IPd MDM2 levels were seen in M(5) and OSA cells, both of which surpassed the similar levels of DN(5) and U2OS co-IPd MDM2.

Normal Western analysis of lactacystin cells clearly revealed lactacystin-mediated increases in both MDM2 and p53 protein levels in M(5), U2OS and OSA cells. In contrast, DN(5) cells showed a possible increase in p53 levels, while MDM2 protein levels were not affected at all (see Figure 3.4 [II]).

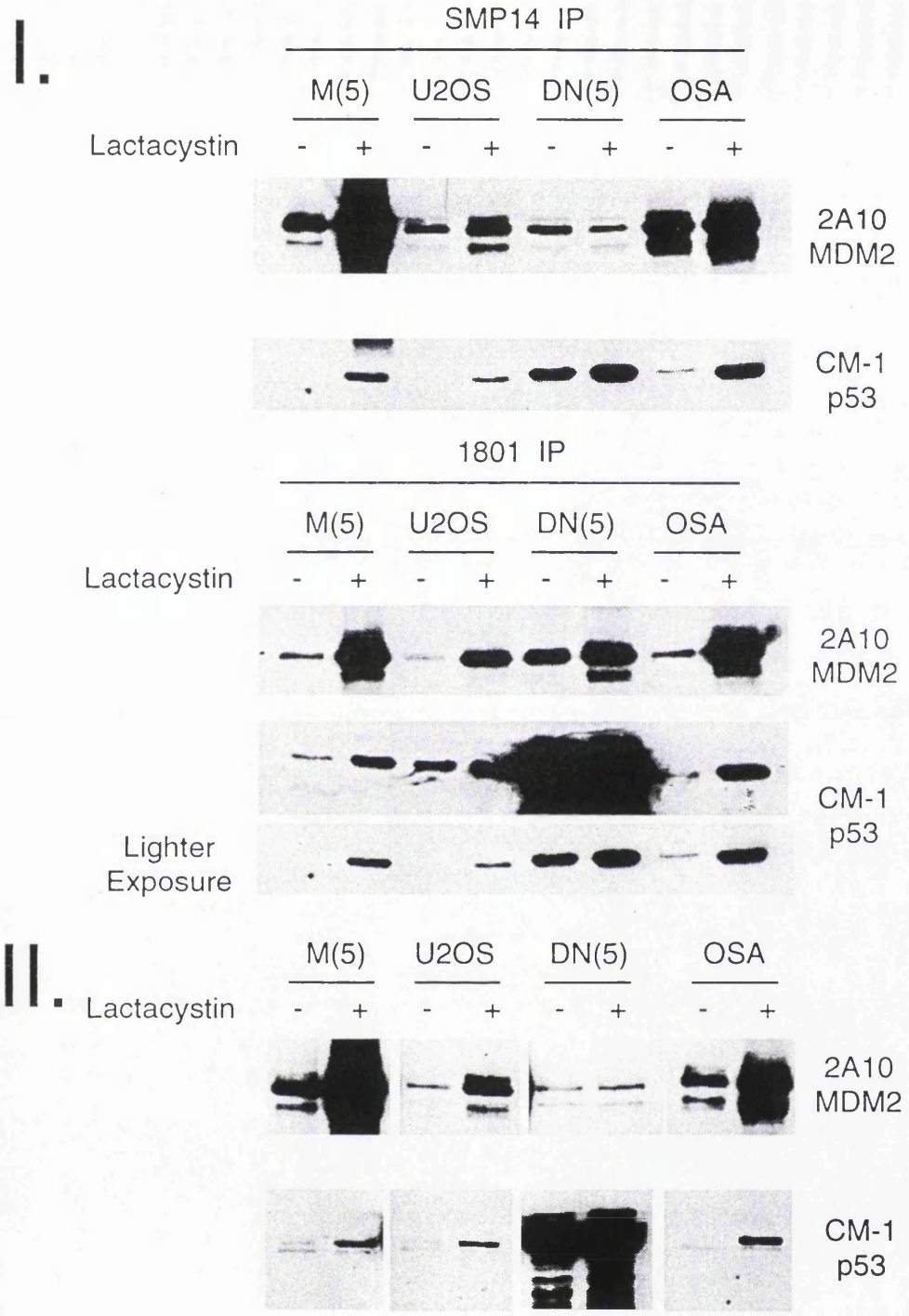

Figure 3.4. Lactacystin-treatment increases p53:MDM2 complex formation. (I) IP analysis of three 10μM lactacystin-treated cell lines reveals elevated p53 and MDM2 proteins levels and p53:MDM2 complexes; Various cell lines (as indicated) were treated with 10μM lactacystin (+) or DMSO (-) for eight hours prior to IP analysis with either agarose-conjugated SMP14 (MDM2) or 1801 (p53) antibodies (as indicated), followed by Western analysis for p53 and MDM2. (II) Western analysis reveals increased p53 and MDM2 protein levels in three cell lines; Various cell lines (as indicated) were treated as above and examined by Western analysis without prior IP analysis.

Transient transfection of MDM2 or p53 increases complex formation

From the work on the various cell lines and the lactacystin results it seemed as though absolute protein levels, and/or perhaps p53 conformation in the case of mutant $p53^{175R \Rightarrow H}$ expressing DN(5) cells, were determining the degree of p53:MDM2 complex formation. To partially address this question, transient transfections of wild-type p53, MDM2 and pcDNA3.1 (vector-only control) were carried out in M(5) and DN(5) cell lines. Direct Western samples were taken and analysed to determine the increase in MDM2 and p53 levels post transfection (see Figure 3.5). MDM2 transients increased MDM2 levels, but reduced p53 levels, while WT p53 transients lead to increased p53 and MDM2 levels – mimicking the X-ray irradiation response (see Chapter Two). IPs were also carried out 48 hours post-transfection and revealed increased complex formation with WT p53 and MDM2 transfected cells relative to vector only (pcDNA3.1) transfectants. Increased complex formation was evident in reciprocal MDM2 and p53 immunoprecipitations.

SMP14 IPs revealed a drastic increase in MDM2:p53 complex formation upon p53 transfection, showing both increased MDM2 and p53 levels (see Figure 3.6). MDM2 transfectants exhibited a slight increase in MDM2:p53 complex levels, reflecting the slight increase in MDM2 levels seen by normal Western analysis. In contrast, transfection of all three plasmids failed to significantly affect complex formation in DN(5) cells, although there was a slight decrease in co-IPd p53 levels upon p53 and MDM2 transfection (see later). The amount of co-IPd p53 seen with MDM2 transfected M(5) cells was similar to the amount seen with all three transfected DN(5) cells, although the amount of MDM2 IPd was significantly lower.

1801 IPs mirrored the SMP14 IP results, with only p53 transfected cells demonstrating a dramatic increase in co-IPd MDM2, while no significant effect was seen in DN(5) cells (see Figure 3.6). However, MDM2-transfectants demonstrated a slight increase in co-IPd MDM2 levels. Comparison of the amount of co-IPd MDM2 between p53 transfected M(5) cells and all three DN(5) transfected cells revealed higher MDM2 levels with lower p53 levels in the MDM2-transfected M(5) cells.

Further IP analysis was carried out on the transfected M(5) and DN(5) cells, with reciprocal and sequential IPs carried out upon the samples. Each sample was twice IPd for 4 hours with either SMP14 or 1801 and then IPd for eight hours once with 1801 or SMP14, respectively. This process was to give an idea of remaining complexes after a single IP and whether SMP14-IPd complexes differed to 1801-IPd complexes.

Sequential SMP14 IP analysis of all three transfected M(5) cell lines revealed similar results, with the 1st and 2nd IPs yielding similar amounts of MDM2 and co-IPd p53 (see Figure 3.7). In keeping with the earlier observations p53 transfected M(5) cell line revealed the most co-IPd p53, followed by MDM2-transfected and p3-transfected M(5) cells. After two rounds of SMP14 IPs, an 1801 IP demonstrated a significant amount of MDM2-complexed p53, the degree of which again mirrored the pattern seen in the SMP14 IPs.

1801 IP analysis demonstrated similar results with respect to earlier observation concerning the degree of MDM2:p53 complexes in the various transfectants (see Figure 3.7). Sequential analysis exhibited reduced direct-IPd p53 and co-IPd MDM2 after the 2nd IP in all three M(5) transfectants. The following SMP14 IP clearly demonstrated that a significant amount of MDM2-complexed p53 was still available.

Analysis of transiently transfected DN(5) cells with MDM2, p53 and pcDNA3.1 revealed a number of similarities with the observation made in the M(5) cell analysis. In agreement with the M(5) results, pre-clearing with the alternative antibody did not significantly affect the levels of subsequently direct or co-IPd proteins (see Figure 3.8). Increased amounts of directly IPd MDM2 were also apparent in MDM2- and p53-transfected cells. However, in contrast to M(5) transfectants, p53 and MDM2 transfected DN(5) cells exhibited significantly lower levels of co-IPd p53, in comparison to vector-only transfected cells.

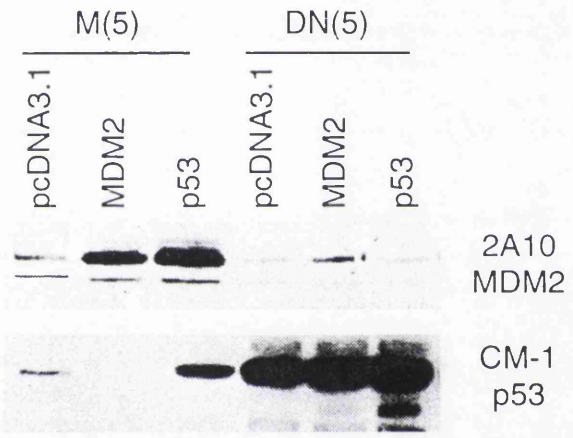

Figure 3.5. Transient transfection of MDM2 and p53 into M(5) and DN(5) cells. M(5) and DN(5) cells were transiently transfected with 5μg of pCMV-MDM2, pCMV-p53 (wild-type) or pcDNA3.1 (vector-only) (as indicated) and examined by Western analysis 48 post-transfection for p53 and MDM2.

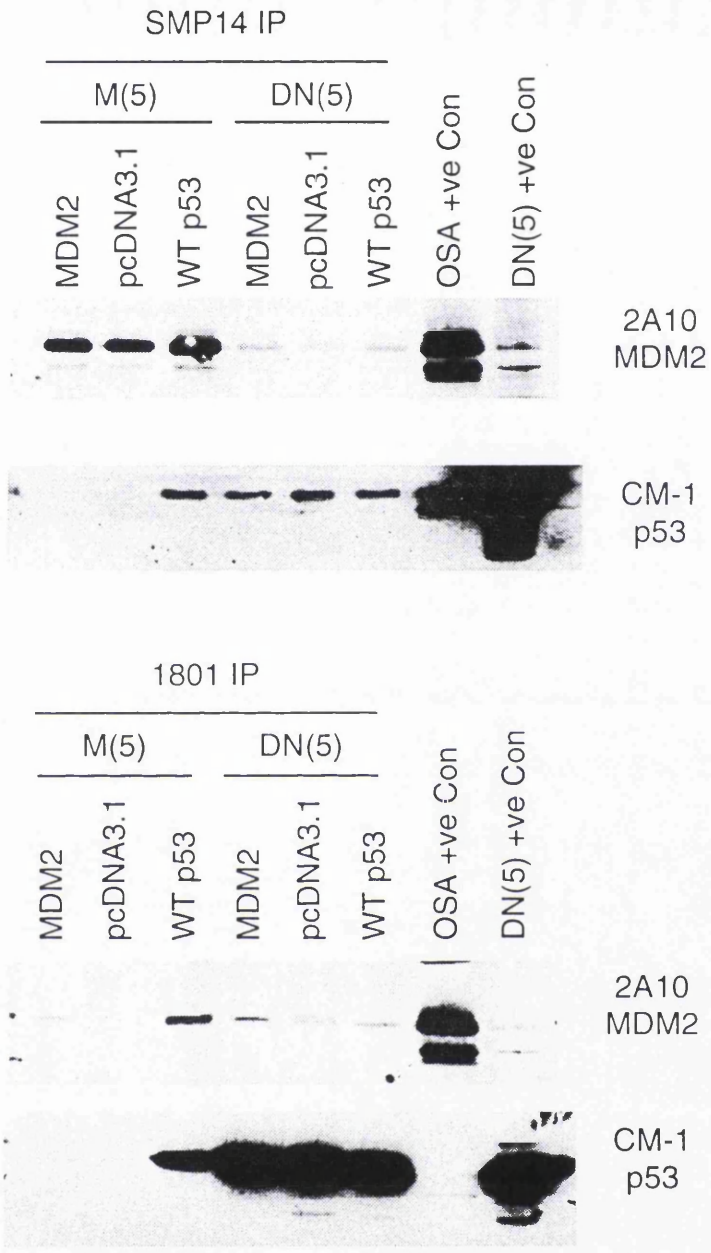

Figure 3.6. Transient transfection of MDM2 and p53 have differential effects on p53:MDM2 complex levels. M(5) and DN(5) cells were transiently transfected with 5μg of pCMV-MDM2, pCMV-p53 (wild-type) or pcDNA3.1 (vector-only) (as indicated) and examined by IP analysis 48 hours post-transfection. Agarose-conjugated SMP14 (MDM2) or 1801 (p53) antibodies (as indicated) were used for IP analysis and subsequently examined by Western analysis for p53 and MDM2. +ve Con = direct Western lysates.

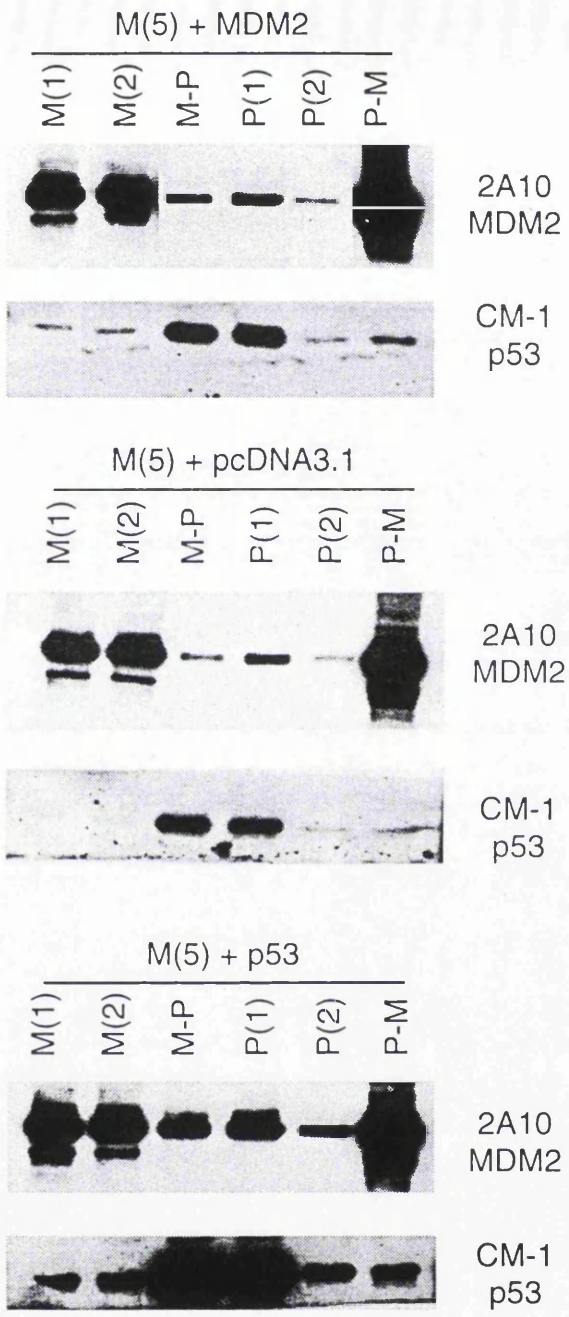

Figure 3.7. Transient transfection of MDM2 and p53 in M(5) cells increases MDM2:p53 complex levels. M(5) cells were transiently transfected with 5µg of pCMV-MDM2, pCMV-p53 (wild-type) or pcDNA3.1 (vector-only) (as indicated) and examined by sequential IP analysis 48 hours post-transfection. Agarose-conjugated SMP14 (MDM2) or 1801 (p53) antibodies were used for IP analysis: M(1) = 1st 4 hour SMP14 IP; M(2) = 2nd 4 hour SMP14 IP; M-P = 1801 8 hour IP post-M(1) and -M(2) IPs and vice versa for P(1), P(2) and P-M. Samples were subsequently examined by Western analysis for p53 and MDM2.

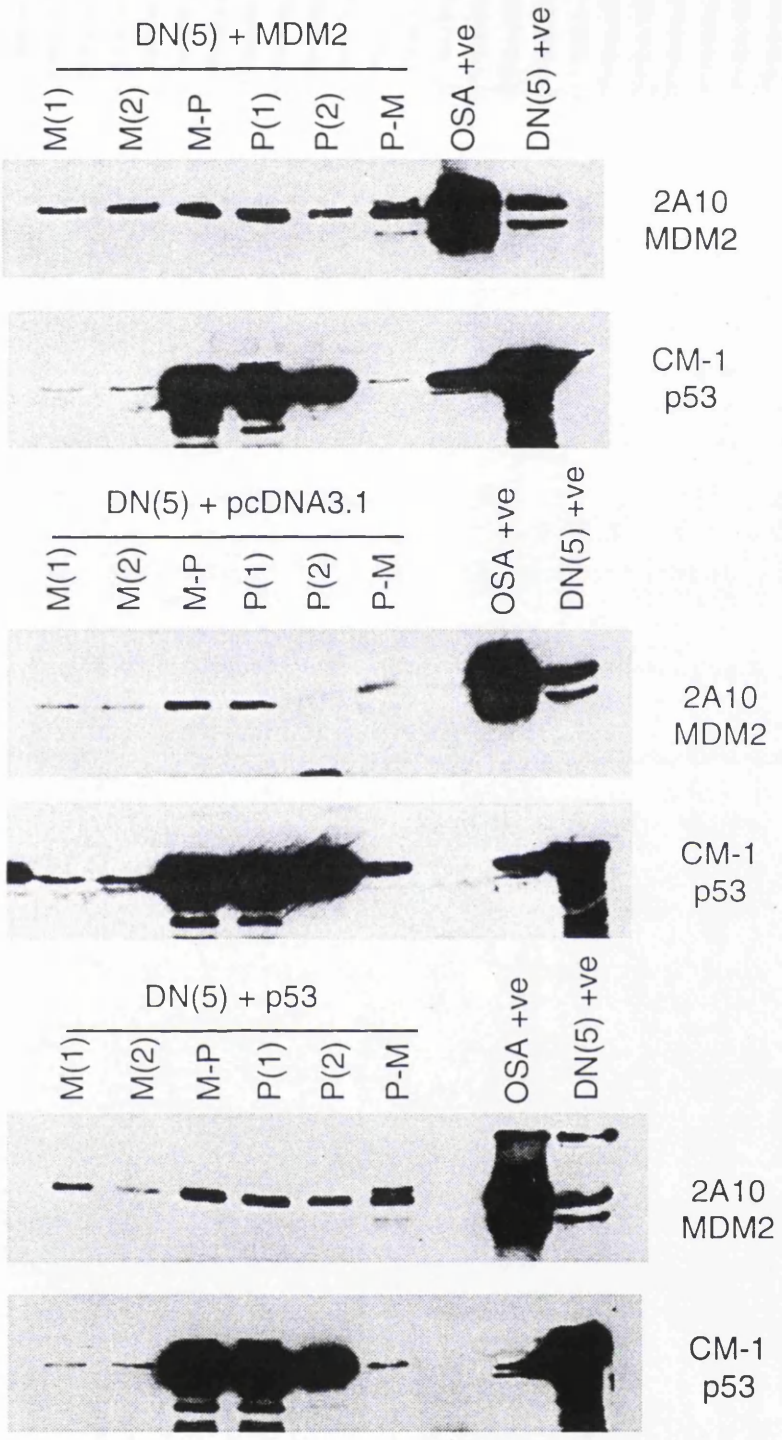

Figure 3.8. Transient transfection of MDM2 and p53 in DN(5) cells have little effect on MDM2:p53 complex levels. DN(5) cells were transiently transfected with 5μg of pCMV-MDM2, pCMV-p53 (wild-type) or pcDNA3.1 (vector-only) (as indicated) and examined by sequential IP analysis 48 hours post-transfection. Agarose-conjugated SMP14 (MDM2) or 1801 (p53) antibodies were used for IP analysis: M(1) = 1st 4 hour SMP14 IP; M(2) = 2nd 4 hour SMP14 IP; M-P = 1801 8 hour IP post-M(1) and -M(2) IPs and vice versa for P(1), P(2) and P-M. Samples were subsequently examined by Western analysis for p53 and MDM2. OSA and DN(5) +ve = direct Western lystates.

Certain mutant p53 conformations influence the degree of p53:MDM2 complex formation

With the observation that DN(5) cells co-IPd a high level of MDM2 , it was of interest to determine whether this was due to a specific conformational state of p53 $175^{A\Rightarrow H}$ or simply a consequence of elevated p53 levels. To address this question transient transfections of wild-type and mutant $248^{R\Rightarrow Q}$, $249^{R\Rightarrow S}$ (a gift from H. Land) and $175^{R\Rightarrow H}$ p53's in pcDNA3.1 were carried out in M(5) cells and compared to vector only transfections by immunoprecipitation analysis. p53 1801-IPs revealed increased co-IPd MDM2 levels in wild-type, $175^{R\Rightarrow H}$ and $248^{R\Rightarrow Q}$ p53-transfected M(5) cells in comparison to vector only controls (see Figure 3.9).

All of the transfected p53 constructs increased the amount of IPd p53, with p53 $175^{R\Rightarrow H}$ and -wild-type producing similar dramatic increases, while only a significantly small increases in both p53 $248^{R\Rightarrow Q}$ and $249^{R\Rightarrow S}$ transfectants (see Figure 3.9). As expected the increased levels of $175^{R\Rightarrow H}$ and wild-type p53 caused an increase in co-IPd MDM2. However the most co-IPd MDM2 was seen with p53 $248^{R\Rightarrow Q}$, which had only exhibited a moderate increase in IPd p53 levels. p53 $249^{R\Rightarrow S}$ had no effect on the amount of co-IPd MDM2 in comparison to vector only control transfections, although p53 levels were elevated.

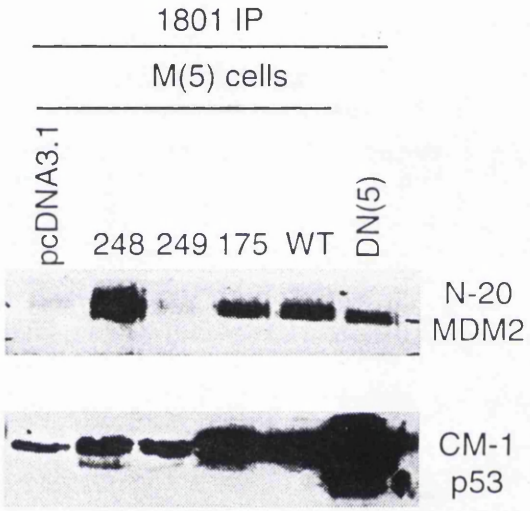

Figure 3.9. p53 point mutants show different binding affinities for MDM2. M(5) cells were transiently transfected with 5μg of pCMV p53 (WT), pCMV p53 175R⇒H, pcDNA3.1 p53 248R⇒Q, pcDNA3.1 p53R⇒S or pCDNA3.1 (vector-only) (as indicated) and examined by IP analysis 48 post-transfection. Agarose-conjugated 1801 (p53) antibody was used for IP and subsequently examined by Western analysis for p53 and MDM2. DN(5) 1801-IP lysate was also included.

Western analysis of glutaraldehyde-treated cells reveals differentially complexed-p53 175$^{R\Rightarrow H}$ in DN(5) cells.

Glutaraldehyde analysis was used in an attempted to analyse the predominant p53-and MDM2-protein complexes in M(5), DN(5) and OSA cell lines. Cells were lysed in NP-40 IP buffer and treated with either 0%, 0.025% or 0.1% glutaraldehyde for 30 minutes (to covalently cross link p53- and MDM2-interacting proteins through their amino-groups), prior to Western analysis. DN(5) cells exhibited very high levels of a high-molecular p53 smear that persevered upon glutaraldeyde-treatment (see Figure 3.10). This smear was absent from M(5) and OSA samples (even upon long film exposure), suggesting the existence of novel p53 175$^{R\Rightarrow H}$ molecular interactions, absent in wild-type p53 cells. The occurrence of high molecular weight bands in the untreated DN(5) sample also suggested the existence of p53 175$^{R\Rightarrow H}$-specific post-translational modifications, such as ubiquitination, sumoylation and phosphorylation (see Introduction). Similar high molecular weight p53 bands were also evident in untreated M(5) and OSA samples (upon higher exposure), although they did not correspond in molecular weight to the heavier p53 175$^{R\Rightarrow H}$-specific bands.

MDM2 analysis revealed a number of differences between the untreated MDM2 expression patterns and the three cell lines examined. A ≅170kDa MDM2 band, unique to the two U2OS-derived cell lines, was absent in the OSA sample (see Figure 3.10), while DN(5) cells exhibited a unique ≅62kDa band, absent from both M(5) and OSA cells. Additionally, two MDM2 bands (≅55 and 75kDa) were absent from DN(5) cells, but present in both OSA and M(5) cells. The occurrence of different MDM2 bands in untreated cell samples could primarily be explained through differential cell-specific post-translational modifications, although differential *mdm2* splicing and/or proteolytic-cleavage could explain the sub-90kDa bands. Upon glutaraldehyde treatment, both OSA and M(5) cells exhibited similar high molecular weight smears, which were also absent from DN(5) samples upon very long exposure times. Overall, these results suggested that the amplified endogenous and exogenous MDM2 proteins in M(5) and OSA cells, respectively, were behaving similarly. However, p53 175$^{R\Rightarrow H}$ expression may have altered MDM2 expression patterns.

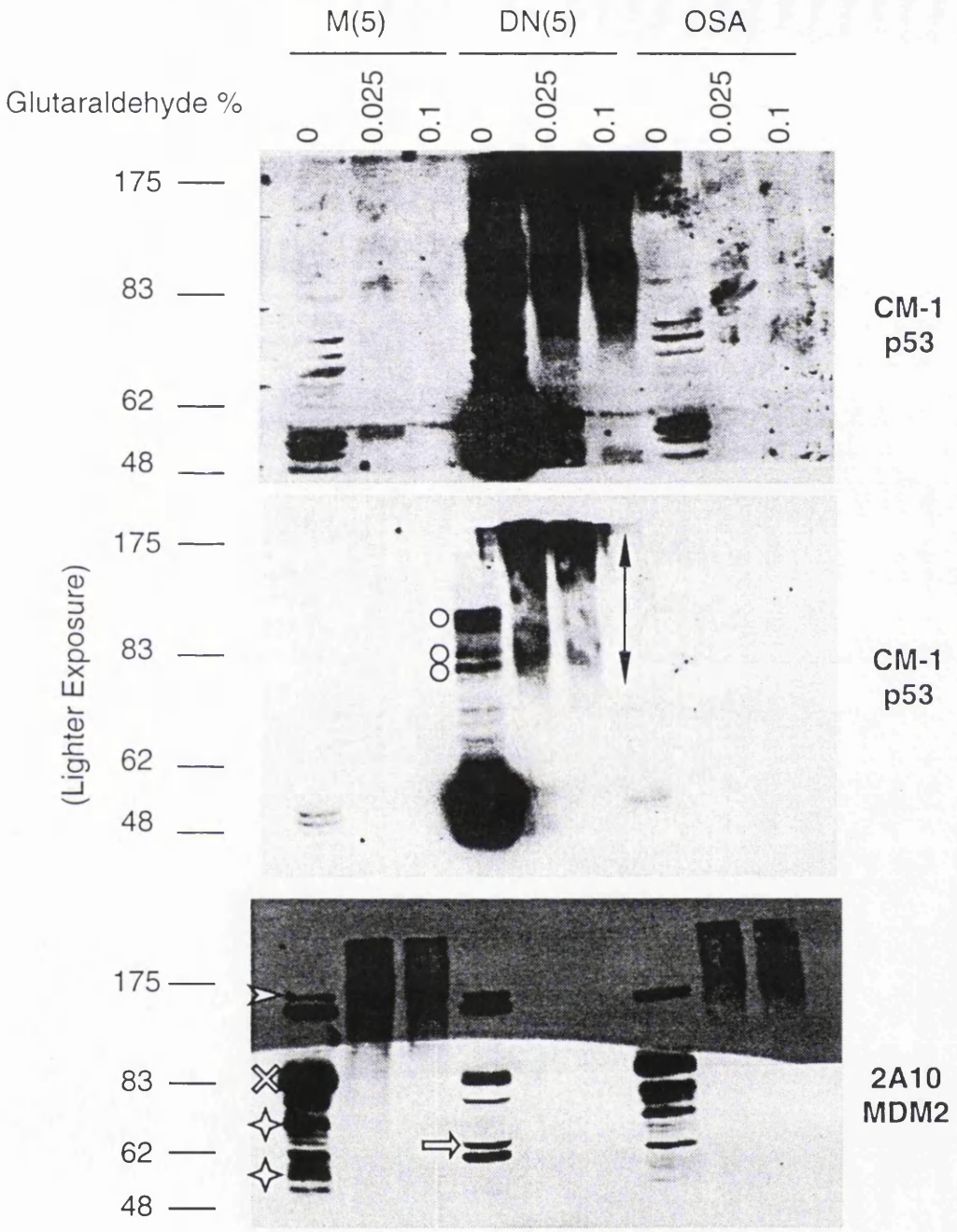

Figure 3.10. Glutaraldehyde-mediated protein cross-linking of p53 and MDM2 proteins. M(5), DN(5) and OSA NP-40 IP buffer cell lysates were treated with either 0%, 0.025% or 0.1% glutaraldehyde for 30 minutes, prior to Western analysis for MDM2 and p53. U2OS-unique MDM2 bands are marked with an arrowhead; the major 90kDa MDM2 band is marked with an cross; M(5)- and OSA-unique bands are marked with a star; a DN(5) unique MDM2 band is marked with a compete arrow; p53 175R⇒H-unique/dominant bands are marked with a circle; p53 175R⇒H smear is marked with arrowheaded vertical line. Size markers are indicated on the left-hand side kDa.

ARF induction does not decrease p53:MDM2 complex formation

With the reports of ARF inducing a cell-cycle arrest and reported inhibition of MDM2-mediated p53 degradation (see Introduction), it was thought that ARF overexpression would mainly bring about these events through abrogation of MDM2-mediated inhibition of p53. Mechanistically this could be achieved either through prevention or disruption of the p53:MDM2 complex or alternative downstream inhibition of MDM2-mediated degradation.

NARF(6) cells were used to investigate the effects of ARF-overexpression on p53:MDM2 complex formation, both with respect to its effects on p53 and MDM2 protein levels and cell cycle arrest. Cells were either induced with 1mM IPTG, or mocked treated and analysed by IP. Time points were taken post-induction and SMP14 and 1801 IPs were carried out on the samples and compared to control samples.

Reciprocal IPs showed that p53 and MDM2 co-immunoprecipitates were increased following ARF induction (see Figure 3.11). As expected, increased levels of direct MDM2 and p53 immunoprecipitates were apparent six to 24 hours post-induction, although no further significant increases were observed at later time points. The increase reflected the ARF-mediated stabilisation of both proteins (see Figure 2.37). Increased complex formation was observed as early as six hours post-induction and continued to increase until the final time point at 72 hrs when the cells were cell cycle arrested. Therefore, increasing co-IPd protein resulted without significant increases in direct IPd protein after the six-hour time point.

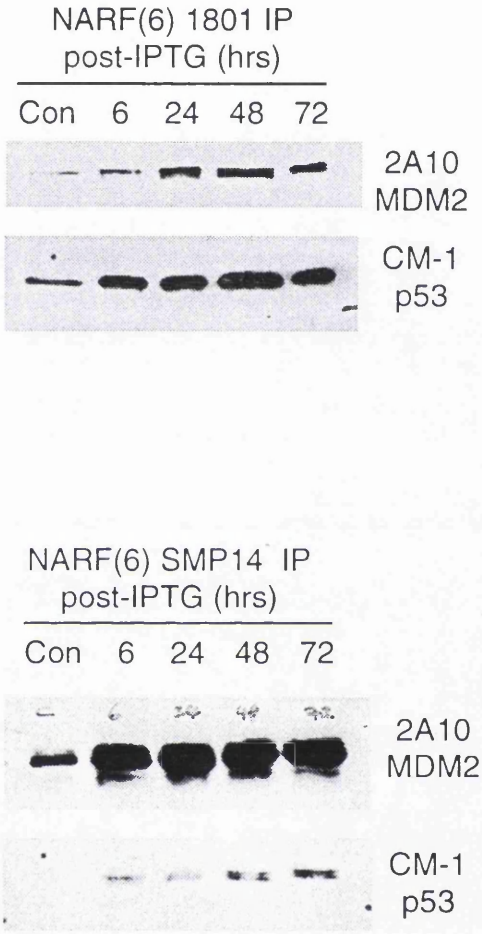

Figure 3.11. p14ARF expression increases p53:MDM2 complex levels. NARF(6) cells were treated with 1mM IPTG and analysed by IP analysis at various time points post-treatment (as indicated). Agarose-conjugated SMP14 (MDM2) and 1801 (p53) antibodies were used for IP and subsequently examined by Western analysis for p53 and MDM2.

Inability to detect MDM2:pRB or MDM2:E2F-1 complexes

A recent report(Hsieh, Chan et al. 1999) had documented the association of MDM2 with pRB and linked the interaction with the regulation of apoptosis. With the earlier observation of M(5) cells exhibiting attenuated apoptosis and cell cycle arrest, an differential MDM2:pRB interaction was a candidate for a second mechanism for such an abrogation. Xin Lu (personal communication) had recommended MCF-7 cells eight hours post-irradiation as a positive control. Furthermore, MDM2 had been reported to bind E2F-1(Martin, Trouche et al. 1995), a transcription factor whose activity may be modulated through MDM2 interaction and is implicated in apoptosis (see Chapter Two). With the evidence that UV-irradiation induced E2F-1 levels approximately eight-ten hours post-irradiation and coincided with apoptosis in U2OS cells, MDM2:E2F-1 complex formation was also analysed.

M(5), DN(5), U2OS, OSA and MCF-7 were UV-irradiated and IP samples were taken eight hours post-irradiation. IF8 (pRB) IPs while successfully immunoprecipitating pRB, failed to show any detectable co-IPd MDM2 (see Figure 3.12). However, E2F-1 was successfully co-IPd, suggesting that the IP conditions were working. 2A10 IPs did reveal a prospective hypo-phosphorylated pRB co-IPd band, running just below the predominantly hyperphosphorylated M(5) positive control pRB. However, no E2F-1 was co-IPd, although a potential faster running E2F-1 band was present in all of the IPs. E2F-1 would have been expected to be complexed specifically with the hypophosphorylated pRB form and hence co-IPd. To ensure that the potential pRB and E2F-1 bands were 'real', 2A10 IPs were carried out on *RB*-null Saos2 cells. Analysis revealed that the potential hypophosphorylated pRB and E2F-1 bands were present in Saos2 IPs, suggesting that they were non-specific contaminating bands most probably derived from the 2A10 ascite fluid (see Figure 3.13).

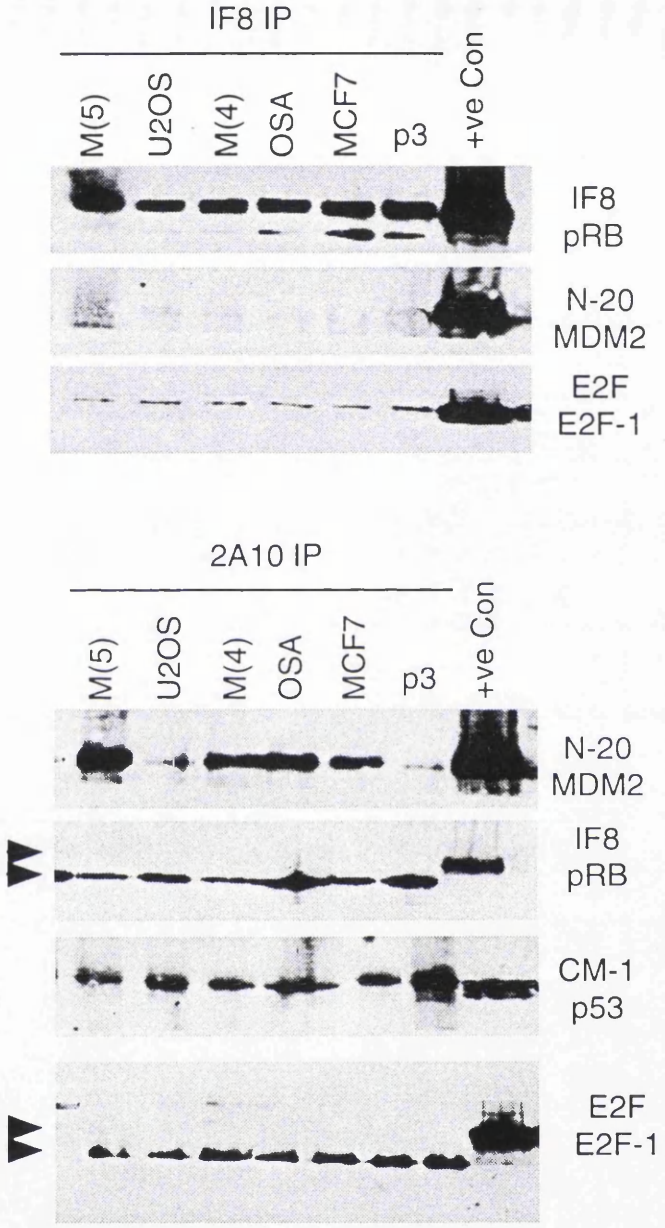

Figure 3.12. Inability to detect pRB:- or E2F-1:MDM2 complexes in a number of cell lines. Various cell lines (as indicated) were 30 Jm-2 UV-irradiated and analysed by IP analysis eight hours post-irradiation. IF8 (pRB) and 2A10 (MDM2) antibodies, in conjunction with protein-G sepharose, were used for IP analysis and subsequently examined by Western analysis for different cellular proteins (as indicated). Arrowheads indicate the difference between potential and real pRB and E2F-1 bands. +ve Con = M(5) direct Western lysate.

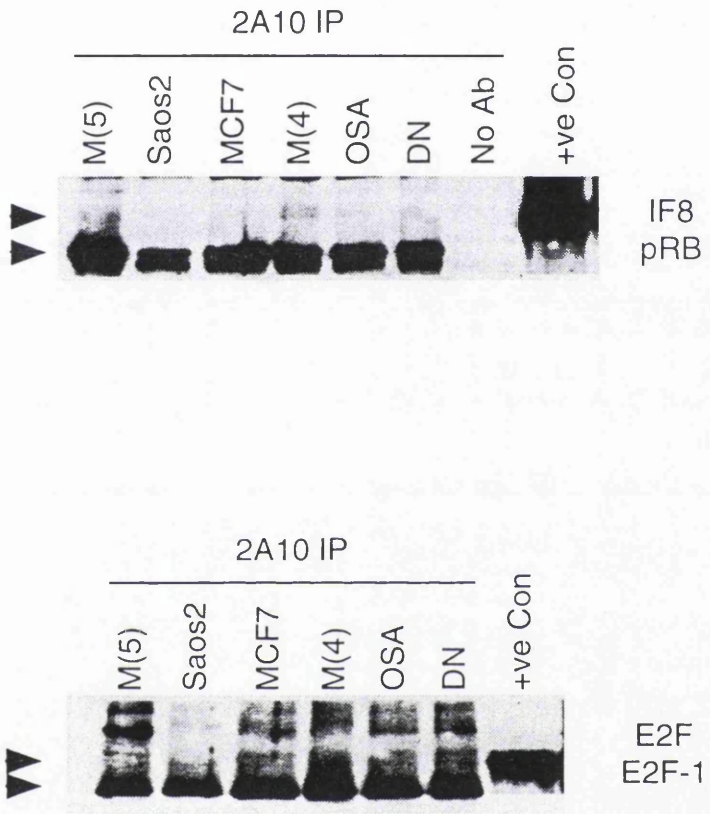

Figure 3.13. Control IPs reveal contaminating IF8- (pRB) and E2F- (E2F-1) immunoreactive bands. Various cell lines (as indicated) were 30 Jm-2 UV-irradiated and analysed by IP analysis eight hours post-irradiation. IF8 (pRB) and 2A10 (MDM2) antibodies, in conjunction with protein-G sepharose, were used for IP analysis and samples were subsequently examined by Western for pRB and E2F-1. Arrowheads indicate the difference between potential and real pRB and E2F-1 bands. +ve Con = M(5) direct Western lysate.

Inability to detect MDM2:ARF complexes

Western blot analysis of a number of cell lines revealed the presence of ARF in a number of U2OS-derived cell lines and in IPTG-induced and un-induced NARF(6) cells (see Chapter Two). As a negative regulator of MDM2, up-regulation of ARF was expected in M(5) cells, although this was not seen. The lack of induction was perhaps due to increased ARF:MDM2 binding affinities and hence complex formation, rather than simple increases in protein levels. A similar explanation could have explained the lack of increased ARF levels in DN(5) cells, where mutant p53 was expected to relieve wild-type p53-mediated repression of ARF expression. To address these questions and generally examine MDM2:ARF binding, IPs were carried out upon M(5), DN(5) cells and compared to IPTG-induced and un-induced NARF(6) cells. FST-13, a rabbit polyclonal anti-peptide antibody developed against His-tagged ARF (kindly donated by F.Stott), was used for ARF immunoprecipitation studies.

Reciprocal SMP14 MDM2 and FST-13 ARF IPs successfully IPd MDM2 and ARF, respectively, but failed to generate any co-IPs (see Figure 3.14). These results suggested that either the two proteins did not interact in these cells, or the IP conditions were not suited to visualise the complex.

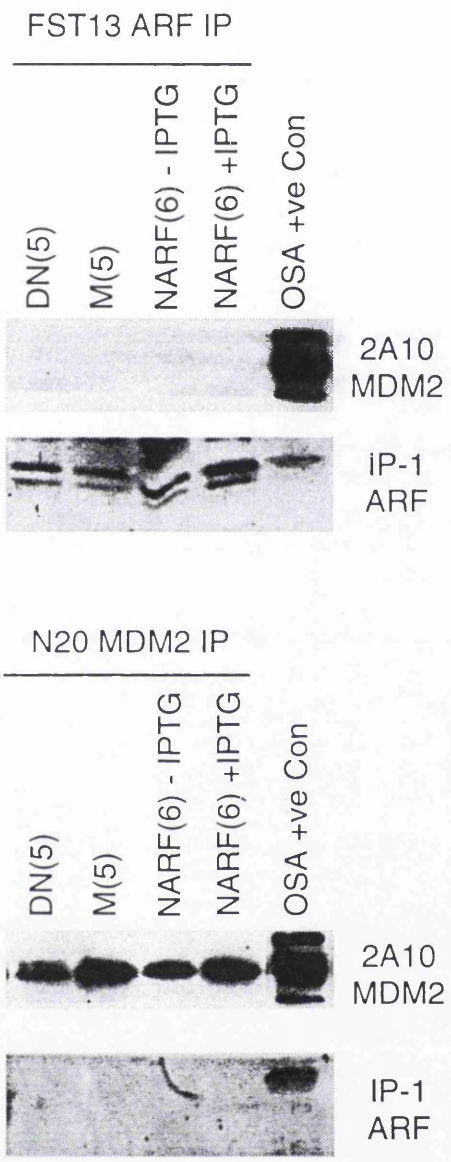

Figure 3.14. Inability to detect MDM2:p14ARF complexes in various cell lines. Untreated or 24 hour post-1mM IPTG-treated NARF(6) cells, DN(5) and M(5) cells were examined by IP analysis. FST-13 (p14ARF) and N-20 (MDM2) antibodies were used for IP analysis and samples were subsequently examined by Western analysis for MDM2 and p14ARF. OSA +ve Con = direct Western lysate.

Summary and Discussion

Correlation between the amount of p53 immunoprecipitated and the amount of co-immunoprecipitated MDM2, supported the idea that control of MDM2:p53 complex formation was heavily influenced by increases in either proteins' level.

Immunoprecipitation analysis of the isogenic cell lines M(5), DN(5) and U2OS revealed the presence of p53:MDM2 complexes in all three lines. In addition the tumour cell line OSA, which exhibited high levels of endogenous MDM2 and detectable wild-type p53 (mimicking M[5] cells), also demonstrated p53:MDM2 complexes. These results clearly show that complex formation between the two proteins takes place in non-stressed cell lines, suggesting a role for the complex in maintaining a 'normal' cellular state. The current view is that MDM2-mediated degradation and transcriptional silencing of p53 prevents p53-dependent activation of target genes, in turn preventing p53-mediated cell cycle arrest or apoptosis. Therefore, in an attempt to prevent cell cycle arrest and apoptosis, and hence maintain a 'normal' state, MDM2 would bind and inactivate any p53 molecules capable of activating such processes.

Comparison between these cell lines revealed a link between increased expression levels of MDM2 and increased p53:MDM2 complexes. Both M(5) and OSA exhibited high levels of MDM2, and generated more co-immunoprecipitates in either MDM or p53 direct-immunoprecipitations, than the parental U2OS cell line. Increased complex formation in M(5) cells suggested that the exogenously expressed MDM2 was functional, with respect to binding p53. Therefore, inhibition of excess MDM2:p53 association, could not explain the lack of excessive p53 degradation seen in M(5) cells. Similar observations of increased complex levels were seen in OSA cells, where MDM2 and wild-type p53 levels are similar. These results strongly suggested that the regulatory mechanism governing the p53:MDM2 interaction were either not responsive to increases in either MDM2 levels, or the responsive cellular action was unable to function in these cell lines; either through mutational events in the pathway or, as in the case of the exogenously expressed protein in M(5) cells, through an inability to modulate transcription of pCMV-driven *mdm2*.

Analysis of DN(5) cells which exogenously expressed extremely high levels of p53 $175^{R\Rightarrow H}$ exhibited the highest degree of p53:MDM2 complexes of all the cell lines examined. The presence of MDM2:p53 complexes suggests that MDM2 is capable of binding the non-DNA binding mutant $p53^{R\Rightarrow H}$. p53 IPs pulled down a vast amount of p53 and a significant amount of co-immunoprecipitated MDM2, while MDM2 IPs pulled down a relatively small amount of MDM2, but still co-IPd an extremely large amount of p53 in comparison to parental U2OS cells. The latter observation can be explained through the potential binding ratios of MDM2 and p53: tetrameric p53 could bind up to four molecules of MDM2, while a single molecule of MDM2 may also co-IP four p53 molecules. Association assays had determined that MDM2's interaction was, unlike HPV E6, significantly impaired by loss of quartenary structure(Marston, Jenkins et al. 1995; Midgley and Lane 1997; Kubbutat, Ludwig et al. 1998; Maki 1999). Therefore a 1:4 ratio could explain the significantly large amount of co-IPd p53 by a significantly small amount of MDM2. DN(5) cells may contain a higher ratio of tetrameric p53, perhaps mediated by p53 $175^{R\Rightarrow H}$, although this could not be determined from this work.

Interestingly, glutaraldehyde analysis revealed differences between the wild-type p53 of M(5) and OSA cells and the mutant p53 $175^{R\Rightarrow H}$ of DN(5) cells. The persistence of high molecular CM-1 reactive smears, suggested the existence of novel p53 $175^{R\Rightarrow H}$ protein-protein interactions that may represent oligomerised p53 or heat shock protein-complexed p53(Pinhasi-Kimhi, Michaalovitz et al. 1986). Nevertheless, the observed differences may promote MDM2 association, accounting for the altered p53:MDM2 binding characteristics seen in DN(5) cells.

Addition of transfected MDM2 or p53 into M(5) cells also lead to increased p53:MDM2 complex formation, supporting the initial observations. Increased complex formation upon MDM2 transfection was detectable, while p53 transfection yielded the most dramatic increase. Increased MDM2 levels and subsequent increased p53:MDM2 complex levels suggest that there was unbound-p53 available for MDM2 complex formation. Addition of extra MDM2 may present a body of MDM2 that initially cannot be regulated with respect to binding p53. Potential p53:MDM2 complex-hindering MDM2 post-translational modification systems may effectively be swamped, allowing un-regulated promiscuous interaction.

Alternatively, as in the case of stable MDM2 expression in M(5) cells, the rate of *de novo* MDM2 production, may be in excess of the rate of negative modification. A simpler explanation relates to simple increased MDM2 levels increasing the likelihood of interaction, although such an unregulated cellular interaction remains unlikely.

The dramatic increase in p53:MDM2 complex formation observed with transfected p53 most probably reflects the two-fold effect on both MDM2 and p53 protein levels. Not only does the transfected p53 increase p53 levels directly, but p53-mediated transcriptional activation presumably also accounts for the increased amounts of direct- and co-IPd MDM2 seen upon SMP14 and 1801 IPs, respectively. Similar arguments used for the MDM2-transfected M(5) cells concerning swamping of inhibitory regulatory systems can be applied to both p53 and MDM2. In addition, activation of an MDM2:p53-complex promoting system may also account for the increased levels, although this seems unlikely. Again, simple increases in protein levels could also explain the increased complex levels.

Interestingly, transient transfection of wild-type p53 and the subsequent increase in both p53 and MDM2 protein levels mimics, in part, the X-ray irradiation response seen in chapter two. In this scenario of increased p53 and MDM2 levels in the absence of any DNA damage, p53-transfection lead to increased levels of p53:MDM2 complexes. However, DNA transfection itself has been shown to generate a cellular stress response(Renzing and Lane 1995). Nevertheless, if that was the case, MDM2:p53 levels would have been expected to be reduced to facilitate p53 activation.

No significant increase in complex formation was observed upon transfection of MDM2 or p53 in DN(5) cells, perhaps suggesting that maximal levels of complex formation were achieved in these cells and increases in either protein could not affect the levels of the MDM2:p53 complexes. Alternatively, mutant-p53-mediated abrogation of an MDM2:p53 complex inhibitory regulatory system could also account for the lack of 'swamping' effects. Nevertheless, the failure of wild-type p53 to mirror the dramatic increase in complex formation see in M(5) cells may be explained through the presence of mutant p53 $175^{R \Rightarrow H}$. Formation of mixed non-DNA binding wild-type:mutant tetramers, would abrogate p53-dependent transcriptional upregulation of the MDM2 gene, thereby reducing the two-fold induction effect of p53 seen in M(5) cells.

Paradoxically, sequential SMP14 IP analysis highlighted an MDM2- and p53-mediated reduction in the amount of co-IPd p53, in comparison to vector-only transfected cells. Both p53 and MDM2 transfections caused similar effects, suggesting that MDM2 (transcriptionally induced by the wild-type p53) may have been the actual effector. A possible explanation for the loss of p53:MDM2 association could lie in selective MDM2-mediated degradation of p53-associated in complexes IPd by SMP14. However, no clear explanation can be provided for these observations.

Generally, the sequential IP analysis revealed a large degree of complexed p53:MDM2 retained in the IP lysis following pre-clearing with either antibody. These observations support the suggestion that either 1801 or SMP14 antibodies exhibit selectively between different types of p53:MDM2 complexes. Such differences may be reflected in the ratio of p53 and MDM2 within these complexes, with SMP14 favouring tetrameric-complexed MDM2 and 1801 favouring lower order p53-complexes.

Western analysis of lactacystin treated cells increased both wild-type p53 and MDM2 expression in M(5), U2OS and OSA cell lines upon Western analysis, while only p53 levels were affected in DN(5) cells. MDM2 immunoprecipitation of similarly treated cells revealed dichotomous results, with increased p53:MDM2 complex formation in M(5), OSA and U2OS cells while no effect was seen in DN(5) cells. These results further supported the link between increased p53 and MDM2 protein levels and increased p53:MDM2 complexes.

p53 IPs mirrored the MDM2 IPs, with increased direct and co-IPd protein levels following lactacystin-treatment. However, DN(5) cells did exhibit more co-IPd MDM2, while alterations in IPd p53 levels were hard to determine due to the intensity of the bands. This observation conflicts with the lack of effect seen with the MDM2 IP results, perhaps suggesting that there may be some antibody-binding preference, with SMP14 preferring non-complexed MDM2 and 1801 preferring complexed p53.

Lactacystin-treated cells in comparison to mock-treated cells revealed parallels between increased levels of IPd MDM2 and increased co-IPd p53. An explanation of the increase in complex formation lies in either general increases in protein levels or the nature of MDM2-mediated ubiquitination of p53. The MDM2:p53 protein-protein interaction is required to

ubiquitinate p53 and transport it to the cytoplasmic proteosomes and once there, may remain complexed until the proteosome has degraded p53. However, in a lactacystin-treated cell, the proteosome is unable to degrade ubiquitinated proteins and hence a block in the terminal stage of MDM2-mediated degradation may occur. Such a block may effectively increase the degree of MDM2-complexed p53 in a temporal window, reducing the inherent transient nature of the interaction. Therefore, in addition to increases in MDM2 levels mediated by transcriptional activation by p53, proteosomal inhibition could also contribute to increased complex levels. However, lactacystin-mediated alterations of complex-promoting or -dissociating/prevention factors could also explain the observations.

The lactacystin results supported the idea that both p53 and MDM2 were regulated by degradation events. However, it could not be determined whether the increased p53 expression was due to inhibition of MDM2 degradation, or perhaps, inhibited degradation of positive p53 transcriptional/translational/stabilising factors. Lack of MDM2 induction in DN(5) cells also suggested that the increased MDM2 levels seen in M(5), U2OS and OSA were a consequence of increased p53-mediated transcription of the *mdm2* gene, rather than inhibition of MDM2 degradation. Hence, lactacystin not only increases p53 levels, but also activates p53 for transcriptional transactivation of the p53-target gene, *mdm2*. Additionally, the increase of lactacystin-mediated p53 $175^{R\Rightarrow H}$ implies that like endogenous wild-type p53, was under some degree of proteosome-mediated degradation control.

High levels of mutant p53 levels may be attributed to the inability of such p53 mutants to be bound and hence degraded by MDM2. Alternatively, mutant p53s' inability to transactivate the *mdm2* gene and hence expression of its negative degradation-mediated regulator can also explain the high expression of mutant p53 proteins. The high degree of p53:MDM2 complexes evident in DN(5) cells, prompted thoughts that regulation of p53 $175^{R\Rightarrow H}$ stability was not impaired at the level of MDM2 interaction, but inhibited at a stage downstream of p53:MDM2 association. Due to lack of accurate quantitative analysis, no clear explanation of the extremely high levels of MDM2 co-IP seen in p53 IPs with DN(5) cells could be made; therefore distinction between a preferred MDM2 binding conformation, DNA-bound or unbound, or simple increased p53 protein levels or a combination of both was not clear. Increased stability of the complex, due to the inability of MDM2 to degrade p53 $175^{R\Rightarrow H}$,

could also explain the increased detectability of the complex. This explanation is similar to the lactacystin explanation, where p53 and MDM2 association is increased due to inhibited degradation of complex.

Analysis of transiently transfected wild-type and mutant $175^{R\Rightarrow H}$ p53s in M(5) cells revealed similar levels of both IPd p53 and co-IPd MDM2. This result suggested that the increased levels of co-IPd MDM2 seen in DN(5) cells was a reflection of increased p53 levels rather than a more favourable MDM2-binding p53 conformation. Although, p53-mediated upregulation of endogenous MDM2 may have slightly confused this observation and conclusion. In contrast to these observations, transient transfection of mutant p53 $248^{R\Rightarrow Q}$ and $249^{R\Rightarrow S}$ only slightly increased the IPd p53 levels, while $248^{R\Rightarrow Q}$, but not $249^{R\Rightarrow S}$, showed increased co-IPd MDM2. Therefore, significantly more MDM2 was co-IPd with mutant p53 $248^{R\Rightarrow Q}$ than with either wild-type or mutant $175^{R\Rightarrow H}$ and in the absence of higher IPd p53 levels. These results suggested that mutant p53 $248^{R\Rightarrow Q}$'s conformation was more efficient at binding MDM2. In addition to intrinsic conformational differences, mutation of certain residues (such as R248) may lead to increased MDM2 association and/or stability either via: inhibition or abrogation of certain MDM2:p53 dissociating or destabilising protein-protein interactions; or alternatively, enhance complex-stabilising protein-protein interactions.

The actual mechanism of ARF as a negative regulator of MDM2 function has not been fully clarified. One potential mode of action concerns prevention or dissociation of p53:MDM2 complexes. Analysis of a ARF-induction time course revealed no loss of p53:MDM2 interaction, but surprisingly a significant increase by six hours post-induction. In light of the ARF-mediated induction of p53 and MDM2 protein levels, these results suggested at the very least that either pre-formed complexes were not dissociated, but either stabilised or increased. Association of nascent p53 and/or MDM2 may be controlled, in part, by ARF upon induction, limiting complex formation and generating free, unbound p53. Nevertheless, no decrease in complex formation was observed, showing that a certain pool of p53 was bound to MDM2 during ARF-mediated cell cycle arrest. Increasing levels of co-IPd p53 and MDM2 proteins were observed throughout the time course, without any clear increases in direct-IPd protein, suggesting *de novo* association of p53 and MDM2 proteins.

Possible similarities can be drawn with mutant p53 $175^{R \Rightarrow H}$ and lactacystin observations which demonstrate easily elevated MDM2:p53 complexes (relative to parental U2OS), but do not exhibit significant p53 degradation. Therefore, ARF may mimic lactacystin's inhibition of p53 degradation downstream of the protein-protein association step.

MDM2:ARF complexes were not readily detected in any of the cell lines tested. Many reported ARF:MDM2 interaction have been reported using cellular systems massively overexpressing both proteins(Kamijo, Weber et al. 1998; Pomerantz, Schreiber-Agus et al. 1998). The need for such overexpression suggests that either the complex was not very stable or there was a negative regulator, which needed to be squelched out. However problems regarding the sensitivity of detection with the ARF polyclonal IP-1 and the IP buffer used was also of concern. Inability of either of the ARF or MDM2 antibodies used to IP their respective complexed proteins, may have also explained the lack of MDM2:ARF complex detection.

pRB was another possible regulator of MDM2 activity, which had been reported to increase MDM2 binding after UV-irradiation(Hsieh, Chan et al. 1999). Unfortunately, no MDM2:pRb interactions were detected in a variety of UV-irradiated cell lines. Again stability of the complex and sensitivity of the IP methods may have hindered MDM2:pRb complex detection, although pRb:E2F-1 complexes, which may be less transient in nature, were detectable. Similarly no MDM2:E2F-1 interactions were observed in UV-irradiated cells.

Overall, a general trend of increased protein level of either MDM2 or p53, matched a general increase in p53:MDM2 complex levels (see Table 3.1). Modulation of this general theme may be affected by p53 conformation, oligomerisation state or DNA-binding status. Nevertheless a large body of evidence suggests that one of the main determinants of MDM2:p53 complex formation is protein level.

Table 3. 1. Summary of the effects of various treatments on p53, MDM2 and p53:MDM complex levels.

Treatment	p53 protein level	MDM2 protein level	p53:MDM2 complex levels
Lactacystin	Increase*	Increase*	Increase*
Stable MDM2 expression	No effect	Increase	Increase
Transient MDM2 expression	Decrease	Increase	Increase
Transient p53 expression	Increase	Increase	Increase
ARF expression	Increase	Increase	Increase
Transient and stable mutant p53 $175^{R \Rightarrow H}$ expression	Increase	Decrease	Increase
*Slight to undetectable increase in DN(5) cells			

Analysis of p53:MDM2 complex formation post UV- and X-ray irradiation

Upon cellular stress p53 responds by either generating a cell cycle arrest, providing a temporal stall to allow DNA repair, or an apoptotic signal, removing the cell from the population and hence, preventing perpetuation of DNA mutations through DNA replication. To generate such signals, MDM2 inhibition is though to be alleviated to allow p53 function either through transcriptional regulation of target genes or protein-protein interactions. Alleviation of the p53:MDM2 protein-protein interaction would in theory remove such inhibition. Therefore, it was of interest to determine whether complex levels were reduced post X-ray or UV-irradiation, which generate a p53-dependent cell cycle arrest and apoptosis, respectively (see Chapter Two). Another point of interest concerned the decrease in the p53 induction-rate post-DNA damage. Increased MDM2-mediated degradation of p53 could explain these findings; perhaps mediated through increased MDM2:p53 binding.

X-ray irradiation does not decrease p53:MDM2 complex formation

OSA, M(5), DN(5) and U2OS cells lines were X-ray irradiated with 12 Gy. Various time points were taken post-irradiation and samples underwent MDM2 and p53 IP analysis. Analysis showed no reduction, but a general increase in co-immunoprecipitates post-irradiation, in both reciprocal p53 and MDM2 IPs. The X-ray mediated dip in MDM2 protein levels 30 minutes post-irradiation observed by Western analysis (see Chapter Two) was reflected with decreased direct IPd MDM2 (see Figure 3.15). Following time points exhibited increasing amounts of direct IPd MDM2 up until 72 hours post-irradiation. M(5) and U2OS cells demonstrated increasing amounts of co-IPd p53 with time, mimicking the increase seen with MDM2. DN(5) cells maintained a near constant level of co-IPd p53, even though the levels of IPd MDM2 varied. Interestingly, OSA cells demonstrated a biphasic pattern of reduced co-IPd p53 from 30 minutes to 24 hours post-irradiation, followed by a return to sub-control levels by 48 hours.

p53 IP analysis of U2OS and M(5) cells revealed a similar pattern of increasing direct IPd p53 and co-IPd MDM2 post-irradiation. DN(5) cells exhibited no major alteration in the degree of IPd p53, while a reduction in co-IPd MDM2 was apparent from 30 minutes to six hours post-irradiation. Following the reduction, co-IPd MDM2 levels returned to and were maintained at control levels. Repeated p53 IP analysis of OSA cells failed to reveal a clear pattern. However, increased IPd p53 and co-IPd MDM2 levels were apparent from 48-72 hours post-irradiation.

UV- irradiation increases p53:MDM2 complex formation

OSA, M(5) U2OS and DN(5) cell lines were UV-irradiated with 30 Jm^{-2} and immunoprecipitation time points were taken two, eight and 24 hours post-irradiation. Samples were subsequently examined by MDM2 and p53 IP analysis.

MDM2 IP analysis of U2OS, M(5) and DN(5) cells revealed decreasing levels of directly IPd MDM2 following UV-irradiation (see Figure 3.16). This observation matched the Western analysis carried out in chapter two, where UV-irradiation dramatically reduced the detection of MDM2 (see Figure 2.29). OSA cells demonstrated a slight reduction in IPd MDM2 levels,

which increased to near control levels 24 hours post-irradiation. Again this MDM2 IP profile mirrored the UV-irradiation MDM2 profiled as determined by Western analysis, where early loss of MDM2 expression was recovered by 24 hours post-irradiation. Therefore, as opposed to OSA, the three U2OS based cell lines demonstrated significant UV-mediated reductions in IPd MDM2 levels. Surprisingly, M(5), U2OS and OSA cell lines demonstrated increasing levels of co-IPd p53 with increasing time post-irradiation, while DN(5) showed a small but significant reduction in co-IPd p53 levels.

p53 IP analysis of OSA, U2OS and M(5) exhibited the expected increase in IPd p53 following UV-irradiation, while DN(5) cells showed no detectable alterations (see Figure 3.16). The increase in IPd p53 levels in M(5) cells was somewhat delayed in comparison to U2OS cells, perhaps reflecting the slightly delayed induction of p53 seen in M(5) cells (see Figure 2.22 [II]). The co-IPd MDM2 levels in M(5) and U2OS cells exhibited quite constant levels, while OSA increased and DN(5) levels decreased with increasing time post-irradiation.

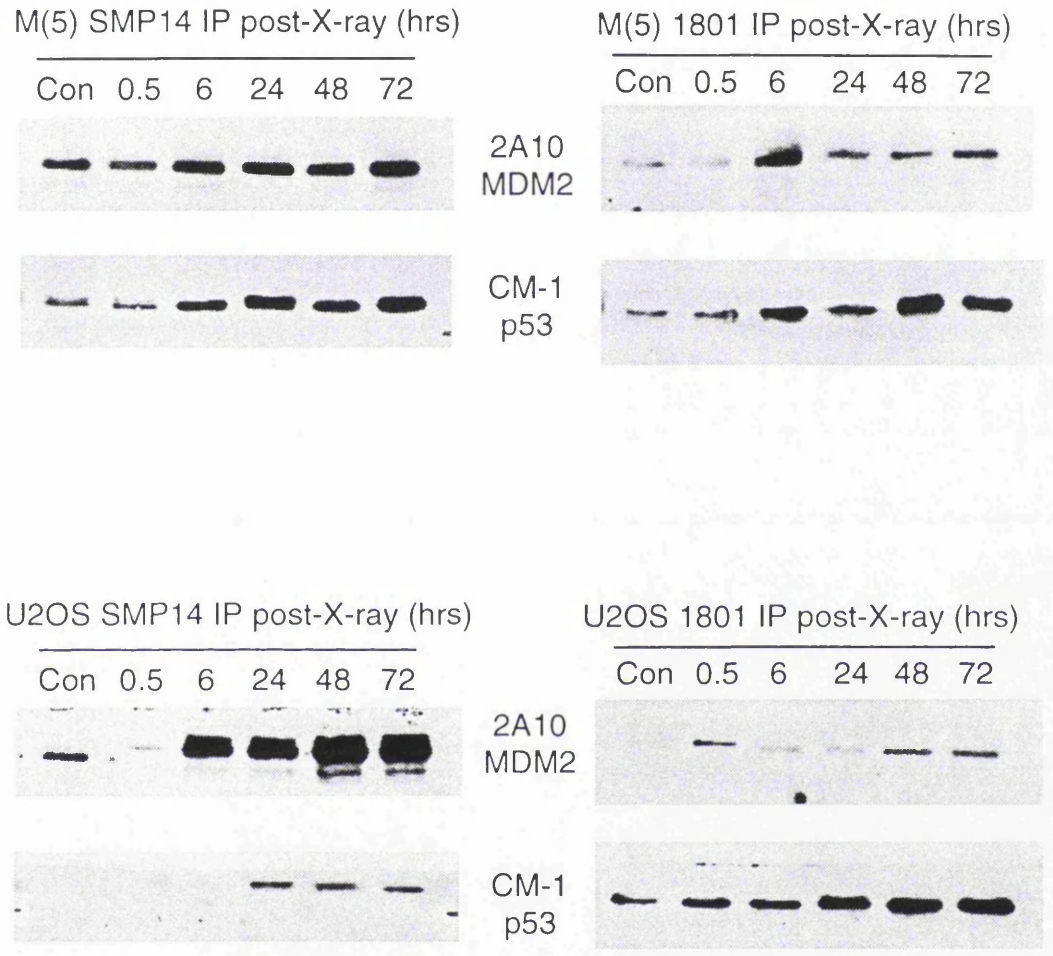

Figure 3.15. 12 Gy X-ray-irradiation of various cell lines generally increases p53:MDM2 complex levels (two pages). Various cell lines (as indicated) were 12 Gy X-ray irradiated and examined by IP analysis at various time points post-irradiation (as indicated). Agarose-conjugated SMP14 (MDM2) and 1801 (p53) antibodies were used for IP analysis and samples were subsequently examined by Western analysis for MDM2 and p53.

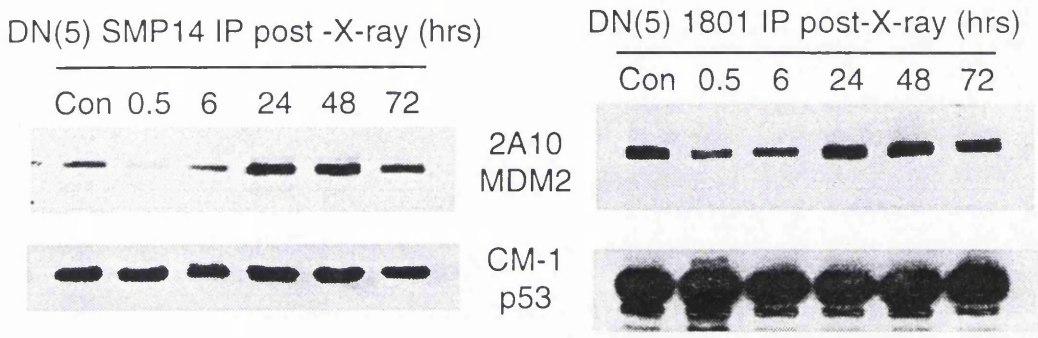
DN(5) SMP14 IP post -X-ray (hrs)
Con 0.5 6 24 48 72
2A10
MDM2
CM-1
p53
DN(5) 1801 IP post-X-ray (hrs)
Con 0.5 6 24 48 72

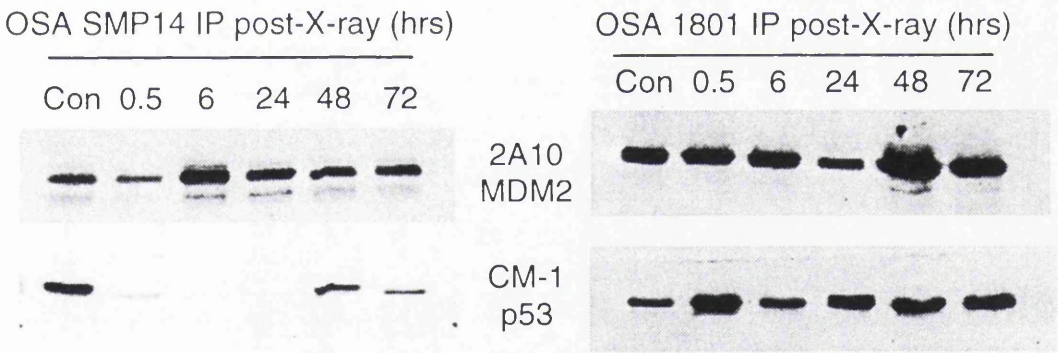
OSA SMP14 IP post-X-ray (hrs)
Con 0.5 6 24 48 72
2A10
MDM2
CM-1
p53
OSA 1801 IP post-X-ray (hrs)
Con 0.5 6 24 48 72

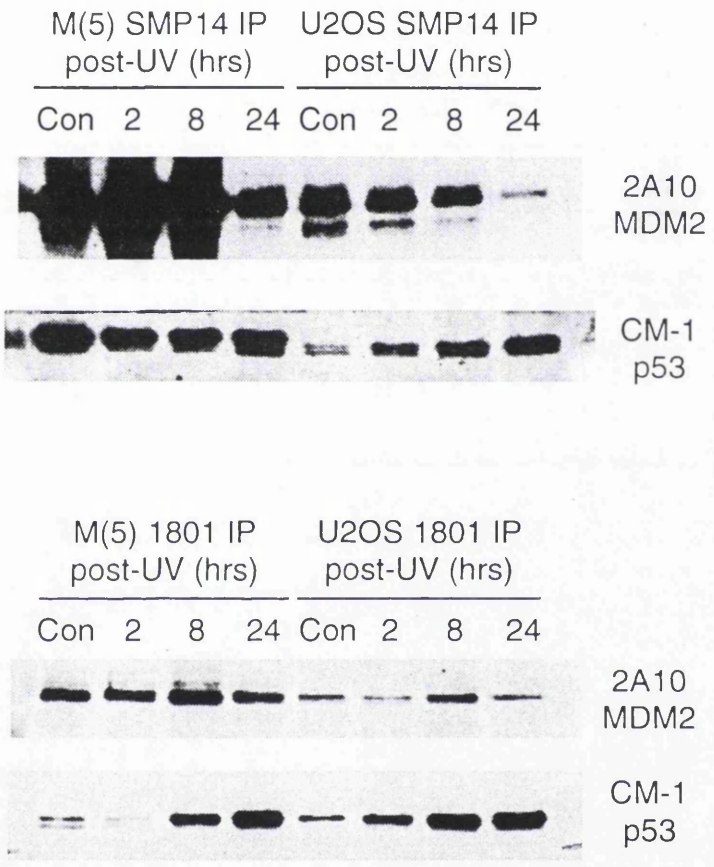

Figure 3.16. 30 Jm-2 UV-irradiation of various cell lines generally increases p53:MDM2 complex levels (two pages). Various cell lines (as indicated) were 30 Jm-2 UV-irradiated and examined by IP analysis at various time points post-irradiation (as indicated). Agarose-conjugated SMP14 (MDM2) and 1801 (p53) antibodies were used for IP analysis and samples were subsequently examined by Western analysis for MDM2 and p53.

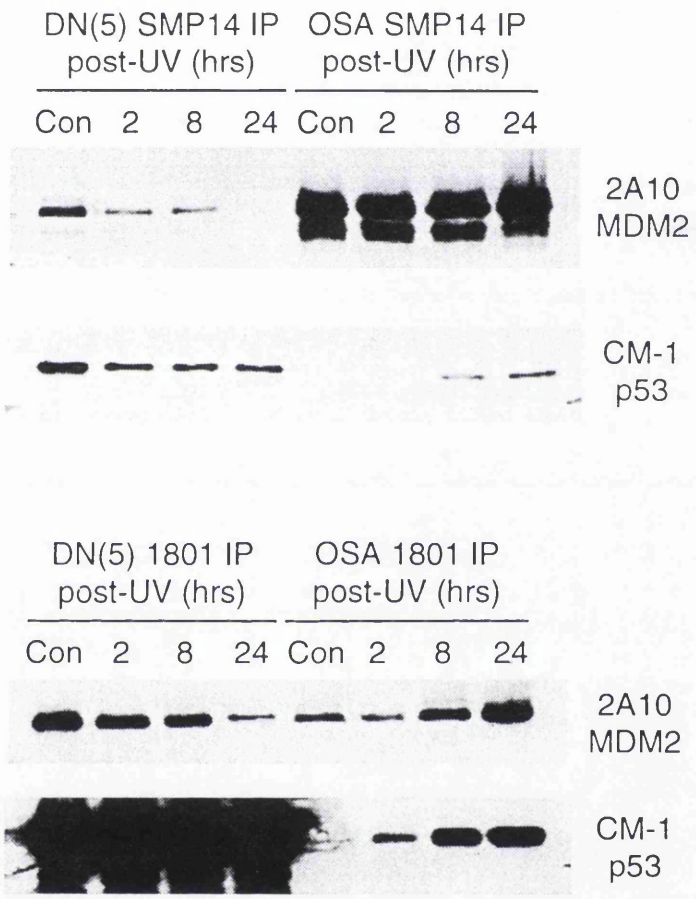
DN(5) SMP14 IP
post-UV (hrs)
OSA SMP14 IP
post-UV (hrs)
Con 2 8 24 Con 2 8 24
2A10
MDM2
CM-1
p53
DN(5) 1801 IP
post-UV (hrs)
OSA 1801 IP
post-UV (hrs)
Con 2 8 24 Con 2 8 24
2A10
MDM2
CM-1
p53

Summary and Discussion

p53 accumulation in response to DNA damage has mainly been attributed to post-transcriptional events. Translational upregulation has been postulated, although increased protein stability is more commonly reported. MDM2-mediated p53 degradation has been placed as the principal negative regulatory mechanism of p53 activity. Two possible mechanisms of preventing MDM2-mediated inhibition rely upon either prevention/dissociation of MDM2:p53 complexes or inhibition of MDM2-mediated ubiquitination or subsequent degradation processes.

As determined by Western analysis, X-ray-irradiation caused the accumulation of both p53 and MDM2 in a variety of cell lines (see Chapter Two). With the observation of increased protein levels leading to increased MDM2:p53 complex formation, X-ray-induced increases in protein levels suggested that p53:MDM2 complex formations would increase. However, this assumption conflicted with the observation that X-ray-mediated cellular stress lead to p53 accumulation and activation of transcriptional target genes, as increased p53:MDM2 complex levels would antagonise such a processes. Upon analysis an increase and/or no loss of complex levels was observed in all of the cell lines examined, except OSA. OSA demonstrated an initial loss of complex formation followed by a recovery 48 hours post-irradiation; a response expected and in agreement with the theory of stress-mediated inhibition of p53:MDM2 interaction and subsequent p53 accumulation. However, the expected reduction in p53:MDM2 complexes in response to cellular stress was not seen in M(5) or parental U2OS cells, mirroring the results seen with ARF-mediated cell cycle arresting cells.

This data suggests that a pool of MDM2-complexed p53 is maintained, tolerated and elevated in response to X-ray irradiation. Excess unbound p53 and MDM2 may also accumulate at greater rate than the rate of complex formation, therefore allowing a significant amount of free p53 to mediate a cell cycle arrest. 72 hours post-irradiation, when the majority of cells have re-entered the cell cycle, maximal complex formation was apparent. Such p53:MDM2 complexes would be expected to inhibit the p53-mediated cell cycle arrest, allowing the cell to re-enter the cell cycle. Additionally, the earliest observed

increase in p53:MDM2 complex levels was six hours post-irradiation, suggesting that p53 may have initiated a cell cycle arrest prior to that time point.

It is possible that a mechanism prevents *de novo* formation of p53:MDM2 complexes, perhaps through modification of either protein or through increased or decreased levels of a complex-dissociating or –promoting protein. A problem with this idea emerges, mainly due to the transient nature of the complex - with p53 being degraded as a result of complex formation. Without some degree of *de novo* MDM2:p53 complex formation, complex levels would rapidly be reduced, therefore a low level of *de novo* complex formation could account for persistent levels of the complex. Alternatively, inhibition of the actual degradation event at the level of the proteosome, downstream of the MDM2:p53 interaction, would allow perpetuation of complexes without *de novo* formation.

The p53-dependent induction of p21and MDM2 observed in X-ray-irradiated U2OS cells (see Chapter Two) suggested that MDM2-uncomplexed and transcriptionally active p53 was required. Hence, with respect to the two potential mechanisms of MDM2 inhibition, the preventative model of p53:MDM2 complex formation could account for both p53 accumulation and increased transcriptional activity.

Western analysis of UV-irradiated U2OS and OSA cells caused an accumulation of p53, while MDM2 and p21 levels dropped (see Figures 2.19 [I] and 2.28). With the high p53 and low MDM2 levels, UV-irradiated U2OS cells mimicked the DN(5) cell line protein profile, which also has very high levels of p53, although mutant, and low MDM2 levels. Immunoprecipitation analysis of the degree of p53:MDM2 complexes between various untreated cell lines revealed DN(5) cells to be the highest observed. Therefore, high p53 and low MDM2 protein levels can generate high levels of complex formation. Accordingly, in UV-irradiated U2OS cells, increased complex formation was observed 24 hours post-irradiation. The observed increase in complex formation with decreasing MDM2 levels suggested that the elevation of p53 more than compensated for the loss of MDM2 expression, perhaps reflecting a shift to one MDM2 molecule binding higher order p53 oligomers. Overall increases in p53:MDM2 complex formation was most drastic in the U2OS MDM2 IPs, ranging to slight in the reciprocal U2OS p53 IPs. However, no reductions in MDM2:p53 complex levels were observed in U2OS, M(5) and OSA cells. In contrast UV-

irradiated DN(5) cells exhibited decreasing p53:MDM2 complex levels in reciprocal IPs. Decreased complex formation in DN(5) cells could possibly be attributed to a reduction of MDM2 levels below a certain threshold of complex formation. DN(5) cells exhibited the lowest starting levels of MDM2 expression, mainly due to abrogated p53-mediated transcriptional induction and hence may have attained that threshold level before the other cell lines.

Overall, Both X-ray- and UV-irradiated cells, with the exception of DN(5) and X-ray-irradiated OSA cells, exhibited increased or stable levels of p53:MDM2 complexes. Therefore, no significant difference in complex formation could account for the differential cellular choice between apoptosis and cell cycle arrest. Ultimately, it seems that the increases in p53:MDM2 complexes observed, if at all, may not significantly attenuate the level of free, unbound p53. However, more accurate quantitative studies would be needed to definitely determine this.

Oligomerisation of p53 has been linked to its activation and stabilisation (see Introduction). Phosphorylation of p53 Ser^{392}, as seen in response to UV-irradiation has been reported to stabilise tetrameric p53(Sakaguchi, Sakamoto et al. 1997; Sakaguchi, Sakamoto et al. 1997). Additionally, MDM2 has a higher binding affinity for tetrameric p53(Marston, Jenkins et al. 1995), which suggests that MDM2 would preferentially inhibit 'active' p53. In the case of UV-induced apoptosis of U2OS, the observed p53 Ser^{392} phosphorylation, lack of *p21* and *mdm2* induction and increased MDM2:p53 association (transcriptionally-masked p53) supports a non-transcriptional role for p53 in apoptosis. Paradoxically, in the case of X-ray mediated cell cycle arrest where p53-dependent transcription was required, p53 Ser^{392} phosphorylation was not observed, in a situation where oligomeric stabilisation of p53 was expected. However, p53 Ser^{392} phosphorylation may not be the sole oligomeric promoting modification, and X-ray mediated oligomerisation may have also accounted for the increased MDM2:p53 complex formation.

The increased Ser^{15} phosphorylation observed upon X-ray- and UV-irradiation (see Figure 2.20) was proposed to be an inhibitory modification with respect to MDM2 association(Shieh, Ikeda et al. 1997). In light of the IP results post-irradiation, such modifications may not provide an inhibitory mechanism, although the existence of

phosphorylated Ser^{15}-p53 in the p53:MDM2 complexes was not determined. The strong UV-mediated induction of p53 Ser^{15} phosphorylation in U2OS-derived cell lines(see Figure 2.29) conflicted with the increased p53:MDM2 complex levels observed. These results suggested p53 Ser^{15} to be a complex promoting modification, rather than an inhibitory one. Interestingly, recent work determined that p53 Ser^{15} phosphorylation did not influence the p53:MDM2, but was involved in stimulation of p53 activity(Dumaz and Meek 1999). However, UV-irradiation of mutant p53 $175^{R\Rightarrow H}$-expressing DN(5) cells did reveal a large increase in p53 Ser^{15} phosphorylation, which coincided with loss of p53:MDM2 complex.

Overall, these finding seem paradoxical as p53:MDM2 complexes would be expected to be prevented or dissociated upon cellular stress and DNA damage. Prevention of new p53:MDM2 associations was possibly apparent, although a consistent level of complex formation was generally observed. An alternative view to MDM2 being the negative regulator of p53 is linked with viewing p53 as a negative-regulator of MDM2 function. Therefore, increased p53:MDM2 complex formation may lead to inhibition of MDM2's function; perhaps inhibiting MDM2 binding other macromolecules. Complex formation may lead to the mutual inactivation of both proteins functions or simply modify their functions. Alternatively, p53 may actively recruit MDM2 to carry out a function, placing MDM2 a positive co-regulator in certain situations. This final view may be more feasible due to the overall observations of a lack of decreasing p53:MDM2 complexes following DNA damage or ARF expression. Some of the anomalous observations made with DN(5) cells suggest that especially in the case of UV-mediated signalling to the MDM2:p53 feedback loop, the presence of mutant p53 $175^{R\Rightarrow H}$ interferes with such a signalling pathway.

Although immunoprecipitation is a direct method of measuring the degree of complex-formation, the method does have its flaws. With the emerging evidence for subcellular compartmentalisation serving as an important mechanism for controlling protein-protein interactions, a process that destroys such protein separation may allow promiscuous interactions. Such destruction of subcellular protein compartmentalisation and subsequent IP analysis may therefore not reflect the true cellular situation. Furthermore, disruption of cellular integrity may also affect the regulation of protein-protein association through the abrogation of spatially separated post-translational regulatory mechanism components. For

example, promiscuous kinases or phosphatase activity during the immunoprecipitation process may alter the true, cellular protein-protein interaction profile.

Additional problems ensuring equal protein loading in immunoprecipitation comparisons, provides an additional degree of uncertainty. Different cell lines exhibit different protein expression profiles and of particular concern is large differences in cytoskeletal protein expression. These proteins can dominate the percentage of total protein present in the sample and may also change in response to certain treatments, skewing equal loading. However, such problems can be minimised through use of isogenic cell lines. Intrinsic problems with different antibody affinities also complicate comparative analysis; for example antibodies may have higher binding affinities for non-complexed proteins over complexed proteins due to allosteric conformational effects of complexed proteins. Overall, immunoprecipitation analysis provides an effective method for observing qualitative protein-protein interactions, although results should not be taken as verbatim.

Chapter Four

Immunofluorescence analysis

In a further attempt to characterise the irradiation responses of U2OS-derived and OSA cell lines, the subcellular localisation of MDM2 and p53 was examined using immunofluorescence (IF). Compartmentalisation of proteins within organelles, the cytoplasm or the nucleus is an effective method of controlling protein-protein interactions, and hence, can determine a number of cellular outcomes.

MDM2 shows punctate nuclear staining, nuclear bodies and nucleolar occlusion

In light of the use of N-20, SMP14 and 2A10 MDM2 antibodies in Western and immunoprecipitation (IP) analysis (see Chapter Two and Three), these antibodies were subsequently used for IF studies. IP analysis had shown that all three antibodies were capable of co-immunoprecipitating p53, excluding selective identification of non-p53-complexed MDM2. Detection of splice variants was also limited due to the absence of some antibody epitopes within certain splice variants, although N-20's epitope is present in all six splice variants (see Figure 1.2).

IF analysis with all three MDM2 antibodies revealed predominant nuclear staining, with limited perinuclear cytoplasmic staining in the four cell lines: U2OS, DN(5), M(5) and OSA (see Figure 4.1). Potential nucleolar occlusion was apparent in all of the cell lines analysed, as determined by co-localisation with the differential DAPI staining of nucleoli. Such differential DAPI staining is characteristic of differential DNA concentrations within the nucleus, such as within nucleoli(Bilinski and Bilinska 1996) which contain high concentrations of RNA and protein components for ribosomal biogenesis. Non-nucleolar MDM2 staining patterns have also been observed in a number of other cell lines(Lain, Midgley et al. 1999; Tao and Levine 1999; Tao and Levine 1999; Weber, Taylor et al. 1999). A punctate, sub-nuclear speckled-pattern, overlaying a weaker general nuclear staining was

observed in OSA, M(5) and U2OS cell lines. N-20 revealed larger, more defined sub nuclear structures that were most apparent in OSA cells. However, all three MDM2 antibodies showed a less well-defined, general nuclear staining pattern in DN(5) cells. Interestingly, detectability of MDM2 in DN(5) cells was significantly higher then U2OS cells.

DO-1 and PAb421 antibody staining reveals nuclear pods in OSA, M(5) and U2OS and general nuclear staining in DN(5)

The amino-terminal DO-1 antibody, which had successfully been used in Western and immunoprecipitation analysis (capable of detecting MDM2-complexed p53) and a carboxyl-terminal PAb421 (421) antibody were used to analyse the four cell lines, U2OS, DN(5), M(5) and OSA. Both antibodies revealed nuclear pod-like body and perinuclear staining patterns, fainter general nuclear and cytoplasmic staining in M(5), U2OS and OSA cell lines (see Figure 4.2). In contrast, DN(5) cells exhibited strong nuclear staining with clear nucleolar occlusion. With the exception of DN(5) cells, DO-1 consistently gave stronger, more defined results in comparison to 421 and was used for the majority of the subsequent work.

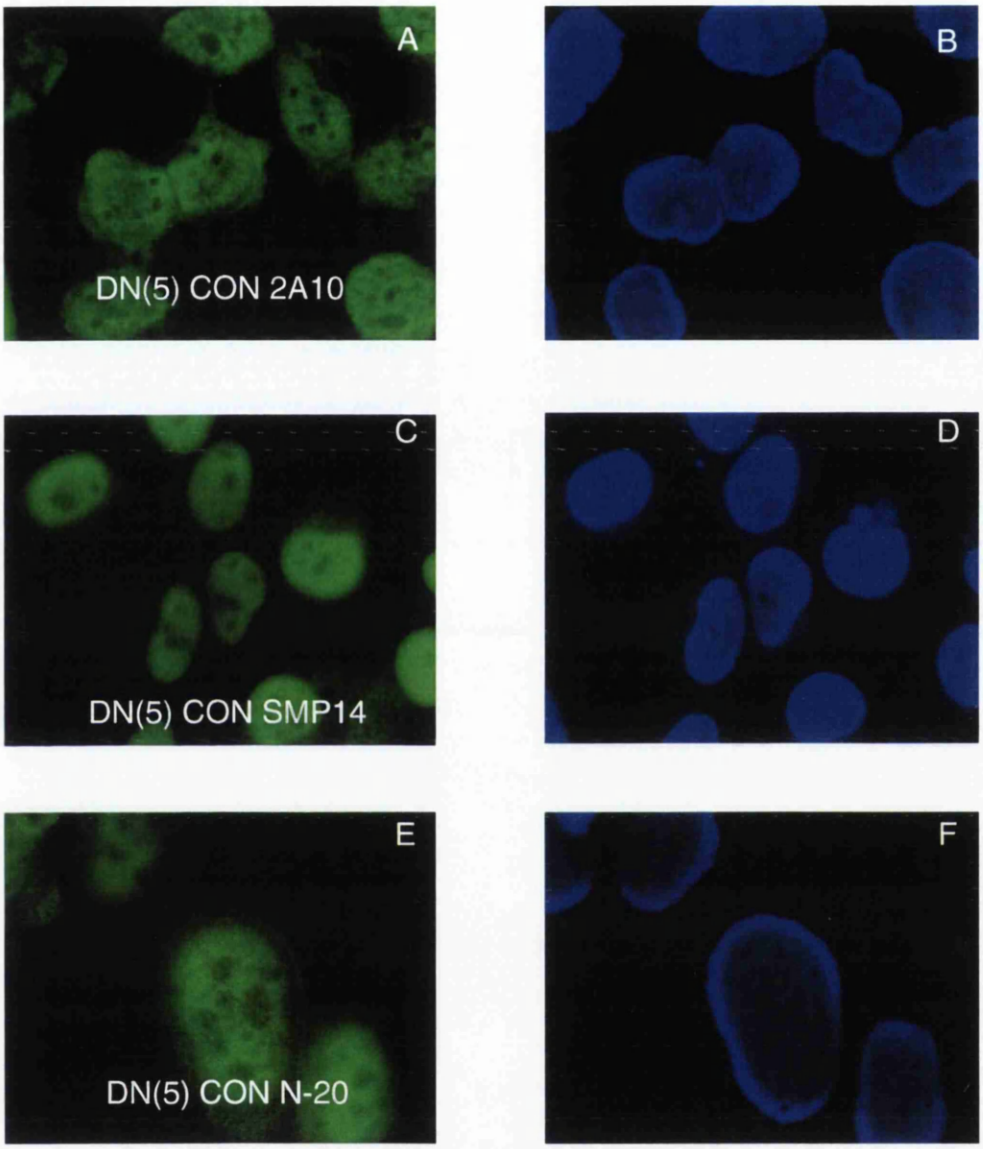

Figure 4.1. Immunofluorescence (IF) analysis of MDM2 subcellular localisation in various cell lines (four pages). Various cell lines (as indicated) were examined by IF using three different MDM2 antibodies, 2A10, SMP14 or N-20 (as indicated). 2A10 and SMP14 antibodies were detected with α-mouse FITC-conjugated 2°-antibody; N-20 antibody was detected with α-rabbit Alexa(GFP)-conjugated 2°-antibody. The right-hand panels represent DAPI (nuclear) stained cells. A-F = DN(5) cells; G-L = M(5) cells; M-R = OSA cells; and S-X = U2OS cells.

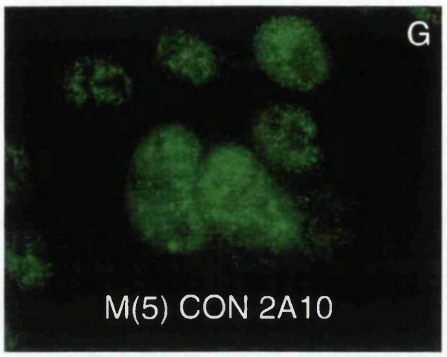
G
M(5) CON 2A10

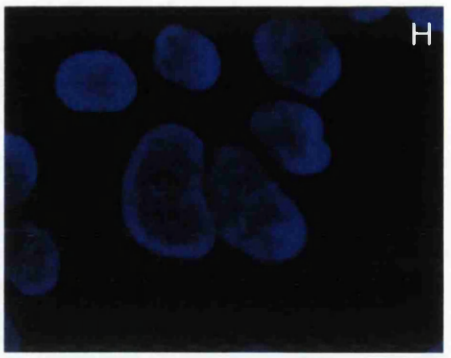
H

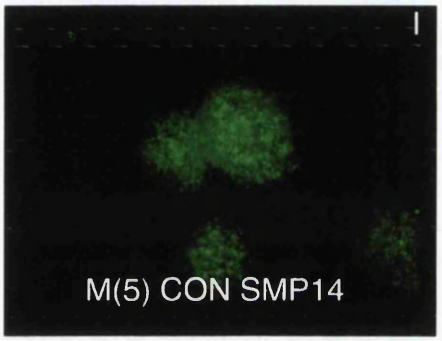
I
M(5) CON SMP14

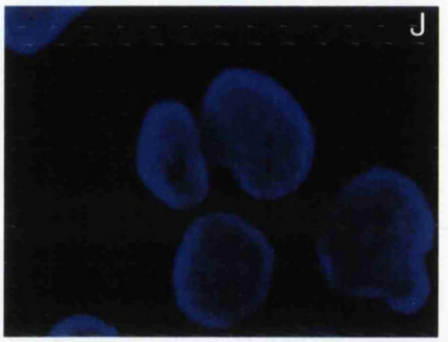
J

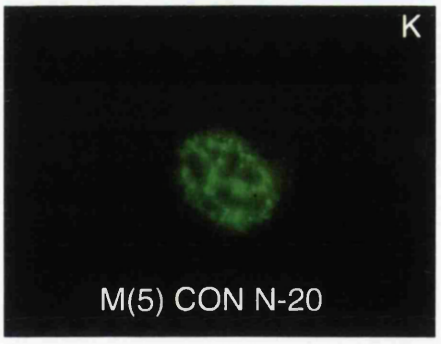
K
M(5) CON N-20

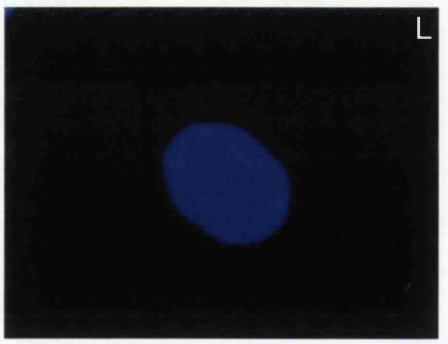
L

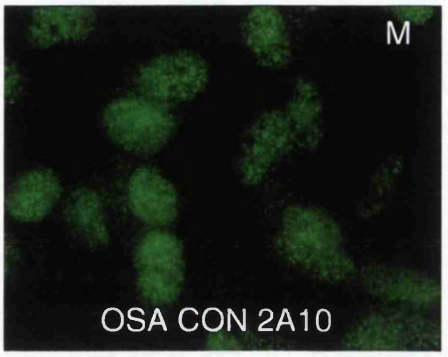
M
OSA CON 2A10

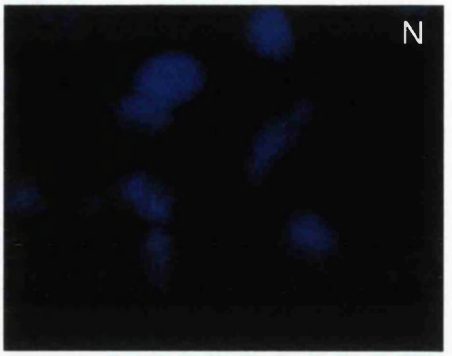
N

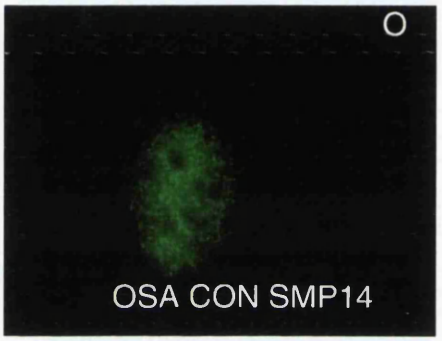
O
OSA CON SMP14

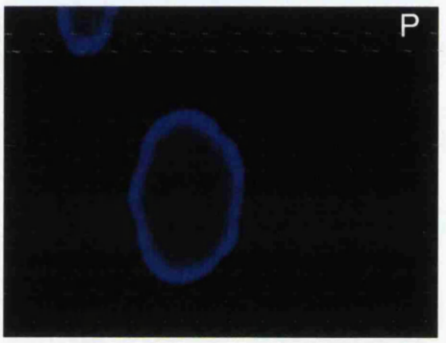
P

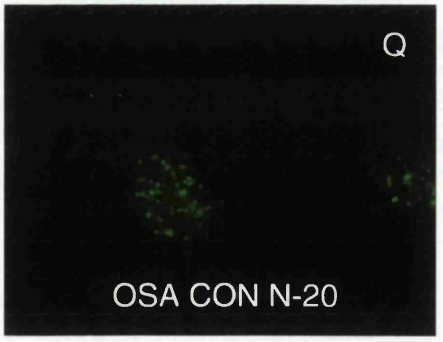
Q
OSA CON N-20

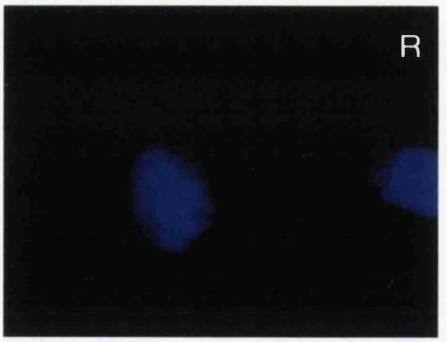
R

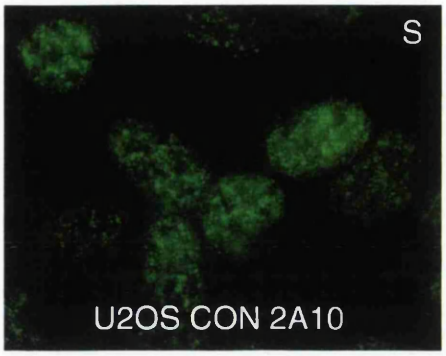
S
U2OS CON 2A10

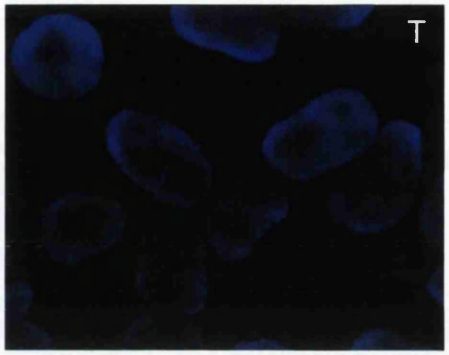
T


U
U2OS CON SMP14

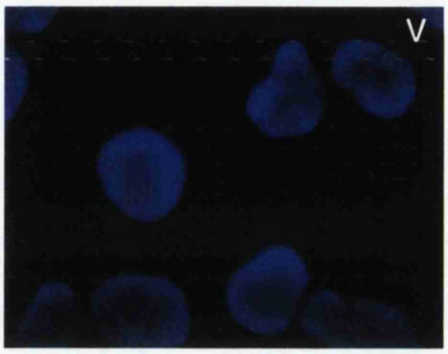
V

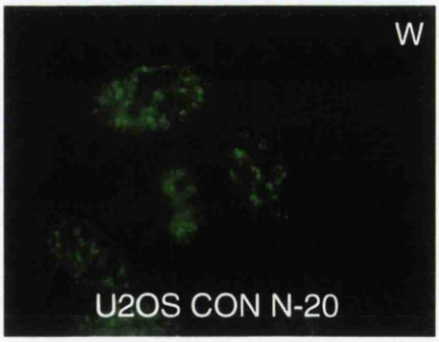
W
U2OS CON N-20

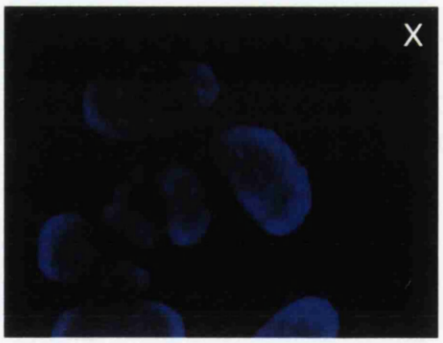
X

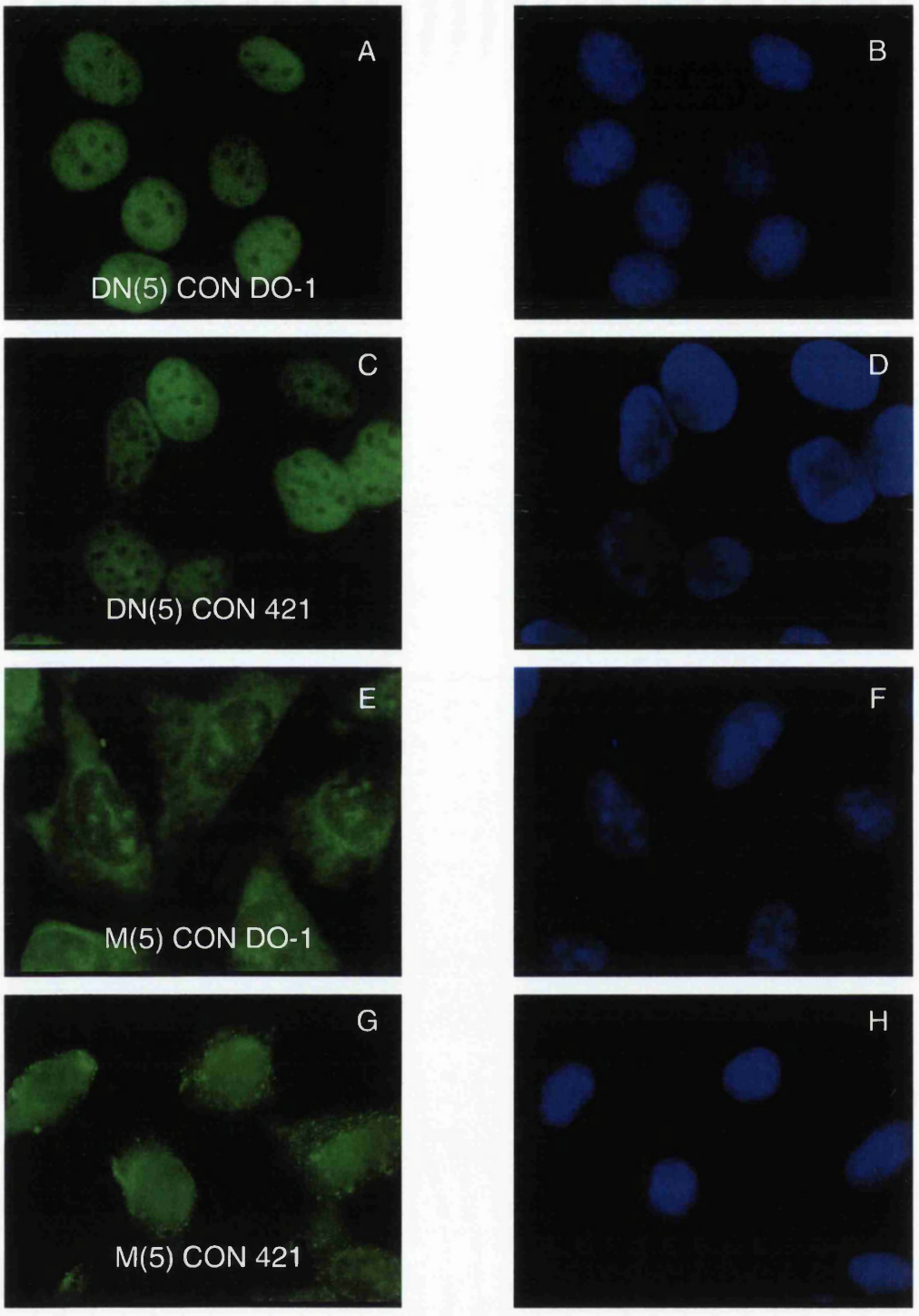

Figure 4.2. Immunofluorescence (IF) analysis of p53 subcellular localisation in various cell lines (two pages). Various cell lines (as indicated) were examined by IF using two different p53 antibodies, DO-1 or 421 (as indicated). Both antibodies were detected with α-mouse FITC-conjugated 2°-antibody. The right-hand panels represent DAPI (nuclear) stained cells. A-D = DN(5) cells; E-H = M(5) cells; I-L = OSA cells; M-P = U2OS cells.

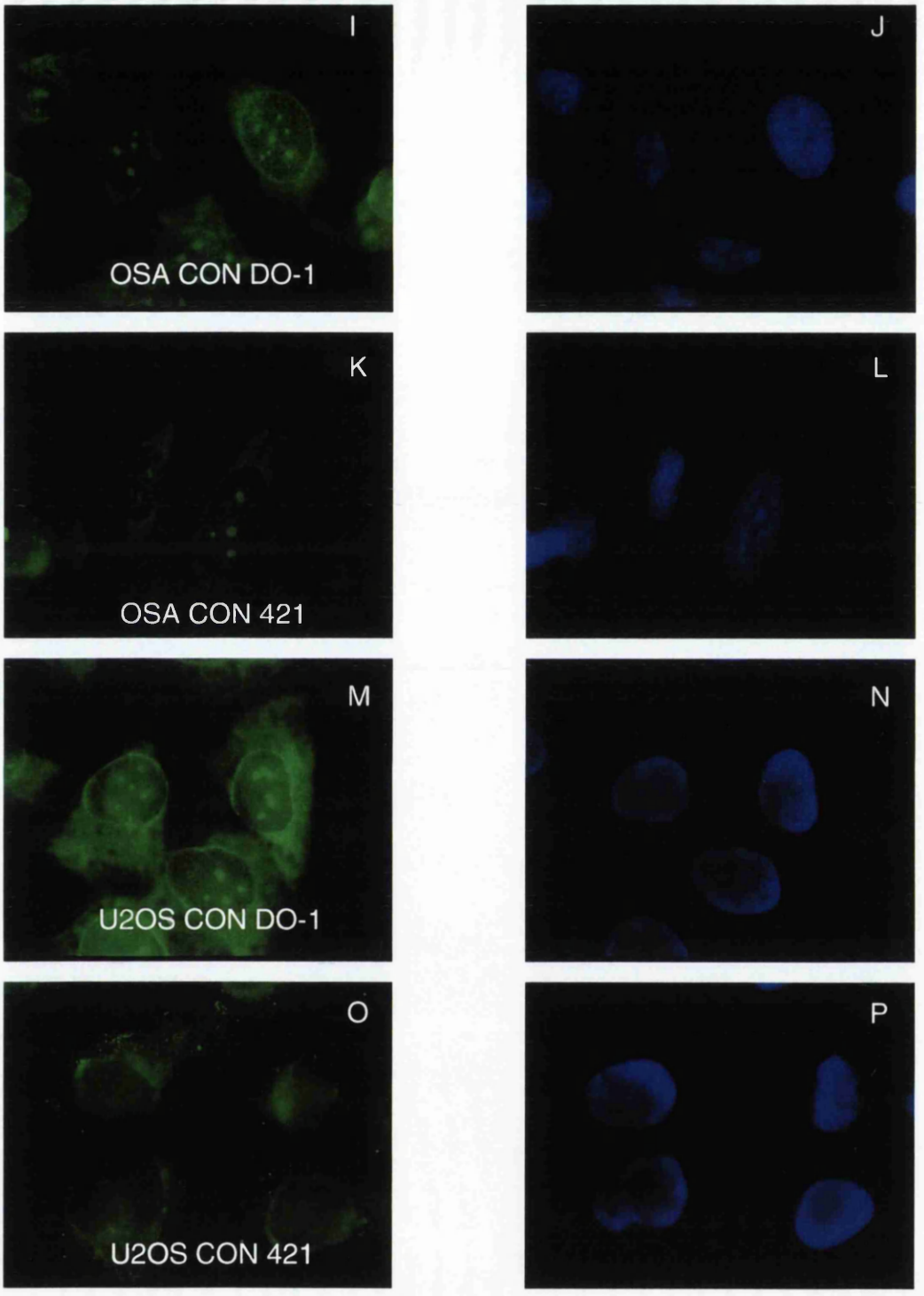
I
J
OSA CON DO-1
K
L
OSA CON 421
M
N
U2OS CON DO-1
O
P
U2OS CON 421

Lactacystin treatment causes MDM2 to generate sub-nuclear structures.

Lactacystin treatment of U2OS, M(5) and OSA cell lines revealed increased p53 and MDM2 protein levels by Western analysis (see Figure 2.31). IF analysis of lactacystin-treated cells eight hours post-treatment, generally increased the levels of nuclear MDM2 fluorescence, while cytoplasmic levels were decreased relative to the nuclear levels (see Figure 4.3). Additionally, lactacystin caused the generation of large sub-nuclear bodies, most prevalent in OSA, M(5) and U2OS cell lines. These novel sub-nuclear structures seemed larger and less in number than the sub-nuclear speckles observed in the control cells (see Figure 4.3 and compare with Figure 4.1). OSA cells exhibited the most radical response, with the formation of extremely discrete sub-nuclear bodies that co-localised with the differentially staining DAPI structures (nucleoli). Nevertheless, general nuclear staining was still evident in all three cell lines. In contrast, DN(5) cells revealed the formation of more defined nuclear speckles, reminiscent of control M(5), U2OS or OSA cells, that were not apparent in DN(5) control cells (see Figure 4.3 [A-D] and compare with Figure 4.1 [A-F]). Nucleolar occlusion was generally reduced in all lactacystin treated cells, with potential well-defined, positive nucleolar staining in OSA cells, although DN(5) cells exhibited a more general nuclear-staining.

Lactacystin treatment generates decreased nuclear, but increased cytoplasmic p53 staining

A dramatic shift in nuclear to cytoplasmic staining was observed in all four of the cell lines treated with lactacystin. Cytoplasmic staining increased, with the most intense staining around the periphery of the nucleus (see Figure 4.4). In some examples, the cytoplasmic staining was polarised and localised to a specific side of the cell. However, the sub-nuclear bodies observed in control cells, remained evident. The most dramatic response was seen with DN(5) cells, with near total relocation of the highly nuclear-localised p53 of control cells, to the cytoplasm (see Figure 4.2 [A-D] and compare with 4.4 [A-B]). Weakly staining sub nuclear bodies were detected in DN(5) cells, reminiscent of the pod-like structures seen in the other cell lines. Overall, IF detection of p53 increased with lactacystin treatment; as was expected due to the increased expression levels detected by Western following treatment.

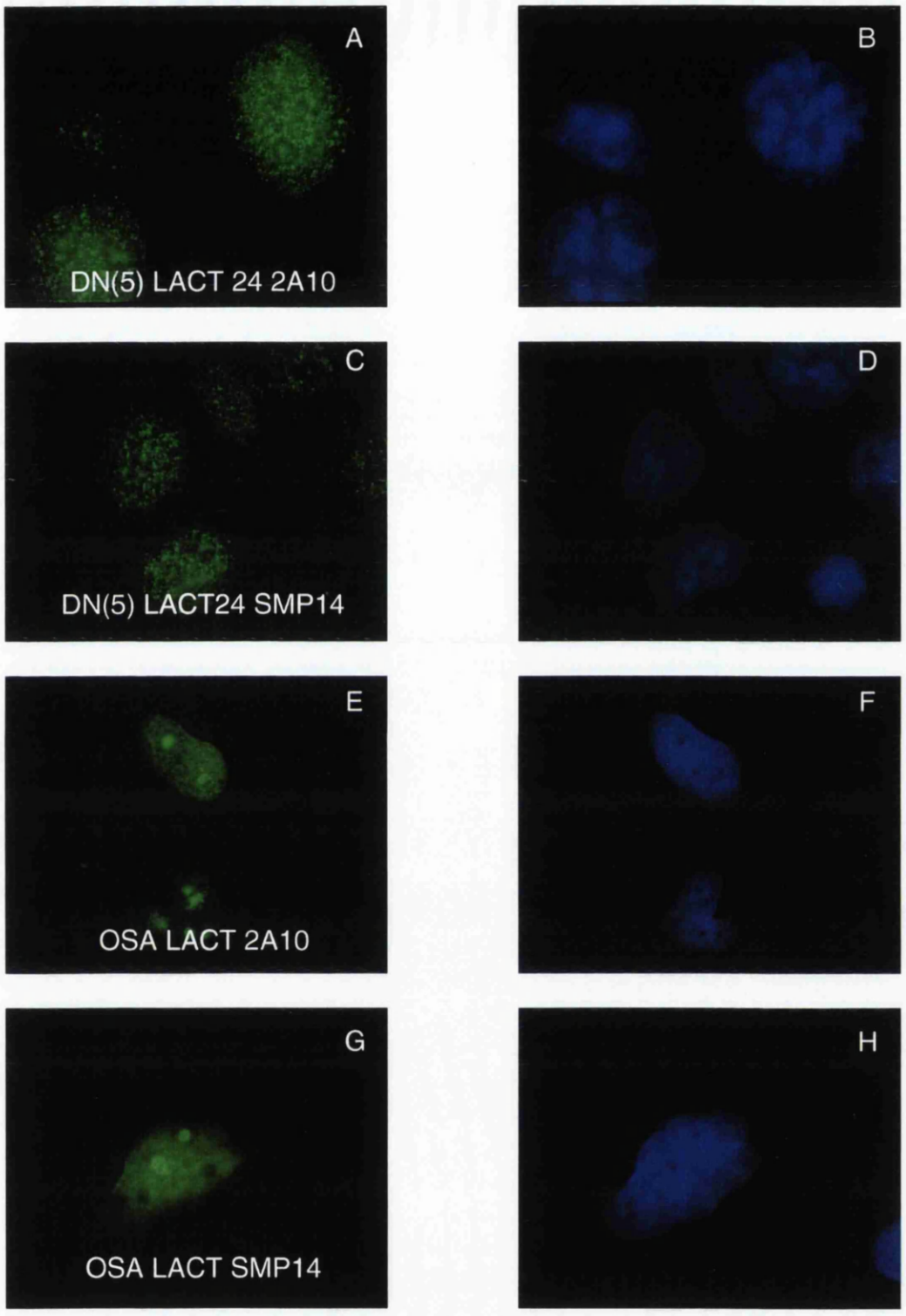

Figure 4.3. Lactacystin-treatment alters MDM2 subcellular localisation (two pages). Various cell lines (as indicated) were treated with 10μM lactacystin for eight hours prior to IF analysis. 2A10 or SMP14 (both MDM2) antibodies (as indicated) were used and subsequently detected with α-mouse FITC-conjugated 2°-antibody. The right-hand panels represent DAPI (nuclear) stained cells.

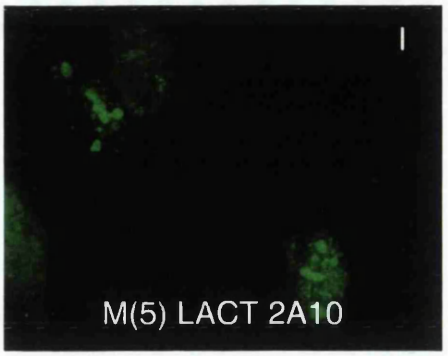

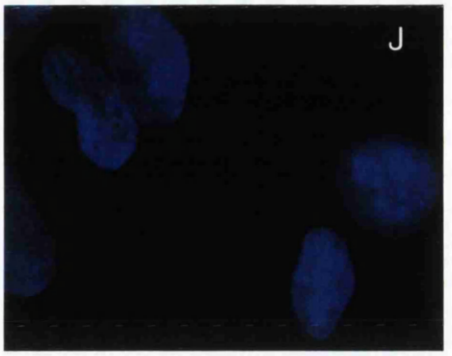

M(5) LACT 2A10

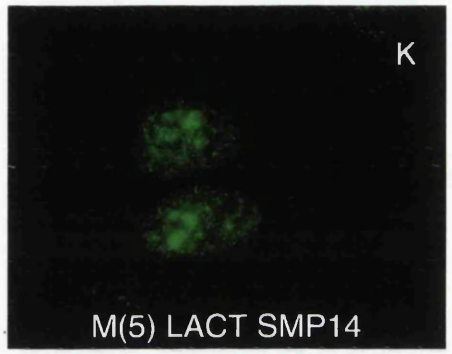

M(5) LACT SMP14

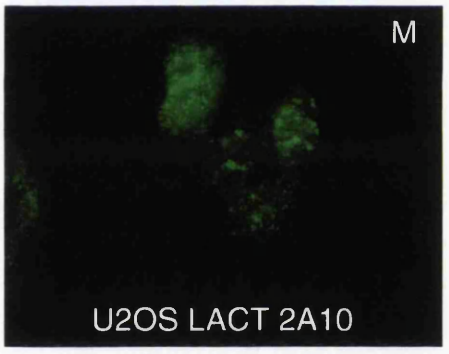

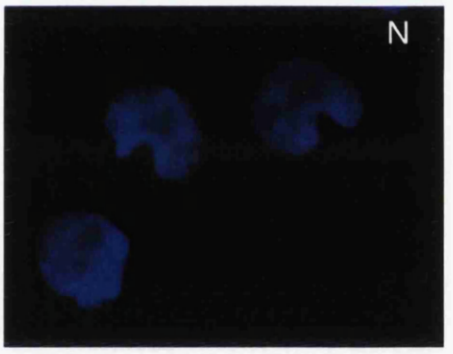

U2OS LACT 2A10

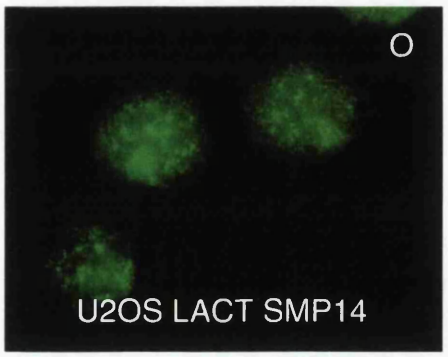

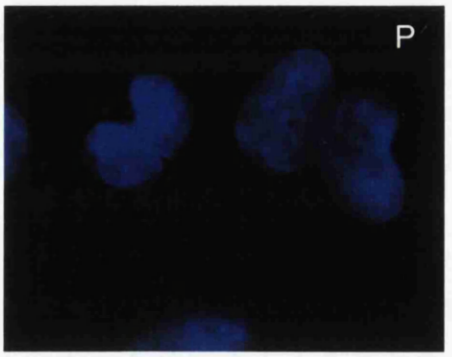

U2OS LACT SMP14

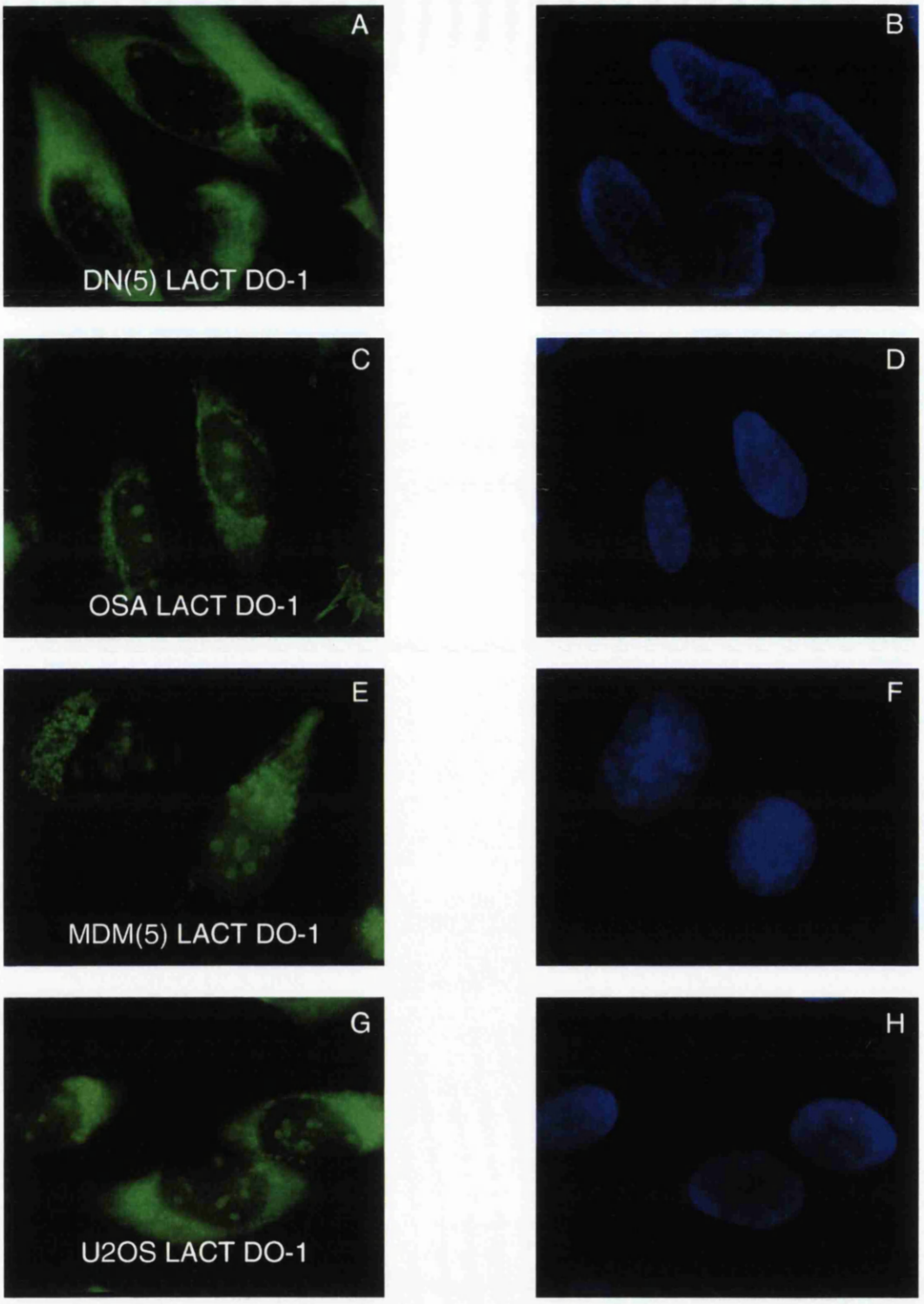

Figure 4.4. Lactacystin-treatment alters p53 subcellular localisation. Various cell lines (as indicated) were treated with 10μM lactacystin for eight hours prior to IF analysis. DO-1 (p53) antibody was used and subsequently detected with α-mouse FITC-conjugated 2°-antibody. The right-hand panels represent DAPI (nuclear) stained cells.

X-ray irradiation does not alter the subcellular localisation of MDM2 or p53

X-ray analysis (12 Gy) of all four cell lines revealed an initial reduction in MDM2 protein levels 30 minutes post-irradiation by Western analysis, followed by induction of both p53 and MDM2 (see Figure 2.26). An increase in MDM2:p53 complex formation had also been observed over an 24 hour time course by IP (see Figure 3.15). IF analysis of all four cell lines at 30 minutes and 24 hours post-irradiation, failed to exhibit any gross alteration in staining patterns of either MDM2 or p53 in comparison to the relative control staining patterns (See Figure 4.6 and 4.6, respectively). However, MDM2 staining and especially p53 staining, which exhibited clearer p53 sub-nuclear structures, was increased in comparison to relative control levels.

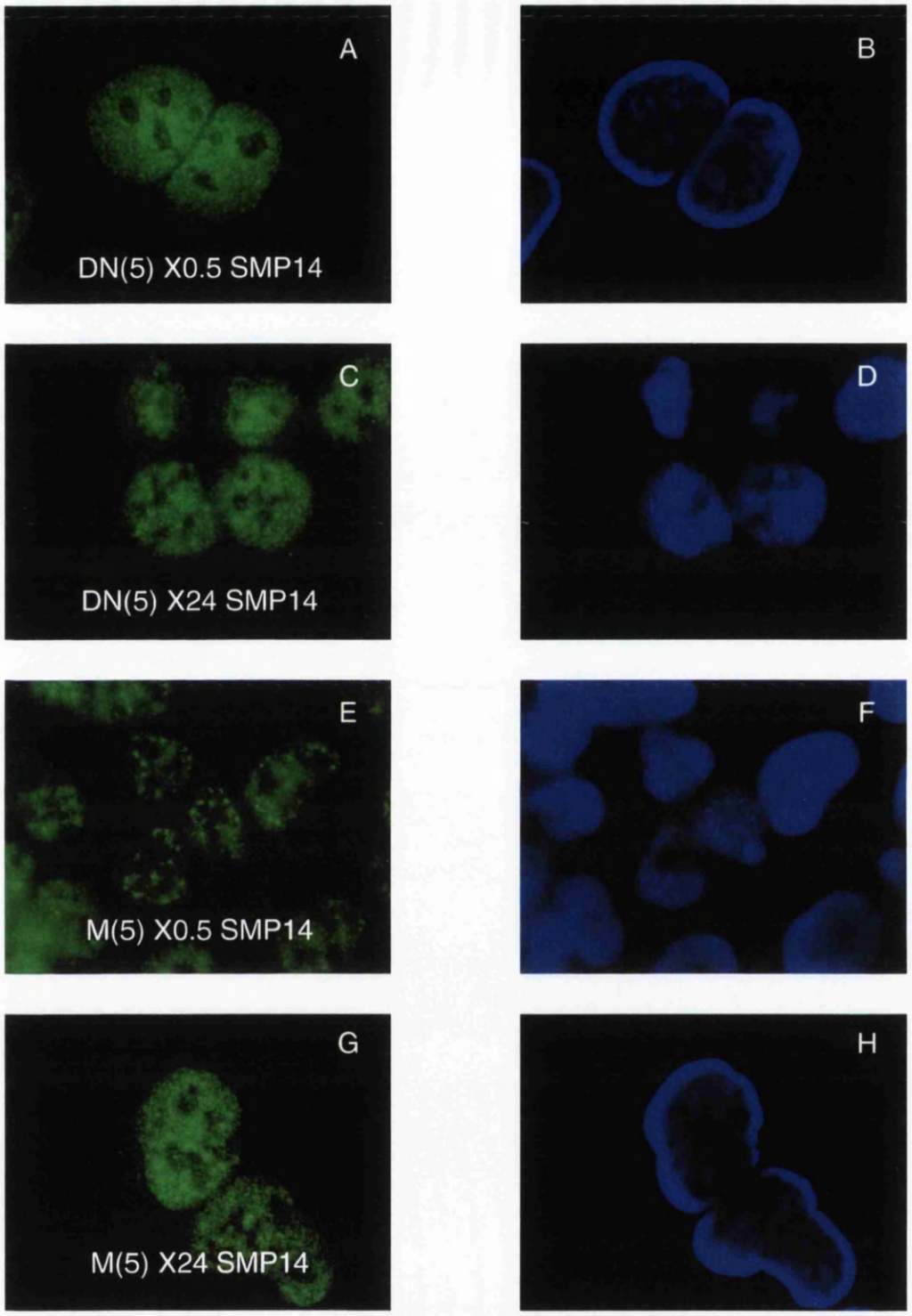

Figure 4.5. 12 Gy X-ray-irradiation fails to significantly alter the subcellular localisation of MDM2 (two pages). Various cell lines (as indicated) were 12 Gy X-ray irradiated and analysed by IF at various time points post-irradiation (as indicated, X0.5 etc [hrs]). SMP14 (MDM2) antibody was used and subsequently detected with α-mouse FITC-conjugated 2°-antibody. The right-hand panels represent DAPI (nuclear) stained cells.

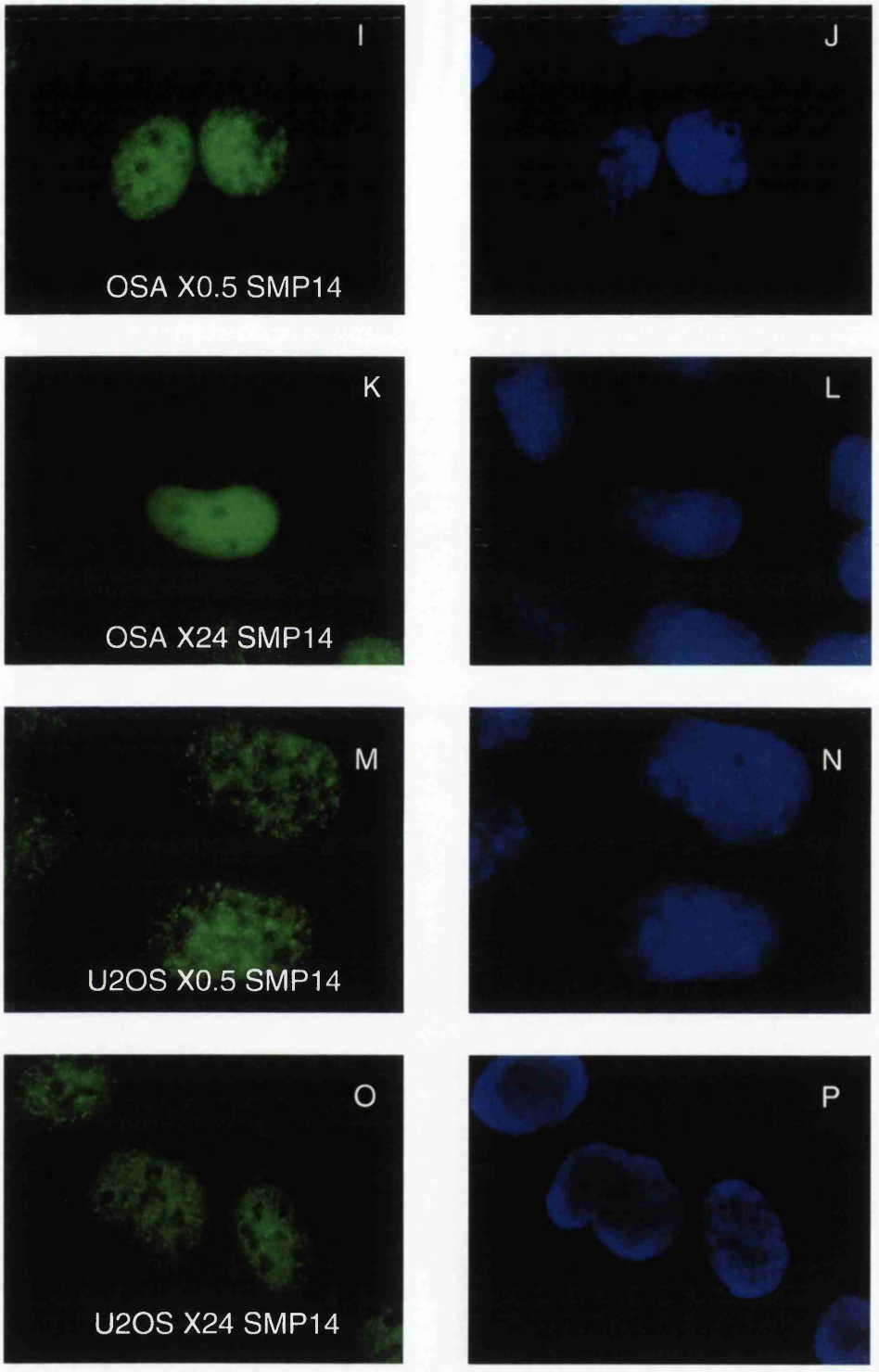
I
J
OSA X0.5 SMP14
K
L
OSA X24 SMP14
M
N
U2OS X0.5 SMP14
O
P
U2OS X24 SMP14

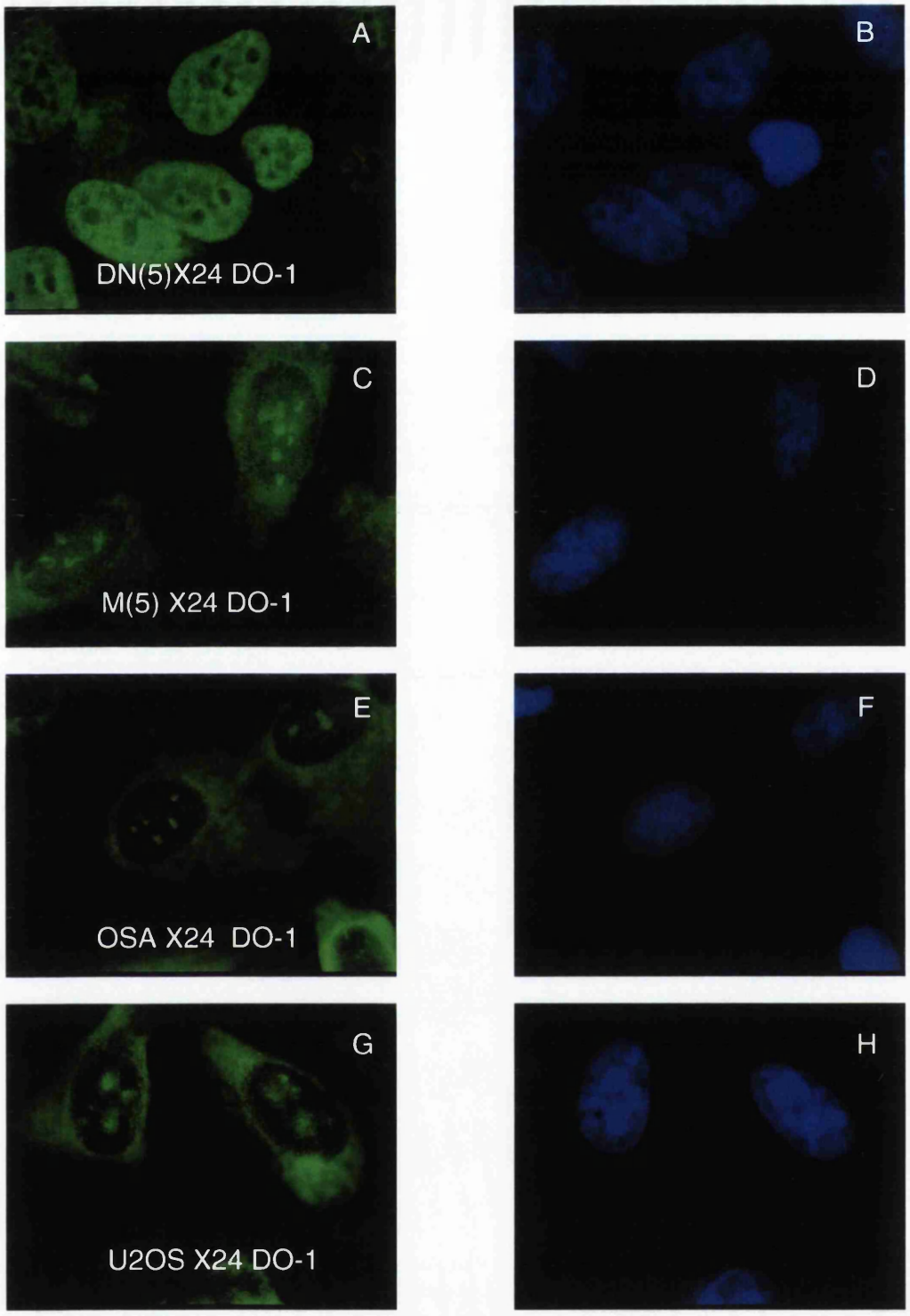

Figure 4.6. 12 Gy X-ray-irradiation fails to significantly alter the subcellular localisation of p53. Various cell lines (as indicated) were 12 Gy X-ray irradiated and analysed by IF at various time points post-irradiation (as indicated, X0.5 etc [hrs]). DO-1 (p53) antibody was used and subsequently detected with α-mouse FITC-conjugated 2°-antibody. The right-hand panels represent DAPI (nuclear) stained cells.

UV-irradiation reveals MDM2-containing sub-nuclear dot-like structures

UV-irradiation (30 Jm^{-2}) analysis of all four cell lines revealed both a significant reduction in MDM2 and induction in p53 protein levels (see Figure 2.29). Interestingly, only OSA cells recovered from the UV-mediated MDM2 reduction, 24 hours post-irradiation. Additionally, all cell lines, with the exception of DN(5), exhibited increased MDM2:p53 complex levels, as determined by IP analysis following a 24 hour UV-irradiation time course (see Figure 3.16). IF analysis of all four cell lines revealed alterations in both MDM2 and p53 sub-cellular location.

MDM2 IF analysis revealed that UV-irradiation of all of the cell lines caused the formation of large sub-nuclear bodies, fewer in number and larger in size than those seen in the respective control cells; reminiscent of lactacystin treated cells (see Figure 4.7 and compare with Figure 4.3). Cells were analysed two, eight and 24 hours post-irradiation and revealed a rapid shift from a poorly defined, general nuclear speckled pattern to a more defined 'dotted' pattern, as early as two hours post-irradiation. As with lactacystin treatment, DN(5) cells shifted from a general to 'speckled' nuclear staining, although larger 'dots' were apparent in some cells. In addition to the two mouse monoclonal antibodies, 2A10 and SMP14, the rabbit polyclonal antibody, N-20, also detected these sub-nuclear bodies.

Overall, MDM2 general nuclear staining (excluding dots), was reduced in all cell lines, where MDM2 detection levels mirrored the Western observations of reduced MDM2 expression. However, Western analysis of OSA cells revealed a bi-phasic response in MDM2 expression, but maintained an altered IF staining pattern relative to control cells.

Parallels between lactacystin and UV-treatment were also observed in the reduction of MDM2 nucleolar occlusion, with potential positive nucleolar staining evident in M(5) and OSA cells (See Figure 4.3 and compare with Figure 4.7).

UV-irradiation reveals increased cytoplasmic p53 staining

p53 analysis revealed increased detection of p53-positive sub-nuclear pods and cytoplasmic staining in OSA, U2OS and M(5) cells, mirroring control patterns, albeit with increased detectability. As with lactacystin treatment, UV-irradiated M(5) and U2OS cells exhibited a partially polarised, perinuclear staining pattern while OSA cell exhibited more general cytoplasmic staining (see Figure 4.4 and compare with Figure 4.8). In contrast, DN(5) cells exhibited almost exclusively nuclear staining with limited cytoplasmic staining, generally retaining the control nuclear staining pattern. As with control DN(5) cells, sub-nuclear pods were undetectable in UV-irradiated DN(5) cells. Interestingly, comparison between UV-irradiated MDM2 and p53 staining patterns in DN(5) cells revealed near opposite patterns, with a 'speckled' MDM2 and 'perforated' p53 nuclear localisation (see Figures 4.7 and 4.8, respectivelty).

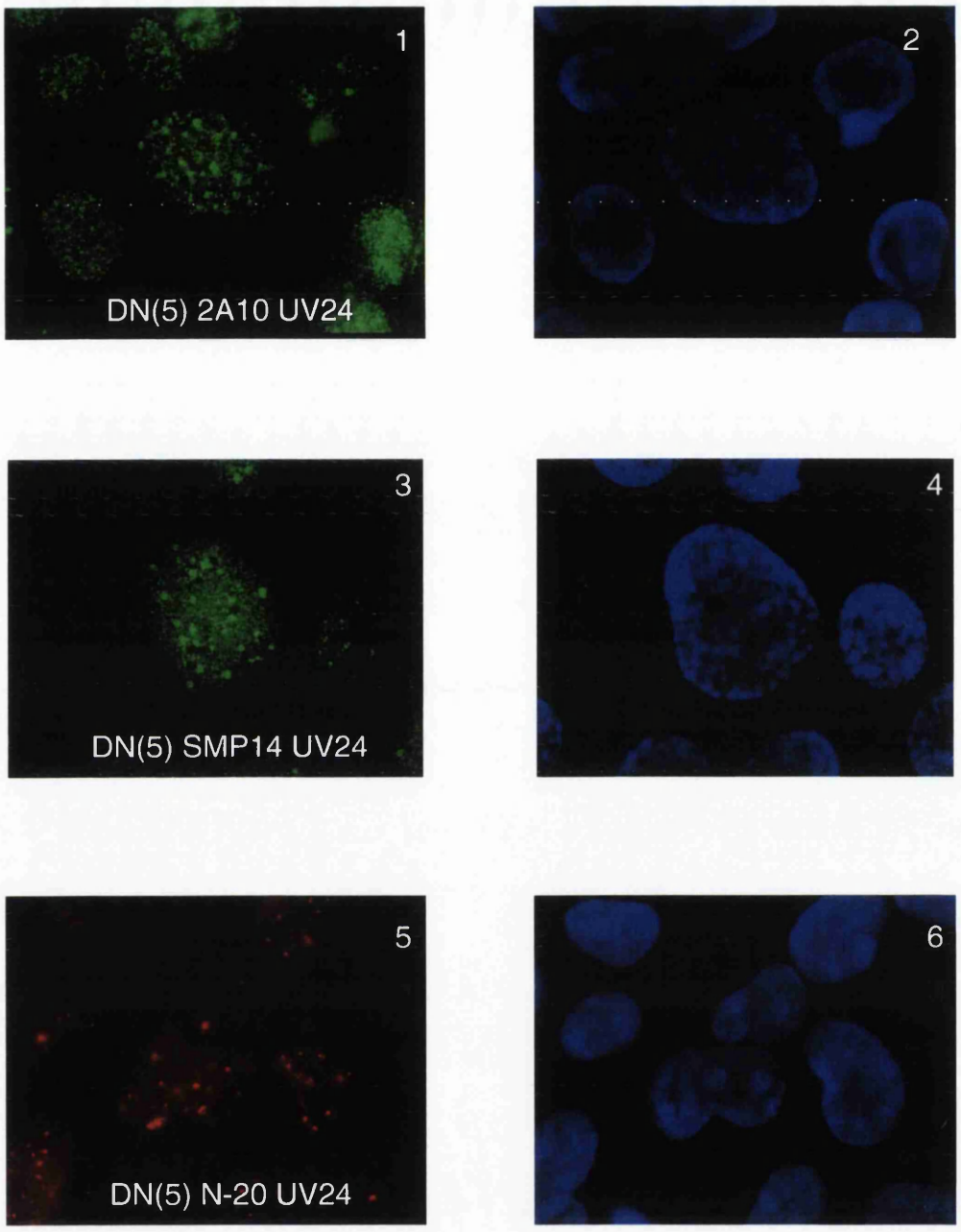

Figure 4.7. 30 Jm-2 UV-irradiation alters MDM2 subcellular localisation (four pages). Various cell lines (as indicated) were 30 Jm-2 UV-irradiated and analysed by IF at various time points post-irradiation (as indicated, UV2 etc [hrs]). 2A10, SMP14 or N-20 (MDM2) antibodies were used; 2A10 and SMP14 were subsequently detected with α-mouse FITC-conjugated 2°-antibody; N-20 was subsequently detected with α-rabbit Cy3-conjugated 2° antibody. The unlabeled right-hand panels represent DAPI (nuclear) stained cells. Panel numbers: 7-8, 11-12, 17-18, 21-22, 27-28 and 31-32 DAPI-associated stained cells are not shown.

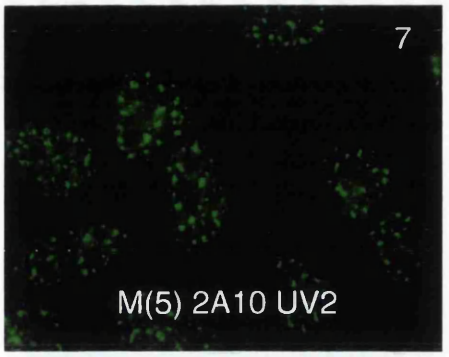
7
M(5) 2A10 UV2

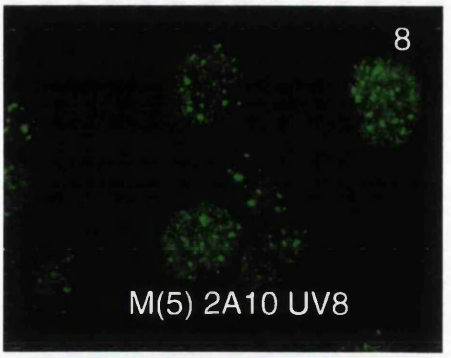
8
M(5) 2A10 UV8

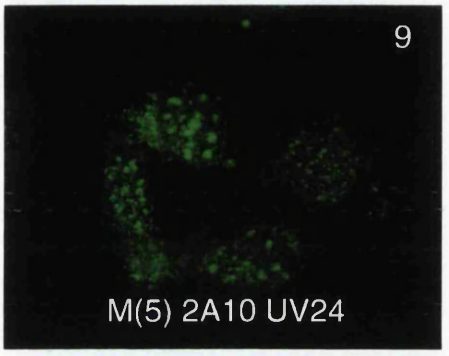
9
M(5) 2A10 UV24

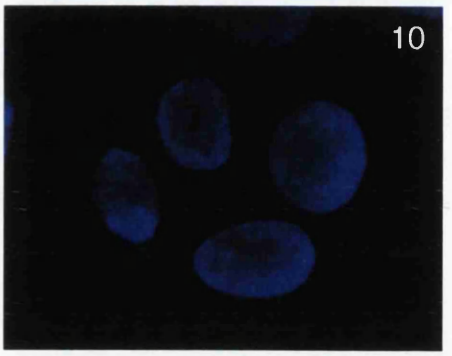
10

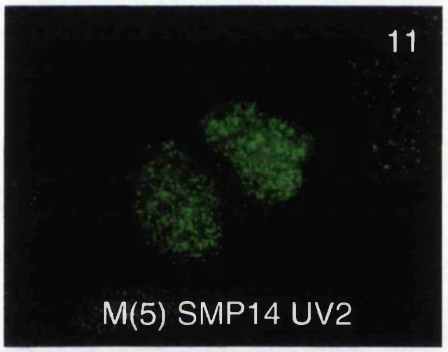
11
M(5) SMP14 UV2

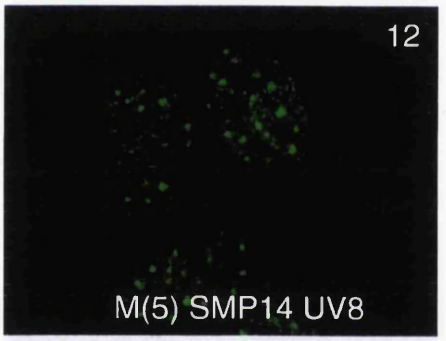
12
M(5) SMP14 UV8

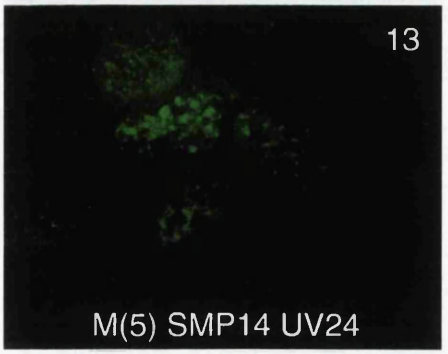
13
M(5) SMP14 UV24

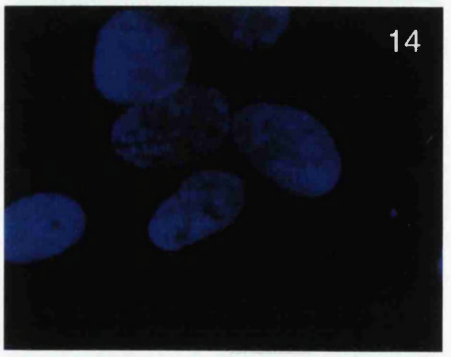
14

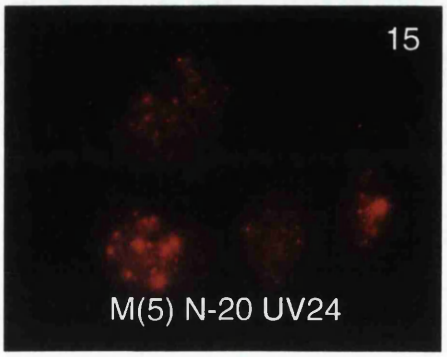
15
M(5) N-20 UV24

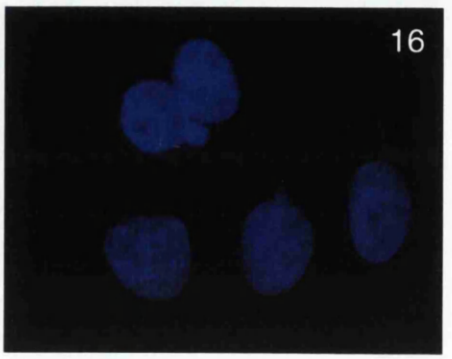
16

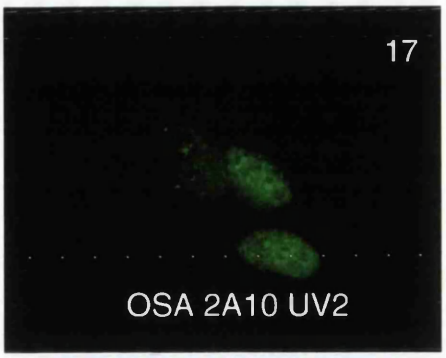
17
OSA 2A10 UV2

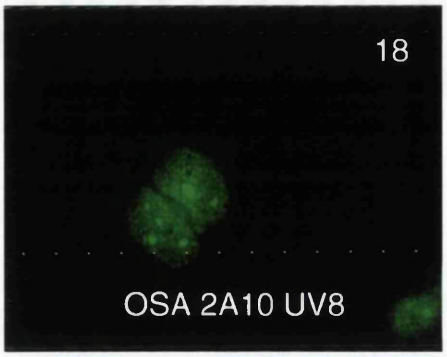
18
OSA 2A10 UV8

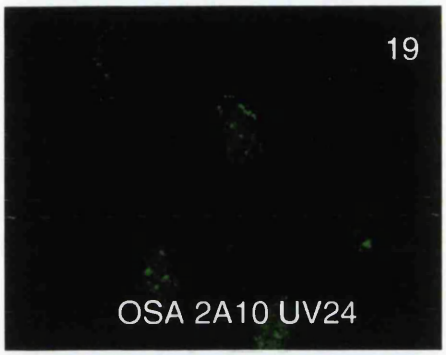
19
OSA 2A10 UV24

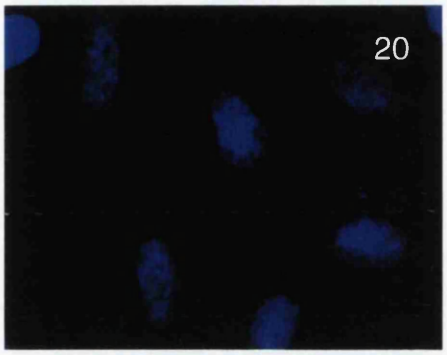
20

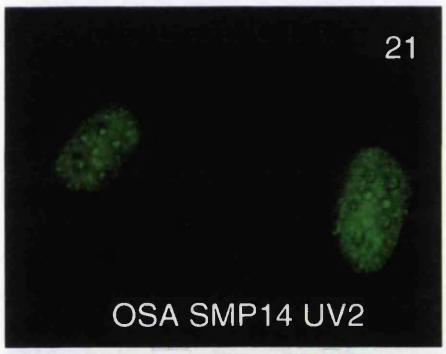
21
OSA SMP14 UV2

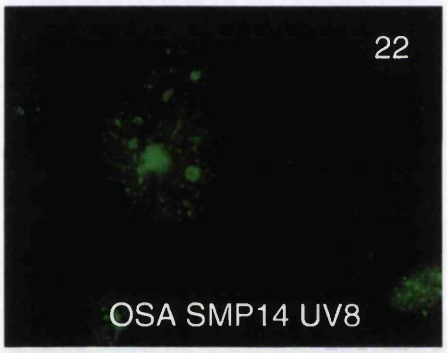
22
OSA SMP14 UV8

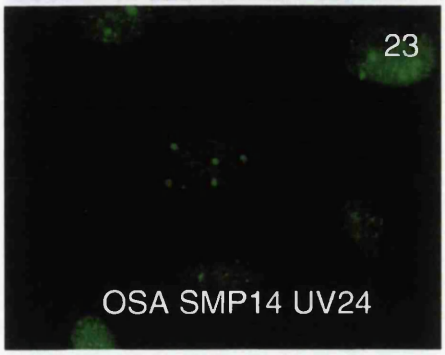
23
OSA SMP14 UV24

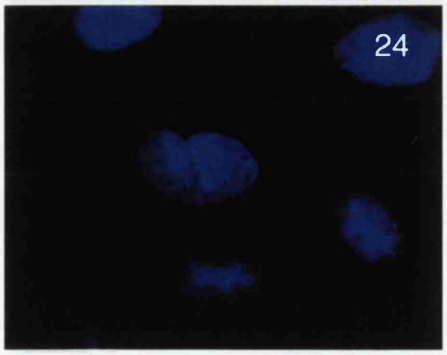
24

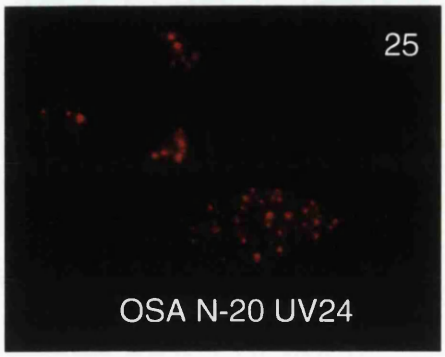
25
OSA N-20 UV24

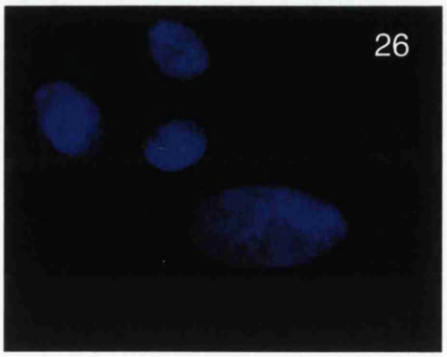
26

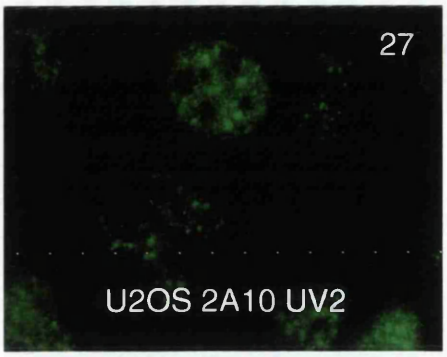
27
U2OS 2A10 UV2

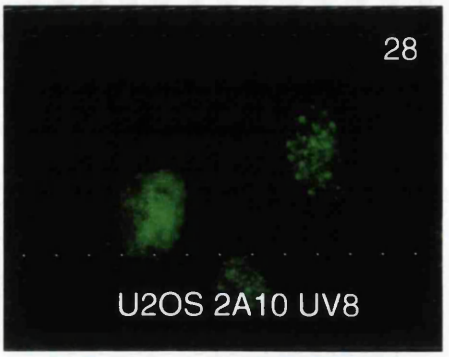
28
U2OS 2A10 UV8

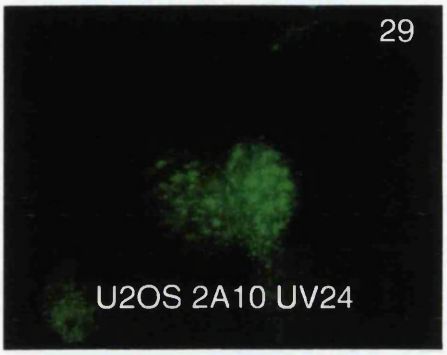
29
U2OS 2A10 UV24

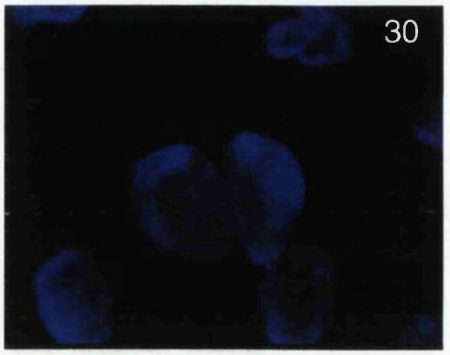
30

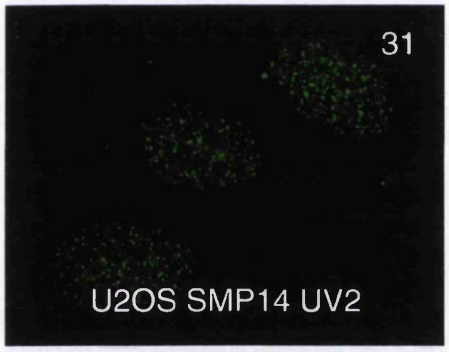
31
U2OS SMP14 UV2

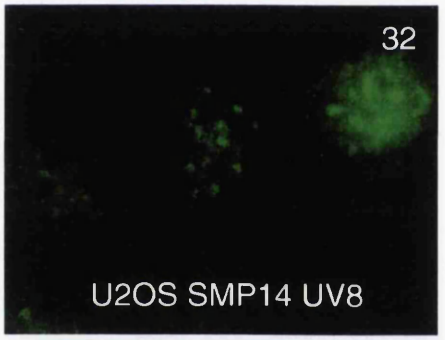
32
U2OS SMP14 UV8

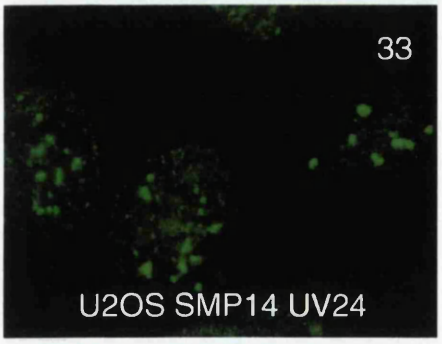
33
U2OS SMP14 UV24


34

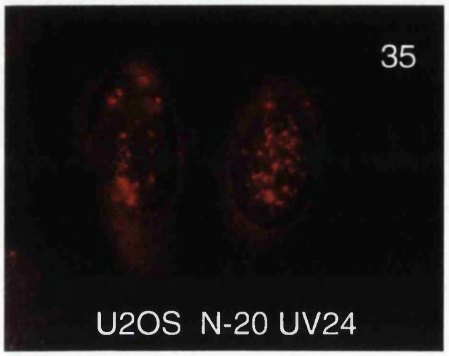
35
U2OS N-20 UV24

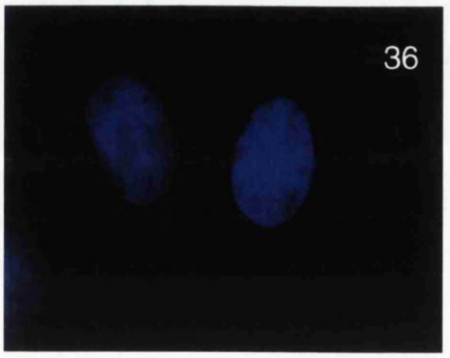
36

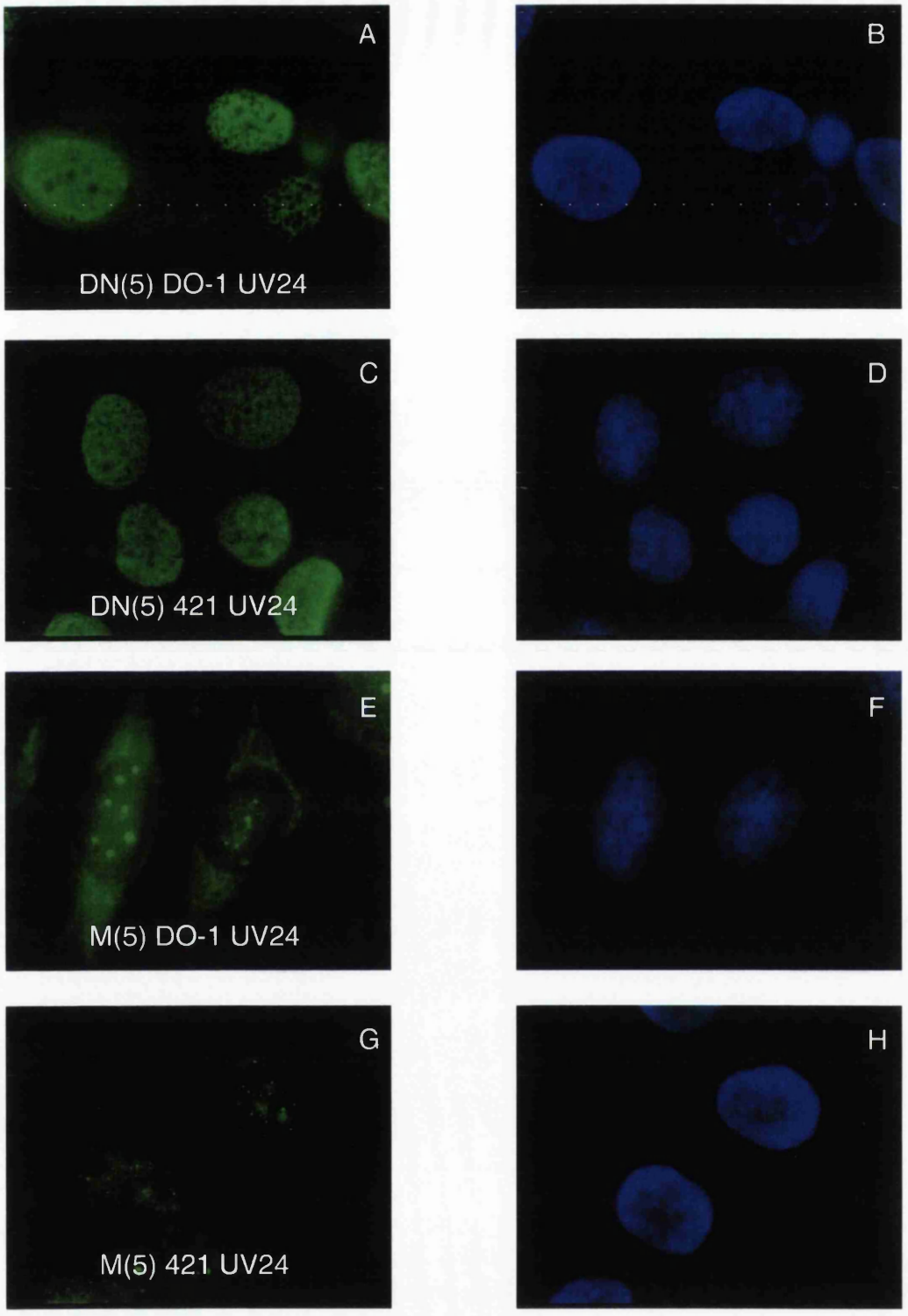

Figure 4.8. 30 Jm-2 UV-irradiation alters p53's subcellular localisation (two pages). Various cell lines (as indicated) were 30 Jm-2 UV-irradiated and analysed by IF at various time points post-irradiation (as indicated, UV2 etc [hrs]). DO-1 or 421 (p53) antibodies were used and subsequently detected with α-mouse FITC-conjugated 2°-antibody. The right-hand panels represent DAPI (nuclear) stained cells.

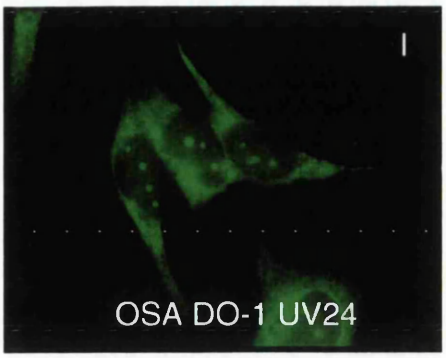
I
OSA DO-1 UV24

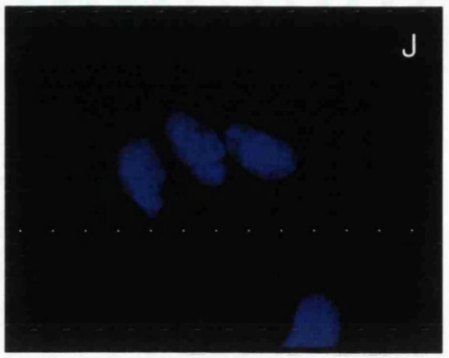
J

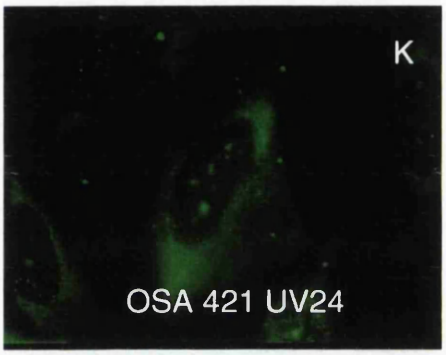
K
OSA 421 UV24

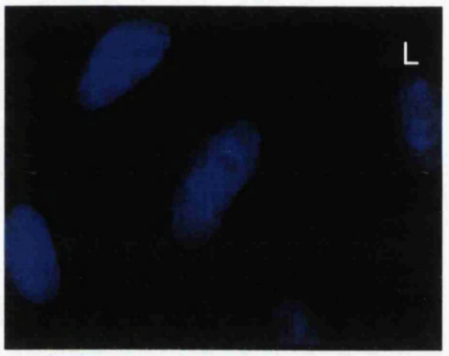
L


M
U2OS DO-1 UV24

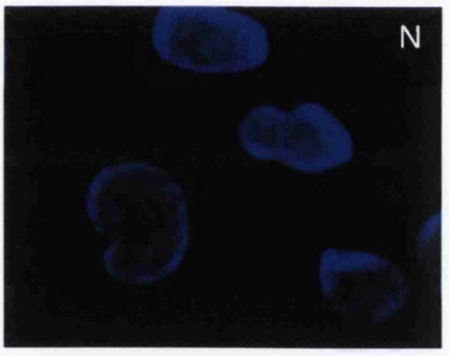
N

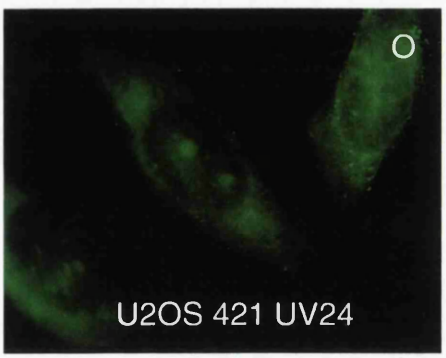
O
U2OS 421 UV24

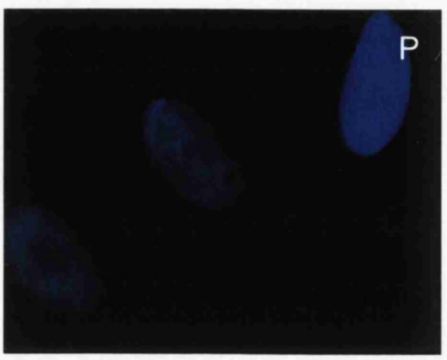
P

UV-treatment reveals co-localisation of PML bodies with MDM2 pods

The 'dotted' nature of the UV-induced MDM2 sub-nuclear structures were similar in number and size to the pattern observed for PML-bodies. PML bodies were examined pre- and post-UV irradiation using a rabbit PML polyclonal antibody (kindly donated by M.Hodges [ICRF]). Analysis revealed the presence of PML bodies in all of the cell lines examined, pre- and post-UV-irradiation, with no detectable differences between cell lines or following treatment (see Figure 4.9). Co-localisation studies post-UV-treatment, with 2A10 and PML antibodies, revealed that M(5) cells exhibited PML bodies that co-localised with MDM2 (see Figure 4.10). However, there was concern over the overlap in fluorescence between the Cy3 and FITC fluorophores (having similar excitation [≅500 nm] and emission [≅ 525 nm] spectra).

To ensure a more accurate determination of PML-MDM2 co-localisation, confocal microscopy was used (see Material and Methods) and revealed a considerable overlap in both M(5) cells pre- and (24 hours) post-UV-irradiation (see Figure 4.11 [I, II and IV]). 3D cellular reconstruction and size measurements were also made, determining the MDM2-postive 'dots' to be approximately 0.5-1μm across and located centrally along the width of the nucleus (see Figure 4.11 [III]).

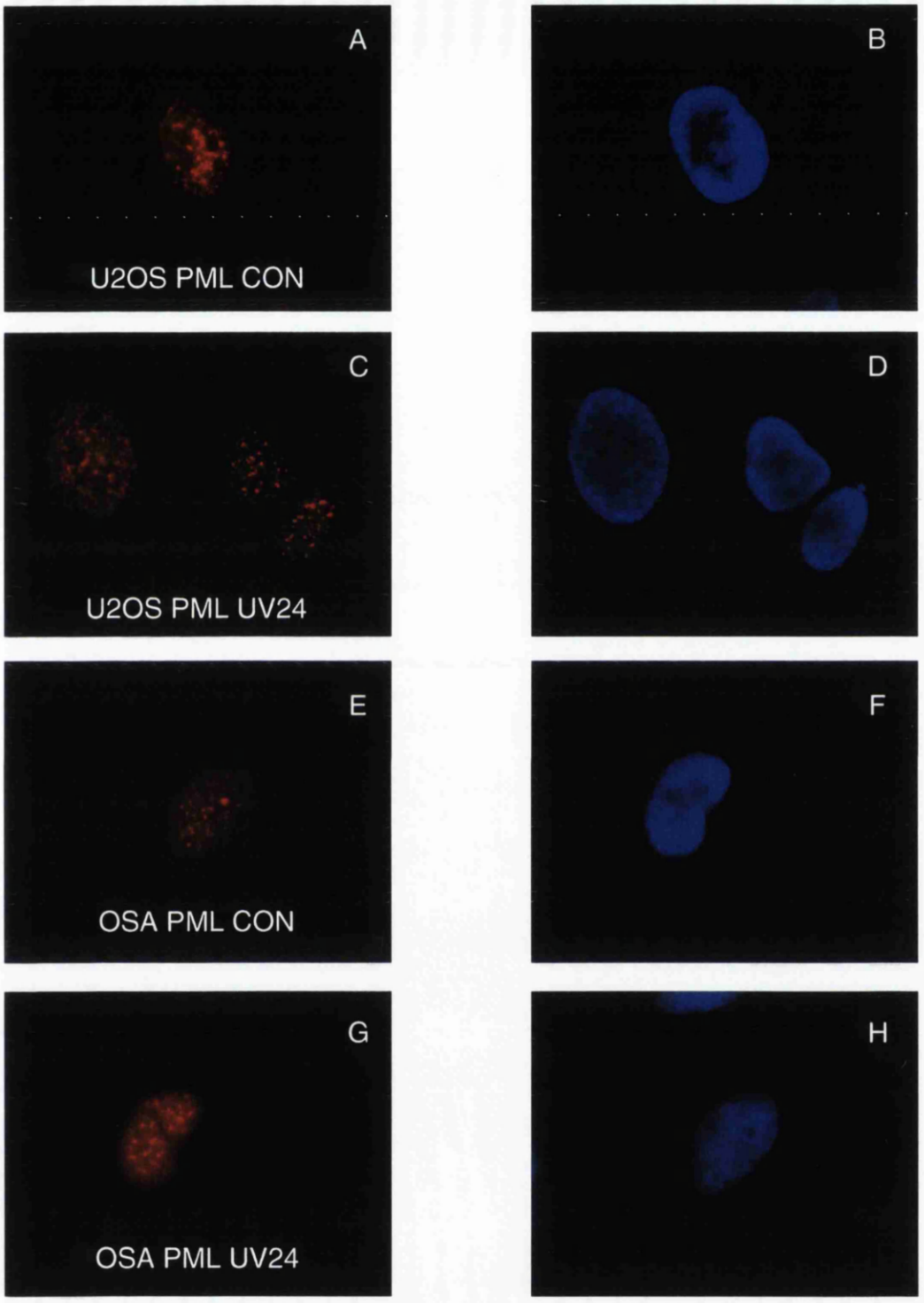

Figure 4.9. Subcellular localisation of PML pre- and post-UV-irradiation (two pages). Un-irradiated (Con) or 30 Jm-2 UV-irradiated (UV24) cell lines (as indicated) were analysed by IF analysis 24 hours post-irradiation. PML (PML) antibody was used and subsequently detected with α-rabbit Cy3-conjugated 2° antibody. The right-hand panels represent DAPI (nuclear) stained cells.

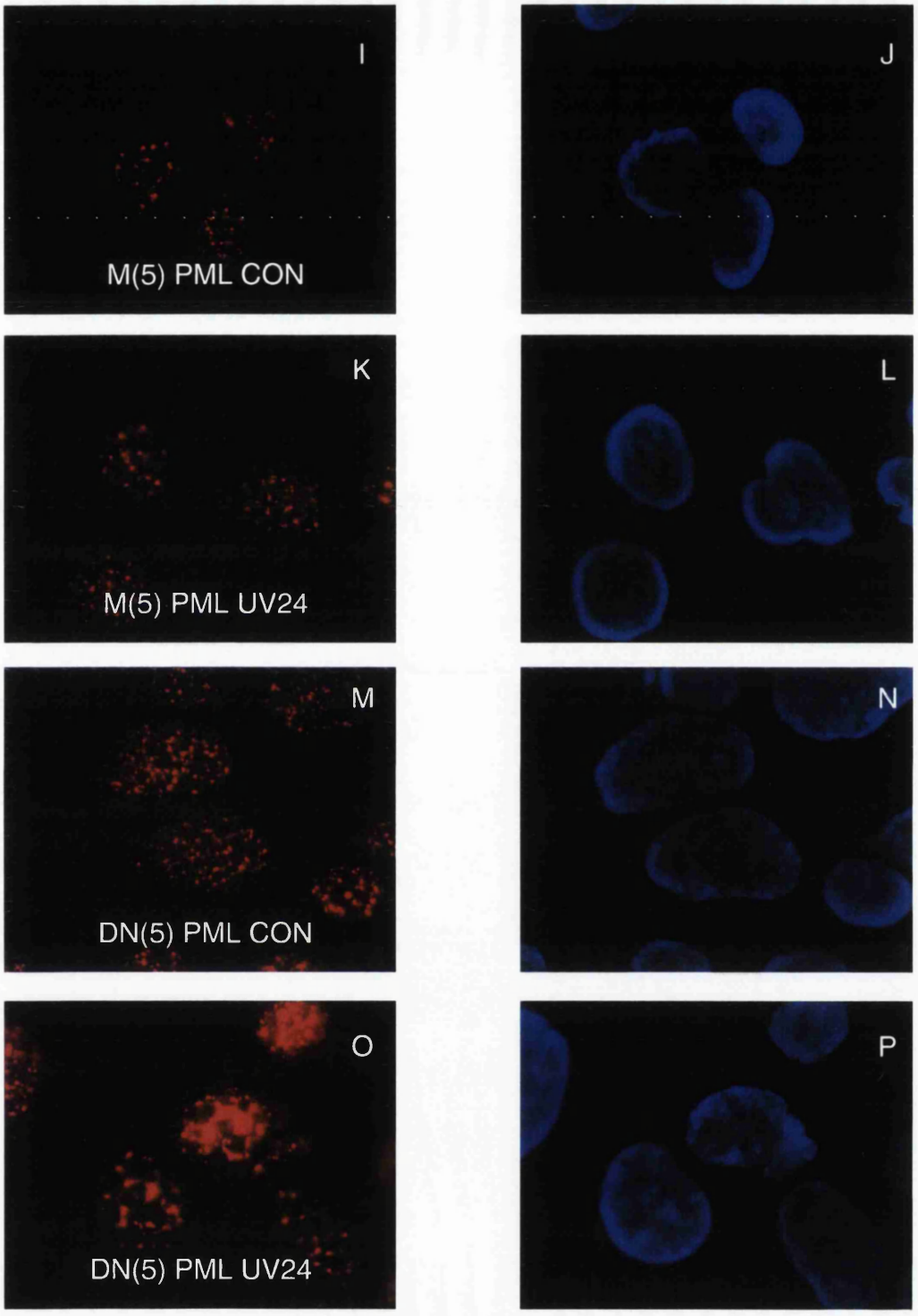
I
M(5) PML CON
J
K
M(5) PML UV24
L
M
DN(5) PML CON
N
O
DN(5) PML UV24
P

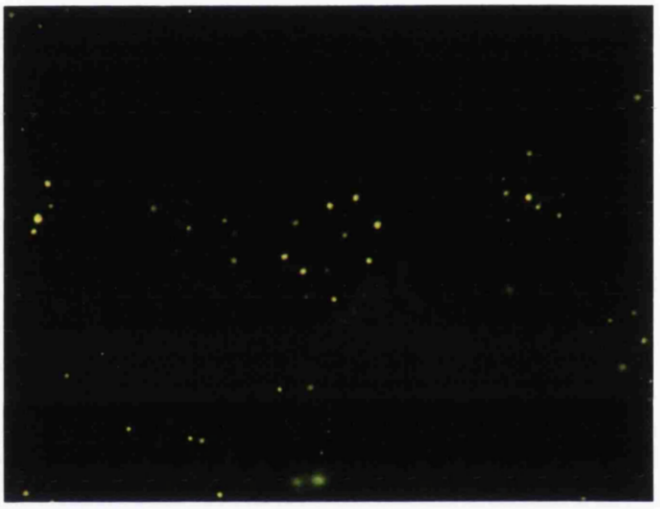

Figure 4.10. MDM2 co-localises with PML post-UV-irradiation. M(5) cells were 30 Jm-2 UV-irradiated and analysed by IF 24 hours post-irradiation. SMP14 (MDM2) and PML (PML) antibodies were used together and subsequently detected with α-mouse FITC-conjugated and α-rabbit Cy3-conjugated 2° antibodies, respectively.

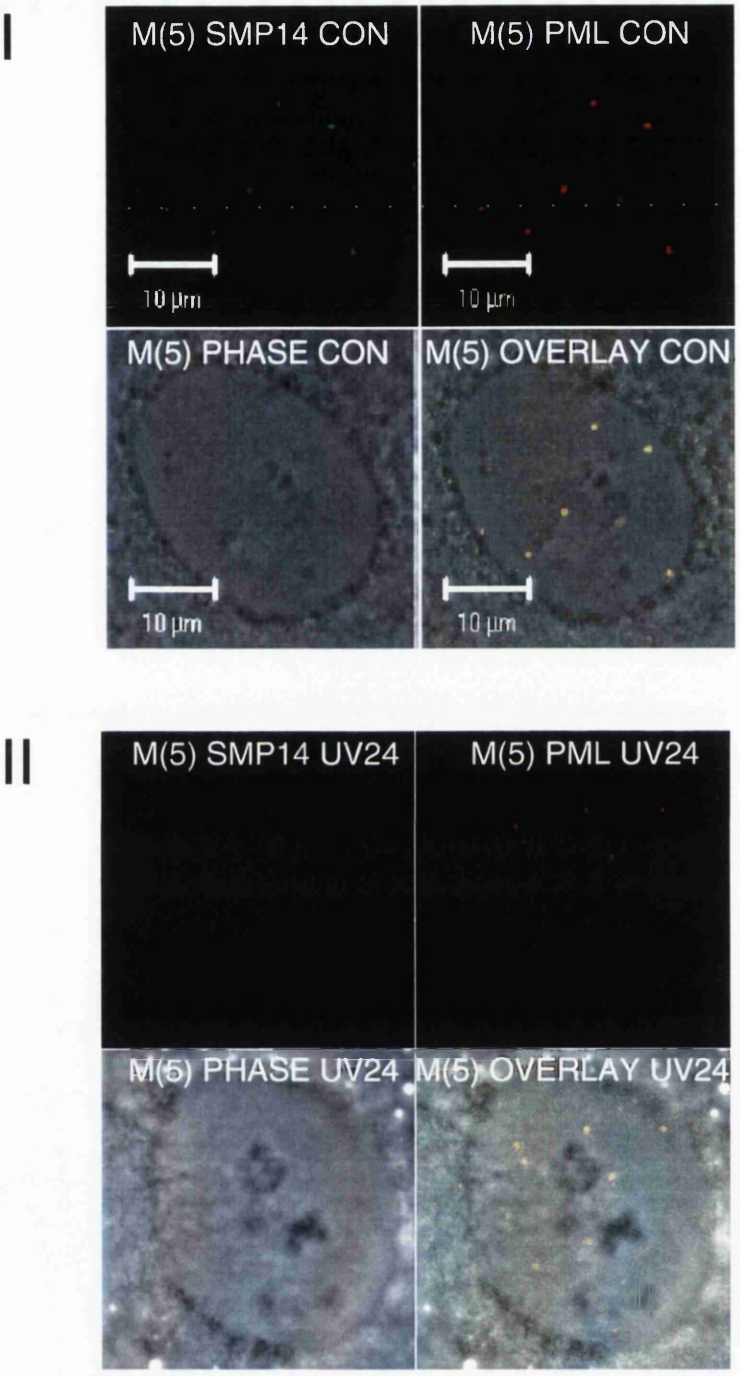

Figure 4.11. MDM2 co-localises with PML pre- and post-UV-irradiation (two pages). M(5) cells were analysed by confocal microscopy pre- and post-30 Jm-2 UV-irradiation. SMP14 (MDM2) and PML (PML) antibodies were used together and subsequently detected with α-mouse FITC-conjugated and α-rabbit Cy3-conjugated 2° antibodies. PHASE – refers to a phase-contrast image and OVERLAY – refers to the single SMP14 and PML images combined. (I) Untreated M(5) cells (CON); (II) UV-irradiated M(5) cells (UV24); (III) UV-irradiated M(5) cells - confocal-generated 'side-on' 'overlay'-image of a PML and SMP14 dual-stained cell; (IV) UV-irradiated M(5) cells - confocal-generated 'overlay'-image of a PML and SMP14 dual-stained cell.

III

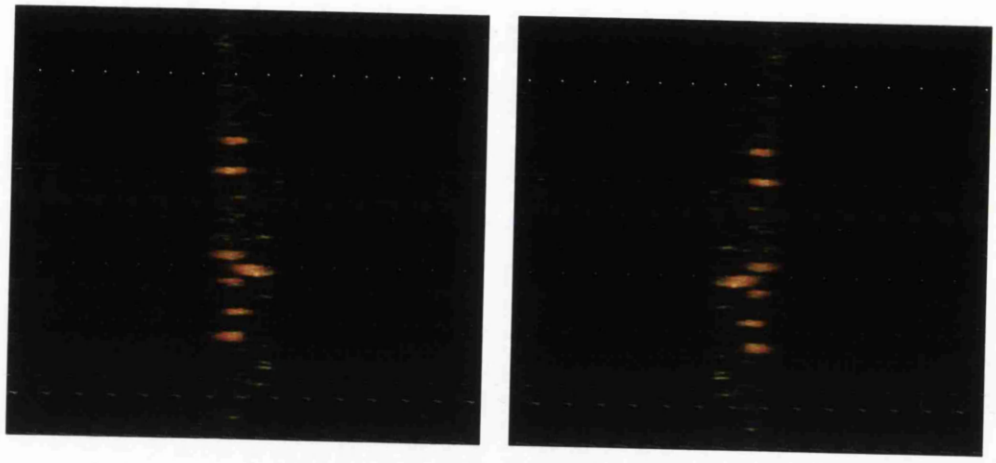

IV

Induced NARF(6) cells show no MDM2 re-localisation while ARF accumulates in the nucleolus

IPTG-mediated ARF-induction in NARF(6) cells caused elevated MDM2 and p53 levels, as well as increased p53:MDM2 complexes, determined by Western and IP analysis, respectively (see Figures 2.37 and 3.11, respectively). Initial analysis of IPTG-induced NARF(6) cells failed to detect ARF using an immuno-purified anti-peptide, rabbit polyclonal antibody (FST-13) (kindly donated by Fran Stott [ICRF]). No gross alterations in MDM2 or p53 subcellular localisation patterns were evident, although detection of both proteins was increased. In an attempt to facilitate visualisation of IPTG-induced ARF, a different fixing protocol was carried out using paraformaldehyde instead of methanol:acetone. Paraformaldehyde fixation 24 hours post-IPTG treatment allowed detection of discretely localised ARF bodies; most probably nucleolar-associated(Stott, Bates et al. 1998; Tao and Levine 1999; Weber, Taylor et al. 1999; Zhang and Xiong 1999), due to the DAPI staining patterns (see Figure 4.12). However, as with the methanol:acetone fixation procedure, no significant differences in sub-cellular staining patterns of either MDM2 or p53 were apparent (see Figure 4.13).

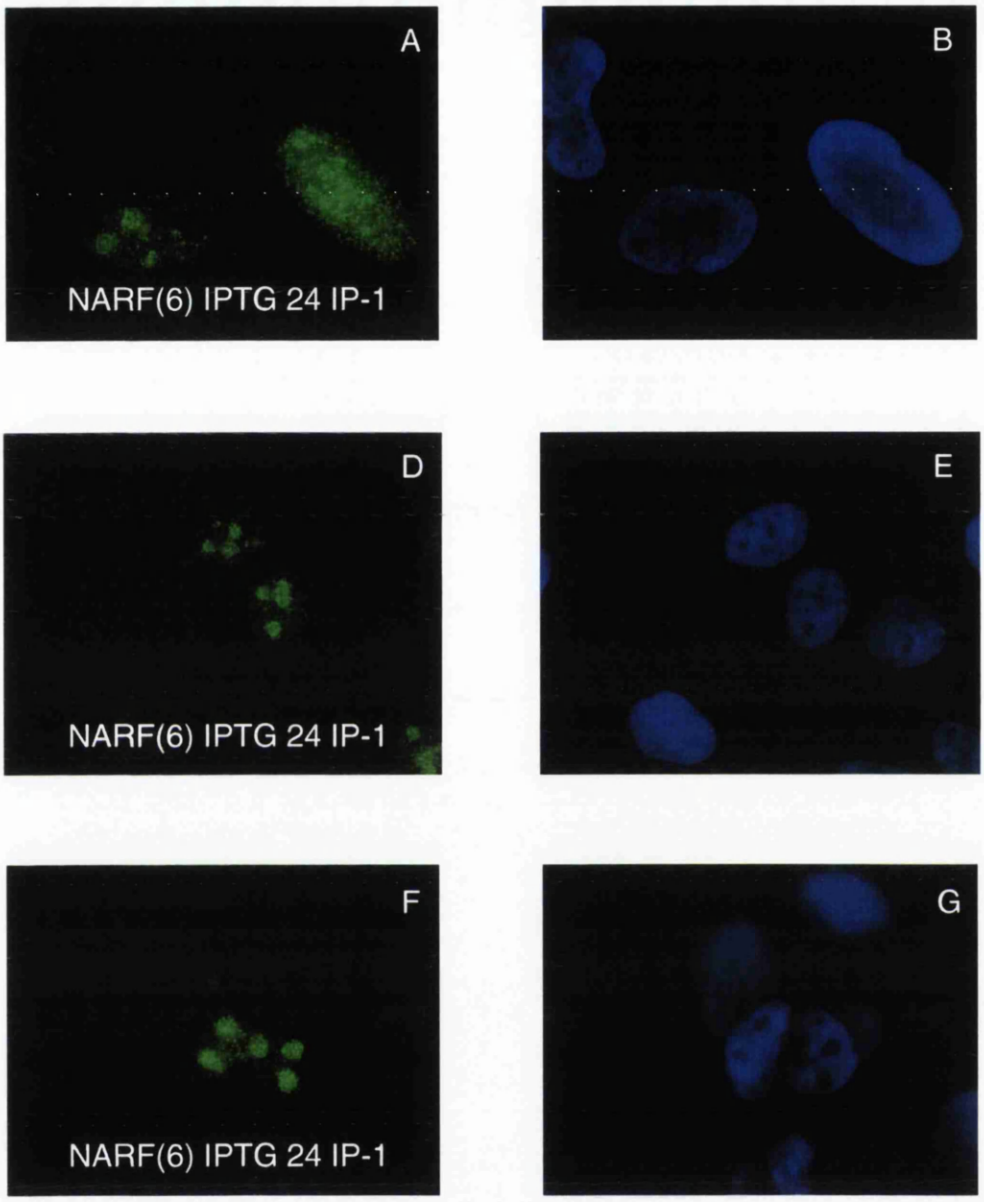

Figure 4.12. Paraformaldeyde fixation reveals discrete sub-nuclear localisation of ARF. NARF(6) cells were treated with 1mM IPTG (IPTG24) and analysed by IF 24 hours post-treatment. Cells were fixed with paraformaldehyde (instead of methanol:acetone – see Materials and Methods). IP-1 (ARF) was used and subsequently detected with α-rabbit Alexa (GFP)-conjugated 2°-antibody. The right-hand panels represent DAPI (nuclear) stained cells.

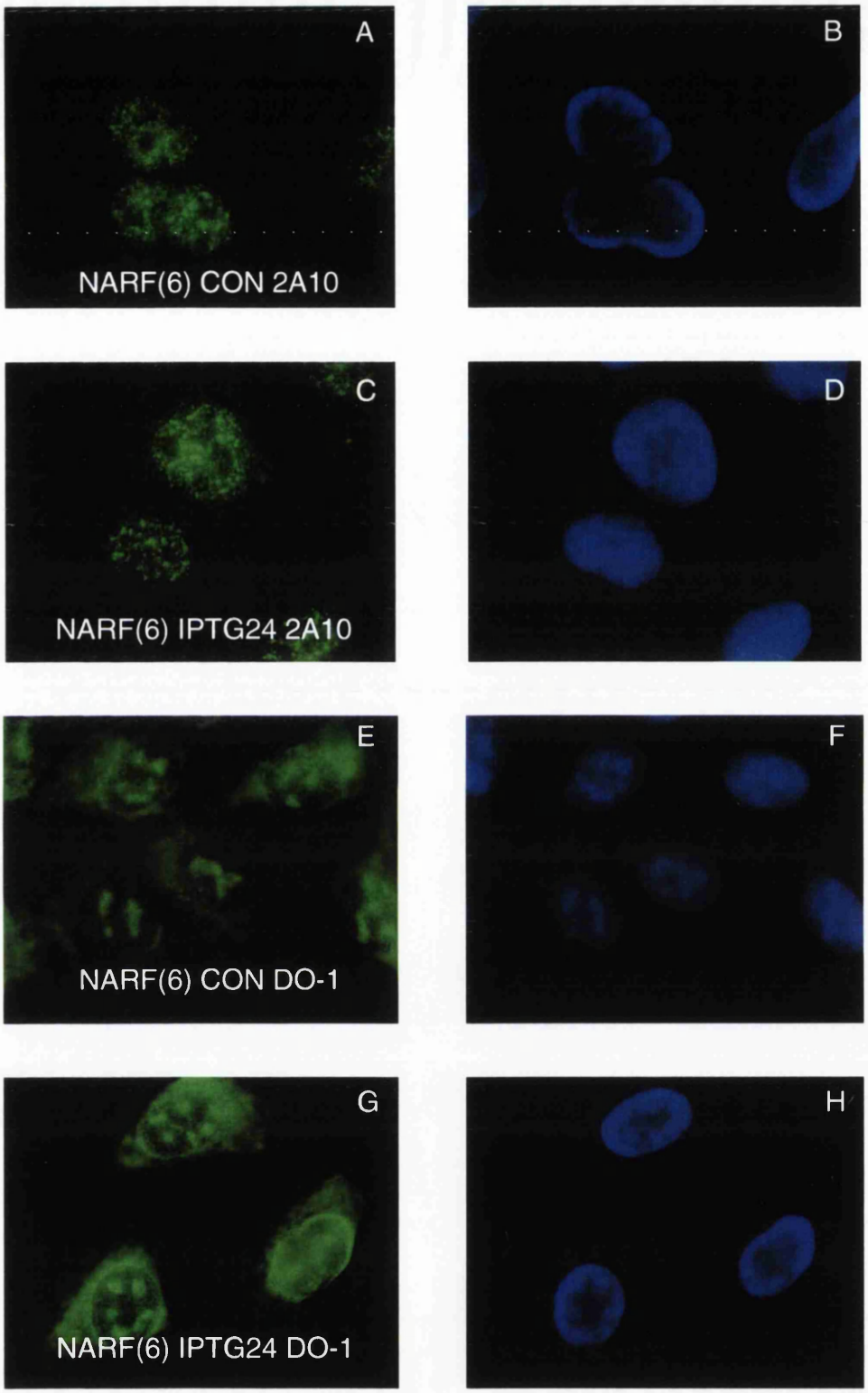

Figure 4.13. ARF-expression does not affect MDM2 and p53 subcellular localisation. NARF(6) cells were treated with 1mM IPTG (IPTG24), or not (Con), and analysed by IF 24 hours post-treatment. Cells were fixed with paraformaldehyde (instead of methanol:acetone – see Materials and Methods). 2A10 (MDM2) and DO-1 (p53) antibodies were used and subsequently detected with α-mouse FITC-conjugated 2°-antibody. The right-hand panels represent DAPI (nuclear) stained cells.

ARF is undetectable in DN/U2OS/MDM2/OSA

Paraformaldehyde fixation was also used on DN(5), U2OS, M(5) and OSA cells lines, which had been shown to contain low levels of ARF, in an attempt to localise the endogenously expressed protein. Repeated attempts with varying antibody concentrations failed to detect significant staining over background levels (results not shown).

Summary and Discussion

Control

All of the cell lines analysed exhibited predominantly nuclear localisation of MDM2. Additionally, both exogenously- and endogenously-expressed MDM2 present in M(5) and U2OS, DN(5) and OSA cells, respectively, generated similar patterns of nuclear staining. These two sets of results suggested that the exogenously expressed MDM2 was behaving in a similar manner to the endogenous protein[15]. Therefore, enforced expression throughout the cell cycle from a CMV-promoter did not cause any major detectable alterations in the sub-nuclear organisation of MDM2 in U2OS cells.

In accordance with Western analysis (see Chapter Two), M(5) and OSA exhibited increased detection of MDM2 by IF in comparison to U2OS and DN(5) cells. Interestingly, DN(5)'s MDM2-staining was higher than U2OS cells, although the opposite was observed by Western analysis, suggesting that DN(5)-specific MDM2 cellular structures may have been more accessible to detection in comparison to U2OS cells. Indeed, DN(5)'s cellular MDM2 staining pattern was significantly different to the other cell lines, with a more constant, uninterrupted, general nuclear staining. In contrast, OSA, M(5) and U2OS cells exhibited a 'speckled' staining pattern, with a high number of discrete sub-nuclear foci, over a lower general nuclear signal. In comparison to U2OS, M(5) cells showed stronger staining of these speckles, suggesting that exogenous MDM2 was capable of entering these structures.

---

[15] The differences between U2OS and M(5) cells was assumed to be due to the effects of the exogenous MDM2 protein, although endogenous and exogenous proteins could not be distinguished.

The presence of differential nuclear staining or 'speckles' suggested that within the nucleus, MDM2 may be specifically targeted to sub-nuclear structures, facilitating a specific role or function of MDM2. An alternative view could determine these 'speckles' as simply storage depots for excess MDM2, while the general nuclear MDM2 may be the 'active' protein. In addition to sites of higher concentrations of MDM2 staining, all the cell lines demonstrated areas of the nucleus devoid of MDM2 staining, most probably corresponding to nucleoli. Therefore, these results also supported the idea of specific sub-nuclear targeting of MDM2. Interestingly, N-20 consistently detected larger well-defined sub nuclear bodies in wild-type p53 expressing cell lines and may reflect the antibodies ability to detect MDM2 splice variants undetectable by the other antibodies (see Figure 4.1 and Figure 1.2 – for antibody epitopes and MDM2 splice variants).

Examination of p53 in all of the cell lines, including both endogenous wild-type p53 and exogenous mutant p53 $175^{R\Rightarrow H}$, revealed both nuclear and cytoplasmic staining. p53's dual subcellular compartmentalisation can be explained through MDM2-mediated nuclear:cytoplasmic shuttling and p53's own nuclear import signal (see Introduction). M(5) and OSA cells exhibited significantly higher cytoplasmic p53 staining than U2OS cells, while DN(5) cells demonstrated the lowest levels of cytoplasmic staining of all four cell lines. The correlation between increased MDM2 expression levels and increased cytoplasmic p53 staining are in agreement with the idea of MDM2-mediating its nuclear export (see Introduction).

OSA, DN(5) and U2OS cells all exhibited strong MDM2 perinuclear staining, discrete nuclear 'speckles' and weaker cytoplasmic staining. However, DN(5) cells showed reduced cytoplasmic staining, increased general nuclear staining and clear nucleolar exclusion (relative to U2OS cells). This staining pattern mirrored the observed MDM2 general-nuclear staining pattern and in conjunction with the IP results of high p53:MDM2 complex (see Chapter Three), suggested that p53 subcellular localisation was influencing the MDM2's staining pattern. The sub-nuclear pods may have been present, but simply masked by excess general nuclear staining and decreasing visible contrast. Alternatively, mutant p53 $175^{R\Rightarrow H}$ may have lost the ability to form sub-nuclear pods, perhaps due to its inability to bind

DNA or other macromolecules important for mediating the formation of these structures. Another view could be a gain of function, where increased binding to a ubiquitous nuclear protein determined its more general nuclear staining. Nevertheless, p53 $175^{R \Rightarrow H}$ had not lost or gained the ability to maintain the sites of nucleolar exclusion.

The biological relevance of these sub-nuclear pods, as with the MDM2 'speckles', may either represent active sites of p53 function, active sequestration of unwanted p53 activity or simple storage areas of latent p53.

Lactacystin

Due to the proteosome mediating the degradation of a large number of proteins, lactacystin-mediated inhibition of proteosome function has the potential to stabilise multiple proteins. Therefore, any specific observations made may be due to an indirect consequence of proteosome inhibition, rather than direct stabilisation of the observed protein. Nevertheless, both p53(Maki, Huibregtse et al. 1996; Fuchs, Adler et al. 1998) and MDM2(Honda, Tanaka et al. 1997; Chang, Lee et al. 1998) proteins have been documented to undergo ubiquitination and proteolysis by the proteosome.

Addition of the 26S proteosome inhibitor, lactacystin, caused a general increase in detection of both p53 and MDM2. Presumably via direct inhibition of ubiquitin-mediated degradation of both proteins and/or p53-mediated transcriptional upregulation of MDM2 (see Figure 2.31). However, in addition to elevating immunofluorescence levels, both MDM2 and p53 sub-cellular localisation were affected.

Lactacystin treatment of OSA, M(5) and U2OS cells caused the formation of large globular sub-nuclear bodies, fewer in number and larger than the speckles observed in control cells. Similar observations were made with both endogenous- and exogenous-MDM2 expressing cells. A decrease in general nuclear staining and nuclear speckles was seen in cells with globular sub-nuclear bodies. These results suggested that MDM2 was redistributed into the globular bodies, although accurate quantitative and qualitative analysis was not carried out. The decreased number of globular foci, suggested that these sub-nuclear bodies were not

enlarged speckles and represented novel sub-nuclear structures. However, selective enlargement of specific speckles through either speckle aggregation or specific addition of excess MDM2 could not be ruled out. In addition, OSA cells seemed to generate globular bodies within potential nucleoli (low DAPI stained areas), providing evidence for lactacystin-induced nucleolar localisation of MDM2. A possible mechanism could have been mediated through stabilisation and activation of MDM2-nucleolar-promoting targeting molecules or macromolecular interactions. These results supported the observations that MDM2 is capable of nucleolar localisation, as seen upon ARF-expression(Weber, Taylor et al. 1999). Indeed, ARF may effectively ubiquitinate and sequester MDM2 in such bodies ready for degradation (mimicking lactacystin treatment) and/or simple sequestration from p53. Nevertheless, these concentrated MDM2-containing structures may represent the results of over-active targeting and/or inhibition of redistribution mechanisms.

Lactacystin can lead to stabilisation of multi-ubiquitinated forms of proteins(Fenteany and Schreiber 1998; Fukuchi, Maruyama et al. 1999) and may provide a non-proteosomal sub-cellular localisation signal. However, lactacystin-induced inhibition of ubiquitin-mediated degradation may cause localisation of ubiquitinated MDM2 at the site of proteosomal degradation, i.e., the globular bodies. The precise location of the proteosomes in mammalian cells is unclear, although they are present in both the nucleus and the nuclear-periphery of fission yeast(Wilkinson, Wallace et al. 1998; Wilkinson, Penney et al. 1999). Nevertheless, this evidence suggested that MDM2 could be degraded by nuclear proteosomes.

In the case of lactacystin treated DN(5) cells, a similar drastic alteration in MDM2 expression pattern was observed. The constant, uninterrupted general nuclear staining pattern observed in control cells was altered to a more 'speckled' pattern, similar to control M(5), OSA and U2OS cells. Again these results suggested that lactacystin-mediated alterations in MDM2's subcellular localisation promoted the formation of more discrete sub-nuclear bodies. The formation of these structures most probably reflects a post-translational modification of MDM2, rather than increased MDM2 levels, as lactacystin treatment of DN(5) failed to upregulate MDM2 expression by Western analysis (see Figure 2.31). Nevertheless, the defined nucleolar exclusion seen in control DN(5) cells was apparently reduced.

Generally, cytoplasmic MDM2 expression was reduced (to varying degrees) in all of the cell lines, with OSA cells showing the greatest loss of cytoplasmic staining. Taken with the observation of increased lactacystin-induced nuclear body formation, lactacystin may also promote the increase in nuclear MDM2 levels at the expense of cytoplasmic MDM2 levels. Stabilisation of ubiquitinated MDM2 forms may provide an extrinsic sub-nuclear localisation signal (targeting MDM2 to nuclear proteosomes) and inhibit MDM2 nuclear export or promote MDM2's intrinsic nuclear import ability. Again, the argument for activation and/or loss of localisation remains relevant.

Analysis of p53 localisation, post-lactacystin treatment, in all four cell lines revealed a significant increase in cytoplasmic staining, the most drastic occurring in DN(5) cells. Both U2OS and M(5) cells clearly exhibited a partial, polarised perinuclear halo. The polarisation of the partial halo did not occur in any particular direction, suggesting that it was not a consequence of plunging the cells into the fixative and subsequent rupturing of the nuclear membrane; phenomena which had not been observed in any other experiments. On closer inspection the halos themselves were not uniform and were made up of a number of discrete bodies. Such polarised movement of discrete bodies, in conjunction with the localisation to the nuclear membrane, suggested targeted movement of vesicles. However, accurate study of the physical and biological nature of these bodies was not carried out. It remains unknown of the halo's directional movement, whether nuclear to cytoplasmic, or vice versa, but with the general observation of lactacystin-mediated cytoplasmic accumulation of p53, the former directional movement seems more likely. Obvious 'halo' formation was not clear in OSA, while DN(5) exhibited a more uniform, non-polarised cytoplasmic accumulation of p53.

Sub-nuclear p53 pods were still detectable in OSA, U2OS and M(5) cell lines post-treatment, although they were slightly weaker than control levels. The most drastic nuclear reduction and concomitant increase in cytoplasmic p53 staining occurred in DN(5) cells. The reduced general nuclear staining of DN(5) cells allowed the detection of faint sub-nuclear pod structures, reminiscent of those seen in OSA, U2OS and M(5) cells. These findings suggested that p53 sub-nuclear pods were present in control DN(5) cells, but simply masked due to lack of contrast generated by the general nuclear staining. Additionally,

these pods seemed relatively unaffected by lactacystin-treatment, perhaps representing a specific pool of p53 unable to be ubiquitinated.

Observation of increased cytoplasmic p53 accumulation can be attributed to either increased nuclear export or a block of nuclear import. MDM2 is required for p53 nuclear export(Freedman and Levine 1998) and lactacystin induced MDM2 expression levels in OSA, M(5) and U2OS cells, while no induction was seen in DN(5) cells. However, all four cell lines exhibited a shift in nuclear to cytoplasmic p53 staining, suggesting that MDM2 upregulation was not absolutely required. Nevertheless, upon lactacystin treatment the existing MDM2 levels in DN(5) cells may have been sufficient to mediate p53 nuclear export. Lactacystin-mediated stabilisation of ubiquitinated p53, through inhibition of cytoplasmic proteosomes, may have provided a nuclear export signal and/or caused accumulation of p53 at the site of cytoplasmic proteosome-mediated degradation. This same explanation can be used on the accumulation of MDM2 into globular nuclear structures (see above).

The cytoplasmic localisation/sequestration of p53 may be an active cellular response in an attempt to limit p53's activity as a nuclear transcription factor. Additionally, in an attempt to repress it own translation and hence reduce it's protein levels(Mosner, Mummenbrauer et al. 1995; Fu, Ma et al. 1999).

Overall the lactacystin results revealed that both MDM2 and p53 were dynamic molecules capable of existing in both the nucleus and cytoplasm. Both molecules were also capable of forming discrete sub-nuclear bodies, which in the case of mutant p53 $175^{R \Rightarrow H}$ was severely altered. However, due to lactacystin's ability to inhibit global ubiquitin-mediated degradation, a whole multitude of ubiquitin-targeted proteins may have been affected, which potentially could directly or indirectly modulate both proteins' subcellular localisation.

X-ray

X-ray-irradiation of all four cell lines caused little overall effect on MDM2 or p53 subcellular localisation. However, p53 and MDM2 detection did slightly increase in OSA, M(5) and U2OS cells. Such increased expression was also seen in these three cell lines by Western

analysis, as a result of a combination of increased transcription and/or translation of both MDM2 and p53 (see Chapter Two).

Both p53's cytoplasmic and nuclear-pod staining was increased in OSA, M(5) and U2OS cells, suggesting that a balance between both subcellular locations may be necessary for mediating the X-ray-mediated cell cycle arrest. p53's role as nuclear transcription factor and cytoplasmic regulator of its own translation may account for its dichotomous localisation. No gross alterations in MDM2 levels or subcellular location were observed in cells 30 minutes post X-ray irradiation; a time point corresponding to the X-ray-mediated reduction in MDM2 protein levels seen by Western analysis (see Chapter Two). However, accurate quantitative immunofluorescence was not carried out. An alternative view to the lack of reduced MDM2 staining concerns the MDM2 epitope remaining detectable in the cell, perhaps as part of a cleavage product, rather than being completely degraded (see below).

UV

IF analysis of UV-irradiated OSA, U2OS and M(5) cells generally lead to reduced detection of MDM2 and increased p53 detection, while only the MDM2 level was significantly reduced in DN(5) cells. Western analysis of UV-irradiated cells revealed clear induction of p53, except in DN(5) cells which showed no clear induction. MDM2 levels, however, exhibited a drastic reduction at 24 hours post-UV-irradiation, except in OSA cells which after an initial dip recovered above control levels (see Figure 2.29). Therefore, with the exception of OSA cells, MDM2 levels were expected to be severely reduced upon IF analysis. Surprisingly, all the cell lines post-UV-irradiation demonstrated easily detectable MDM2 signals. Possible explanations were perhaps due to the maintenance of the three MDM2 epitopes (2A10, N-20 and SMP14) within MDM2 cleavage products or sub-90kDa MDM2 splice variants (see Introduction). Reductions in the 90kDa MDM2 level occurred in apoptotic cells via caspase-mediated cleavage(Chen, Marechal et al. 1997). This report supported the idea of the persistence of antibody epitopes, as all three antibodies epitopes used in this study are present in the major caspase-mediated MDM2 cleavage product (see Figure 1.2).

In addition to the general reduction in MDM2 detection, its staining pattern was also altered in response to UV-irradiation. OSA, M(5) and U2OS cells all exhibited the formation of novel sub-nuclear structures, similar to those formed by lactacystin treatment (see above). UV-irradiation of DN(5) cells, as with lactacystin treatment, caused the formation of more discrete sub-nuclear MDM2 speckles, similar to those observed in non-treated control OSA, M(5) and U2OS cells. In the case of UV-irradiated cells, the emergence of discrete nuclear bodies may be due to a general reduction of MDM2 levels, unmasking stronger staining, pre-existing structures. However, with the Western evidence of reduced full length MDM2 expression (see Chapter Two), it remained more likely that the nuclear bodies were formed from UV-mediated MDM2 cleavage products or alternative splice variants (see above). An alternative explanation could lie in post-translational modifications masking the MDM2 antibodies epitopes upon Western analysis. Nevertheless, UV-mediated induction of novel structures in the cell lines cannot be ruled out, although aggregation of nuclear speckles may also explain the emergence of the larger structures.

UV-irradiated OSA cells, as with lactacystin-treatment, yielded the most dramatic alterations in the MDM2 staining pattern. Approximately one to five discrete, intensely staining sub-nuclear structures were apparent following UV-irradiation and were, in some instances, clearly located within the centre of low DAPI-staining, nucleoli-like 'holes'. These results further support the possibility of nucleolar-localised MDM2, consistent with observations seen with lactacystin treatment (see above) and ARF-mediated nucleolar sequestration(Weber, Taylor et al. 1999), but in this case in response to UV-irradiation.

Analysis of p53 in OSA, M(5) and U2OS cells revealed increased cytoplasmic detection, with polarised cytoplasmic p53 expression evident in M(5) and U2OS cells. These results suggested that the UV-mediated induction of both p53 in sub-nuclear pods and the cytoplasm, may have potentially mediated UV-specific processes. Increases in both cellular locations again mirrored the increase seen upon lactacystin treatment. However, the cytoplasmic accumulation may have simply reflected an accumulation of *de novo* translated p53 in the process of being transferred to the nucleus. Nevertheless, the similarity between the UV- and lactacystin-treated immunofluorescence results provides evidence for the utilisation of similar pathways of p53 and MDM2 subcellular reorganisation. Similar discussion points made for lactacystin results can be made concerning the formation and

detection of these structures and the control of nuclear:cytoplasmic shuttling (see above). However, DN(5) p53 $175^{R\Rightarrow H}$'s behaviour in response to the two treatments was not identical, with a lack of nuclear to cytoplasmic shift upon UV-irradiation. These observations suggested that either the cellular response to the two treatments utilised different mechanisms or that p53 $175^{R\Rightarrow H}$ was defective in the UV-response. Perhaps, such a defect could explain DN(5)'s delayed UV-mediated apoptotic response.

Analysis of the ubiquitination status of p53 following (10 Gy) γ- and ($20Jm^{-2}$) UV-irradiation in U2OS cells revealed that γ-irradiation enhanced(Maki, Huibregtse et al. 1996; Maki and Howley 1997), while UV-irradiation decreased p53 ubiquitination(Maki and Howley 1997). Therefore, differential ubiquitination of p53, and possibly MDM2, in a non-degradatory role (see Introduction) may have explained the differential irradiation-mediated subcellular localisations of these proteins.

In addition to ubiquitination, p53 also undergoes post-translational modification by a small ubiquitin-like protein SUMO-1(Boddy, Howe et al. 1996), pre- and post-UV-irradiation(Gostissa, Hengstermann et al. 1999; Rodriguez, Desterro et al. 1999). Sumoylation enhanced p53's transcriptional activity, activating a p21-reporter plasmid pre-UV-irradiation in 293 cells(Gostissa, Hengstermann et al. 1999) and an artificial p53-responsive reporter post-UV-irradiation (25 Jm^{-2}) in U2OS cells(Rodriguez, Desterro et al. 1999). However, no transcriptional activation (measured through increases in protein levels) of p21 or MDM2 was seen in (30 Jm^{-2}) UV-irradiated U2OS cells (see Chapter Two). In addition to SUMO-1's ability to activate p53's transcriptional activity, the modification can protect proteins from ubiquitin-dependent degradation through direct competition with ubiquitin for covalent attachment with lysine residues(Desterro, Rodriguez et al. 1998). However, this was not shown to be true for p53(Rodriguez, Desterro et al. 1999). Alternatively, sumolylation may also affect the subcellular localisation of proteins and could explain the UV-mediated effects on p53's subcellular distribution.

Post-translational modifications mediated by UV-irradiation, such as ubiquitination, sumoylation, phosphorylation and acetylation (as well as their opposing actions), may effect p53's oligomeric state, conformation and activity of p53. Such modifications may therefore

regulate nuclear import and export of p53 through MDM2-interaction or it's intrinsic NES (see Introduction), as well as its subnuclear localisation. Similar post-translational modifications are also applicable to MDM2, adding further complexity to MDM2-mediated nucleoplasmic shuttling of p53.

The observed cytoplasmic accumulation of p53 in response to UV-irradiation supports the idea of p53 transcriptionally-independent apoptosis and perhaps supports an active role for p53 in the cytoplasm. Such a role could concern translational repression of specific mRNAs, as is seen in p53's autoinhibition of translation(Fu, Ma et al. 1999). However, the presence of the p53 sub-nuclear pods maintained the possibility for p53-mediated nuclear transcription of target genes.

In light of the observed UV-mediated reduction in MDM2 protein levels, it was unlikely that full-length MDM2 was responsible for mediating the nuclear export of p53 into the cytoplasm. p53-binding MDM2 alternative splice variant (e) MDM2 and cleavage products (see Figure 1.2) may have provided a IF signal. However, although MDM2 (e) is the only splice form capable of binding p53, it lacks the NES and IF antibody epitopes. Therefore, a caspase cleavage product (retaining both the p53 binding domain and NES)(Chen, Marechal et al. 1997; Pochampally, Fodera et al. 1998; Pochampally, Fodera et al. 1999), remains the likely candidate. Additionally, other protein-protein interactions may influence p53 subcellular localisation (see Introduction).

Alterations in a protein's subcellular localisation can be influenced by active or passive measures. For example, inhibition of a nuclear mechanism could result in cytoplasmic localisation, while active nuclear export could achieve the same result and *vice versa*.

IP analysis had revealed increased p53:MDM2 association following lactacystin, X-ray and UV-irradiation treatment. Generally, immunofluorescence analysis revealed that MDM2 maintained a nuclear subcellular localisation upon various treatments, while p53 showed a strong increase in cytoplasmic induction in response to lactacystin and UV-irradiation. Therefore, no clear mutual overlap between their subcellular localisations were apparent, although both proteins did show clear nuclear/sub nuclear localisation. In the case of lactacystin and UV-irradiation, concentration of MDM2 and p53 in sub-nuclear regions,

whose formations was perhaps mediated through increased association, may have also facilitated increased protein-protein interaction. However, direct co-localisation studies of p53 and MDM2 were not carried out. An alternative idea concerns UV-mediated selective loss of non-p53-complexed MDM2, thereby concentrating p53:MDM2 complexes.

The function of the p53 and MDM2 sub-nuclear structures formed upon UV-irradiation can either be attributed to an active or passive pro-apoptotic effect. For example, p53 and MDM2 (independently or complexed) may be required to suppress transcription or translation of anti-apoptotic genes at specific locations, as both proteins have transcriptional and RNA binding abilities (see Introduction). In contrast, a more passive role in the formation of sub-nuclear structures may be concerned with simple subcellular compartmentalisation, sequestering the proteins away from anti-apoptotic macromolecular components. In comparison with the X-ray-irradiated cells, only the formation of MDM2 sub-nuclear structures were specific to UV-irradiation and hence apoptosis, supporting either a causal or consequential role. The apparently delayed formation of these MDM2 structures in DN(5) cells may have been linked to it's delayed UV-mediated apoptotic response.

UV-irradiated MDM2 co-localisation with PML bodies

MDM2's nuclear staining pattern observed in UV-irradiated cells was similar to the nuclear staining pattern of PML bodies(Dyck, Maul et al. 1994). Immunofluorescence analysis of PML bodies pre- and post-UV-irradiation in four cell lines, revealed no major alterations in expression patterns. Dual PML/MDM2 immunofluorescence co-localisation studies revealed a significant overlap of MDM2 and PML signals post- UV-irradiation in M(5) cells. Confocal analysis of the PML bodies and 'speckled' MDM2 structures revealed partial co-localisation in control cells, although the excess general MDM2 staining did not. After UV-irradiation the general MDM2 staining seemed to be reduced and the MDM2 speckles remained co-localised with PML. Taken with the observed UV-mediated increase in MDM2 sub-nuclear structure size, these results suggested that the larger UV-induced MDM2 containing bodies were simply enlarged versions of the un-irradiated MDM2 'speckles'. Interestingly, leptomycin B-treatment of human foreskin fibroblasts caused the formation of p53 and

MDM2 containing foci that colocalised with each other and were juxtaposed with Sp-100-containing 'nuclear speckles' and PML bodies(Lain, Midgley et al. 1999).

The protein PML has been found concentrated in many small round nuclear domains, called PML bodies, ND10, or PODs(Dyck, Maul et al. 1994) and occur in higher numbers, usually 10-30 per nucleus, in virtually every cell type. They are enriched in several proteins, including sp100(Szostecki, Krippner et al. 1987), PIC1 or SUMO-1(Boddy, Howe et al. 1996) and Int-6(Stuurman, de Graaf et al. 1992), which can be continuously released and incorporated from these domains(Stuurman, Floore et al. 1997). PML bodies are also found associated with other nuclear domains(Gongora, David et al. 1997) and can suppress cell growth and suppress oncogenic transformation by co-operating oncogenes(Mu, Chin et al. 1994; Mu, Le et al. 1996). Therefore, PML bodies may be associated with sub-nuclear structures and/or genes that need to be carefully regulated or suppressed, such as regions controlling/containing oncogenes and viral genes(Carvalho, Seeler et al. 1995; Lavau, Marchio et al. 1995).

MDM2's association with PML bodies may be mediated through RING finger protein-protein interactions(Sadoul, Fernandez et al. 1996) between the two proteins' RING finger motifs. Interestingly, such a RING:RING-mediated protein-protein interaction has been demonstrated with MDM2 and MDMX association(Tanimura, Ohtsuka et al. 1999) and stabilises MDM2(Sharp, Kratowicz et al. 1999). Therefore, a RING-RING protein interaction with PML in PML bodies may stabilise MDM2 and explain the perseverance of MDM2 staining post UV-irradiation. Another method of PML-body targeting of MDM2 involves possible post-translational modification with SUMO-1, which targets PML (Boddy, Howe et al. 1996; Duprez, Saurin et al. 1999) and Sp100(Sterndorf, Jensen et al. 1997) proteins to such bodies.

The function of the PML bodes remains unclear, although MDM2 association with these structures may represent 'sink holes' drawing MDM2 from the general nucleoplasm. Sub-nuclear targeting of MDM2 may facilitate its destruction, sequestration, degradation of target proteins (as a ubiquitin-protein ligase, E3) or in transcriptional control of genes (utilising it's transcriptional silencing domain or acidic domain), ultimately in a pro-apoptotic manner. The actual act of sumoylation may protect MDM2 from ubiquitin-mediated degradation, either

through competitive binding for lysine residues with ubiquitin or sequestration from caspases and other degradative systems. Therefore explaining the persistence of MDM2 in such SUMO-1-containing structures.

NARF

ARF IF analysis of OSA, U2OS, M(5) and DN(5) cells, using both methanol:acetone and paraformaldeyde fixation, failed to reveal any specific staining pattern above background levels, suggesting that the combination of the antibody's (IP-1) binding affinity, immunofluorescence conditions and low ARF expression were unfavourable for detection. However, IPTG-treated, but not untreated NARF(6) cells, revealed nucleolar localisation of ARF upon induction. Due to the inability to detect any specific ARF staining pattern in control, untreated NARF(6) cells, it was impossible to determine whether the *de novo* ARF formed novel nucleolar structures or simply facilitated detection of pre-existing structures. Nevertheless, ARF's two potential nuclear and/or nucleolar localisation signals may explain its subcellular localisation(Zhang and Xiong 1999).

Subcellular localisation of ARF was originally reported to localise to nuclear speckles(Quelle, Zindy et al. 1995), although upon further analysis were identified as nucleoli(Pomerantz, Schreiber-Agus et al. 1998). Nucleolar localisation of exogenously expressed ARF was observed in a variety of cell lines with varying p53, MDM-2 and ARF status(Pomerantz, Schreiber-Agus et al. 1998; Stott, Bates et al. 1998; Tao and Levine 1999; Weber, Taylor et al. 1999; Zhang and Xiong 1999). *p53/mdm2*-null and *ARF*-null MEFs exhibited nucleolar staining upon exogenous ARF expression, suggesting that sub-nuclear localisation of ARF did not depend on the presence of endogenous ARF, p53 or MDM2 proteins(Weber, Taylor et al. 1999).

Immunofluorescence analysis of MDM2 and p53 in IPTG-induced NARF(6) cells failed to reveal any gross alterations in subcellular localisation of either protein, although detection of both proteins was increased. These results conflicted with the observations that ARF-overexpression caused either MDM2-nucleolar localisation(Tao and Levine 1999; Weber, Taylor et al. 1999) or ARF:p53:MDM2 sub-nuclear complex formation(Zhang and Xiong

1999). However, the majority of these studies utilised ectopic transient-overexpression of ARF and MDM2, therefore expressing massive levels of both proteins. In contrast, the IPTG-induced NARF(6) cells produced only moderate increases in MDM2, p53 and ARF levels, perhaps explaining why similar observation were not made. A problem of gross protein overexpression concerns the potential formation of abnormal structures, due to overloading 'bottleneck' points in protein distribution pathways, or simple protein precipitation, however it can also facilitate 'normal' protein subcellular visualisation.

The range of MDM2- and p53-subnuclear bodies reflects both the diversity of the proteins' nuclear roles and functions of subnuclear structures. The functional organisation or architecture of the nucleus is based on the dynamic interplay of nucleic acids and protein components. Therefore, the view of the nucleus as being an unstructured subcellular compartment is beginning to change through numerous observations of specific subcellular localisation of proteins.

Interdependency of three major nuclear processes, methylation, replication and transcription, have been demonstrated with genomic and nuclear architecture. Transcribed genes, in contrast to inactive genes, are preferentially associated with subnuclear compartments enriched in splicing factors (speckled compartments) and transcription and splicing of these genes occur at the border of these speckles(Xing, Johnson et al. 1995). Also, highly methylated chromatin, such as centromeric chromatin, replicates late in S phase(Leonhardt, Page et al. 1992). These major metabolic processes occurring in the nucleus, though not separated by membranes, are organised into discrete subnuclear domains attached to an underlying nuclear matrix, providing active sites for enzymatic and nucleic acid functions.

Of the various different nuclear domains that have been identified, the most prominent and well characterised is the nucleolus. The nucleolus itself shows different compartments: fibrillar, dense fibrillar and granular centres. Each has its own morphology and protein composition(Scheer and Benavente 1990) and function(Scheer, Thiry et al. 1993). Ribosomal RNA genes on different chromosomes are grouped together in the nucleolus to facilitate the expression and maturation of the rRNA. Several nuclear domains have been reported to be closely associated with the nucleolus: the perinuclear compartment (PNC),

the hnRNP L domain, the OPT domain and coiled bodies (reviewed(Schul, de Jong et al. 1998)). However, the function of these sub-nuclear domains remains unclear.

Therefore, proteins and RNAs are not only concentrated in domains in the nucleus, but these domains are also organised relative to each other. The spatial association between nuclear domains can be temporary and dynamic and reflects the state of the cell(Huang, Deerinck et al. 1997; Misteli, Caceres et al. 1997). In addition, the nuclear domains can be associated with specific genes, probably to facilitate or regulate the production and maturation of RNA. The spatial and functional organisation of different domains and specific genomic loci in higher-order structures as found in the nucleolus is a probably a common organisational principle for controlled and efficient gene expression in the cell nucleus.

Chapter Five

General Discussion

A central dogma has arisen within p53 biology, based firmly in the observation of post-transcriptional induction of p53 upon cellular stress. Discovery of the p53-responsive gene, *mdm2* and its ability to negatively regulate both p53-dependent transcription and protein levels revealed a likely candidate for post-transcriptional stress-mediated inhibition. MDM2's mode of action is mediated through its protein-protein interaction with p53, masking p53's transcriptional transactivation domain and facilitating p53 ubiquitination and subsequent degradation. Therefore, the abolishment of the p53:MDM2 interaction was proposed as a mechanism of stress-mediated p53 stabilisation and transcriptional activation.

One paradox exists where p53 actually upregulates its own negative regulator in response to a variety of stress-stimuli. This negative feedback loop can be explained through controlled temporal expression and/or negative regulation of the p53:MDM2 interaction throughout the response, allowing p53 accumulation and activity. However, no convincing universal evidence has been provided to support any of these theories.

Identification of a number of sarcomas exhibiting elevated *mdm2* copy number as well as elevated mRNA and protein levels, which also harboured wild-type *p53* genes, supported the idea that such a situation could create a p53-compromised cell. Over the last few years intensive research has concentrated on potential regulatory mechanisms governing p53:MDM2 protein-protein interaction, with the intention of generating potential therapeutic agents. Application of an MDM2:p53 'dissociating' agent would allow activation of p53 in cells overexpressing MDM2 or cells defective in upstream p53-activational pathways; ultimately resulting in apoptosis or cell cycle arrest.

Phosphorylation of both p53 and MDM2 initially provided a promising regulatory mechanism, controlling the interaction between the two proteins. However, controversy remains over its true relevance.

The importance of MDM2 as an *in vivo* cellular regulator of p53 level and activity was elegantly demonstrated using a p53-derived MDM2-binding competing peptide(Bottger, Bottger et al. 1997). A 12 amino-acid peptide derived from a MDM2-binding phage display insert was shown to bind and occupy the p53-binding pocket of MDM2. Expression of the peptide *in vivo* efficiently competed with native p53 for binding to MDM2, increased p53-dependent activation of reporter constructs, elevated p53 protein levels and lead to a reduction in S-phase. Independent analysis with a similar MDM2 competing peptide or antibody revealed activation of p53 levels(Midgley and Lane 1997) and activity(Blaydes, Gire et al. 1997), culminating in apoptosis(Wasylyk, Salvi et al. 1999). These experiments also clearly demonstrated that additional post-translational modifications of p53 were not needed to increase p53's protein levels and activity and to mediate a cell cycle arrest or apoptosis(Bottger, Bottger et al. 1997).

It is possible that the normal p53 response to genotoxic damage and other stress signals are mediated by inhibition of the p53:MDM2 interaction, perhaps by competitive inhibition. The experiment cited above clearly support this theory, as treatment with MDM2-competing peptides replicated the p53 effects and subsequent cellular outcomes seen with many DNA damaging agents. If this is the case, the target for p53 activation is purely the dissociation or the prevention of formation of the MDM2:p53 complex, rather than other p53 'activating events'. Nevertheless, 'activating' events may modulate the degree, or specificity of activation. Whether such a mechanism actually occurs in response to cellular stress-events remains to be seen.

Overall, the MDM2:p53 relationship has revealed itself to be an important regulatory component of the p53 response. Potential regulatory pathways and mechanisms are only beginning to be exposed and concern virtually every conceivable regulatory mode of gene expression available to the cell.

The main aim of this study was to investigate the molecular decisions governing the choice between irradiation-mediated apoptosis and cell cycle arrest in the U2OS cell line. The effects of MDM2 and mutant p53 $175^{R \Rightarrow H}$ overexpression were also examined through the creation of isogenic U2OS cell lines and analysis of OSA cells, which endogenously

overexpress MDM2. A p53-centric view was taken, with specific interest in the MDM2:p53 relationship and the effects of MDM2 overexpression on p53's activity. Hence, partially addressing the p53:MDM2 dogma mentioned above. Five techniques were used in an attempt to construct a complimentary picture of apoptotic and cell cycle arresting cells, consisting of FACS, Western, Northern, immunoprecipitation and immunofluorescence analysis.

The effects of four different treatments on various cell lines are discussed below:

UV

30 Jm^{-2} UV(C)-irradiation of U2OS cells revealed a partial p53-dependent apoptotic cellular response. Analysis of a variety of cell lines showed an apoptotic response even in the presence of mutant p53, while the U393 and MG-63 cell lines showed no signs of apoptosis. These findings demonstrated that the same dose and dose rate could generate differential cellular responses in different cell types, supporting the idea of cell-specific- and p53-independent-apoptosis in response to irradiation. Nevertheless, delayed apoptosis was evident in U2OS cell lines overexpressing MDM2 (M[5]) and p53 $175^{R\Rightarrow H}$ (DN[5]) in comparison to parental U2OS cells. Such anti-apoptotic action was consistent with their p53 inhibitory actions, although both proteins failed to reverse the UV-mediated apoptotic response.

Western analysis of UV-irradiated cells revealed loss of MDM2 and p21 protein expression and concomitant induction of p53 and E2F-1. Northern analysis revealed the UV-mediated loss of MDM2 to be partially attributed to loss of *mdm2* mRNA, while *p21* mRNA levels were unaffected. A potential UV-mediated p21-protein degradation event was revealed, with lactacystin protecting p21 from UV-mediated reductions in protein levels. MDM2-overexpressing U2OS M(5) cells demonstrated a slightly delayed p53 induction in comparison to vector-only, p3 U2OS cells. Furthermore, M(5) cells exhibited greater persistence of MDM2 expression post-UV-irradiation which most probably reflected the higher exogenous-derived steady-state MDM2 levels in comparison to vector-only U2OS cells. The combination of MDM2's persistent expression and reduced p53 induction seen in

M(5) cells could have explained their delayed UV-mediated apoptotic response. However, a similar explanation could not be applied to DN(5) cells, which exhibited very low levels of MDM2 expression, suggesting that apoptosis may be regulated at multiple levels. E2F-1 induction in all of the cells analysed suggested that the induction was independent of p53 and supportive of E2F-1's pro-apoptotic role. UV-mediated phosphorylation of p53 Ser^{15} was most evident in the DN(5) cells lines, but detectable in all of the other cell lines examined, demonstrating that both mutant p53 $175^{R\Rightarrow H}$ and wild-type p53 were capable of being phosphorylated.

Immunoprecipitation analysis surprisingly revealed increased p53:MDM2 complexes post-UV-irradiation, in spite of the decreasing MDM2 levels seen by western analysis in all of the cell lines analysed. However, determination of the relative increases of MDM2-associated and free p53 was not possible. An exception to this observation was in the DN(5) cell line which actually decreased p53:MDM2 complex formation, revealing a major difference between wild-type and mutant $175^{R\Rightarrow H}$ p53 forms. The observation of UV-mediated induction of p53 Ser^{15} phosphorylation in all of the cell lines, failed to totally agree with the reports of its negative regulatory role of the p53:MDM2 interaction.

Immunofluorescence analysis of UV-irradiated cells revealed a striking alteration in MDM2's subcellular localisation. Relatively large and well defined subnuclear structures, or 'pods', formed in all of the cell lines analysed, except DN(5) cells, which showed more general 'speckled' nuclear staining. Furthermore, OSA cells exhibited potential nucleolar-associated MDM2 'pods'. Confocal analysis of M(5) cells revealed that MDM2 co-localised with PML-bodies, pre- and post-UV-irradiation, but preferentially concentrated with PML post-irradiation. Increased cytoplasmic p53 localisation was revealed in all of the cell lines examined except DN(5) cells, which showed predominately nuclear localisation. Therefore, DN(5) cells exhibited differential subcellular localisation of both MDM2 and p53 following UV-irradiation.

The effects of UV-irradiation on the different cell lines are summarised in Table 5.1.

Table 5. 1. Summary of UV-irradiation effects.

	Cell lines examined post-30Jm^{-2}-UV-irradiation			
UV-mediated effect on:	U2OS	DN(5)*	M(5)§	OSA
p53 levels and subcellular localisation	Increases. Sub-nuclear bodies and cytoplasmic	No effect. Nuclear.	Increases. Sub nuclear bodies and cytoplasmic	Increases. Sub nuclear bodies and cytoplasmic
MDM2 levels and subcellular localisation	Decreases. Discrete sub-nuclear pods.	Decreases. 'Speckled' general nuclear.	Attenuated decrease. Discrete sub-nuclear pods (PML-associated)	Decrease and Increase. Discrete sub-nuclear pods (nucleolar-associated)
E2F-1 levels	Increase.	Increase.	Increase.	Increase.
p21 levels	Decreased	Decreased	Decreased	Decreased
p53:MDM2 Complexes	Increases.	Decreases.	Increases	Increases
Cellular response	Apoptosis	Delayed apoptosis	Delayed apoptosis	Apoptosis
*** Expressing p53 175$^{R\Rightarrow H}$**				
§Expressing both endogenous and exogenous MDM2				

X-ray

12 Gy X-ray-irradiation of U2OS cells revealed a transient G_1/S and G_2/M cell cycle arrest. The growth arrest was shown to be p53-dependent, with both M(5) and DN(5) cell lines showing an abrogated G_1/S arrest. However, the G_2/M arrest was still apparent in both of these cell lines. The same X-ray-irradiation dose and dose rate caused apoptosis in some of

the other cell lines analysed (HOS, MG63 and U393), again supporting the idea that the cellular response to irradiation is cell type specific.

Western analysis revealed an X-ray-mediated increase in p53, MDM2 and p21 levels. Early analysis of a variety X-ray irradiated cell lines revealed a transient reduction in MDM2 levels, which was not a result of reduced *mdm2* mRNA levels. Its occurrence in M(5) (pCMV-driven *mdm2* expressing) and DN(5) (mutant p53 $175^{R \Rightarrow H}$-expressing) cell lines suggested that the reduction was not effected through specific transcriptional control and was p53-independent, respectively. Furthermore, lactacystin and cycloheximide analysis supported a post-translational degradation event as the mechanism for the X-ray-mediated reduction. Additionally, cycloheximide treatment abrogated the X-ray-mediated p53 induction, suggesting that translational upregulation was responsible for the increased p53 protein levels.

Immunoprecipitation analysis revealed increased or no loss of p53:MDM2 complex levels post-X-ray-irradiation in all of the cell lines examined, except OSA cells, which showed an initial reduction followed by a recovery. Immunofluorescence analysis failed to reveal any significant alterations in the subcellular localisation of either p53 or MDM2.

The effects of X-ray-irradiation on the different cell lines are summarised in Table 5.2.

Table 5. 2. Summary of X-ray-irradiation effects.

	Cell lines examined post-12 (Gy)-irradiation			
X-ray-mediated effect on:	U2OS	DN(5)*	M(5)§	OSA
p53 levels and subcellular localisation	Increases. Nuclear pods and some cytoplasmic.	No effect. Nuclear.	Attenuated increase. Nuclear pods and some cytoplasmic.	Increases. Nuclear pods and some cytoplasmic.
MDM2 levels and subcellular localisation	Initial dip then increases. Speckled nuclear.	Initial dip then increases. General nuclear.	Initial dip then attenuated increase. Speckled nuclear.	Initial dip then increases. Speckled nuclear.
E2F-1 levels	Transient Increase 8 hrs post-X-ray	Transient Increase 8 hrs post-X-ray	Transient Increase 8 hrs post-X-ray	Transient Increase 8 hrs post-X-ray
p21 levels	Increases	Slight increase	Increases	Increases
p53:MDM2 Complexes	Increase after initial loss.	Slight increase after initial loss.	Increase after initial loss.	Initial loss followed by recovery.
Cellular response	G_1/S and G_2/S arrest.	Attenuated G_1/S and maintained G_2/M arrests	Attenuated G_1/S and maintained G_2/M arrests	G_1/S and G_2/S arrest.
*** Expressing p53 $175^{R \Rightarrow H}$**				
§Expressing both endogenous and exogenous MDM2				

Lactacystin

Lactacystin treatment of all the cell lines analysed increased MDM2, p53 and p21 levels, except in DN(5) cells which exhibited only slightly elevated p21 levels. The failure of mutant p53-containing DN(5) cells, but not wild-type p53 cells, to elevate MDM2 levels suggested that the induction was mediated through p53-dependent transcriptional upregulation of the *mdm2* gene. Therefore, suggesting that MDM2 was not a direct target for ubiquitin-dependent degradation.

Immunoprecipitation analysis of lactacystin treated cells revealed greatly increased p53:MDM2 complexes in all of the cell lines examined, except DN(5) cells which showed only a small increase. Therefore, lactacystin-mediated inhibition of the proteosome lead to increased p53 protein levels and p53:MDM2 complex levels, mimicking the results obtained seen in X-ray- and UV-irradiated cells. These results clearly suggested that increases in p53 can accompany increased p53:MDM2 complex formation.

Lactacystin-treated cell lines exhibited a drastic increase in cytoplasmic p53 and in the case of DN(5) cells, clearly at the expense of nuclear p53. Although, sub-nuclear p53 pods were also evident in all of the cell lines. A certain degree of polarised p53 cytoplasmic staining was also apparent. The radical shift in p53 subcellular localisation suggested that p53's nuclear:cytoplasmic shuttling pathway was interfered with. Analysis of lactacystin-treated cells showed the formation of large, novel MDM2 sub-nuclear structures showing potential nucleolar localisation (especially clear in OSA cells). Overall, lactacystin caused drastic alterations in the immunofluorescence-staining pattern of both p53 and MDM2, highlighting the importance of ubiquitin-dependent degradation in the maintenance of these proteins' subcellular localisation. However, lactacystin-mediated global inhibition of proteosome-dependent function would have affected many proteins. Therefore, no specific inferences can be made towards the individual role of increased p53 or MDM2 ubiquitination.

The effects of lactacystin-treatment on the different cell lines are summarised in Table 5.3.

Table 5. 3. Summary of lactacystin effects.

	Cell lines treated with Lactacystin			
Lactacystin-mediated effect on:	U2OS	DN(5)*	M(5)§	OSA
p53 levels and subcellular localisation	Increases. Nuclear pods and strong cytoplasmic.	Slight increase. Reduced nuclear and strong cytoplasmic .	Increases. Nuclear pods and strong cytoplasmic.	Increases. Nuclear pods and strong cytoplasmic.
MDM2 levels and subcellular localisation	Increase. Discrete sub-nuclear bodies.	No effect. Speckled nuclear.	Increase. Discrete sub-nuclear bodies.	Increase. Discrete sub-nuclear bodies (including nucleoli).
p21 levels	Increases	Slight increase.	Increases	Increases
p53:MDM2 Complexes	Increase.	Slight increase^.	Increase.	Increase.

* Expressing p53 $175^{R \Rightarrow H}$.

§Expressing both endogenous and exogenous MDM2.

^ Increase only detected with co-IPd MDM2.

ARF

Induction of ARF in IPTG-inducible U2OS (NARF[6]) cells revealed a G_1/S and G_2/M cell cycle arrest and increased p53, p21 and MDM2 protein levels. Therefore, the cellular and partial molecular response of ARF-induced NARF(6) cells mimicked the X-ray mediated effects on U2OS cells.

Immunoprecipitation analysis of IPTG-induced NARF(6) cells revealed increased p53 and MDM2 complexes, although ARF:MDM2 complexes could not be detected in reciprocal

MDM2 and ARF IPs. pRB: and E2F-1:MDM2-interactions were also examined, but IP analysis failed to detect any complex formation. However, differences in the use of IP buffers and antibodies to aid detection of protein-protein complexes, could explain the lack of visualisation.

Immunofluorescence analysis of IPTG-induced NARF(6) cells revealed no significant effects on p53 and MDM2 localisation, although ARF accumulated in nucleolar-like bodies. The lack of ARF-mediated re-localisation of MDM2 and p53 reported previously may simply reflect the lower expression levels of all three proteins, hence reducing the detectability.

The effects of ectopic ARF-expression are summarised in Table 5.4.

Table 5. 4. Summary of ARF effects.

ARF-mediated effect on:	IPTG-induced NARF(6) cells
p53 levels and subcellular localisation	Increase. Nuclear pods and cytoplasmic.
MDM2 levels and subcellular localisation	Increase. Speckled nuclear.
p21 levels	Increase.
p53:MDM2 Complexes	Increase.
Cellular response	G_1/S and G_2/M arrest.

Overall

U2OS cells are capable of undergoing both a transient cell cycle arrest and apoptosis in response to X-ray- and UV-irradiation, respectively(Allan and Fried 1999). Both of these partially p53-dependent processes were examined in U2OS and other cell lines by FACS, Western, Northern, immunoprecipitation and immunofluorescence analysis. Examination of UV and X-ray-irradiated cells revealed a number of irradiation- and cellular-specific responses that may have actively contributed to the specific cellular outcome, or may have merely been consequential.

Examination of four major protein components of the cellular growth regulatory pathways revealed a partial protein file for the apoptotic and cell cycle arrested cells examined. ARF expression and X-ray- and UV-irradiation lead to the accumulation of wild-type p53 protein, supporting a role for this protein in oncogene- and genotoxic-mediated cell cycle arrest and apoptosis. Furthermore, attenuated/delayed UV-mediated apoptotic and X-ray-mediated cell cycle arrest responses were apparent in p53 $175^{R \Rightarrow H}$ and MDM2 overexpressing U2OS cells. However, these cells eventually succumbed to UV-mediated apoptosis, suggesting the presence of slower acting p53-independent apoptotic pathways.

In addition to p53 itself, the p53-responsive gene products p21 and MDM2 were differentially regulated in cell cycle arresting or apoptotic cells. In wild-type p53-expressing U2OS cells, both proteins' expression levels increased in response to X-ray irradiation and ARF-expression, but decreased in response to UV-irradiation. These results suggested that p21, and perhaps MDM2, may have been required for cell cycle arrest, but actively reduced to facilitate apoptosis. Furthermore, in comparison with parental cells, MDM2-overexpressing U2OS cells showed attenuated UV-mediated apoptosis with concomitant persistence of MDM2 expression and reduced X-ray-mediated G_1/S arrest with reduced p21 induction.

The anti-UV-mediated-apoptotic effect of p21 in U2OS cells was clearly demonstrated with enforced expression of inducible p21. However, p53 $175^{R \Rightarrow H}$ expressing U2OS cells showed attenuated UV-mediated apoptosis without showing upregulation or persistence of p21 or MDM2 expression, stressing the existence of multiple apoptotic steps accessible to regulatory control.

Cellular regulation of protein activity and function is basically controlled via chronic and acute regulatory mechanisms:

Chronic, quantitative changes in protein levels, especially in the most extreme sense of the presence or absence of a protein, can affect its ability to carry out its role in a cell. Alteration in protein levels can be thought of being a balance between protein production and degradation. Indeed, regulation of both protein synthesis and degradation occurs at multiple levels. Transcriptional and translational control govern the rate of protein production in a

'normal' eukaryotic cellular environment, although alterations in gene dose and copy number are apparent in some developmental situations and disease states. Opposing the rate of protein production are independent degradation mechanisms, including caspase- and proteosome-mediated degradation events, which can determine the half-life of a protein, effectively removing it from the cellular environment.

Acute, qualitative changes in protein function can mostly be viewed as activational or inhibitory events, rapidly modulating or enhancing protein activity; thus regulating functional activity temporally and spatially. Four basic models of acute regulatory mechanisms exist: allosteric; reversible covalent-modification of proteins; stimulation and inhibition by control proteins, including co-factors; and irreversible proteolytic alteration of proteins, such as pro-enzyme activation.

Overall, chronic regulatory systems governing the basic mechanisms of production and removal are in are turn determined by molecular events, initially instigated by acute mechanisms of regulation. Therefore, the two modes of control can be intimately linked, being both causal and consequential, generating elaborate feedback mechanism.

Irradiation-mediated reductions in both p21 and MDM2 proteins revealed potential transcriptional and post-translational regulatory control mechanisms. An early X-ray-mediated transient reduction in MDM2 protein levels was detected in a number of wild-type and mutant-p53 cell lines, suggesting a p53-independent event. Such a reduction in MDM2 levels may have facilitated a transient reduction in MDM2-mediated inhibition of p53 activity, allowing initiation of p53-dependent cell cycle arrest. The X-ray mediated effect on MDM2 was independent of reductions in *mdm2* mRNA; co-operating with cycloheximide-mediated MDM2 reduction and partially abrogated through lactacystin-treatment. Such a reduction in MDM2 levels may have facilitated a transient reduction in MDM2-mediated inhibition of p53 activity, allowing initiation of p53-dependent cell cycle arrest. Similar observations were also made with UV-mediated loss of p21 expression, supporting a role for post-translational control mechanisms, with the likely candidates being caspase- or ubiquitin-mediated degradation.

Both X-ray-irradiation and ARF-overexpression lead to the increase of both p53 and MDM2, demonstrating concomitant increase in p53 and its negative regulator, MDM2. These results suggested that a regulatory mechanism was inhibiting MDM2-mediated degradation of p53, although a net increase in production of p53 could also have explained its accumulation.

Of the known mechanisms governing MDM2 activity in relation to p53, two main control points exist, namely: regulation of the physical protein-protein interaction between MDM2 and p53 and MDM2-mediated ubiquitin-dependent degradation of p53, although a comprehensive picture is far from clear.

MDM2 has been branded the 'inhibitor' of the 'target' protein p53, due to its ability abrogate a number of well-established p53 functions. A simplistic view of controlling this relationship can be seen as either: inhibition of the inhibitor and protection of the target from the inhibitor; or the opposite, but interrelated method of activation of the inhibitor and increasing the susceptibility of the target to the inhibitor.

Due to the necessity of the p53:MDM2 protein-protein interaction in facilitating both MDM2-mediated transcriptional inactivation and degradation of p53, prevention of the association would clearly stabilise and potentially activate p53. Mechanisms for such abrogation can be envisioned, one through alteration of either protein, generating proteins incapable of interaction or a simple steric-hindrance competitive model, where a third macromolecule may bind to either protein at the expense of the other.

Immunoprecipitation analysis of ARF-overexpressing and irradiation- and lactacystin-treated wild-type p53-expressing cells generally revealed an increase in p53:MDM2 complex levels. These results suggested that ARF- and irradiation-mediated p53 accumulation was independent of dissociation of the p53:MDM2 complex, however accurate quantitation of un-complexed p53 and MDM2 levels were not determined. Therefore, the increased p53:MDM2 complex levels and concomitant p53 induction seen with ARF- and irradiation-treatment could be explained through inhibition of degradatory events downstream of the protein-protein association. Supporting such a theory, lactacystin-treatment, which directly inhibits proteosomal degradation, mimicked the X-ray- and ARF-mediated increases in p53 and MDM2 protein levels and p53:MDM2 complex levels. Overall, these results revealed an

exception to the simplistic idea of increasing MDM2 levels leading to decreased p53 levels; furthermore, the probable existence of alternative regulatory steps, downstream of p53:MDM2 association, involved in MDM2-mediated p53 degradation.

Alternatively, MDM2-mediated degradation of p53 may only be required for maintenance of basal p53 levels(Bottger, Bottger et al. 1997) or p53:MDM2 complex-dissociating and/or -preventative mechanisms may regulate non-genotoxic- or oncogene-mediated p53 responses. Nevertheless, upon cellular stress p53 may be upregulated through a combination of increased translation (as seen in the U2OS X-ray-irradiation response) and inhibition of p53 degradation.

Immunoprecipitation analysis revealed various p53 mutants to co-immunoprecipitate significant levels of MDM2 and exhibit elevated expression levels. Additionally, MDM2-overexpressing U2OS cells failed to exhibit any significant reduction in p53 levels, but demonstrated elevated levels of p53:MDM2 complexes in comparison to vector only and parental U2OS cells. These observations further enforced the idea that wild type and mutant p53 expression levels were not mediated through inhibition of MDM2:p53 association.

Wild type p53 is normally present in small quantities in most cells, displaying a rapid turnover rate that is in the order of minutes(Reich, Oren et al. 1983; Reihsaus, Kohler et al. 1990). The inductive response upon various stress signals is generally believed to be post-translational(Kastan, Onyekwere et al. 1991; Fritsche, Haessler et al. 1993) and somewhat cell-type dependent(Midgley, Owens et al. 1995). However, there are cell lines that exhibit constitutively high levels of apparently wild-type p53, including colon adenomas(Tominaga, Hamelin et al. 1993; Williams, Browne et al. 1993), the F9 teratocarcinoma line and cells transformed with DNA viruses(Zantema, Schrier et al. 1985; Reihsaus, Kohler et al. 1990). Therefore, mutation of the p53 gene is not necessary for protein accumulation, although the majority of cell lines expressing mutant proteins exhibit elevated levels of p53.

Initial experiments revealing MDM2 as a mediator of p53 ubiquitination and destruction(Haupt, Maya et al. 1997; Kubbutat, Jones et al. 1997; Midgley and Lane 1997), also demonstrated that both endogenous wild-type and tumour-derived mutant p53 could be degraded by exogenous expression of MDM2. Supporting work revealed a limited inverse

relationship between endogenous MDM2 inducibility and protein levels, and the wild-type or mutant status and protein levels of p53 levels(Kubbutat, Jones et al. 1997)(Haupt, Maya et al. 1997)(Midgley and Lane 1997). A model proposed that mutant p53s' inability to transcriptionally upregulate *mdm2*, would lead to low MDM2 levels, abrogating the MDM2:p53 autoregulatory feedback loop(Midgley and Lane 1997). Such an absence of MDM2 would therefore allow p53 levels to accumulate, through lack of MDM2-mediated degradation. However, cancer-derived transcriptionally-inactive p53 mutants, $143^{V\Rightarrow A}$, $248^{R\Rightarrow H}$ and $273^{R\Rightarrow H}$, varied in their susceptibility to MDM2-mediated ubiquitination. p53 $273^{R\Rightarrow H}$ showed lower levels of ubiquitination, which was not attributed to decreased MDM2 binding, suggesting that factors other than MDM2 binding can affect p53 ubiquitination(Maki 1999). Hence, the scenario of increased p53 stability could be achieved in addition to abrogation of p53's transcriptional function or MDM2 binding.

Establishment of wild-type, $p53^{Phe121}$ and $p53^{22Q,23S,121F}$ tetracycline-inducible H1299 cell lines revealed inconsistencies with the p53-MDM2 negative feedback model(Saller, Tom et al. 1999). $p53^{Phe121}$, defective in MDM2 induction, exhibited similar protein stability in comparison with MDM2-inducing, wild-type p53. Measurement of p53 stability revealed that wild-type p53 and $p53^{Phe121}$ were both as stable as the transcriptionally-dead, non-MDM2 binding $p53^{22Q,23S,121F}$ mutant. Thus, in contrast to overexpressed exogenous MDM2(Haupt, Maya et al. 1997; Kubbutat, Jones et al. 1997), endogenous MDM2 was unable to induce p53 degradation in H1299 cells. Therefore, transfection of cells with huge excesses of MDM2 may swamp or squelch out any of the negative-regulatory controls governing MDM2-mediated p53 degradation.

Potential regulatory mechanisms downstream of the p53:MDM2 protein-protein interaction, regard the processes of ubiquitination and subsequent proteosomal degradation. MDMX, MDM2 splice variants and <60kDa MDM2 caspase cleavage products are all potentially capable of interacting with components of the ubiquitin system (mainly through their RING finger(Honda, Tanaka et al. 1997; Kubbutat, Ludwig et al. 1999)). Therefore, these proteins may effectively compete with full-length MDM2 for ubiquitin, hence, inhibiting subsequent p53 ubiquitination. Alternatively, MDM2 splice variants retaining the carboxyl-terminal ARF-

binding domain may squelch out the negative effects of ARF on full-length MDM2, facilitating p53 ubiquitination.

Most damaged or abnormal proteins are recognised and destroyed by the ubiquitin system, as improper protein folding may expose their normally buried degradation signal(s). To prevent unwanted degradation of nascent, immature proteins, chaperonins (including members of the Hsp 70p family), play a role in correctly folding proteins(Miyata and Yahara 1992; Wiech, Buchner et al. 1992). Therefore, a kinetic battle between degradation and protein folding processes at the earliest stages of protein production, may add an extra level of regulation of protein expression. Furthermore, treatment of mutant-p53 containing cells with the benzoquinone ansamycin, geldanamycin, which dissociates p53 from hsp70, caused a marked reduction in p53 levels(Whitesell, Sutphin et al. 1997; Whitesell, Sutphin et al. 1998; Nagata, Anan et al. 1999). These results enforced a role for Hsp70 in the regulation of p53 ubiquitination and degradation.

The existence of ubiquitin-specific processing proteases (UBPs), which are ATP-independent proteases, capable of cleaving the covalent isopeptide bond between ubiquitin and other proteins(Hochstrasser 1996), provide an additional level of control of ubiquitin-dependent degradation. A wide diversity of UBP targets exist, targeting precursor ubiquitin-chain proteins, or substrate-linked ubiquitin, yielding free, reusable, monomeric ubiquitin. A 26S proteosome-linked UBP functions as an editing enzyme, with the ability to regulate degradation of ubiquitin-conjugated target proteins through ubiquitin removal(Lam, Xu et al. 1997). Interestingly, the junctions in linear ubiquitin adducts are structurally different from the junctions in branched, determining specificity to UBPs and therefore adding specificity to de-ubiquitination of ubiquitinated proteins(Hochstrasser 1996).

It is proposed that a major function of a substrate-linked multi-ubiquitin chain is to decrease the rate of dissociation of a substrate:proteosome complex, thereby increasing the probability of substrate degradation(Varshavsky 1992). A rate-limiting step of a proteosome-bound substrate cleavage may be the unfolding of a relevant domain of the substrate, driven by thermal fluctuations and/or ATPases of the 26S proteosome. Therefore, increased stability of the proteosome-substrate complex would facilitate substrate degradation. Hence,

the degree of ubiquitination may determine the rate of substrate degradation by the 26S proteosome.

Immunofluorescence analysis of MDM2 and p53 subcellular localisation in a number of cell lines revealed predominantly nuclear localisation of both proteins. Of particular interest were the large, discrete sub-nuclear p53 bodies detected by both DO-1 and 421 antibodies, which perhaps reflected specific sites for p53 function (DNA repair, replication, transcription etc). X-ray- and UV-irradiation analysis, as with Western analysis, revealed different effects on p53 and MDM2. UV-irradiation caused a general increase in cytoplasmic p53 staining, while gross alterations in MDM2's nuclear staining pattern was observed. Specific PML-co-localising MDM2 sub-nuclear bodies persisted post-UV-irradiation, while other MDM2 nuclear staining was reduced. In contrast, X-ray-irradiation and ARF-expression, both of which mediated cell cycle arrest, failed to mediate any alterations in either proteins' subcellular localisation. Hence, such differences in irradiation-mediated protein subcellular localisation may reflect the difference between UV- and X-ray-mediated apoptosis and cell cycle arrest, respectively. Furthermore, p53 $175^{R \Rightarrow H}$ DN(5) cells failed to exhibit the parental-U2OS apoptotic- or cell cycle arrest-associated subcellular localisation of p53 and MDM2; perhaps reflecting its attenuated UV and X-ray cellular responses. However, MDM2-overexpressing M(5) cells (which also exhibited attenuated UV and X-ray responses) showed no radical differences in p53 or MDM2 subcellular localisation, supporting the existence of multiple mechanism of apoptotic and cell cycle arrest abrogation.

Immunoprecipitation analysis of lactacystin and X-ray- and UV-irradiated cells revealed significant p53:MDM2 association, although immunofluorescence analysis did not reveal a great degree of subcellular co-localisation. A possible explanation, in addition to the inherent limitation of immunoprecipitation processes respecting subcellular compartmentalisation of proteins, lies in the possible transient nature of the MDM2:p53 interaction. Both proteins, as a consequence of the interaction, may rapidly dissociate and separate into different subcellular localisations. Alternatively, the immunofluorescence technique may specifically reduce the detectability of p53:MDM2 complexed proteins.

Overall, this work has partially characterised a number of cell lines' responses to a variety of different treatments. Molecular analysis revealed dichotomous responses between cell cycle

arresting and apoptotic cells, as well as between cells overexpressing p53 inhibitory proteins. Immunoprecipitation analysis revealed the regulatory complexities of the p53:MDM2 interaction in the context of the p53-MDM2 negative feedback loop. While immunofluorescence analysis of MDM2 and p53 subcellular localisation, revealed the dynamic nature of these molecules, adding further regulatory considerations to the p53-MDM2 relationship.

The respective potential mechanisms for UV- and X-ray-mediated apoptosis and cell cycle arrest are illustrated in Figures 5.1 and 5.2, respectively.

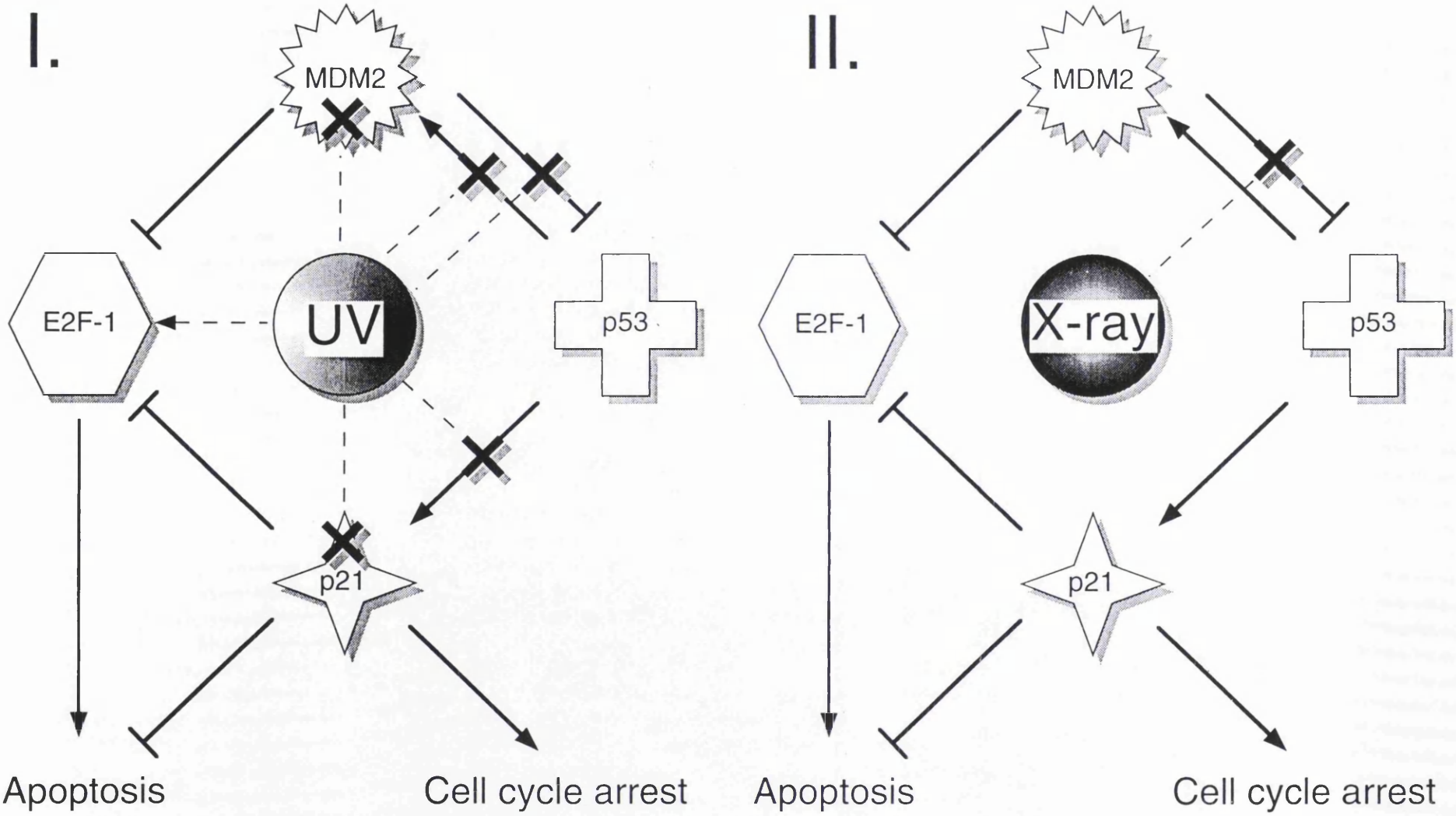

Figure 5.1 Potential model for the respective UV- and X-ray-irradiation mediated apoptosis and cell cycle arrest in U2OS cells. (I) UV-mediated apoptosis. (II) X-ray-mediated cell cycle arrest. MDM2, p53, E2F-1 and p21 proteins are represented by different shapes (as indicated). Flat-head lines represent inhibtiory actions; arrowheads represent activating actions; black crosses represent potential UV-specific inhibitory actions on gene expression or protein function. Please see Discussion text for details.

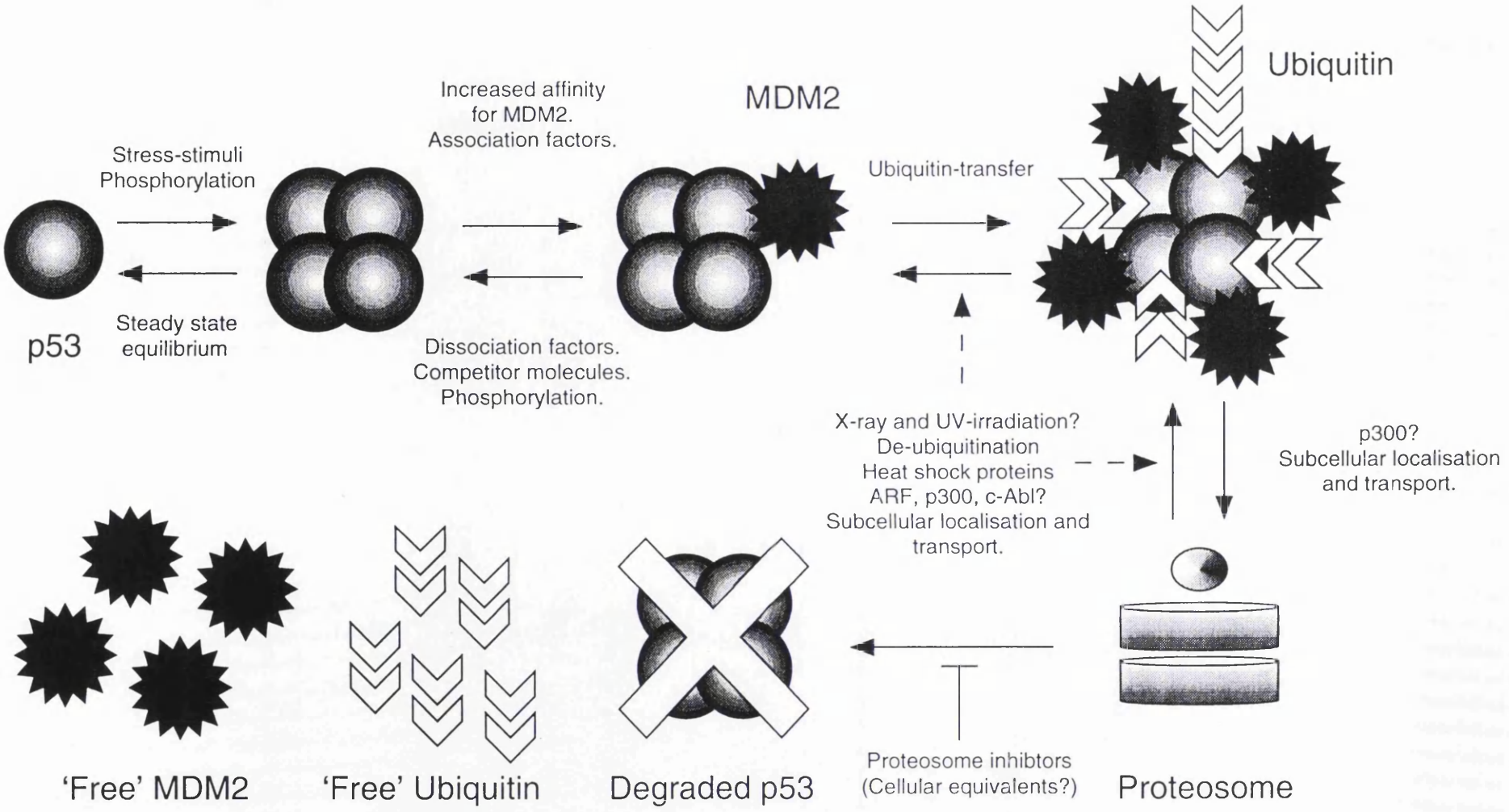

Figure 5.2 Regulatory model of MDM2-mediated degradation of p53. p53 is represented by a sphere; MDM2 is repressented as a spiked circle; and ubiquitn molecules are represented by chevrons. Directionally opposing arrows reflect the two-way regulatory nature of each event. Please see Discussion text for details.

Future

The major core of this work has focused on the cellular and molecular consequences of X-ray- and UV-irradiation. In addition to irradiation, cells are exposed to, and respond to, various other stress-stimuli. Therefore, it would be of interest to determine whether the observed responses reported herein, are similar to non-irradiation-mediated cellular stress stimuli (especially viral and oncogene-mediated).

A major limitation of this work was the use of immortalised tumour-derived cell lines that may not reflect either 'true' tumour or normal cells. Therefore, examination of primary tumour or normal cells would be of interest, in an attempt to support and compare the observations made with the cell lines herein. Additionally, the use of MDM2 or p53 $175^{R \Rightarrow H}$ 'knock-in' murine cells would also be beneficial, in an attempt to consolidate some of the queries over the roles of the endogenous MDM2 or p53 proteins.

p300(Grossman, Perez et al. 1998; Yuan, Huang et al. 1999) and c-Abl (Sionov, Moallem et al. 1999), which are implicated in the regulation of p53 ubiquitination and degradation, may provide support for theory of regulatory control of p53 degradation downstream of the p53:MDM2 protein-protein interaction. Therefore, further investigation of their roles in MDM2-mediated degradation of p53 would also be of interest.

Given the heterogeneous responses of different cell lines to genotoxic stress and the cross talk between the many molecules known to be involved, a reductionist approach may be inadequate for understanding p53 function. Hence, modern integrative approaches are necessary to understand the importance and roles of the many interacting factors in the p53 and cellular stress response pathways in different cell types and individuals. Furthermore, such analysis may help to explain conflicting observations seen in different cell types.

The techniques and approaches used in this study give only a partial insight into the p53:MDM2 relationship. Recent developments have revealed a plethora of regulatory mechanisms that utilise many of the strategies available to the cell. Therefore, Western data cannot be accurately interpreted without evaluation of protein-protein interaction and

subcellular localisation data. Progress is rapidly being made with the introduction of a number of important large scale screening techniques: CHIP technology, which can provide a near complete mRNA profile of the specifically treated cells; 2D-gel electrophoresis, allowing separation and identification of multiple differentially regulated proteins; Fluorescence Resonance Energy Transfer (FRET)(Gordon, Berry et al. 1998) and GFP-tagging allow *in vivo*, real-time analysis of protein-protein interactions and subcellular localisation. Integration of such approaches may also reveal the apparent discordance between mRNA and protein levels, highlighting the importance of translational control mechanisms. Overall, the proteomics revolution should facilitate the elucidation of the dynamic and complex regulatory mechanisms governing protein function and activity.

Chapter Six

Materials and Methods

All solutions, unless otherwise stated, were made up using de-ionised water (dH_2O). All chemical reagents were supplied by Sigma, unless stated otherwise.

Materials

Oligonucleotides

All oligonucleotides were synthesised by the ICRF Oligonucleotide Synthesis service. See table 5.1 for primers used in DNA sequencing and PCR cloning protocols.

Table 6. 5. Primers used for DNA sequencing and PCR cloning

Name	5' Sequence 3'	Tm °C
DNA Sequencing Primers		
T7	GTAATACGACTCACTATAGGGC	52
SP6	CATACGATTTAGGTGACACTATAG	52
5'MDMSeq	GAAAAGGAATAAGCCCTGCCC	54
3'MDMSeq	CCAGGGTCTCTTGTTCCGAAGC	58
PCR Cloning Primers		
5'BamMDM	GGCGGATCCATGTGCAATACCAACATGTCTG	62
5'BamCTMDM	GGCGGATCCATGCAAGTTACTGTGTATCAGGC AGG	68
3'BamNTMDM	CCGGGATCCCTAAGGAACATCAAAGCCCTCTT CAGC	72
3'BamMDM	CCGGGATCCCTAGGGGAAATAAGTTAGCAC	60

Bacterial strains and Mammalian Cell lines

Bacterial Strains

RecA$^-$ (recombination deficient) *E. coli* strains DH5α and XL1-Blue were used for all propagation of plasmids. See Sambrook et al., 1989(Sambrook, Fritsch et al. 1989), for genotypes.

Mammalian Cell lines

U2OS, Saos-2 and JAR cell lines were provided by ICRF Cell Production; MG63, HOS and U393 cell lines were kindly provided by G. Peters, ICRF; and the OSA cell line was generously provided by C. Midgely, CRC. NARF(6) and pIND p21 (1-3) were kindly provided by F.Stott (ICRF) and L. Allan (ICRF), respectively. Please see table 2.1 for more details.

Formulation of frequently used solutions and buffers

All of the following solutions were prepared as described(Sambrook, Fritsch et al. 1989), except PBS and 20X SSC, which were made and supplied by the ICRF central services.

Table 6. 6. Formulation of frequently used solutions and buffers

Solution	Components
PBS (Phosphate Buffered Saline)	0.8% w/v NaCl, 0.02% w/v KCl, 0.114% w/v Na_2HPO_4, 0.02% w/v KH_2PO_4 adjusted to pH 7.3 with 10 M NaOH.
TE	1 mM EDTA, 10 mM Tris-HCl pH 7.4 to 8.0.
1x TBE	89 mM Tris-base, 89 mM boric acid, 2 mM EDTA.
20x SSC	3 M NaCl, 0.3 M Na_3 citrate.
20x SSPE	3.6 M NaCl, 0.2 M sodium phosphate, 20 mM EDTA pH 7.7
Denaturing solution	1.5 M NaCl, 0.5 M NaOH.
Neutralising solution	1.5 M NaCl, 0.5 M Tris-HCl pH 8.0, 1 mM EDTA.

1x Denhardt's solution	0.02% w/v Bovine Serum Albumin (BSA), 0.02% w/v Ficoll 400, 0.02% w/v polyvinylpyrrolidone
Formamide loading buffer	95% v/v formamide, 20 mM EDTA, 0.05% w/v bromophenol blue, 0.05% w/v xylene cyanol.
Pre-hybridisation solution	5X Denhardt's solution, 5X SSPE, 0.5% SDS and 50µg/ml sonicated denatured salmon sperm DNA
2x SDS gel-loading buffer	100 mM Tris-HCl pH 6.8, 200 mM DTT, 4% SDS, 0.2% bromophenol blue, 20% glycerol

Formulation of bacterial media (supplied pre-made by ICRF central services)

L-Broth (LB):	1% w/v Bactotryptone, 0.5% w/v Bacto yeast extract, 1% w/v NaCl.
LB agar:	LB supplemented with 1.5% w/v Bactoagar.

Formulation of mammalian cell culture media and reagents

Dulbecco's modified Eagle medium (DMEM)*: (All values per L, unless otherwise stated).	*Inorganic Salts*: $CaCl_2.2H_20$ 265.00g; $Fe(NO_3)_3$ 0.1g; KCl, 400.00g; $MgSO_4.7H_2O$, 200.00g; NaCl, 6400.00g; $NaH_2PO_4.2H_2O$, 140.00g. *Amino Acids*: L- Arginine mono.HCl, 84.00g; L- Cystine, 48.00g; L-Histidine mono.HCl, 42.00g; L-Glutamine, 584.00g; Glycine, 30.00g; L-Isoleucine, 104.80g; L-Leucine, 104.80g; L-Lysine mono.HCl, 146.20g; L-Methionine, 30.00g; L-Phenylalanine, 66.00g; L-Serine, 42.00g; L-Threonine, 95.20g; L-Tryptophan, 16.00g; L-Tyrosine, 72.40g; L-Valine, 93.60g; Inositol, 7.00g. *Vitamins*: Choline Chloride, 4.00g; Folic acid, 4.00g; Nicotinamide, 4.00g; DL-pantothenic acid, Ca salt, 4.00g; Pyridoxal HCl, 4.00g; Riboflavin, 0.40g; Thiamine HCl (aneurine), 4.00g.

	Other Compounds: D-Glucose, 4500.00g; Phenol red, 15.00g; NaHCO3, 3700.00g; Penicillin, 100,000 units; Streptomycin Sulphate, 100.00g; Sodium pyruvate, 110.00g; Antimycotic (Butyl-p-hydroxybenzoate), 0.2g.
Trypsin*:	NaCl, 8g; Na2HPO4, 0.1g; D-glucose, 1g; Trizma Base, 3g; KCl (19%), 2ml; Phenol Red (1%), 1.25ml; Trypsin, 2.25g.
Versene*:	NaCl, 8g; KCl, 0.25g; Na2HPO4, 1.2g; KH2PO4, 0.25g; EDTA, 0.25g;
Foetal Calf Serum (Autogen Bioclear)	
*(supplied pre-made by ICRF Cell services)	

Plasmids

Table 6. 7. Summary of plasmid DNAs used in this study.

Plasmid	Source	Comment
pCMV-9927	C. Midgely	Neo^R plasmid expressing mutant p53 $175^{R\Rightarrow H}$
pCMV-MDM2	B. Vogelstein(Baker, Markowitz et al. 1990)	Neo^R plasmid expressing full-length human MDM2
pcDNA249	H. Land	Neo^R plasmid expressing mutant p53 $249^{R\Rightarrow S}$
pcDNA248	H. Land	Neo^R plasmid expressing mutant p53 $248^{R\Rightarrow Q}$
pcDNA3.1	Invitrogen	Neo^R pCMV mammalian expression vector
pCMV-CD8	D. Mann	Plasmid expressing CD8 cell surface marker
pGEM T-Easy	Promega	Bacterial PCR-product cloning vector
pBluescript	Stratagene	Bacterial cloning vector

Methods

DNA and RNA methods

Quantitation of DNA and RNA

DNA and RNA concentrations were determined by spectrophotometry at 260ηm, using a Beckman spectrophotometer. An OD_{260} of 1 equates to 50μg/μl of dsDNA or 40μg/μl RNA.

Precipitation of DNA

DNA was generally concentrated by ethanol precipitation. 0.1 volumes of 3M sodium acetate, pH5.0, were added to DNA solutions to adjust the monovalent cation concentration to 0.3M. DNA was precipitated by adding 3.5 volumes of -20°C ethanol and incubated at –20°C for 10 minutes, followed by centrifugation at 13,000 rpm for 1-20 minutes, washed in 70% ethanol, air dried and then re-suspended in TE or H_2O.

Enzymatic DNA Manipulations

Enzymatic manipulations of DNA molecules were performed as described(Sambrook, Fritsch et al. 1989). Restriction endonuclease digests of plasmid DNA were mostly performed for 2 hours using 5-20 units of enzyme (New England Biolabs [NEB], GibcoBRL or Boehriger Mannheim) in the appropriate buffer. Ligation of DNA molecules using T4 DNA ligase (NEB) were performed in 10μl reactions for a total DNA content of up to 1μg with a plasmid:insert ratio generally between 1:5 and 1:3. When the plasmid was capable of self-ligation, the compatible ends were dephosphorylated prior to use, using calf intestinal alkaline phosphatase (Boehringer Mannheim). Ligations were performed overnight at 16°C (blunt-ended) or for 2 hours at room temperature (cohesive termini) in T4 DNA ligase buffer (NEB). Amino- and carboxyl-terminal MDM2 pcDNA3.1 were constructed using primers incorporating BamHI and subsequent ligation into BamHI cut and phosphatased pcDNA3.1 vector. A SalI restriction digest was used to determine the correct orientation of the MDM2 insert.

Propagation and maintenance of plasmid DNA

Plasmids were propagated in DH5α and XL1-Blue bacterial cells in LB (or on LB-agar plates) in the presence of the appropriate antibiotic - 50μg/μl ampicillin (Penbritin) for most plasmids. Sterile glycerol was added to liquid cultures to a final concentration of 20% for long-term storage at -80°C.

Preparation and storage of competent bacteria

Bacteria were rendered competent for the uptake of DNA by treatment with $CaCl_2$. A 10 ml culture of bacteria grown overnight in 2YT (1% w/v Bacto-tryptone, 1% w/v Bacto-yeast extract, 0.5% w/v NaCl) without shaking were inoculated into 100mls of P-media (15.9 mM K_2PO_4, 6.3 mM KH_2PO_4, 15 mM $(NH_4)_2SO_4$, 10 mM $MgSO_4$, 1.8 mM $FeSO_4$, 1% casamino acids and 0.25% glucose) and grown to an OD_{600} of 0.4 as measured by spectrophotometry. Bacteria were pelleted at 6,000g for 10 minutes in a JA-10 rotor. Cells were washed in 100 mls of 10 mM NaCl at 4°C and re-pelleted. Bacteria were resuspended in 100 mls of 50 mM $CaCl_2$ and incubated at 4°C for 15 minutes. Finally cells were pelleted and resuspended in 10 mls of 50 mM $CaCl_2$, 16% (v/v) glycerol, aliquotted and snap frozen in a dry ice/ethanol bath before being stored at -80°C. The transformation efficiency of the resulting cells was approximately 5×10^6 to 5×10^7 colonies/mg of plasmid DNA.

Plasmid DNA transformation of $CaCl_2$ competent bacteria

Frozen competent-bacteria were thawed on ice and 10-1000 ηg of DNA was added to 100-200 μl of the cells on ice. Bacteria were kept on ice for 20 minutes and heat shocked at 42°C for 90 seconds. After being cooled on ice for 2 minutes, 800 ml of LB was added to the cells and the mixture was incubated at 37°C for 45-60 minutes. Bacteria were then plated out onto LB-agar plates containing the appropriate antibiotic and, when necessary, 0.1mM IPTG (Isopropylthio-β-D-galactoside) and 20μg/ml X-Gal (5-Bromo-4-chloro-3-indoyl-β-D-galactoside) for blue/white selection.

Small-scale preparation of plasmid DNA

A TENS minipreparation was mostly used. 1.5 mls of overnight bacterial culture was centrifuged briefly in a microcentrifuge (MSA Microcentaur) and the pellet resuspended by vortexing in the liquid remaining (≅50 μl) after decanting most of the LB . 300 μl of TENS solution (0.1 M NaOH, 0.5% SDS) was added and the tube inverted ~6 times followed by

150 µls of 3M sodium acetate, pH 5.5, and vigorous inversion. After a 2 minutes centrifugation at 13,000 rpm the supernatant was removed and nucleic acids ethanol precipitated and the pellet was resuspended in H_2O containing 0.1 µg/µl RNase A. In all other cases minipreparations of plasmid and cosmid DNAs were made using the Qiagen Miniprep Kit (using microcentrifuge spin columns) using the protocol and reagents provided by the manufacturer. DNAs were eluted in 50 µl of distilled H_2O.

Large-scale preparation of plasmid DNA

Solution I	50 mM glucose, 10 mM EDTA, 25 mM Tris pH 8.0.
Solution II	1% SDS, 0.2 M NaOH
Solution III	3 M K acetate pH 5.5
Solution IV	5 M LiCl

For general plasmid preparations LiCl based maxi-preps were used. 200 mls of bacterial cells were pelleted in a Sorvall superspeed centrifuge (4000 rpm for 10 minutes) and resuspended in 5 mls of Solution I. 10 mls of Solution II was added and tubes inverted 6-12 times followed by 5 mls of Solution III and 6-12 inversions. Following centrifugation for 15 minutes at 2500 rpm in a Jouan benchtop centrifuge, the supernatant was removed and nucleic acids precipitated with 20 mls of -20°C isopropanol. Precipitated nucleic acids were then recovered by centrifugation (15 minutes at 2500 rpm). The supernatant was discarded and the pellet re-dissolved in 1.5 mls of TE (pH 8.0) and 2 mls of -20°C 5M LiCl added to precipitate the RNA. Samples were then left on ice for 5 minutes and then centrifuged at 2500 rpm for 10 minutes. The supernatant was transferred to a 15 ml Falcon tube and DNA precipitated with 2 volumes of cold ethanol. This was recovered by centrifugation at 2500 rpm for 10 minutes, the pellet was then washed once with 95% ethanol and then re-dissolved in 0.8 mls of TE pH 8.0. RNase was added to 40 µg/ml and samples incubated at 37°C for 15 minutes. DNA was then precipitated by addition of 0.5 volumes of 20% PEG 8000, 2.5 M NaCl with a 5 min incubation on ice. DNA was recovered by centrifugation in a microcentrifuge and the pellet resuspended in 0.6 mls of TE (pH 8.0). Separate chloroform and phenol extractions(Baker, Markowitz et al. 1990) were performed twice each before DNA was ethanol precipitated. DNA was resuspended in H_2O to a concentration of ~1 µg/µl.

For transfection of mammalian cells either Qiagen 'Endo-free' tip-500 columns (carried out according to the manufacturer's protocol) were used.

Extraction of RNA from mammalian cell lines

Total cellular RNA was extracted from cell lines and yeast using the TRIZOL® reagent (GibcoBRL) following the supplied protocol. RNA samples were stored at -70°C at the 75% ethanol wash stage.

Agarose gel electrophoresis of DNA and RNA

DNA: Large submarine agarose gels (150-200 ml) and mini submarine agarose gels (50 ml) were made and run in 1 x TBE using ATTO gel electrophoresis equipment. The agarose concentration of gels varied from 0.7-3.0% w/v depending on the size of the DNA fragments being resolved. 0.7-1.5% agarose gels were made using standard agarose and 1.5-3.0% agarose gels were made with NuSieve® agarose (FMC Bioproducts/Flowgen). Gels contained 0.5 μg/ml ethidium bromide to enable visualisation of DNA using a UV-camera (Mitsubishi electronics). DNA samples were loaded into gels after addition of 0.1 volumes of 10x DNA sample loading buffer (0.25% w/v bromophenol blue, 40% w/v sucrose). Mini-gels were run at 40-100 V and large gels at 40-150 V. 1 kb DNA ladder (GibcoBRL) was used as size markers in all gels.

RNA: 1% agarose RNA gels were cast from a solution composed of 1-1.5 g of agarose, 73 mls of H_2O, 10 mls of 10x MOPS running buffer (200 mM MOPS, 10 mM EDTA, 500 mM Na acetate, pH adjusted to 7.0 with glacial acetic acid) and 17 mls of 37% formaldehyde (for 100 mls). The agarose was melted and cooled in water alone before the addition of buffer and formaldehyde. Gel tanks/other apparatus components were treated with 3% H_2O_2 prior to usage to inactivate RNases. Gel tanks were filled with 1 x MOPS running buffer. RNA samples were incubated at 65% for 5 minutes in a solution containing 50% formamide, 1 x MOPS buffer and 6% formaldehyde before being chilled briefly on ice and loaded into the gel after the addition of 0.1 volumes of 10x RNA loading buffer (50% glycerol, 1 mM EDTA (pH 8.0), 0.25% bromophenol blue, 0.25% xylene cyanol). Gels were pre-run for 5 minutes prior to loading and after loading at 120 V.

Purification of DNA fragments from agarose gels

DNA was purified from agarose gels using the Geneclean II kit (BIO 101) using the supplied protocol. DNA fragments were excised from agarose gels with a scalpel and placed in a 1.5 ml Eppendorf tube. Gel volumes were estimated by sight. TBE modifier was added in all cases. DNA was eluted into a final volume of 20 µl.

Denaturing polyacrylamide gel electrophoresis of DNA

Acrylamide solutions for sequencing gels contained 19:1 acrylamide:bisacrylamide (Anachem). Gels contained 7% polyacrylamide in 1x TBE buffer containing 46% w/v urea. 250 µl of 10% ammonium persulphate and 50 µl of TEMED were used to polymerise 50 mls of gel mix (for a sequencing gel 0.4 mm thick). Gels were pre-run for 1 hr before use and electrophoresed in 1x TBE at 1600-1800V. Dideoxy sequencing reactions were treated as outlined in the Sequenase manual before loading (see below). After electrophoresis, gels were fixed for 15 minutes in a tray of 10% v/v methanol, 10% v/v acetic acid, and then dried onto 3 MM paper at 80°C for 30 minutes.

DNA sequencing and analysis

Sequencing was performed from plasmid clones using standard vector primers or designed insert-specific primers (see Table 5.1). Early sequence analysis was performed using the Sequenase Version 2.0 kit from U. S. Biochemical (USB) based upon the dideoxy chain termination method(Sanger, Nicklen et al. 1977). Double-stranded templates were used and the supplied protocol was followed. Reactions were separated on 7% denaturing polyacrylamide gels (see above). ^{35}S dATP was supplied by Amersham. Latterly sequence was generated from clean double-stranded DNA templates (maxipreps and Qiagen minipreps) using ABI PRISM™ Dye Terminator Cycle Sequencing (Perkin Elmer Corp.) following the supplied protocol and using the supplied reagents. Cycling reactions of 25 cycles were performed on a DNA Thermal Cycler as instructed with a primer annealing temperature of 50°C in all cases. Reactions were run on an automated ABI PRISM™ 377 DNA sequencer (Applied Biosystems). Sequence data was entered directly into the MacVector™ 6.0.1 program (Oxford Molecular Group Plc.) on an Apple Macintosh computer.

Polymerase Chain Reaction (PCR)

PCR reactions were routinely carried out in the following conditions: 25 µl (for a Techne PTC-100 thermal cycler - M.J. Research Inc.) or 50 µl (for a Trio thermoblock thermal cycler - Biometra) reactions contained 50 mM KCl, 10 mM Tris-HCl pH 8.3, 1.5 mM $MgCl_2$, 10% DMSO, 200 µM dNTPs, 1 µM of each primer, 5 units of *Taq* DNA polymerase (Perkin-Elmer Cetus) and ~20-100 ng template DNA. Reactions performed in thermal cyclers without a heated lid were overlaid with light mineral oil to prevent evaporation. Where reaction numbers were manageable, the reaction was usually heated to 94°C for 1 minute prior to adding the *Taq* polymerase in order to inhibit non-specific amplification. Typical cycling conditions typically used were: denaturation at 94°C for 30 seconds, annealing at 45-68°C (dependent on the melting temperature - T_m - of the oligonucleotide primers being used) for 20 seconds, and extension at 72°C for 0.5-4.0 minutes (generally 1 minute for every 1 kb to be amplified). In general, for oligonucleotides less than 23 nucleotides in length T_m values were based on the G + C = 4°C plus A + T = 2°C rule but for longer oligonucleotides the equation $T_m = 81.5°C + 16.6 (\log M) + 0.41(\% GC) - 500/n$ was used to estimate T_m where M is the molarity of salt in the buffer and n is the primer length(Sanger, Nicklen et al. 1977). 17-25 nt oligonucleotide primers were designed avoiding long stretches of the same nucleotide, unusual base composition and obvious propensities to form secondary structures or cross-hybridise with one another.

Cloning of PCR products

PCR products were sometimes cloned directly into a vector with 3' overhangs of a single T residue (T-vector). T-vector was generated by cleavage of pBluescript II KS+ with *Eco*RV followed by enzyme inactivation (65°C for 20 minutes) and then incubation at 72°C for 2 hrs in PCR buffer (see above) containing only dTTP in the presence of *Taq* polymerase. T-vector was then purified using the Geneclean II kit (see above). Latterly the pre-made vector pGEM T-Easy (Promega) was used. Restriction sites were placed at the 5' end of the oligonucleotides with a 3 bp preceding trailer in order to facilitate cloning of products after restriction endonuclease digestion of the amplified product.

Northern (RNA) blotting

Blotting of RNA from agarose gels was performed essentially as described in the protocol booklet accompanying Hybond-N membrane (Amersham) which was used in all cases.

Typically, 5-20 µgs of total RNA was blotted per lane. After electrophoresis, denaturing agarose gels used for electrophoresis of RNA were soaked in many changes of H_2O to remove as much formaldehyde as possible. RNA was blotted onto Hybond-N by capillary action from a reservoir containing 20x SSC(Sambrook, Fritsch et al. 1989). Following overnight transfer of RNA, the filters were baked at 80°C for 2 hours (or 1 hour under vacuum).

Random hexa-nucleotide labelling of DNA with ^{32}P

The random priming method(Feinberg and Vogelstein 1984) was used to label DNA probes. Up to 200 ng of plasmid DNA or purified DNA fragments were denatured at 100°C for 5 minutes in 5 µl OLB buffer (see below) made up to 18 µl with H_2O and then put on ice immediately for 2-3 minutes. Labelling was initiated by addition of 1 µl of 10 mg/ml BSA (enzyme grade), 2.5 µl each of ^{32}P α-dATP and ^{32}P α-dCTP (10 mCi/ml) and 2 units Klenow enzyme (Boehringer). After 2-8 hrs at room temperature the reaction was passed through a G50 column (see below). Oligo-labelling buffer (OLB) consists of a mixture of solutions A:B:C in the ratio 10:25:15

Solution A:	1 ml of 1.25 M Tris-HCl, 0.125 M $MgCl_2$, 18 µl 2-mercaptoethanol, 5 µl 0.1 M dGTP and dTTP.
Solution B:	2M HEPES (pH to 6.6 with 4 M NaOH).
Solution C:	Hexadeoxynucleotides pd$(N)_6$ (Pharmacia), in TE (90 OD units/ml).

Non-incorporated radioactive nucleotides were removed from labelling reactions using G50 gel filtration. Single nucleotides and oligonucleotides up to 16 nt in length are retained in the gel. A 1ml syringe was sealed with a plug of siliconised glass wool and filled with a suspension of G50 (Pharmacia) in H_2O. The syringe was placed within a 15ml falcon tube and spun at 1000 rpm for 5 minutes at RT in a Jouan centrifuge. The syringe was topped up with 100 µl H_2O and re-spun. A cap-less microcentrifuge tube was placed below the syringe within the 15ml tube and the syringe loaded with the sample in 100 µl. Centrifugation was repeated. The contents of the microcentrifuge tube (the probe) was then assessed for radioactive incorporation using a Geiger counter.

Hybridisation of labelled probes to RNA blots

Northern blots were pre-hybridised in 20-50 mls of pre-hybridisation solution containing 50% formamide at 42°C O/N. After removal of pre-hybridisation fluid, filters were hybridised at a temperature 5-10°C below the T_m of the oligonucleotide probe for 3-4 hours in 10-30 mls of pre-hybridisation solution containing the heat-denatured probe DNA (heated to 100°C for 5 minutes and cooled rapidly on ice). Filters were routinely washed twice in 2 x SSC, 0.5% w/v SDS for 15 minutes each and twice in 0.1 x SSC, 0.5% w/v SDS for 15 minutes each at RT. Following washing filters were covered with Saran wrap and exposed to autoradiographic film (Kodak XAR-5 X-ray film) with intensifying screens (Du Pont) at -80°C. All hybridisations were performed in Hybaid hybridisation ovens and bottles.

Blots were stripped of radioactive probe by incubation in 0.4 M NaOH for 30 minutes at 45°C (to denature probe and target) followed by neutralisation in 0.1x SSC, 0.1% w/v SDS, 0.2 M Tris-HCl pH 7.5 at 45°C for 15 minutes. Autoradiography was performed to check that the probe had been removed prior to re-use.

Protein methods

Preparation of mammalian cell extracts for Western analysis

Monolayer mammalian cell lysates for 'direct' western analysis were prepared as follows (all stages of lysis were carried out on ice): culture medium was aspirated from the culture plates and washed twice with 4°C PBS. After extensive aspiration, 50-200 µl of 1X SDS gel-loading buffer (50mM Tris-HCl, pH6.8, 2% w/v SDS, 10% v/v glycerol and lacking both 0.1% w/v bromophenol blue and 0.1M DTT – which were added post protein concentration determination) was added to the dish, mixed and scraped with a rubber policeman, then aliqouted into eppendorfs. Samples were then heated at 100°C for 5 minutes, repeatedly passed through a 23G needle (to shear chromosomal DNA and reduce viscosity), centrifuged at 13,000 rpm in a microcentrifuge (to remove cellular debris) and the supernatant removed to a fresh tube and stored at -20°C.

Immunoprecipitation analysis

Monolayer mammalian cell lines were lysed for immunoprecipitation analysis as follows (all stages were carried out with ice-cold reagents, on ice or at 4°C): culture medium was aspirated from the culture plates and washed twice with 4°C PBS. After extensive aspiration, 3 ml of IP lysis buffer, containing protease and phosphatase inhibitors (see IP buffer formulations table below), was added to the plate and incubated for 10 minutes. Cells were scraped into 15 ml falcon tubes using a rubber policeman, snap frozen in dry ice and stored at –70°C (if required) and de-frozen in wet ice (when required), repeatedly passed through a 23G needle and centrifuged at 3,000 rpm for 20 minutes in a Jouan refrigerated centrifuge (to remove cell debris). Samples then underwent protein concentration determination (see below) and appropriate volumes/mass of total protein was added to eppendorfs. 0.5-1.0 mg of total protein was added to immunoprecipitation reactions and made up to 1ml total volume with IP buffer (to ensure equal protein concentrations). Initially, samples were pre-cleared with either 50 µl of 50% v/v protein A or G sepharose (Pharmacia) slurry and rotated on a blood mixer at for one hour, prior to antibody addition (to remove non-specific background interactions). However, in later experiments, this pre-clearing step was not used in conjunction with agarose-conjugated antibodies.

Table 6. 8. Formulation of IP buffers used in this study.

Buffer Name	Formulation
Pomerantz	10mM NaF, 50mM β-glycerophosphate, 10% Glycerol, 1% NP-40 (in PBS)
RIPA	150mM NaCl, 1.0% NP-40, 0.5% DOC, 0.1% SDS, 50mM Tris (pH8.0)
NP-40	150mM NaCl, 1.0% NP-40, 50mM Tris (pH 8.0)
Protease inhibitors	Aprotinin (50µg/ml), PMSF (100µg/ml) and 'complete Mini' protease inhibitor cocktail tablets (Boehringer Mannheim)
Phosphatase inhibitor	Sodium Orthovanadate (50µg/ml)

The appropriate mass of monoclonal or polyclonal, agarose-conjugated or 'free' antibody (see Table 6.6) was added to the IP lysis mix and incubated for one hour on a blood mixer,

before addition of 25µl of protein A or G sepharose 50% v/v slurry (this step was omitted with the agarose-conjugate antibodies). Immunoprecipitations were then incubated for 4 hours on a blood mixer, spun at 2,500 rpm in a microcentrifuge for 2 minutes. Supernatants were either discarded or used for subsequent immunoprecipitations, while the pellet was repeatedly washed with IP buffer, agitated and re-centrifuged (x4). After the final wash, the pellet was carefully aspirated of excess IP buffer and resuspended in 20µl of 2xSDS Gel-loading buffer, incubated at 100°C for 5 minutes and centrifuged at 6,000 rpm in a microcentrifuge. The resulting supernatant was either used immediately for PAGE analysis or kept frozen at -20°C.

Glutaraldehyde treatment of protein lysates

0.1 and 0.025% glutaraldehyde treatment was carried on NP-40 IP-buffer lysates in a 20µl total volume. After addition, samples were incubated at room temperature for 30 minutes and then 20µl of 2X SDS gel loading buffer was added. Samples were then treated as 'normal' western sample.

Protein concentration determination

Protein determination for both IP samples and 'direct' western samples was carried out (prior to DTT and bromophenol blue addition) as described in the Bio-Rad 'DC protein Assay' instruction manual. Protein ODs were measured using Bio-Rad disposable polystyrene cuvettes in a Beckmann spectrophotometer and converted into protein concentrations through the use of a BSA protein-standard curve (see Figure 2.18).

Denaturing polyacrylamide gel electrophoresis of proteins

When quantitative loading was required, all protein samples were made up to 20-25µl with 1xSDS Gel-loading buffer. Prior to loading on the gel (20-25 µl per lane), 10% 1M DTT (to reduce disulphide bonds) and 0.1% bromophenol blue (to aid visualisation upon loading) were added to the samples and heated to 100°C for 10 minutes. Samples were left to cool to room temperature before loading (to ensure quantitative pipetting and loading). Cell extracts were separated under denaturing conditions by SDS polyacrylamide gel electrophoresis (SDS-PAGE) - essentially as described(Sambrook, Fritsch et al. 1989) - using Miniprotean II™ electrophoresis equipment (Bio-Rad). Various percentage 'separating' polyacrylamide gels were prepared according the molecular weight of interested

proteins (see Table 5.5). For example, a 12% polyacrylamide gel was prepared with 1.6 ml of water, 2.0 ml of 30% 37.5:1 acrylamide:bisacrylamide mix (Anachem), 1.3 ml of 1.5 M Tris-HCl pH 8.8, 50 µl of 10% SDS, 50 µl of 10% ammonium persulphate and 2 µl of TEMED were mixed and poured between two vertical glass plates separated by 0.75 mm thick spacers (sealed at the bottom) leaving a 1 cm gap between the top of the gel and the glass plates. The space at the top of the gel was overlaid with 0.1% SDS. After 10-20 minutes the gel had set and the 0.1% SDS was discarded. Then, 0.68 ml of water, 0.17 ml of 30% acrylamide, 0.13 ml of 1.0M Tris (pH 6.8), 10 µl of 10% SDS, 10 µl of 10% ammonium persulphate and 1 µl of TEMED were mixed and the solution was poured into the space above the previously polymerised gel. A comb was inserted into the solution between the glass plates. After 15 minutes the gel had set and the stacking gel was ready for use. Gels were run in Tris-glycine electrophoresis buffer (25 mM Tris, 250 mM glycine, 0.1% SDS) at 100-150V. Low and high molecular weight Rainbow size markers (Amersham) were run alongside for later reference. To assess amounts of protein loaded, gels were sometimes stained after electrophoresis with Coomassie brilliant blue staining solution (45% ethanol, 10% glacial acetic acid, 0.25% Coomassie brilliant blue R250 in H_2O). Gels were immersed in the staining solution and rotated on a shaking platform for several hrs. Gels were then de-stained by immersion in several changes of the same solution used for staining, lacking Coomassie brilliant blue.

Table 6. 9. Percentage of polyacrylamide gel used for Western analysis of various proteins.

Protein of interest	Polyacrylamide gel (%)
p53:53kDa	10-12
MDM2:90kDa	8-10
pRB:110kDa	8-10
E2F-1:≅60kDa	10-12
Bax:23kDa	15
Bcl2:29kDa	15
$p14^{ARF}$:14kDa	15
p21:21kDa	15

Actin:≅50kDa	10-12

Western blotting

Proteins were blotted from SDS-PAGE gels to Hybond-ECL membrane (Amersham) by semi-dry transfer using a Transblot® semi-dry transfer apparatus (Bio-Rad). A sandwich for transfer was made by first placing three pieces of 3MM filter paper cut to the size of the gel and soaked in blotting buffer (20 mM Tris-HCl pH 8.3, 150 mM glycine, 20% methanol and 0.1% SDS in H_2O) on the bottom plate of the apparatus (anode). Next were placed a piece of Hybond-ECL cut to size and soaked in blotting buffer and then the gel similarly soaked in buffer. Finally three more pieces of blotting buffer-soaked 3MM were placed on top as the final layer. As each layer was added any air bubbles were rolled out. The lid was then placed on the top of the apparatus and transfer performed at 10 V for 30 minutes. Once transfer was complete the membrane was washed briefly in H_2O. Ponceau S in PBS (0.5g/100 ml) was used to stain the membranes to ensure efficient and quantitative transfer. Membranes were de-stained by repeated washing in PBS. Membranes were pre-blocked in a 5% w/v Marvel (milk powder) in TBS (Tris-Buffered Saline - 150 mM NaCl, 20 mM Tris-HCl pH 8.3) solution for 1 hr at RT and then rinsed briefly in 5% Marvel, 1x TBS, 0.5% Tween 20. The membrane was then incubated for 2 hrs at RT in 5% Marvel, 1x TBS, 0.5% Tween 20 with the appropriate antibody (see Table 6.6). Membranes were washed three times in 5% Marvel, 1x TBS, 0.5% Tween 20 for 10 minutes each. The membrane was then incubated in 5% Marvel, 1x TBS, 0.5% Tween 20 containing a 1:1000 dilution of the appropriate donkey or sheep peroxidase (HRP)-conjugated anti-mouse, -goat or -rabbit IgG (Amersham) for 1 hour at RT in a sealed bag. Afterwards the membrane was washed four times in 1x TBS, 0.5% Tween 20 and subjected to ECL. 1:1 volumes of ECL Solutions 1 and 2 (Amersham) were mixed and applied to the membrane for 1 minute. The membrane was then dried, wrapped in Saran wrap and exposed to film for a few seconds to several minutes to obtain the best exposure.

Table 6. 10. Summary of antibodies used in this study.

Antibody	Protein	Concentration used
Rabbit polyclonal CM-1 (Novocastra)	p53	W: 1:2500 IP: 1µl
Mouse monoclonal DO-1 (ICRF)	p53	W: 1µg/ml IP: 1µg IF: 1:50
Mouse monoclonal 421 (ICRF)	p53	W: 1µg/ml IP: 1µg IF: 1:50
Mouse monoclonal 1801 (ICRF)	p53	W: 1µg/ml IP: 1µg
Agarose-conjugated 1801 (Santa-Cruz)	p53	IP: 20µl
Rabbit polyclonal Ser^{392} (NEB)	p53	W: 1:1000
Rabbit polyclonal Ser^{15} (NEB)	p53	W: 1:1000
Rabbit polyclonal N-20 (Santa-Cruz)	MDM2	W: 0.25µg/ml IP: 0.25µg IF: 1:50
Mouse monoclonal 2A10 (gift from A. Levine)	MDM2	W: 30µl/ml IP:150µl IF: 1:20
Mouse monoclonal SMP-14 (Santa-Cruz)	MDM2	IF: 1:20
Agarose-conjugated SMP-14 (Santa-Cruz)	MDM2	IP: 20µl
Mouse monoclonal Ab-3 (Neomarkers)	p21	W: 1µg/ml
Goat polyclonal N-20 (Santa-Cruz)	Bax	W: 0.5µg/ml
Mouse monoclonal Ab-1 (Neomarkers)	Bcl-2	W: 1µg/ml
Mouse monoclonal IF8 (Santa-Cruz)	pRB	W: 0.5µg/ml IP: 0.5µg
Rabbit polyclonal IP-1 (gift from F.Stott)	$p14^{ARF}$	W: 1:1000 IF: 1:100
Rabbit polyclonal FST-13 (gift from F.Stott)	$p14^{ARF}$	IP:5µl

Mouse monoclonal E2F (Pharmingen)	E2F-1	W: 1μg/ml
Rabbit polyclonal α-Actin (Sigma)	α-Actin	W: 1μg/ml
W=Western; IP=Immunoprecipitation; and IF=Immunofluorescence		

Mammalian cell culture methods

General propagation

All tissue culture reagents were filter sterilised by passage through a 0.22μm filter (Nalgene). Monolayer cell lines were propagated using standard procedures. All cell lines used were grown in DMEM media, supplemented with L-glutamine and bovine foetal calf serum (Autogen Bioclear) generating 'complete' E4, at 37°C in 10% CO_2. Generally, cells were split 1:5 two-three times per week. Frozen cell stocks were made using freezing media: 70% complete E4, 20% FCS and 10% DMSO and kept short term at -80°C and long-term in liquid nitrogen. For recovery, frozen cells were rapidly thawed at 37°C, plated in complete E4, allowed to adhere after 3-4 hrs, then fluid changed with complete E4 (to remove the DMSO). Cell lines were generally refreshed from frozen stocks every two months. Cells were counted by haemocytometry.

Induction of NARF(6) and pIND p21 U2OS cell lines

1mM IPTG was added to NARF(6) culture media every 24 hours, as needed. 5 μM of Ponasterone A (PonA, Invitrogen) dissolved in ethanol was added to pIND p21 U2OS cell lines every 24 hours, as needed. Control pIND p21 U2OS cells were mock-treated with an equivalent volume of ethanol. Care was taken to avoid adding PonA or ethanol directly onto the cells.

Transfection of plasmid DNA

Transient and stable transfections were carried out using Superfect (Qiagen), a class of activated-dendrimer transfection reagent, which assembles DNA into a compact structure, facilitates binding and uptake by negatively-charged receptors and buffers lysomal nucleases. 70% confluent cells (approx. $1x10^6$ cells for a 9 cm plate and $5x10^5$ for a 5 cm plate, incubated overnight) were transfected with either $CsCl_2$ or Endo-free (Qiagen) purified

DNA according to the manufacturers instructions. Optimem-GlutMax (Gibco-BRL) serum-free chemically-defined DMEM was used for the transfection mix.

Selection of CD8-positive Transfected cells

For CD8 selection, cells were co-transfected with pCMV-CD8 (David Mann, ICRF) 1:5 with the plasmid of interest. 48 hours post-transfection cells were tyrpsinised, washed and selected using biomagnetic separation with anti-CD8 beads (Dynal) according to manufacturers instructions. CD8-positive cells were lysed in 1xSDS Gel-loading buffer on the beads, boiled at 100°C for 5 minutes, centrifuged at 13,000 rpm in a microcentrifuge and the supernatant removed to a fresh tube. These samples were then treated as normal western lysates.

Stable selection of plasmid-transfected cell lines

5 cm plates were seeded with 5 $x10^5$ cells overnight, prior to transfection with 2.5 µg of DNA. Following transfection approximately 12 hours post-transfection, cells were tyrpsinised and split between 4 x 9 cm plates. Cells were allowed to adhere overnight before the addition of the selective antibiotic. For the selection of stable cell clones following transfection of selectable antibiotic markers, Zeocin (500 µg/ml) (Invitrogen), G418/Neo (800 µg/ml) were used appropriately. Approximately 7 days post-antibiotic addition isolated colonies were picked using trypsin/versene soaked 3MM discs and gradually expanded into larger culture volumes.

UV-irradiation of mammalian cell lines

Cells at 80% confluency were irradiated using a laminar flow hood-based germicidal UV(C) bulb, which generates 254 ηM wavelength UV light (UVC). Zonal UV measurements at the hood's work surface revealed a central area, large enough for 2 x 9cm plates, with consistent readings of 2 Jm^{-2}. Pre-conditioned cell media was removed and retained, before the cells were twice washed with PBS, in an attempt to remove proteins and chemicals that might absorb UV and create free radicals. 2 mls of PBS was added to the cells prior to irradiation to prevent drying out. Culture plate lids were also removed upon irradiation, due to plastic absorbing UV irradiation. Plates were irradiated for 15 seconds, delivering 30 Jm^{-2} and the PBS was aspirated. Pre-conditioned media was added to the plates and replaced in

the incubator until processed. Control plates were mock-irradiated, undergoing the same procedures, but excluding UV-irradiation.

X-ray-irradiation of mammalian cells

Cells were grown to 70% confluency and then irradiated in culture media with 6 Gray/minute, 17 cm from the source for various times using a Pantax HS320 X-ray generator. Culture plate lids were not removed due to negligible X-ray absorbence and non-sterile conditions. Care over control mock-irradiated cells ensured that the temperature and CO_2 fluctuations and the relatively long exposure times (including transport to the X-ray generator) were taken into account. Controls were set to broad focus at 320 kV and 10 mA and exposure times were varied accordingly. Post-irradiation, cells were returned to the incubator until processed.

Cycloheximide and Lactacystin treatment

Cells were grown to 70% confluency and 10μg/ml cycloheximide was added directly to the media and mixed thoroughly. Cells were left in cycloheximide-containing media until processed. 10μM lactacystin (Calbiochem) dissolved in DMSO was added directly to cell media and mixed thoroughly. Control cells were mock-treated with an equivalent volume of DMSO. Care was taken to avoid adding lactacystin or DMSO directly onto the cells. Cells were left in cycloheximide-containing media until processed.

Cell biology methods

FACS cell cycle analysis

Cells at various time points post-treatment were analysed for cell cycle distribution through addition of 10μM bromodeoxyuridine (BrdU). 30 minutes post-BrdU-addition, cells were harvested by trypsinisation, washed twice with PBS and then fixed in ice cold 70% ethanol. BrdU-treated cells were subsequently incubated with fluorescin isothiocyanate (FITC)-conjugated anti-BrdU antibody and propidium iodide (PI) and analysed using a FACSCalibur cell analyser (Becton-Dickinson).

FACS apoptosis analysis

Terminal deoxynucleotidyl transferase-mediated dUTP-biotin nick end-labelling (TUNEL)(Gavrieli, Sherman et al. 1992) and sub-G_1 were used to assay apoptosis. For both TUNEL and sub-G_1 analysis, cells at various times post-treatment were harvested, washed twice in PBS and fixed in 1% paraformaldehyde or 70% ethanol, respectively. TUNEL analysis was carried out using the APO-BRDU kit according to the manufacturer's protocol (Pharmingen). Both TUNEL and sub-G_1 analysed cells were counter-stained with PI and analysed using a FACSCalibur cell analyser.

Immunofluorescence analysis

$3x10^4$ cells were seeded per well on an 8-well chamber slide (Becton-Dickinson) and grown overnight and treated the following morning. At desired time-points post-treatment (where applicable) cell media and the plastic chambers were removed. The slide was washed multiple times in PBS and then fixed in either -20°C methanol:acetone (1:1) or 4% paraformaldehyde (in PBS) for 10 minutes at room temperature or -20°C, respectively. Slides were then left to air dry for approximately 10 minutes. Once dry, slides were twice washed and re-hydrated with PBS then blocked and permeabilised in block buffer (5% milk powder (Marvel), 10% foetal calf serum, 0.5% bovine serum albumin and 0.1% Triton X-100 in PBS) for 1 hour. All incubations from this point were carried out in a moist, dark box. Block buffer was removed with multiple PBS washes, prior to addition of 1° antibody (see Table 5.6) diluted in incubation buffer (3% BSA in PBS). For double-staining, both antibodies were added together and processed together. After 1 hour the 1° antibody incubation buffer was removed with multiple washes (0.1% Tween-20 in PBS). The appropriate anti-rabbit or –mouse fluorophore-conjugated 2° antibodies (1:200 fluorescin FITC-conjugated anti-mouse and 1:800 Cy3-[both Jackson Immuno-Research Lab] or 1:250 Alexa(GFP)-conjugated [Molecular Probes] anti-rabbit antibodies) were then diluted in incubation buffer and added to the slide for 1 hour. Slides were then washed multiple times (0.1% Tween-20 in PBS) and then the excess liquid was shaken off. Slides were then mounted in mounting solution [CitiFluor] containing 0.1µg/ml DAPI stain and sealed using nailpolish (MaxFactor). Immunofluorescence images were analysed and captured using the IPlab programme and a Nikon 'Axioplot' microscope. Confocal analysis was carried out on a Zeiss LSM 510 using sequential line scanning. The sample was scanned line by line, one wavelength at a time;

488 ηm followed by 543 ηm with pass filters in front of the two detectors (Band Pass 505-530 – Green emission and Long Pass 585 - Red). These precautions minimised the risk of overlap in fluorescence and subsequent detection with FITC and Cy3.

References

Adams, P. D., W. R. Seller, et al. (1996). Mol. Cell Biol. **16**: 6623-6633.

Agarwal, M. L., A. Agarwal, et al. (1995). Proc Natl Acad Sci U S A **92**(18): 8493-7.

Agoff, S. N., J. Hou, et al. (1993). Science **259**(5091): 84-7.

Aladjem, M. I., B. T. Spike, et al. (1998). Curr Biol **8**(3): 145-55.

Alkhalaf, M., G. Ganguli, et al. (1999). Oncogene **18**(7): 1419-34.

Allan, L. A. and M. Fried (1999). Oncogene **18**(39): 5403-12.

Alnemri, E. S., D. J. Livingston, et al. (1996). Cell **87**: 171.

Amundson, S. A., T. G. Myers, et al. (1998). Oncogene **17**(25): 3287-99.

Andres, J. L., S. Fan, et al. (1998). Oncogene **16**(17): 2229-41.

Ashcroft, M., M. H. Kubbutat, et al. (1999). Mol Cell Biol **19**(3): 1751-8.

Askew, D. S., R. A. Ashmun, et al. (1991). Oncogene **6**: 1915-1922.

Attardi, L. D., S. W. Lowe, et al. (1996). Embo J **15**(14): 3693-701.

Avantaggiati, M. L., V. Ogryzko, et al. (1997). Cell **89**(7): 1175-84.

Bakalkin, G., G. Selivanova, et al. (1995). Nucleic Acids Res **23**(3): 362-9.

Bakalkin, G., T. Yakovleva, et al. (1994). Proc Natl Acad Sci U S A **91**(1): 413-7.

Baker, S., E. Fearon, et al. (1989). Science **249**: 217-221.

Baker, S. J., S. Markowitz, et al. (1990). Science **249**(4971): 912-5.

Balagurumoorthy, P., H. Sakamoto, et al. (1995). Proc Natl Acad Sci U S A **92**(19): 8591-5.

Balint, E., S. Bates, et al. (1999). Oncogene **18**(27): 3923-9.

Ball, K. L., S. Lain, et al. (1997). Curr. Biol. **7**: 71-80.

Ballester, R., D. Marchuk, et al. (1990). Cell **63**: 851-859.

Barak, Y., E. Gottlieb, et al. (1994). Genes Dev **8**(15): 1739-49.

Barak, Y., T. Juven, et al. (1993). Embo J **12**(2): 461-8.

Bargonetti, J., A. Chicas, et al. (1997). Cell Mol Biol (Noisy-le-grand) **43**(7): 935-49.

Bargonetti, J., J. J. Manfredi, et al. (1993). Genes Dev **7**(12B): 2565-74.

Barinaga, M. (1997). Science **278**(5340): 1036-9.

Bates, S., A. C. Phillips, et al. (1998). Nature **395**(6698): 124-5.

Baudier, J., C. Delphin, et al. (1992). Proc Natl Acad Sci U S A **89**(23): 11627-31.

Bayle, J. H., B. Elenbaas, et al. (1995). Proc Natl Acad Sci U S A **92**(12): 5729-33.

Beer-Romero, P., S. Glass, et al. (1997). Oncogene **14**(5): 595-602.

Beham, A., M. C. Marin, et al. (1997). Oncogene **15**(23): 2767-72.

Ben-Yosef, T., O. Yanuka, et al. (1998). Oncogene **17**(2): 165-71.

Benedict, W. F., A. L. Murphree, et al. (1983). Science **219**: 973-975.

Benveniste, P. and A. Cohen (1995). Proc Natl Acad Sci U S A **92**(18): 8373-7.

Berberich, S. and M. Cole (1994). Oncogene **9**: 1469-1472.

Bhat, M. K., C. Yu, et al. (1997). J Biol Chem **272**(46): 28989-93.

Bienz-Tadmor, B., R. Zakut-Houri, et al. (1985). EMBO Journal **4**: 3209-3213.

Bilinski, S. M. and B. Bilinska (1996). Histochem J **28**(9): 651-6.

Billiau, A. (1977). Antimicrob. Agents Chemother. **12**: 11-15.

Bischoff, J. R., P. N. Friedman, et al. (1990). Proc Natl Acad Sci U S A **87**(12): 4766-70.

Bischoff, J. R., D. H. Kirn, et al. (1996). Science **274**(5286): 373-6.

Bissonnette, N. and D. J. Hunting (1998). Oncogene **16**(26): 3461-9.

Blagosklonny, M. V., W. G. An, et al. (1998). J Biol Chem **273**(20): 11995-8.

Blagosklonny, M. V., G. S. Wu, et al. (1996). Biochem Biophys Res Commun **227**(2): 564-9.

Blaszyk, H., A. Hartmann, et al. (1996). Oncogene **13**(10): 2159-66.

Blattner, C., A. Sparks, et al. (1999). Mol Cell Biol **19**(5): 3704-13.

Blattner, C., E. Tobiasch, et al. (1999). Oncogene **18**(9): 1723-32.

Blaydes, J. P., V. Gire, et al. (1997). Oncogene **14**(15): 1859-68.

Blaydes, J. P. and T. R. Hupp (1998). Oncogene **17**(8): 1045-52.

Boddy, K. L., P. S. Freemont, et al. (1994). Trends Biochem. Sci. **19**: 198-199.

Boddy, M. N., K. Howe, et al. (1996). Oncogene **13**: 971-982.

Bogerd, H. P., R. A. Fridell, et al. (1996). Mol. Cell Biol. **16**: 4207-4214.

Bottger, A., V. Bottger, et al. (1997). J Mol Biol **269**(5): 744-56.

Bottger, A., V. Bottger, et al. (1997). Curr Biol **7**(11): 860-9.

Bottger, V., A. Bottger, et al. (1999). Oncogene **18**(1): 189-99.

Brachmann, R. K., M. Vidal, et al. (1996). Proc Natl Acad Sci U S A **93**(9): 4091-5.

Brady, H. J., G. S. Salomons, et al. (1996). Embo J **15**(6): 1221-30.

Brain, R. and J. R. Jenkins (1994). Oncogene **9**(6): 1775-80.

Brown, D. R., C. A. Thomas, et al. (1998). Embo J **17**(9): 2513-25.

Brugarolas, J., C. Chandrasekaran, et al. (1995). Nature **377**(6549): 552-7.

Buchhop, S., M. K. Gibson, et al. (1997). Nucleic Acids Res **25**(19): 3868-74.

Buckbinder, L., R. Talbott, et al. (1995). Nature **377**(6550): 646-9.

Bueso-Ramos, C. E., Y. Yang, et al. (1993). Blood **82**(9): 2617-23.

Butz, K., C. Geisen, et al. (1998). Oncogene **17**(6): 781-7.

Caelles, C., A. Helmberg, et al. (1994). Nature **370**(6486): 220-3.

Cahilly-Snyder, L., T. Yang-Feng, et al. (1987). Somatic Cell Mol **13**: 235-244.

Calmels, S., P. Hainaut, et al. (1997). Cancer Res **57**(16): 3365-9.

Candau, R., D. M. Scolnick, et al. (1997). Oncogene **15**(7): 807-16.

Canman, C. E., T. M. Gilmer, et al. (1995). Genes Dev **9**(5): 600-11.

Canman, C. E. and M. B. Kastan (1998). Oncogene **16**(8): 957-66.

Canman, C. E., D. S. Lim, et al. (1998). Science **281**(5383): 1677-9.

Caron de Fromentel, C. and T. Soussi (1992). Genes Chromosomes and Cancer **4**: 1-15.

Carroll, P. E., M. Okuda, et al. (1999). Oncogene **18**(11): 1935-44.

Carvalho, T., J. S. Seeler, et al. (1995). J. Cell Biol. **131**: 45-56.

Casiano, C. A., S. J. Martin, et al. (1996). J. Exp. Med. **184**: 765-770.

Cayrol, C., M. Knibiehler, et al. (1998). Oncogene **16**(3): 311-20.

Chandar, N., B. Billig, et al. (1992). Br J Cancer **65**(2): 208-14.

Chang, T. H., F. A. Ray, et al. (1997). Oncogene **14**(20): 2383-93.

Chang, Y. C., Y. S. Lee, et al. (1998). Cell Growth Differ **9**(1): 79-84.

Chellappan, S. P., S. Hiebert, et al. (1991). Cell **65**: 1053-1061.

Chen, C. A., Y. H. Chen, et al. (1994). Carcinogenesis **15**(10): 2221-3.

Chen, C. Y., J. D. Oliner, et al. (1994). Proc Natl Acad Sci U S A **91**(7): 2684-8.

Chen, J., V. Marechal, et al. (1993). Mol Cell Biol **13**(7): 4107-14.

Chen, J., X. Wu, et al. (1996). Mol Cell Biol **16**(5): 2445-52.

Chen, L., V. Marechal, et al. (1997). J Biol Chem **272**(36): 22966-73.

Chen, P. L., Y. M. Chen, et al. (1990). Science **250**(4987): 1576-80.

Chenevix-Trench, G., N. G. Martin, et al. (1990). Oncogene **5**(8): 1187-93.

Chin, K. V., K. Ueda, et al. (1992). Science **255**: 459-462.

Cho, Y., S. Gorina, et al. (1994). Science **265**(5170): 346-55.

Clarke, A. R., C. A. Purdie, et al. (1993). Nature **362**(6423): 849-52.

Clayman, G. L., A. K. el-Naggar, et al. (1998). J Clin Oncol **16**(6): 2221-32.

Clore, G. M., J. Ernst, et al. (1995). Nat Struct Biol **2**(4): 321-33.

Cohen, G. B., R. Ren, et al. (1995). Cell **80**: 237-248.

Conradt, B. and H. R. Horovitz (1998). Cell **93**: 518-529.

Cordon-Cardo, C., E. Latres, et al. (1994). Cancer Res **54**(3): 794-9.

Crook, T., J. A. Tidy, et al. (1991). Cell **67**(3): 547-56.

Cross, S. M., C. A. Sanchez, et al. (1995). Science **267**(5202): 1353-6.

Dameron, K. M., O. V. Volpert, et al. (1994). Science **265**(5178): 1582-4.

Dang, C. and W. Lee (1989). The Journal of Biological Chemistry **264**: 18019-18023.

David-Pfeuty, T., F. Chakrani, et al. (1996). Cell Growth Differ **7**(9): 1211-25.

Dazard, J. E., D. Augias, et al. (1997). Oncogene **14**(9): 1123-8.

de Stanchina, E., M. E. McCurrach, et al. (1998). Genes Dev **12**(15): 2434-42.

Debbas, M. and E. White (1993). Genes Dev **7**(4): 546-54.

DeGregori, J., T. Kowalik, et al. (1995). Mol. Cell. Biol. **15**: 4215-4224.

DeGregori, J., G. Leone, et al. (1997). Proc. Natl. Acad. Sci. USA **94**(7245-7250).

Del Sal, G., E. M. Ruaro, et al. (1995). Mol Cell Biol **15**(12): 7152-60.

Delic, J., P. Masdehors, et al. (1998). Br J Cancer **77**(7): 1103-7.

Deng, C., P. Zhang, et al. (1995). Cell **82**(4): 675-84.

Desdouets, C., C. Ory, et al. (1996). FEBS Lett **385**(1-2): 34-8.

Desterro, J. M., M. S. Rodriguez, et al. (1998). Mol Cell **2**(2): 233-9.

Di Leonardo, A., S. P. Linke, et al. (1994). Genes Dev **8**(21): 2540-51.

Diller, L., J. Kassel, et al. (1990). Mol Cell Biol **10**(11): 5772-81.

Dimri, G. P., K. Itahana, et al. (2000). Mol Cell Biol **20**(1): 273-85.

Dittmer, D., S. Pati, et al. (1993). Nat Genet **4**(1): 42-6.

Dobner, T., N. Horikoshi, et al. (1996). Science **272**(5267): 1470-3.

Donahue, B. A., S. Yin, et al. (1994). Proc. Natl. Acad. Sci. USA **91**: 8502-8506.

Donehower, L. A., L. A. Godley, et al. (1995). Genes Dev **9**(7): 882-95.

Donehower, L. A., M. Harvey, et al. (1992). Nature (London) **356**: 215-221.

Dracopoli, N. C., P. Harnett, et al. (1989). Cell **75**: 817-825.

Dragovich, T., C. M. Rudin, et al. (1998). Oncogene **17**(25): 3207-13.

Dubs-Poterszman, M. C., B. Tocque, et al. (1995). Oncogene **11**(11): 2445-9.

Dumaz, N. and D. W. Meek (1999). Embo J **18**(24): 7002-10.

Duprez, E., A. J. Saurin, et al. (1999). J. Cell Sci. **112**: 381-393.

Dutta, A., J. M. Ruppert, et al. (1993). Nature **365**(6441): 79-82.

Dyck, J. A., G. G. Maul, et al. (1994). Cell **76**: 333-343.

Eckner, R., J. W. Ludlow, et al. (1996). Mol. Cell. Biol. **16**: 3454-3464.

El-Deiry, W., S. Kern, et al. (1992). Nature Genetics **1**: 45-49.

El-Deiry, W. S., J. W. Harper, et al. (1994). Cancer Res **54**(5): 1169-74.

El-Deiry, W. S., T. Tokino, et al. (1993). Cell **75**(4): 817-25.

Elenbaas, B., M. Dobbelstein, et al. (1996). Mol Med **2**(4): 439-51.

Eliyahu, D., D. Michalovitz, et al. (1989). Proc. Natl. Acad. Sci. USA. **86**: 8763-8767.

Eliyahu, D., A. Raz, et al. (1984). Nature **312**: 646-649.

Elkind, N. B., N. Goldfinger, et al. (1995). Oncogene **11**(5): 841-51.

Elledge, S. J. (1996). Science **274**: 1664-1672.

Enari, M., H. Hug, et al. (1995). Nature **375**: 78-81.

Evans, G. I., A. H. Wyllie, et al. (1992). Cell **69**: 119-128.

Fakharzadeh, S. S., S. P. Trusko, et al. (1991). Embo J **10**(6): 1565-9.

Fan, S., M. L. Smith, et al. (1995). Cancer Res **55**(8): 1649-54.

Fanger, G., P. Gerwins, et al. (1997). Curr. Opin. Genet. Dev. **7**: 67-74.

Fearon, E. R., S. R. Hamilton, et al. (1987). Science **238**: 193-197.

Feinberg, A. P. and B. Vogelstein (1984). Anal Biochem **137**(1): 266-7.

Feitelson, M. A., M. Zhu, et al. (1993). Oncogene **8**(5): 1109-17.

Fenteany, G. and S. L. Schreiber (1998). J Biol Chem **273**(15): 8545-8.

Fenteany, G., R. F. Standaert, et al. (1995). Science **268**: 726-731.

Fiddler, T. A., L. Smith, et al. (1996). Mol Cell Biol **16**(9): 5048-57.

Fields, S. and S. K. Jang (1990). Science **249**(4972): 1046-9.

Finlay, C., P. Hinds, et al. (1989). Cell **57**(1083-1093).

Finlay, C. A. (1993). Mol Cell Biol **13**(1): 301-6.

Finley, D., B. Bartel, et al. (1989). Nature **338**(6214): 394-401.

Fiscella, M., H. Zhang, et al. (1997). Proc Natl Acad Sci U S A **94**(12): 6048-53.

Fischer, U., J. Huber, et al. (1995). Cell **82**: 475-483.

Florenes, V. A., G. M. Maelandsmo, et al. (1994). J Natl Cancer Inst **86**(17): 1297-302.

Ford, J. C. (1994). Science **265**(533-535).

Ford, J. M. and P. C. Hanawalt (1995). Proc Natl Acad Sci U S A **92**(19): 8876-80.

Ford, J. M. and P. C. Hanawalt (1997). J Biol Chem **272**(44): 28073-80.

Fornace, A. J. J. (1992). Annu. Rev. Genet. **26**: 507-526.

Fornerod, M., M. Ohno, et al. (1997). Cell **90**: 1051-1060.

Forrester, K., S. Ambs, et al. (1996). Proc Natl Acad Sci U S A **93**(6): 2442-7.

Fraser, A. and G. Evan (1996). Cell **85**(781-784).

Freedman, D. A., C. B. Epstein, et al. (1997). Mol Med **3**(4): 248-59.

Freedman, D. A. and A. J. Levine (1998). Mol Cell Biol **18**(12): 7288-93.

Freytag, S. O., K. R. Rogulski, et al. (1998). Hum Gene Ther **9**(9): 1323-33.

Friedlander, P., Y. Haupt, et al. (1996). Mol Cell Biol **16**(9): 4961-71.

Friedman, P. N., X. Chen, et al. (1993). Proc Natl Acad Sci U S A **90**(8): 3319-23.

Fritsche, M., C. Haessler, et al. (1993). Oncogene **8**(2): 307-18.

Fritsche, M., M. Mundt, et al. (1998). Mol Cell Endocrinol **143**(1-2): 143-54.

Fu, L. and S. Benchimol (1997). Embo J **16**(13): 4117-25.

Fu, L., W. Ma, et al. (1999). Oncogene **18**(47): 6419-24.

Fuchs, S. Y., V. Adler, et al. (1998). Genes Dev **12**(17): 2658-63.

Fuchs, S. Y., L. Dolan, et al. (1996). Oncogene **13**: 1531-1535.

Fuchs, S. Y., B. Xie, et al. (1997). J. Biol. Chem. **272**: 32163-32168.

Fukada, M., S. Asano, et al. (1997). Nature **390**: 308-311.

Fukasawa, K., T. Choi, et al. (1996). Science **271**(5256): 1744-7.

Fukuchi, K., H. Maruyama, et al. (1999). Biochim Biophys Acta **1451**(1): 206-10.

Funk, W., D. Pak, et al. (1992). Molecular and Cellular Biology **12**: 2866-2871.

Furlong, E. E., T. Rein, et al. (1996). Mol Cell Biol **16**(10): 5933-45.

Furuhata, T., T. Tokino, et al. (1996). Oncogene **13**(9): 1965-70.

Gadbois, D. M., E. M. Bradbury, et al. (1997). Cancer Res **57**(6): 1151-6.

Gannon, J. V., R. Greaves, et al. (1990). Embo J **9**(5): 1595-602.

Gannon, J. V. and D. P. Lane (1991). Nature **349**(6312): 802-6.

Garkavtsev, I., I. A. Grigorian, et al. (1998). Nature **391**(6664): 295-8.

Garkavtsev, I. A., A. R. Kazarov, et al. (1996). Nature Genet. **14**: 415-420.

Gartel, A. L. and A. L. Tyner (1999). Exp Cell Res **246**(2): 280-9.

Gavrieli, Y., Y. Sherman, et al. (1992). J Cell Biol **119**(3): 493-501.

Gerach, L. (1995). Cell **82**: 341-344.

Ginsberg, D., F. Mechta, et al. (1991). Proc Natl Acad Sci U S A **88**(22): 9979-83.

Ginsberg, D., D. Michael-Michalovitz, et al. (1991). Mol Cell Biol **11**(1): 582-5.

Ginsberg, D., M. Oren, et al. (1990). Oncogene **5**(9): 1285-90.

Giorello, L., L. Clerico, et al. (1998). Cancer Res **58**(16): 3654-9.

Goga, A., X. Liu, et al. (1995). Oncogene **11**(4): 791-9.

Goi, K., M. Takagi, et al. (1997). Cancer Res **57**(10): 1895-902.

Gongora, C., G. David, et al. (1997). J. Biol. Chem. **272**: 19457-19463.

Gopalkrishnan, R. V., E. W. F. Lam, et al. (1998). J Biol Chem **273**(18): 10972-8.

Gordon, G. W., G. Berry, et al. (1998). Biophys J **74**(5): 2702-13.

Gorlich, D. and I. W. Mattaj (1996). Science **271**: 1513-1518.

Gorospe, M., C. Cirielli, et al. (1997). Oncogene **14**(8): 929-35.

Gorospe, M., X. Wang, et al. (1996). Mol Cell Biol **16**(12): 6654-60.

Gorospe, M., X. Wang, et al. (1998). Mol Cell Biol **18**(3): 1400-7.

Gostissa, M., A. Hengstermann, et al. (1999). Embo J **18**(22): 6462-71.

Gottlieb, E., R. Haffner, et al. (1994). Embo J **13**(6): 1368-74.

Gottlieb, E., S. Lindner, et al. (1996). Cell Growth Differ **7**(3): 301-10.

Gottlieb, E. and M. Oren (1998). Embo J **17**(13): 3587-96.

Gottlieb, T. M. and M. Oren (1996). Biochim Biophys Acta **1287**(2-3): 77-102.

Graeber, T. G., C. Osmanian, et al. (1996). Nature **379**(6560): 88-91.

Graeber, T. G., J. F. Peterson, et al. (1994). Mol Cell Biol **14**(9): 6264-77.

Greenblatt, M. S., W. P. Bennett, et al. (1994). Cancer Res **54**(18): 4855-78.

Grimm, L. M. and B. A. Osborne (1999). Results Probl Cell Differ **23**: 209-28.

Grossman, S. R., M. Perez, et al. (1998). Mol Cell **2**(4): 405-15.

Gu, W. and R. G. Roeder (1997). Cell **90**(4): 595-606.

Gu, W., X. L. Shi, et al. (1997). Nature **387**(6635): 819-23.

Gualberto, A., K. Aldape, et al. (1998). Proc Natl Acad Sci U S A **95**(9): 5166-71.

Gualberto, A. and A. S. Baldwin, Jr. (1995). J Biol Chem **270**(34): 19680-3.

Gudas, J., H. Nguyen, et al. (1995). Oncogene **11**: 253-261.

Gudas, J. M., H. Nguyen, et al. (1995). Clin Cancer Res **1**(1): 71-80.

Guenal, I., Y. Risler, et al. (1997). J Cell Sci **110**(Pt 4): 489-95.

Gujuluva, C. N., J. H. Baek, et al. (1994). Oncogene **9**(7): 1819-27.

Hainaut, P., A. Hall, et al. (1994). Oncogene **9**(1): 299-303.

Hainaut, P., T. Hernandez, et al. (1998). Nucleic Acids Res **26**(1): 205-13.

Hainaut, P. and J. Milner (1993). Cancer Res **53**(19): 4469-73.

Hainaut, P. and J. Milner (1993). Cancer Res **53**(8): 1739-42.

Haines, D. S., J. E. Landers, et al. (1994). Mol Cell Biol **14**(2): 1171-8.

Halaban, R., E. Cheng, et al. (1998). Oncogene **16**(19): 2489-501.

Halazonetis, T. D., L. J. Davis, et al. (1993). Embo J **12**(3): 1021-8.

Halazonetis, T. D. and A. N. Kandil (1993). Embo J **12**(13): 5057-64.

Hall, S. R., L. E. Campbell, et al. (1996). Nucleic Acids Res **24**(6): 1119-26.

Harper, J. W., G. R. Adami, et al. (1993). Cell **75**: 805-816.

Harper, J. W., S. J. Elledge, et al. (1995). Mol. Biol. Cell **6**: 387-400.

Hartwell, L. H. and M. B. Kastan (1994). Science **266**(5192): 1821-8.

Harvey, M., M. J. McArthur, et al. (1993). Nat Genet **5**(3): 225-9.

Harvey, M., A. T. Sands, et al. (1993). Oncogene **8**(9): 2457-67.

Harvey, M., H. Vogel, et al. (1995). Cancer Res **55**(5): 1146-51.

Hassig, C. A., T. C. Fleischer, et al. (1997). Cell **89**: 341-347.

Haupt, Y., Y. Barak, et al. (1996). Embo J **15**(7): 1596-606.

Haupt, Y., R. Maya, et al. (1997). Nature **387**(6630): 296-9.

Haupt, Y., S. Rowan, et al. (1995). Genes Dev **9**(17): 2170-83.

Havre, P. A., J. Yuan, et al. (1995). Cancer Res **55**(19): 4420-4.

Hecker, D., G. Page, et al. (1996). Oncogene **12**(5): 953-61.

Helbing, C. C., C. Veilette, et al. (1997). Cancer Res. **57**: 1255-1258.

Hengartner, M. O. and H. R. Horovitz (1994). Cell **76**: 665-676.

Henglein, B., X. Chenivesse, et al. (1994). Proc. Natl. Acad. Sci. USA. **91**: 5490-5494.

Hermeking, H. and D. Eick (1994). Science **265**(5181): 2091-3.

Hermeking, H., J. O. Funk, et al. (1995). Oncogene **11**(7): 1409-15.

Hermeking, H., C. Lengauer, et al. (1997). Mol Cell **1**(1): 3-11.

Hershko, A. (1996). Trends. Biochem. Sci. **21**: 445-449.

Hicke, L. and H. Riezman (1996). Cell **84**: 277-287.

Hinds, P. W., C. A. Finlay, et al. (1990). Cell Growth Differ **1**(12): 571-80.

Hirai, H. and C. J. Sherr (1996). Mol. Cell. Biol. **16**: 6457-6467.

Hirsch, T., P. Marchetti, et al. (1997). Oncogene **15**: 1573-1581.

Hiyama, H., A. Lavarone, et al. (1998). Oncogene **16**(12): 1513-23.

Hochstrasser, M. (1996). Cell **84**: 813-815.

Hochstrasser, M. (1996). Annu Rev Genet **30**: 405-39.

Hofferer, M., C. Wirbelauer, et al. (1999). Nuc. Acid Res. **27**: 491-495.

Hollander, M. C., I. Alamo, et al. (1993). J Biol Chem **268**(32): 24385-93.

Hollstein, M., K. Rice, et al. (1994). Nucleic Acids Res **22**(17): 3551-5.

Honda, R., H. Tanaka, et al. (1997). FEBS Lett **420**(1): 25-7.

Horak, J. and D. H. Wolf (1997). J. Bacteriol. **179**: 1541-1549.

Horikoshi, N., A. Usheva, et al. (1995). Mol Cell Biol **15**(1): 227-34.

Howes, K. A., N. Ransom, et al. (1994). Genes Dev **8**(11): 1300-10.

Hsiao, M., J. Low, et al. (1994). Am J Pathol **145**(3): 702-14.

Hsieh, J. K., F. S. Chan, et al. (1999). Mol Cell **3**(2): 181-93.

Huang, L. C., K. C. Clarkin, et al. (1996). Proc Natl Acad Sci U S A **93**(10): 4827-32.

Huang, S., T. J. Deerinck, et al. (1997). J. Cell Biol. **137**: 965-974.

Hudson, J. M., R. Frade, et al. (1995). DNA and Cellular Biology **14**: 759-766.

Huibregtse, J. M., M. Scheffner, et al. (1991). Embo J **10**(13): 4129-35.

Hupp, T. R. and D. P. Lane (1994). Curr Biol **4**(10): 865-75.

Hupp, T. R., D. W. Meek, et al. (1992). Cell **71**(5): 875-86.

Hupp, T. R., A. Sparks, et al. (1995). Cell **83**(2): 237-45.

Ibrahim, A. P., P. H. Gallimore, et al. (1997). Biochim Biophys Acta **1350**(3): 306-16.

Imajoh-Ohmi, S., T. Kawaguchi, et al. (1995). Biochem Biophys Res Commun **217**(3): 1070-7.

Inoue, K. and C. J. Sherr (1998). Mol. Cell. Biol. **18**: 1590-1600.

Ip, Y. T. and R. J. Davis (1998). Curr. Opin. Cell. Biol. **10**: 205-219.

Isfort, R. J., D. B. Cody, et al. (1995). Mol Carcinog **14**(3): 170-8.

Ishioka, C., H. Shimodaira, et al. (1997). Biochem Biophys Res Commun **232**(1): 54-60.

Ishioko, C., C. Engler, et al. (1993). Oncogene **10**: 1485-1492.

Ishizaki, K., Y. Ejima, et al. (1994). Int J Cancer **58**(2): 254-7.

Israeli, D., E. Tessler, et al. (1997). Embo J **16**(14): 4384-92.

Itoh, N., Y. Tsujimoto, et al. (1993). J. Immunol. **151**: 621-627.

Iwabuchi, K., P. L. Bartel, et al. (1994). Proc Natl Acad Sci U S A **91**(13): 6098-102.

Jacks, T., L. Remington, et al. (1994). Curr Biol **4**(1): 1-7.

Jackson, S. P. (1996). Cancer Surv. **28**: 261-279.

Jarpe, M. B., C. Widmann, et al. (1998). Oncogene **17**(11 Reviews): 1475-82.

Jayaraman, J. and C. Prives (1995). Cell **81**(7): 1021-9.

Jayaraman, L., N. C. Moorthy, et al. (1998). Genes Dev **12**(4): 462-72.

Jayaraman, L., K. G. Murthy, et al. (1997). Genes Dev **11**(5): 558-70.

Jeffrey, P. D., S. Gorina, et al. (1995). Science **267**(5203): 1498-502.

Jenkins, J. R., K. Rudge, et al. (1984). Nature **312**: 651-654.

Jentsch, S. and S. Schlenker (1995). Cell **82**: 881-884.

Johnson, D. G., J. K. Schwartz, et al. (1993). Nature **365**: 349-352.

Johnson, D. G., J. K. Schwarz, et al. (1993). Nature **365**(6444): 349-52.

Johnson, P., S. Chung, et al. (1993). Mol Cell Biol **13**(3): 1456-63.

Jones, J. M., L. Attardi, et al. (1997). Cell Growth Differ **8**(8): 829-38.

Jones, S. N., M. A. Ansari-Lari, et al. (1996). Gene **175**(1-2): 209-13.

Jones, S. N., A. R. Hancock, et al. (1998). Proc Natl Acad Sci U S A **95**(26): 15608-12.

Jones, S. N., A. E. Roe, et al. (1995). Nature **378**(6553): 206-8.

Jost, C. A., M. C. Marin, et al. (1997). Nature **389**(6647): 191-4.

Ju, J., J. Pedersen-Lane, et al. (1999). Proc Natl Acad Sci U S A **96**(7): 3769-74.

Juven, T., Y. Barak, et al. (1993). Oncogene **8**(12): 3411-6.

Juven-Gershon, T., O. Shifman, et al. (1998). Mol Cell Biol **18**(7): 3974-82.

Kaghad, M., H. Bonnet, et al. (1997). Cell **90**(4): 809-19.

Kamei, Y., L. Xu, et al. (1996). Cell **85**: 403-414.

Kamijo, T., J. D. Weber, et al. (1998). Proc Natl Acad Sci U S A **95**(14): 8292-7.

Kamijo, T., F. Zindy, et al. (1997). Cell **91**: 649-659.

Kao, C. C., P. R. Yew, et al. (1990). Virology **179**(2): 806-14.

Kastan, M. B., O. Onyekwere, et al. (1991). Cancer Res **51**(23 Pt 1): 6304-11.

Kastan, M. B., Q. Zhan, et al. (1992). Cell **71**(4): 587-97.

Katahira, J., T. Ishizaki, et al. (1995). J. Virol. **69**: 3125-3133.

Kato, M. V., H. Sato, et al. (1997). Blood **90**(4): 1373-8.

Kazantsev, A. and A. Sancar (1995). Science **270**(5238): 1003-4; discussion 1005-6.

Kearsey, J. M., P. J. Coates, et al. (1995). Oncogene **11**: 1675-1683.

Kearsey, J. M., M. K. Shivji, et al. (1995). Science **270**(5238): 1004-5; discussion 1005-6.

Kelman, Z. (1997). Oncogene **14**: 629-640.

Kern, S. E., K. W. Kinzler, et al. (1991). Science **252**(5013): 1708-11.

Kerr, J. F. K., A. H. Wyllie, et al. (1972). British Journal of Cancer **26**: 239-245.

Khanna, K. K. and M. F. Lavin (1993). Oncogene **8**(12): 3307-12.

Khatib, Z. A., H. Matsushime, et al. (1993). Cancer Res **53**(22): 5535-41.

Kim, E., N. Albrechtsen, et al. (1997). Oncogene **15**(7): 857-69.

Kitagawa, H., E. Tani, et al. (1999). FEBS Lett **443**(2): 181-6.

Klotzsche, O., D. Etzrodt, et al. (1998). Oncogene **16**(26): 3423-34.

Knippschild, U., M. Oren, et al. (1996). Oncogene **12**(8): 1755-65.

Ko, L. J. and C. Prives (1996). Genes Dev **10**(9): 1054-72.

Kobayashi, T., U. Consoli, et al. (1995). Oncogene **11**(11): 2311-6.

Kolling, R. and S. Losko (1997). EMBO J. **16**: 2251-2261.

Kolodner, R. D. and G. T. Marsischky (1999). Curr Opin Genet Dev **9**(1): 89-96.

Kondo, S., B. P. Barna, et al. (1996). Oncogene **13**(6): 1279-85.

Kondo, S., G. H. Barnett, et al. (1995). Oncogene **10**(10): 2001-6.

Kondo, S., Y. Kondo, et al. (1996). Br J Cancer **74**(8): 1263-8.

Kondo, Y., S. Kondo, et al. (1997). Exp Cell Res **236**(1): 51-6.

Kowalik, T. F., J. DeGregori, et al. (1998). Cell Growth Differ **9**(2): 113-8.

Kowalik, T. F., J. DeGregori, et al. (1995). J Virol **69**(4): 2491-500.

Kozak, M. (1981). Nucleic Acids Res **9**(20): 5233-62.

Kubbutat, M. H., S. N. Jones, et al. (1997). Nature **387**(6630): 299-303.

Kubbutat, M. H., R. L. Ludwig, et al. (1998). Mol Cell Biol **18**(10): 5690-8.

Kubbutat, M. H., R. L. Ludwig, et al. (1999). Cell Growth Differ **10**(2): 87-92.

Kubbutat, M. H. and K. H. Vousden (1997). Mol Cell Biol **17**(1): 460-8.

Kulesz-Martin, M. F., B. Lisafeld, et al. (1994). Mol Cell Biol **14**(3): 1698-708.

Kurdistani, S. K., P. Arizti, et al. (1998). Cancer Res **58**(19): 4439-44.

Kurokawa, K., T. Tanaka, et al. (1999). Oncogene **18**(17): 2718-27.

Kussie, P. H., S. Gorina, et al. (1996). Science **274**(5289): 948-53.

Ladanyi, M., R. Lewis, et al. (1995). J. Pathol **175**: 211-217.

Laherty, C. D., W.-M. Yang, et al. (1997). Cell **89**: 349-356.

Lain, S., C. Midgley, et al. (1999). Exp Cell Res **248**(2): 457-72.

Lakin, N. D., B. C. Hann, et al. (1999). Oncogene **18**: 3989-3995.

Lam, Y. A., W. Xu, et al. (1997). Nature **385**(6618): 737-40.

Lamb, P. and L. Crawford (1986). Mol. Cell. Biol. **6**: 1379-1285.

Land, H., L. F. Parada, et al. (1983). Nature **304**: 596-602.

Landers, J. E., S. L. Cassel, et al. (1997). Cancer Res **57**(16): 3562-8.

Landers, J. E., D. S. Haines, et al. (1994). Oncogene **9**(9): 2745-50.

Lane, D. (1992). Nature **358**: 15-16.

Lane, D. P. and L. Crawford (1979). Nature **278**: 261-263.

Lanni, J. S. and T. Jacks (1998). Mol Cell Biol **18**(2): 1055-64.

Lavau, C., A. Marchio, et al. (1995). Oncogene **11**: 871-876.

Leach, S. D., C. D. Scatena, et al. (1998). Cancer Res **58**(15): 3231-6.

Lee, S., B. Elenbaas, et al. (1995). Cell **81**(7): 1013-20.

Lee, T. C., L. Li, et al. (1997). Proc. Natl. Acad. Sci. USA **94**: 12866-12891.

Lee, W., T. S. Harvey, et al. (1994). Nat Struct Biol **1**(12): 877-90.

Lees-Miller, S. P., Y. R. Chen, et al. (1990). Mol Cell Biol **10**(12): 6472-81.

Lehar, S. M., M. Nacht, et al. (1996). Oncogene **12**(6): 1181-7.

Leonhardt, H., A. W. Page, et al. (1992). Cell **71**: 865-873.

Leveillard, T., L. Andera, et al. (1996). Embo J **15**(7): 1615-24.

Leveillard, T. and B. Wasylyk (1997). J Biol Chem **272**(49): 30651-61.

Levkau, B., H. Koyama, et al. (1999). Mol. Cell **1**: 553-563.

Li, F. and J. J. Fraumeni (1969). Annals of Internal Medicine **71**: 747-752.

Li, P., D. Nijhawan, et al. (1997). Cell **91**: 479-489.

Li, R., S. Waga, et al. (1994). Nature **371**(6497): 534-7.

Li, Z., A. Rakkar, et al. (1998). Gene Ther **5**(5): 605-13.

Lill, N. L., S. R. Grossman, et al. (1997). Nature **387**(6635): 823-7.

Lin, J., J. Chen, et al. (1994). Genes Dev **8**(10): 1235-46.

Lin, J., X. Wu, et al. (1995). Cold Spring Harbour Symposia on Quantitative Biology ***LIX***: 215-223.

Linke, S. P., K. C. Clarkin, et al. (1996). Genes Dev **10**(8): 934-47.

Linke, S. P., K. C. Clarkin, et al. (1997). Cancer Res **57**(6): 1171-9.

Linzer, D. I. and A. J. Levine (1979). Cell **17**: 43-52.

Liu, P. K., E. Kraus, et al. (1996). Oncogene **12**(11): 2267-78.

Livingstone, L. R., A. White, et al. (1992). Cell **70**: 923-935.

Ljungman, M. and P. C. Hanawalt (1992). Mol Carcinog **5**(4): 264-9.

Ljungman, M. and P. C. Hanawalt (1995). Nucleic Acids Res **23**(10): 1782-9.

Ljungman, M. and F. Zhang (1996). Oncogene **13**(4): 823-31.

Lomax, M. E., D. M. Barnes, et al. (1998). Oncogene **17**(5): 643-9.

Lowe, S. W. and H. E. Ruley (1993). Genes Dev **7**(4): 535-45.

Lowe, S. W., H. E. Ruley, et al. (1993). Cell **74**(6): 957-67.

Lowe, S. W., E. M. Schmitt, et al. (1993). Nature **362**(6423): 847-9.

Lu, H., R. P. Fisher, et al. (1997). Mol Cell Biol **17**(10): 5923-34.

Lu, H. and A. J. Levine (1995). Proc Natl Acad Sci U S A **92**(11): 5154-8.

Lu, X., S. A. Burbidge, et al. (1996). Oncogene **13**: 413-418.

Lu, X. and D. P. Lane (1993). Cell **75**(4): 765-78.

Lu, Y., N. Yamagishi, et al. (1998). Oncogene **16**(6): 705-12.

Luchnik, A. N., T. A. Hisamutdinov, et al. (1988). Nucleic Acids Res **16**(11): 5175-90.

Ludwig, R. L., S. Bates, et al. (1996). Mol Cell Biol **16**(9): 4952-60.

Lundgren, K., R. Montes de Oca Luna, et al. (1997). Genes Dev **11**(6): 714-25.

Luo, R. X., A. A. Postigo, et al. (1998). Cell **92**: 463-473.

Lutzker, S. G. and A. J. Levine (1996). Nat Med **2**(7): 804-10.

Mack, D. H., J. Vartikar, et al. (1993). Nature **363**(6426): 281-3.

Macleod, K. F., N. Sherry, et al. (1995). Genes Dev **9**(8): 935-44.

Maheswaran, S., S. Park, et al. (1993). Proc Natl Acad Sci U S A **90**(11): 5100-4.

Maki, C. G. (1999). J Biol Chem **274**(23): 16531-5.

Maki, C. G. and P. M. Howley (1997). Mol Cell Biol **17**(1): 355-63.

Maki, C. G., J. M. Huibregtse, et al. (1996). Cancer Res **56**(11): 2649-54.

Malkin, D. (1994). Biochim Biophys Acta **1198**(2-3): 197-213.

Malkin, D., F. P. Li, et al. (1990). Science **250**(4985): 1233-8.

Maltzman, W. and L. Czyzyk (1984). Mol. Cell Biol. **4**: 1689-1694.

Marechal, V., B. Elenbaas, et al. (1994). Mol Cell Biol **14**(11): 7414-20.

Marechal, V., B. Elenbaas, et al. (1997). Oncogene **14**(12): 1427-33.

Marhin, W., S. Chen, et al. (1997). Oncogene **14**(2825-2834).

Marks, D. I., E. C. Vonderheid, et al. (1996). Br J Haematol **92**(4): 890-9.

Marston, N. J., T. Crook, et al. (1994). Oncogene **9**(9): 2707-16.

Marston, N. J., J. R. Jenkins, et al. (1995). Oncogene **10**(9): 1709-15.

Martin, K., D. Trouche, et al. (1995). Nature **375**(6533): 691-4.

Martinez, J. D., M. T. Craven, et al. (1997). Oncogene **14**(21): 2511-20.

Matsumoto, R., M. Tada, et al. (1998). Cancer Res **58**(4): 609-13.

Matsushime, H., M. E. Ewen, et al. (1992). Cell **71**: 323-334.

Mayo, L. D., J. J. Turchi, et al. (1997). Cancer Res **57**(22): 5013-6.

McAllister, R. M. (1971). Cancer **27**: 397-402.

McCormack, S. J., Z. Weaver, et al. (1998). Oncogene **16**(21): 2755-66.

McDonald, E., G. S. Wu, et al. (1996). Cancer Res. **56**: 2250-2255.

McKay, B. C., M. Ljungman, et al. (1998). Oncogene **17**(5): 545-55.

McLure, K. G. and P. W. Lee (1998). Embo J **17**(12): 3342-50.

Medema, R. H., R. Klompmaker, et al. (1998). Oncogene **16**(4): 431-41.

Meek, D. W. (1998). Cell Signal **10**(3): 159-66.

Meek, D. W., S. Simon, et al. (1990). Embo J **9**(10): 3253-60.

Mellon, I., G. Spivak, et al. (1987). Cell **51**: 241-249.

Mercer, W. E., M. Amin, et al. (1990). Oncogene **5**(7): 973-80.

Mercer, W. E., M. T. Shields, et al. (1990). Proc Natl Acad Sci U S A **87**(16): 6166-70.

Middeler, G., K. Zerf, et al. (1997). Oncogene **14**(12): 1407-17.

Midgley, C. A. and D. P. Lane (1997). Oncogene **15**(10): 1179-89.

Midgley, C. A., B. Owens, et al. (1995). J Cell Sci **108**(Pt 5): 1843-8.

Milne, D. M., D. G. Campbell, et al. (1994). J Biol Chem **269**(12): 9253-60.

Milne, D. M., L. E. Campbell, et al. (1995). J Biol Chem **270**(10): 5511-8.

Milne, D. M., R. H. Palmer, et al. (1992). Nucleic Acids Res **20**(21): 5565-70.

Milner, J., A. Cook, et al. (1990). Embo J **9**(9): 2885-9.

Milner, J. and E. A. Medcalf (1991). Cell **65**(5): 765-74.

Milner, J., E. A. Medcalf, et al. (1991). Mol Cell Biol **11**(1): 12-9.

Mirzayans, R., L. Enns, et al. (1996). Carcinogenesis **17**(4): 691-8.

Misteli, T., J. F. Caceres, et al. (1997). Nature **387**: 523-527.

Miura, M., H. Zhu, et al. (1993). Cell **75**(4): 653-60.

Miyashita, T., M. Harigai, et al. (1994). Cancer Res **54**(12): 3131-5.

Miyashita, T., S. Krajewski, et al. (1994). Oncogene **9**(6): 1799-805.

Miyashita, T. and J. C. Reed (1995). Cell **80**(2): 293-9.

Miyata, Y. and I. Yahara (1992). J. Bio. Chem. **267**: 7042-7047.

Moll, U. M., M. LaQuaglia, et al. (1995). Proc Natl Acad Sci U S A **92**(10): 4407-11.

Moll, U. M., A. G. Ostermeyer, et al. (1996). Mol Cell Biol **16**(3): 1126-37.

Momand, J. and G.P. Zambetti (1992). Cell **69**(7): 1237-1245.

Momand, J. and G. P. Zambetti (1997). J Cell Biochem **64**(3): 343-52.

Montes de Oca Luna, R., A. D. Tabor, et al. (1996). Genomics **33**: 352-357.

Montes de Oca Luna, R., D. S. Wagner, et al. (1995). Nature **378**(6553): 203-6.

Moore, M., N. Horikoshi, et al. (1996). Proc. Natl. Acad. Sci. USA **93**(11295-11301).

Morgan, S. E. and M. B. Kastan (1997). Adv Cancer Res **71**: 1-25.

Morgenbesser, S. D., B. O. Williams, et al. (1994). Nature **371**(6492): 72-4.

Mosner, J., T. Mummenbrauer, et al. (1995). Embo J **14**(18): 4442-9.

Mu, Z. M., K. V. Chin, et al. (1994). Mol. Cell Biol. **14**: 6858-6867.

Mu, Z. M., X. F. Le, et al. (1996). Leuk. Lymphoma **23**: 277-285.

Murphy, M., J. Ahn, et al. (1999). Genes & Dev. **13**: 2490-2501.

Murphy, M., A. Hinman, et al. (1996). Genes Dev **10**(23): 2971-80.

Nagaich, A. K., E. Appella, et al. (1997). J Biol Chem **272**(23): 14842-9.

Nagata, S. (1997). Cell **88**: 355-365.

Nagata, Y., T. Anan, et al. (1999). Oncogene **18**(44): 6037-49.

Nagy, L., H.-Y. Kao, et al. (1997). Cell **89**: 373-380.

Nelson, W. G. and M. B. Kastan (1994). Mol Cell Biol **14**(3): 1815-23.

Nevels, M., S. Rubenwolf, et al. (1997). Proc. Natl. Acad. Sci. USA **94**(2008-2012).

Nevins, J. R. and P. K. Vogt (1996). Virology, Vol.1 (Lippencott-Raven: New York): 301-343.

Niculescu, A. B., 3rd, X. Chen, et al. (1998). Mol Cell Biol **18**(1): 629-43.

Nishimori, H., T. Shiratsuchi, et al. (1997). Oncogene **15**(18): 2145-50.

Nozaki, T., M. Masutani, et al. (1997). Biochem Biophys Res Commun **233**(1): 216-20.

Nuber, U., S. E. Schwarz, et al. (1998). Eur. J. Biochem. **254**: 643-649.

Nunez, G., M. A. Benedict, et al. (1998). Oncogene **17**(25): 3237-45.

O'Connor, D. J., E. W. Lam, et al. (1995). Embo J **14**(24): 6184-92.

O'Connor, P. M. (1997). Cancer Surv **29**: 151-82.

O'Connor, P. M., J. Jackman, et al. (1997). Cancer Res **57**(19): 4285-300.

O'Connor, P. M., J. Jackman, et al. (1993). Cancer Res **53**(20): 4776-80.

Oberosler, P., P. Hloch, et al. (1993). Embo J **12**(6): 2389-96.

Okamoto, K. and D. Beach (1994). Embo J **13**(20): 4816-22.

Oleinick, N. L. (1977). Arch Biochem Biophys **182**(1): 171-80.

Oliner, J. D. (1993). Bioessays **15**(11): 703-7.

Oliner, J. D., K. W. Kinzler, et al. (1992). Nature **358**(6381): 80-3.

Oliner, J. D., J. A. Pietenpol, et al. (1993). Nature **362**(6423): 857-60.

Olson, D. C., V. Marechal, et al. (1993). Oncogene **8**(9): 2353-60.

Oltavi, Z. N., C. L. Milliman, et al. (1993). Cell **74**: 609-619.

Osada, M., M. Ohba, et al. (1998). Nat Med **4**(7): 839-43.

Ossareh-Nazari, B., F. Bachelerie, et al. (1997). Science **278**: 141-144.

Owen-Schaub, L. B., W. Zhang, et al. (1995). Mol Cell Biol **15**(6): 3032-40.

Palmero, I., C. Pantoja, et al. (1998). Nature **395**(6698): 125-6.

Pan, G., J. Ni, et al. (1997). Science **277**: 815-818.

Pan, H. and A. E. Griep (1994). Genes Dev **8**(11): 1285-99.

Pan, H., C. Yin, et al. (1998). Mol Cell **2**(3): 283-92.

Pan, Z. Q., J. T. Reardon, et al. (1995). J Biol Chem **270**(37): 22008-16.

Parada, L. F., H. Land, et al. (1984). Nature **312**: 649-651.

Pariat, M., S. Carillo, et al. (1997). Mol Cell Biol **17**(5): 2806-15.

Pavletich, N. P., K. A. Chambers, et al. (1993). Genes Dev **7**(12B): 2556-64.

Pawson, T. (1995). Nature **373**: 573-580.

Pellegata, N. S., R. J. Antoniono, et al. (1996). Proc Natl Acad Sci U S A **93**(26): 15209-14.

Peng, C. Y., P. R. Graves, et al. (1997). Science **277**: 1501-1505.

Perry, M. E., J. Piette, et al. (1993). Proc Natl Acad Sci U S A **90**(24): 11623-7.

Pesch, J., U. Brehm, et al. (1996). J Interferon Cytokine Res **16**(8): 595-600.

Peterson, J. M., J. J. Skalicky, et al. (1995). Science **269**: 1866-1869.

Phillipp, A., A. Schneider, et al. (1994). Mol. Cell. Biol. **14**: 4032-4043.

Pietenpol, J. A., T. Tokino, et al. (1994). Proc Natl Acad Sci U S A **91**(6): 1998-2002.

Piette, J., H. Neel, et al. (1997). Oncogene **15**(9): 1001-10.

Pinhasi-Kimhi, O., D. Michaalovitz, et al. (1986). Nature **320**: 182-184.

Plummer, S. J., L. Adams, et al. (1997). Oncogene **14**(19): 2339-45.

Pochampally, R., B. Fodera, et al. (1999). J Biol Chem **274**(21): 15271-7.

Pochampally, R., B. Fodera, et al. (1998). Oncogene **17**(20): 2629-36.

Polyak, K., T. Waldman, et al. (1996). Genes Dev **10**(15): 1945-52.

Polyak, K., Y. Xia, et al. (1997). Nature **389**(6648): 300-5.

Pomerantz, J., N. Schreiber-Agus, et al. (1998). Cell **92**(6): 713-23.

Ponten, J. and E. Saksela (1967). Int. J. Cancer **2**: 434-447.

Powell, S. N., J. S. DeFrank, et al. (1995). Cancer Res **55**(8): 1643-8.

Price, A. (1993). Semin Cancer Biol **4**(2): 61-71.

Price, B. D., L. Hughes-Davies, et al. (1995). Oncogene **11**(1): 73-80.

Price, B. D. and S. J. Park (1994). Cancer Res **54**(4): 896-9.

Prisco, M., A. Hongo, et al. (1997). Mol Cell Biol **17**(3): 1084-92.

Prives, C., J. Bargonetti, et al. (1994). Cold Spring Harb Symp Quant Biol **59**: 207-13.

Prokocimer, M., N. Harris, et al. (1987). Recent Advances in Leukemia Lymphoma: 164-243.

Purdie, C. A., D. J. Harrison, et al. (1994). Oncogene **9**(2): 603-9.

Qin, X. Q., D. M. Livingston, et al. (1994). Proc Natl Acad Sci U S A **91**(23): 10918-22.

Quelle, D. E., F. Zindy, et al. (1995). Cell **83**(993-1000).

Rabizadeh, S., D. J. LaCount, et al. (1993). J Neurochem **61**(6): 2318-21.

Radford, I. R. (1994). Int J Radiat Biol **66**(5): 557-60.

Radford, I. R., T. K. Murphy, et al. (1994). Int. J. Radiat. Biol. **65**: 217-227.

Rallapalli, R., G. Strachan, et al. (1999). J Biol Chem **274**(12): 8299-308.

Rao, L., M. Debbas, et al. (1992). Proc. Natl. Acad. Sci. USA **89**: 7742-7746.

Ravi, R., B. Mookerjee, et al. (1998). Cancer Res **58**(20): 4531-6.

Raycroft, L., H. Y. Wu, et al. (1990). Science **249**(4972): 1049-51.

Reed, J. C. (1997). Nature **387**: 773-776.

Reed, M., B. Woelker, et al. (1995). Proc Natl Acad Sci U S A **92**(21): 9455-9.

Reich, N. C., M. Oren, et al. (1983). Mol Cell Biol **3**(12): 2143-50.

Reihsaus, E., M. Kohler, et al. (1990). Oncogene **5**(1): 137-45.

Reinke, V., D. M. Bortner, et al. (1999). Cell Growth Differ **10**(3): 147-54.

Reisman, D., e. Balint, et al. (1996). Genomics **38**(3): 364-70.

Reisman, D., N. B. Elkind, et al. (1993). Cell Growth Differ **4**(2): 57-65.

Reisman, D., M. Greenburg, et al. (1988). Proc Natl Acad Sci USA **85**: 5146-5150.

Reisman, D. and W. T. Loging (1998). Semin Cancer Biol **8**(5): 317-24.

Renzing, J. and D. P. Lane (1995). Oncogene **10**(9): 1865-8.

Rochlitz, C. F., I. Heide, et al. (1995). Ann Oncol **6**(10): 981-6.

Rock, K. L., A. L. Goldberg, et al. (1994). Cell **78**: 761-772.

Rodriguez, A. and E. K. Flemington (1999). Analytical Biochemistry **272**: 171-181.

Rodriguez, M. S., J. M. Desterro, et al. (1999). Embo J **18**(22): 6455-61.

Rolley, N., S. Butcher, et al. (1995). Oncogene **11**(4): 763-70.

Romano, J. W., J. C. Ehrhart, et al. (1989). Oncogene **4**(12): 1483-8.

Roperch, J. P., V. Alvaro, et al. (1998). Nat Med **4**(7): 835-8.

Roth, J., M. Dobbelstein, et al. (1998). Embo J **17**(2): 554-64.

Rouault, J. P., D. Prevot, et al. (1998). J Biol Chem **273**(35): 22563-9.

Rousseau, D., D. Cannella, et al. (1999). Oncogene **18**(30): 4313-25.

Rowan, S., R. L. Ludwig, et al. (1996). Embo J **15**(4): 827-38.

Roy, B., J. Beamon, et al. (1994). Mol Cell Biol **14**(12): 7805-15.

Ruley, H. E. (1983). Nature **304**(602-606).

Ryan, J. J. and M. F. Clarke (1994). Leuk Res **18**(8): 617-21.

Sabbatini, P., J. Lin, et al. (1995). Genes Dev **9**(17): 2184-92.

Sadoul, R., P. A. Fernandez, et al. (1996). Embo J **15**(15): 3845-52.

Saido, T. C., H. Sorimachi, et al. (1994). FASEB J. **8**: 814-822.

Saitoh, H., R. T. Pu, et al. (1997). Trends. Biochem. **22**: 374-376.

Sakaguchi, K., J. E. Herrera, et al. (1998). Genes Dev **12**(18): 2831-41.

Sakaguchi, K., H. Sakamoto, et al. (1997). Biochemistry **36**(33): 10117-24.

Sakaguchi, K., H. Sakamoto, et al. (1997). J Protein Chem **16**(5): 553-6.

Sakamoto, H., M. S. Lewis, et al. (1994). Proc Natl Acad Sci U S A **91**(19): 8974-8.

Sakamuro, D., P. Sabbatini, et al. (1997). Oncogene **15**(8): 887-98.

Saller, E., E. Tom, et al. (1999). EMBO J. **18**: 4424-4437.

Sambrook, J., E. F. Fritsch, et al. (1989). Cold Spring Harbour Laboratory Press (CSH).

Sands, A. T., M. B. Suraokar, et al. (1995). Proc Natl Acad Sci U S A **92**(18): 8517-21.

Sang, B. C., J. Y. Chen, et al. (1994). Oncogene **9**(3): 853-9.

Sanger, F., S. Nicklen, et al. (1977). Proc Natl Acad Sci U S A **74**(12): 5463-7.

Santhanam, U., A. Ray, et al. (1991). Proc Natl Acad Sci U S A **88**(17): 7605-9.

Sarnow, P., P. Hearing, et al. (1984). J. Virol. **49**(692-700).

Saucedo, L. J., B. P. Carstens, et al. (1998). Cell Growth Differ **9**(2): 119-30.

Saucedo, L. J., C. D. Myers, et al. (1999). J Biol Chem **274**(12): 8161-8.

Saurin, A. J., K. L. Borden, et al. (1996). Trends Biochem. Sci. **21**: 208-214.

Savitsky, K., A. Bar-Shira, et al. (1995). Science **268**: 1749-1753.

Scheer, U. and R. Benavente (1990). Bioessays **12**: 14-21.

Scheer, U., M. Thiry, et al. (1993). Trends Cell Biol. **3**: 236-241.

Scheffner, M., J. M. Huibregtse, et al. (1993). Cell **75**(3): 495-505.

Scheffner, M., U. Nuber, et al. (1995). Nature **373**: 81-83.

Scheffner, M., T. Takahashi, et al. (1992). J. Virol. **66**: 5100-5105.

Scheffner, M., B. A. Werness, et al. (1990). Cell **63**(6): 1129-36.

Schlegel, J., I. Peters, et al. (1996). J. Biol. Chem. **271**: 1841-1844.

Schlesinger, D. H., G. Goldstein, et al. (1975). Biochemistry **14**: 2214-2218.

Schlott, T., S. Reimer, et al. (1997). J Pathol **182**(1): 54-61.

Schmale, H. and C. Bamberger (1997). Oncogene **15**(11): 1363-7.

Schott, A. F., I. J. Apel, et al. (1995). Oncogene **11**(7): 1389-94.

Schul, W., L. de Jong, et al. (1998). J Cell Biochem **70**(2): 159-71.

Schwartz, D. and V. Rotter (1998). Semin Cancer Biol **8**(5): 325-36.

Selivanova, G., V. Iotsova, et al. (1996). Nucleic Acids Res **24**(18): 3560-7.

Selvakumaran, M., H. K. Lin, et al. (1994). Oncogene **9**(6): 1791-8.

Serrano, M., H.-W. Lee, et al. (1996). Cell **85**: 27-37.

Seto, E., A. Usheva, et al. (1992). Proc Natl Acad Sci U S A **89**(24): 12028-32.

Shan, B. and w. Lee (1994). Mol. Cell. Biol. **14**: 8166-8173.

Sharp, D. A., S. A. Kratowicz, et al. (1999). J Biol Chem **274**(53): 38189-96.

Shaulian, E., I. Haviv, et al. (1995). Oncogene **10**(4): 671-80.

Shaulian, E., A. Zauberman, et al. (1993). Embo J **12**(7): 2789-97.

Shaulsky, G., A. Ben-Ze'ev, et al. (1990). Oncogene **5**(11): 1707-11.

Shaulsky, G., N. Goldfinger, et al. (1990). Mol Cell Biol **10**(12): 6565-77.

Shaw, P., J. Freeman, et al. (1996). Oncogene **12**(4): 921-30.

Shibasaki, F., E. Kondo, et al. (1997). Nature **386**: 728-731.

Shieh, S. Y., M. Ikeda, et al. (1997). Cell **91**(3): 325-34.

Shivji, K. K., S. J. Grey, et al. (1994). Curr. Biol. **4**: 1062-1068.

Shivji, K. K., M. K. Kenny, et al. (1992). Cell **69**: 367-374.

Shivji, M. K., V. N. Podust, et al. (1995). Biochemistry **34**: 5011-5017.

Shvarts, A., M. Bazuine, et al. (1997). Genomics **43**(1): 34-42.

Shvarts, A., W. T. Steegenga, et al. (1996). Embo J **15**(19): 5349-57.

Sigalas, I., A. H. Calvert, et al. (1996). Nat Med **2**(8): 912-7.

Sionov, R. V., E. Moallem, et al. (1999). J Biol Chem **274**(13): 8371-4.

Slansky, J. E. and P. J. Farnham (1996). Curr. Top. Microbiol. Immunol. **208**: 1-30.

Slingerland, J. M., J. R. Jenkins, et al. (1993). Embo J **12**(3): 1029-37.

Smith, M. L., I. T. Chen, et al. (1994). Science **266**(5189): 1376-80.

Smith, M. L., I. T. Chen, et al. (1995). Oncogene **10**(6): 1053-9.

Smith, M. L. and A. J. Fornace, Jr. (1997). Proc Natl Acad Sci U S A **94**(23): 12255-7.

Somasundaram, K. and W. S. El-Deiry (1997). Oncogene **14**(9): 1047-57.

Somasundaram, K., H. Zhang, et al. (1997). Nature **389**(6647): 187-90.

Soussi, T., C. Caron de Fromentel, et al. (1990). Oncogene **5**(7): 945-52.

Speir, E., R. Modali, et al. (1994). Science **265**(5170): 391-4.

Srivastava, S., Z. Q. Zou, et al. (1990). Nature **348**(6303): 747-9.

Stanchina, E., M. E. McCurrach, et al. (1998). Gene & Dev. **12**: 2434-2442.

Steitz, J. A., C. Berg, et al. (1988). J. Cell. Biol. **106**: 545-556.

Stenger, J., G. Mayr, et al. (1992). Mol. Carcinogenesis **5**: 102-106.

Stenger, J. E., P. Tegtmeyer, et al. (1994). Embo J **13**(24): 6011-20.

Sterndorf, T., K. Jensen, et al. (1997). J. Cell. Biol. **139**: 1621-1634.

Stewart, N., G. G. Hicks, et al. (1995). Oncogene **10**(1): 109-15.

Stillman, B. (1994). Cell **78**: 725-728.

Stommel, J. M., N. D. Marchenko, et al. (1999). Embo J **18**(6): 1660-72.

Stott, F. J., S. Bates, et al. (1998). Embo J **17**(17): 5001-14.

Stuart, E. T., R. Haffner, et al. (1995). Embo J **14**(22): 5638-45.

Sturzbecher, H.-W., R. Brain, et al. (1992). Oncogene **7**: 1513-1523.

Stuurman, N., A. de Graaf, et al. (1992). J. Cell Sci. **101**: 773-784.

Stuurman, N., A. Floore, et al. (1997). Cell. and Mol. Biol. Letters **2**: 137-150.

Sun, P., P. Dong, et al. (1998). Science **282**(5397): 2270-2.

Sun, X., H. Shimizu, et al. (1995). Mol Cell Biol **15**(8): 4489-96.

Sun, X. F., J. M. Carstensen, et al. (1992). Lancet **340**(8832): 1369-73.

Symonds, H., L. Krall, et al. (1994). Cold Spring Harb Symp Quant Biol **59**: 247-57.

Symonds, H., L. Krall, et al. (1994). Cell **78**(4): 703-11.

Szekely, L., G. Selivanova, et al. (1993). Proc Natl Acad Sci U S A **90**(12): 5455-9.

Szostecki, C., H. Krippner, et al. (1987). Clin. Exp. Immunol. **68**: 108-116.

Takei, Y., S. Ishikawa, et al. (1998). Genes Chromosomes Cancer **23**(1): 1-9.

Takenaka, I., F. Morin, et al. (1995). J Biol Chem **270**(10): 5405-11.

Tanimura, S., S. Ohtsuka, et al. (1999). FEBS Lett **447**(1): 5-9.

Tao, W. and A. J. Levine (1999). Proc Natl Acad Sci U S A **96**(6): 3077-3080.

Tao, W. and A. J. Levine (1999). Proc Natl Acad Sci U S A **96**(12): 6937-41.

Tarunina, M. and J. R. Jenkins (1993). Oncogene **8**(11): 3165-73.

Tewari, M. and V. M. Dixit (1995). J. Biol. Chem. **270**: 3255-3260.

Thomas, M., P. Massimi, et al. (1995). Oncogene **10**(2): 261-8.

Thompson, D. A., G. Belinsky, et al. (1997). Oncogene **15**(25): 3025-35.

Thut, C. J., J. L. Chen, et al. (1995). Science **267**(5194): 100-4.

Thut, C. J., J. A. Goodrich, et al. (1997). Genes Dev **11**(15): 1974-86.

Tibbetts, R. S., K. M. Brumbaugh, et al. (1999). Genes Dev **13**(2): 152-7.

Timchenko, N. A., T. E. Harris, et al. (1997). Mol Cell Biol **17**(12): 7353-61.

Timchenko, N. A., M. Wilde, et al. (1996). Genes Dev **10**(7): 804-15.

Tokino, T., S. Thiagalingam, et al. (1994). Hum Mol Genet **3**(9): 1537-42.

Tominaga, O., R. Hamelin, et al. (1993). Oncogene **8**(10): 2653-8.

Tornaletti, S. and G. P. Pfeifer (1996). Bioessays **18**(3): 221-8.

Trotter, M. J., L. Tang, et al. (1997). J Cutan Pathol **24**(5): 265-71.

Ueda, H., S. J. Ullrich, et al. (1995). Nat Genet **9**(1): 41-7.

Uittenbogaard, M. N., H. A. Giebler, et al. (1995). J Biol Chem **270**(48): 28503-6.

Ullman, K. S., M. A. Powers, et al. (1997). Cell **90**: 967-970.

Unger, T., M. Nau, et al. (1992). EMBO J. **11**: 1383-1390.

Urashima, M., G. Teoh, et al. (1998). Blood **92**(3): 959-67.

Utrera, R., L. Collavin, et al. (1998). Embo J **17**(17): 5015-25.

Van Meir, E. G., P. J. Polverini, et al. (1994). Nat Genet **8**(2): 171-6.

Varley, J. M., G. McGown, et al. (1996). Oncogene **12**(11): 2437-42.

Varley, J. M., G. McGown, et al. (1997). Cancer Res **57**(15): 3245-52.

Varmeh-Ziaie, S., I. Okan, et al. (1997). Oncogene **15**(22): 2699-704.

Varshavsky, A. (1992). Cell **69**: 725-735.

Varshavsky, A. (1997). Trends. Biochem. **22**: 383-387.

Venanzoni, M. C., L. R. Robinson, et al. (1996). Oncogene **12**(6): 1199-1204.

Venkatachalam, S., Y. P. Shi, et al. (1998). Embo J **17**(16): 4657-67.

Ventatachalam, S. and L. A. Donehower (1998). Mutat. Res. **400**: 392-407.

Wadgaonkar, R. and T. Collins (1999). J. Biol. Chem. **274**: 13760-13767.

Waga, S., G. J. Hannon, et al. (1994). Nature **369**: 574-578.

Wagenknecht, B., M. Hermisson, et al. (1999). Cell Physiol Biochem **9**(3): 117-125.

Wagner, A. J., J. M. Kokontis, et al. (1994). Genes Dev **8**(23): 2817-30.

Wahl, G. M., S. P. Linke, et al. (1997). Cancer Surv **29**: 183-219.

Waldman, T., K. W. Kinzler, et al. (1995). Cancer Res **55**(22): 5187-90.

Wales, M. M., M. A. Biel, et al. (1995). Nat Med **1**(6): 570-7.

Walker, K. K. and A. J. Levine (1996). Proc Natl Acad Sci U S A **93**(26): 15335-40.

Wang, Q., S. Fan, et al. (1996). J Natl Cancer Inst **88**(14): 956-65.

Wang, Q., G. P. Zambetti, et al. (1997). Mol Cell Biol **17**(1): 389-97.

Wang, X. W., W. Vermeulen, et al. (1996). Genes Dev **10**(10): 1219-32.

Wang, X. W., H. Yeh, et al. (1995). Nat Genet **10**(2): 188-95.

Wang, X. W., Q. Zhan, et al. (1997). Proc. Amer. Assoc. Ca. Res. **38**: 201.

Wang, X. W., Q. Zhan, et al. (1999). Proc Natl Acad Sci U S A **96**(7): 3706-11.

Wang, Y., G. Blandino, et al. (1999). Oncogene **18**: 2643-2649.

Wang, Y. and C. Prives (1995). Nature **376**(6535): 88-91.

Wang, Y., M. Reed, et al. (1993). Genes Dev **7**(12B): 2575-86.

Wasylyk, C., R. Salvi, et al. (1999). Oncogene **18**(11): 1921-34.

Watanabe, T., T. Hotta, et al. (1994). Blood **84**(9): 3158-65.

Waterman, J. L., J. L. Shenk, et al. (1995). Embo J **14**(3): 512-9.

Waterman, M. J., E. S. Stavridi, et al. (1998). Nat Genet **19**(2): 175-8.

Weber, J. D., L. J. Taylor, et al. (1999). Nat. Cell Biol. **1**: 20-26.

Webster, N. J., J. L. Resnik, et al. (1996). Cancer Res **56**(12): 2781-8.

Whitaker, S. J. (1992). Eur J Cancer **28**(1): 273-6.

Whitaker, S. J., S. N. Powell, et al. (1991). Eur J Cancer **27**(7): 922-8.

White, A. E., E. M. Livanos, et al. (1994). Genes Dev **8**(6): 666-77.

White, E. (1996). Genes & Dev. **10**: 1-15.

Whitesell, L., P. Sutphin, et al. (1997). Oncogene **14**(23): 2809-16.

Whitesell, L., P. D. Sutphin, et al. (1998). Mol Cell Biol **18**(3): 1517-24.

Wiech, H., J. Buchner, et al. (1992). Nature **358**: 169-170.

Wilcock, D. and D. P. Lane (1991). Nature **349**(6308): 429-31.

Wilkinson, C. R., M. Penney, et al. (1999). Philos Trans R Soc Lond B Biol Sci **354**(1389): 1523-32.

Wilkinson, C. R., M. Wallace, et al. (1998). Embo J **17**(22): 6465-76.

Williams, A. C., S. J. Browne, et al. (1993). Oncogene **8**(11): 3063-72.

Wold, M. S. (1997). Annu. Rev. Biochem. **66**: 61-92.

Wolkowicz, R., A. Peled, et al. (1995). Proc Natl Acad Sci U S A **92**(15): 6842-6.

Woo, R. A., K. G. McLure, et al. (1998). Nature **394**(6694): 700-4.

Wu, G. S., T. F. Burns, et al. (1997). Nat Genet **17**(2): 141-3.

Wu, G. S., P. Saftig, et al. (1998). Oncogene **16**(17): 2177-83.

Wu, L., J. H. Bayle, et al. (1995). Mol Cell Biol **15**(1): 497-504.

Wu, L. and A. J. Levine (1997). Mol Med **3**(7): 441-51.

Wu, X., J. H. Bayle, et al. (1993). Genes Dev **7**(7A): 1126-32.

Wu, X. and A. J. Levine (1994). Proc Natl Acad Sci U S A **91**(9): 3602-6.

Wu, Y., Y. Liu, et al. (1994). Embo J **13**(20): 4823-30.

Wyllie, A. H., G. J. Beattie, et al. (1981). Histochem J **13**(4): 681-92.

Xiao, H., A. Pearson, et al. (1994). Mol Cell Biol **14**(10): 7013-24.

Xiao, Z. X., J. Chen, et al. (1995). Nature **375**(6533): 694-8.

Xing, Y., C. V. Johnson, et al. (1995). J. Cell Biol. **131**: 1635-1647.

Xiong, Y., G. J. Hannon, et al. (1993). Nature **366**(6456): 701-4.

Xiong, Y., H. Zhang, et al. (1993). Genes Dev **7**(8): 1572-83.

Xu, J. and G. F. Morris (1999). Mol Cell Biol **19**(1): 12-20.

Yin, Y., M. A. Tainsky, et al. (1992). Cell **70**: 937-948.

Yin, Y., Y. Terauchi, et al. (1998). Nature **391**(6668): 707-10.

Yonish-Rouach, E., D. Resnitzky, et al. (1991). Nature **352**(6333): 345-7.

Yu, C. L., P. Driggers, et al. (1997). Biochem Biophys Res Commun **239**(2): 617-20.

Yu, H., J. Chen, et al. (1994). Cell **76**: 933-945.

Yuan, J., S. Shaham, et al. (1993). Cell **75**: 641-652.

Yuan, Z. M., Y. Huang, et al. (1999). J Biol Chem **274**(4): 1883-6.

Yuan, Z. M., Y. Huang, et al. (1996). Nature **382**(6588): 272-4.

Zakut-Houri, R., B. Bienz-Tadmor, et al. (1985). EMBO J. **4**: 1251-1255.

Zantema, A., P. I. Schrier, et al. (1985). Mol Cell Biol **5**(11): 3084-91.

Zastawny, R. L., R. Salvino, et al. (1993). Oncogene **8**(6): 1529-35.

Zeng, X., A. J. Levine, et al. (1998). Proc Natl Acad Sci U S A **95**(12): 6681-6.

Zhan, Q., I. Alamo, et al. (1996). Oncogene **13**(10): 2287-93.

Zhan, Q., M. J. Antinore, et al. (1999). Oncogene **18**(18): 2892-900.

Zhan, Q., I. T. Chen, et al. (1998). Mol Cell Biol **18**(5): 2768-78.

Zhan, Q., S. Fan, et al. (1994). Oncogene **9**(12): 3743-51.

Zhan, Q., S. Fan, et al. (1996). DNA Cell Biol **15**(10): 805-15.

Zhang, H., K. Somasundaram, et al. (1998). Oncogene **16**(13): 1713-21.

Zhang, Y., N. Fujita, et al. (1999). Oncogene **18**(5): 1131-8.

Zhang, Y. and Y. Xiong (1999). Mol Cell **3**(5): 579-91.

Zhang, Y., Y. Xiong, et al. (1998). Cell **92**(6): 725-34.

Zhu, J. W., D. DeRyckere, et al. (1999). Cell Growth Differ **10**(12): 829-38.

Ziegler, A., A. S. Jonason, et al. (1994). Nature **372**(6508): 773-6.

Zindy, F., C. M. Eischen, et al. (1998). Genes Dev **12**(15): 2424-33.

Zuo, Z., N. M. Dean, et al. (1998). J Biol Chem **273**(20): 12250-8.

zur Hausen, H. (1991). Virology **184**: 9-13.